DRAFT

Summary Report of
HVS Testing of the Palmdale Test Site, North Tangent Sections:
Evaluation of Long Life Pavement Rehabilitation Strategies—Rigid

Report prepared for the California Department of Transportation by:

Louw du Plessis, Fritz Jooste, Steve Keckwick, Wynand Steyn

CSIR Transportek
PO Box 395
Pretoria, Republic of South Africa

Technical Edit: John Harvey, Bill Nokes

Pavement Research Center
Institute of Transportation Studies
University of California Berkeley
University of California Davis

August 2005

EXECUTIVE SUMMARY

As part of the Caltrans Long Life Pavement Rehabilitation Strategies (LLPRS), a concrete pavement constructed with fast setting strength hydraulic cement concrete (FSHCC) and Portland cement concrete (PCC) blend was constructed on State Route 14 about 5 miles south of Palmdale, California. The test pavement was evaluated under Heavy Vehicle Simulator (HVS) testing beginning June 1999 and finishing December 2001. This report summarizes part of the testing program which was undertaken on three 70-m long test sections with a 200-mm thick FSHCC and the following design features:

- Section 7 was constructed with plain joints (no dowels), relying on aggregate interlock for joint load transfer, with an asphalt concrete shoulder and a normal lane width of 3.66 m.
- Section 9 was constructed with dowels and a concrete shoulder with tie bars and a normal lane width of 3.66 m.
- Section 11 was constructed using a widened truck lane (4.26 m wide) and doweled joints with an asphalt concrete shoulder.

The most significant observations are briefly discussed subsequently.

Environmental Influences on the Behavior of the Concrete Slab

Temperature played a significant role in the behavior of the concrete slab in two ways:

1. Daily variations in slab temperatures cause the slabs to go through cycles of expansion and contraction, which had a noticeable effect on the measured load transfer efficiency (LTE) at joints. During the hotter part of the day, the slabs expanded, the joints locked up, and LTE values close to 100 percent were commonly

calculated. At night when slab contraction took place, the opposite occurred: LTE values dropped to lower than 80 percent.

2. Owing to temperature differentials (temperature at the surface of the slab minus the temperature at the bottom of the slab) the concrete slabs went through cycles of being curled upwards (at night when the top is cooler than the bottom) and being curled downwards (during the day when the top is warmer than the bottom). Analysis of deflections and temperatures indicated that high deflection measurements were associated lower surface temperatures (and negative temperature differentials) and vice versa. An inversely proportional relationship was observed between surface temperature, the temperature difference between the top and the bottom of the PCC layer, and the measured deflections.

These two effects played major roles in the behavior of the concrete under accelerated loading. Throughout this study, the influence of the above-mentioned slab movements were visible on the parameters used to determine the extent and degree of damage on each test. The surface deflections measured at night were at least double those recorded during the day at the same locations. It is obvious that deflection measurements were highly dependent on the time of day. It is therefore very important that slab curl resulting from temperature variations should be built into any deflection analysis on concrete pavements.

Permanent Warping Due to Differential Shrinkage

Although concrete shrinkage was limited in some cases by the inclusion of design features (i.e., dowels and tie bars), the observations made during this study show that slab warping due to differential shrinkage between the upper and the lower part of the concrete layer

played a significant role in the measured deflections. Deflection sensors placed just below the concrete in the base layer close to the edge registered very small deflections, even with the application of test loads greater than 90 kN. Deflections recorded in the base layer were typically less than 0.2 mm, while the surface mount modules recorded deflections between 1 and 1.2 mm for the same test. This means that less than 20 per cent of the surface deflections were passed on to the base layer. One explanation for this observation is that, due to differential shrinkage, the slabs were slightly curled upwards all along its longitudinal edge which created a cavity between the bottom of the PCC layer and the base. The high deflections measured at the top were a direct result of this loss in support from the sub-structure.

Traffic-Induced Changes in the Behavior of the Concrete Slabs

From this study it is clear that in almost all the cases, deflection variations caused by daily and seasonal temperature changes masked the damaging effect caused by repetitive loading. At night (low surface temperatures), the slabs were warmer at the bottom than the top, causing the slabs to curl upwards and slab lift-off from the base layers occurred. Nighttime deflection measurements were high due to the loss in support from the underlying layers. During the day, the slabs were warmer at the top than the bottom, resulting in downward curling of the slabs and low deflections.

A significant drop in surface deflections and subsequent increase in base layer deflections occurred after the appearance of cracks on the undoweled test sections. The cracks caused the slabs to come into full contact with the base layer. This resulted in increased support from the underlying layers and, therefore, an increase in base layer deflections and a subsequent reduction in the measured surface deflections.

Comparing the Performance of the Three Different Structures

Because different loading regimes for different tests were used, direct one-to-one comparisons of all tests is not possible. The performance of the two main structural response parameters, edge surface deflections and load transfer efficiency (LTE) is briefly discussed below.

Section 7, Plain Joints (Relying on Aggregate Interlock for Joint Load Transfer), Normal Lane Width

Edge surface deflections under the influence of a 90-kN test load were on the order of 2 to 4 mm before any cracks appeared, and dropped to approximately 1 to 2.2 mm after edge and corner cracks appeared.

LTE values started around 99 percent and dropped to as low as 20 percent after corner cracks appeared

Section 9, Doweled with Concrete Shoulder and Tie Bars, Normal Lane Width

Edge surface deflections under the influence of a 90-kN test load were on the order of 0.8 to 1.8 mm, before any cracks appeared. No dramatic difference in edge deflections could be detected after the appearance of cracks.

LTE values varied between 80 and 100 percent for the duration of testing. The appearance of cracks did not cause any reduction in LTE values; in fact in a few cases, it caused an increase in LTE values.

Section 11, Doweled, Asphalt Shoulder, Widened Truck Lane (4.26 m)

Edge deflections under the influence of a 90-kN test load were on the order of 0.6 to 1.4 mm, before any cracks appeared and 0.8 to 1.5 mm after the appearance of cracks.

LTE values varied between 97 and 100 percent for the duration of testing. The appearance of cracks did not cause any reduction in LTE values.

Conclusion

The advantages of dowels, tie bars, and a widened (4.26-m) lane are clearly illustrated in the study. Even after the application of aggressive 150-kN loading onto the test sections, no obvious LTE deterioration could be detected from the sections constructed with dowels, tie bars, and widened lanes. Although significant cracks developed during the testing period, no significant drop in LTE values could be detected after the formation of the cracks, which is an indication of the effectiveness of the dowels to transfer load across joints, even after extensive joint deterioration. The dowels had a significant influence in controlling slab edge movements.

In contrast to this, the plain aggregate interlock sections (no dowels or tie bars) experienced significant reductions in LTE after the appearance of corner cracks. The damaging effect of repetitive loading caused a significant reduction in the life of the pavement in comparisons with the reinforced jointed sections.

TABLE OF CONTENTS

Executive Summary i

Environmental Influences on the Behavior of the Concrete Slab i

Permanent Warping Due to Differential Shrinkage ii

Traffic-Induced Changes in the Behavior of the Concrete Slabs iii

Comparing the Performance of the Three Different Structures iv

Section 7, Plain Joints (Relying on Aggregate Interlock for Joint Load Transfer), Normal Lane Width iv

Section 9, Doweled with Concrete Shoulder and Tie Bars, Normal Lane Width iv

Section 11, Doweled, Asphalt Shoulder, Widened Truck Lane (4.26 m) v

Conclusion v

Table of Contents vii

List of Figures xiii

List of Tables xxvii

1.0 Introduction 1

2.0 HVS Test Objectives and Scope Of Work 3

3.0 HVS Test Program 5

3.1 HVS Instrumentation 8

3.1.1 Joint Deflection Measuring Device (JDMD) 9

3.1.2 Multi-Depth Deflectometer (MDD) 10

3.1.3 Thermocouples 22

3.2 HVS Loading Plan 22

4.0 HVS Results 27

4.1 Test 532FD 28
4.1.1 Visual Observations 29
4.1.2 Joint Deflection Measuring Device (JDMD) Results 31
4.1.3 Joint Load Transfer Efficiency (LTE) 33
4.2 Test 533FD 35
4.2.1 Visual Observations 35
4.2.2 Joint Deflection Measuring Device (JDMD) Results 36
4.2.3 Joint Load Transfer Efficiency (LTE) 38
4.2.4 Multi-Depth Deflectometer (MDD) Results 41
4.3 Test 534FD 45
4.3.1 Visual Observations 46
4.3.2 Joint Deflection Measuring Device (JDMD) Results 46
4.3.3 Joint Load Transfer Efficiency (LTE) 51
4.3.4 Multi-Depth Deflectometer (MDD) Results 51
4.4 Test 535FD 57
4.4.1 Visual observation 57
4.4.2 Joint Deflection Measuring Device (JDMD) Results 59
4.4.3 Joint Load Transfer Efficiency (LTE) 62
4.4.4 Multi-Depth Deflectometer (MDD) Results 64
4.5 Test 536FD 69
4.5.1 Visual Observations 70
4.5.2 Joint Deflection Measuring Device (JDMD) Results 71
4.5.3 Multi-Depth Deflectometer (MDD) Results 86

4.5.4 Joint Load Transfer Efficiency (LTE) 92
4.6 Test 537FD 97
4.6.1 Visual Observations 97
4.6.2 Joint Deflection Measuring Device (JDMD) Results 100
4.6.3 Multi-Depth Deflectometer (MDD) Results 107
4.6.4 Load Transfer Efficiency (LTE) 120
4.7 Test 538FD 125
4.7.1 Visual Observations 126
4.7.2 Joint Deflection Measuring Device (JDMD) Results 128
4.7.3 Multi-Depth Deflectometer (MDD) Results 140
4.7.4 Load Transfer Efficiency (LTE) 141
4.8 Test 539FD 145
4.8.1 Visual Observations 146
4.8.2 Joint Deflection Measuring Device (JDMD) Results 148
4.8.3 Joint Load Transfer Efficiency (LTE) 151
4.8.4 Multi-Depth Deflectometer (MDD) Elastic Deflection Results 152
4.8.5 Multi-Depth Deflectometer (MDD) Permanent Deformation Results 157
4.9 Test 540FD 161
4.9.1 Visual Observations 161
4.9.2 Joint Deflection Measuring Device (JDMD) Results 163
4.9.3 Joint Load Transfer Efficiency (LTE) 166
4.9.4 Multi-Depth Deflectometer (MDD) Elastic Deflection Results 167
4.9.5 Multi-Depth Deflectometer (MDD) Permanent Deformation Data 171

4.10 Test 541FD 175
4.10.1 Visual Observations 175
4.10.2 Joint Deflection Measuring Device (JDMD) Results 176
4.10.3 Joint Load Transfer Efficiency (LTE) 179
4.11 Test 541FD Phase II 180
4.11.1 Visual Observations 181
4.11.2 Joint Deflection Measuring Device (JDMD) Results 182
4.11.3 Joint Load Transfer Efficiency (LTE) 189
4.11.4 Permanent Deformation 190
5.0 Falling Weight Deflectometer (FWD) Results 195
5.1 Available Data and Analysis Methodology 196
5.2 Test Configuration 199
5.2.1 Principal Effects 199
5.3 Analysis of Maximum Deflections 202
5.3.1 Measurements Recorded Prior to Concrete Construction 202
5.3.2 Measurements Taken After Concrete Construction 204
5.4 Load Transfer Efficiency Across Joints 213
5.5 Deflections Before and After HVS Testing 229
5.5.1 Test 532FD (Section 7: No Dowels or Tie Bars) 230
5.5.2 Test 533FD (Section 7: No Dowels or Tie Bars) 231
5.5.3 Test 534FD (Section 7: No Dowels or Tie Bars) 232
5.5.4 Test 535FD (Section 7: No Dowels or Tie Bars) 233
5.5.5 Test 536FD (Section 9: Dowels and Tie Bars) 234

5.5.6 Test 537FD (Section 9: Dowels and Tie Bars) 235
5.5.7 Test 538FD (Section 9: Dowels and Tie Bars) 236
5.5.8 Test 539FD (Section 11: Dowels, No Tie Bars, Widened Truck Lane) 237
5.5.9 Test 540FD (Section 11: Dowels, No Tie Bars, Widened Truck Lane) 238
5.5.10 Test 541FD (Section 11: Dowels, No Tie Bars, Widened Truck Lane) 239
5.5.11 Observations and Conclusions 240
5.6 Back-calculated Stiffnesses 240
5.7 Summary and Conclusions 249
6.0 PCC Core Measurements (North Tangent) 251
6.1 Cores taken 40 days after construction 251
6.1.1 Slab Thickness 254
6.1.2 Core Densities 254
6.1.3 Compressive Strength 255
6.2 Observations from Cores Taken After HVS Testing 256
6.2.1 Slab Thickness 256
6.2.2 Instrument Positioning 260
6.2.3 Crack Mechanisms 262
6.3 Observations and Comments on Day/Night Cores Taken in February 2001 267
6.3.1 Day/Night Measurements of Cores at Joints 268
6.3.2 Day/Night Measurements of Cracks through Joints 269
6.3.3 Day/Night Measurements of Normal Surface Cracks 271
6.3.4 Dowel Bar Placement Measurements 272
7.0 Discussion of HVS Test Results and Conclusions 275

7.1 Deflection Profiles 276
7.1.1 Section 7: No Dowels, No Tie Bars, Asphalt Shoulder (Tests 532–535FD) 288
7.1.2 Section 9: Dowels, Tied Concrete Shoulder (Tests 536FD–538FD) 289
7.1.3 Section 11: Dowels, Asphalt Shoulder, Widened (4.26-m) Truck Lane (Tests 539FD–541FD) 291
7.2 Influence of Main Test Variables 292
7.2.1 Dowels 292
7.2.2 Widened (4.26-m) Truck Lane Slabs 293
7.3 General Conclusions 295
8.0 References 297
9.0 Appendix A: Stripmaps Showing FWD Deflections 299

LIST OF FIGURES

Figure 1. Layout of HVS testing areas on the North Tangent. 6

Figure 2. Illustration of the placement of JDMD instruments and their numbering with respect to the test sections. 10

Figure 3. Instrumentation layout of Test Section 532FD. 12

Figure 4. Instrumentation layout of Test Section 533FD. 13

Figure 5. Instrumentation layout of Test Section 534FD. 14

Figure 6. Instrumentation layout of Test Section 535FD. 15

Figure 7. Instrumentation layout of Test Section 536FD. 16

Figure 8. Instrumentation layout of Test Section 537FD. 17

Figure 9. Instrumentation layout of Test Section 538FD. 18

Figure 10. Instrumentation layout of Test Section 539FD. 19

Figure 11. Instrumentation layout of Test Section 540FD. 20

Figure 12. Instrumentation layout of Test Section 541FD. 21

Figure 13. Schematic of crack pattern, Test 532FD. 30

Figure 14. Composite image of Test 532FD showing cracks. 30

Figure 15. Plot of JDMD deflections and temperature versus load repetitions, Test 532FD. 32

Figure 16. Plot of LTE and temperature versus load repetitions, Test 532FD. 34

Figure 17. Schematic of crack pattern, Test 533FD. 37

Figure 18. Composite image of Test 533FD showing cracks. 37

Figure 19. Plot of JDMD deflections and temperature versus load repetitions, Test 533FD. 39

Figure 20. Plot of LTE and temperature versus load repetitions, Test 533FD. 40

Figure 21. Plot of MDD 14 deflections and temperature versus load repetitions, Test 533FD. ...43

Figure 22. Plot of MDD 15 deflections and temperature versus load repetitions, Test 533FD. ...44
Figure 23. Schematic of crack pattern, Test 534FD. 47
Figure 24. Composite image of Test 534FD showing cracks. 47
Figure 25. Plot of JDMD deflections and temperature versus load repetitions (entire loading sequence), Test 534FD. 48
Figure 26. Plot of JDMD deflections and temperature versus load repetitions (1M repetitions to end of test), Test 534FD. 50
Figure 27. Plot of LTE and temperature versus load repetitions, Test 534FD. 52
Figure 28. Plot of MDD 12 deflections and temperature versus load repetitions, Test 534FD. ...53
Figure 29. Plot of MDD 13 deflections and temperature versus load repetitions, Test 534FD. ...54
Figure 30. Plot of MDD 12 permanent deformation and temperature versus load repetitions, Test 534FD....56
Figure 31. Schematic of crack pattern, Test 535FD. 58
Figure 32. Composite image of Test 535FD showing cracks. 58
Figure 33. Plot of JDMD deflections and temperature versus load repetitions, Test 535FD. 60
Figure 34. Plot of LTE and temperature versus load repetitions, Test 535FD. 63
Figure 35. Plot of MDD 11 deflections and temperature versus load repetitions, Test 535FD. ...66
Figure 36. Plot of MDD 11 permanent deformation and temperature versus load repetitions, Test 535FD....68
Figure 37. Composite image of Test 536FD....70
Figure 38. Plot of JDMD deflections and temperature versus load repetitions, 90-kN test load, Test 536FD....72

Figure 39. Plot of JDMD deflections and temperature versus load repetitions; 90-, 110-, 130-, and 150-kN test loads; Test 536FD. 73
Figure 40. Plot of JDMD deflections and temperature versus load repetitions, 150-kN test load, Test 536FD. 74
Figure 41. Joint deflections and the effect of wheel load repetitions, Test 536FD. 75
Figure 42. Effect of wheel load repetitions on midspan and horizontal deflections, Test 536FD. 79
Figure 43. Effect of temperature on joint deflections, Test 536FD. 81
Figure 44. Effect of temperature on midspan and horizontal deflections, Test 536FD. 84
Figure 45. Relationship between temperature and joint deflection, Test 536FD. 85
Figure 46. Effect of wheel load repetitions on MDD deflections, Test 536FD. 87
Figure 47. Plot of MDD 10 permanent deformation and temperature versus load repetitions, Test 536FD. 89
Figure 48. Plot of MDD permanent deformation differentials and temperature versus load repetitions, Test 536FD. 91
Figure 49. Joint load transfer efficiency at Joints 26 and 27, Test 536FD. 93
Figure 50. Comparison of joint deflections on either side of Slab 27 (Joints 26 and 27), Test 536FD. 94
Figure 51. Plot of LTE and temperature versus load repetitions, Test 536FD. 95
Figure 52. Joint load transfer efficiency at Joints 26 and 27, Test 536FD. 96
Figure 53. Schematic of crack pattern, Test 537FD. 98
Figure 54. Composite image of Test 537FD showing cracks. 98
Figure 55. Plot of JDMD deflections and temperature versus load repetitions, Test 537FD. 101

Figure 56. Effect of wheel load repetitions on joint deflections, Test 537FD. 102

Figure 57. Effect of wheel load repetitions on mid-span and horizontal deflections, Test 537FD. 106

Figure 58. Effect of temperature on joint deflections, Test 537FD. 108

Figure 59. Effect of temperature on mid-span and horizontal deflections, Test 537FD. 109

Figure 60. Effect of temperature and joint deflections, Test 537FD. 110

Figure 61. Plost of MDD 8 deflections and temperature versus load repetitions, Test 537FD. .. 112

Figure 62. Plot of MDD 9 deflections and temperature versus load repetitions, Test 537FD. ... 113

Figure 63. Plot of MDD 8 permanent deformation and temperature versus load repetitions, Test 537FD. 115

Figure 64. Plot of MDD 8 permanent deformation differentials and temperature versus load repetitions, Test 537FD. 116

Figure 65. Plot of MDD 9 permanent deformation and temperature versus load repetitions, Test 537FD. 117

Figure 66. Plot of MDD 9 permanent deformation differentials and temperature versus load repetitions, Test 537FD. 118

Figure 67. Joint load transfer efficiency at Joints 22 and 23, Test 537FD. 121

Figure 68. Comparison of joint deflections on either side of Slab 23 (Joints 22 and 23), Test 537FD. 123

Figure 69. Plot of LTE and temperature versus load repetitions, Test 537FD. 124

Figure 70. Joint load transfer efficiency at Joints 22 and 23, Test 537FD. 125

Figure 71. Schematic of crack pattern, Test 538FD. 127

Figure 72. Composite image of Test 538FD showing cracks. 127

Figure 73. Plot of JDMD deflections and temperature versus load repetitions, Test 538FD. 129
Figure 74. Effect of wheel load repetitions on joint deflections, Test 538FD.....130
Figure 75. Effect of wheel load repetitions on mid-span and horizontal deflections, Test 538FD. 133
Figure 76. Effect of temperature on joint deflections, Test 538FD. 135
Figure 77. Effect of temperature on mid-span and horizontal deflections, Test 538FD. 136
Figure 78. Relationship between temperature and joint deflection, Test 538FD. 137
Figure 79. Plot of JDMD permanent deformation and temperature versus load repetitions, Test 538FD.....139
Figure 80. Comparison of deflections on both sides of Joints 18 and 19, Test 538FD. 142
Figure 81. Comparison of deflections on either side of Slab 19 (Joints 18 and 19), Test 538FD. 143
Figure 82. Plot of LTE and temperature versus load repetitions, Test 538FD. 144
Figure 83. Comparison of LTE at each end of Slab 19 (Joints 18 and 19), Test 538FD.....145
Figure 84. Schematic of crack pattern, Test 539FD. 147
Figure 85. Composite image of Test 539FD showing cracks. 147
Figure 86. Plot of JDMD deflections and temperature versus load repetitions, Test 539FD. 150
Figure 87. Plot of MDD 5 deflections and temperature versus load repetitions, Test 539FD. ...154
Figure 88. Plot of MDD 4 deflections and temperature versus load repetitions, Test 539FD. ...155
Figure 89. Plot of MDD 5 permanent deformation and temperature versus load repetitions, Test 539FD.....159
Figure 90. Plot of MDD 4 permanent deformation and temperature versus load repetitions, Test 539FD.....160

Figure 91. Schematic of crack pattern, Test 540FD. 162

Figure 92. Composite image of Section 540FD showing crack pattern. 162

Figure 93. Plot of JDMD deflections and temperature versus load repetitions, Test 540FD. 165

Figure 94. Plot of MDD 2 deflections and temperature versus load repetitions, Test 540FD. ...169

Figure 95. Plot of MDD3 deflections and temperature versus load repetitions, Test 540FD. 170

Figure 96. Plot of MDD 2 permanent deformation and temperature versus load repetitions, Test 540FD.....173

Figure 97. Plot of MDD 3 permanent deformation and temperature versus load repetitions, Test 540FD.....174

Figure 98. Composite image of Test Section 541FD.....176

Figure 99. Plot of JDMD deflections and temperature versus load repetitions, Test 541FD. 178

Figure 100. Composite image of Test 541FD phase II. 181

Figure 101. Plot of JDMD deflections versus test load at the start of Test 541FD Phase II. 183

Figure 102. Plot of JDMD deflections and temperature versus load repetitions (40-kN test load), Test 541FD Phase II. 185

Figure 103. Plot of JDMD deflections and temperature versus load repetitions (90-kN test load), Test 541FD Phase II. 186

Figure 104. Plot of JDMD deflections and temperature versus load repetitions (150-kN test load), Test 541FD Phase II. 187

Figure 105. Plot of JDMD permanent deformation and temperature versus load repetitions (first 125,000 repetitions), Test 541FD Phase II. 191

Figure 106. Plot of JDMD permanent displacement and temperature versus load repetitions, Test 541FD Phase II. 192

Figure 107. FWD measurement program relative to HVS program.....196
Figure 108. General setup for FWD measurement locations.....200
Figure 109. Sensor setup for measurements across transverse and longitudinal joints.....200
Figure 110. Maximum deflection measured along slab centerline prior to concrete construction.....203
Figure 111. Maximum deflection measured along K-rail edge prior to concrete construction...203
Figure 112. Central deflection along centerline at different concrete ages, Section 11 (doweled joints with asphalt concrete shoulder and widened truck lane). 206
Figure 113. Central deflection along centerline at different surface temperatures, Section 11 (doweled joints with asphalt concrete shoulder and widened truck lane), ...207
Figure 114. Central deflection along centerline at different concrete ages, Section 9 (doweled joints and tie bars at concrete shoulder).....207
Figure 115. Central deflection along centerline at different temperatures, Section 9 (doweled joints and tie bars at concrete shoulder). 208
Figure 116. Central deflection along centerline at different concrete ages, Section 7 (no dowels or tie bars, asphalt concrete shoulder). 208
Figure 117. Central deflection along centerline at different temperatures, Section 7 (no dowels or tie bars, asphalt concrete shoulder). 209
Figure 118. Central deflection along K-rail at different concrete ages, Section 11 (doweled joints with asphalt concrete shoulder and widened truck lane). 210
Figure 119. Central deflection along K-rail at different temperatures, Section 11 (doweled joints with asphalt concrete shoulder and widened truck lane). 211

Figure 120. Central deflection along K-rail at different concrete ages, Section 9 (doweled joints and tie bars at concrete shoulder). 211
Figure 121. Central deflection along K-rail at different temperatures, Section 9 (doweled joints and tie bars at concrete shoulder). 212
Figure 122. Central deflection along K-rail at different concrete ages, Section 7 (no dowels or tie bars, asphalt concrete shoulder). 212
Figure 123. Central deflection along K-rail at different temperatures, Section 7 (no dowels or tie bars, asphalt concrete shoulder). 213
Figure 124. Typical deflection profile measured across a transverse joint along slab centerline. 214
Figure 125. Typical deflection profile measured across a transverse joint along slab edge (K-rail side). 214
Figure 126. LTE across transverse joints at concrete ages of less than 300 days. 218
Figure 127. LTE across transverse joints at concrete ages of more than 900 days (only day measurements are shown). 219
Figure 128. Transverse joint LTE versus concrete age, Section 11 (doweled joints with asphalt concrete shoulder and widened truck lane). 219
Figure 129. Transverse joint LTE versus surface temperature, Section 11 (doweled joints with asphalt concrete shoulder and widened truck lane). 220
Figure 130. Transverse joint LTE versus concrete age, Section 9 (doweled joints and tie bars at concrete shoulder). 220
Figure 131. Transverse joint LTE versus surface temperature, Section 9 (doweled joints and tie bars at concrete shoulder). 221

Figure 132. Transverse joint LTE versus concrete age, Section 7 (no dowels or tie bars, asphalt concrete shoulder). 221
Figure 133. Transverse joint LTE versus surface temperature, Section 7 (no dowels or tie bars, asphalt concrete shoulder).....222
Figure 134. Longitudinal joint LTE versus concrete age at slab center along K-rail edge, Section 11 (doweled joints with asphalt concrete shoulder and widened truck lane). 223
Figure 135. Longitudinal joint LTE versus surface temperature at slab center along K-rail edge, Section 11 (doweled joints with asphalt concrete shoulder and widened truck lane). 223
Figure 136. Longitudinal joint LTE versus concrete age at slab center along K-rail edge, Section 9 (doweled joints and tie bars at concrete shoulder).....224
Figure 137. Longitudinal joint LTE versus surface temperature at slab center along K-rail edge, Section 9 (doweled joints and tie bars at concrete shoulder). 224
Figure 138. Longitudinal joint LTE versus concrete age at slab center along K-rail edge, Section 7 (no dowels or tie bars, asphalt concrete shoulder).....225
Figure 139. Longitudinal joint LTE versus surface temperature at slab center along K-rail edge, Section 7 (no dowels or tie bars, asphalt concrete shoulder). 225
Figure 140. Longitudinal joint LTE versus concrete age at slab corner along K-rail edge, Section 11 (doweled joints with asphalt concrete shoulder and widened truck lane). 226

Figure 141. Longitudinal joint LTE versus surface temperature at slab corner along K-rail edge, Section 11 (doweled joints with asphalt concrete shoulder and widened truck lane). 227
Figure 142. Longitudinal joint LTE versus concrete age at slab corner along K-rail edge, Section 9 (doweled joints and tie bars at concrete shoulder).....227
Figure 143. Longitudinal joint LTE versus surface temperature at slab corner along K-rail edge, Section 9 (doweled joints and tie bars at concrete shoulder). 228
Figure 144. Longitudinal joint LTE versus concrete age at slab corner along K-rail edge, Section 7 (no dowels or tie bars, asphalt concrete shoulder).....228
Figure 145. Longitudinal joint LTE versus surface temperature at slab corner along K-rail edge, Section 7 (no dowels or tie bars, asphalt concrete shoulder). 229
Figure 146. Impact of HVS testing on central deflection measured at slab center (Test 532FD). 230
Figure 147. Impact of HVS testing on LTE at transverse joints measured along slab centerline (Test 532FD). 230
Figure 148. Impact of HVS testing on central deflection measured at slab center (Test 533FD). 231
Figure 149. Impact of HVS testing on LTE measured at transverse joints along slab centerline (Test 533FD). 231
Figure 150. Impact of HVS testing on central deflection measured at slab center (Test 534FD). 232
Figure 151. Impact of HVS testing on LTE measured at transverse joints along slab centerline (Test 534FD). 232

Figure 152. Impact of HVS testing on central deflection measured at slab center (Test 535FD). 233
Figure 153. Impact of HVS testing on LTE measured at transverse joints along slab centerline (Test 535FD). 233
Figure 154. Impact of HVS testing on central deflection measured at slab center (Test 536FD). 234
Figure 155. Impact of HVS testing on central LTE measured at transverse joints along slab centerline (Test 536FD). 234
Figure 156. Impact of HVS testing on central deflection measured at slab center (Test 537FD). 235
Figure 157. Impact of HVS testing on LTE measured at transverse joints along slab centerline (Test 537FD). 235
Figure 158. Impact of HVS testing on central deflection measured at slab center (Test 538FD). 236
Figure 159. Impact of HVS testing on LTE measured at transverse joint along slab centerline (Test 538FD). 236
Figure 160. Impact of HVS testing on central deflection measured at slab center (Test 539FD). 237
Figure 161. Impact of HVS testing on LTE measured at transverse joints along slab centerline (Test 539FD). 237
Figure 162. Impact of HVS testing on central deflection measured at slab center (Test 540FD). 238

Figure 163. Impact of HVS testing on LTE measured at transverse joints along slab centerline (Test 540FD). 238
Figure 164. Impact of HVS testing on central deflection measured at slab center (Test 541FD). 239
Figure 165. Impact of HVS testing on LTE measured at transverse joints along slab centerline (Test 541FD). 239
Figure 166. Back-calculated stiffness 1 day after concrete construction. 242
Figure 167. Back-calculated stiffness 7 days after concrete construction. 242
Figure 168. Back-calculated stiffness 49 days after concrete construction. 243
Figure 169. Back-calculated stiffness 90 days after concrete construction. 243
Figure 170. Back-calculated stiffness 200 days after concrete construction. 244
Figure 171. Back-calculated stiffness 270 days after concrete construction. 244
Figure 172. Back-calculated stiffness 966 days after concrete construction (daytime measurement). 245
Figure 173. Back-calculated stiffness 966 says after concrete construction (daytime measurement). 245
Figure 174. Concrete stiffness at different ages, Section 11 (doweled joints with asphalt concrete shoulder and widened truck lane) 246
Figure 175. Concrete stiffness at different ages, Section 9 (doweled joints and tie bars at concrete shoulder). 246
Figure 176. Concrete stiffness at different ages, Section 7 (no dowels or tie bars, asphalt concrete shoulder). 247

Figure 177. Subgrade stiffness at different ages, Section 11 (doweled joints with asphalt concrete shoulder and widened truck lane).....247
Figure 178. Subgrade stiffness at different ages, Section 7 (no dowels or tie bars, asphalt concrete shoulder).....248
Figure 179. Subgrade stiffness at different ages, Section 9 (doweled joints and tie bars at concrete shoulder).....248
Figure 180. Relationship between compressive strength and concrete density.....255
Figure 181a. Variation in deflection with respect to N10, Section 7 (no dowels or tie bars, asphalt concrete shoulder), Test 532FD. 278
Figure 181b. Variation in deflection with respect to N10, Section 7 (no dowels or tie bars, asphalt concrete shoulder), Test 534FD. 279
Figure 181c. Variation in deflection with respect to N10, Section 7 (no dowels or tie bars, asphalt concrete shoulder), Test 533FD. 280
Figure 181d. Variation in deflection with respect to N10, Section 7 (no dowels or tie bars, asphalt concrete shoulder), Test 535FD. 281
Figure 182a. Variation in deflection with respect to N10, Section 9 (doweled joints and tie bars at concrete shoulder), Test 536FD. 282
Figure 182b. Variation in deflection with respect to N10, Section 9 (doweled joints and tie bars at concrete shoulder), Test 537FD. 283
Figure 182c. Variation in deflection with respect to N10, Section 9 (doweled joints and tie bars at concrete shoulder), Test 538FD. 284
Figure 183a. Variation in deflection with respect to N10, Section 11 (doweled joints with asphalt concrete shoulder and widened truck lane). Test 539FD. 285

Figure 183b. Variation in deflection with respect to N10, Section 7 (no dowels or tie bars, asphalt concrete shoulder), Test 540FD. 286
Figure 183c. Variation in deflection with respect to N10, Section 7 (no dowels or tie bars, asphalt concrete shoulder), Test 541FD. 287

LIST OF TABLES

Table 1 HVS Tests on the North Tangent 6

Table 2 Slab Dimensions 7

Table 3 Location of MDDs Placed on the North Tangent HVS Sections 11

Table 4 Loading Plan for the HVS Tests 23

Table 5 JDMD Deflections, Test 532FD 31

Table 6 Load Transfer Efficiency, Test 532FD 33

Table 7 JDMD Deflections, Test 533FD 36

Table 8 Load Transfer Efficiency, Test 533FD 41

Table 9 MDD Deflections, Test 533FD 42

Table 10 JDMD Deflections, Test 534FD 46

Table 11 MDD Deflections, Test 534FD 51

Table 12 MDD 12 Permanent Deformation, Test 534FD 55

Table 13 JDMD Deflections, Test 535FD 59

Table 14 Load Transfer Efficiency, Test 535FD 62

Table 15 MDD Deflections, Test 535FD 65

Table 16 MDD Permanent Deformation, Test 535FD 67

Table 17 JDMD Deflections to 750,000 repetitions, 90-kN Load, Test 536FD 76

Table 18 Deflections After 500 Repetitions of Various Aircraft Wheel Loads, Test 536FD) 77

Table 19 Test Temperature Conditions, Test 536FD 82

Table 20 JDMD Deflections (Test loads 40 kN, 70 kN, 90 kN), Test 539FD 149

Table 21 Load Transfer Efficiency, Test 539FD 152

Table 22 MDD 5 Deflections (Test Loads 40 kN, 70 kN, 90 kN), Test 539FD.....153

Table 23 MDD 4 Deflections (Test loads 40 kN, 70 kN, 90 kN) Test 539FD.....153

Table 24 MDD 5 Permanent Deformation, Test 539FD.....158

Table 25 MDD 4 Permanent Deformation, Test 539FD.....158

Table 26 JDMD Deflections, (Test Load 40 kN, 90 kN, 150 kN) Test 540FD.....164

Table 27 Load Transfer Efficiency, Test 540FD.....166

Table 28 MDD 2 Deflections (Test load 40 kN, 90 kN, 150 kN), Test 540FD.....168

Table 29 MDD 3 Deflections (Test load 40 kN, 90 kN, 150 kN), Test 540FD.....168

Table 30 MDD 2 Permanent Deformation, Test 540FD.....172

Table 31 MDD 3 Permanent Deformation, Test 540FD.....172

Table 32 JDMD Deflections (Test Loads 70 kN, 90 kN, 150 kN) Test 541FD.....177

Table 33 Load Transfer Efficiency, Test 541FD.....179

Table 34 Relationship between Test Loads and Measured Deflections, Test 541FD Phase II.....182

Table 35 JDMD Deflections, Test Load 40 kN, Test 541FD Phase II.....183

Table 36 JDMD Deflections, Test Load 90 kN, Test 541FD Phase II.....184

Table 37 Average of all 40-kN Deflection, Test 541FD.....188

Table 38 Load Transfer Efficiency at Various Loads, Test 541FD Phase II.....189

Table 39 Load Transfer Efficiency, Test Load 40 kN, Test 541FD Phase II.....189

Table 40 Summary of Relevant FWD Tests Performed on North Tangent.....197

Table 41 Summary of Average Central Deflections Along Slab Centerline.....205

Table 42 Summary of Average Central Deflection Measured Along Slab Edge (K-rail Side).....206

Table 43 Summary of LTE Across Transverse Joints Along Slab Centerline 215
Table 44 Summary of LTE Across Longitudinal Joints Along K-Rail Edge, Slab Center.....216
Table 45 Summary of LTE Across Longitudinal Joints Along K-Rail Edge, At Slab Corner 216
Table 46 Properties and Statistics of Cores Taken Approximately 40 Days After Construction.....252
Table 47 Core Height Statistics of Cores Taken after HVS Testing on Section 7 257
Table 48. Core Height Statistics of Cores Taken After HVS Testing on Section 9 258
Table 49 Core Height Statistics of Cores Taken After HVS Testing on Section 11 259
Table 50 Summary of Core Height Statistics.....259
Table 51 Strain Gauge Positioning as Measured from Cores after HVS Testing.....261
Table 52 Observations from Cores Taken Through Cracks on Section 7 263
Table 53 Observations from Cores Taken Through Cracks on Section 9 264
Table 54 Observations from Cores Taken Through Cracks on Section 11 265
Table 55 Saw-cut and Core Height Statistics, Day/Night Cores 268
Table 56 Day/Night Crack Widths at Bottom of Cores Drilled through Joints on the North Tangent.....269
Table 57 Day/Night Crack Widths at Bottom of Cores Drilled through Joints on the South Tangent.....270
Table 58 Day/Night Crack Widths from Cores Drilled on Cracks on the South Tangent..271
Table 59 Dowel Bar Placement Statistics.....272
Table 60 Deflection Comparison: Plain Jointed versus Doweled Sections.....290

Table 61 Summary of JDMD Deflections for All Sections, 90-kN Test Load.....294

1.0 INTRODUCTION

As part of the Caltrans Long Life Pavement Rehabilitation Strategies (LLPRS), a concrete pavement was constructed with a blend of fast-setting hydraulic cement concrete (FSHCC) and Portland cement concrete (PCC) on sections tangent to State Route 14 in Palmdale, California. This pavement was evaluated using the Heavy Vehicle Simulator (HVS). The tests followed plans detailed in the Test Plan for CAL/APT Goal LLPRS - Rigid Phase III (*1*). The concrete was specified to obtain a flexural strength of 2.8 MPa within 4 to 8 hours of placement.

Two full-scale test sites, each approximately 210 m in length, were constructed. Each site included three 70-m long test sections, for a total of six sections. The site tangent to the southbound direction of SR 14 ("South Tangent") included sections with different thicknesses of concrete placed on compacted granular base. The site tangent to the northbound direction ("North Tangent") included three 200-mm thick concrete on cement treated base, with varying design features: dowels, tied shoulders, widened lanes (*2*).

This report documents the results of the North Tangent test sections Another report presents the results of the HVS tests on the South Tangent (*3*).

2.0 HVS TEST OBJECTIVES AND SCOPE OF WORK

The objectives of the accelerated pavement testing performed with HVS No. 2 (HVS2) at the Palmdale north tangent test sections were to evaluate the performance of full-scale pavements with the selected design features (dowels, tied slabs, and widened truck lanes) under traffic loading with respect to fatigue cracking, corner cracking, and joint distress to determine whether they will provide the performance desired by Caltrans. HVS trafficking is intended to accelerate damage as much as possible within the time available, without overloading to an extent that the distress mechanism is significantly different from that which would occur in the field.

Ten HVS tests were undertaken on the North Tangent, State Route 14. This report summarizes the results and first-level analysis of all HVS tests conducted on the North Tangent at Palmdale. The primary purpose of a first-level HVS report is to present a complete and validated set of HVS data without detailed analysis and interpretation of the data. The first-level report is confined to the HVS data and associated test results from the HVS site. The conclusions of the first-level report are therefore site specific with little interpretation and should not be generalized.

Also documented are weather data during each test, visual distress, pavement response measured by in-situ instrumentation (thermocouples, joint deflection measuring devices, multi-depth deflectometers), and periodic testing using the heavy weight deflectometer (HWD). A first-level summary is provided for each type of data.

All data presented in this report are included in the Caltrans/University of California Pavement Research Center electronic database (*4*).

3.0 HVS TEST PROGRAM

Three 70-m long test sections with 200-mm thick FSHCC were constructed at the north tangent as follows:

- Section 7 was constructed with plain joints (no dowels, relying on aggregate interlock for load transfer across the joint) with an asphalt concrete shoulder and a normal lane width of 3.66 m.
- Section 9 was constructed with dowels and tie bars and a normal lane width of 3.66 m. The dowels were placed parallel to the direction of trafficking (i.e., square joints) and the section was constructed with tie bars connected to a concrete shoulder.
- Section 11 consisted of a "widened lane" (lane width of 4.26 m) and doweled joints. The dowels were placed parallel to the direction of trafficking and the section was constructed with an asphalt concrete shoulder.

The aim of this series of tests was to evaluate the performance of the three different pavement structures under the influence of accelerated trafficking, to do a direct comparison between the performance of a plain jointed aggregate interlock structure, a doweled pavement structure, and a concrete pavement constructed with a widened truck lane.

The HVS tests on the North Tangent are summarized in Table 1.

The layout of all sections with respect to the 210-m long full scale test section on the northbound side is detailed in an earlier report (*2*). A graphical representation of the various sections with respect to the 210-m long North Tangent testing area can be seen in Figure 1. Slab dimensions, numbers, joint numbers, and joint spacing are summarized in Table 2. Complete construction and dimension details for the various sections are found in Reference (*2*) and are not repeated here.

Table 1 HVS Tests on the North Tangent

HVS Test	North Tangent Section Number	Slab Number*	Start Date	End Date	Type of structure
532FD	7D	43	7-Jun-99	26-Jul-99	
533FD	7C	39	6-Aug-99	1-Nov-99	No dowels, asphalt shoulder
534FD	7B	35	15-Dec-99	14-Mar-00	
535FD	7A	32	29-Jan-00	4-Apr-00	
536FD	9A	27	17-Apr-00	12-Jul-00	Dowels, tied concrete shoulder
537FD	9C	23	20-Jul-00	21-Aug-00	
538FD	9D	19	3-Jan-01	18-Jan-01	
539FD	11C	11	1-Sep-01	29-Sep-01	Dowels, asphalt shoulder, widened truck lane
540FD	11B	7	8-Oct-01	28-Nov-01	
541FD	11A	3	2-Dec-01	27-Dec-01	

* The HVS test was centered around this slab. Some areas of the adjacent slabs were also subjected to HVS trafficking.

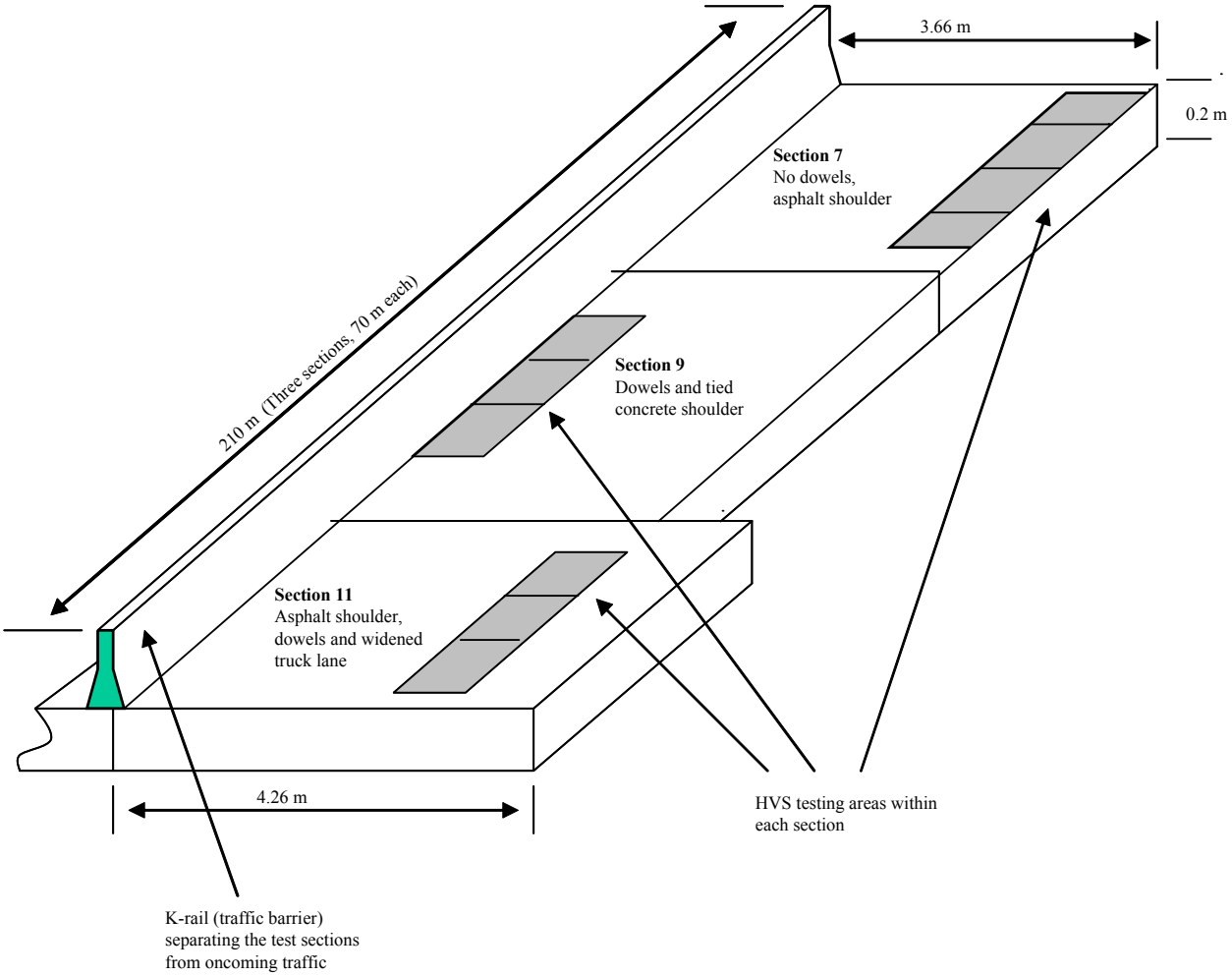

Figure 1. Layout of HVS testing areas on the North Tangent.

Table 2 Slab Dimensions

Test Number	Section Number	Slab Number	Joint Number	Slab Dimensions (m)		Type of Structure
				Length	Width	
532FD	7	42		5.82	3.66	no dowels, asphalt shoulder
			42			
		43		3.95	3.66	
			43			
		44		3.64	3.66	
533FD	7	38		5.79	3.66	
			38			
		39		4.03	3.66	
			39			
		40		3.65	3.65	
534FD	7	34		5.91	3.68	
			34			
		35		3.86	3.66	
			35			
		36		3.90	3.66	
535FD	7	31		4.11	3.66	
			31			
		32		3.71	3.66	
			32			
		33		5.35	3.66	
536FD	9	26		5.81	3.66	dowels and tied to a concrete shoulder
			26			
		27		3.96	3.66	
			27			
		28		3.62	3.66	
537FD	9	22		5.78	3.66	
			22			
		23		3.94	3.66	
			23			
		24		3.66	3.66	
538FD	9	18		5.86	3.66	
			18			
		19		3.92	3.66	
			19			
		20		3.75	3.66	

Table 2 (continued)

Test Number	Section Number	Slab Number	Joint Number	Slab Dimensions (m)		Type of Structure
				Length	Width	
539FD	11	10		5.86	4.26	dowels, asphalt shoulder, and widened truck lane
			10			
		11		3.85	4.26	
			11			
		12		3.71	4.26	
540FD	11	6		5.86	4.26	
			6			
		7		3.80	4.26	
			7			
		8		3.80	4.26	
541FD	11	2		5.91	4.26	
			2			
		3		3.89	4.26	
			3			
		4		3.67	4.26	

3.1 HVS Instrumentation

Test instruments used to monitor the functional and structural behavior of the pavement under accelerated loading include the following:

- Joint Deflection Measuring Devices (JDMD)
- Multi-depth Deflectometers (MDD)
- Thermocouples (TC)
- Visual surveys and photographs

The description and function of these instruments and their recording mechanisms are described in previous reports (*1–3*).

The HVS test pad (8 m × 1 m) extends over 3 slabs, the greater part of the test section being over the middle slab as illustrated in Figure 2. During Tests 532FD and 533FD, the same data acquisition system was used as during the South Tangent tests. From Test 534FD onwards, a new automatic data acquisition system was implemented. This new system enabled data

recording on the fly (automatically and without any operator intervention) and was able to record more data from more instruments simultaneously than the previous system. As a result, more instruments were installed and a different testing program was used than during the South Tangent tests and the first two tests (532FD and 533FD) on the North Tangent.

3.1.1 Joint Deflection Measuring Device (JDMD)

Joint Deflection Measuring Devices (JDMDs) are linear variable displacement transducers (LVDTs) mounted on the concrete slab to measure joint movement, as shown in Figure 2. Six of these instruments were used per test section (JDMD numbers refer to layout shown in Figure 2):

- one at the middle of the edge of the center slab (JDMD 3),
- one on either side of the center slab at the corners (two total – JDMD 2 and 4),
- one at the corners of the adjacent slabs bordering the center slab (two total – JDMD 1 and 5), and
- a sixth JDMD (JDMD 6) oriented horizontally to record the differential movement across the transverse joint of the center slab and an adjacent slab.

During Test 532FD, only three JDMDs were used (two for corner deflections on one joint, and one for midspan edge deflections). During Test 533FD, only five JDMDs were used (four for the measurement of corner deflections on the joints, and one for midspan edge deflections).

The vertical JDMDs were anchored in the shoulder of the pavement with an anchor rod isolated from the movement of the slabs. Thus, they provide measurements of the absolute deflection of the slab. JDMD 6 measures the relative horizontal movement of the slab across the

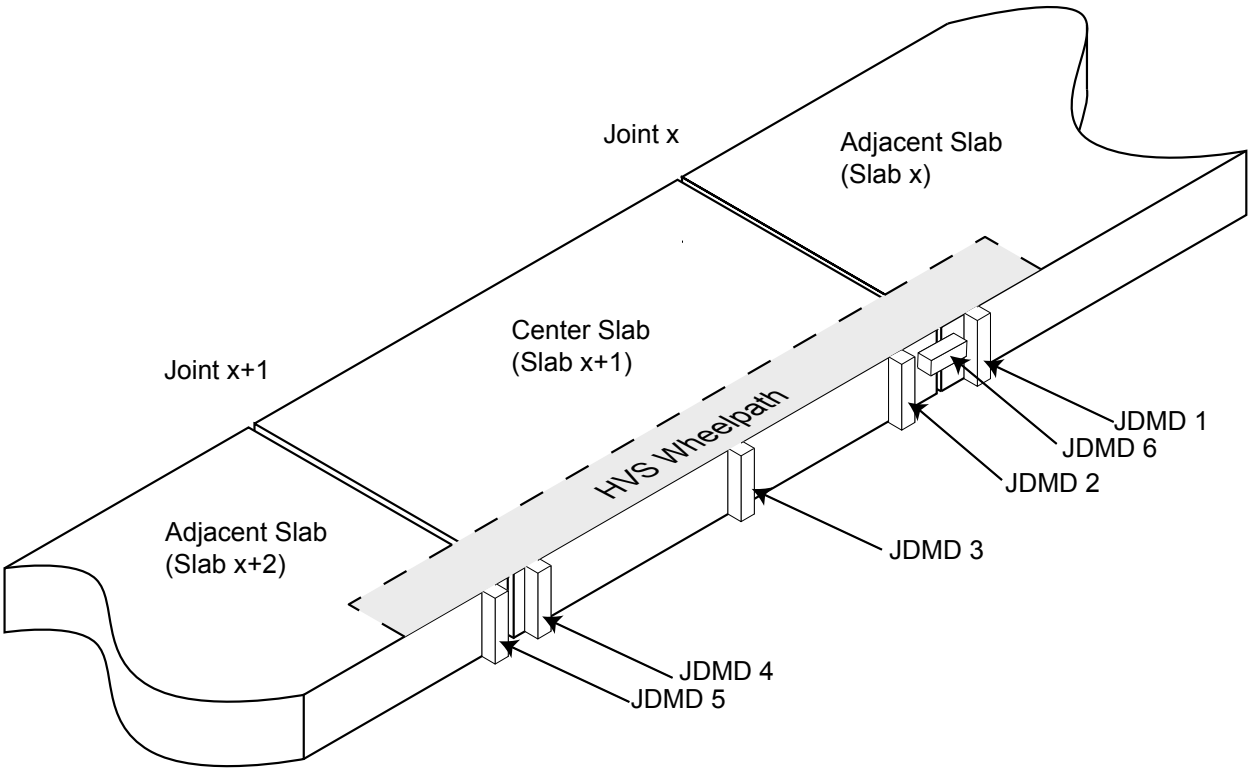

Figure 2. Illustration of the placement of JDMD instruments and their numbering with respect to the test sections.

joint. JDMD 3 is also referred to as an "edge deflection measuring device" (EDMD) because it is placed at an edge rather than a joint. Placement of the JDMDs in each section is shown in Figures 3–12.

3.1.2 Multi-Depth Deflectometer (MDD)

MDDs were placed between the two wheel paths of the dual HVS loading wheels, approximately 300 mm from the edge of the concrete slab. All MDDs were fitted with 4 in-depth LVDTs, placed at various depths.

Seven of the ten HVS sections were instrumented with MDDs. MDDs were installed on the tests and locations shown in Table 3. The complete instrument placement and locations are also shown for all 10 tests in Figures 3 through 12.

Table 3 Location of MDDs Placed on the North Tangent HVS Sections

Test Number	MDD ID Numbers	Test Slab Numbers	300 mm from Joint Number	Type of Structure
532FD	No MDDs installed	42		Section 7: No dowels, asphalt shoulder
			42	
		43		
			43	
		44		
533FD	14	39		
			39	
	15	40		
534FD	12	35		
			35	
	13	36		
535FD	11		between Joints 31 and 32 (midspan Slab 32)	
		32		
536FD	10	27	between Joints 26 and 27 (midspan Slab 27)	Section 9: Dowels and tied to a concrete shoulder
537FD	8	23		
			23	
	9	24		
538FD	No MDDs installed	18		
			18	
		19		
			19	
		20		
539FD	4	11		Section 11: Dowels, asphalt shoulder, and widened truck lane
			11	
	5	12		
540FD	2	7		
			7	
	3	8		
541FD	No MDDs installed	2		
			2	
		3		
			3	
		4		

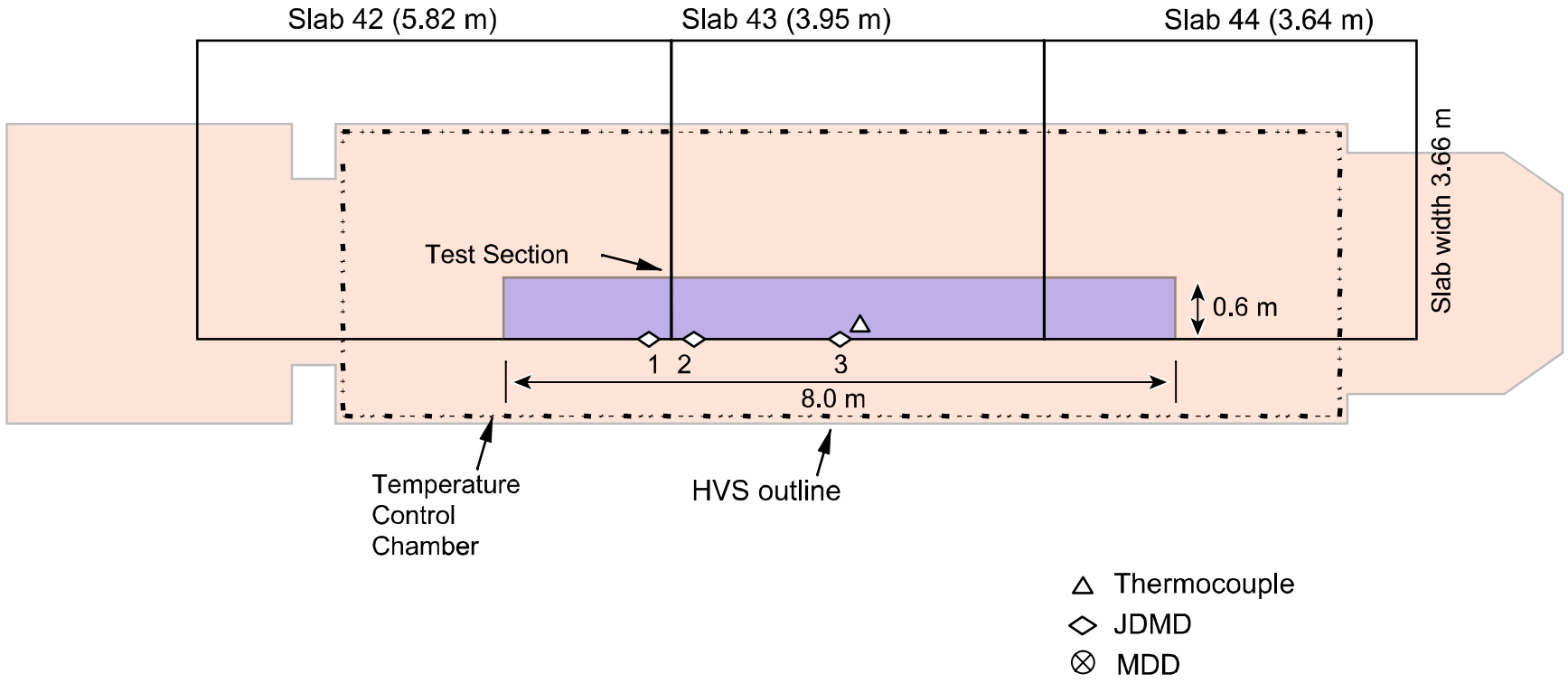

Figure 3. Instrumentation layout of Test Section 532FD.

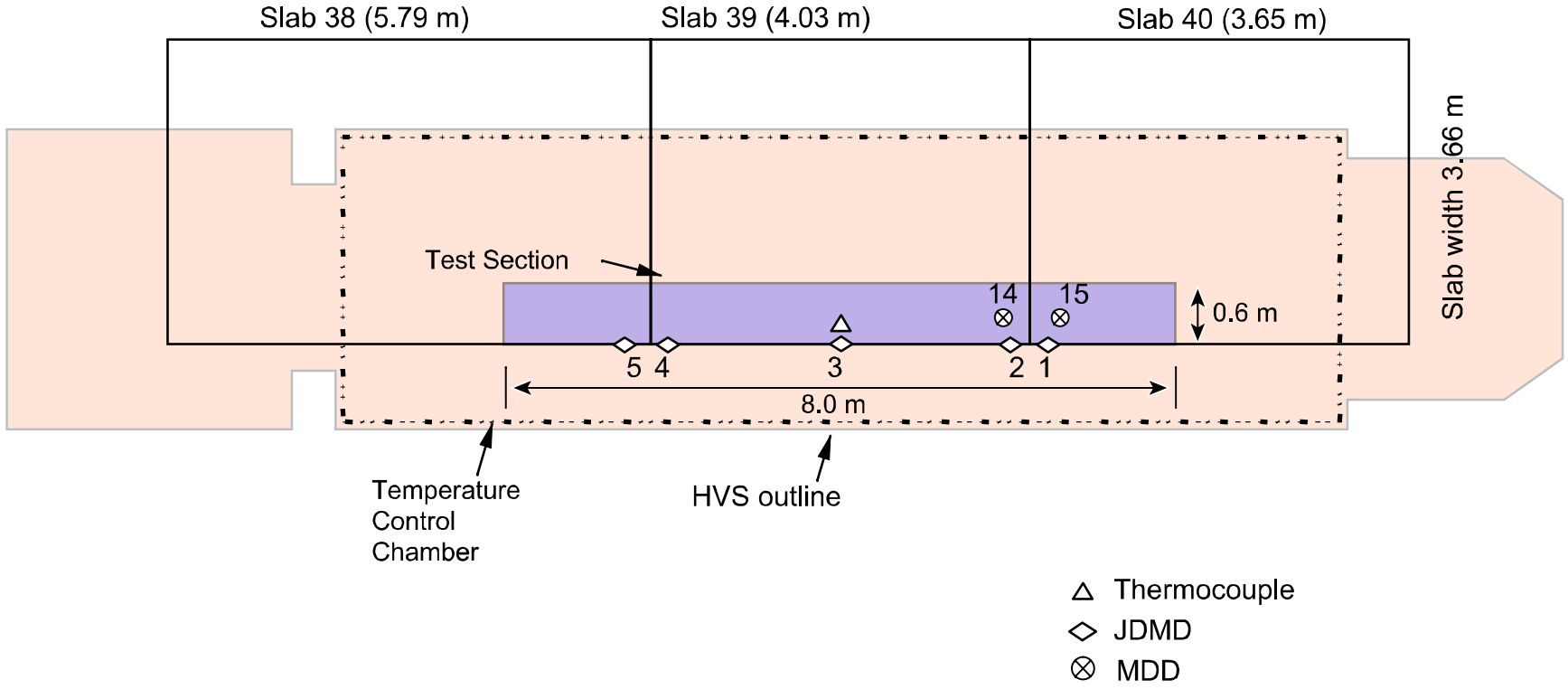

Figure 4. Instrumentation layout of Test Section 533FD.

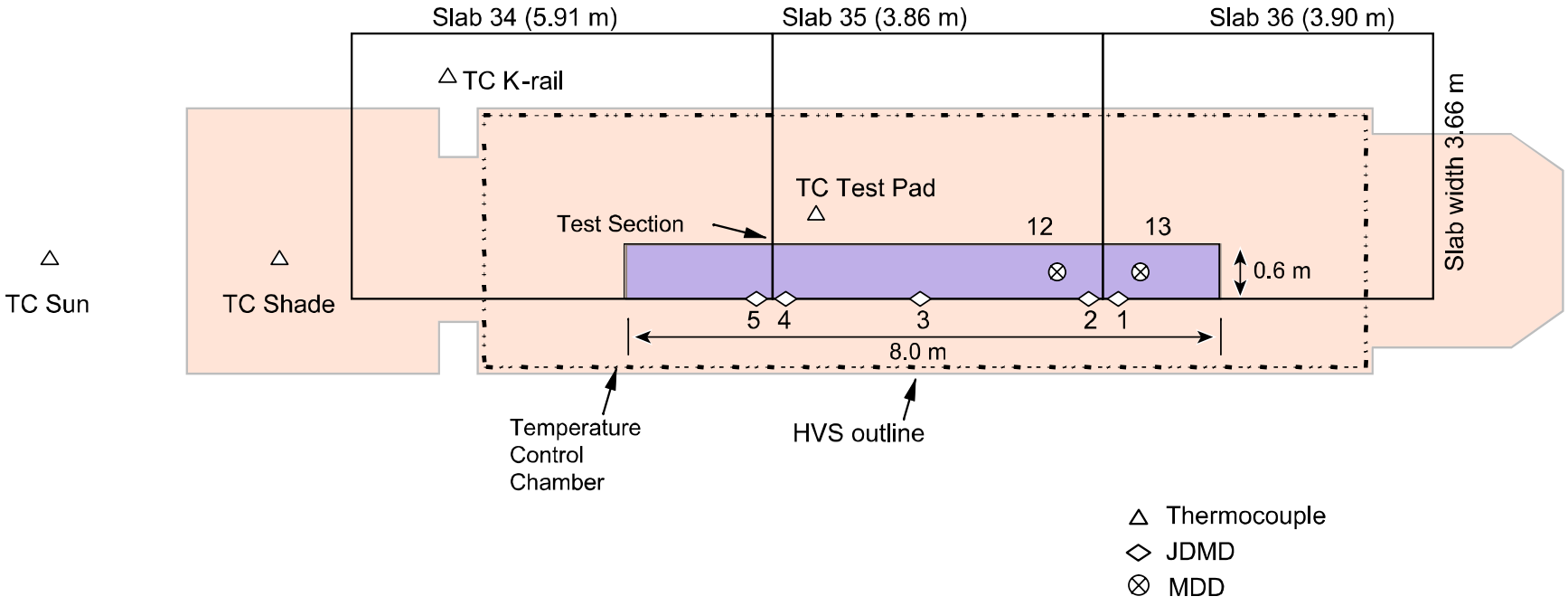

Figure 5. Instrumentation layout of Test Section 534FD.

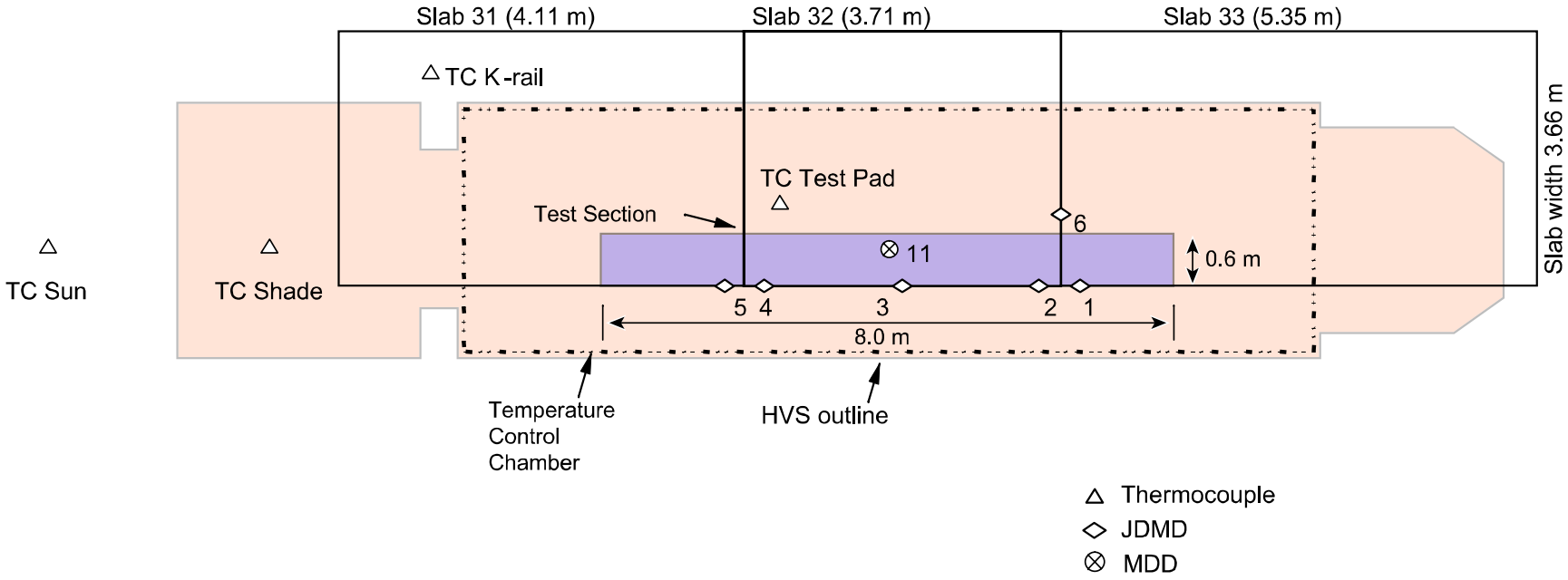

Figure 6. Instrumentation layout of Test Section 535FD.

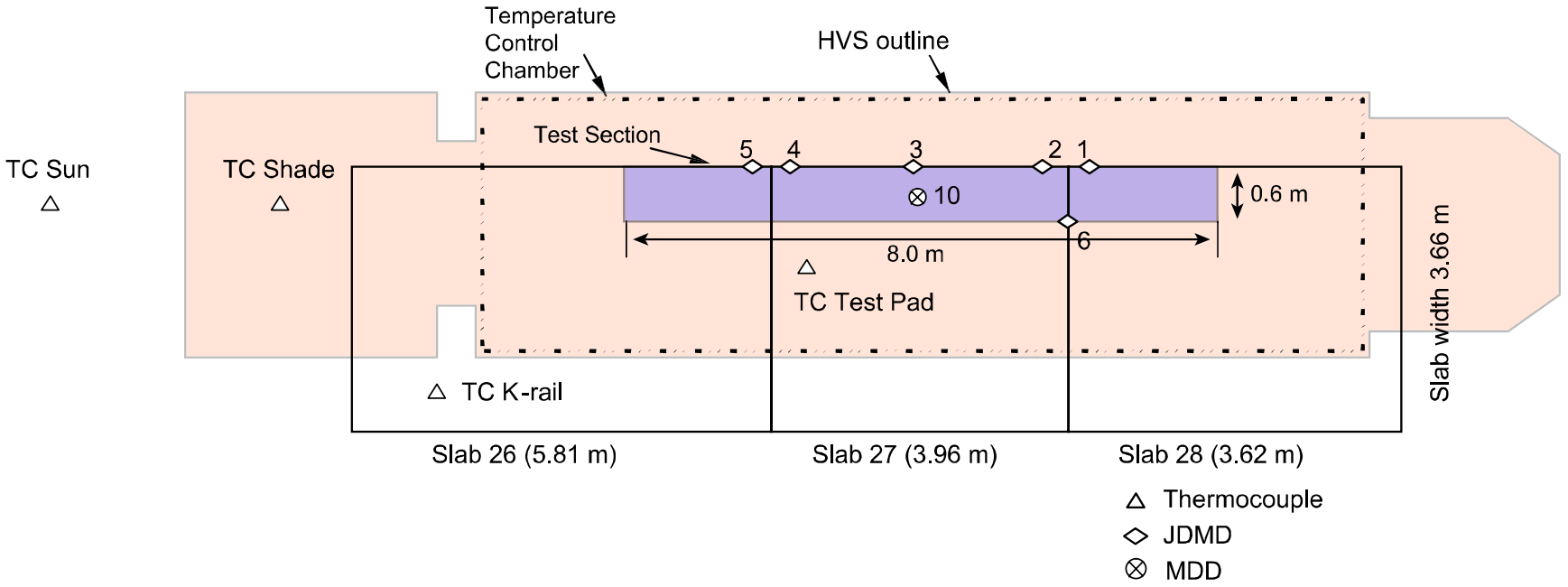

Figure 7. Instrumentation layout of Test Section 536FD.

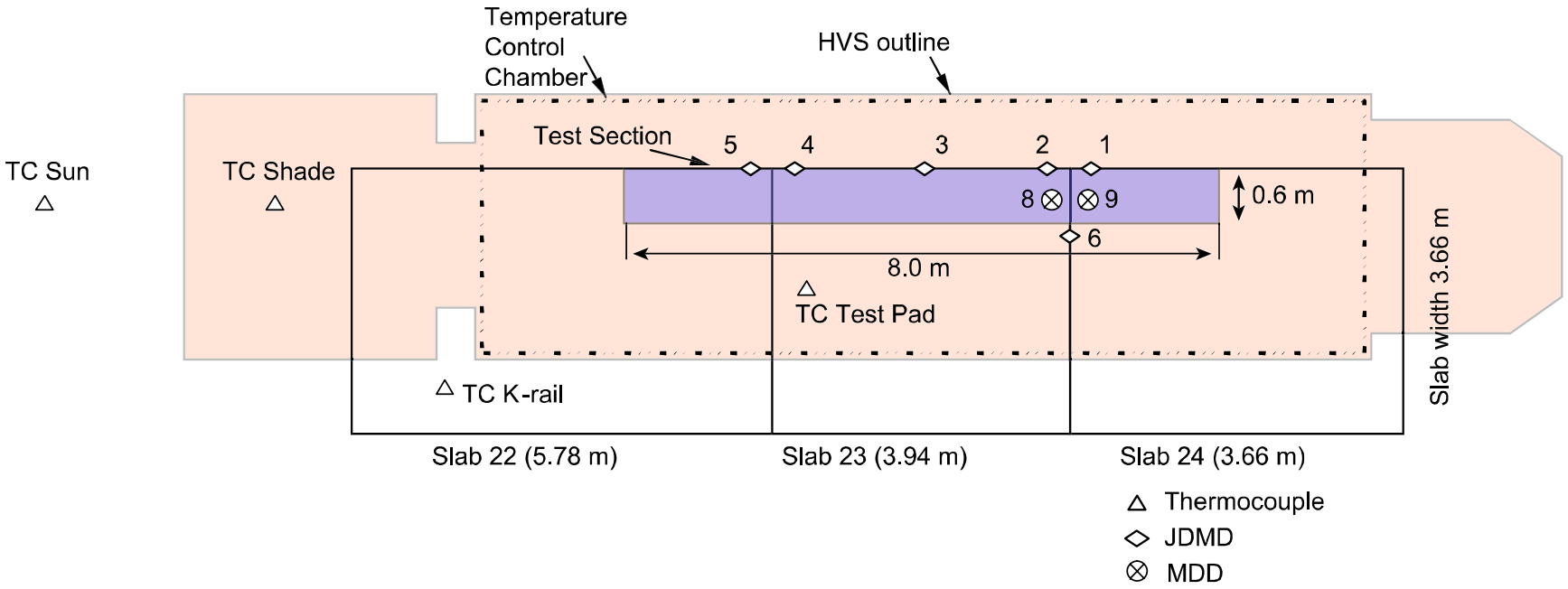

Figure 8. Instrumentation layout of Test Section 537FD.

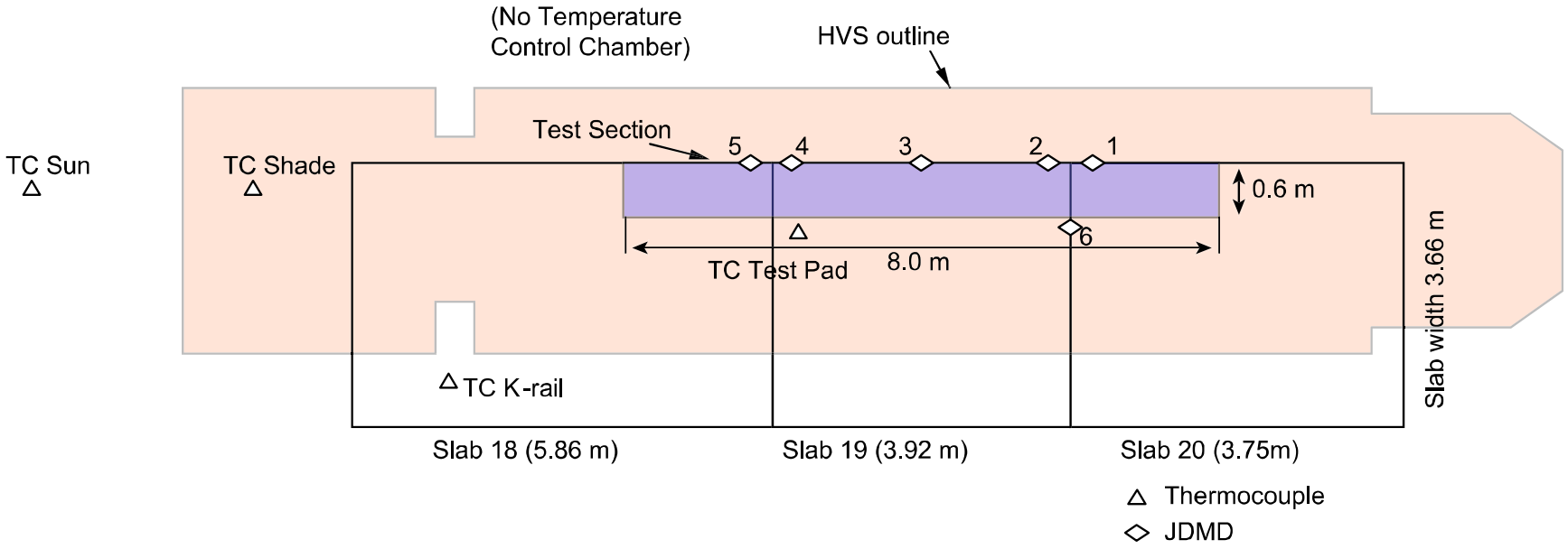

Figure 9. Instrumentation layout of Test Section 538FD.

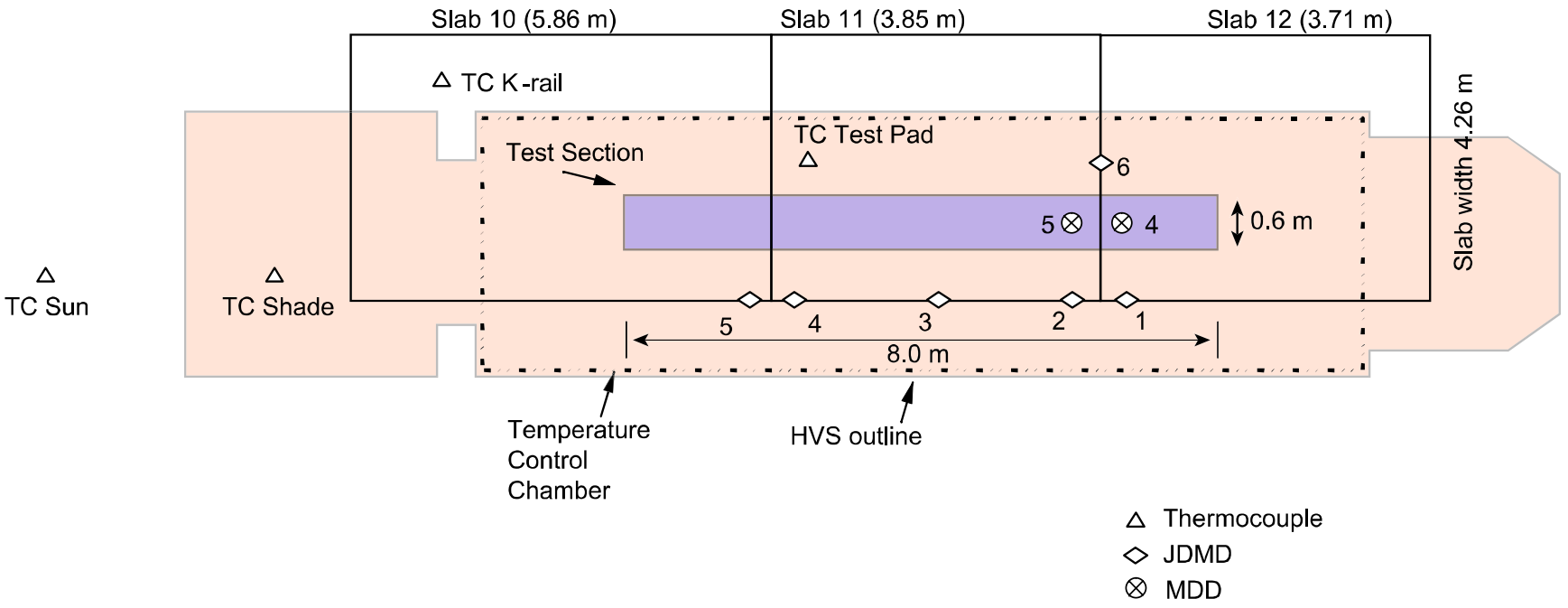

Figure 10. Instrumentation layout of Test Section 539FD.

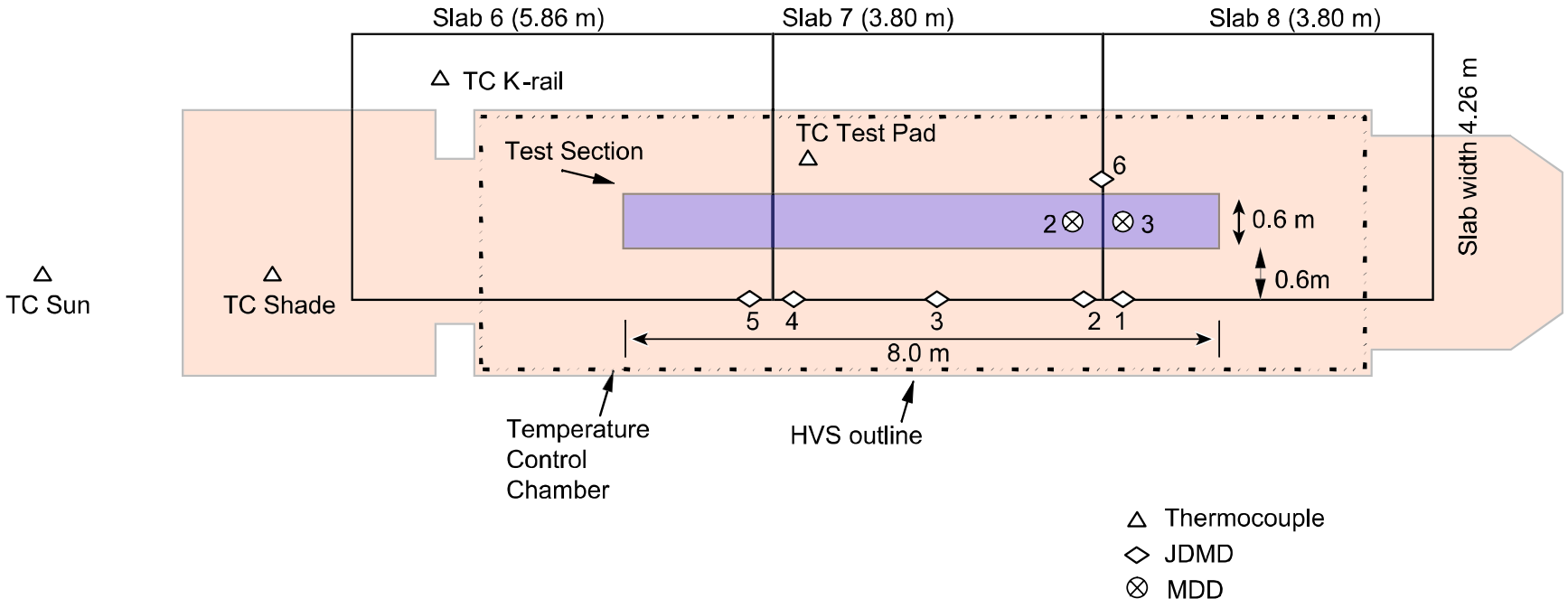

Figure 11. Instrumentation layout of Test Section 540FD.

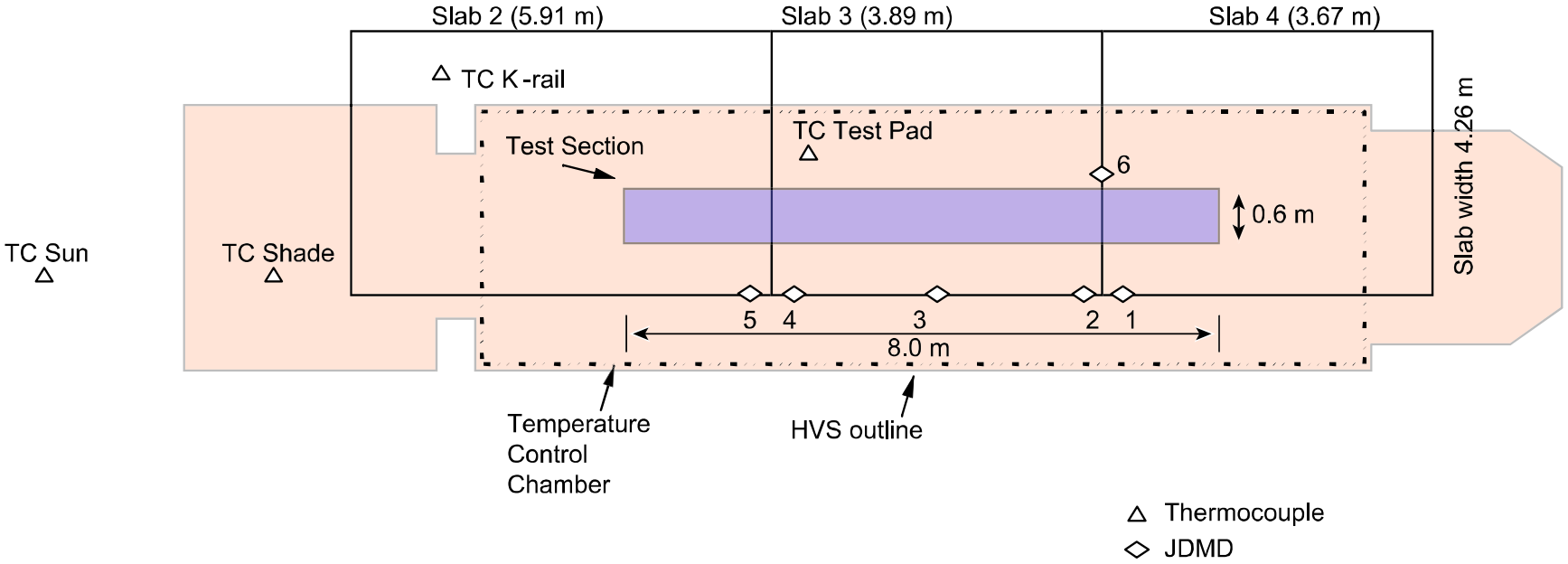

Figure 12. Instrumentation layout of Test Section 541FD.

3.1.3 Thermocouples

Thermocouples were placed to measure temperatures in the 200-mm thick concrete slabs at the surface and at depths of 100 and 200 mm at the following positions:

- inside the temperature box ("TC Test Pad"),
- under the HVS in the shade (TC Shade),
- at a location in which the thermocouple was completely exposed to direct sunlight 100 percent of the day (TC Sun), and
- at a location between the HVS and the adjacent K-rail, partially exposed to the sun but shaded part of the day from the HVS and the K-rail (TC K-rail).

This thermocouple configuration was used for Test Sections 534FD through 541FD.

Sections 532FD and 533FD were tested using the old data acquisition system and a different thermocouple layout was used. During Test 532FD, one thermocouple "stack" (0, 100, 200-mm depths) was installed at the edge of Slab 43 inside the temperature control box. During Test 533FD, one stack was installed at the edge of Slab 39, also inside the temperature control box. The detailed layouts of all sections, including placement of all instrumentation with relation to the various concrete slabs, are presented in Figures 3–12.

3.2 HVS Loading Plan

To investigate the various effects of temperature, water, and loading, the test sections were subjected to different loading and environmental conditions. Table 4 details the various combinations which were used during the tests on the North Tangent. The normal dual wheel configuration (tire pressure = 690 kPa) was used during the tests except in certain cases where the aircraft wheel (tire pressure = 1,100 kPa) was used (see Table 4). The aircraft wheel was used

Table 4 Loading Plan for the HVS Tests

Test Number	Repetitions from	Repetitions to	Load kN Dual Wheel	Temperature Control	Water Added?	Loading Type	Actual Repetitions per Load Cycle	Actual Repetitions Total
532FD	0	7,794	40	yes	dry	unidirectional	7,794	202,302
	7,794	16,543	40		wet		8,749	
	16,543	202,302	70				185,759	
533FD	0	44,164	40	yes	dry	unidirectional	44,164	371,150
	44,164	254,167	70				210,003	
	254,167	371,150	90				116,983	
534FD	0	126,580	40	yes	dry	bi-directional	126,580	1,284,360
	126,580	984,602	70				858,022	
	984,602	1,284,360	90				299,758	
535FD	0	80,002	90	yes	dry	bi-directional	80,002	80,002
536FD	0	750,000	90	yes	dry	bi-directional	750,000	992,782
	750,000	750,500	70 aircraft				500	
	750,500	751,000	90 aircraft				500	
	751,000	751,500	110 aircraft				500	
	751,500	752,000	130 aircraft				500	
	752,000	840,450	150 aircraft				88,450	
	840,450	992,782	150 aircraft	ambient			152,332	
537FD	0	13,230	40	ambient	dry	bi-directional	13,230	388,736
	13,230	13,730	70				500	
	13,730	323,734	90				310,004	
	323,734	388,736	150 aircraft				65,002	
538FD	0	500	70	ambient	dry	bi-directional	500	189,382
	500	189,382	90				188,882	
539FD	0	13,342	40	ambient	dry	bi-directional	13,342	318,846
	13,342	13,842	70				500	
	13,842	318,846	90				305,004	
540FD	0	13,003	40	yes	dry	bi-directional	13,003	547,463
	13,003	405,065	90				392,062	
	405,065	547,463	150 aircraft				142,398	
541FD	0	500	70	ambient	dry	bi-directional	500	278,288
	500	168,277	90				167,777	
	168,277	278,288	150 aircraft				110,011	

for cases in which the pavement response under a heavy load (150 kN) was investigated. The normal dual tires may only carry loads of up to 100 kN.

It is important to note the following:

- During HVS Tests 532FD and 533FD (and all tests done on the South Tangent), the old data acquisition system (DAS) was used. In order to perform data collection with the old DAS, the HVS test wheel was set at creep speed (2 km/h). All data collection and subsequent responses measured by the various instruments were performed under the influence of this slow moving wheel.
- During Tests 534FD through 541FD, the new DAS was used. This DAS takes readings on the fly at the regular traffic speed of about 7 km/h.

Although not as critical for concrete as for flexible pavement structures, the difference in wheel speed make direct comparison between the responses measured during tests performed with the old DAS (Test 519FD through 533FD) and the new DAS (534FD onwards) more complex, as the time of loading was different.

The stress and strain states in concrete slabs are not only influenced by the induced traffic loads, but also by other significant factors such as temperature. In order to minimize the effects of outside temperature, some sections on the North Tangent were conducted with a temperature control box erected over each section. The target surface temperature was 20ºC and a variation of ± 7ºC was allowed.

Tests were conducted with the HVS trafficking in either the unidirectional or bi-directional traffic mode. All tests were performed with a channelized traffic pattern, meaning that no lateral wander of the test wheel was introduced, and the wheel always traveled along the

edge of the slabs next to the asphalt shoulder. Wander was not introduced because it would have prolonged the time required to achieve fatigue cracking on each test section.

In the case of loading the widened truck lane sections (Tests 539FD through 541FD), the HVS loading wheel traveled 0.6 m from the edge of the concrete slab as shown in Figures 10–12

4.0 HVS RESULTS

The results of the individual HVS tests are summarized in this section. A previously published report on the construction of the test sections at Palmdale gives complete details of the instrumentation layout, which will not be repeated here (*1*). Data collection was undertaken at various intervals for the various tests and is summarized for each test section. For fatigue analysis purposes, the appearance of a crack on the middle slab signified fatigue failure. In certain cases, the HVS tests were run longer to monitor the performance of the middle and adjacent slabs after the first fatigue crack.

During all tests on the North Tangent, data collection took place with the HVS wheel traveling in the same direction (HVS cabin to tow-end direction). Load transfer efficiency (LTE) was therefore also calculated with the HVS wheel running only in one direction (unlike the South Tangent where LTE was calculated for the wheel running in both directions). LTE values were calculated using two methods at each joint. Because two JDMDs were placed on either side of the joint, it was possible to calculate LTE when the HVS wheel is right over the one JDMD and again when the wheel has crossed the joint and is right over the second JDMD. In the subsequent tables and graphs, both calculations of LTE are presented.

Because temperature differentials inside the concrete slab significantly affect the stress and strain state, which in turn influences surface deflections, the temperature difference between the surface and the bottom of the PCC layer at the time of deflection measurements is also given with the tabulated deflection data. Thermocouple data collection was not always in synchronization with regular data collection so in some cases, no data are available.

Because data collection took place at 2-hour intervals, it is not possible to present all the collected data in table format. The complete data set is available on the HVS database located at

The Pavement Research Center at the University of California, Berkeley. The results are, nevertheless given in graphical format and summary tables are given throughout this report.

To assist in the interpretation of the effects of temperature on the measured responses, all graphs detailing pavement response data consists of two parts: the top part presents the thermocouple temperature data and the bottom part the response data.

All temperature graphs show two types of data: the surface temperature on the test pad as well as the temperature difference (difference between top and bottom temperature of the 200-mm PCC sections) at various places as described in Chapter 3.2.3. To improve the clarity of the temperature data plots, a second vertical axis showing the temperature differential (top – bottom), is included on the right hand side of all graphs used in this report.

4.1 Test 532FD

Test 532FD was undertaken on Slabs 42, 43, and 44 on Section 7 of the North Tangent. Slab 43 (total length 3.95 m) was fully tested, together with some area on either side of Joints 42 and 43 in Slabs 42 (total length 5.82 m) and Slab 44 (total length 3.65 m). In order to minimize stresses and strains caused by temperature effects, the temperature control chamber was used during this test. Unidirectional trafficking was applied throughout the test. This was the first of four tests on Section 7. The section was constructed of 200-mm FSHCC pavement without dowels and with an asphalt shoulder.

The test was conducted in three phases: Phase I started with a 40-kN dual wheel load and was kept constant up to 7,794 unidirectional repetitions, as which point loading was paused for 18 hours. While loading was stopped, the joints were saturated with water at a rate of 4.92 l/hour per joint. A total of 88.6 l/joint was poured during this 18-hour period.

Phase II resumed loading at 40 kN for another 16,543 repetitions while water continued to be added at the joints as in Phase I.

Phase III consisted of 177,965 load repetitions with the load increased to 70 kN together with water being added at the same rate as in Phase I and Phase II. A total of 202,302 unidirectional load repetitions were applied to the section.

4.1.1 Visual Observations

The crack pattern, as it developed with time, can be seen in Figure 13. The figure shows the outer shoulder at the bottom of the page (the trailer side). The inner shoulder, near the K-rail (the opposing traffic side), is at the top of the figure.

Prior to the start of the test, a mid-slab crack existed right through Slab 42 (See Figure 13). After the first two loading cycles (Phases I and II), no visible cracks could be found. A corner crack in Slab 44 (towards Joint 43) developed after another 20,875 load applications of 70 kN at a total of 45 121 load applications. This crack was immediately followed by a smaller corner crack on the same slab (44) towards Joint 43. The ingress of water had a very detrimental effect on the support of the slab and visible pumping could be seen at Joint 43. This pumping led to the complete loss of support under Slab 44 and a huge chunk of concrete broke loose in the corner of Slab 44. In order not to damage the trafficking wheels, a piece of wood was put in place where the concrete chunk broke loose. Another corner crack developed in Slab 43 towards Joint 43. A composite image of the final crack pattern can be seen in Figure 14.

The number of load repetitions at which each crack appeared was not noted but the sequence was recorded as seen in Figure 13.

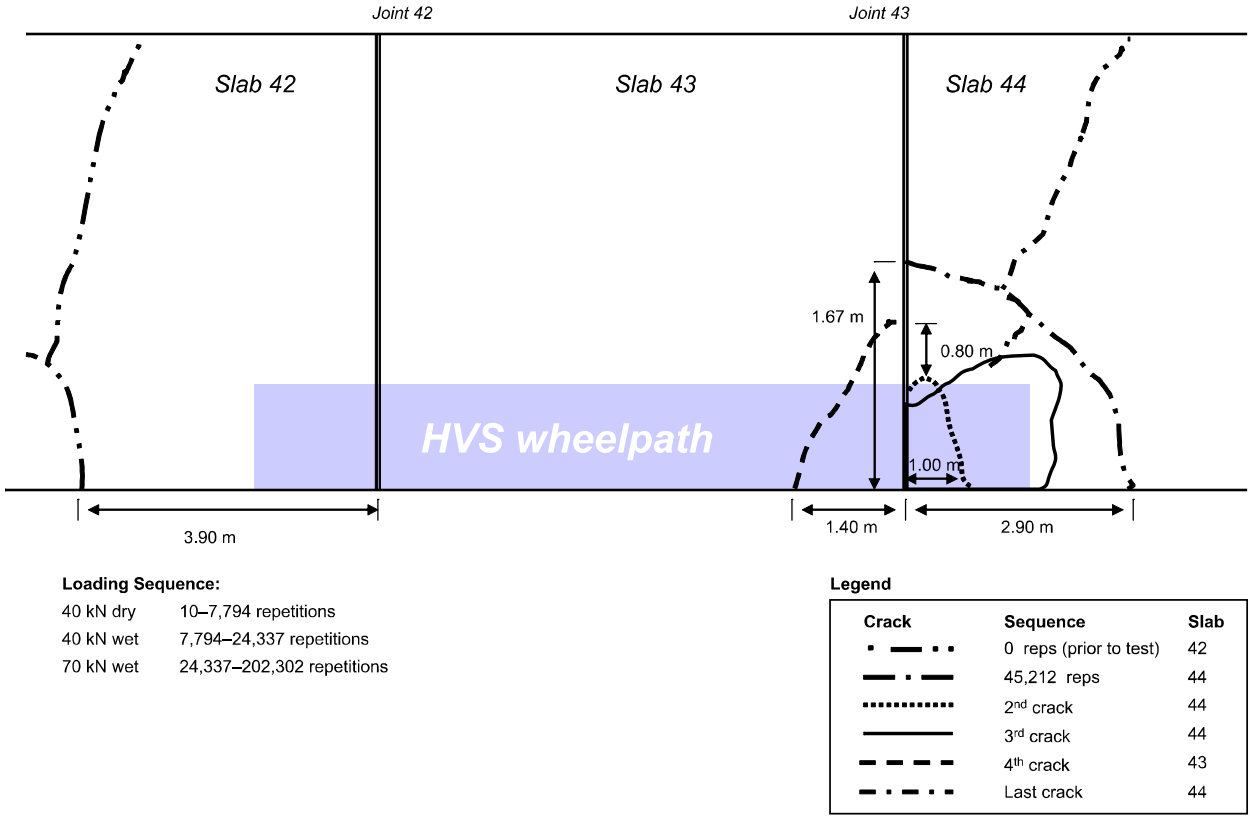

Figure 13. Schematic of crack pattern, Test 532FD.

Figure 14. Composite image of Test 532FD showing cracks.

4.1.2 Joint Deflection Measuring Device (JDMD) Results

Two Joint Displacement Monitoring Devices (JDMDs) were placed on either side of Joint 42 (the right-hand joint of Slab 43) and one was placed on the edge of Slab 43 at its midspan (midway between the two joints). A summary of the peak deflections at the beginning and end of each loading phase can be seen in Table 5.

Table 5 JDMD Deflections, Test 532FD

		Deflection (mm)						Temperature (ºC)	
	Test Load	Corner, Joint 42		Mid-span, Slab 43	Corner, Joint 43		Horizontal Joint 43		Difference (top - bottom)
		Slab 42	Slab 43		Slab 43	Slab 44			
Repetitions	kN	JDMD 1	JDMD 2	JDMD 3	JDMD 4	JDMD 5	JDMD 6	Surface	
10– 7,794	40, dry	1.726 1.751	1.606 1.572	0.656 0.527	N/A	N/A	N/A	17.3 15.6	0.6 -1.5
7,799– 24,337	40, wet	1.683 1.681	1.570 1.169	0.505 0.509				15.4 18.2	-1.0 -0.6
24,342– 202,302	70	2.079 1.764	1.273 2.462	0.632 0.585				17.8 21.4	-0.9 -0.4

The data are also graphically displayed in Figure 15. To properly interpret these values, they should be analyzed together with the crack pattern as displayed in Figure 13.

It seems as if the crack development at Joint 43 (see Figures 13 and 14) had little effect on the deflections measured at the other joint (Joint 42). Even after water was added and the load increased to 70 kN (from 40 kN), deflections stayed relatively constant and no sudden increase was detected.

After 202,302 repetitions, Joint 43 had deteriorated to such an extent that the test was stopped. However, no instruments were placed at this joint so performance data are not available.

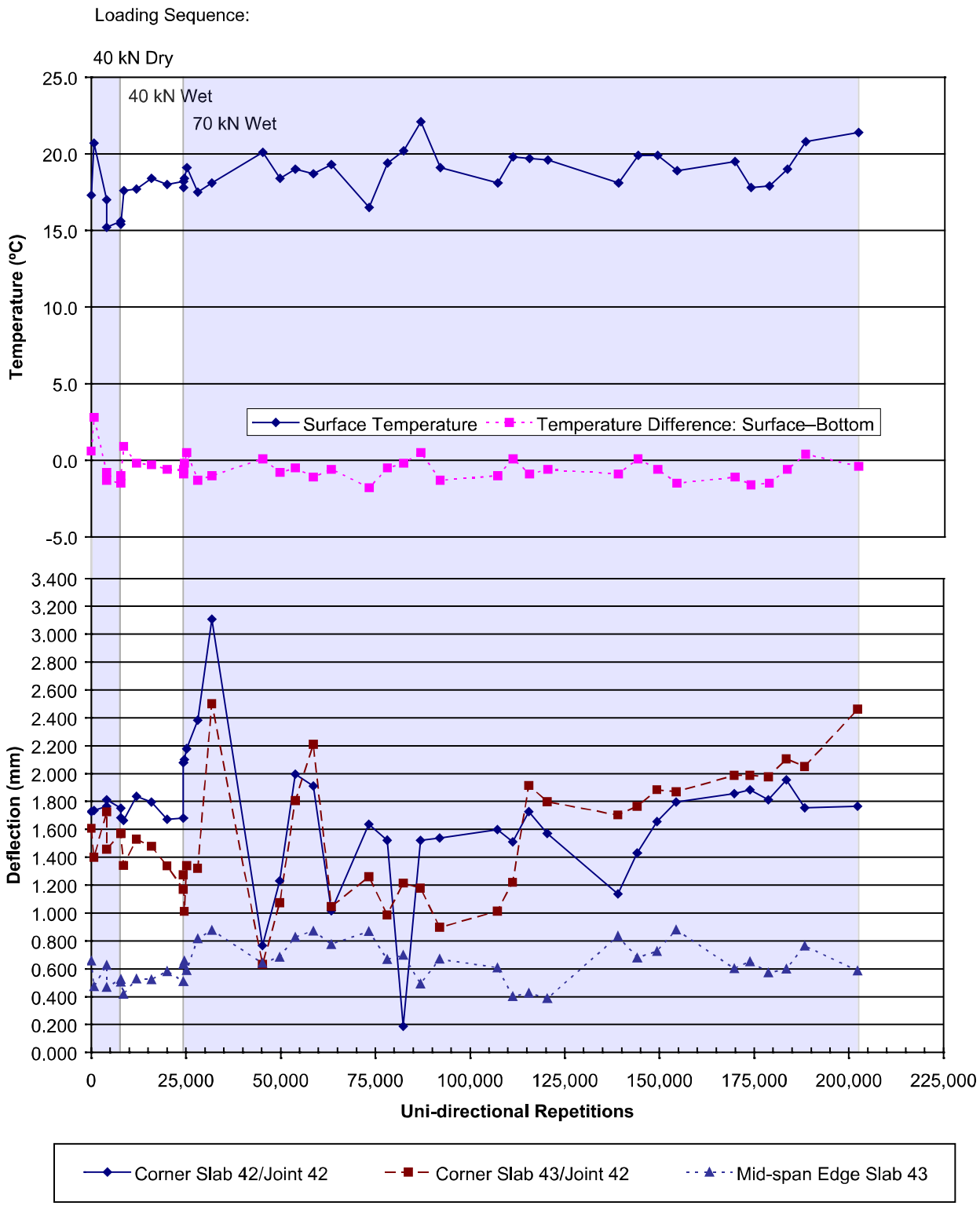

Figure 15. Plot of JDMD deflections and temperature versus load repetitions, Test 532FD.

4.1.3 Joint Load Transfer Efficiency (LTE)

The Load Transfer Efficiency (LTE) was calculated at the left-hand joint of the middle slab (Joint 42 between Slab 42 and Slab 43). The joint deterioration with number of load applications can be seen in Figure 16. Summary results are presented in Table 6.

Table 6 Load Transfer Efficiency, Test 532FD

		Load Transfer Efficiency (%)				**Temperature (ºC)**	
	Test	**Corner, Joint 42**		**Corner, Joint 43**			**Difference**
	Load,	**Slab 42**	**Slab 43**	**Slab 43**	**Slab 44**		**(top –**
Repetitions	**kN**	**JDMD 1**	**JDMD 2**	**JDMD 4**	**JDMD 5**	**Surface**	**bottom)**
10 – 7,794	40, dry	73.5	69.2	N/A	N/A	17.3	0.6
		72.5	53.8			15.6	-1.5
7,799 – 24,337	40, wet	67.7	52.3			15.4	-1.0
		76.8	73.3			18.2	-0.6
24,342 – 202,302	70	98.5	97.1			17.8	-0.9
		87.5	75.5			21.4	-0.4

The reason why the LTE values increased from around 70 percent to 90 percent after about 24,000 repetitions is not known. One possible reason is the influence of temperature variations. Although the variations in surface temperature are not substantial (Figure 16) at the position where the thermocouple was placed (see Figure 3), it is possible that more dramatic temperature changes took place at the joint were the LTE values were calculated. Higher surface temperatures cause concrete slabs to expand. This expansion can lead to an increased degree of aggregate interlock as reported by the increased LTE values.

After about 120,000 repetitions, the area in the proximity of Joint 43 had extensive cracking (see Figure 13). This crack pattern had an effect on the LTE calculated at the right-hand side of Joint 42, which is clearly visible in Figure 16.

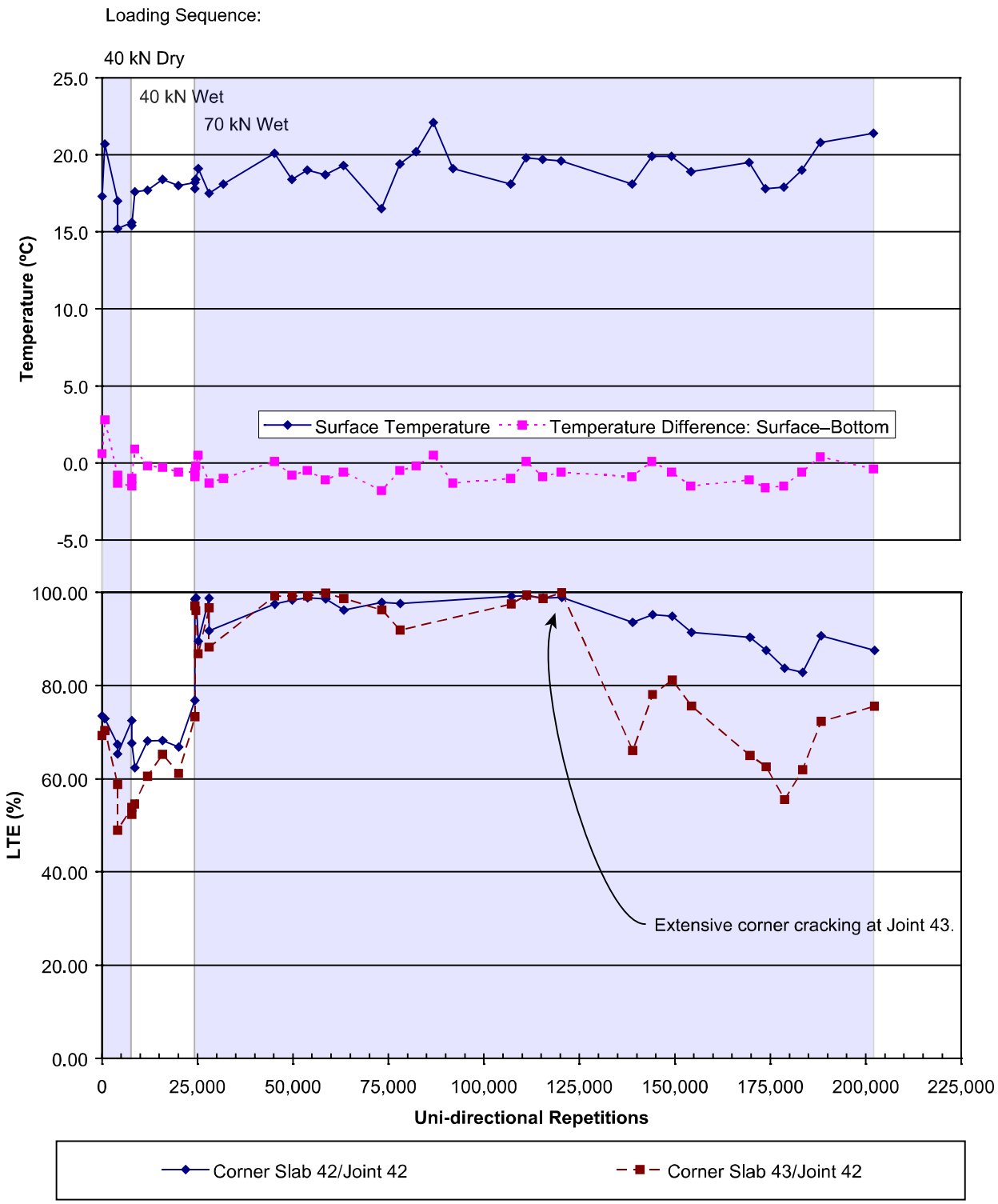

Figure 16. Plot of LTE and temperature versus load repetitions, Test 532FD.

The LTE calculated from JDMD 2 was 75.5 percent after 202,302 repetitions compared to that of JDMD 1 of 87.5 percent after the same number of repetitions. It is obvious that the extensive cracking at Joint 43 had a significant effect on the LTE measured by JDMD 2. The reason for this is probably due to the extensive cracking which took place on Slab 44. The LTE at Joint 43 was obviously reduced to zero after the piece of concrete broke loose, and this had an effect on the LTE values measured at the other joint (Joint 42).

4.2 Test 533FD

Test 533FD was the second HVS test performed on the undoweled 200-mm PCC sections with an asphalt shoulder.

HVS Test Section 533FD was located on Slabs 38, 39, and 40, with the 8 × 1 m test pad placed in such a way that Slab 39 (total length 4.03 m) was fully tested along its edge plus some area from Slab 38 (total length 5.79 m) and Slab 40 (total length 3.65 m). The temperature control chamber was used during this test. The test was completed without the use of water; trafficking was unidirectional. The test started with a 40-kN dual wheel load, which was kept constant to 44,164 repetitions, after which it was increased to 70 kN for 210, 003 repetitions. The test was stopped after another 116,983 loading repetitions at 90 kN, for a total of 371,150 unidirectional load applications.

4.2.1 Visual Observations

Prior to the start of Test 533FD, a cracks existed that ran through the complete width of the Slab 38 (3.66 m) starting 3,707 mm left of Joint 38. The crack pattern that developed with

time is shown in Figure 17. A composite image of the completed test section is shown in Figure 18.

No additional cracks developed during the 40-kN or 70-kN loading cycles. The first load-related crack was detected after 33,631 repetitions of 90-kN loading, which is after a total of 287,798 total load applications. This crack started at Joint 38 about 200 mm outside the wheelpath and ran parallel to the edge of the slab, towards the existing crack at the start of the test on Slab 38.

After another 52,789 90-kN load repetitions (total of 340,587), a second longitudinal crack developed through the length of Slab 40 between Joints 39 and 40, about 1.5 m away from the edge. The center slab (Slab 39) did not crack and testing was stopped after a total of 371,150 unidirectional load applications.

4.2.2 Joint Deflection Measuring Device (JDMD) Results

Five JDMDs were placed on Section 533FD: on either side of both the joints (Joints 38 and 39), and on the edge at midpoint of Slab 39 (Figure 4). The results can be seen in Figure 19 and are summarized in Table 7.

Table 7 JDMD Deflections, Test 533FD

		Deflection (mm)						Temperature (ºC)	
	Test Load	Corner, Joint 39		Mid-span, Slab 39	Corner, Joint 40		Horizontal		Difference (top - bottom)
		Slab 40	Slab 39		Slab 39	Slab 38	Joint 39		
Repetitions	kN	JDMD 1	JDMD 2	JDMD 3	JDMD 4	JDMD 5	JDMD 6	Surface	
10–44,164	40	1.282	1.089	0.452	1.345	1.221	N/A	17.1	-2.5
		1.499	1.472	0.505	1.410	1.368		18.4	-1.1
44,169–254,167	70	2.306	2.276	0.721	2.070	1.988		17.6	-1.9
		2.036	2.273	0.705	2.264	2.091		18.4	-0.7
254,172–371,149	90	2.251	2.557	0.767	2.382	2.189		18.0	-1.1
		2.567	2.485	0.807	2.402	1.976		19.9	-0.3

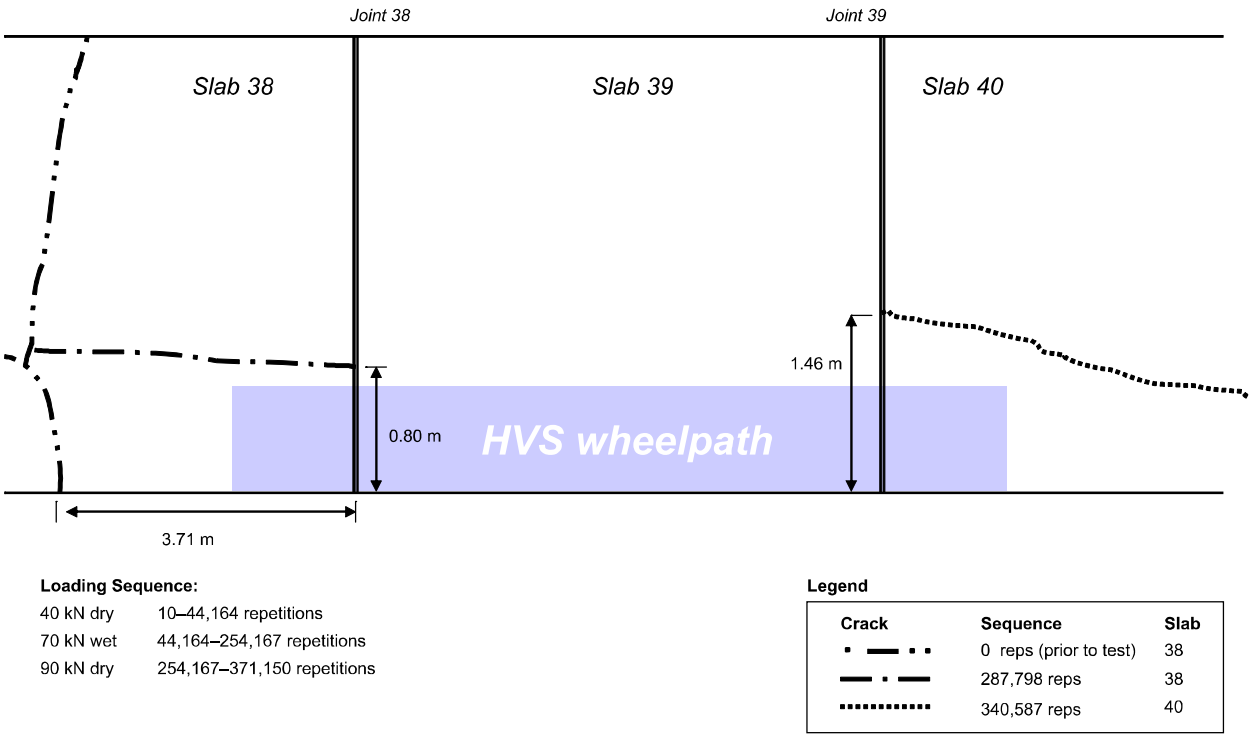

Figure 17. Schematic of crack pattern, Test 533FD.

Figure 18. Composite image of Test 533FD showing cracks.

The surface deflections were very similar at all joints, starting at around 1.2 mm under the influence of the 40-kN load. This increased to around 1.4 mm at the end of the 40-kN phase. The increase in deflections from one loading phase to another (from 40 kN to 70 kN and then again to 90 kN) is expected because of the increase test load.

From Figure 19, it is clear that the existing crack in Slab 38 had little effect on the deflections measured in the vicinity of the crack. The deflections on either side of Joint 38 are not significantly different from those measured at Joint 39 where no cracks existed. The middle slab (Slab 39) edge deflections are significantly lower than the corner deflections. This behavior is expected as these sections were constructed without dowels and the free corners are expected to exhibit more deflection than the middle of the slab.

Towards the end of the test, the corner deflections measured on Slab 38 (Joint 38) show a significant drop, whereas all the other deflections stayed relatively constant for the remainder of the test. One explanation for this behavior may be the influence of the longitudinal crack that developed in Slab 38 (see Figure 17) on the corner deflection of that slab. It is possible that the corner of the slab was not in full contact with the base course due to differential shrinkage and warping. After the crack developed the one piece of the slab fully in contacted the base course, which caused a drop in the corner deflections because of increased support from below.

4.2.3 Joint Load Transfer Efficiency (LTE)

The Load Transfer Efficiency (LTE) was calculated at either side of the middle slab (Joints 38 and 39). The joint deterioration with number of load applications can be seen in Figure 20. Summary results are presented in Table 8.

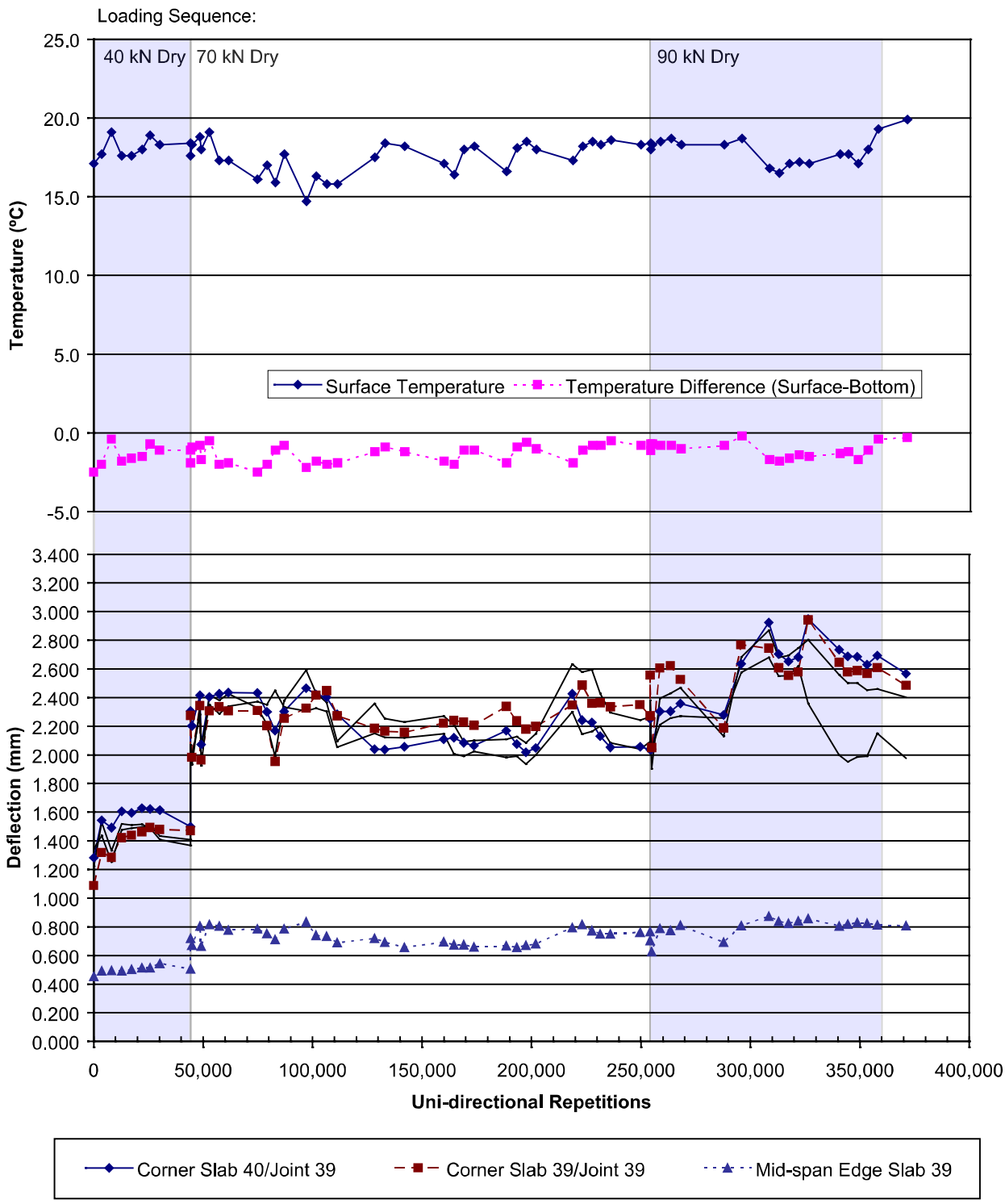

Figure 19. Plot of JDMD deflections and temperature versus load repetitions, Test 533FD.

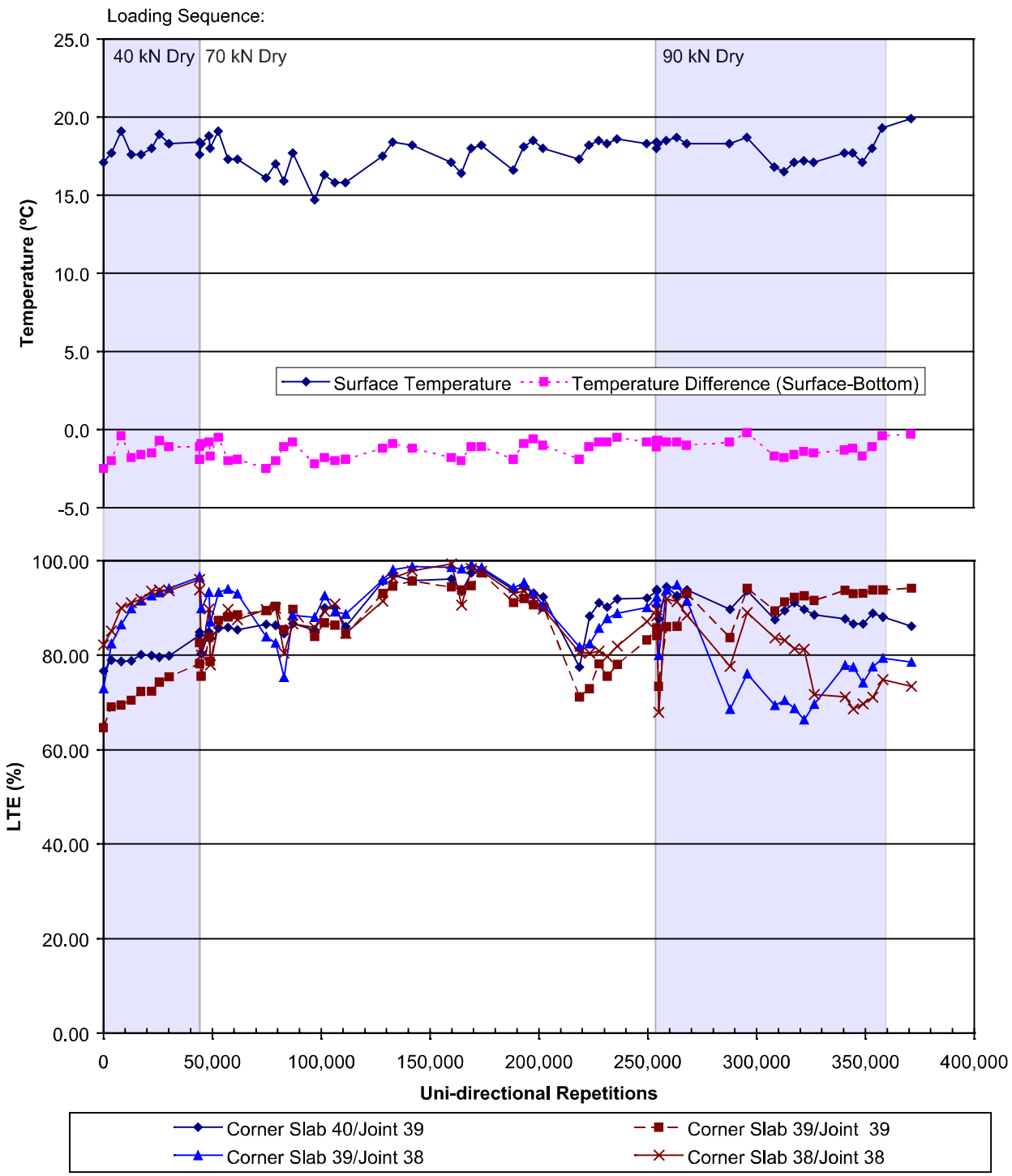

Figure 20. Plot of LTE and temperature versus load repetitions, Test 533FD.

Table 8 Load Transfer Efficiency, Test 533FD

Repetitions	Test Load, kN	Load Transfer Efficiency (%)				Temperature (ºC)	
		Corner, Joint 39		Corner, Joint 38			
		Slab 40	Slab 39	Slab 39	Slab 38		
		JDMD 1	JDMD 2	JDMD 4	JDMD 5	Surface	Difference (top – bottom)
10 – 44,164	40	76.6 84.2	64.6 78.2	73.0 96.5	82.2 96.0	17.1 18.4	-2.5 -1.1
44,169 – 254,167	70	84.9 93.5	82.6 85.8	96.6 92.3	93.8 89.6	17.6 18.4	-1.9 -0.7
254,172 – 371,149	90	93.9 86.1	84.1 94.2	91.1 78.5	88.4 73.4	18.0 19.9	-1.1 -0.3

Steady rises in LTE values were observed from the beginning of the test until around 150,000 load application. The reason for this behavior is not known; it may be due to the same reasons as for Test 532 (Chapter 4.1.3). After 150,000 repetitions, LTE gradually decreased. This suggests that the load transfer due to aggregate interlock was deteriorating under the influence of the trafficking load. But even at the end of the test, the LTE values were still high. The only noticeable drop in LTE values took place at the right hand side of the middle slab at Joint 38. The crack which developed after 340,000 repetitions caused a drop where values as low as 73 percent were recorded at the end of the test.

4.2.4 Multi-Depth Deflectometer (MDD) Results

Two MDDs were installed on Test 533FD. MDD 14 and 15 were placed on either side of Joint 39, one in Slab 39 and the other in Slab 40 (see Chapter 3.2.2). Each MDD had 4 modules measuring deflection at depths of 0 mm (surface), 200 mm, 425 mm and 650 mm. The data measured by MDD 14 and 15 can be seen in Figures 21 and 22. An abbreviated summary of the deflections of the upper two modules appears in Table 9.

Table 9 MDD Deflections, Test 533FD

Repetitions	Test Load, kN	Deflection (mm)				Temperature (ºC)	
		MDD 14, Slab 39		MDD 15, Slab 40			
		0 mm	200 mm	0 mm	200 mm	Surface	Difference (top – bottom)
10 – 44,164	40	0.895 1.036	0.042 0.036	1.130 1.796	0.008 0.118	17.1 18.4	-2.5 -1.1
44,169 – 254,167	70	1.515 1.772	0.079 0.112	1.829 1.810	0.120 0.178	17.6 18.4	-1.9 -0.7
254,172 – 371,149	90	1.878 1.823	0.135 0.227	1.857 1.823	0.182 0.227	18.0 19.9	-1.1 -0.3

The deflections in both slabs show similar trends. The deflections recorded with the MDDs are, as expected, lower than those recorded with the corner JDMDs. Because the MDDs were placed approximately 300 mm from the edge of the slab, they are not substantially influenced by the edge curling effects that cause high corner deflections.

More important is the deflections recorded in the sub-structure. From Table 9 and Figure 21, it is clear that almost all the deflection measured at the surface originated in the concrete slabs and very little deflection was detected in the base layer. Because concrete is a stiff, incompressible material, the only logical reason for this observation is that differential shrinkage created significant slab curling and warping. This curling caused the slabs to loose contact with the underlying layers, which explains why very little deflection was recorded in the base.

During Test 533FD, temperature control was exercised with the aid of the temperature control chamber. This is evident by the constant surface temperatures and relatively small temperature gradient (no more than –2ºC, as shown in Figures 21 and 22). Differential shrinkage after construction probably caused these slabs to be permanently warped upwards along the sides and edges of the slab. This caused the slabs to lose contact with the base layer along the free edges of the slabs. From the responses measured by the MDDs it is clear that even with the

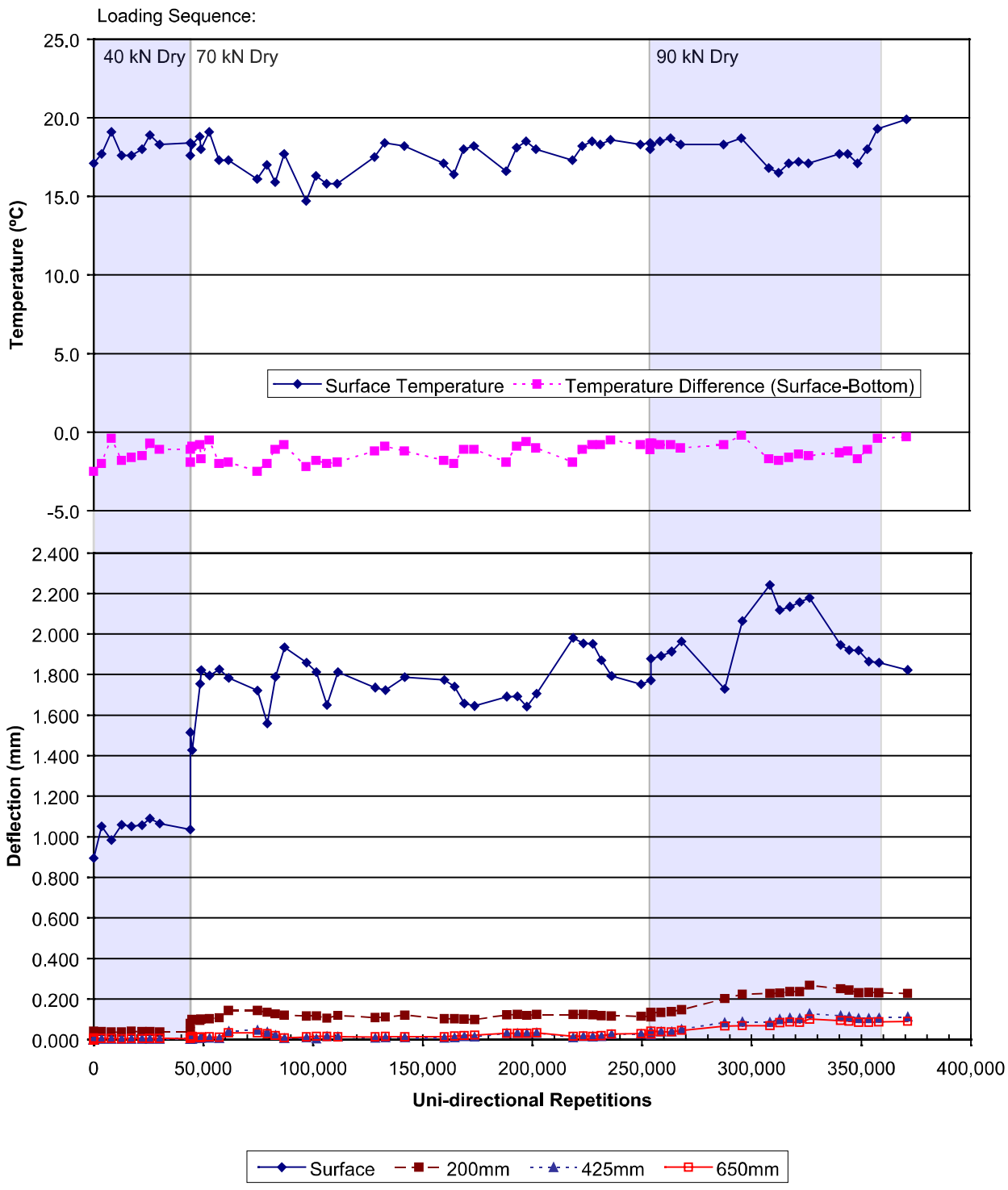

Figure 21. Plot of MDD 14 deflections and temperature versus load repetitions, Test 533FD.

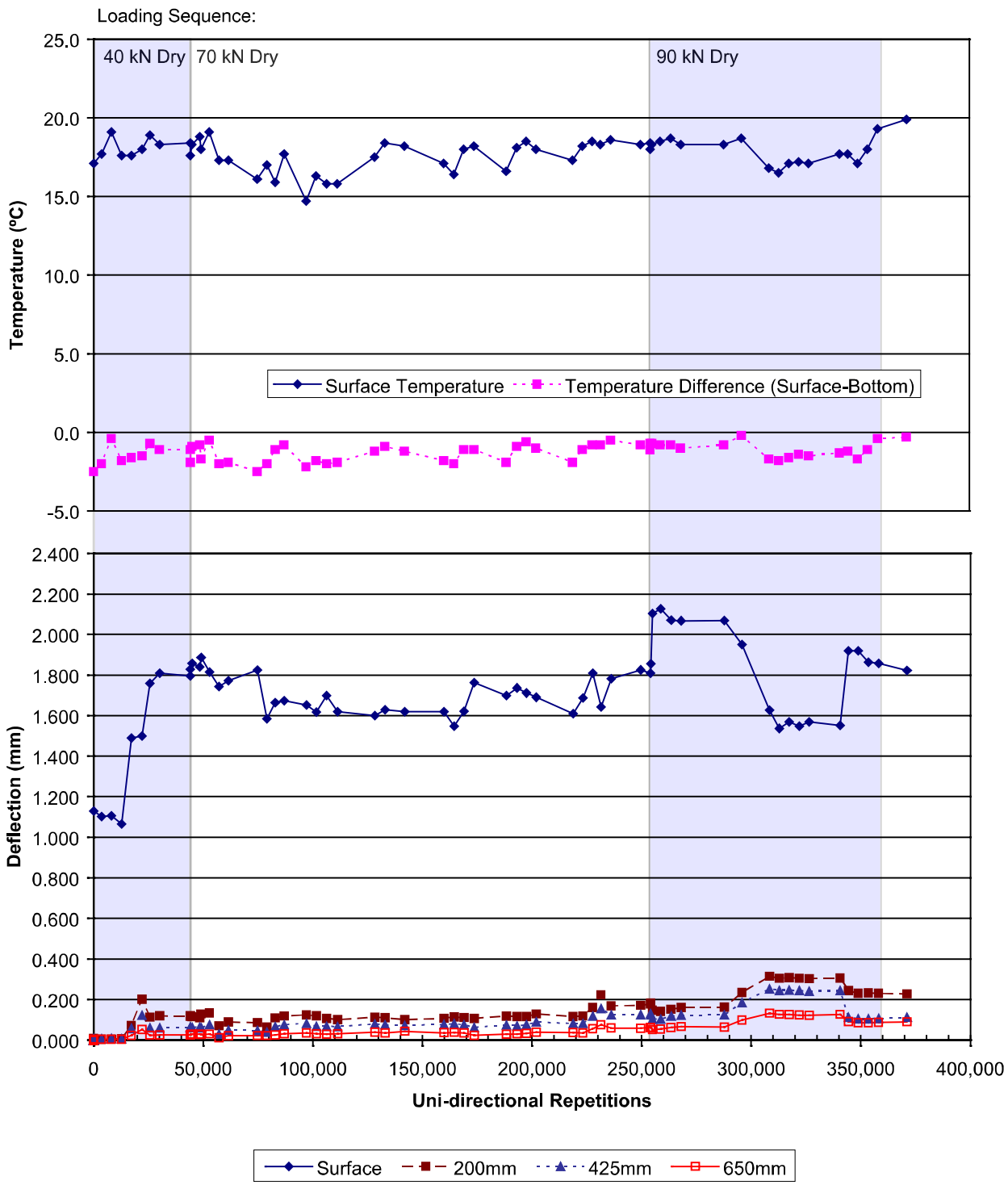

Figure 22. Plot of MDD 15 deflections and temperature versus load repetitions, Test 533FD.

application of a 90-kN load, very little deflection occurred in the base layer. This suggests that even under this high load, the edges of the 200-mm slabs were not in full contact with the base layer. If the slabs were in full contact with the base, the MDD module placed just below the PCC slab inside the base layer (MDD level 2) would have recorded significantly higher deflections.

It is interesting to note that MDD 15, level 2 (placed in the base under Slab 40) did show a slight increase in deflections after the development of the longitudinal crack at 340,587 repetitions (see Figure 22). This crack then caused the slab to have a higher degree of contact between the bottom of the slab and the base, which in turn caused a subsequent drop in the surface deflection as recorded by the surface MDD (Figure 22).

These observations are in agreement with findings from test sections on the South Tangent as well as an environmental study which was conducted to investigate the influences of temperature changes on slab curling (*1,2*).

4.3 Test 534FD

Test 534FD was the first test in which the new data acquisition system was used (discussed in Chapter 3.1). Data was recorded on the fly with the HVS trafficking wheel moving at a typical speed of about 7 km/h. Data collection was performed at regular 2-hour intervals on a 24-hour basis. From Test 534FD onwards, trafficking was applied bi-directionally, however, data collection was only performed when the HVS loading wheel traveled in the cabin-to-tow-end direction of the HVS.

Trafficking was begun with a 40-kN load for 126,580 repetitions followed by a 70-kN phase of 858,022 repetitions. The last phase consisted of 299,758 repetitions of a 90-kN load. The test was stopped after a total of 1,284,360 repetitions.

The test was conducted on Slab 34 (total length 5.91 m), Slab 35 (total length 3.86 m) and Slab 36 (total length 3.90 m). Slab 35 (the center slab) was fully tested together with some areas on either side of Joints 34 (in Slab 34) and 35 (in Slab 36) (Figure 5).

4.3.1 Visual Observations

No cracks existed on any of the slabs prior to starting the test. The section stayed intact for nearly the duration of the whole test. After 1,278,568 repetitions, a corner crack developed in the middle of the center slab (Slab 35), about 1,900 mm from Joint 34. The crack started at the midspan edge of the middle slab immediately to the left of the edge JDMD placed in the middle of Slab 35. The crack propagated towards Joint 34 and is symmetrically placed around the outside corner of Slab 35. The final crack pattern can be seen in the schematic of the crack pattern (Figure 23) and the composite image of the test section (Figure 24).

4.3.2 Joint Deflection Measuring Device (JDMD) Results

Five JDMDs were installed on Section 534FD; all were along the edge of the test pad. A summary of the most significant results can be seen in Table 10; complete results appear in Figure 25. Temperatures were only recorded from 1,269,356 repetitions until the end of the test.

Table 10 JDMD Deflections, Test 534FD

		Deflection (mm)						Temperature (ºC)	
	Test Load	Corner, Joint 35		Mid-span, Slab 35	Corner, Joint 34		Horizontal		Difference (top - bottom)
		Slab 36	Slab 35		Slab 35	Slab 34	Joint 35		
Repetitions	kN	JDMD 1	JDMD 2	JDMD 3	JDMD 4	JDMD 5	JDMD 6	Surface	
10 – 126,580	40	1.401 1.451	1.503 1.183	0.635 0.560	1.688 1.412	2.094 1.428	N/A	N/A	N/A
126,628 – 974,602	70	1.802 1.814	1.862 1.817	0.718 0.843	2.071 2.438	2.110 1.947			
989,441 – 1,284,360	90	2.190 3.421	1.748 2.857	0.761 1.392	2.312 1.971	1.909 3.726		22.7	0.8

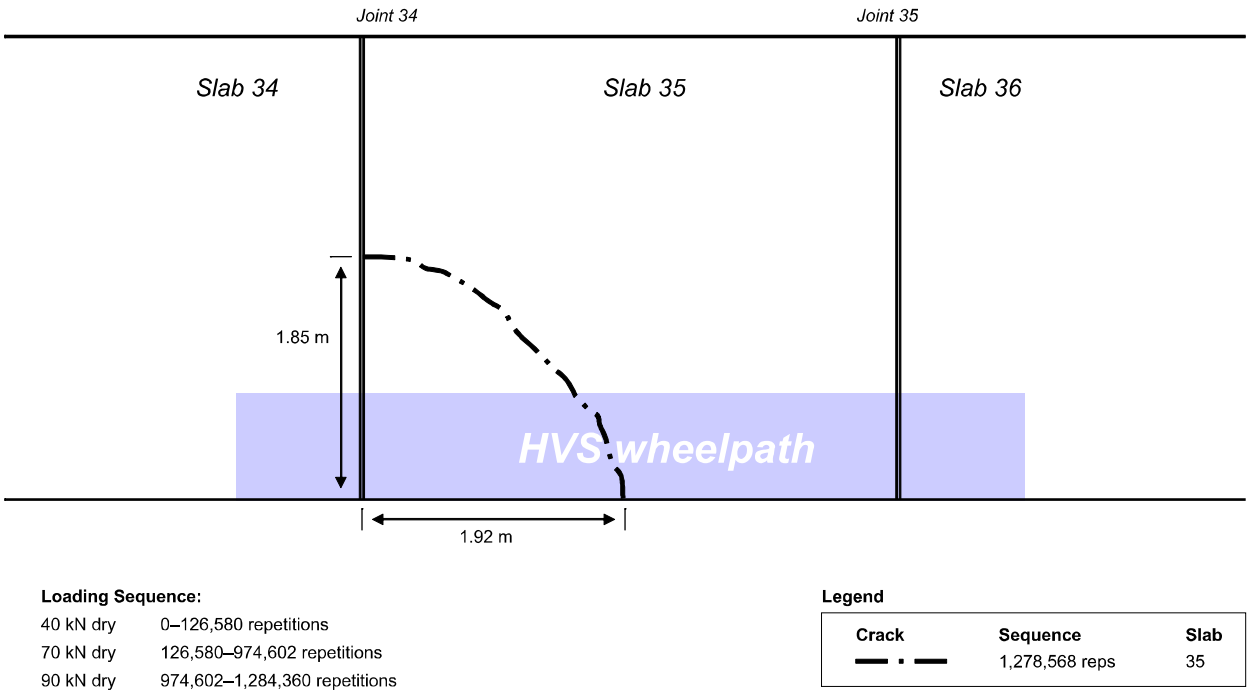

Figure 23. Schematic of crack pattern, Test 534FD.

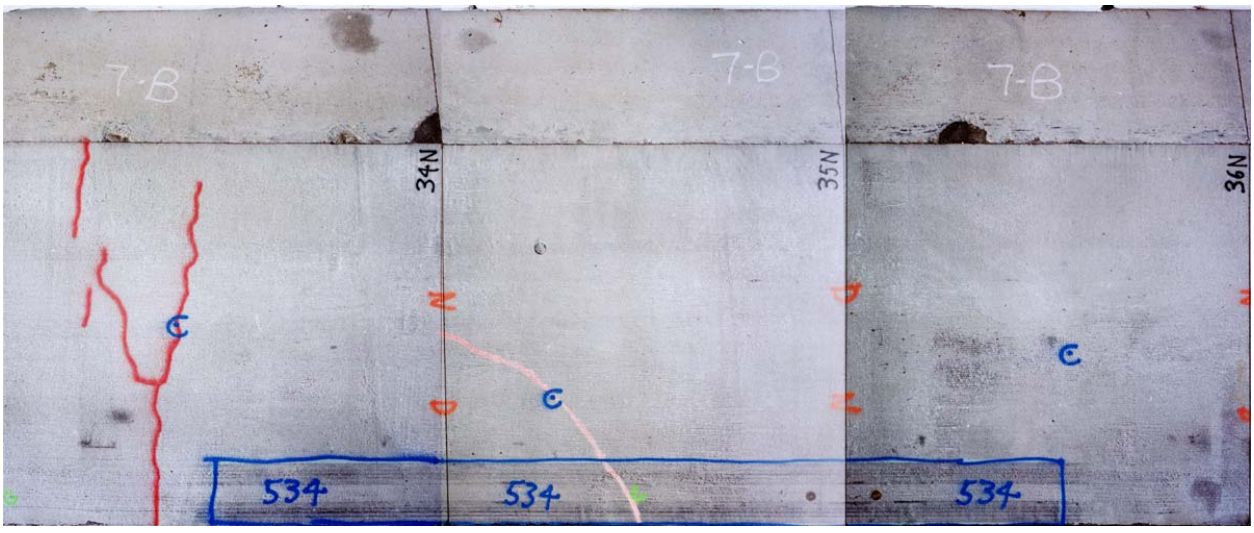

Figure 24. Composite image of Test 534FD showing cracks.

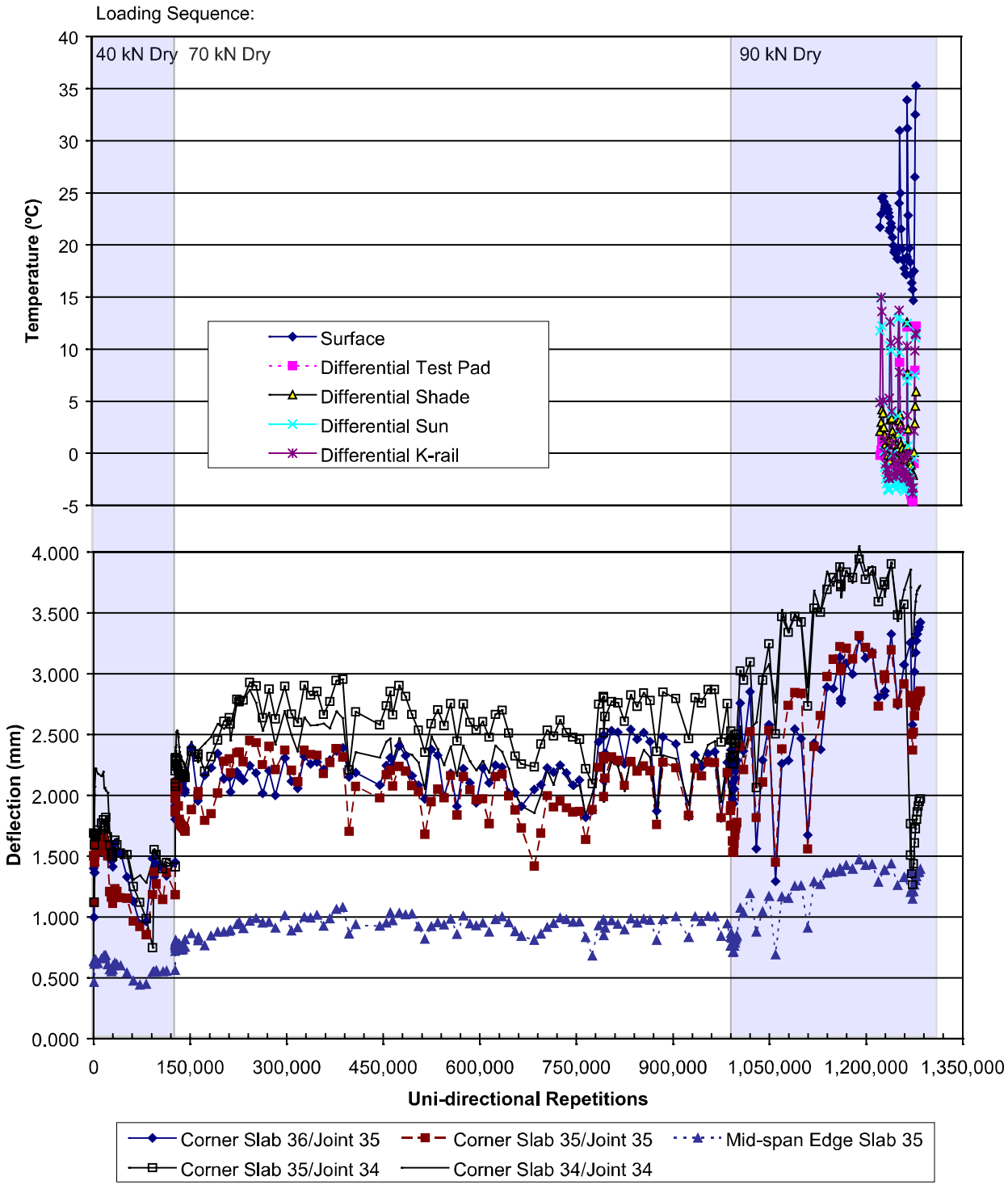

Figure 25. Plot of JDMD deflections and temperature versus load repetitions (entire loading sequence), Test 534FD.

The corner and edge deflections values with the 40-kN load are significantly higher than their counterparts in Test Sections 532FD and 533FD (compare Table 10 with Tables 7 and 5), although the slab lengths are almost the same (see Table 2). One possible explanation for this is the condition of the test section prior to the start of the test. Tests 532 and 533 had cracks in the slabs prior to the start of those tests, but the slabs of Test 534FD had no cracks. Differential shrinkage may have caused slab lift-off and the fact that all these slabs were fully intact may have caused a higher degree of lift-off along the edges. This would explain why higher initial deflections were recorded on Test 534FD than on Tests 534FD and 533FD.

As expected, deflections increased with increasing test load. Deflection values as high as 3.2 mm were recorded towards the end of the test.

An important observation is the behavior of the surface deflections just before and after the crack occurred after about 1.28 million load applications (see Figure 26). First, the corner deflections at Joint 34 experienced a significant drop in values from before to after the crack. Prior to the crack, the deflection measured with the corner JDMD on Slab 35, Joint 34 was almost 4 mm. After Slab 35 cracked, deflections dropped to 1.2 mm. This relates to a 66 percent drop in deflection. All the other JDMDs recorded drops in deflections, but not to the same degree as the corner JDMD at Slab 35.

Second, Figure 26 clearly show that after the crack developed, the deflection readings recovered somewhat. Deflections did not return to the same level as before the crack appeared. It is likely that after settlement of the slab and its loose cracked piece, the deflections increased again due to the heavier (90 kN) loading that was applied to the section until the test was stopped.

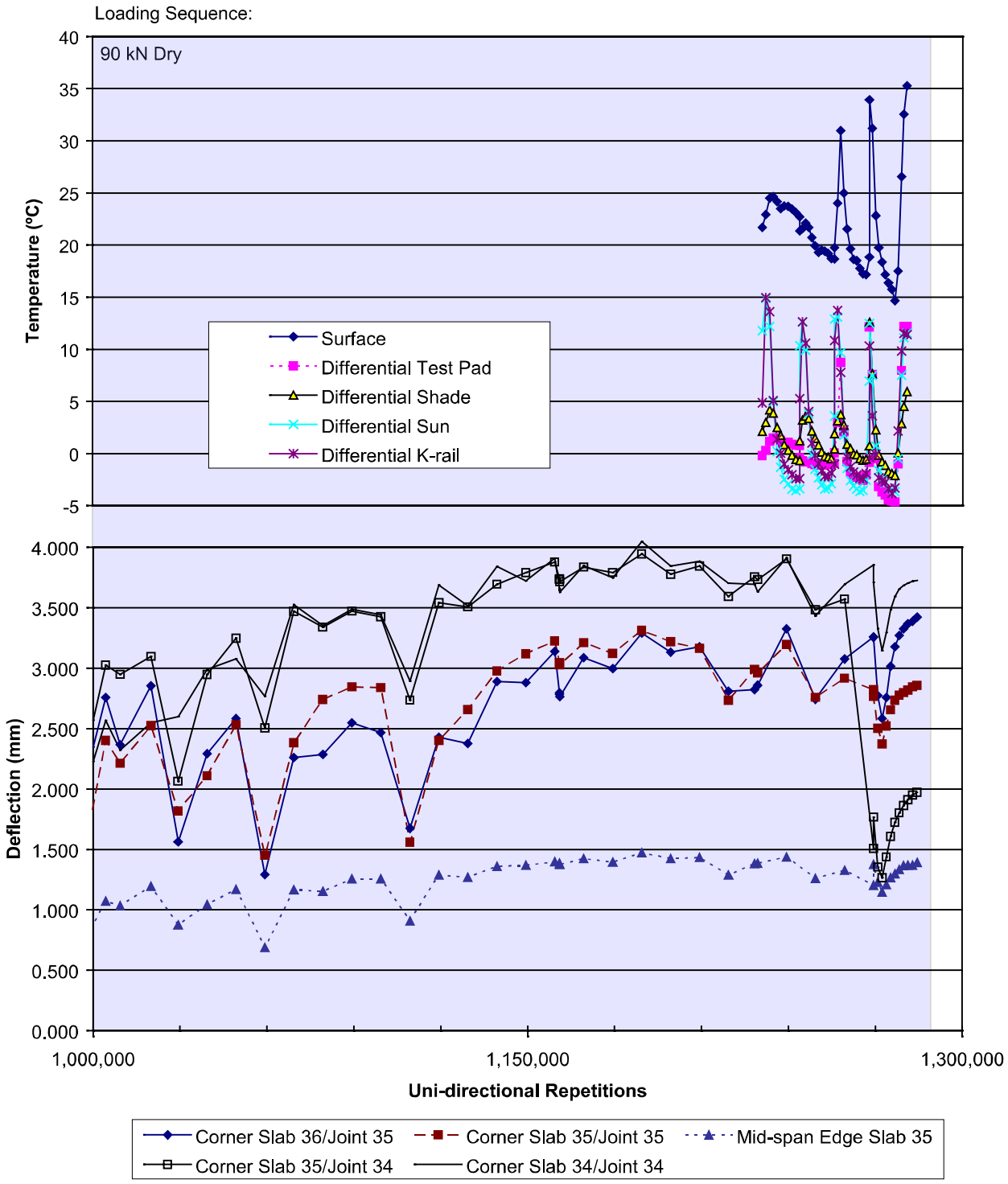

Figure 26. Plot of JDMD deflections and temperature versus load repetitions (1M repetitions to end of test), Test 534FD.

4.3.3 Joint Load Transfer Efficiency (LTE)

LTE values with repetitions can be seen in Figure 27. The effect of accelerated loading on the load transfer efficiency is clearly visible. LTE values between 80 and 100 percent were calculated at the beginning of the test but deterioration of aggregate interlock had a negative effect the load transfer efficiency.

The high corner deflections (see Table 10) had a rapid detrimental effect on the aggregate interlock at the joints. From Figure 27, it is clear that the accelerated loading destroyed the required aggregate interlock with the resulting drop in load transfer. Toward the end of the test LTE values less than 20 percent were observed.

4.3.4 Multi-Depth Deflectometer (MDD) Results

Two MDDs were placed in the vicinity of Joint 35. MDD 12 was placed approximately 300 mm from the joint in Slab 35 (the center slab). MDD 13 was placed approximately 300 mm from the joint in Slab 36. The module depths were the same as the MDDs in Test 533FD: at the surface (0 mm), 200 mm, 425 mm and 650 mm.

The MDD data are shown in Figures 28 and 29 and summarized in Table 11 and Table 12 for the deflections and the permanent deformation data, respectively.

Table 11 MDD Deflections, Test 534FD

Repetitions	Test Load, kN	Deflection (mm)				Temperature (ºC)	
		MDD 12, Slab 35		MDD 13, Slab 36			
		0 mm	200 mm	0 mm	200 mm	Surface	Difference (top – bottom)
10 – 126,580	40	1.039 1.119	0.058 0.070	1.146 0.960	0.016 0.021	N/A	N/A
126,628 – 974,602	70	1.341 1.439	0.051 0.060	1.437 1.524	0.018 0.045		
984,602 – 1,284,360	90	1.649 2.581	0.253 0.247	1.809 2.085	0.380 0.260	22.7	0.8

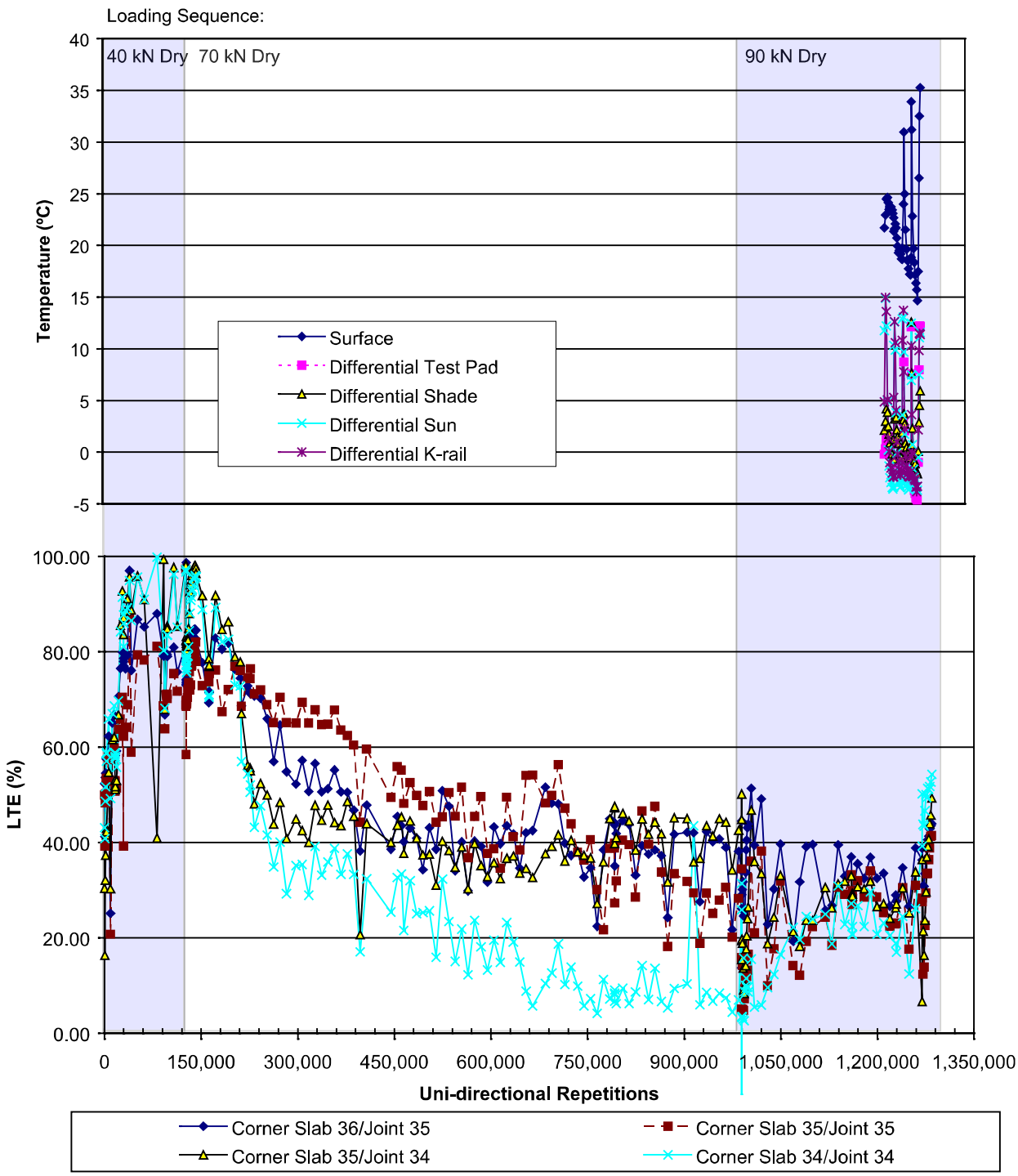

Figure 27. Plot of LTE and temperature versus load repetitions, Test 534FD.

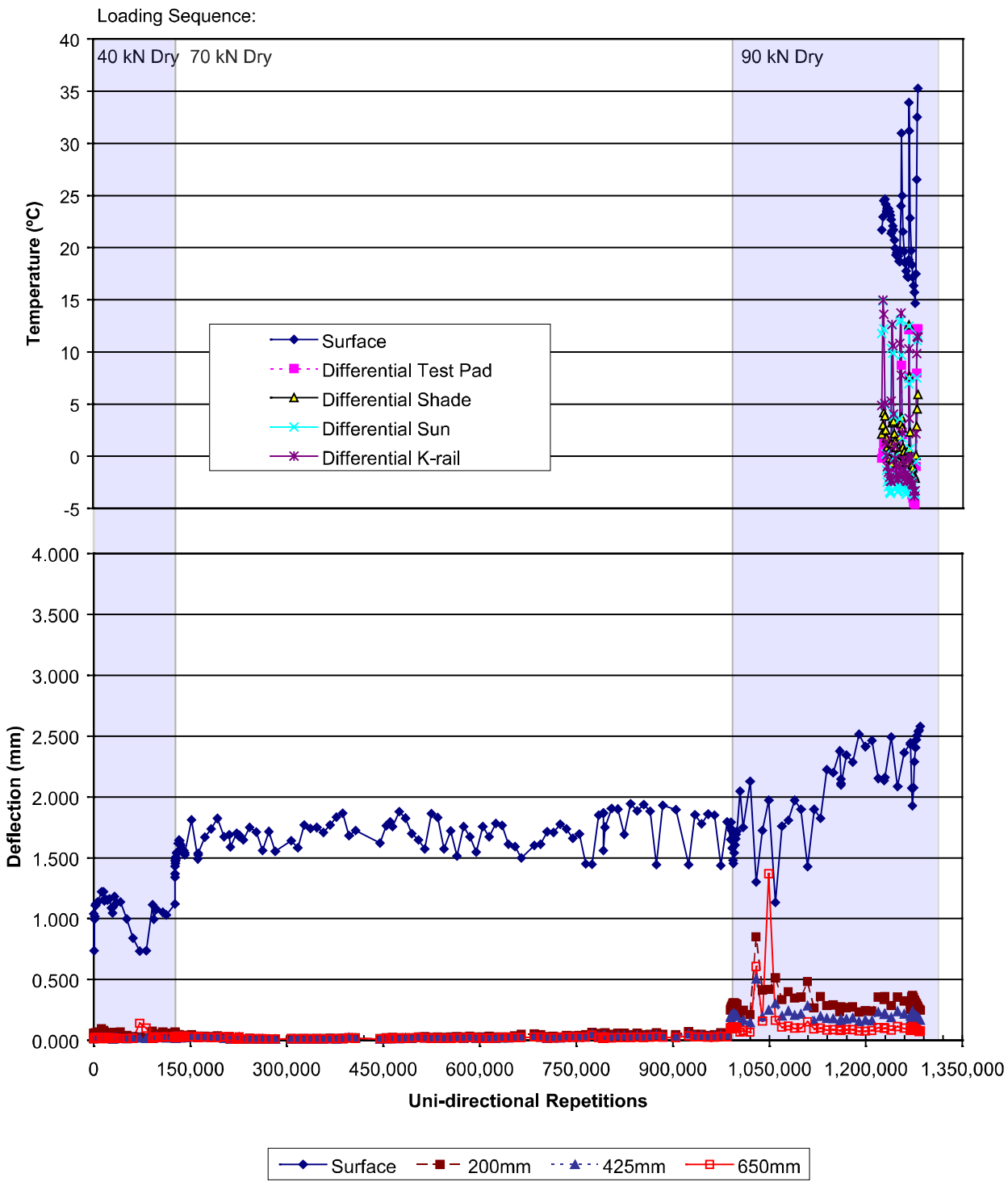

Figure 28. Plot of MDD 12 deflections and temperature versus load repetitions, Test 534FD.

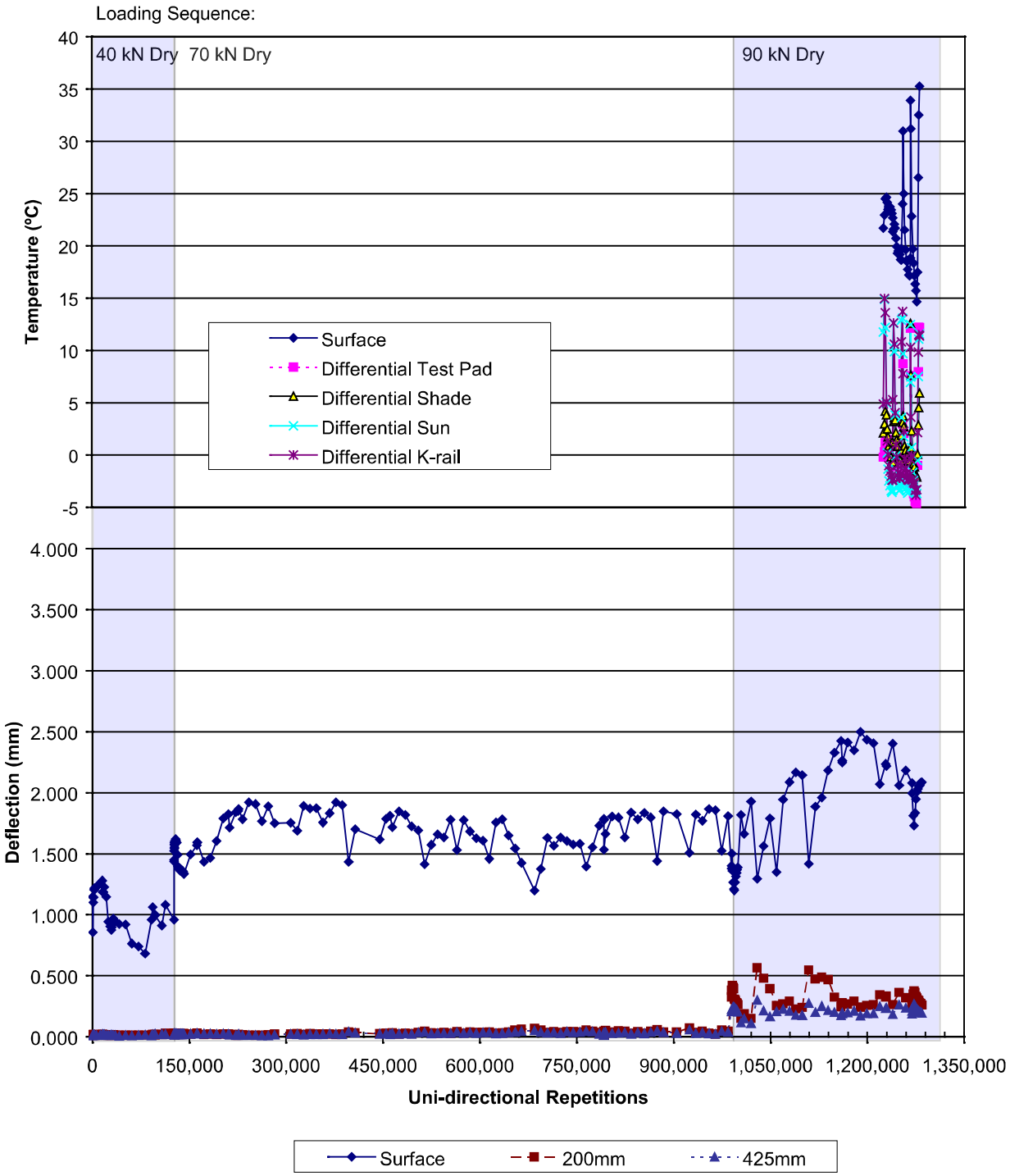

Figure 29. Plot of MDD 13 deflections and temperature versus load repetitions, Test 534FD.

The deflection values are very similar to those measured during Test 533FD and the trends are the same. It is clear that for the duration of the test, all the deflections originated from the PCC layer while very little deflections were recorded in the underlying layers. After the development of the corner crack in Slab 35, some noticeable deflections were recorded from the deeper levels in MDD 12 (placed in the base under Slab 35). These increasing deflections suggest that the crack in the concrete caused the slab to make contact with the base layer which then caused deflections in the underlying layers (see Figure 28).

The permanent deformation data reveal the same result. Figure 30 shows the permanent deformation data recorded by MDD 12 in Slab 35. The data are summarized in Table 12. The permanent movement in level 2 (placed just below the 200-mm concrete layer) had very little permanent movement until the crack started to develop. Subsequent increase in contact of the slab on the base layer led to the effects of the loading on the underlying layers, including deformations measured at MDD 12 level 2.

Table 12 MDD 12 Permanent Deformation, Test 534FD

		Permanent Deformation (mm)				**Temperature (°C)**	
		MDD 12, Slab 35					
Repetitions	**Test Load, kN**	**0 mm**	**200 mm**	**425 mm**	**650 mm**	**Surface**	**Difference (top – bottom)**
10 – 126,580	40	0.000 0.971	0.000 0.217	0.000 0.059	0.000 0.000	N/A	N/A
126,628 – 974,602	70	1.000 1.206	0.217 0.186	0.061 0.059	0.000 0.000		
984,602 – 1,284,360	90	1.589 3.411	0.160 0.197	-0.039 -0.095	0.000 0.000	22.7	0.8

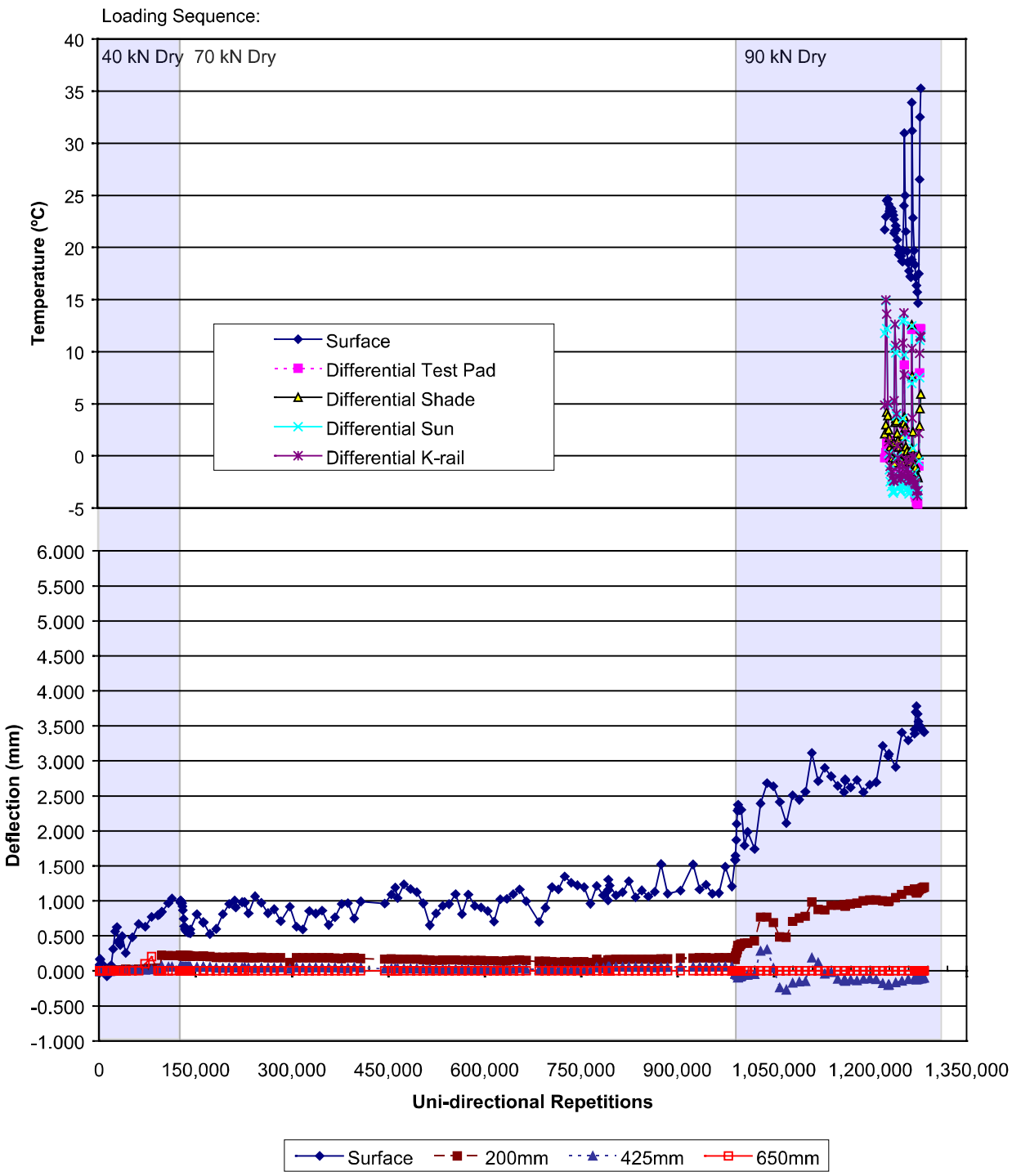

Figure 30. Plot of MDD 12 permanent deformation and temperature versus load repetitions, Test 534FD.

4.4 Test 535FD

Test 535FD was the last test conducted on Section 7 (slabs with no dowels and with an asphalt shoulder). Because of the performance of the previous tests, loading started with a 90 kN wheel load and was stopped after 80,000 load applications. The test was conducted on Slabs 31 (total length 4.11 m), 32 (the center slab with a total length of 3.71 m) and 33 (total length 5.35 m).

During this test the new DAS was fully operational and automatically recording of all the thermocouple, JDMD, and MDD data.

4.4.1 Visual observation

The final crack pattern of Section 535FD is shown in Figure 31. Figure 32 presents a composite image of the test section after the completion of HVS trafficking.

Before starting the test, a series of cracks existed through the width of Slab 33. These cracks occurred at midspan approximately 2,700 mm from Joint 32 (Slab 33 total length 5.35 m).

On Slab 32, the first structural crack appeared after 67,935 load applications. A corner crack on Slab 32 developed approximately 0.5 m from Joint 32. This crack extended right across the length of the center slab (total length = 3.71 m) and ended up at Joint 31 about 1,600 mm from the edge.

The last crack appeared in Slab 31 at the end of the test after 80,000 repetitions. This was a corner crack, which started at about mid-span of Slab 31 and ended at Joint 31 in the middle of Slab 31.

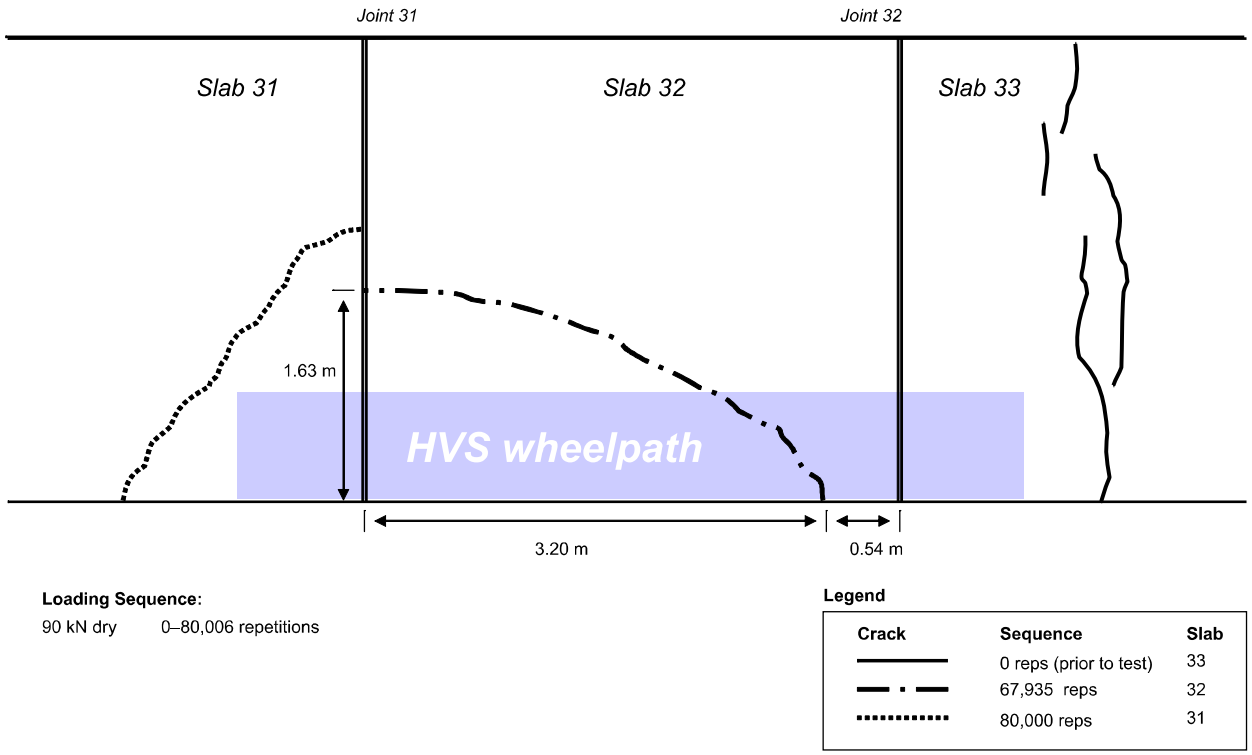

Figure 31. Schematic of crack pattern, Test 535FD.

Figure 32. Composite image of Test 535FD showing cracks.

4.4.2 Joint Deflection Measuring Device (JDMD) Results

Six JDMDs were installed for Test 535FD, of which five recorded edge deflections and one recorded horizontal movements across Joint 32 just outside the trafficking area (Figure 6). The summary data can be seen in Table 13 and the complete data set is graphically displayed in Figure 33.

The upper part of Figure 33 displays the surface temperature (recorded inside the temperature control box) as well as the temperature differentials (temperature at the top of the concrete layer – the temperature at the bottom) of all the installed thermocouples for the duration of the test. From the graph, the day-night cyclic effect is clearly visible. The thermocouples

Table 13 JDMD Deflections, Test 535FD

		Deflection (mm)						Temperature (ºC)	
	Test Load kN	Corner, Joint 32		Mid-span, Slab 32	Corner, Joint 31		Horizontal		
		Slab 33	Slab 32		Slab 32	Slab 31	Joint 33		Difference (top - bottom)
Repetitions		JDMD 1	JDMD 2	JDMD 3	JDMD 4	JDMD 5	JDMD 6	Surface	
0	90	1.930	2.089	1.048	2.924	2.777	0.072	14.9	-1.3
11		1.868	2.093	1.036	2.919	2.756	0.074	15.5	-1.0
101		1.911	2.104	1.094	2.935	2.776	0.071	15.7	-0.8
502		1.950	2.128	1.066	2.989	2.765	0.073	16.4	-0.3
1,002		1.923	2.129	1.102	2.989	2.713	0.077	17.0	0.3
2,003		1.867	2.067	1.074	2.934	2.592	0.080	18.2	1.3
3,003		1.852	2.022	1.042	2.849	2.543	0.065	19.6	1.9
4,003		1.940	2.075	1.039	2.885	2.656	0.059	20.3	2.3
5,003		2.072	2.165	1.061	2.956	2.865	0.065	19.5	2.2
6,002		2.160	2.238	1.068	3.043	3.029	0.067	19.0	2.0
7,002		2.202	2.283	1.115	3.055	3.146	0.069	18.4	1.8
8,002		2.246	2.310	1.055	2.993	3.327	0.075	18.0	1.4
9,002		2.261	2.326	1.048	2.932	3.451	0.081	18.4	1.2
10,002		2.270	2.326	1.010	2.890	3.530	0.083	18.8	1.3
11,002		2.265	2.331	1.024	2.864	3.578	0.083	18.9	1.1
12,002		2.248	2.295	0.971	2.742	3.649	0.088	19.6	1.5
13,002		2.219	2.265	0.946	2.607	3.713	0.081	20.4	2.0
14,002		2.190	2.221	0.895	2.550	3.709	0.081	21.9	3.2
15,002		2.148	2.166	0.863	2.466	3.669	0.075	22.2	2.6
20,003		2.264	2.132	0.893	2.463	3.734	0.063	21.7	2.4
30,002		2.166	2.198	1.056	2.873	3.249	0.068	21.3	0.3
40,003		2.392	2.380	1.040	3.038	3.763	0.076	20.1	0.3
50,002		2.464	2.239	1.110	3.143	3.241	0.062	21.0	0.8
60,002		2.468	1.993	1.005	2.889	3.092	0.040	23.2	1.5
70,002		2.191	1.753	0.511	1.392	1.956	0.016	22.5	0.6
80,002		2.676	2.199	0.596	1.617	2.305	0.007	20.9	-0.4

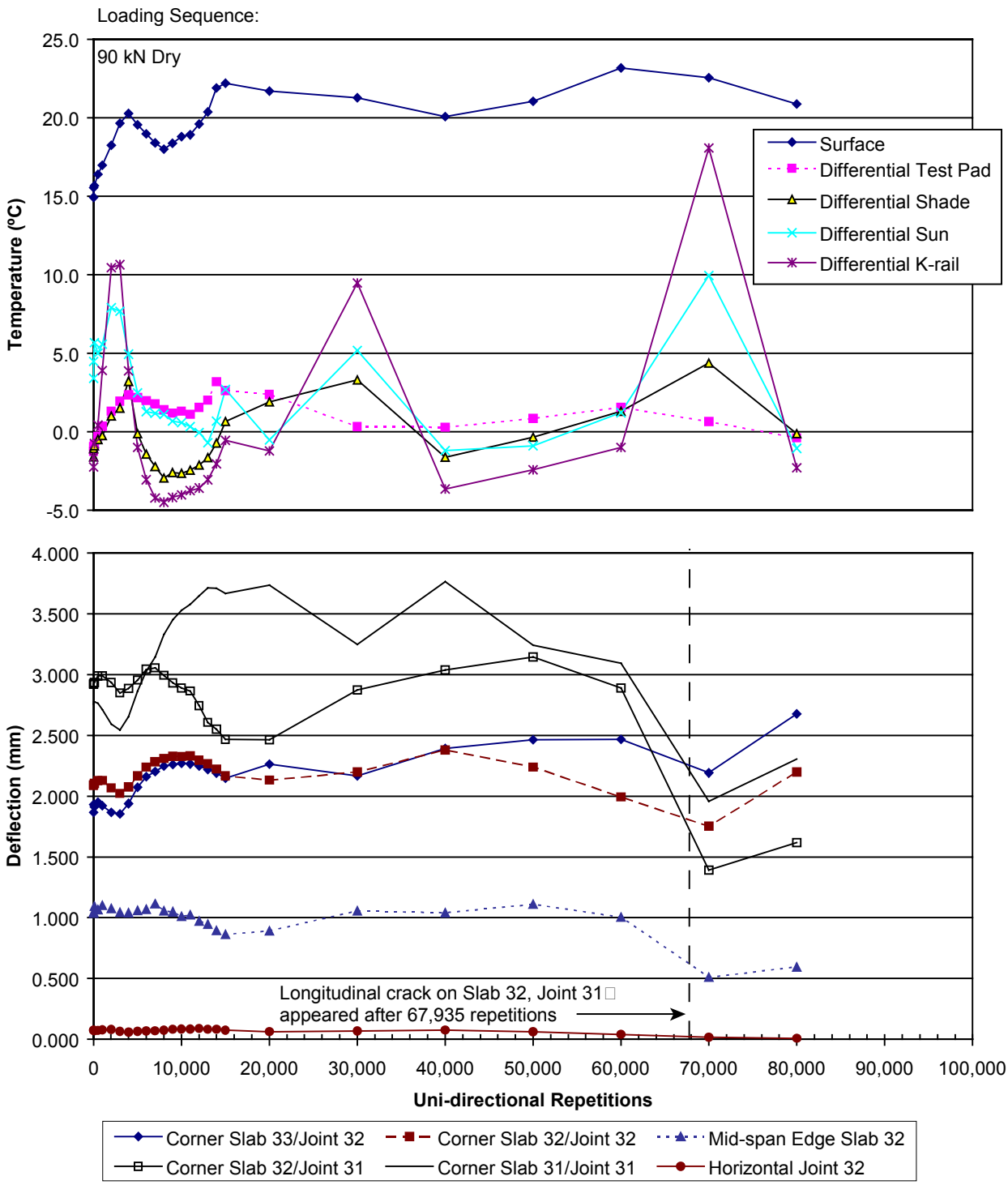

Figure 33. Plot of JDMD deflections and temperature versus load repetitions, Test 535FD.

outside the temperature control box (TC Sun and TC K-rail) show maximum temperature differentials of up to 18ºC, whereas the temperature differentials inside temperature control are lower than 5ºC.

Figure 33 shows an inverse correlation between deflection data and the corresponding temperature data (TC Sun, TC Test Pad, TC K-rail, and TC Shade). An increase in temperature difference leads to a decrease in deflections. One possible explanation for this behavior is that differential shrinkage, warping, and curling caused the initial position of the slab to be curled upwards, preventing the slab from full contact with the base. The lack of support from the underlying layers leads to high deflection values. As the surface temperature increases during the day, the slab heats up on the surface and expands, causing it to curl downwards. The downward curl causes the slab to come in contact with the base, which then leads to reduced deflections.

The JDMD deflections started off higher that in previous tests. However, this test started with a 90-kN load, which was higher than in previous tests. The deflections recorded at Joint 31 were higher than those recorded at the other joint (Joint 32). The midspan edge deflections were the lowest of the five measured locations, which is in agreement with all other previous tests.

The corner crack at Joint 31 had a significant influence on the measured deflections at the same joint. Deflections at this joint prior to the crack were on the order of 3.5 mm; after the crack developed, they dropped to as low as 1.4 mm. This observation supports the hypothesis that the slabs along its edges were not in contact with the base course, resulting in initial high deflections. As in previous tests, once the slab made contact with the base (after the crack developed), the measured deflections dropped.

The elastic horizontal movement measured at Joint 31 displayed similar behavior. Maximum movement on the order of 0.083 mm dropped to 0.02 mm after the crack developed.

4.4.3 Joint Load Transfer Efficiency (LTE)

The LTE is shown in Table 14 and Figure 34. The changes in LTE are somewhat unexpected. Studying the graph, one would expect the LTE values to drop as aggregate interlock deteriorates. The LTE values, calculated at the joint where the crack developed, should display a dramatic drop after the corner crack developed, however according to the data this did not happen. A likely explanation is that slab rocking caused by irregular edge movements as indicated by the various JDMDs at the corners of the joints caused the calculation of the LTE values to be erroneous.

Table 14 Load Transfer Efficiency, Test 535FD

Repetitions	Test Load, kN	Load Transfer Efficiency (%)				Temperature (ºC)	
		Corner, Joint 32		Corner, Joint 31			
		Slab 33	Slab 32	Slab 32	Slab 31		
		JDMD 1	JDMD 2	JDMD 4	JDMD 5	Surface	Difference (top – bottom)
0	90	64.9	62.2	66.2	67.5	14.9	-1.3
11		63.9	64.9	65.7	65.1	15.5	-1.0
101		63.3	64.0	68.6	61.9	15.7	-0.8
502		61.4	63.6	68.2	65.7	16.4	-0.3
1,002		60.6	67.3	70.6	65.8	17.0	0.3
2,003		60.5	61.7	69.9	68.9	18.2	1.3
3,003		58.7	62.2	66.8	69.7	19.6	1.9
4,003		62.5	67.3	69.8	70.2	20.3	2.3
5,003		67.4	70.7	73.9	69.1	19.5	2.2
6,002		68.3	71.1	68.9	69.7	19.0	2.0
7,002		69.5	72.6	68.7	68.8	18.4	1.8
8,002		70.8	73.3	67.2	69.6	18.0	1.4
9,002		72.4	72.3	66.1	66.6	18.4	1.2
10,002		73.9	76.6	66.3	66.1	18.8	1.3
11,002		75.1	76.0	65.4	67.0	18.9	1.1
12,002		75.7	77.7	63.0	64.4	19.6	1.5
13,002		77.3	80.8	62.6	64.4	20.4	2.0
14,002		78.6	82.5	60.7	64.5	21.9	3.2
15,002		80.2	83.6	59.9	71.1	22.2	2.6
20,003		80.5	82.3	53.0	68.0	21.7	2.4
30,002		71.5	76.8	52.1	56.0	21.3	0.3
40,003		79.6	82.7	47.1	58.4	20.1	0.3
50,002		81.7	82.0	44.9	53.1	21.0	0.8
60,002		83.7	79.8	42.2	57.0	23.2	1.5
70,002		83.2	80.0	52.4	63.7	22.5	0.6
80,002		85.6	82.9	51.5	68.2	20.9	-0.4

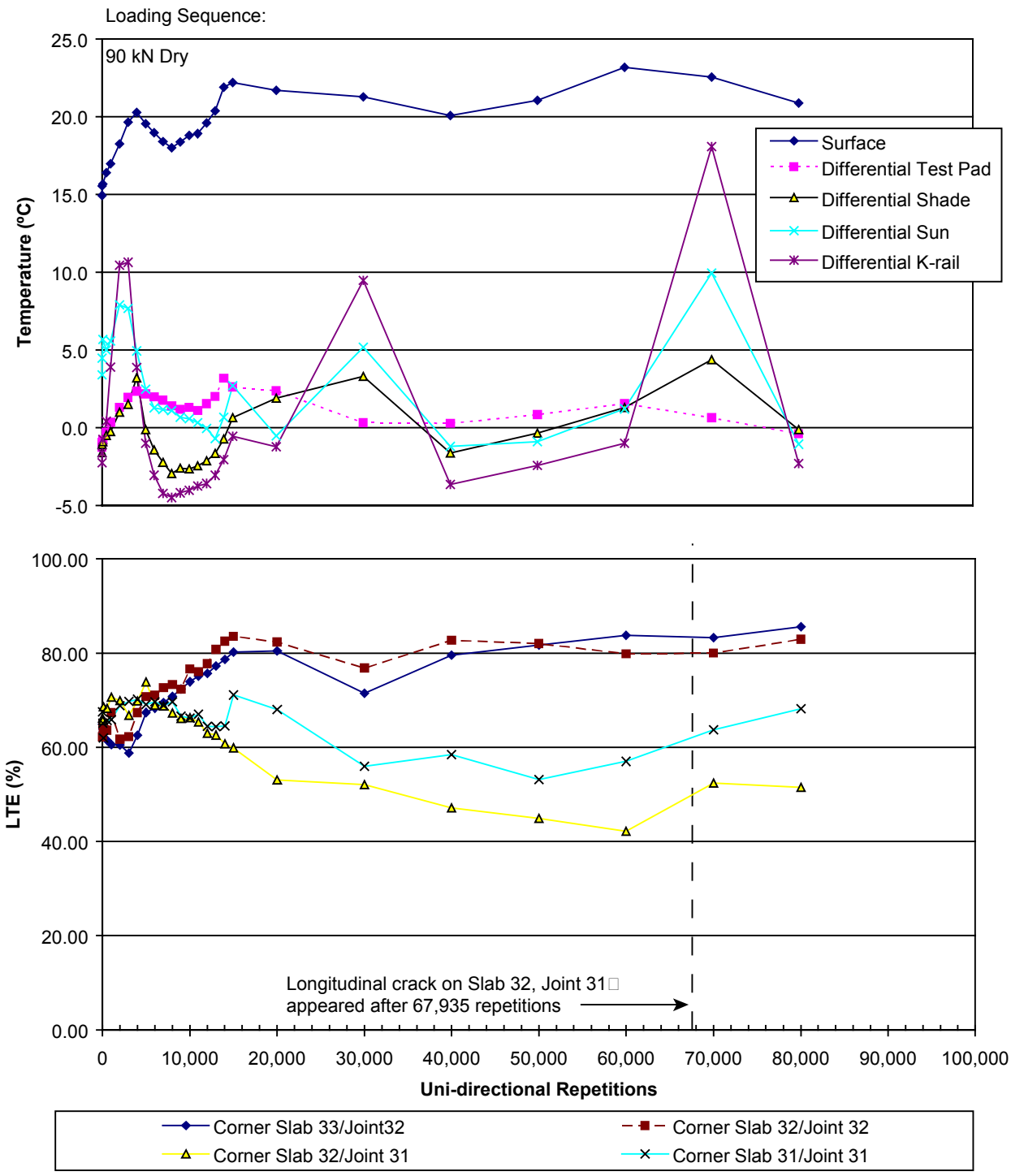

Figure 34. Plot of LTE and temperature versus load repetitions, Test 535FD.

4.4.4 Multi-Depth Deflectometer (MDD) Results

Only one MDD (MDD 11) was installed on this test section. It was placed at the midspan of the center slab in the middle of the HVS wheelpath (see Figure 6). Modules were placed at depths of 0 mm (at the surface), 200 mm, 425 mm and 650 mm. The MDD values are lower than those recorded at the other test sections; however, this MDD was at the midspan of the center slab, away from the joints where high deflections would be expected. MDD data are shown in Table 15 and graphically presented in Figure 35.

One interesting observation from this data set is the deflections recorded by MDD modules in the underlying layers. Figure 35 shows that approximately half of the total deflection measured at the surface originated at a depth of 200 mm. This means a considerable amount of deflection occurred in the base course.

As expected, a significant drop in surface deflection occurred after the crack at Joint 31 appeared accompanied by increased deflections measured by the level 2 MDD (200-mm depth).

The deflections measured at the end of the test (after 80,000 repetitions) revealed that the deflection measured at the surface was almost the same as the deflection measured at 200 mm (0.59 mm versus 0.51 mm in Table 15). This shows that after the crack appeared, the slab was in full contact with the base course. As a result almost all the deflection measured at the surface originated from the underlying layers.

The permanent deformation data from MDD 11 in Table 16 and Figure 36 show the same pattern. Figure 36 shows that during the first part of the test, almost all permanent deformation took place above the depth of 425 mm. The top two MDD modules have very similar movements, suggesting that the bulk of the deformation occurred in the base course between the depth of 200 mm and 425 mm.

Table 15 MDD Deflections, Test 535FD

Repetitions	Test Load, kN	Deflection (mm) MDD 11, Slab 32				Temperature (ºC)	
		0 mm	200 mm	425 mm	650 mm	Surface	Difference (top – bottom)
0	90	0.817	0.363	0.224	0.161	14.9	-1.3
11		0.817	0.363	0.224	0.161	15.5	-1.0
101		0.834	0.364	0.220	0.166	15.7	-0.8
502		0.835	0.378	0.232	0.170	16.4	-0.3
1,002		0.824	0.394	0.243	0.172	17.0	0.3
2,003		0.803	0.428	0.270	0.176	18.2	1.3
3,003		0.788	0.423	0.277	0.176	19.6	1.9
4,003		0.801	0.419	0.277	0.175	20.3	2.3
5,003		0.807	0.405	0.267	0.165	19.5	2.2
6,002		0.853	0.403	0.262	0.164	19.0	2.0
7,002		0.874	0.388	0.253	0.164	18.4	1.8
8,002		0.888	0.383	0.249	0.161	18.0	1.4
9,002		0.904	0.386	0.248	0.160	18.4	1.2
10,002		0.904	0.375	0.240	0.154	18.8	1.3
11,002		0.904	0.373	0.236	0.155	18.9	1.1
12,002		0.893	0.368	0.236	0.155	19.6	1.5
13,002		0.889	0.366	0.236	0.153	20.4	2.0
14,002		0.881	0.375	0.238	0.162	21.9	3.2
15,002		0.861	0.382	0.229	0.160	22.2	2.6
20,003		0.879	0.394	0.241	0.161	21.7	2.4
30,002		0.953	0.413	0.239	0.178	21.3	0.3
40,003		1.014	0.371	0.239	0.161	20.1	0.3
50,002		0.966	0.384	0.255	0.162	21.0	0.8
60,002		0.866	0.402	0.251	0.172	23.2	1.5
70,002		0.531	0.470	0.332	0.221	22.5	0.6
80,002		0.593	0.513	0.403	0.251	20.9	-0.4

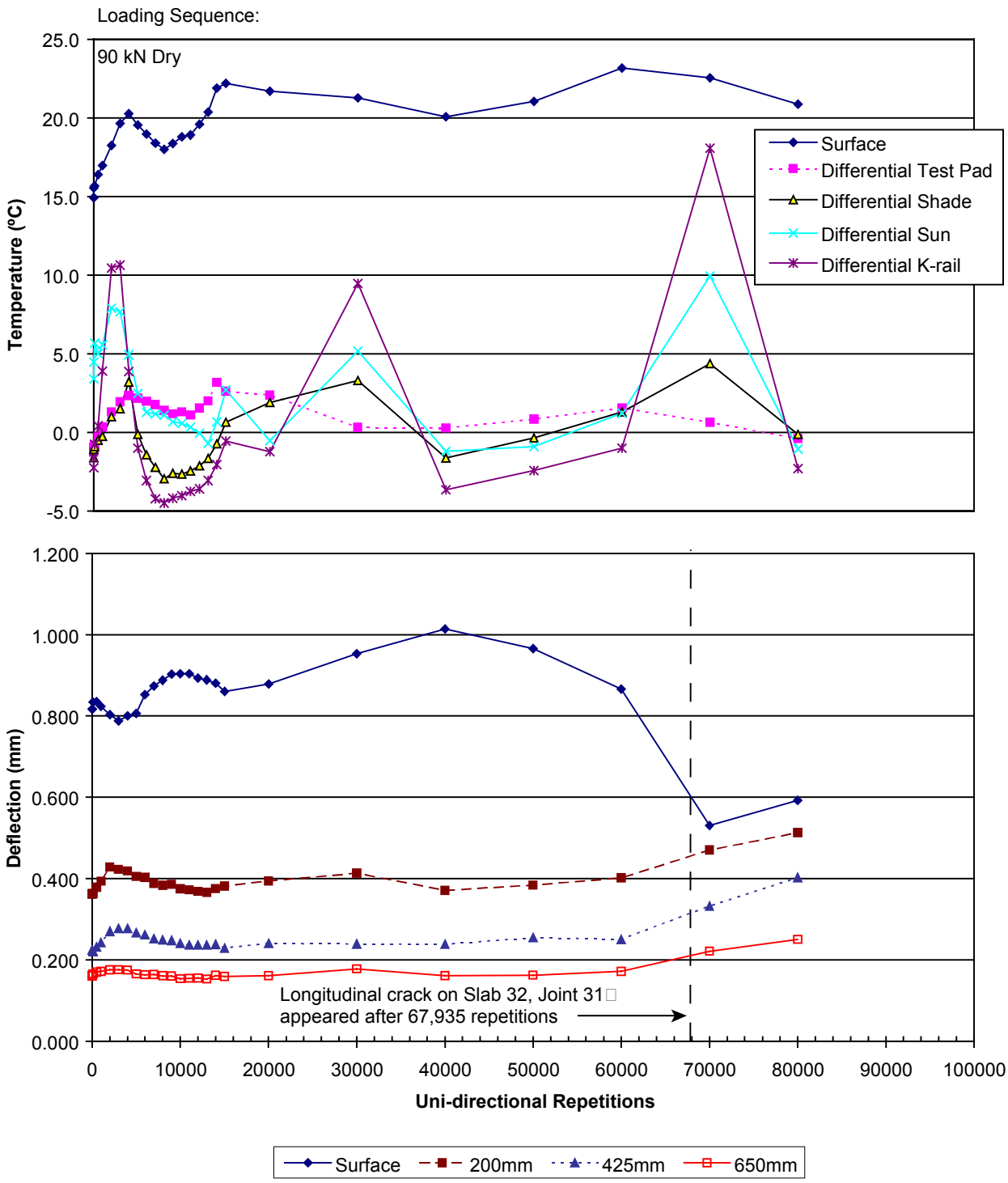

Figure 35. Plot of MDD 11 deflections and temperature versus load repetitions, Test 535FD.

Table 16 MDD Permanent Deformation, Test 535FD

Repetitions	Test Load, kN	Deflection (mm) MDD 11, Slab 32 0 mm	200 mm	425 mm	650 mm	Temperature (ºC) Surface	Difference (top – bottom)
0	90	0.000	0.000	0.000	0.000	14.9	-1.3
11		0.002	0.002	-0.002	-0.001	15.5	-1.0
101		0.012	0.022	0.005	0.005	15.7	-0.8
502		0.073	0.044	0.001	0.011	16.4	-0.3
1,002		0.142	0.071	0.010	0.017	17.0	0.3
2,003		0.281	0.141	0.032	0.039	18.2	1.3
3,003		0.370	0.180	0.041	0.051	19.6	1.9
4,003		0.404	0.193	0.050	0.056	20.3	2.3
5,003		0.406	0.208	0.053	0.049	19.5	2.2
6,002		0.381	0.227	0.052	0.043	19.0	2.0
7,002		0.375	0.246	0.061	0.037	18.4	1.8
8,002		0.369	0.239	0.059	0.034	18.0	1.4
9,002		0.365	0.254	0.062	0.029	18.4	1.2
10,002		0.375	0.271	0.064	0.029	18.8	1.3
11,002		0.380	0.268	0.067	0.028	18.9	1.1
12,002		0.405	0.281	0.072	0.029	19.6	1.5
13,002		0.427	0.296	0.078	0.033	20.4	2.0
14,002		0.454	0.303	0.081	0.031	21.9	3.2
15,002		0.484	0.308	0.085	0.030	22.2	2.6
20,003		0.565	0.370	0.116	0.060	21.7	2.4
30,002		0.609	0.430	0.132	0.067	21.3	0.3
40,003		0.591	0.485	0.139	0.043	20.1	0.3
50,002		0.727	0.544	0.173	0.055	21.0	0.8
60,002		0.928	0.622	0.231	0.091	23.2	1.5
70,002		1.873	1.089	0.466	0.207	22.5	0.6
80,002		1.957	1.150	0.462	0.171	20.9	-0.4

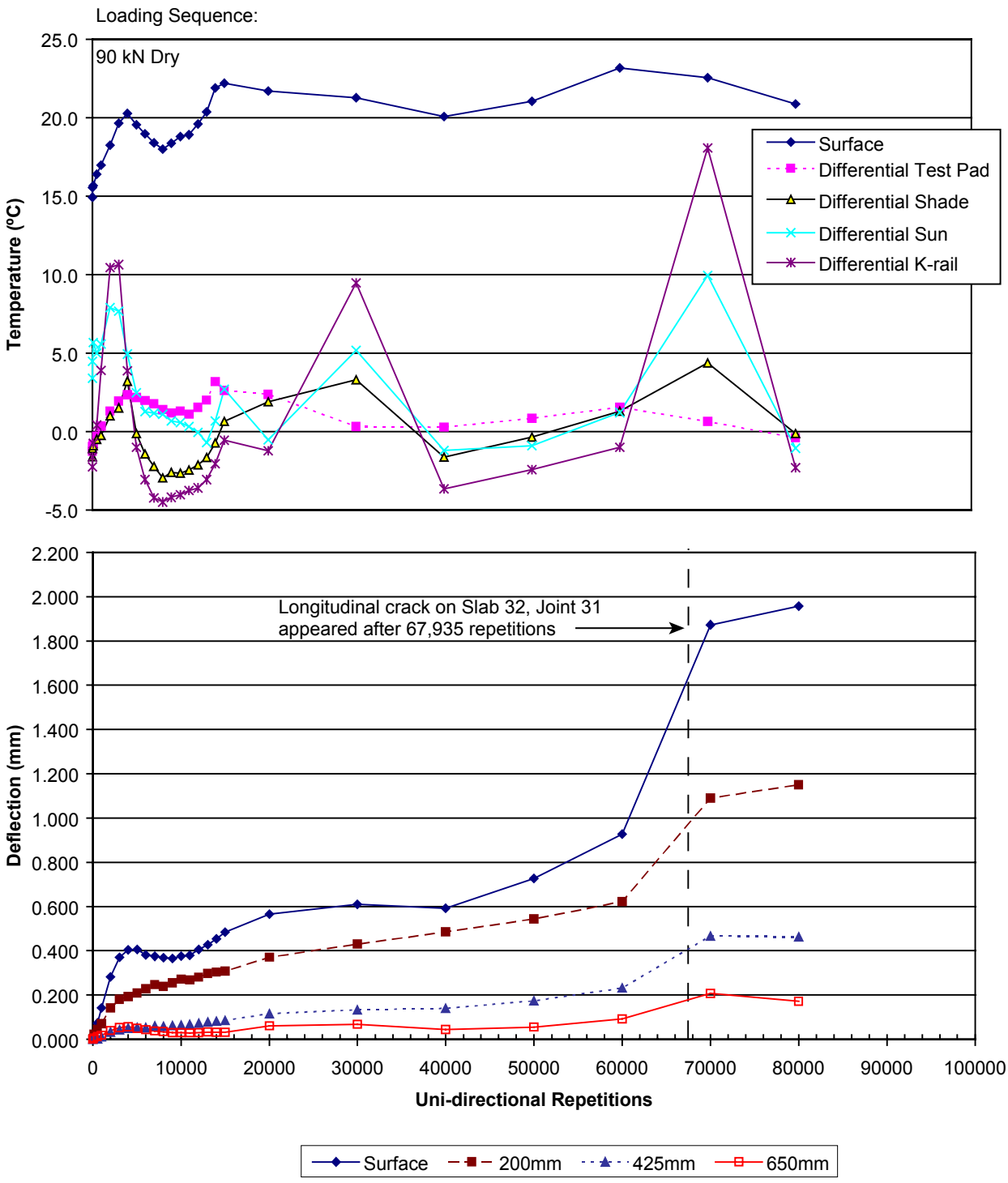

Figure 36. Plot of MDD 11 permanent deformation and temperature versus load repetitions, Test 535FD.

It also can be concluded that although the crack wasn't observed until after 67,000 repetitions, the effect of the crack can already be seen after 60,000 repetitions. After 60,000 repetitions, the rate of permanent deformation recorded by the surface and the 200-mm deep modules show a significant increase. This means that structurally, the crack already existed from 60,000 repetitions onward but was only visually detected on the surface at 67,000 repetitions. As expected, the permanent deformation increased significantly after the crack appeared. The total permanent deformation at the surface was 2.0 mm at the end of the test, after 80,000 load applications.

4.5 Test 536FD

HVS Test 536FD was the first of the series of three HVS tests on the 200-mm FSHCC slabs with dowels and a tied concrete shoulder. Testing proceeded from April 7 to June 12, 2000. The other two HVS tests in the series are 537FD and 538FD and are reported in Chapters 4.6 and 4.7.

The main objective of this series of tests was to evaluate the influence of various factors, including slab length and load transfer devices (dowels), on the effectiveness of joint load transfer and joint deterioration under repetitive loading and controlled temperature. The fatigue behavior of the Fast Setting Hydraulic Cement Concrete (FSHCC) slabs in this series of three tests was monitored under bi-directional wheel loadings of at least 90 kN and in dry conditions (no water added).

Test 536FD was conducted on Slabs 26, 27, and 28 so that the full length (3.96 m) of Slab 27 and approximately 2 m on each of the adjacent slabs (Slabs 26 and 28) was trafficked (Figure 7). Initially, approximately 750,000 wheel load repetitions were applied with a 90-kN

dual wheel. An aircraft tire was then fitted and about 500 repetitions were applied at each of a series of increasing loads (70, 90, 110 and 130 kN). An additional 88,000 repetitions of a 150-kN (still with temperature control) load were then applied. Following this sequence, a final 150,000 repetitions at the same 150-kN wheel load were applied under ambient temperature. A total of almost one million channelized wheel load repetitions were applied in this test.

4.5.1 Visual Observations

No cracks were observed throughout Test 536FD and no visible changes in condition were reported. This is in keeping with a strong, well restrained, pavement slab configuration that was able to carry almost a million repetitions of heavily overloaded wheel loads (90 and 150 kN for just over 990,000 repetitions of the total number of load repetitions) prior to stopping the test. Figure 37 shows a composite image of the section.

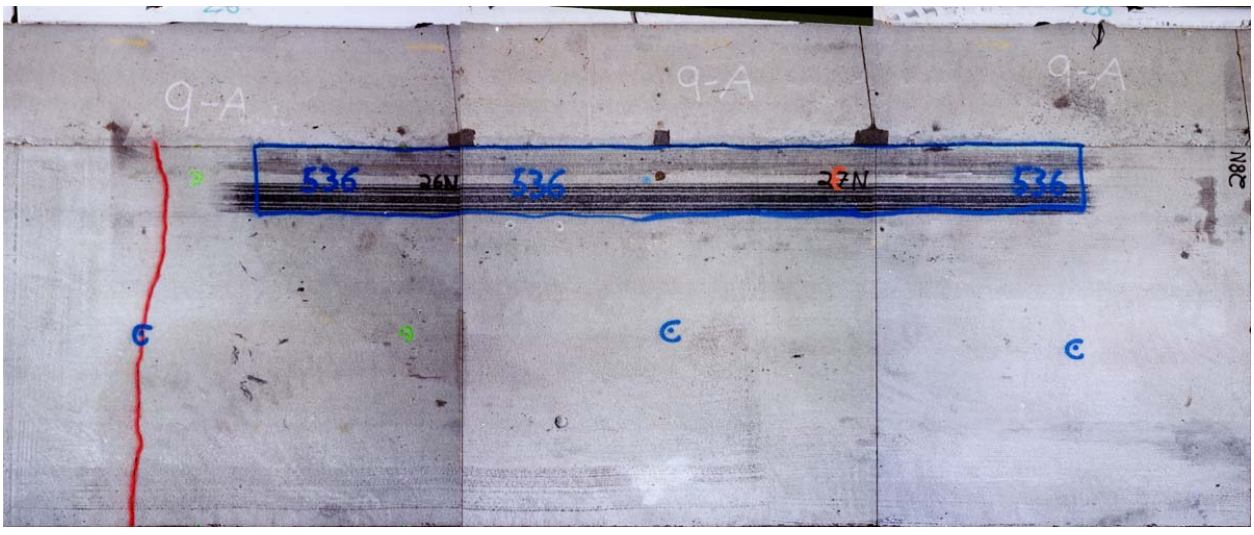

Figure 37. Composite image of Test 536FD.

4.5.2 Joint Deflection Measuring Device (JDMD) Results

4.5.2.1 Elastic deflections and trafficking

Figures 38–40 present the elastic deflection data for the test. These three figures corresponds with three stages of trafficking: the initial 750,000 repetitions at the 90-kN dual wheel load; the next 2,000 repetitions with aircraft wheel loads increasing from 70 to 130 kN; and the final 240,000 repetitions with a 150-kN aircraft wheel load. These figures also show the test slab surface temperatures and the temperature differentials between slab top and bottom at four locations around the test area. The expanded scale helps examine the data and evaluate changes throughout each stage of the test.

Deflections cannot be compared directly because measurements were recorded at the trafficking wheel load, rather than at a selected standard wheel load (normally 40 kN as the equivalent standard axle load). All the joint measurements fluctuate considerably and show a similar distinct "saw-tooth" variation in values rather than smooth gradual changes. Temperature fluctuations would seem to be a contributing factor but, before examining this more closely, the effect of trafficking will be evaluated.

Figure 41 shows deflections recorded by JDMDs 1, 2, 4 and 5 versus trafficking history. The figure shows deflections recorded on either side of Joints 27 and 26 at each end of Slab 27. The graphs show the various trafficking (and test) wheel loads applied and the very narrow trafficking band during which the 70-, 90-, 110-, and 130-kN aircraft wheel loadings were applied.

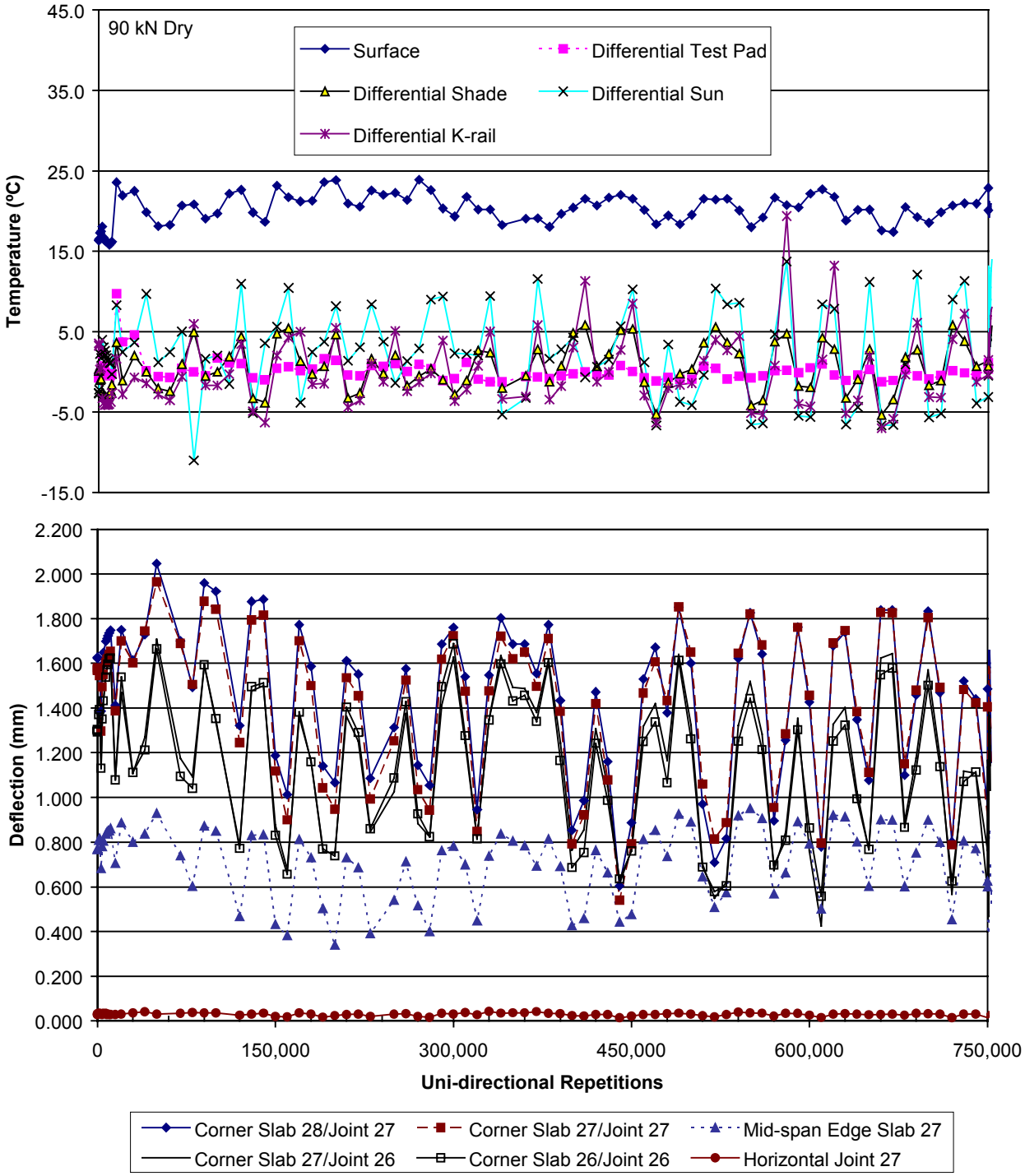

Figure 38. Plot of JDMD deflections and temperature versus load repetitions, 90-kN test load, Test 536FD.

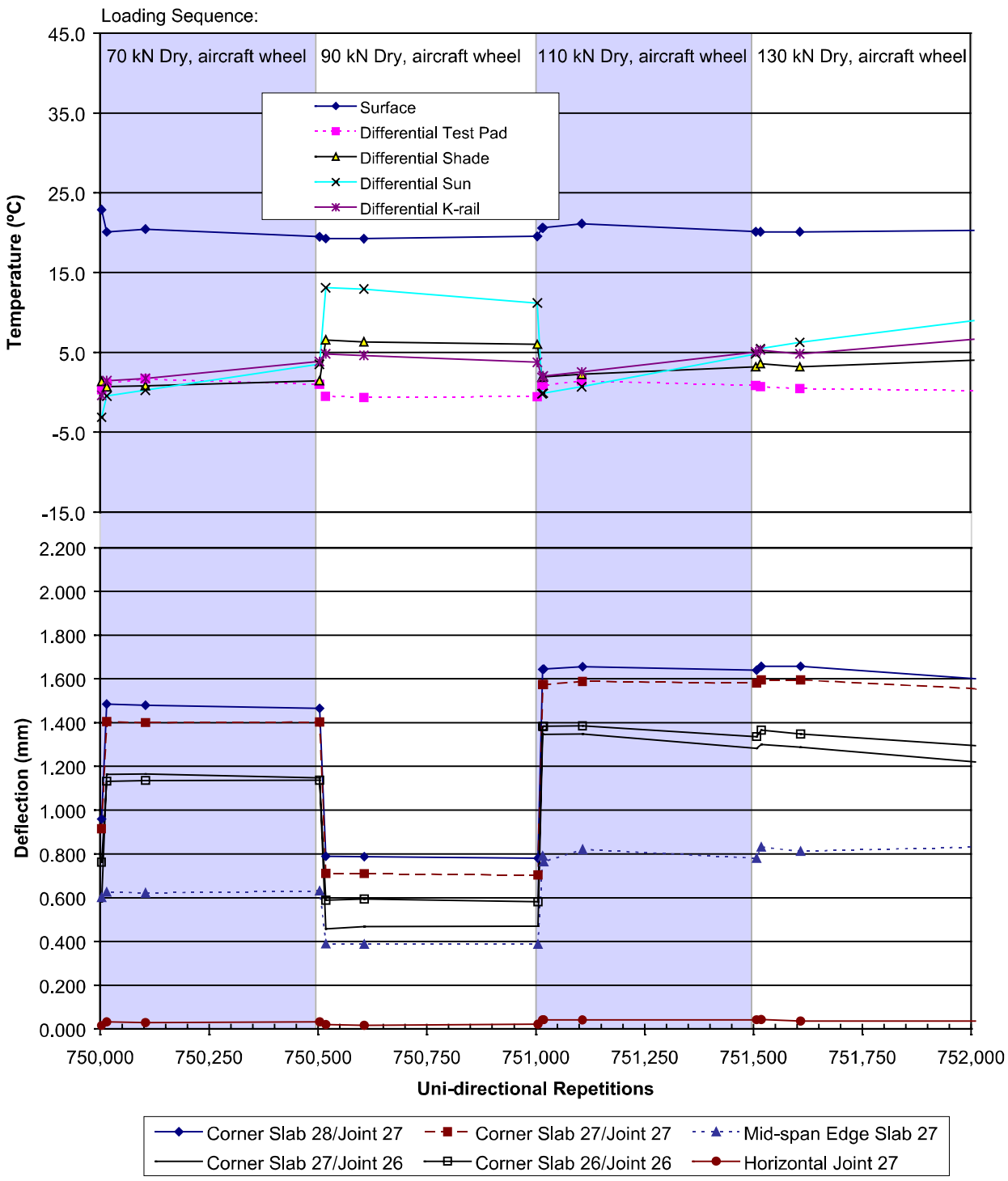

Figure 39. Plot of JDMD deflections and temperature versus load repetitions; 90-, 110-, 130-, and 150-kN test loads; Test 536FD.

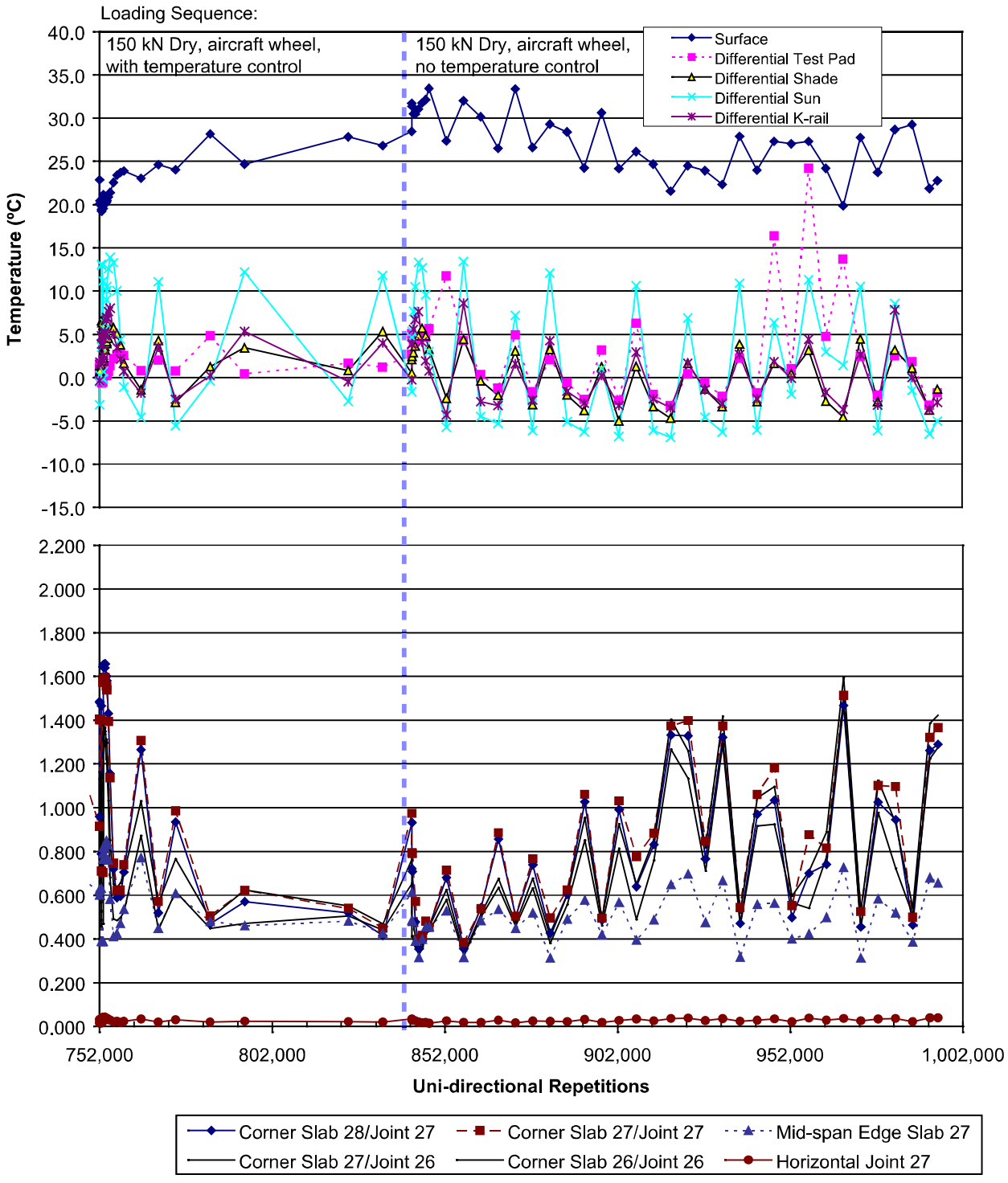

Figure 40. Plot of JDMD deflections and temperature versus load repetitions, 150-kN test load, Test 536FD.

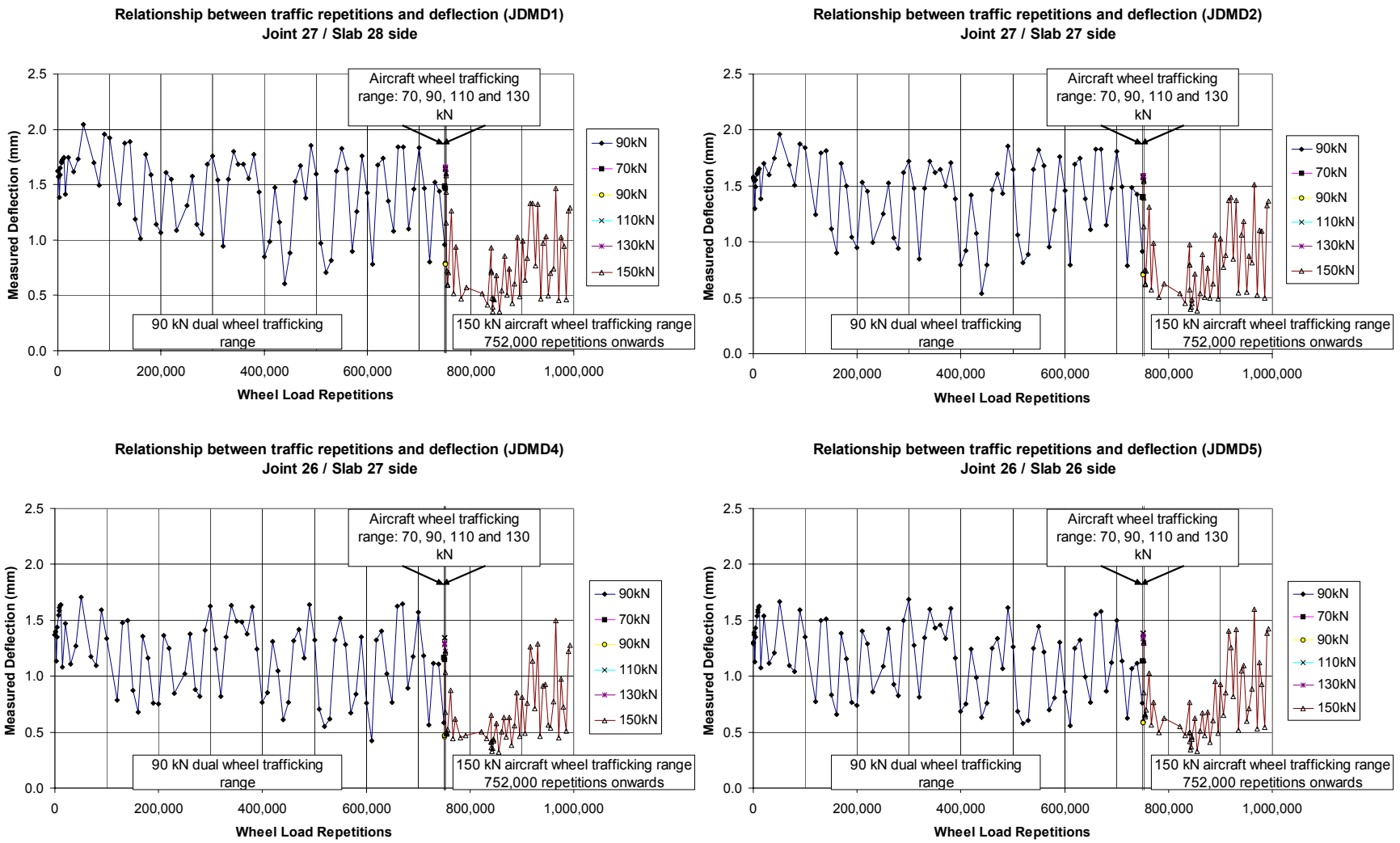

Figure 41. Joint deflections and the effect of wheel load repetitions, Test 536FD.

The overall behavior is similar for all JDMDs. The spread between consecutive peak and trough values during the first 750,000 repetitions (with 90-kN dual wheel load) is largely in the range 0.5 to 1 mm. This is extremely high and clearly indicates that the slab is not fully supported. This trend continues throughout the whole trafficking history, though variability of deflections decreases at higher repetitions.

Generally, deflections at Joint 27 (during approximately the first 750,000 repetitions) are significantly higher than those at Joint 26. Table 17 compares the descriptive statistics for deflections at the four corner joint JDMDs.

Table 17 JDMD Deflections to 750,000 repetitions, 90-kN Load, Test 536FD

	Deflection, mm			
	Corner, Joint 27		**Corner, Joint 26**	
	Slab 28	**Slab 27**	**Slab 27**	**Slab 26**
	JDMD 1	**JDMD 2**	**JDMD 4**	**JDMD 5**
Mean	1.462	1.423	1.190	1.174
Standard Deviation	0.337	0.332	0.332	0.318
Maximum	2.047	1.964	1.707	1.687
Mininum	0.605	0.539	0.425	0.558
n	85	85	85	85

The statistics in Table 17 show that deflections on each side of a joint are very similar (this observation is examined in Chapter 4.5.4 in terms of Load Transfer Efficiency). Average and maximum deflections at Joint 27 are approximately 0.25 to 0.3 mm higher than at Joint 26. Minimum deflections are generally similar. This is an expected result if these values represent more fully supported conditions for all slabs.

Within the wide scatter of results, Figure 41 provides a clear pattern of slab response under accelerated traffic loading. At each joint the deflections start relatively high, increasing

slightly during 50,000 or so repetitions, and subsequently dropping slightly from about 150,000 repetitions and staying reasonably consistent to just over 700,000 repetitions.

Statistics for deflections are summarized in Table 18.

Table 18 Deflections After 500 Repetitions of Various Aircraft Wheel Loads, Test 536FD)

		Deflection, mm			
		Corner, Joint 27		Corner, Joint 26	
		Slab 28	Slab 27	Slab 27	Slab 26
		JDMD 1	JDMD 2	JDMD 4	JDMD 5
70-kN aircraft wheel, (nominally 750,000–750,500 repetitions) n = 3	Mean	1.477	1.403	1.159	1.135
	Standard Deviation	0.008	0.002	0.008	0.002
	Maximum	1.486	1.405	1.166	1.137
	Minimum	1.466	1.400	1.148	1.133
90-kN aircraft wheel (nominally 750,500–751,000 repetitions) n = 3	Mean	0.786	0.707	0.464	0.587
	Standard Deviation	0.004	0.004	0.006	0.005
	Maximum	0.789	0.710	0.469	0.593
	Minimum	0.780	0.702	0.456	0.581
110-kN aircraft wheel (nominally 751,000–751,500 repetitions) n = 3	Mean	1.646	1.579	1.331	1.372
	Standard Deviation	0.006	0.006	0.028	0.020
	Maximum	1.656	1.589	1.347	1.385
	Minimum	1.640	1.574	1.283	1.337
130-kN aircraft wheel (nominally 751,500–752,000 repetitions) n = 3	Mean	1.639	1.582	1.270	1.336
	Standard Deviation	0.027	0.019	0.035	0.030
	Maximum	1.658	1.595	1.300	1.366
	Minimum	1.601	1.555	1.220	1.295

Subsequent loading with the aircraft wheel at 150 kN produced a distinct drop in deflections within the first 1,000 repetitions or so. Deflections fell from typically 1 to 1.5 mm to around 0.5 mm in each case (Figure 41). The variation in deflection also dropped significantly, especially until about 840,000 repetitions at which point the temperature control was stopped and the test was continued with exposure to ambient temperature fluctuation. This suggests that loading with the 150-kN aircraft wheel (a single wheel with higher tire pressure than normal

road traffic) caused significant deterioration of the slabs even though no visible cracking was evident.

Intriguingly, the minimum deflections, which dropped in every case to between 0.4 and 0.5 mm by 850,000 repetitions (the transition from controlled to ambient temperature), seemed to increase slightly to closer to 0.5 mm for the remainder of the test. Together with the greater variation in deflection values during the final 150,000 repetitions (at ambient temperature), it would seem that while distinctly deteriorated compared with the previous condition, the slabs retained integrity (no visible cracks). It is not possible to estimate how much more trafficking could have been applied before visible cracking would have occurred. It is clear that the test slab performed very well under extreme traffic loadings.

Figure 42 shows corresponding results for the mid-span deflection of Slab 27 and the horizontal joint movement at Joint 27. Note that the mid-span deflection scale is the same as for the joint deflections, while the horizontal deflection movement scale is only 1/50. The overall responses of both show similar characteristics to the joint deflections and is discussed in greater detail.

Mean mid-span deflections in the range of 0.7 to 0.8 mm (up to 750,000 repetitions) represent approximately 50 percent of the Joint 27 corner deflections and 65 percent of the Joint 26 corner deflections. From 752,000 repetitions (with the application of the 150-kN aircraft wheel load), the deflections settle to an average of approximately 0.5 mm with minimum values of 0.3 to 0.4 mm.

The horizontal movement at Joint 27 is roughly 2 to 3 percent of the corner deflections at Joint 27 throughout the test, averaging 0.029 mm during the first 750,000 repetitions (90-kN dual wheel load) and averaging 0.027 mm over the final 240,000 repetitions (150-kN aircraft wheel).

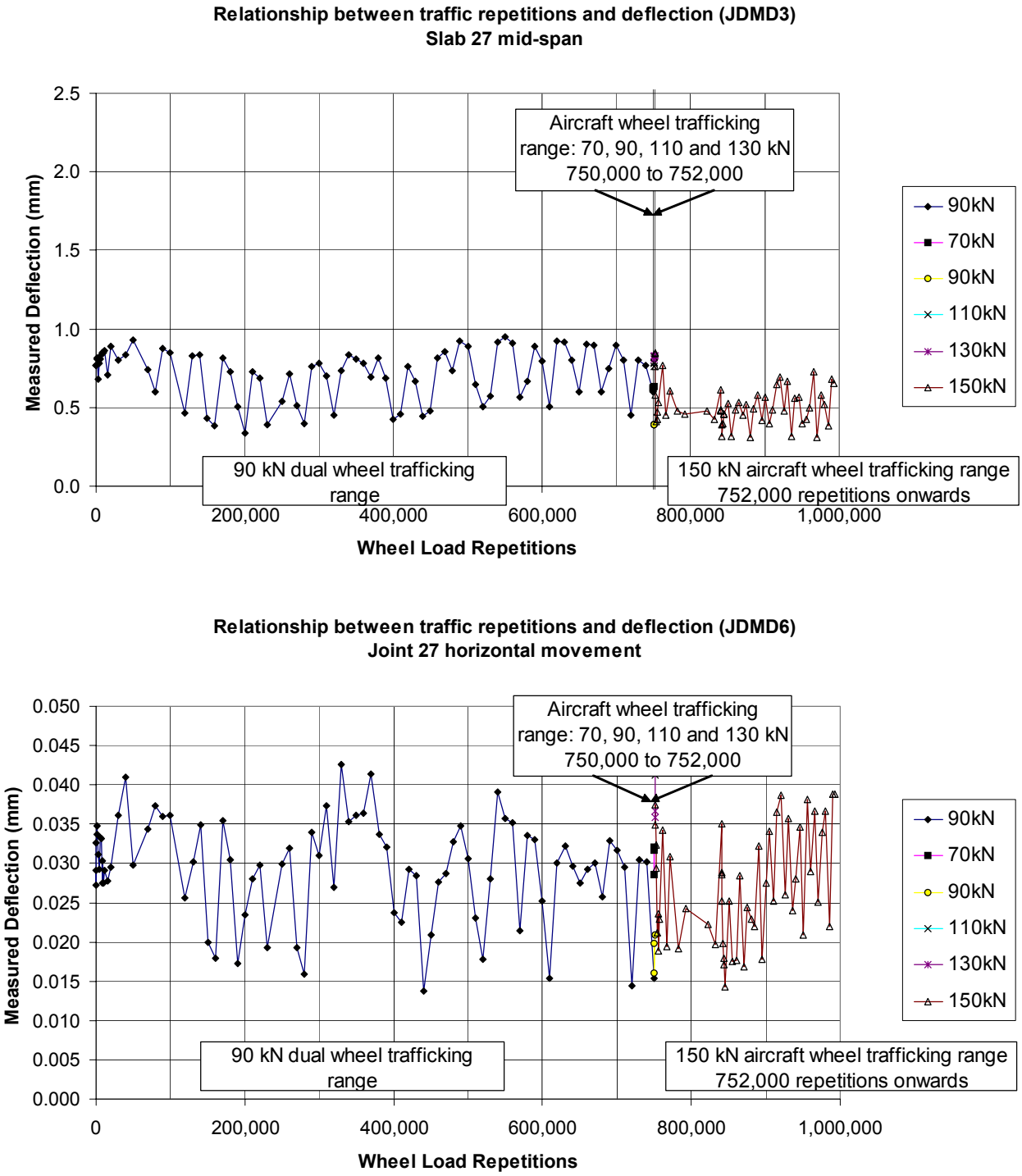

Figure 42. Effect of wheel load repetitions on midspan and horizontal deflections, Test 536FD.

4.5.2.2 Elastic deflections and temperature

As discussed in Chapter 4.6.2.1, all the JDMD deflection results have a "saw-tooth" pattern that suggests factors other than loading are affected the observed behavior. While long-term seasonal variations that could affect the pavement structural responses may be expected to have some influence (particularly moisture and temperature conditions), it is evident that these short-term variations are more likely attributable to daily temperature extremes and variation, as well as temperature differentials (from slab top to bottom).

As discussed earlier, the lack of deflection data sets taken at comparable loads precludes direct comparison. Nevertheless, differences in the deflection response characteristics are marked enough to provide some insight.

Figure 43 shows the deflection responses for JDMDs 1, 2, 4, and 5 plotted against measured slab surface temperature. Even allowing for the differences in applied loads and the influence of trafficking history, it is clear that temperature had a significant effect on pavement deflections. Bearing in mind that the most of the test was conducted with temperatures controlled around 20ºC, it seems that even a variation of two or three degrees led to significant differences in deflection. As previously observed, an inverse relationship of deflection with temperatures exists (i.e., higher deflections at lower temperatures). This trend is probably due to differential shrinkage and slab curling.

Table 19 summarizes the temperature conditions throughout the test shown graphically in Figures 38–40.

For most of the test, through 752,000 repetitions, the temperature was controlled to maintain the desired 20ºC test temperature. Wide temperature fluctuation in this phase of the test occurred during the first 20,000 repetitions when the most frequent readings were taken over a

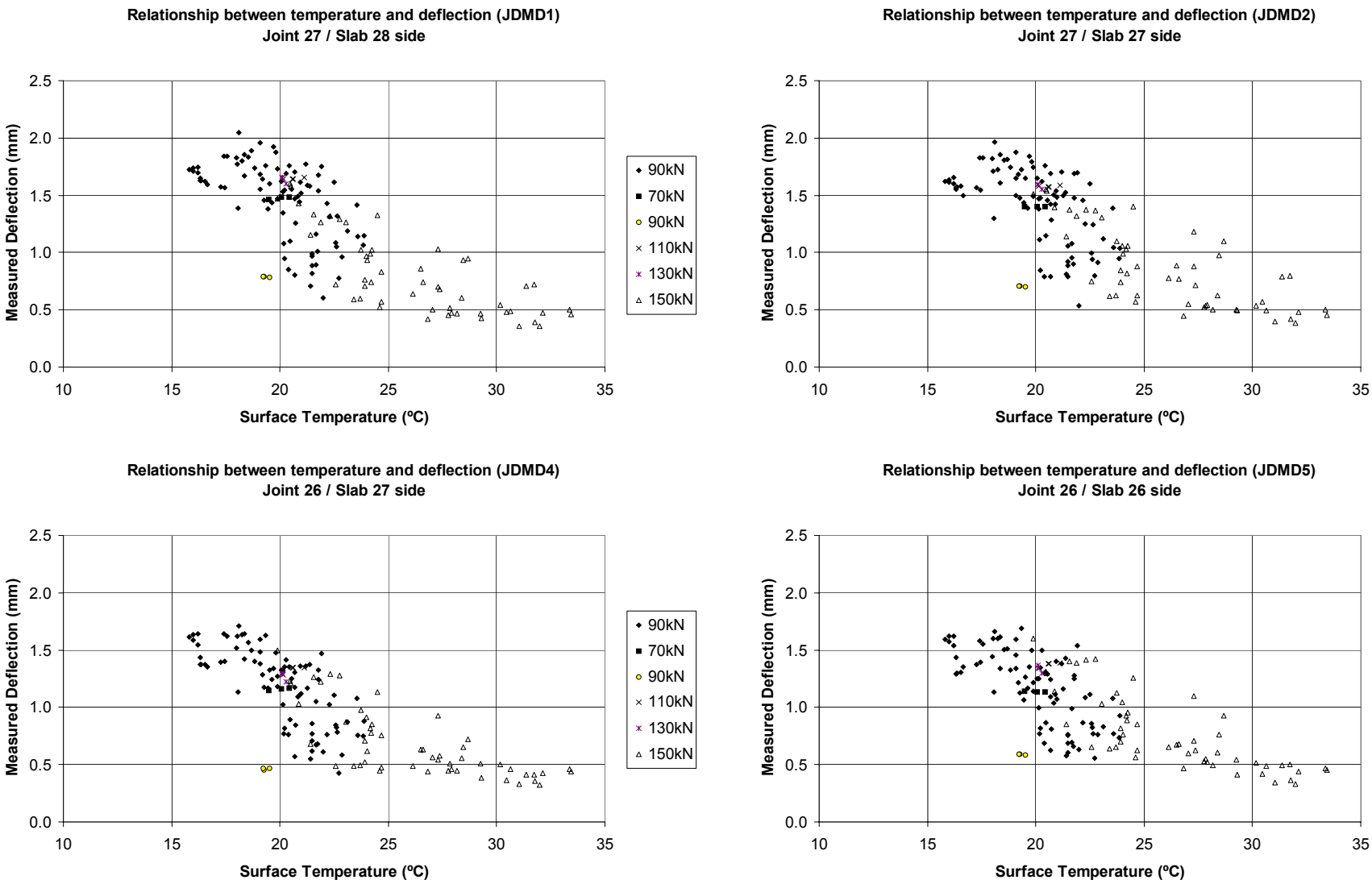

Figure 43. Effect of temperature on joint deflections, Test 536FD.

Table 19 Test Temperature Conditions, Test 536FD

		Temperature (ºC)	
		Surface	Differential (slab top–slab bottom)
90-kN dual wheel load (nominally to 750,000 repetitions)	Mean	20.0	0.1
	Standard Deviation	2.1	1.4
	Maximum	23.9	9.7
	Minimum	15.8	(1.2)
70-kN aircraft wheel (nominally 750,000–750,500 repetitions)	Mean	20.0	1.3
	Standard Deviation	0.4	0.3
	Maximum	20.4	1.7
	Minimum	19.5	1.0
90-kN aircraft wheel (nominally 750,500–751,000 repetitions)	Mean	19.3	(0.6)
	Standard Deviation	0.1	0.1
	Maximum	19.5	(0.5)
	Minimum	19.2	(0.6)
110-kN aircraft wheel (nominally 751,000–751,500 repetitions)	Mean	20.6	1.0
	Standard Deviation	0.4	0.2
	Maximum	21.1	1.4
	Minimum	20.1	0.9
130-kN aircraft wheel (nominally 751,500–752,000 repetitions)	Mean	20.2	0.5
	Standard Deviation	0.1	0.2
	Maximum	20.3	0.7
	Minimum	20.1	0.2
150-kN aircraft wheel (nominally 752,000–840,000 repetitions)	Mean	24.0	1.7
	Standard Deviation	2.6	1.2
	Maximum	28.5	4.8
	Minimum	20.5	0.3
150-kN aircraft wheel (ambient temp.) (nominally 840,000–993,000 repetitions)	Mean	27.3	3.0
	Standard Deviation	3.6	5.7
	Maximum	33.4	24.2
	Minimum	19.9	(3.2)

three day period. During this period manual interventions to ensure instrumentation and equipment functionality were frequent.

During the final phase of testing with temperature control, under the 150-kN aircraft wheel, the temperature increased to approximately 25ºC. This was followed by testing under ambient conditions that varied from roughly 20 to 33 ºC with an average of just over 27°C.

Figure 44 shows the Slab 27 mid-span deflections and Joint 27 horizontal movement in relation to surface temperature. The influence of surface temperature is still evident, although less distinct than for the joint corner deflections shown in Figure 43. Correlation is less clear because of the lower deflection values.

In order to give a more meaningful insight, Figure 45 shows the data for JDMDs 2 and 4 (at each end of Slab 27, as previously shown in Figure 43) in which the data points are connected chronologically for both the 90-kN dual wheel load phase (to 750,000 repetitions) and the 150-kN aircraft wheel phase (752,000 to 993,000 repetitions).

These figures show that a variation of only 2 to 3 degrees in surface temperature may cause a difference of 0.5 mm in deflection for the particular conditions evident during the initial 750,000 repetition trafficking period, (before the apparent deterioration of the slab and while temperatures were well controlled within the 15–25 ºC range).

Numerous factors influence this response including the temperature regime within the concrete slab. The most interesting observation arises from the nature of the observed response: both corner and edge deflections *decrease* with increase in surface temperature. This implies that the slabs were curled up at least during the majority of the testing and almost certainly at temperatures below 25ºC. Thus, they were not fully and evenly supported, which is a common practical and analytical assumption when evaluating concrete pavements.

For future HVS testing of these types of pavements it would be extremely useful to conduct a comprehensive deflection survey over a selection of the test slabs prior to HVS testing. The survey should include at least corner and mid-span deflections for the whole slab (four measurements for each) and a central slab deflection. Surface temperature measurement must be

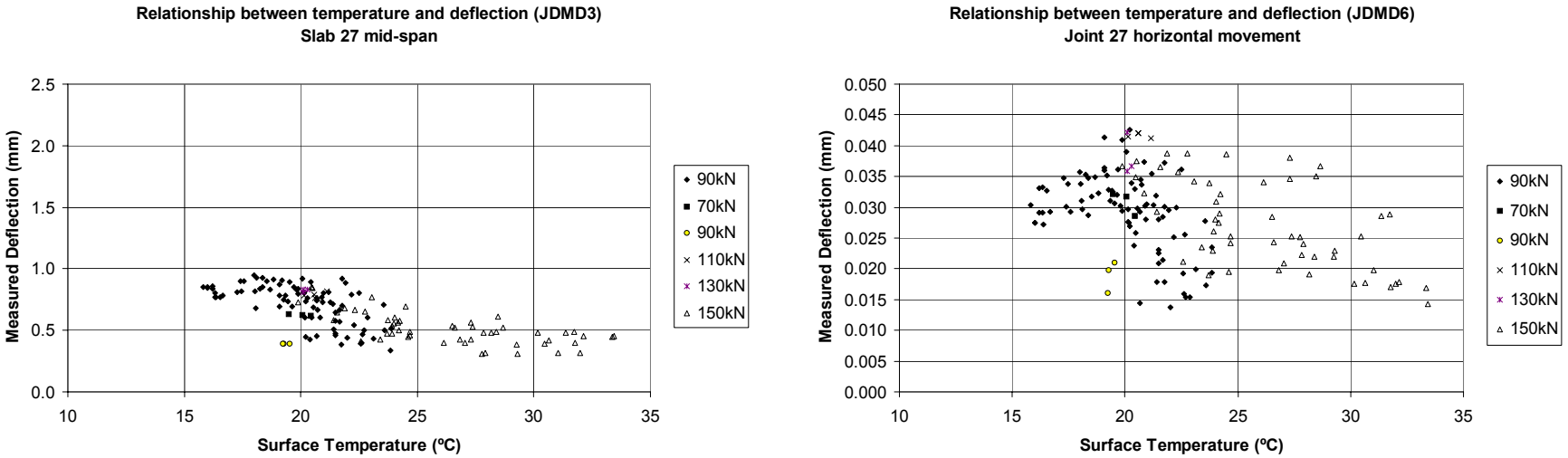

Figure 44. Effect of temperature on midspan and horizontal deflections, Test 536FD.

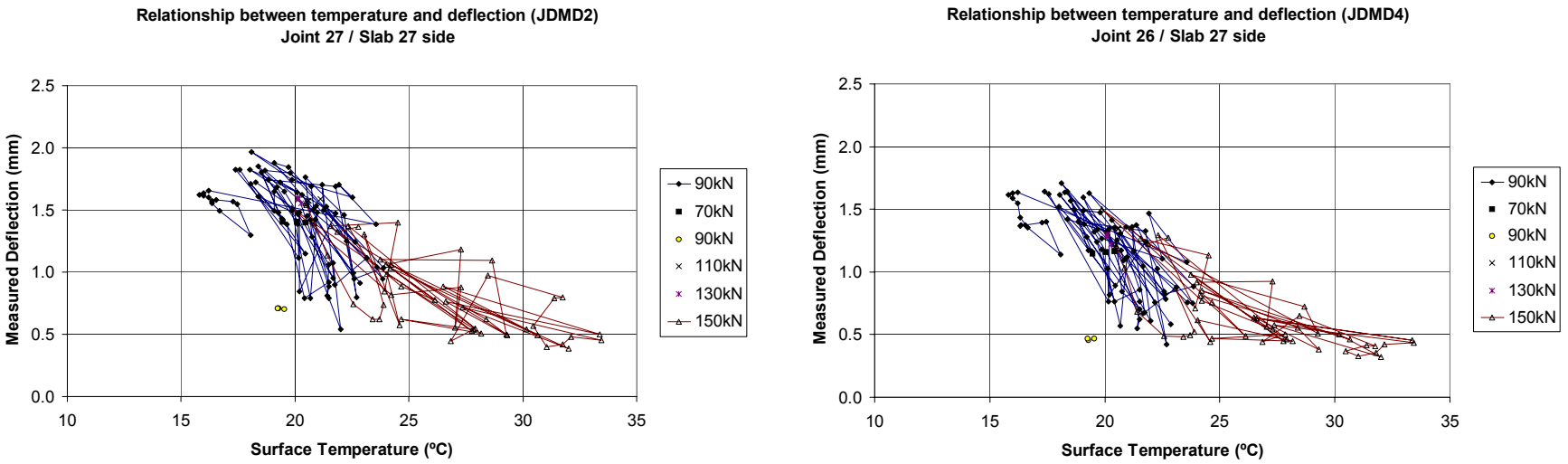

Figure 45. Relationship between temperature and joint deflection, Test 536FD.

taken during deflection testing and the survey should take place over at least three or four days with measurements taken at various times (and therefore temperatures) each day.

This pre-HVS test survey would establish baseline conditions for the slab and provide an indication of its current state. In line with earlier discussion, a standard (probably 80-kN) axle load should be used and subsequent HVS monitoring should also then include the same load for deflection testing. This would provide a very good basis on which to make subsequent performance evaluations.

4.5.3 Multi-Depth Deflectometer (MDD) Results

4.5.3.1 Elastic Deflections and Trafficking

A single MDD was installed in Slab 27 midway along its length and in the center of the HVS wheelpath, adjacent to the mid-span JDMD 3 (Figure 7). MDD modules were installed at depths of 100 mm (mid-depth in the concrete pavement slab), 300 mm, 450 mm, and 650 mm (in the unbound supporting layers beneath the slab).

Figure 46 shows both the elastic deflections as measured and the deflection differences between successive MDD modules. Note that the general range of deflections measured by the module located mid-depth in the slab (0.5 to 1 mm) is similar to that measured at the adjacent mid-span edge by JDMD 3 (see Figure 42). Likewise, the "saw-tooth" temperature-influenced pattern previously discussed is evident in Figure 46.

Also note that the major part of the total deflection occurs between the slab and the module at 300 mm depth. The deflection data differences highlight this. They show that just over 0.5 mm of the average total deflection of 0.78 mm occurs between the slab module and the 300

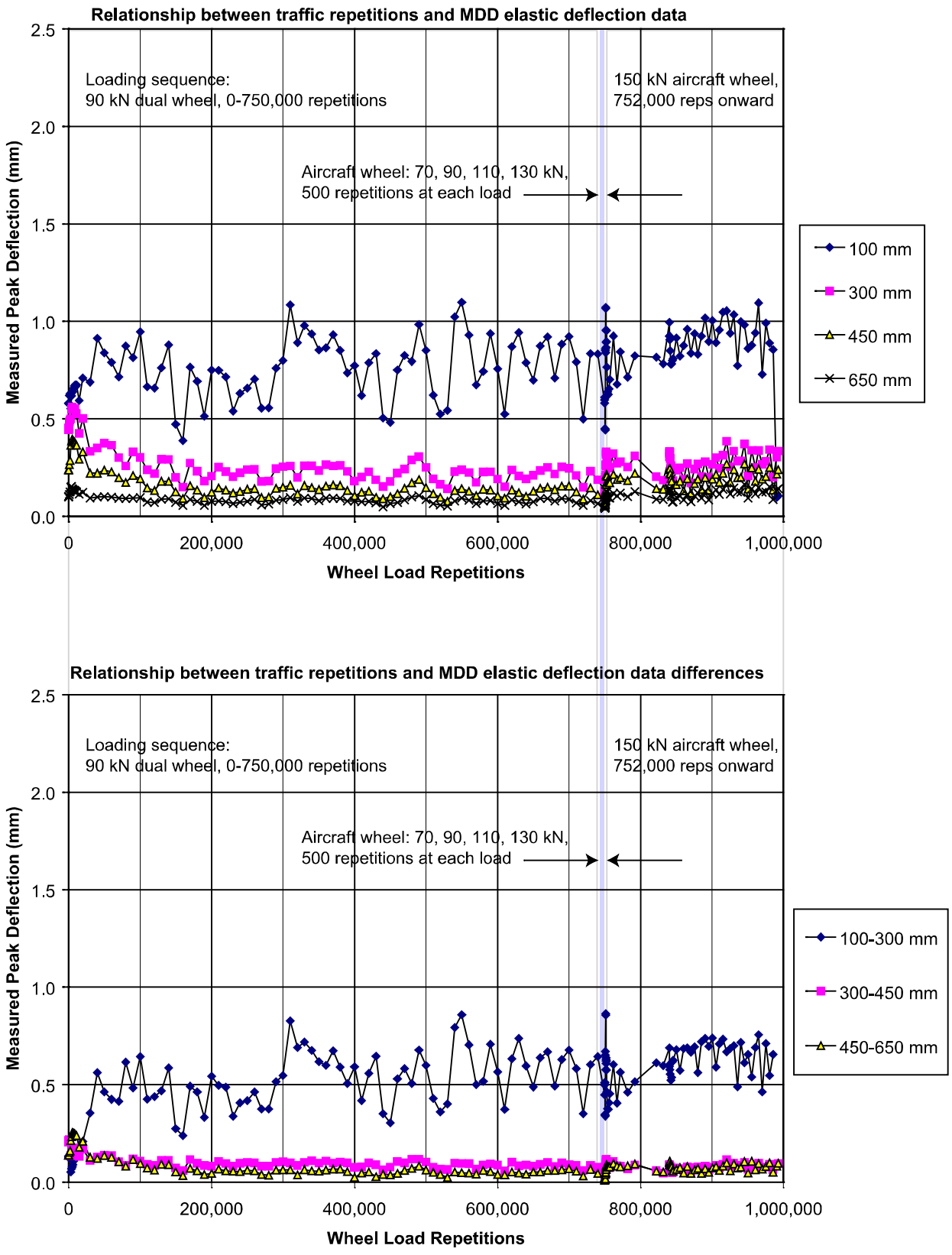

Figure 46. Effect of wheel load repetitions on MDD deflections, Test 536FD.

mm module while just under 0.1 and 0.08 mm occurs between 300 to 450 mm and 450 to 650 mm, respectively.

This supports the earlier observation about the upward curling of the slab through MDD level 2 (placed at a depth of 300 mm, which includes approximately 100 mm of the subbase material under the concrete slab).

In contrast to the JDMD 3 mid-span deflection measurement (Figure 42), the MDD slab deflection measurement (module at nominal depth 100 mm) shows a marginal increase in deflection for the 150-kN aircraft wheel traffic loading from 752,000 repetitions, although with the same reduction in variation. This is not considered as significant in the context of this test (given the previously mentioned difficulties of comparing deflections) but probably is attributable to positioning of the load wheel in relation to the measuring device.

4.5.3.2 Permanent Deformation and Trafficking

Figure 47 presents the permanent deformations recorded at the four MDD modules and shows temperature history.

The slab module shows the same temperature effect as noted for the elastic deflection data, confirming the MDD module placement within the slab and the influence of temperature on the "permanent" deformation recorded there. Because it is unlikely for permanent deformation of the underlying layers (modules 300, 450 and 650 mm) to really decrease, Figure 47 shows initial traffic induced consolidation of the pavement layers above 650 mm during the first approximately 20,000 repetitions.

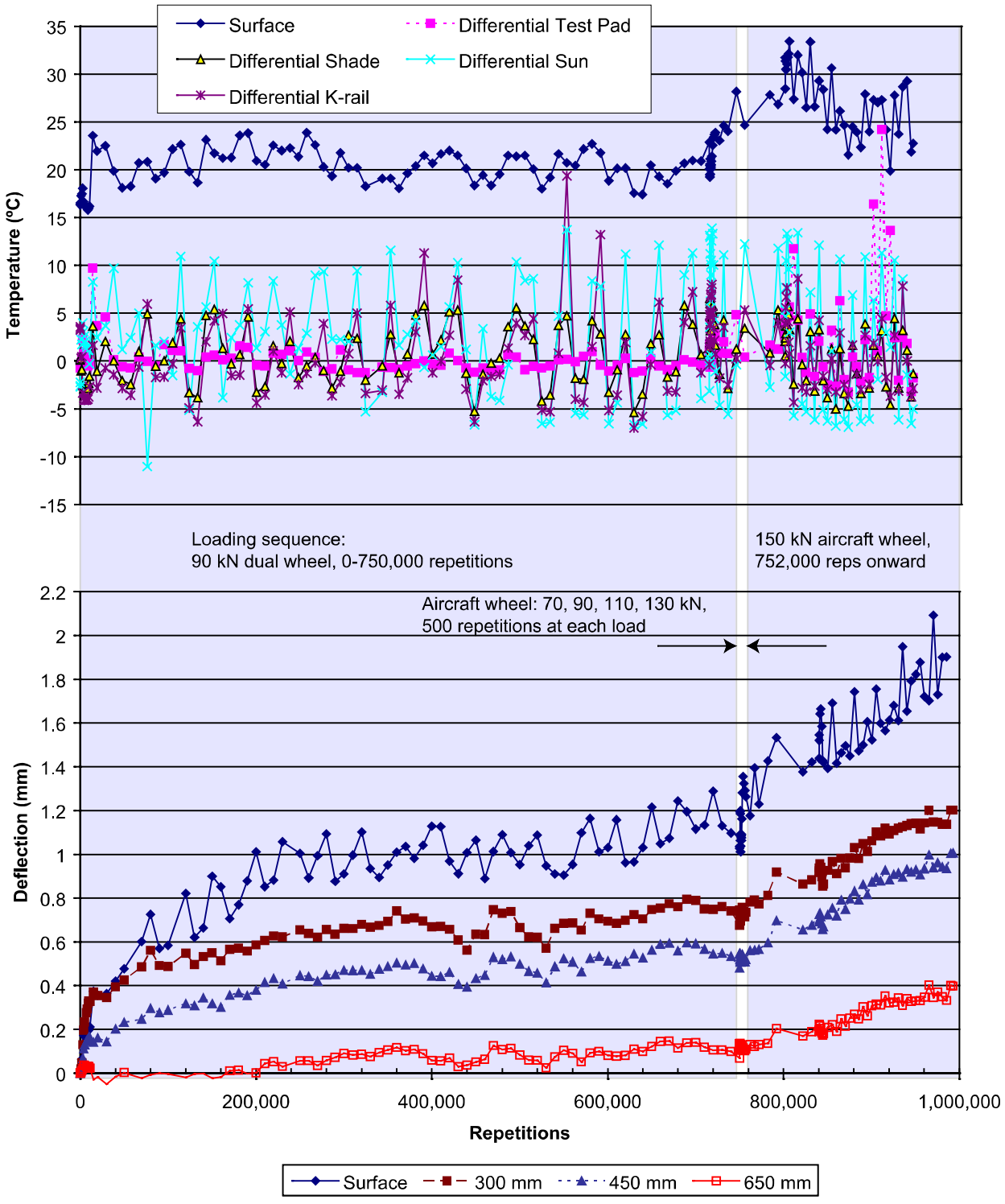

Figure 47. Plot of MDD 10 permanent deformation and temperature versus load repetitions, Test 536FD.

From about 50,000 repetitions, the permanent deformation at all levels gradually increases, as would be expected under the heavy channelized wheel trafficking. The permanent deformation kicks up again markedly with the change to the 150-kN aircraft wheel and then tends to flatten off, showing the transmission of the heavier load through to the supporting layers and another phase of consolidation.

Figure 48 shows the difference in permanent deformation between modules. This shows that approximately 0.2 mm deformation (consolidation) occurred over the first 20,000 or so repetitions between both the 300 to 450 mm and 450 to 650 mm depths. While the 300 to 450 mm depth then showed virtually no change, remaining at 0.2 mm, the deeper 450 to 650 mm layer consolidated further to almost 0.4 mm during the first 200,000 repetitions then at a lower rate to 750,000 repetitions reaching just over 0.4 mm. With the application of the heavier 150-kN aircraft wheel load (from 752,000 repetitions) the layer further consolidated, reaching 0.6 mm at the end of the test and appearing to have additional capacity to densify.

The slab mid-depth to 300 mm layer deforms about 0.2 mm up to 200,000 repetitions, then to approximately 0.4 mm by 750,000 repetitions. It then also shows slight additional consolidation with the application of the 150-kN aircraft wheel load through to the end of the test, also reaching some 0.6 mm at that stage.

These results suggest that, while the 300 to 450 mm layer showed initial consolidation, it attained its equilibrium density quickly and subsequent permanent deformation occurred in both the over- and underlying layers.

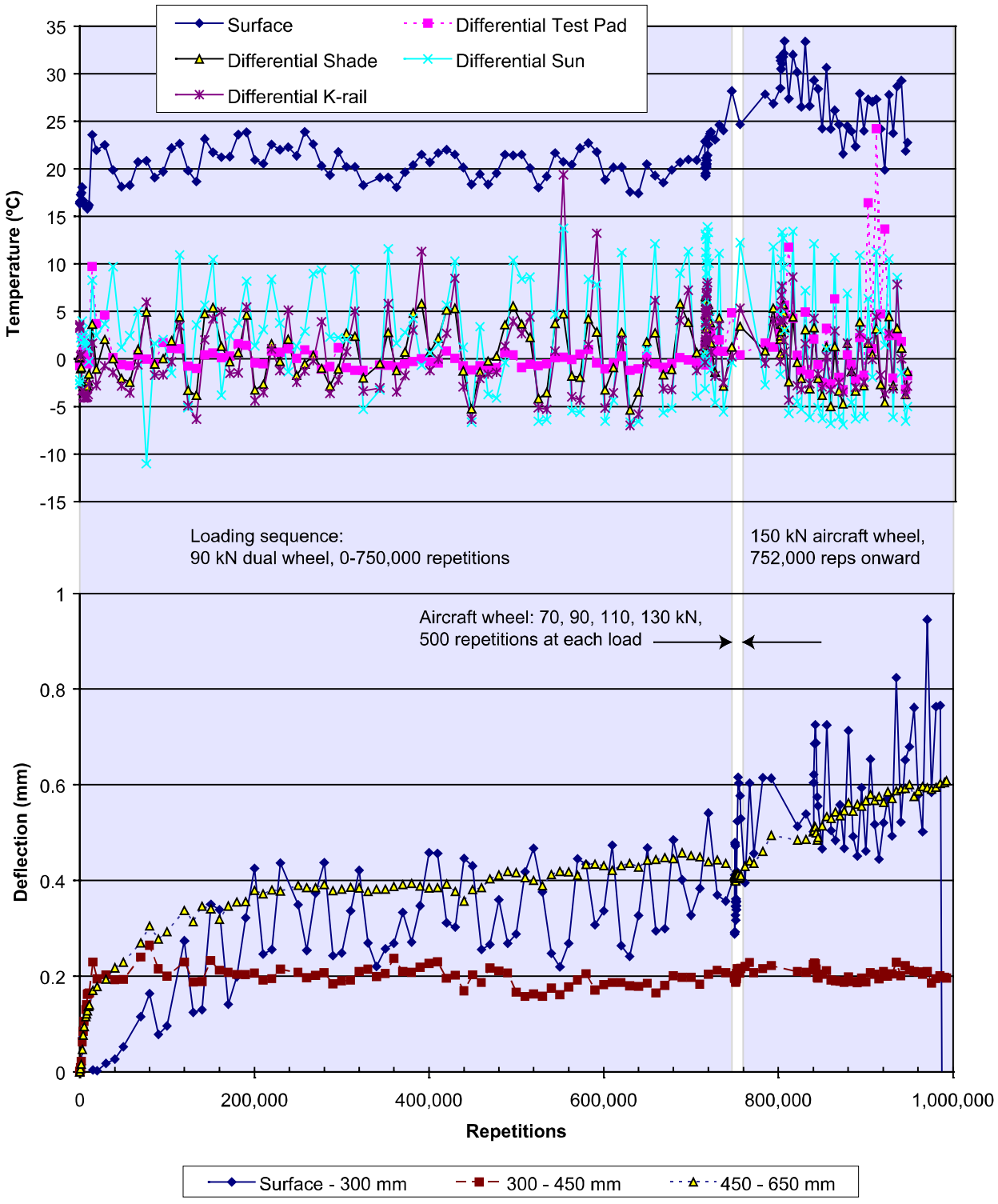

Figure 48. Plot of MDD permanent deformation differentials and temperature versus load repetitions, Test 536FD.

4.5.4 Joint Load Transfer Efficiency (LTE)

Figure 49 shows the peak deflections on each side of Joints 26 and 27 as previously shown plotted against repetitions (Figure 41) and surface temperatures (Figure 43). In this case, the deflections are those measured on each side of the particular joint at the same repetitions and applied test load. The data are grouped in terms of traffic load/test load as described previously, so the predominant data sets are those for the 90-kN dual wheel load trafficking phase (to 750,000 repetitions) and for the 150-kN aircraft wheel trafficking phase (from 752,000 repetitions to the end of test).

Note that over a significant range of deflections, the data points lie close to the line of equality for both joints. This pattern suggests LTEs close to 100 percent in general. Further scrutiny shows that at each joint, the deflections for the 90-kN dual wheel loading phase tend to be slightly above the line of equality and those for the 150-kN aircraft wheel loading phase tend to be below the line of equality.

As discussed previously, the deflection and MDD data confirm that there was a distinct deterioration with the application of this heaviest wheel load and these data suggest some minor deterioration in the load transfer. From Figure 49, it appears that at Joint 27 the Slab 27 deflections were slightly higher laterally, while at Joint 26 the Slab 27 deflections were slightly lower than those on the adjacent slab.

Figure 50 gives deflections at each end of Slab 27 (Joint 26 and Joint 27) which shows that on the slab itself, deflections on the Joint 26 side were almost always lower than those on the Joint 27 side. Thus it is evident that some difference existed in support condition (which includes underlying layers and the joint load transfer) of Slab 27.

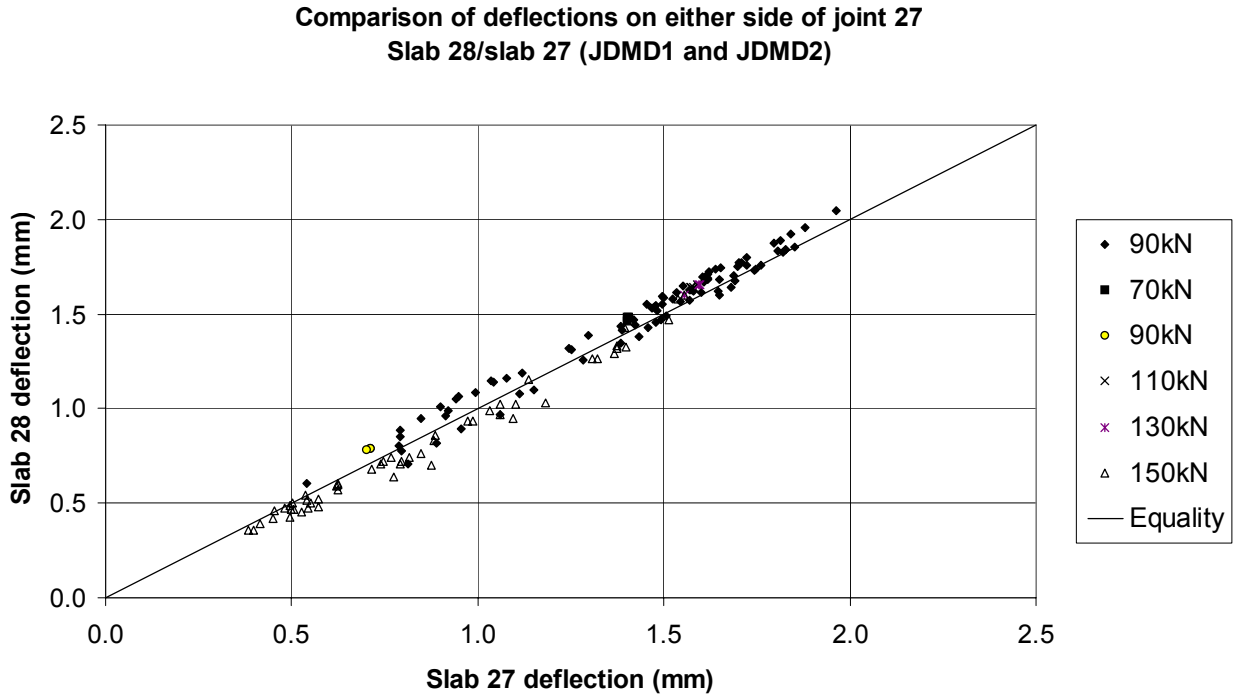

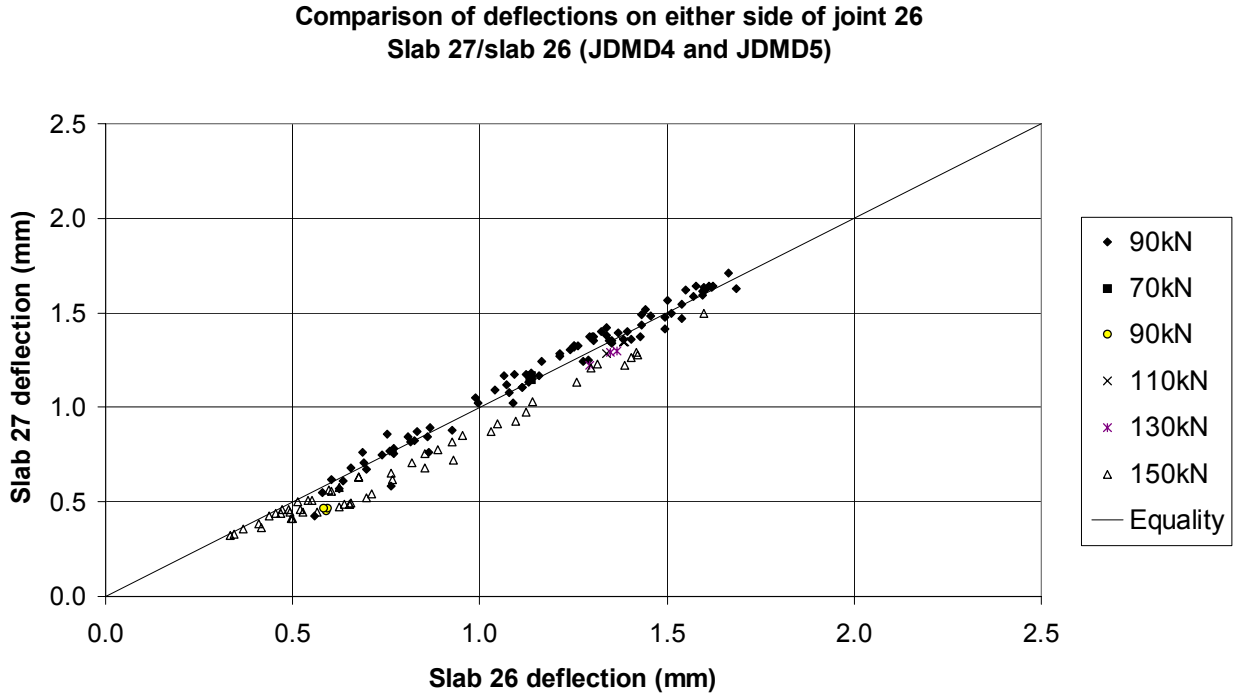

Figure 49. Joint load transfer efficiency at Joints 26 and 27, Test 536FD.

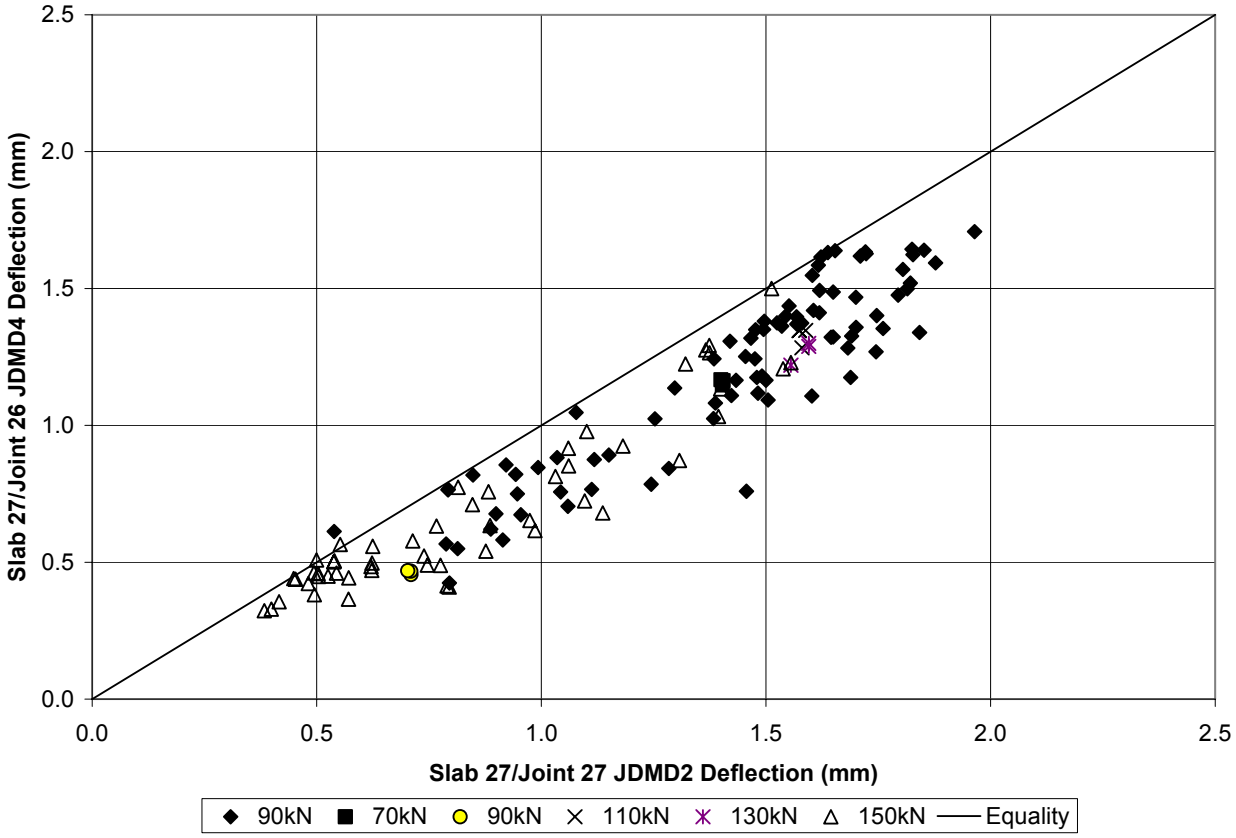

Figure 50. Comparison of joint deflections on either side of Slab 27 (Joints 26 and 27), Test 536FD.

Since the underlying layer support should be uniform for practical purposes, it could therefore be conjectured that the lower deflections at the Joint 26 end of Slab 27 could be attributable to a greater support/resistance to deflection from the longer Slab 26 (5.81 m versus 3.62 m for Slab 28 providing support at Joint 27).

Figure 51 gives the calculated LTEs for both sides of each joint, together with the surface temperature and slab temperature differential. This confirms that the LTEs are generally close to unity (100 percent). Closer inspection shows that the LTEs for Joint 26 are generally slightly lower than those for Joint 27. Figure 52 highlights this, showing the LTEs for each adjacent slab against the corresponding LTEs for Slab 27 (i.e., at Joint 26 and Joint 27).

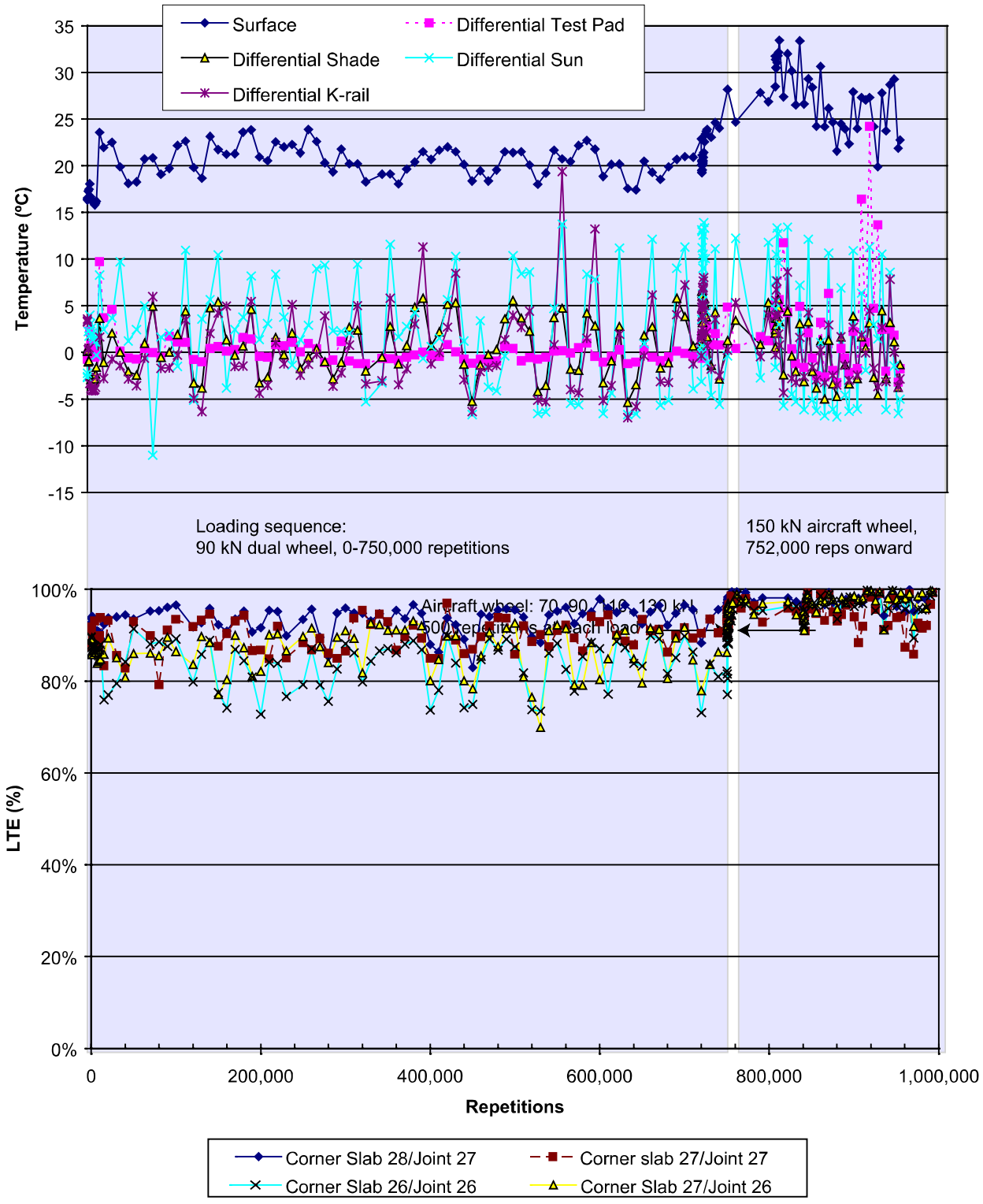

Figure 51. Plot of LTE and temperature versus load repetitions, Test 536FD.

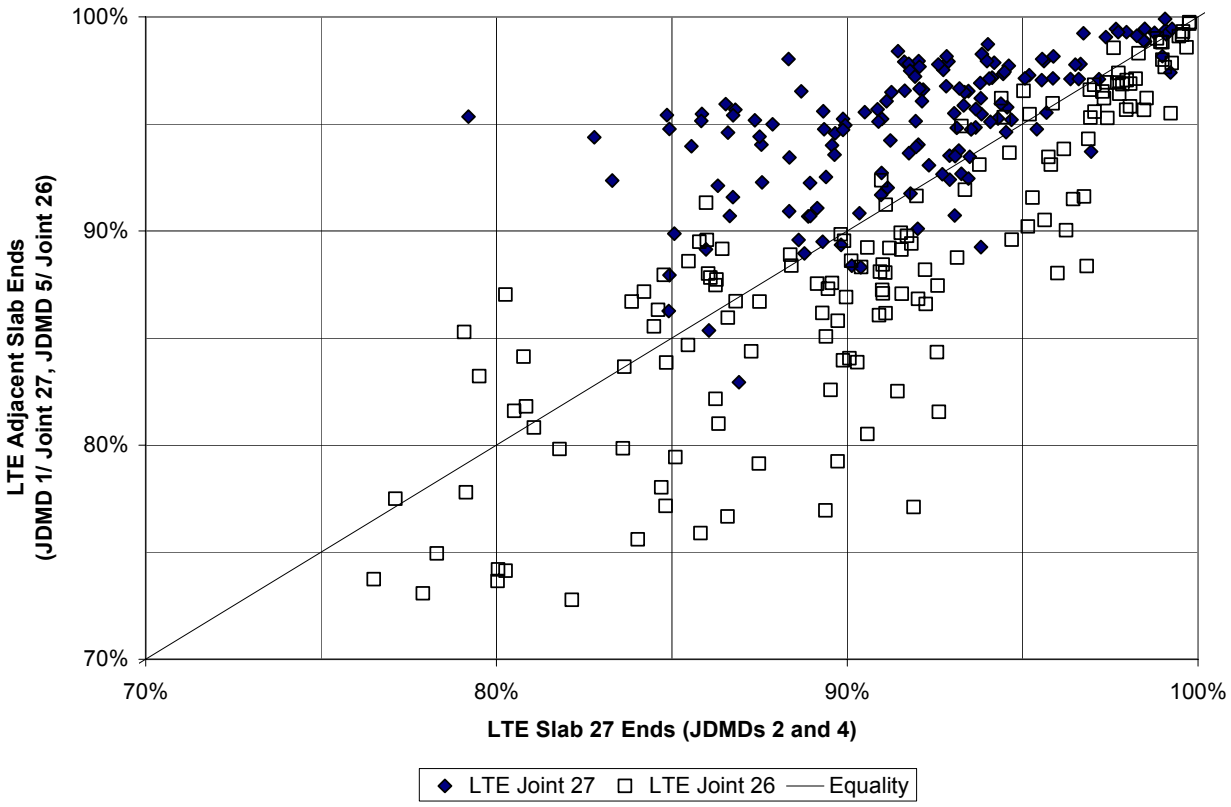

Figure 52. Joint load transfer efficiency at Joints 26 and 27, Test 536FD.

Figure 51 also shows that in each case, LTEs increase very close to unity after trafficking with the 150-kN aircraft wheel load. Since this has previously been identified as a phase in which distinct deterioration occurred, it clearly draws into question the definition and meaningfulness of the LTE as currently used as it would not be expected for LTEs to improve to virtually 100 percent.

The definition and calculation of LTE should therefore be reviewed. It seems that the present definition and calculation will return values of 100 percent if uniform deterioration takes place on each side of a given joint, implying similar changes in deflection responses, but not necessarily identifying joint deterioration per se.

4.6 Test 537FD

HVS Test 537FD was the second of the series of three HVS tests on the 200-mm PCC slabs with dowels and tied concrete shoulders. It was carried out in the period July 20 to August 19, 2000. The other two HVS tests on this section were 536FD and 538FD reported in Chapters 4.5 and 4.7. The main objective of this series of tests is similar to that of the previous test, as discussed in Chapter 4.5.

The fatigue behavior of the Fast Setting Hydraulic Cement Concrete (FSHCC) slabs in this series of three tests was monitored under bi-directional wheel loadings of mainly 90 kN and greater and in dry conditions (no water added).

Test 537FD was undertaken on Slabs 22, 23, and 24 such that the full length (3.94 m) of Slab 23 and some 2 m on each of the adjacent slabs, 22 and 24 was trafficked (Figure 8). The test was conducted under ambient temperature conditions.

Initially some 13,000 wheel load repetitions were applied with a 40-kN dual wheel, followed with just 500 repetitions at 70 kN, then a further 320,000 repetitions at 90 kN. An aircraft tire was then fitted and about 55,000 repetitions were applied at a load of 150 kN to the end of the test. A total of almost 400,000 channelized (i.e., no wander) wheel load repetitions were therefore applied in this test.

4.6.1 Visual Observations

Figure 53 shows the crack patterns as they developed during the test. Figure 54 presents a composite image of the test section after the completion of HVS trafficking. The observed cracking on Test 537FD is in contrast with Test 536FD, an ostensibly similar pavement which carried significantly more load without cracks being observed (discussed in Chapter 4.5). Note

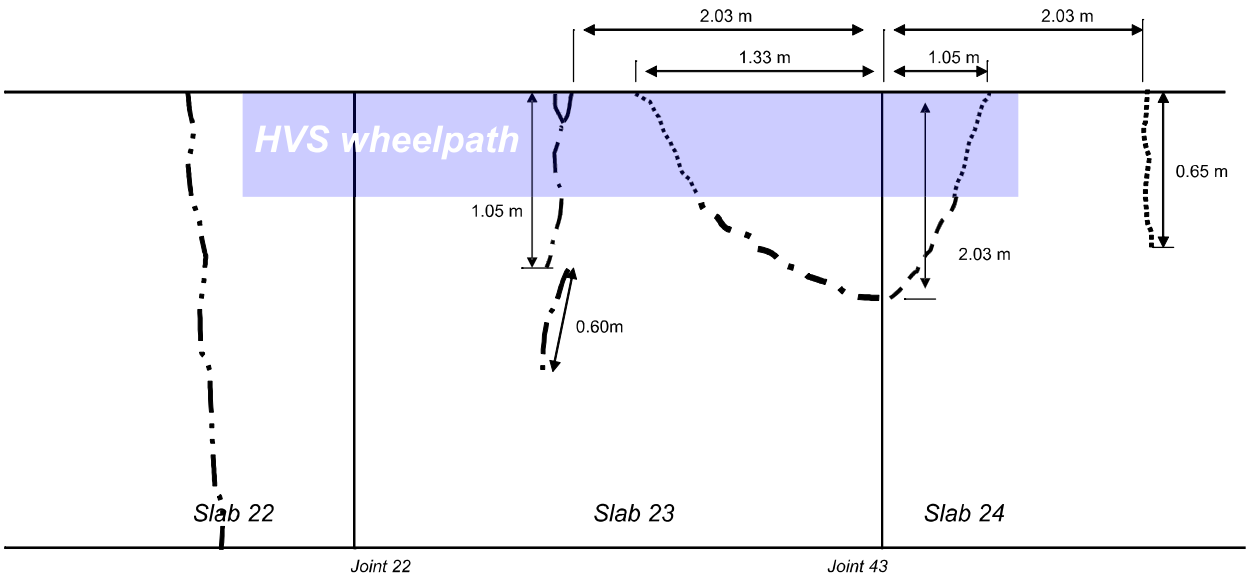

Loading Sequence:

40 kN dry	0–13,240 repetitions
70 kN dry	13,240–13,740 repetitions
90 kN dry	13,740–333,740 repetitions
150 kN dry aircraft wheel	333,740–388,746

Legend

Crack	Sequence	Slab
	0 reps (prior to test)	22
	43,740 reps	23
	73,740 reps	24
	83,740 reps	24
	193,740	23

Figure 53. Schematic of crack pattern, Test 537FD.

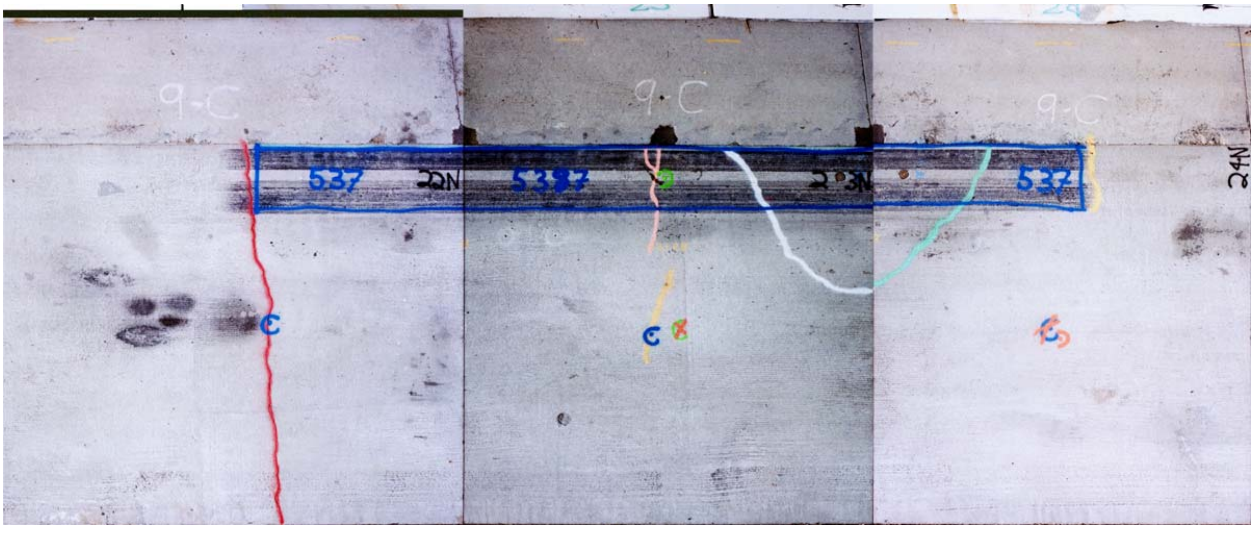

Figure 54. Composite image of Test 537FD showing cracks.

that Slab 22 had a transverse crack across its full width from the outset (approximately 2 m from Joint 22). This crack was just outside the trafficked area. This would give a marked reduction in possible slab support across the joint compared with Test 536FD.

The first HVS traffic-induced crack was observed after 43,740 repetitions, during the early part of the 90-kN dual wheel load test phase. This crack was effectively a mid-span transverse crack from the test section towards the slab center. Although not visibly connected, it is apparent that the two observed cracks must form part of the same discontinuity.

After an additional 30,000 load repetitions, corner cracks emanating from the test section were identified on both sides of Joint 23. The crack on Slab 24 side of the joint visibly propagated to the joint within the next 10,000 repetitions, completing the corner break. This rapid propagation could be due to a reduction in stiffness and support of the slab evidenced by the nominal mid-slab transverse crack that also started at about the same number of load repetitions, propagating from the slab edge about 650 mm towards the center. However, in the case of the main trafficked slab (Slab 23), which had the earlier and more extensive mid-span transverse crack, the corner crack was not visibly complete until a further 110,000 repetitions. Both cracks propagated to the same point on each side of the joint approximately 2 m in from the slab edge.

The final HVS trafficking-induced crack pattern can therefore be summarized as nominal mid-span transverse fractures of both Slabs 23 and 24 (Slab 22 was already transversely cracked prior to testing) and corresponding corner breaks on both slabs. Somewhat surprisingly, given the existing crack on Slab 22 and the anticipated loss of support across Joint 22, no corner breakage occurred during the test on Slab 22 at that joint. This would suggest that the support remained relatively good and better than that at Joint 23.

4.6.2 Joint Deflection Measuring Device (JDMD) Results

4.6.2.1 Elastic Deflections and Trafficking

Figure 55 gives the elastic deflection data for the test, also showing the test slab surface temperatures and the temperature differentials between slab top and bottom at four locations around the test area.

The recorded deflections were taken at the trafficking wheel load rather than at other selected wheel loads (normally including 40 kN as the equivalent standard axle load) so deflections cannot be compared directly. All the joint measurements fluctuate considerably and show a similar distinct "saw-tooth" variation in measured values as noted on Test 536FD (Chapter 4.5).

Figure 56 shows the deflections recorded by JDMDs 1, 2, 4, and 5 against trafficking history. These represent deflections recorded on either side of Joints 23 and 22 at each end of Slab 23.

Comparison of the JDMD pairs on each side of a joint (JDMDs 1 and 2, and 4 and 5) shows notably similar responses. However, it is also clear that the monitored responses at each joint differ.

For Joint 23, the deflections increase from about 0.5 mm during the first 25,000 or so repetitions to peak at just over 1.5 mm (90-kN test load). In each case, the deflections slightly and consistently decrease during the first 3,000 repetitions with the 40-kN wheel load, prior to the increase that continues through the short 70-kN load phase and the start of the 90-kN load phase.

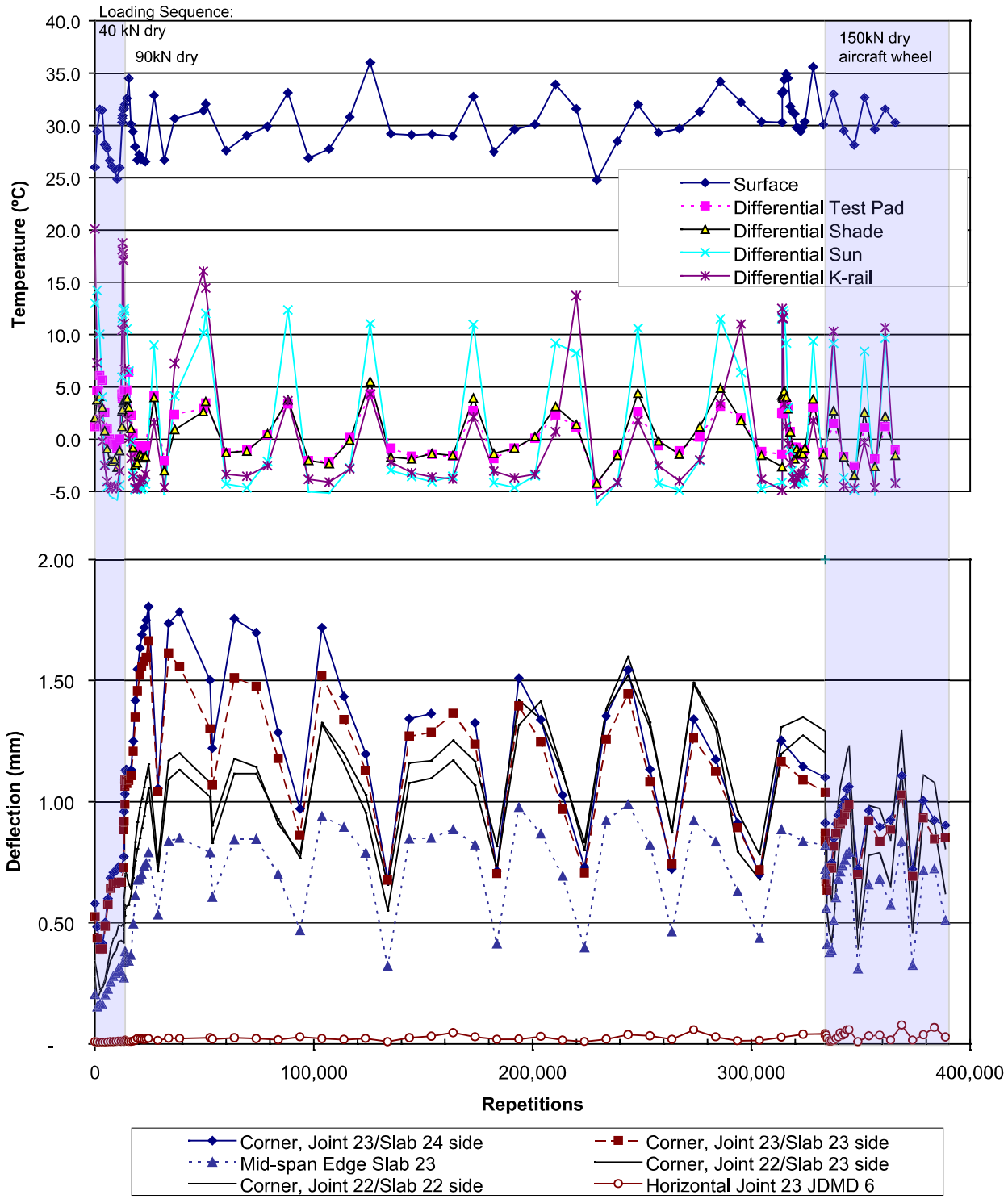

Figure 55. Plot of JDMD deflections and temperature versus load repetitions, Test 537FD.

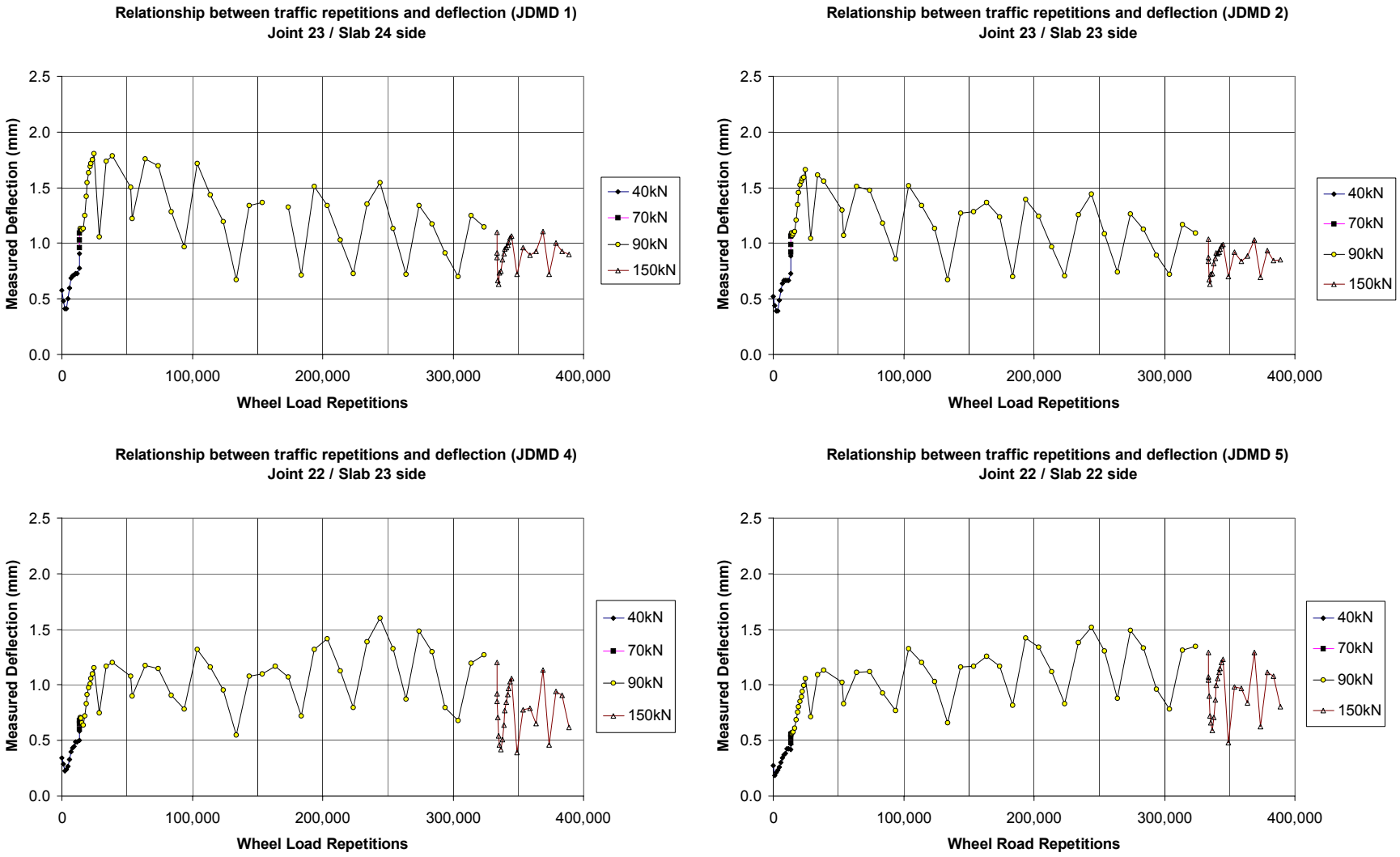

Figure 56. Effect of wheel load repetitions on joint deflections, Test 537FD.

Within the data variation, it is apparent that the deflections then tend toward an overall decrease to an average of about 1 mm by the end of the 90-kN load phase (about 325,000 repetitions). The spread between consecutive peak and trough values during this 90-kN dual wheel load is largely in the range 0.5 to 1 mm in each case. This again is high and clearly indicates that the slab is not fully supported.

The application of the 150-kN aircraft wheel load for the last 55,000 repetitions gives perhaps an initial slight reduction in deflections that tend to then remain about 0.8 mm or so to the end of test. The variation in readings also drops to about 0.5 mm. Within normal flexible pavement parameters, a decrease in deflection for an increased test load is impossible for practical purposes. Consequently, this behavior alone highlights the difference between conventional flexible-type pavements and the more structural configuration of the tied and doweled concrete slabs under the influence of daily temperature variations and traffic.

These results show no clear correlation of deflection changes with the occurrence of the corner cracks at Joint 23 (initial visible cracks on the section at 70,000 to 80,000 repetitions, completion of Slab 23 corner crack around 190,000 repetitions) nor with the mid-slab transverse crack (about 40,000 repetitions). While somewhat surprising, it is considered to be an indication that the joint load transfer was effective at Joint 23 precluding noticeable changes in deflection.

The deflection profile for Joint 22 is slightly different, as might be expected from the crack patterns. Broad similarities to Joint 23 also exist. Again there is an initial increase in deflections for the first 25,000 or so repetitions, with the slight decrease after 2,000 to 3,000 repetitions. At Joint 22, the maximum deflection at this stage is about 1.2 mm, roughly 0.5 mm less than for Joint 23 at the same stage. In contrast to Joint 23, the deflections at Joint 22 then seem to increase through about 250,000 repetitions, although they exhibit similar variations.

Deflections peak at similar levels (about 1.6 mm) for both joints. From 250,000 repetitions to the end of the test, the deflection profile is similar to that for Joint 23 except that the deflection variation for the final 150-kN aircraft wheel load phase is significantly higher at Joint 22.

As noted on previous occasions, the high deflection variation is thought to be (1) an indicator of the continued basic integrity of the slab structure (2) highlighting a variation in support probably attributable to temperature-induced slab movements. Thus, the difference in the deflection profiles for each joint is therefore regarded as indicating greater integrity of the slab structure at Joint 22, which is in accordance with the observed crack pattern.

Again, there is no clear correlation of the deflection responses at Joint 22 and the observed crack history, but it is nonetheless considered that the increasing deflections (until 250,000 repetitions) could reflect a weakening of the slab caused by the mid-span transverse crack and its propagation. For Joint 23, this effect would have been offset by the corner weakening and distinct breakage.

The final deflection range at each joint, basically on the order of 0.5 to 1 mm, can still be regarded as high for a properly seated concrete pavement slab and thus suggests that the load transfer devices were continuing to provide “spring” across the joints. It would be expected that if there was little or no load transfer, then measured deflections would be lower and certainly the variation (trough to peak) reduced because the slab sections would be better seated on the underlying layers.

It can be concluded that the application of the 150-kN aircraft wheel load caused more deterioration at both joints than was observed at the end of the previous 90-kN dual wheel load phase. As with Test 536FD, the significantly greater impact from this extreme loading condition is evident.

Figure 57 shows the corresponding results for the mid-span deflection of Slab 23 and the horizontal joint movement at Joint 23. Note that the mid-span deflection scale is the same as for the joint deflections while the horizontal deflection movement scale is only 1/25. The overall response for the mid-span deflection shows similar characteristics to the joint deflections as discussed subsequently.

Mean mid-span deflections are in the range 0.7 to 0.8 mm as for Test 536FD and are very similar to the deflection profile for Joint 22. For the last load phase (150-kN aircraft wheel load), the deflections settle to an average of roughly 0.5 mm with minimum values of 0.3 mm or so.

Although the horizontal movement at Joint 23 is only 2 or 3 percent of the vertical deflections, it has a rather different profile in that the variation between readings seems to increase throughout the test, particularly in the final 150-kN load phase. The general trend is also for a seeming increase in nominal average value.

Similar to the other deflections, the joint movement increased during the first 25,000 or so repetitions (also with a slight early dip) from about 0.01 mm to approximately 0.025 mm. Given the overall similarities in deflection behavior, it is conjectured that an initial slab weakening occurred around 25,000 repetitions probably related to the formation of the nominal transverse mid-span crack visible after 43,000 repetitions.

However, it is difficult to equate the reduction in variation of vertical deflections during the final 150-kN load phase (attributed to possibly better slab seating under the very heavy wheel load) with the increase at the joint in the horizontal direction.

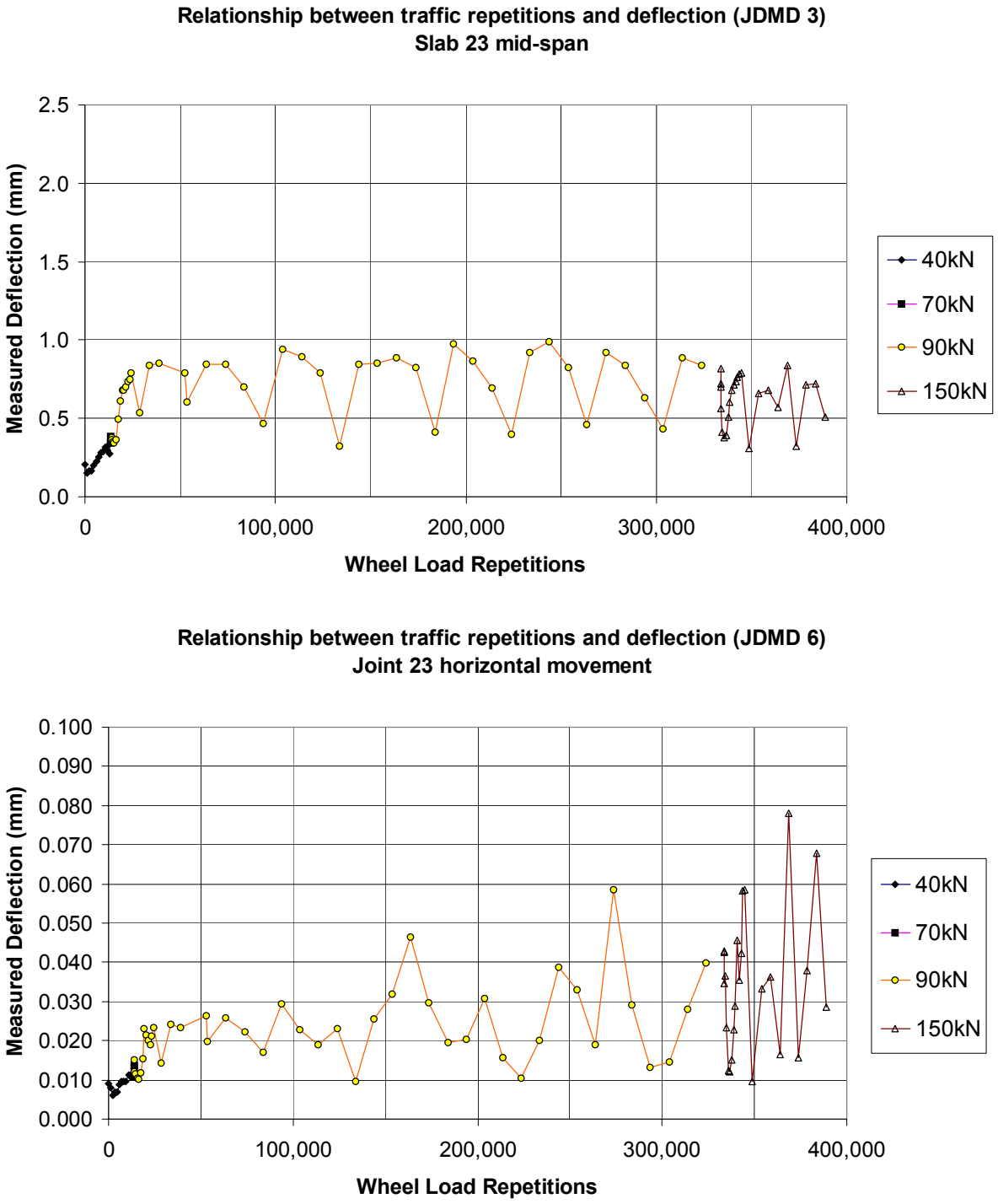

Figure 57. Effect of wheel load repetitions on mid-span and horizontal deflections, Test 537FD.

4.6.2.2 Elastic deflections and temperature

The "saw-tooth" pattern for the deflections is again prominent and likely attributable to temperatures and temperature differentials. This test was conducted throughout under ambient conditions so it provides a spread of test temperatures. However, as mentioned previously, the lack of deflection data sets taken at comparable loads restricts direct comparison and evaluation.

Figure 58 shows the corner deflection responses for JDMDs 1, 2, 4, and 5 plotted against measured slab surface temperature. Figure 59 gives the data for mid-span deflection (JDMD 3) and horizontal movement (JDMD 6). Figure 60 shows the data for JDMDs 2 and 4 (at each end of Slab 23, as previously given in Figure 58) in which the data points are connected chronologically.

Bearing in mind the generally increasing deflections during the first 25,000 repetitions of the test, attributed primarily to some structural deterioration, the results for the 40- and 70-kN load phases (to 13,740 repetitions) can be ignored in this comparison. However, even allowing for the differences in applied loads and the influence of trafficking history, it seems clear that temperature had a significant effect on the pavement behavior.

As observed from the results of Test 536FD (Chapter 4.5) for a similar structure, both corner and edge deflections decrease with increasing surface temperature. This suggests that the slabs were curled up during the majority of testing.

4.6.3 Multi-Depth Deflectometer (MDD) Results

4.6.3.1 Elastic Deflections and Trafficking

Two MDDs were were installed in Slabs 23 and 24 on each side of Joint 23, in similar locations to JDMDs 1 and 2, but further from the slab edge in the center of the HVS wheelpath

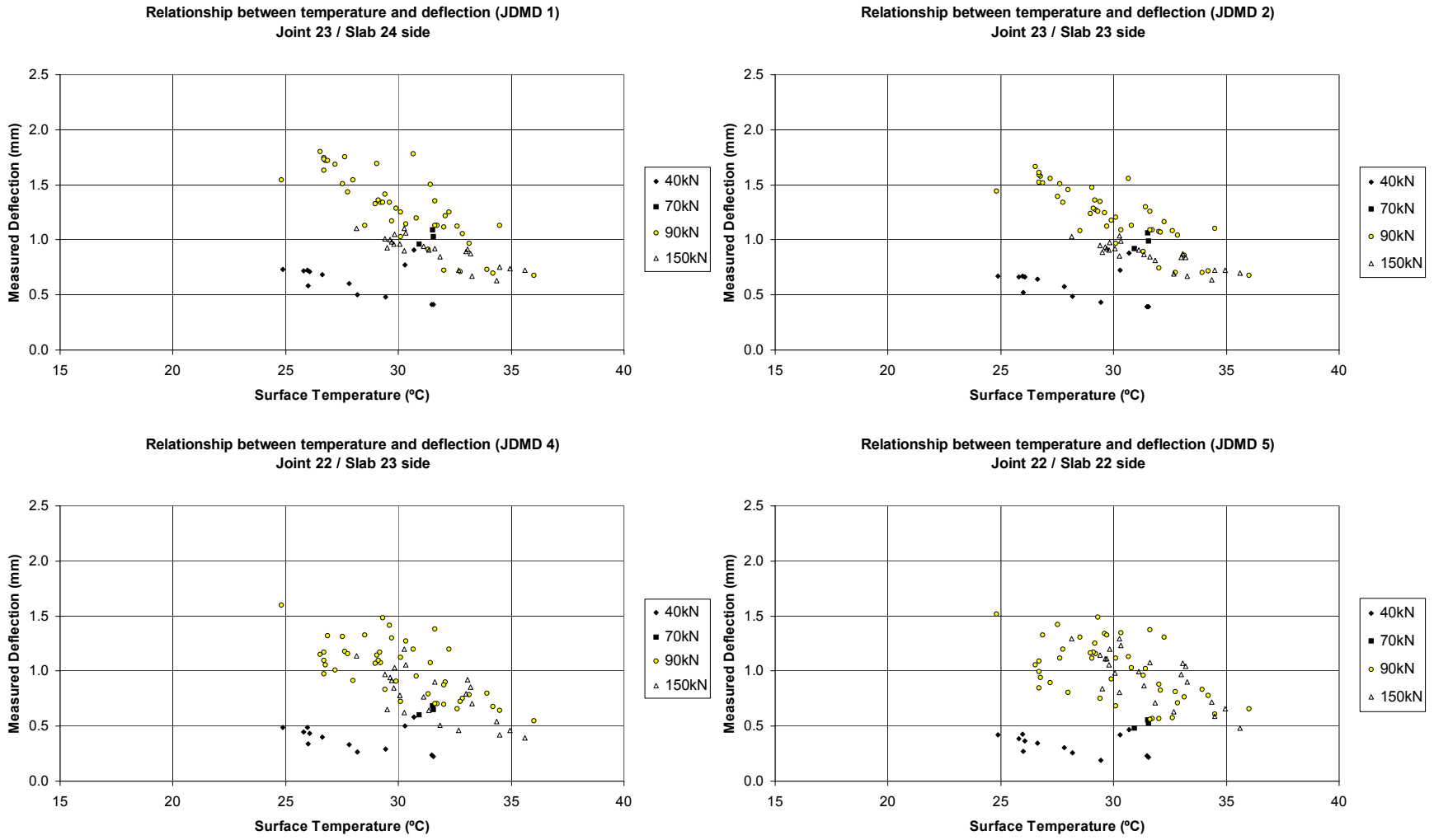

Figure 58. Effect of temperature on joint deflections, Test 537FD.

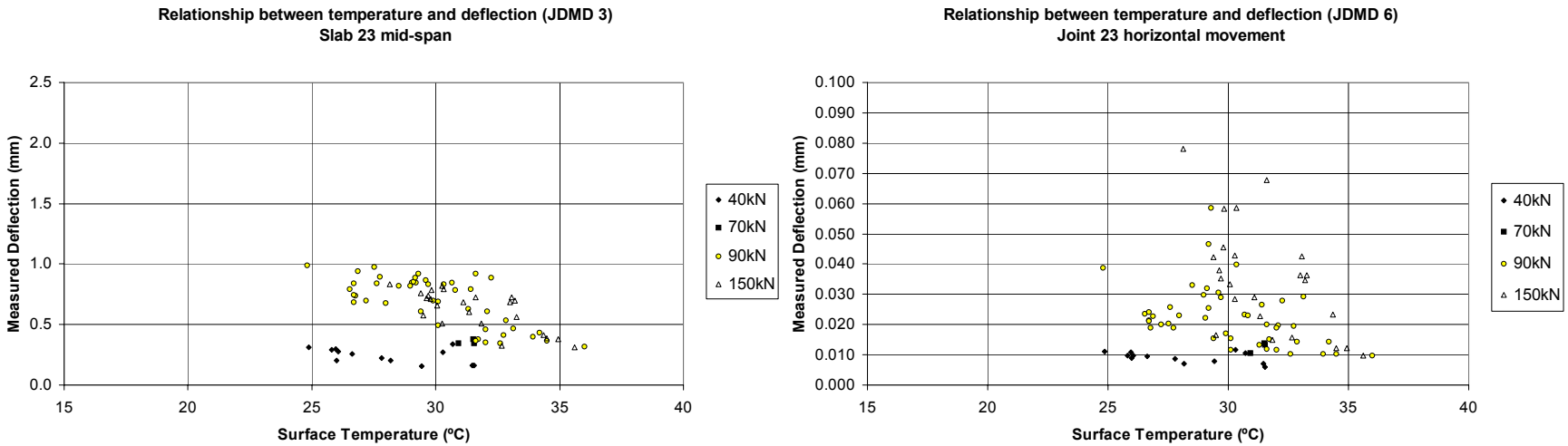

Figure 59. Effect of temperature on mid-span and horizontal deflections, Test 537FD.

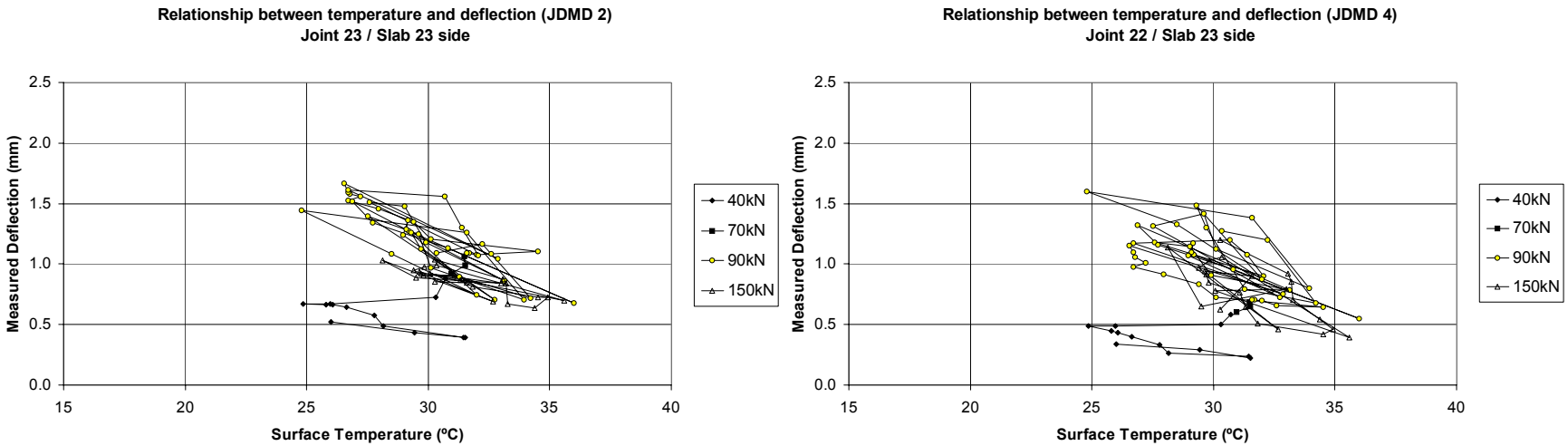

Figure 60. Effect of temperature and joint deflections, Test 537FD.

(Figure 8). They were designated MDD 8 and MDD 9, respectively. MDD modules were installed at the surface of the concrete pavement slab and at depths of 300, 450, and 650 mm below the surface (in the unbound supporting layers beneath the slab).

Figures 61 and 62 show elastic deflections as measured and the deflection differences between successive MDD modules. The deflections measured by the surface (slab) module exhibit the "saw-tooth" temperature influenced pattern previously discussed. The maximum deflections, however, are significantly lower, being typically 0.3 to 0.5 mm compared with 1 mm and more for the corresponding JDMDs 1 and 2 (Figure 56). One possible explanation for this is the transverse position of the MDDs in comparison with that of the JDMDs. The MDDs were placed approximately 300 mm from the longitudinal edge of the slabs whereas the JDMDs were placed right at the edge. Any degree of slab lift-off measured by the JDMDs will be less significant 300 mm towards the center of the slab. Assuming the slab was curled upwards during most of the test, it is expected that the deflections recorded by the MDDs would be lower that those recorded with the JDMDs. The significant difference in maximum deflections measured by the JDMDs and the MDDs can be attributed to (1) the differences in location of the measuring devices relative to the possible localized slab movement near the joint and cracks, and (2) the positioning of the load wheel in relation to the measuring devices.

It also appears that, with the application of 150-kN aircraft wheel loading (from about 334,000 repetitions onward), the deflections tend to increase slightly whereas they decreased at the JDMDs. This effect is more pronounced for MDD 9 on the Slab 23 side of the joint. Final deflections under this wheel load are approximately 0.3 mm (MDD 8) to 0.5 mm (MDD 9), compared with 0.8 to 1 mm at the JDMDs. The same apparent reduction in variation of the deflections is also recorded during this final load phase.

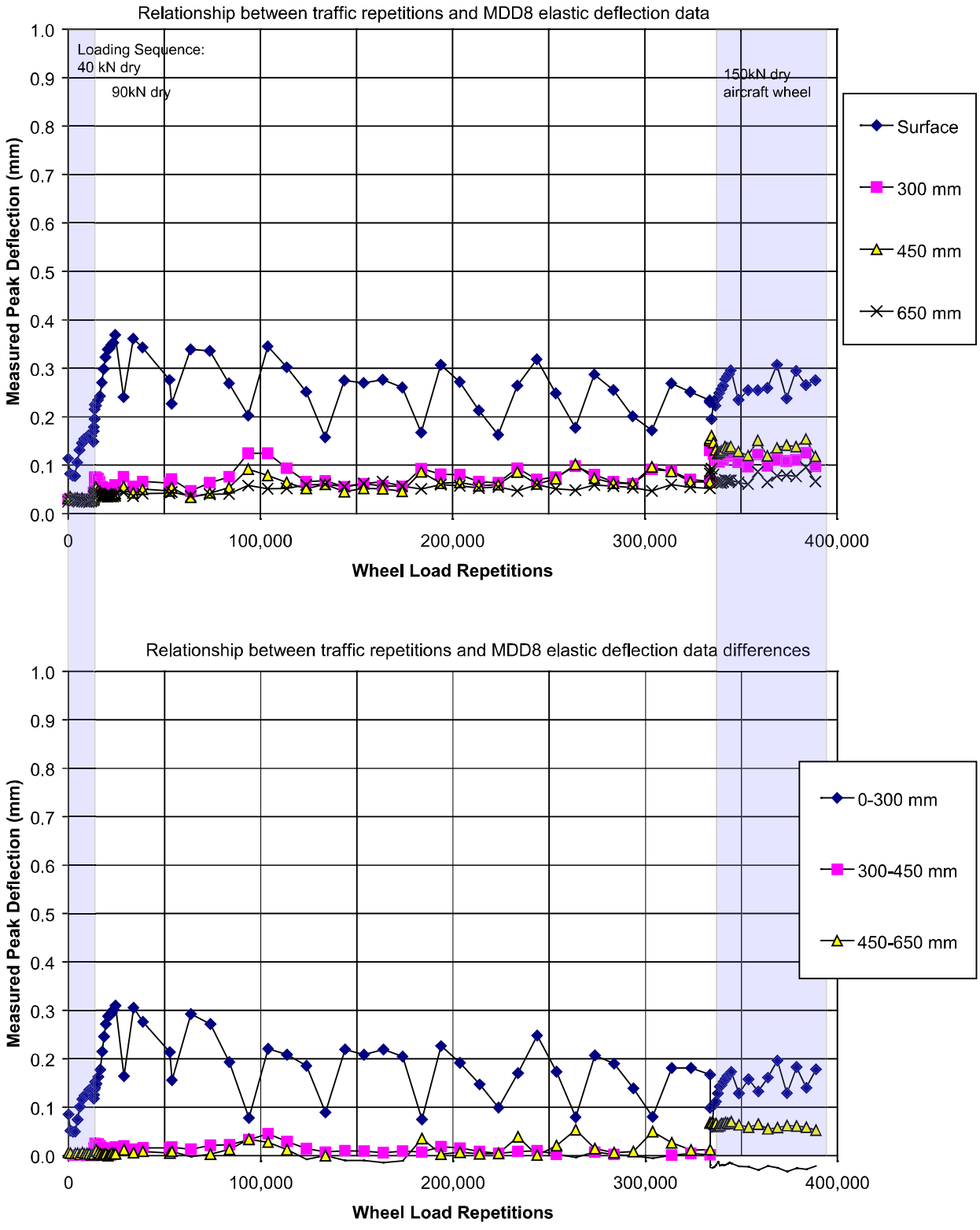

Figure 61. Plost of MDD 8 deflections and temperature versus load repetitions, Test 537FD.

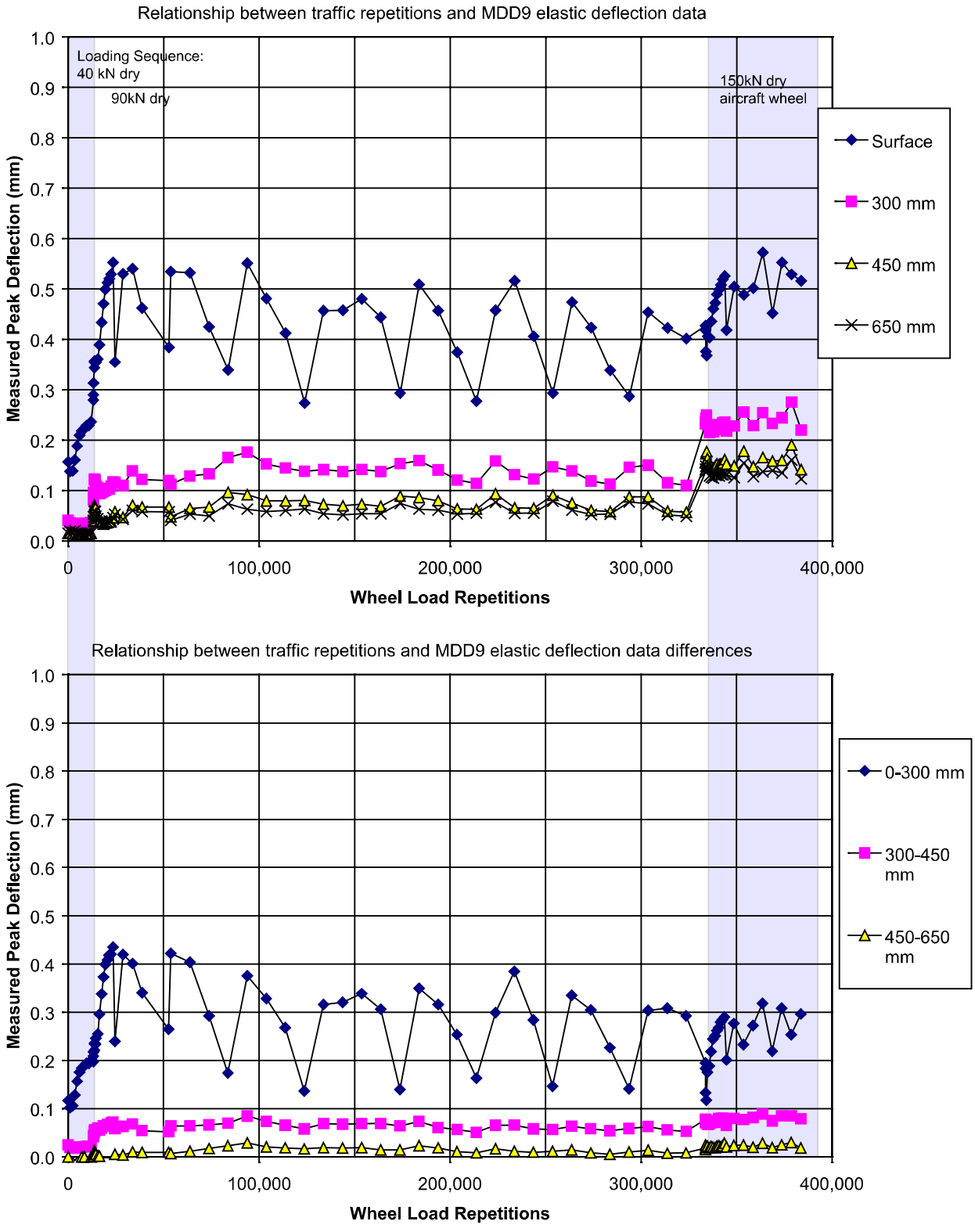

Figure 62. Plot of MDD 9 deflections and temperature versus load repetitions, Test 537FD.

Note that the major share of the total deflection occurs between the slab surface and the module at 300 mm depth. The differences in deflection data highlight this, showing that up to the final loading phase (from 340,000 repetitions with the 150-kN load), only about 0.1 mm of the total deflections can be attributed to the structure below 300 mm. While this remains true for MDD 8 (Slab 24 side), the portion of deflections attributed to the structure below 300 mm increases to about 0.2 mm for MDD 9 (Slab 23 side). This corresponds with increased surface deflections, indicating some weakening of the slab and transmission of greater stress/deflection to the supporting layers. No further cracking was observed during this traffic loading phase.

The major deflection component between the slab surface and 300 mm below, of which 200 mm is concrete slab, tends to support the earlier observation regarding the upward curling of the slab.

4.6.3.2 Permanent Deformation and Trafficking

Figures 63 and 64 show temperature history and the permanent deformations and differences in deformation recorded at the four layers of MDD 8 plotted against repetitions. Figures 65 and 66 give the results for MDD 9 in the same manner.

In both cases, the slab module shows the same temperature effect as noted for the elastic deflection data, seemingly confirming the MDD module placement within the slab and the influence of temperature on the "permanent" deformation recorded there. As would be expected, this effect is not evident in the measurements obtained from modules in the granular materials because the granular materials are less temperature susceptible than concrete.

The permanent deformation of the underlying layers (modules at 300, 450, and 650 mm) is very similar for both MDDs. In each case, the deformation increases to about 0.6 mm at 300

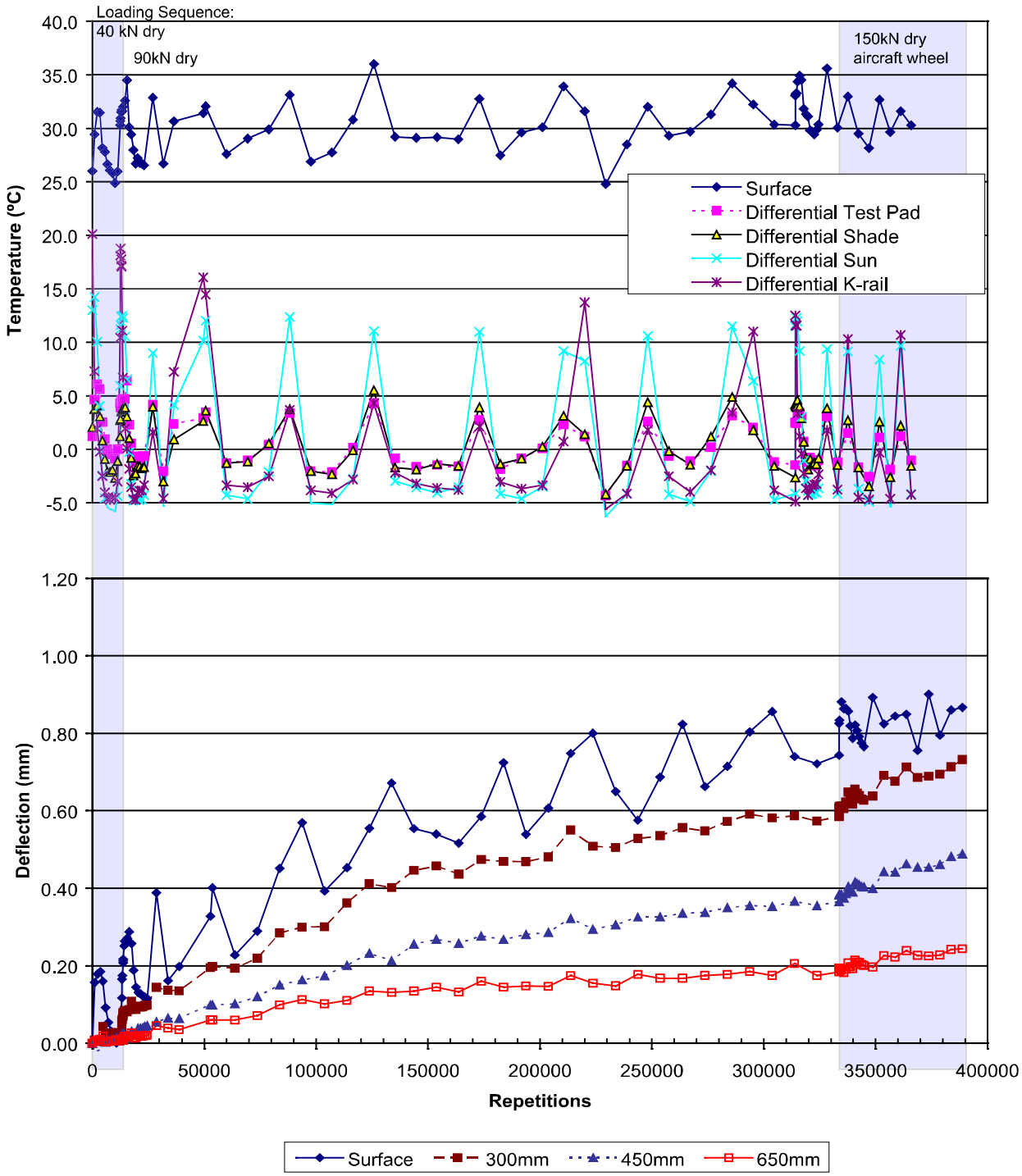

Figure 63. Plot of MDD 8 permanent deformation and temperature versus load repetitions, Test 537FD.

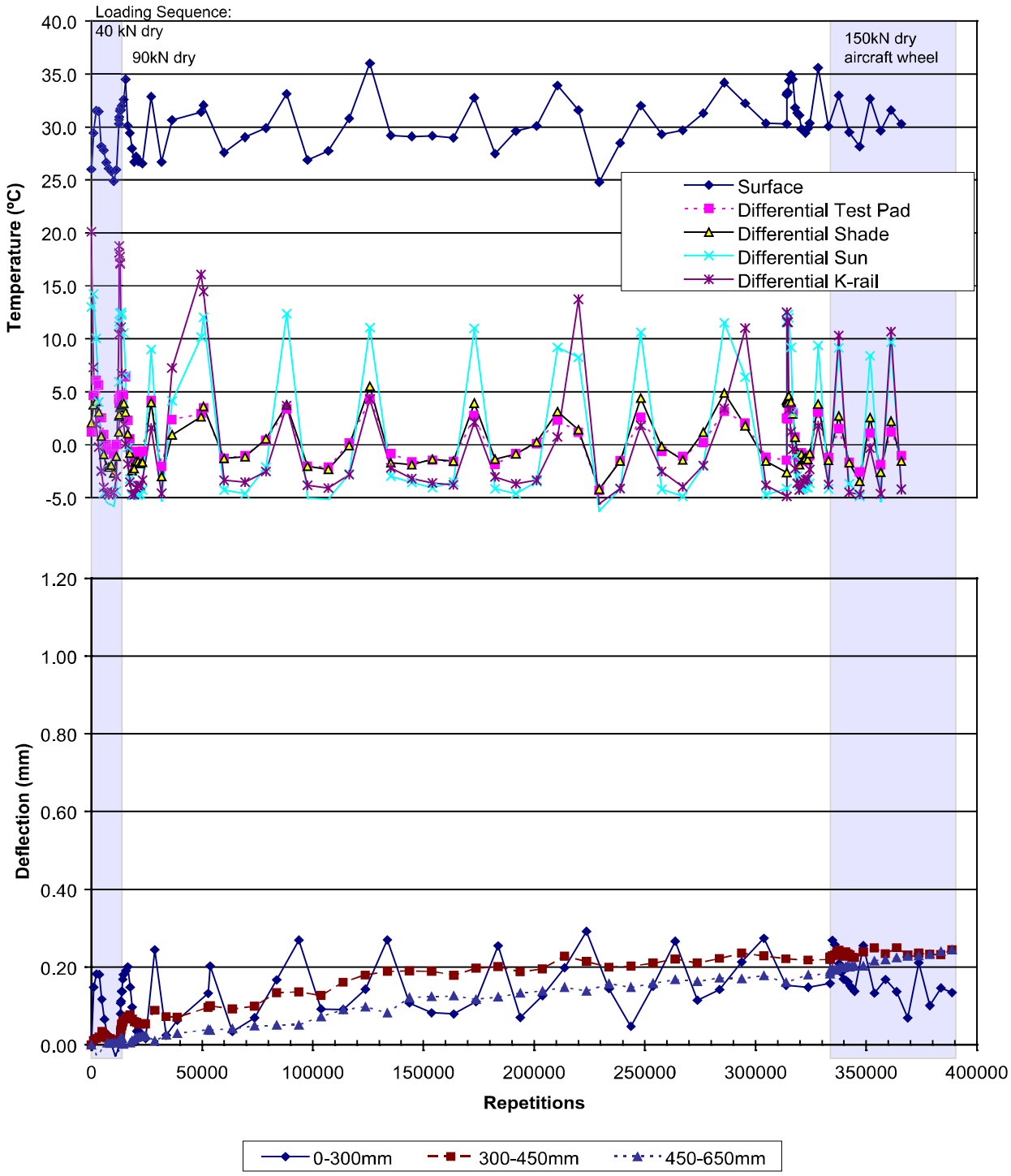

Figure 64. Plot of MDD 8 permanent deformation differentials and temperature versus load repetitions, Test 537FD.

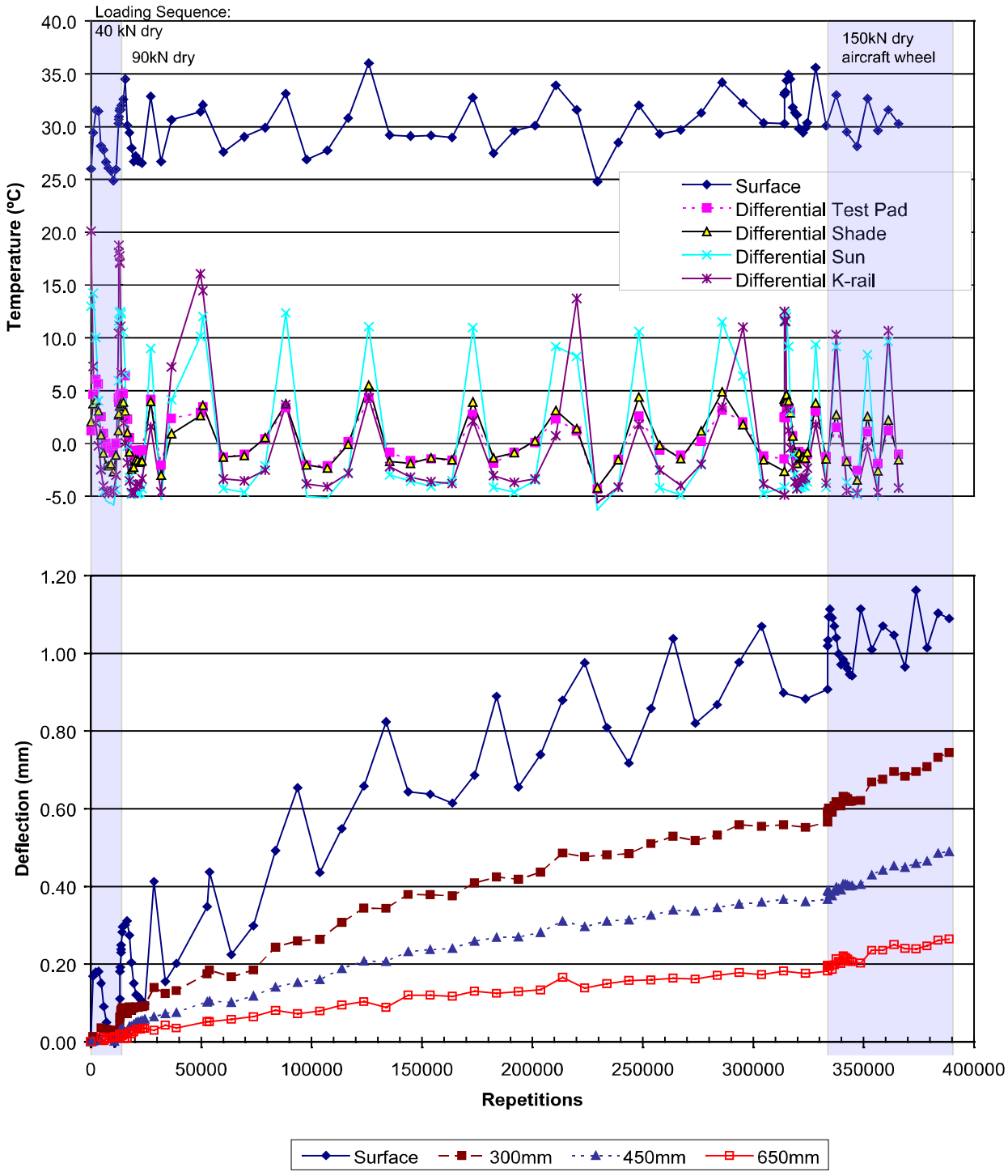

Figure 65. Plot of MDD 9 permanent deformation and temperature versus load repetitions, Test 537FD.

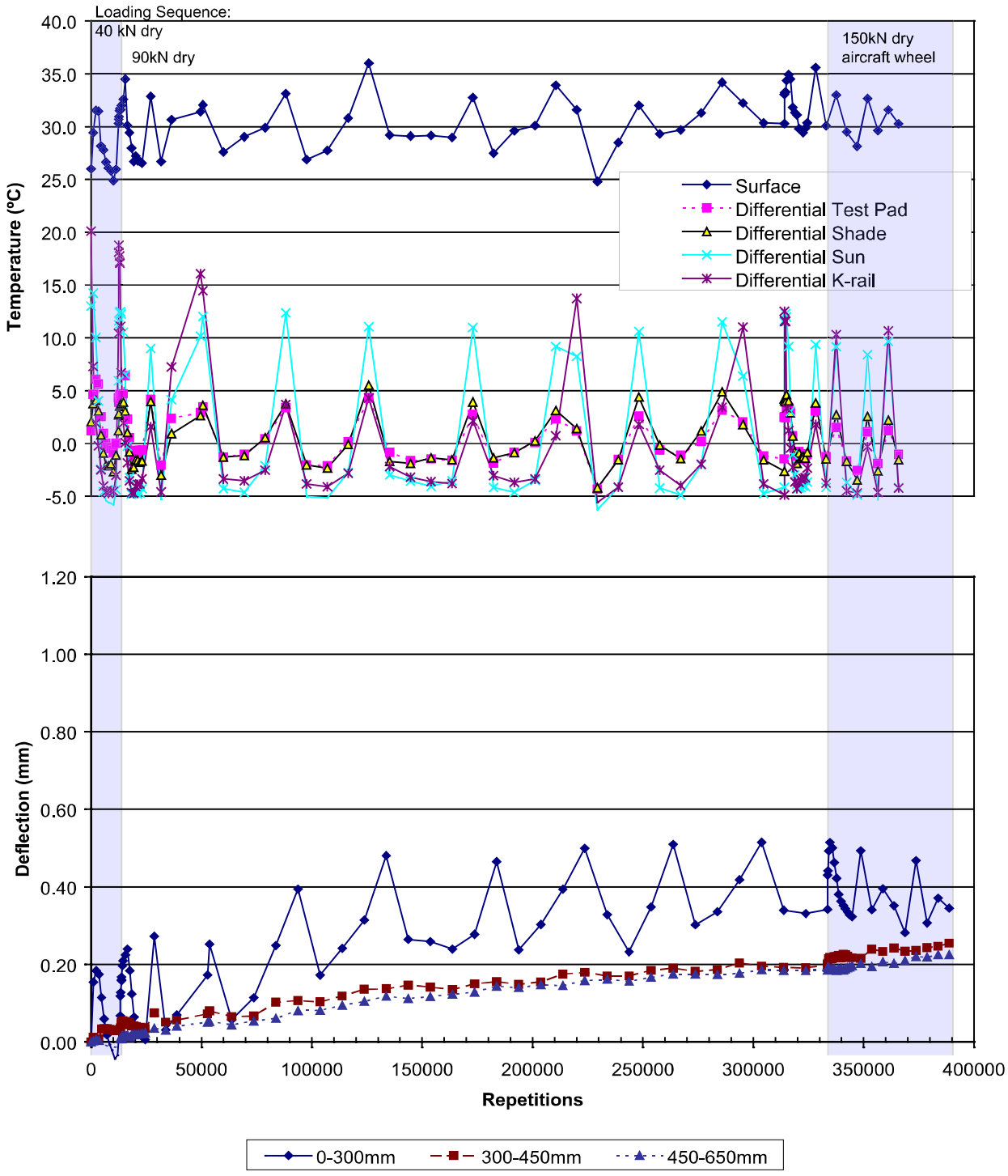

Figure 66. Plot of MDD 9 permanent deformation differentials and temperature versus load repetitions, Test 537FD.

mm depth after 340,000 repetitions (before the 150-kN aircraft wheel load). Lower level modules increase to about 0.4 mm at 450 mm depth and about 0.2 mm at 650 mm depth. The application of the heavier load causes an initial increase in rate of permanent deformation, suggesting further consolidation and continuing increase in permanent deformation to the end of the test. Again, response of the underlying layers is very similar.

The differential deformations between the depths (Figures 64 and 66) clarify that the consolidation between 300 to 450 mm at MDD 8 (Slab 24 side) was similar to consolidation on the other side of the joint (Slab 23, MDD 9), while the consolidation at lower layers (450 to 650 mm) was slightly less than that at MDD 9. However, the differences are small. These figures also show that increased consolidation caused by the 150-kN aircraft wheel load took place below 650 mm with little change in the differential deformations between the modules above.

In contrast to the marked similarities for the underlying layers, the permanent deformation response between the surface and the 300-mm depth module is distinctly different on either side of the joint. While the variation in readings associated with temperature effects is evident for both MDDs, again indicating a thermal-induced movement in the slab, the permanent deformation at MDD 9 (Slab 23 side of Joint 23) is significantly higher than on the other side of the joint at MDD 8.

The initial response is quite similar, however from 50,000 to 150,000 repetitions, the consolidation between the slab and the depth of 300 mm increases markedly at MDD 9. Both MDDs then show only minor increases in deformation and virtually no further increase from 250,000 repetitions or so. Permanent deformations measured at the surface are in the order of 1.1 mm for MDD 9 and 0.9 mm for MDD 8 at the end of test and, as noted previously, the trend of higher deflections comes from the underlying layers not the uppermost layers.

The marked increase in apparent permanent deformation on the Slab 23 side (MDD 9) of the joint between 50,000 and 150,000 repetitions can only be attributed to a structural weakening of the slab and increased load transfer to the support layers. Note that the final part of the corner break on this slab was observed around 190,000 repetitions whereas the corner break on the adjacent slab (Slab 24) was complete by about 80,000 repetitions.

The 0.2-mm difference in measured consolidation in the top 300 mm of the structure on each side of the joint is significant. Although the cracking behavior may have suggested that permanent deformation on the Slab 24 side of the joint would increase because corner break formed sooner than on the other side, this was not the case. This response highlights the complexity of the structural slab interaction and load transfer.

4.6.4 Load Transfer Efficiency (LTE)

Figure 67 shows peak deflections on each side of Joints 23 and 22 as measured in the same data set and previously shown against repetitions (Figure 56) and surface temperatures (Figure 58). The deflections are therefore those measured on each side of the particular joint at the same repetitions and applied test load.

The data are grouped in terms of test load as discussed previously. The predominant data sets are those for the 90-kN dual wheel load trafficking phase (from 14,000 to 334,000 repetitions) and for the 150-kN aircraft wheel trafficking phase (from 334,000 repetitions to the end of test).

At Joint 23 the data points for deflections up to about 1.1 mm lie reasonably close to the line of equality. For higher deflections (which tend to have been measured during the 90-kN phase) the Slab 23 side deflections are slightly lower than those on the Slab 24 side. The general

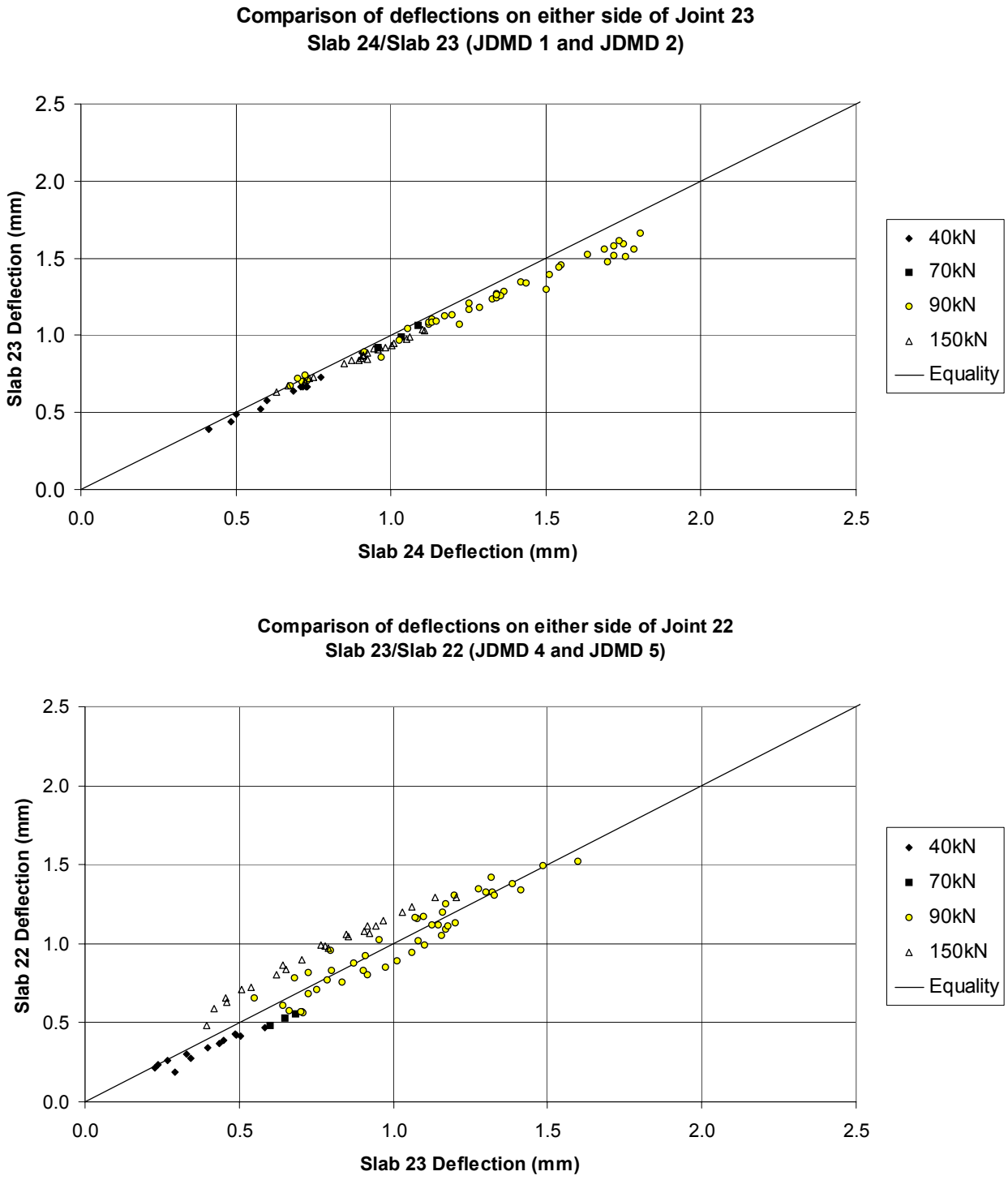

Figure 67. Joint load transfer efficiency at Joints 22 and 23, Test 537FD.

trend, however, shows high correlation and LTEs in the order of unity (100 percent) would be anticipated.

In contrast, although the average value for Joint 22 is closer to the line of equality, the scatter of results is notably higher than at Joint 23. Closer scrutiny shows that the apparent variability is more attributable to deflections on the Slab 22 side, which tend to be lower than those on the Slab 23 side during the initial traffic loading phases and higher after the application of the 150-kN aircraft wheel load. This type of response can only be interpreted as indicating lower LTEs at this joint. This also draws attention to the fact that the load transfer mechanism changed markedly so that the Slab 22 side of the joint began with better load transfer but ended up worse than the Slab 23 side.

Figure 68 gives the comparable deflections at each end of Slab 23 (Joint 22 and Joint 23). On the slab itself, deflections on the Joint 22 side were slightly lower for the major part of the test but became comparable during the 150-kN load phase. This implies that some difference initially existed in the support condition (which includes underlying layers and joint load transfer), but that during the 150-kN aircraft wheel loading phase the Joint 22 side weakened.

Figure 69 gives the calculated LTEs for both sides of each joint together with the surface temperature and slab temperature differential. This confirms that the LTEs are generally close to unity (100 percent) across Joint 23 and lower (80 to 95 percent) at Joint 22. The figure further shows that the load transfer efficiency decrease during 50,000 or so repetitions before generally increasing at around 100,000 repetitions. LTE for the corner of Slab 22/Joint 22 was poorest overall and varied more than for the other positions.

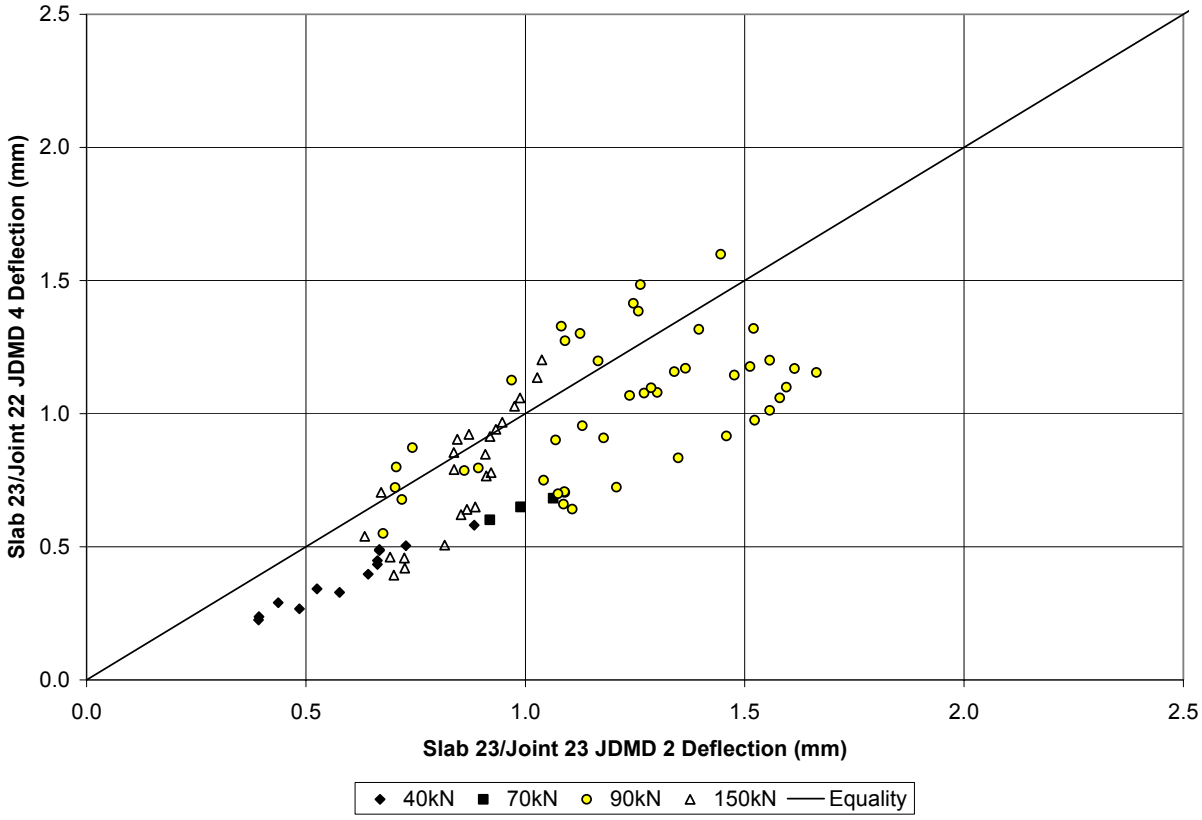

Figure 68. Comparison of joint deflections on either side of Slab 23 (Joints 22 and 23), Test 537FD.

As noted in the previous discussion, the mechanism of load transfer across Joint 22 changed during the final loading phase. This can be inferred from Figure 70, which shows the LTEs for Joint 22 broadly spread around the line of equality. Figure 70 also shows that LTEs for Joint 22 were significantly lower than those for Joint 23 (shown in Figure 69).

In line with the discussion for Test 536FD, it seems that the present definition and calculation of LTE will result in values of 100 percent even if uniform deterioration takes place on each side of a given joint. This implies similar changes in deflection responses but does not necessarily identify joint deterioration per se. In addition, it appears that the calculation gives no indication of a change in mechanism of load transfer in the case (such as for Joint 22) where the greatest degree of deterioration shifts from one side of the joint to the other.

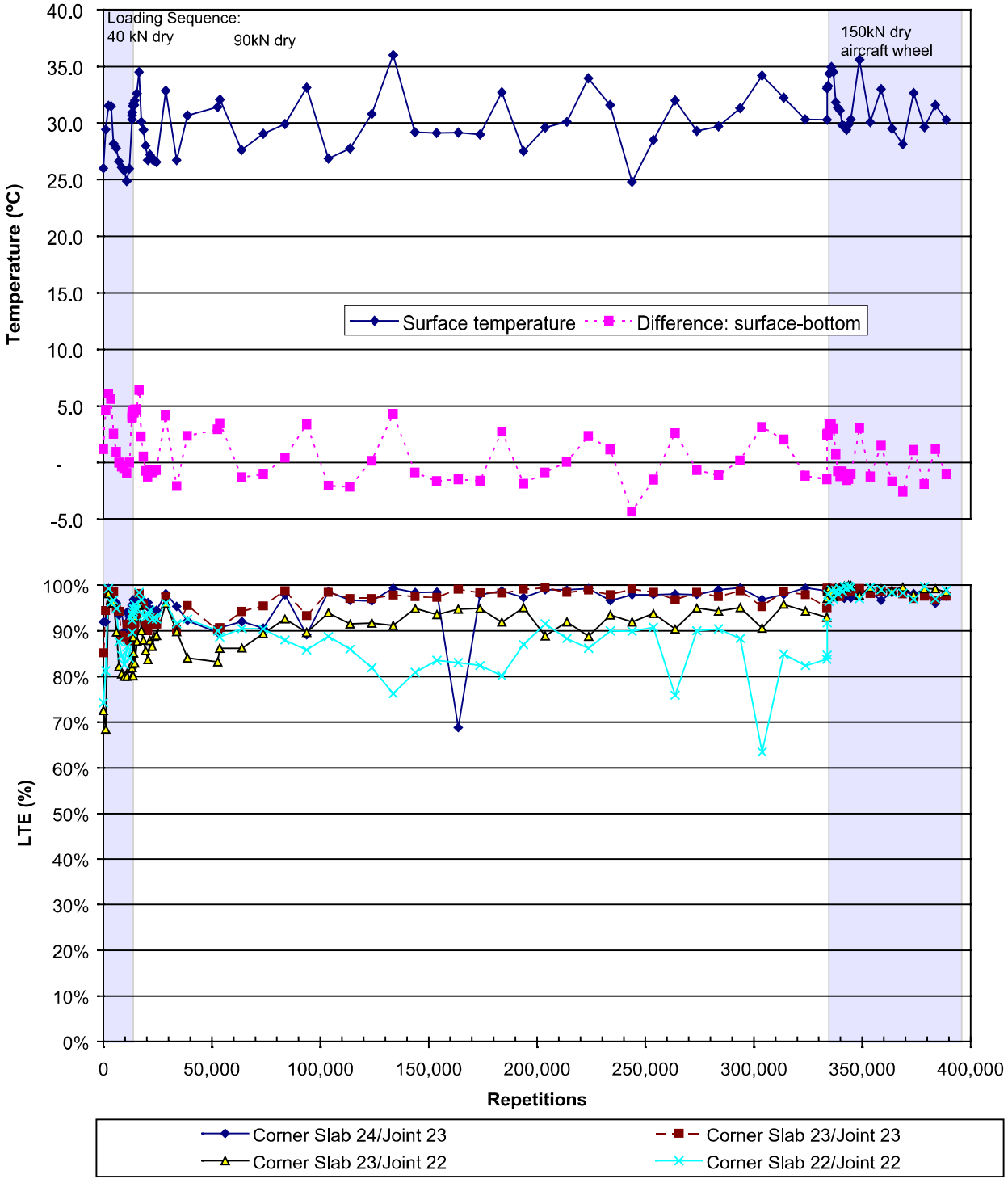

Figure 69. Plot of LTE and temperature versus load repetitions, Test 537FD.

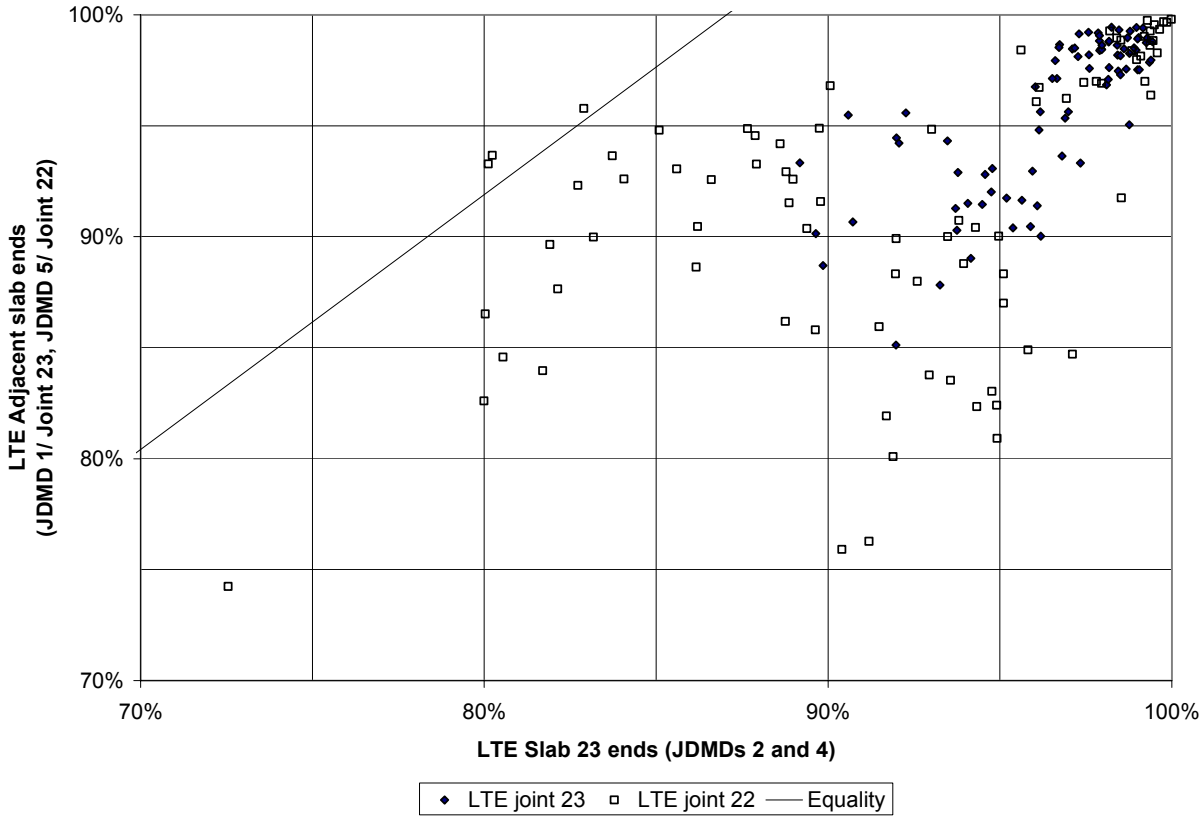

Figure 70. Joint load transfer efficiency at Joints 22 and 23, Test 537FD.

4.7 Test 538FD

HVS Test 538FD was the final of the series of three HVS tests on the 200-mm PCC slabs with dowels and tied concrete shoulders. The test was carried out from January 3 to January 18, 2001. The other two HVS tests on this section were 536FD and 537FD (reported in Chapters 4.5 and 4.6).

The main objective of this test was similar to the previous two tests: to evaluate the influence of various factors, including slab length and load transfer devices (dowels), on the effectiveness of joint load transfer and joint deterioration under the influences of repetitive loading at ambient temperature conditions. The fatigue behavior of the Fast Setting Hydraulic

Cement Concrete (FSHCC) slabs in this series of three tests was monitored under bi-directional primarily 90 kN and greater wheel loadings in dry conditions (no water added).

Test 538FD was undertaken on Slabs 18, 19, and 20 (Figure 9) such that the full length (3.92 m) of Slab 19 and approximately 2 m on each of the adjacent slabs (Slabs 18 and 20). The test was conducted under ambient temperature conditions without the temperature control chamber in place.

Initially, just 500 wheel load repetitions were applied with a 70-kN dual wheel followed by a further 189,000 repetitions at 90 kN. A total of almost 190,000 channelized wheel load repetitions were applied in this test.

4.7.1 Visual Observations

Figure 71 shows the crack patterns as they developed during the test. Figure 72 presents a composite image of the test section after the completion of HVS trafficking. Note that Slab 18 had a transverse crack across its full width approximately 2.25 m from Joint 18 before the start of HVS testing. This is similar to the initial condition in Test 537FD (Chapter 4.6).

During the test, no cracks were observed on the main trafficked slab (Slab 19) and HVS traffic-induced cracking was limited to a transverse crack on Slab 20 approximately 1.5 m from Joint 19. This crack tended to mirror the existing transverse crack on Slab 18, providing a degree of symmetry on each side of Slab 19, however, it did not run completely across the slab. The crack ended approximately 2.1 m from the originating slab edge, so it still had approximately 1.5 m to propagate to the opposite edge of the 3.66-m wide slab. Although visibly discontinuous, it is apparent that the two observed cracks are part of the same discontinuity.

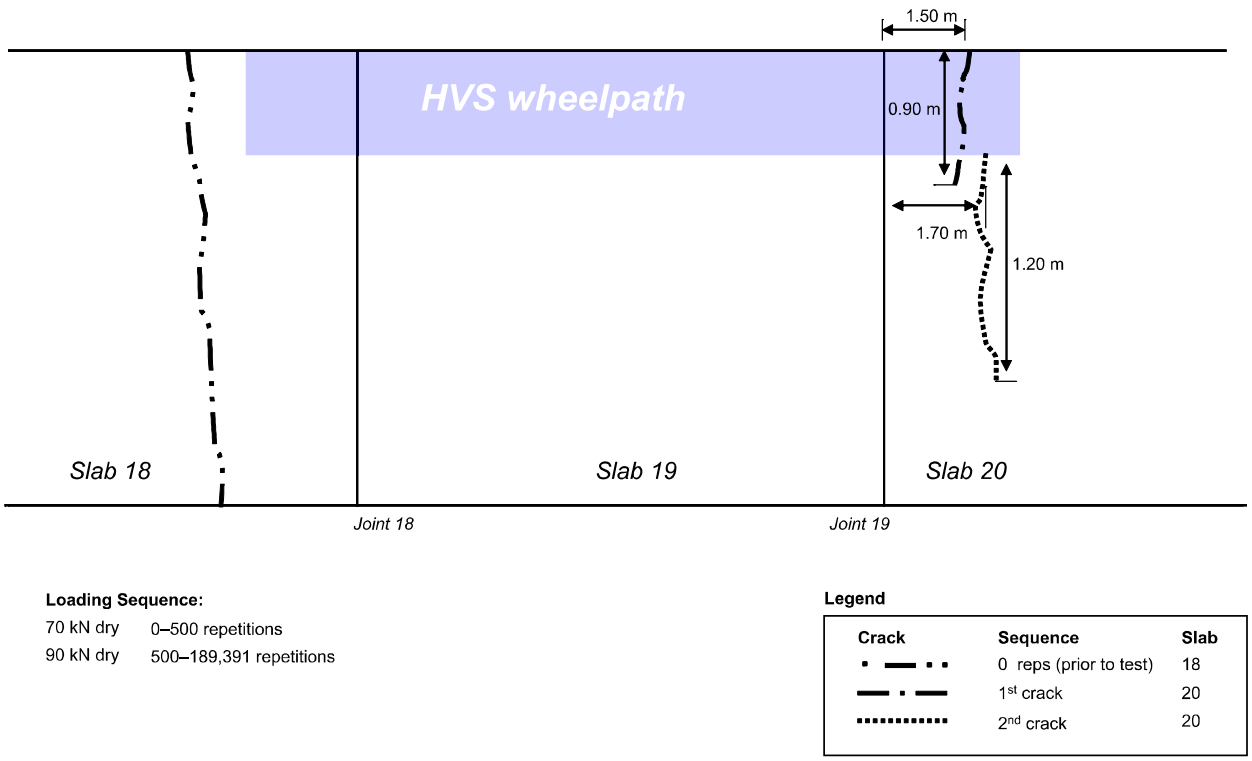

Figure 71. Schematic of crack pattern, Test 538FD.

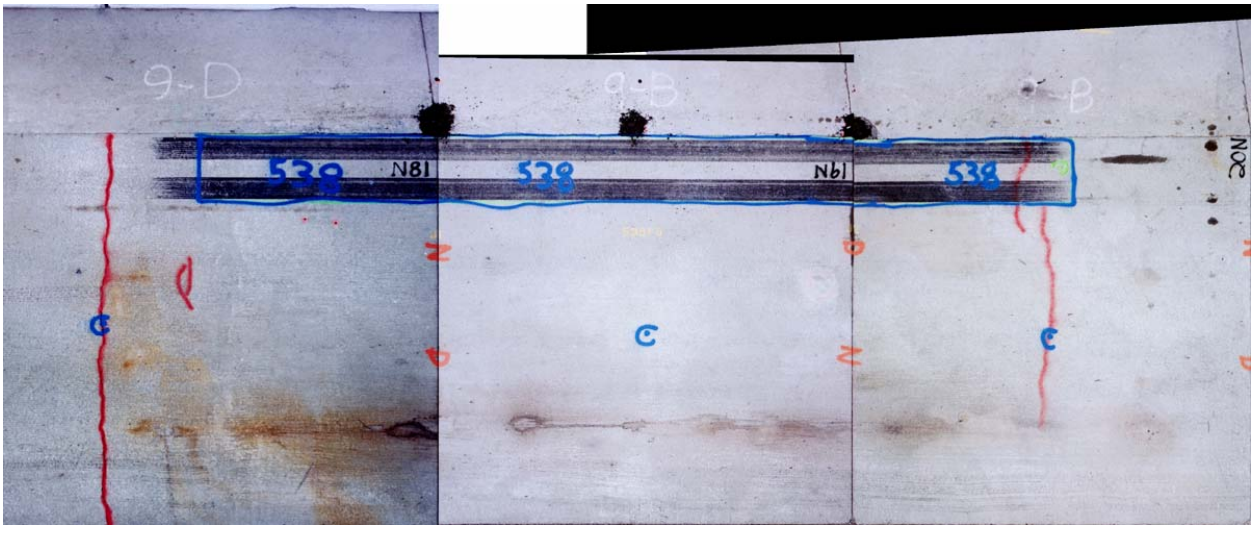

Figure 72. Composite image of Test 538FD showing cracks.

The final HVS trafficking-induced crack pattern can therefore be summarized as a nominal mid-span transverse fracture on Slab 20 (Slab 18 was already transversely cracked prior to testing). There was no evidence of corner breaks and the main trafficked slab (Slab 19) appeared sound at the end of the test.

4.7.2 Joint Deflection Measuring Device (JDMD) Results

4.7.2.1 Elastic Deflections and Trafficking

Figure 73 presents the elastic deflection data for the test, the test slab surface temperatures, and the temperature differentials between slab top and bottom at four locations around the test area.

The deflections were recorded at the trafficking wheel load rather than at other selected wheel loads (normally including 40 kN as the equivalent standard axle load) so deflections cannot be compared directly. All the joint measurements fluctuate considerably and show the distinct "saw-tooth" variation in deflections also observed on Tests 536FD and 537FD (Chapters 4.5 and 4.6).

Figure 74 gives separate graphs of deflections recorded by JDMDs 1, 2, 4, and 5 against trafficking history. These show deflections recorded on either side of Joints 19 and 18 at each end of Slab 19.

Comparing the JDMD pairs on each side of a joint (JDMDs 1 and 2; 4 and 5) reveals very similar responses. The deflections at Joint 18 remain slightly lower throughout than those at Joint 19.

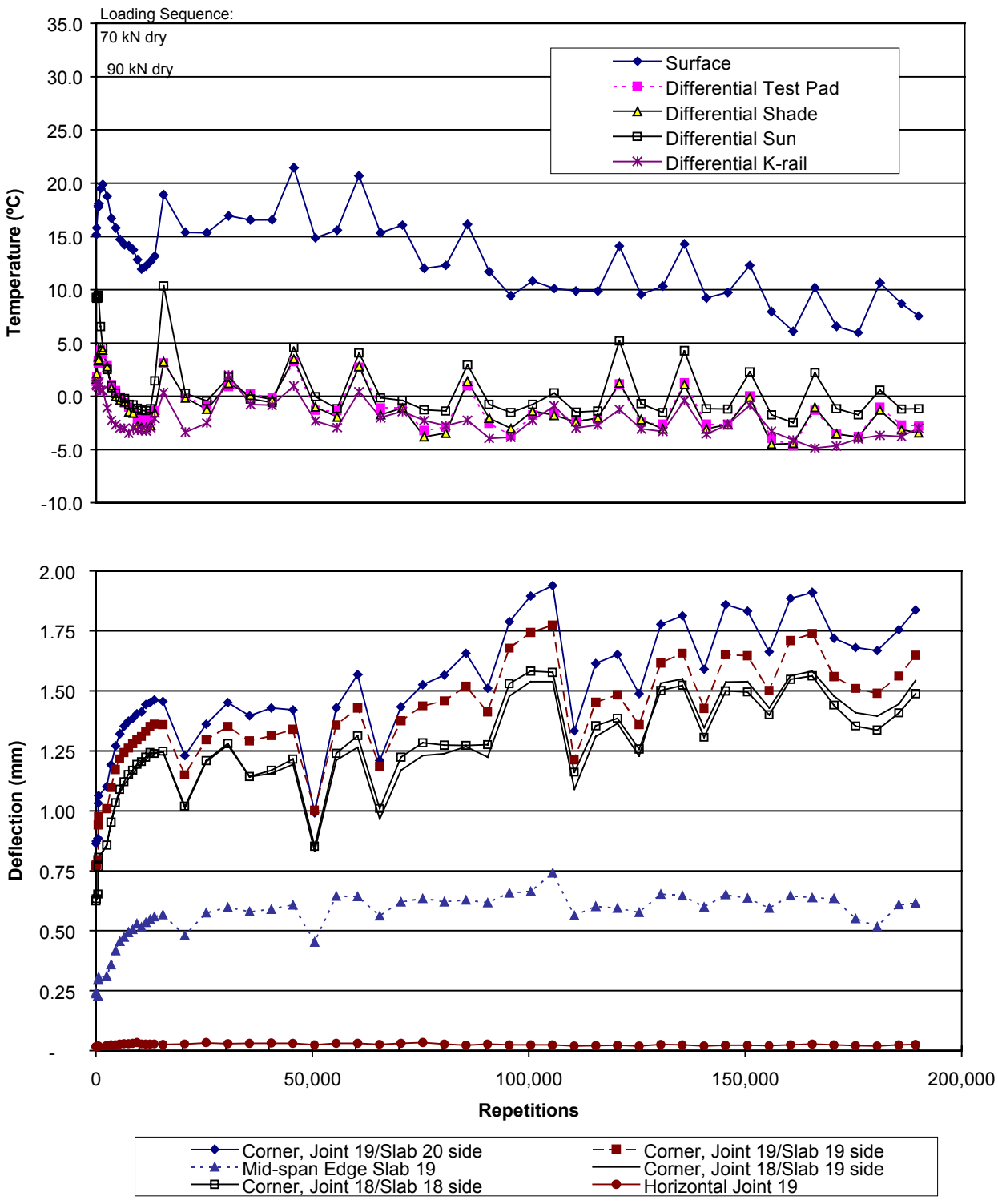

Figure 73. Plot of JDMD deflections and temperature versus load repetitions, Test 538FD.

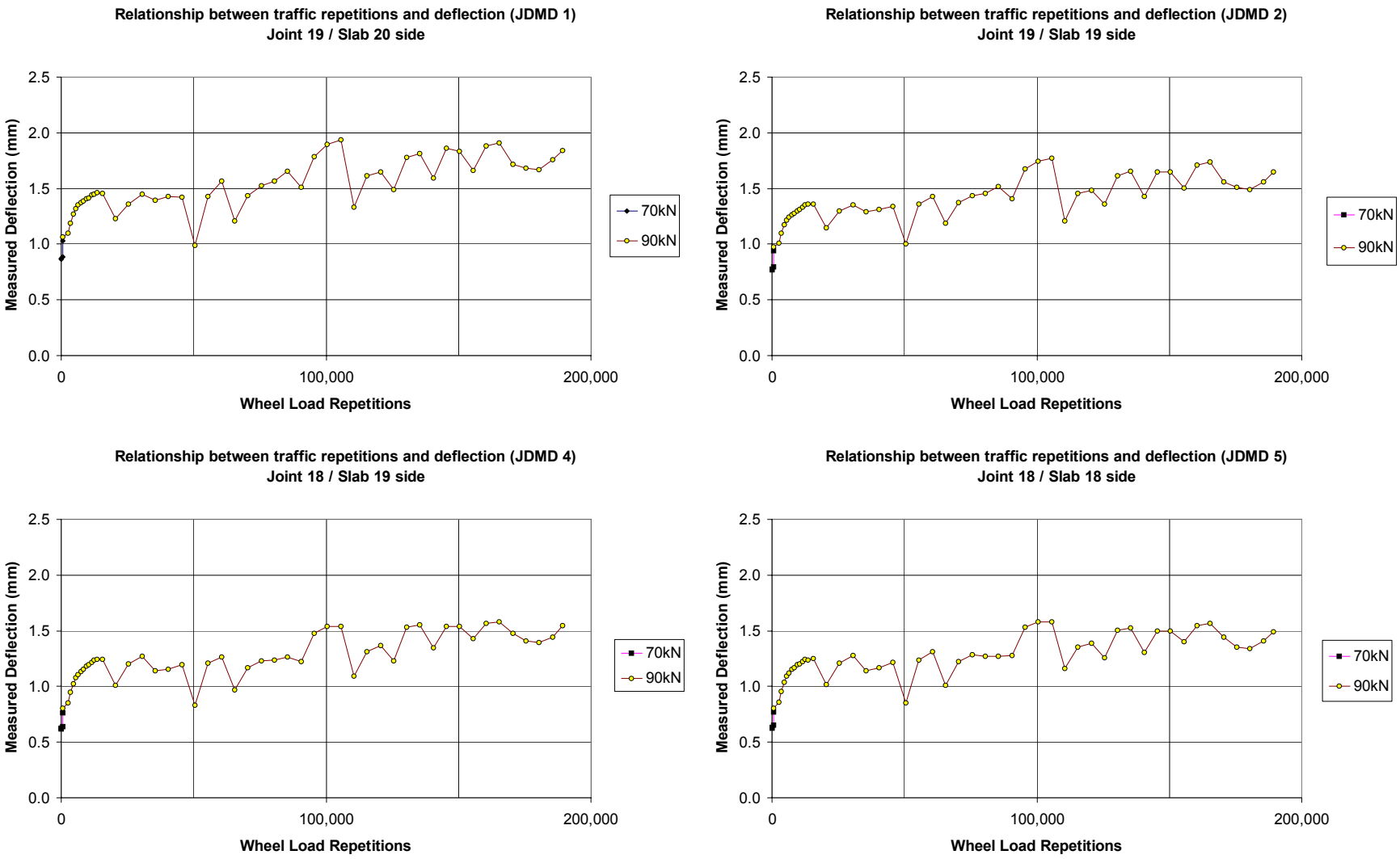

Figure 74. Effect of wheel load repetitions on joint deflections, Test 538FD

For Joint 19, the deflections increase from about 0.8 mm during the first 15,000 or so repetitions to about 1.4 mm (90-kN test load). The deflections appear reasonably constant until about 50,000 repetitions and then tend to increase slightly to the end of test. The deflections on the Slab 20 side of the joint remain slightly higher than those on the Slab 18 side throughout by about 0.2 mm and final deflections are about 1.8 and 1.5 mm, respectively.

The deflection profile for Joint 18 is only slightly different and this is mainly in the magnitude of deflections being slightly lower than those observed at Joint 19 (on the order of 0.2 to 0.4 mm). Again, there is an initial increase in deflections for the first 50,000 or so repetitions, from roughly 0.6 mm to about 1.3 mm, followed by gradually increasing deflections throughout the rest of the test and ending at about 1.5 mm.

The data variation among values (the spread between consecutive peak and trough values) during this test is generally less than 0.5 mm, which is significantly lower than on the previous two tests on this structure (536FD and 537FD). This is undoubtedly attributable to the lower temperatures and temperature variations during this short winter test (16 days in early to mid-January).

A distinct decrease in all deflections was observed at about 105,000 repetitions. Within the variation of readings, this could indicate some deterioration attributable to cracking. Note that this was detected on all three adjacent slabs and on both sides of the two joints. The increasing deflections throughout the test reflect weakening of the slab possibly caused by micro-crack propagation.

The final deflection range (1.5 to 2.0 mm) is high and comparable with those observed during Tests 536FD and 537FD before significant deterioration began under the very heavy aircraft wheel load.

These responses suggest that continuation of the test may have led to more visible cracking within 100,000 repetitions or so. Alternatively, the application of a 150-kN aircraft wheel load (as used on the previous two tests) probably would have caused even faster deterioration.

Figure 75 shows the corresponding results for the mid-span deflection of Slab 19 and the horizontal joint movement at Joint 19. Note that the mid-span deflection scale is the same as for the joint deflections, while the horizontal deflection movement scale is only one-fiftieth of that. The overall response for the mid-span deflection shows characteristics similar to the joint deflections as discussed previously. However, the mid-span deflections remain essentially constant from 50,000 or so repetitions rather than continuing to increase slightly as seen for joint deflections.

Mid-span deflections remain in the range 0.5 to 0.6 mm after the first 50,000 or so repetitions, having increased fairly rapidly from about 0.25 mm initially. Mid-span deflections are in the order of one-third of the corner deflections.

The horizontal movement at Joint 19 is only about 2 percent of the vertical corner deflections. Initially increasing from about 0.017 to 0.030 mm, deflections stay fairly constant until about 75,000 repetitions. Subsequent deflections drop to about 0.023 mm for the remainder of the test. This apparent change in response was not reflected in any of the other JDMDs so is not deemed significant.

4.7.2.2 Elastic Deflections and Temperature

The “saw-tooth” pattern for deflections is less prominent for this test than for Tests 536 and 537. This difference is likely attributable to the lower overall temperatures and temperature

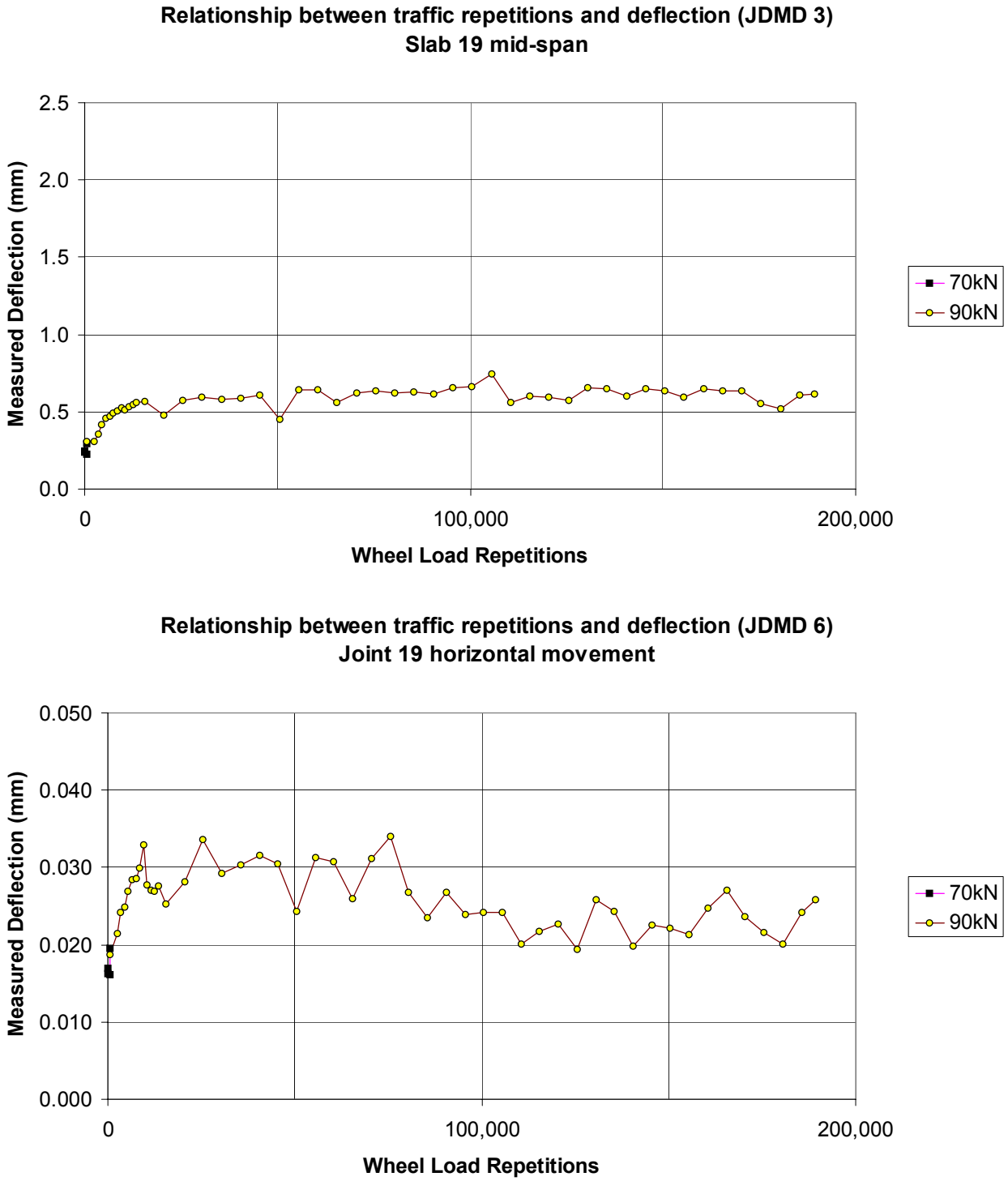

Figure 75. Effect of wheel load repetitions on mid-span and horizontal deflections, Test 538FD.

differentials during this short winter test. In contrast to the previous two tests, this test was conducted at the dual wheel load of 90 kN (except for the first 500 repetitions) so direct comparison of responses is possible.

Figure 76 shows the corner deflection responses for JDMDs 1, 2, 4, and 5 plotted against measured slab surface temperature. Figure 77 gives the data for mid-span deflection (JDMD 3) and horizontal movement (JDMD 6). Figure 78 shows the data for JDMDs 2 and 4 (at each end of Slab 19, as previously given in Figure 76) in which the data points are connected chronologically.

Ignoring the four readings at 70 kN (i.e., during the first 500 repetitions when deflections increased rapidly), it is again apparent that temperature has a significant effect on the pavement behavior at the corners near the joints. As noted earlier, the level of deflections alone (1 mm and higher) is extremely high and indicates lack of support under the slab. This response could be attributed to initial upward curling of the corners.

In contrast to the previous tests, however, mid-span deflections appear clearly independent of temperature. It seems likely that the slab is uniformly supported so that deflections of about 0.5 mm (under a 90-kN dual wheel load) represent full support conditions. This independence from temperature is also apparent from the joint horizontal movement.

While the results of Tests 536FD and 537FD for a similar structure (discussed in Chapters 4.5 and 4.6) showed both corner and edge deflections decreasing with increase in surface temperature (implying that the slabs were curled up at least during the major part of the testing), only the corner deflections exhibit this response in this test. Again this is viewed as an indication of upward curl. However, the results also show that there was little or no curl at the mid-span.

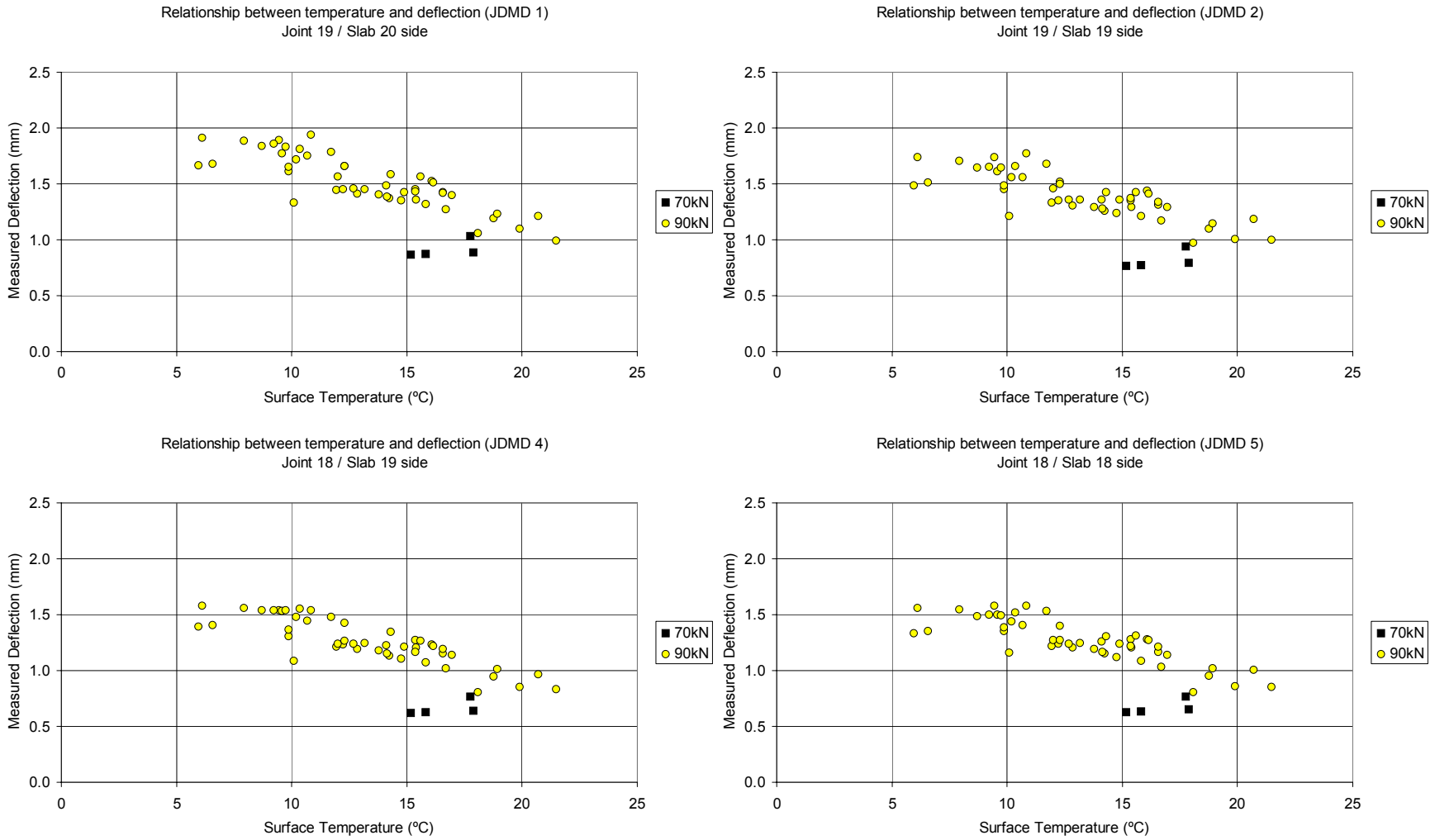

Figure 76. Effect of temperature on joint deflections, Test 538FD.

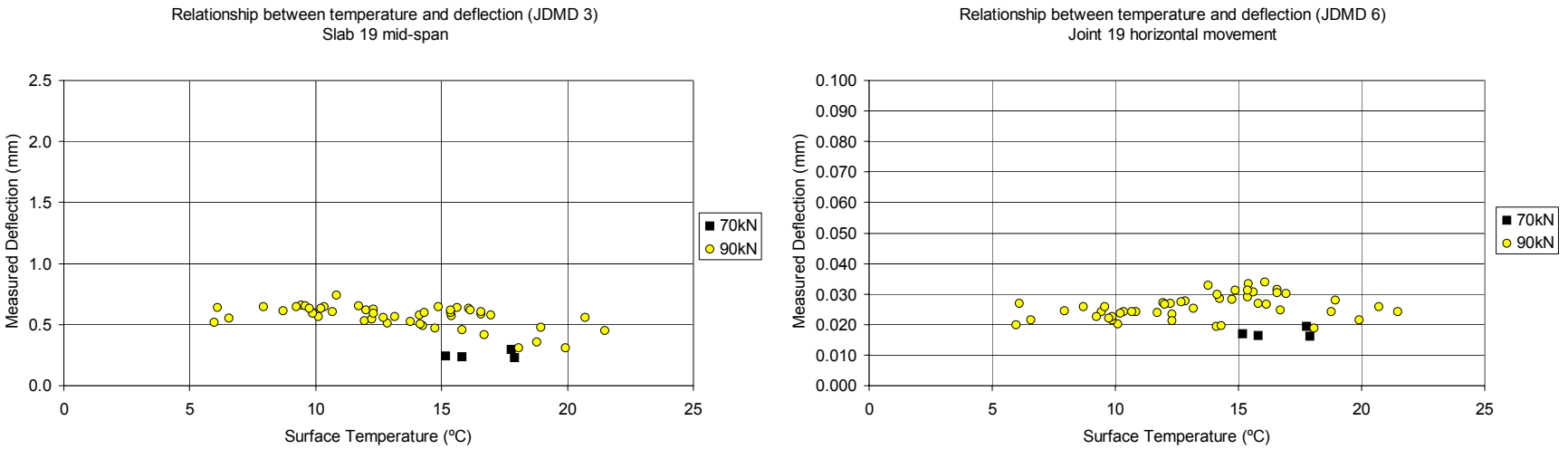

Figure 77. Effect of temperature on mid-span and horizontal deflections, Test 538FD.

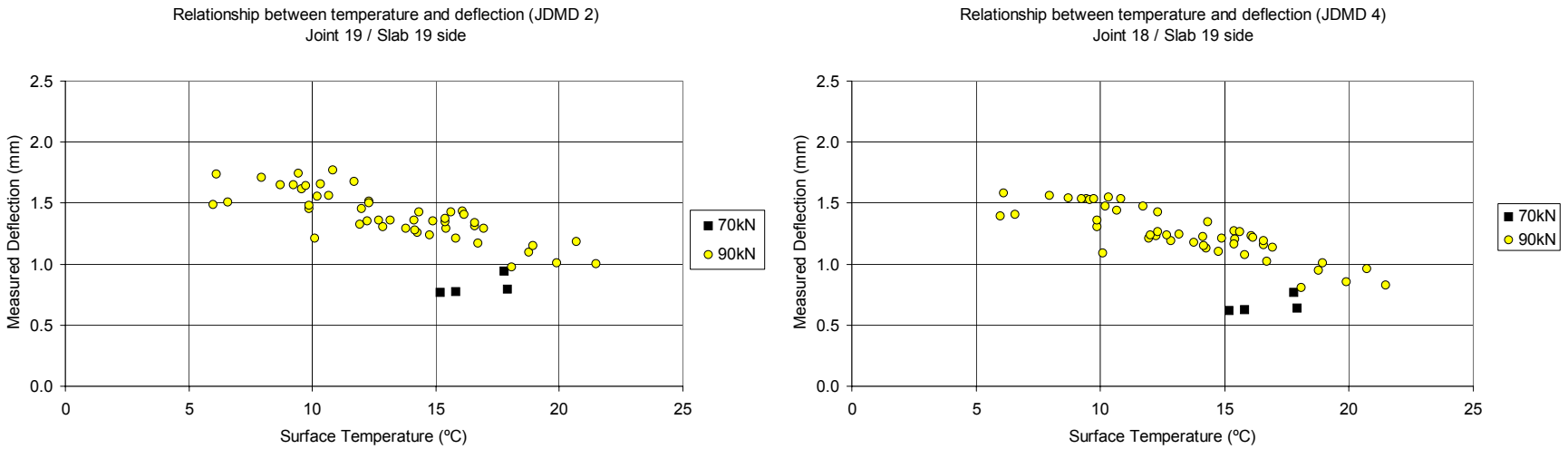

Figure 78. Relationship between temperature and joint deflection, Test 538FD.

This reflects the lower overall temperature regime during this test because there is nothing to suggest behavior should differ from Tests 536FD and 537FD, which were conducted at higher temperatures.

4.7.2.3 Permanent Deformation

The JDMD and EDMD monitoring of permanent deformation based on these surface-mounted gauges was reviewed and not found satisfactory. Apart from possible physical displacements of the gauges, the effects of temperature further complicate the results. However, JDMD results are reviewed here because permanent deformation was not monitored by MDD during this test.

Figure 79 gives the permanent deformation data from all six JDMDs together with the surface temperature and temperature differential profiles.

The large drop in JDMD 2 readings at around 70,000 repetitions can only be attributed to an artificial shift in reading in the order of 1 to 1.2 mm, which should be added to all subsequent JDMD 2 readings.

The significant increase in deflections between 100,000 to roughly 105,000 repetitions cannot be discounted because it is recorded on all five of the vertical JDMDs but not on the horizontal one (JDMD 6). The movement is on the order of 0.7 to 0.8 mm at each end of Slab 19 and on the ends of the adjacent slabs across the joints. Movement is about 0.4 mm at the mid-span position of Slab 19.

For JDMDs 4 and 5 (either side of Joint 18), the responses are very similar throughout and the rate of permanent deformation noticeably increases after this apparent displacement. The response is not so marked for JDMDs 1 and 2 (either side of Joint 19). However, for these

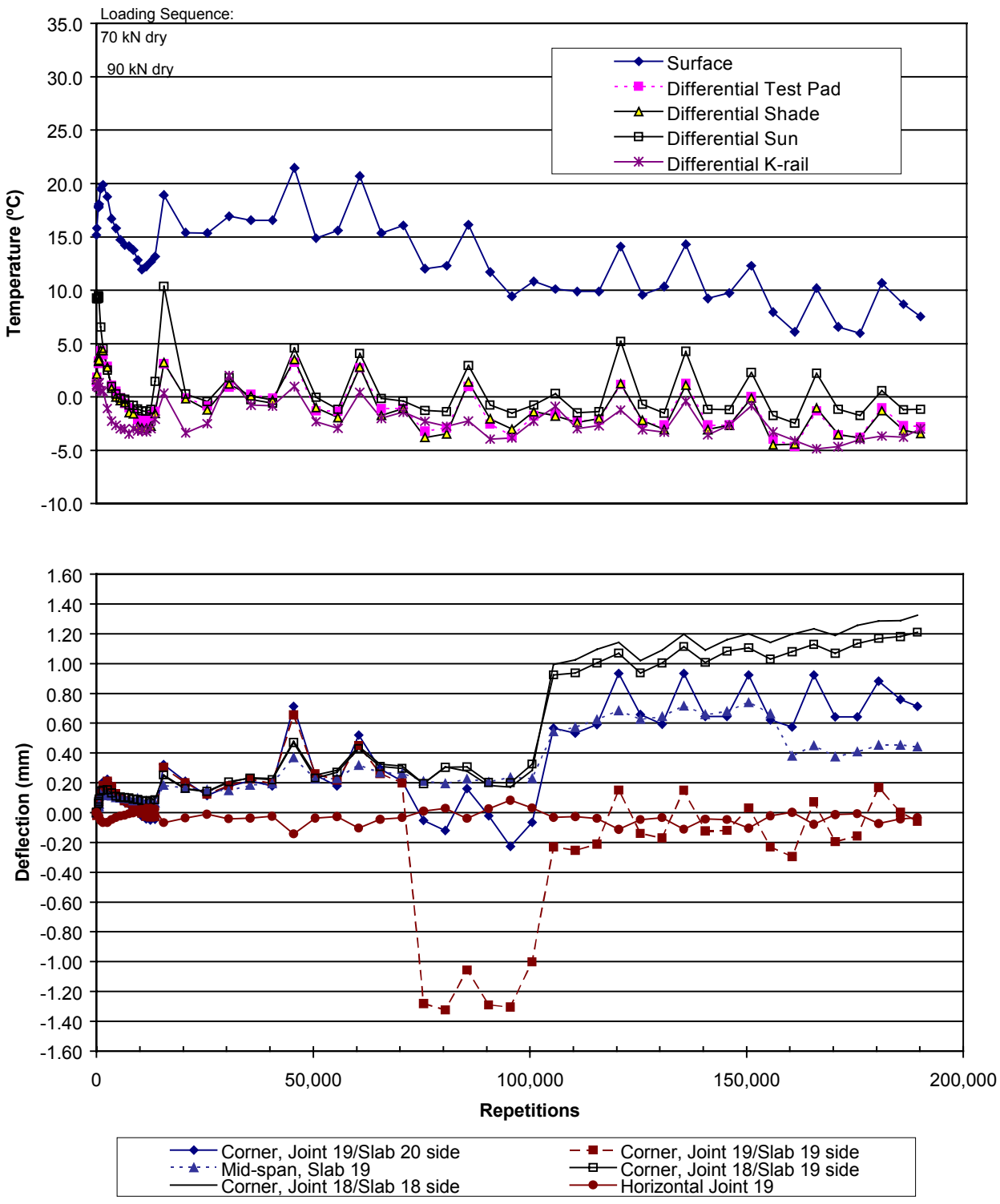

Figure 79. Plot of JDMD permanent deformation and temperature versus load repetitions, Test 538FD.

gauges, the temperature-induced variation is much more evident (from about 75,000 repetitions) whereas it is almost lacking for JDMDs 4 and 5.

The mid-span gauge (JDMD 3) shows a response closer to those at Joint 18 (JDMDs 4 and 5) with little temperature-induced variability and a markedly increased rate of deformation after the large displacement. At about 160,000 repetitions, it shows a distinct decrease in "permanent deformation" (an uplift).

Accepting these data as essentially a valid record of the long-term movements at the top of the pavement, it seems that there was a significant drop/displacement of the slabs in the test section between about 100,000 and 105,000 repetitions. At this stage, the surface temperature at the time of monitoring was consistently about 10ºC. The subsequent increasing permanent deformation suggests that the slabs did in fact displace downwards, making better contact with the support and transmitting more stresses to the underlying layers. This scenario could be attributed to the lower temperature and thermal shrinkage easing possible binding at the joints. However, it seems more likely to be caused by longitudinal weakening of the test section and subsequent movement under HVS trafficking. No longitudinal cracking was observed during the test but this is not regarded as necessarily significant.

As noted previously, the elastic deflections (shown in Figures 74 and 75) were increasing but then all dropped significantly after 105,000 repetitions or so. This is consistent with a partial reseating of the slab followed by better support.

4.7.3 Multi-Depth Deflectometer (MDD) Results

No MDDs were installed on this test section.

4.7.4 Load Transfer Efficiency (LTE)

Figure 80 shows the peak deflections on each side of Joints 19 and 18 as measured in the same data set and previously shown against repetitions (Figure 74) and surface temperatures (Figure 76). The deflections were measured on each side of a particular joint at the same repetitions and applied test load.

As before, the data are grouped in terms of traffic load/test load. Thus, the predominant data set is from the 90-kN dual wheel load trafficking phase, from 500 to the end of the test (189,000 repetitions).

At Joint 19, the data points lie distinctly away from the line of equality with the Slab 19 side deflections slightly lower than those on the Slab 20 side. The general trend shows high correlation. The consistency in response suggests constant LTEs, but also suggests values less than unity (100 percent).

The results for Joint 18 are consistent and lie on the line of equality. This again suggests constant LTEs. However, LTE values in this case are around unity (100 percent).

Figure 81 gives the deflections at each end of Slab 19 (Joints 18 and 19) which shows that, on the slab itself, deflections on the Joint 18 side were slightly lower throughout. This implies that some difference existed in the support condition (which includes underlying layers and the joint load transfer) that remained throughout the test.

Figure 82 gives the calculated LTEs for both sides of each joint together with the surface temperature and slab temperature differential. This shows that the LTEs are generally close to 80 percent across both joints. This contrasts with the inference (from Figure 80) that LTEs for Joint 18 should be close to 100 percent.

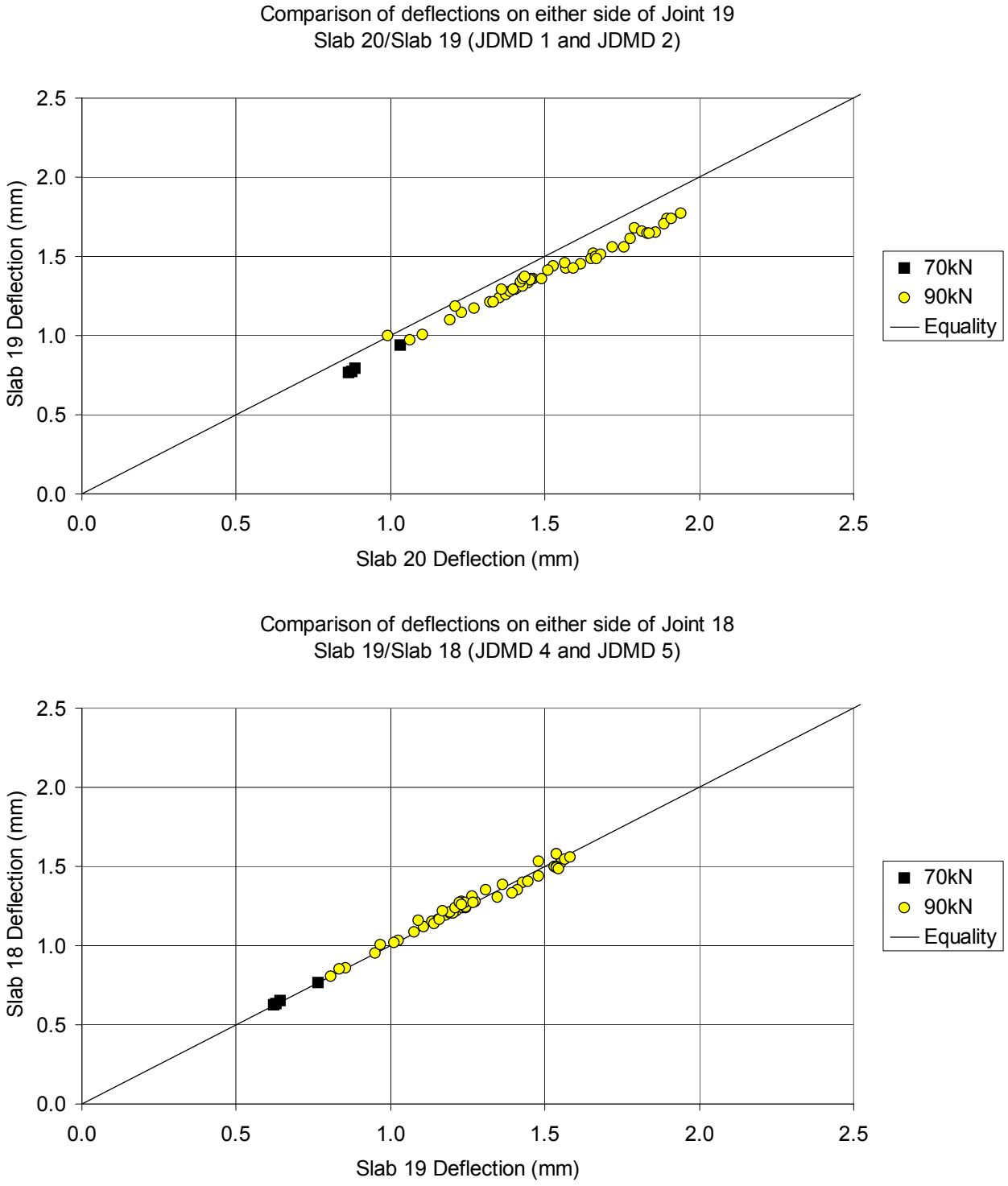

Figure 80. Comparison of deflections on both sides of Joints 18 and 19, Test 538FD.

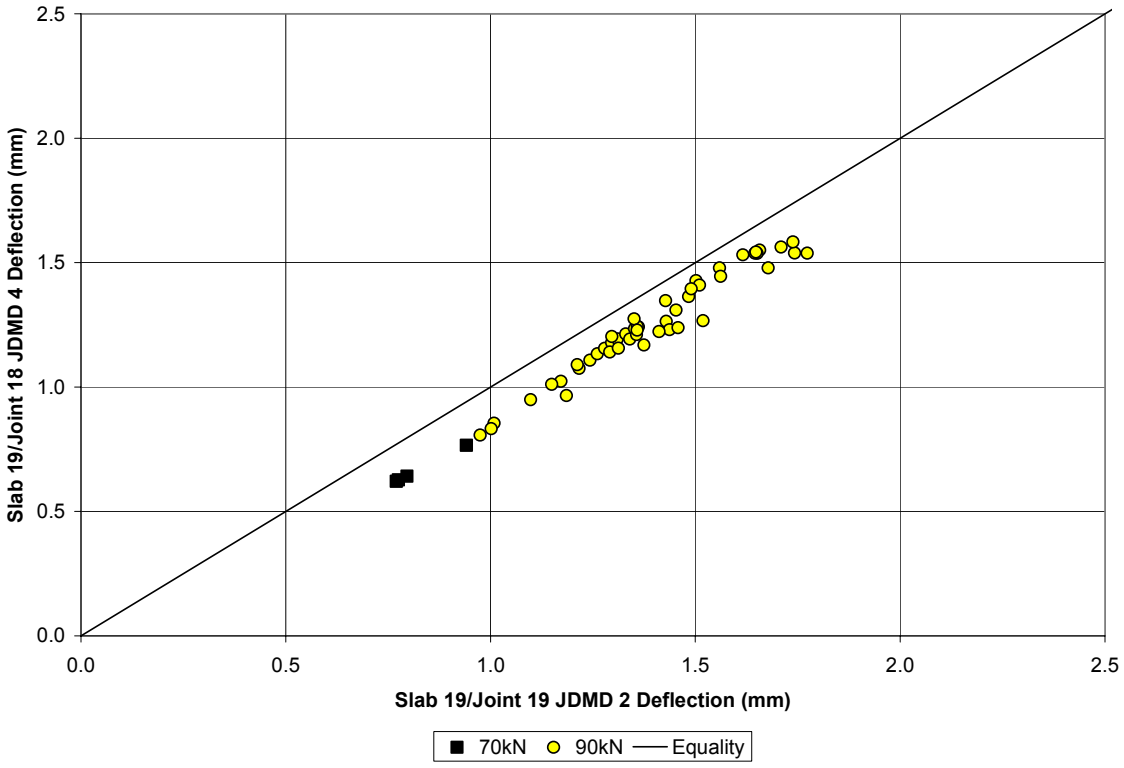

Figure 81. Comparison of deflections on either side of Slab 19 (Joints 18 and 19), Test 538FD.

Figure 83 also confirms that the LTEs for both joints were essentially in the range of 80 to 87 percent with Joint 18 having slightly better LTEs.

In line with the discussion for Test 536FD, it seems that the present definition and calculation of LTE will return values of 100 percent if uniform deterioration takes place on each side of a given joint. This implies similar changes in deflection responses but not necessarily identifying joint deterioration per se.

The disparity of LTEs with the comparison of maximum deflections on either side of the joints suggests cautious interpretation of calculated LTEs and the need for more detailed inspection of the method and its use.

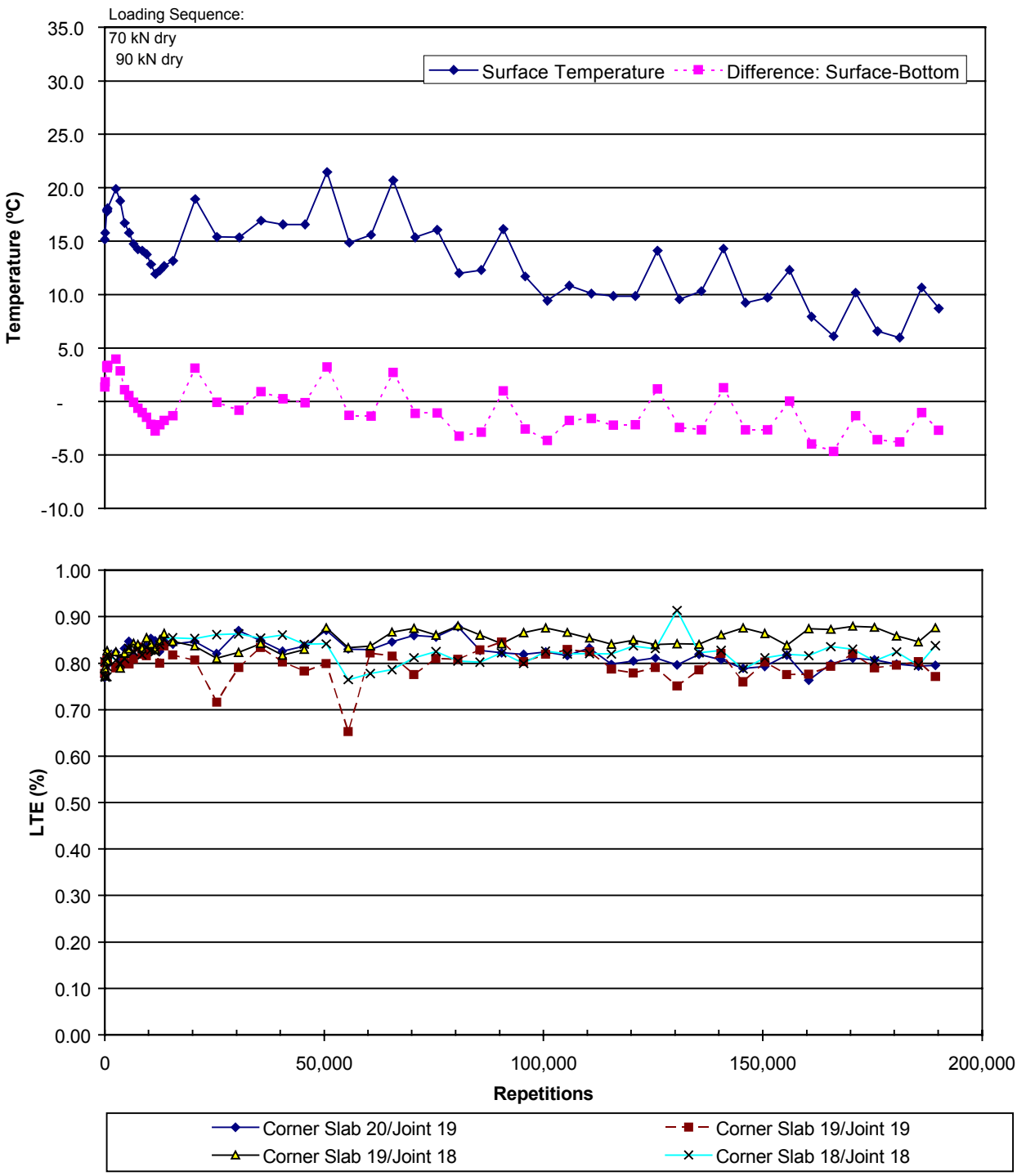

Figure 82. Plot of LTE and temperature versus load repetitions, Test 538FD.

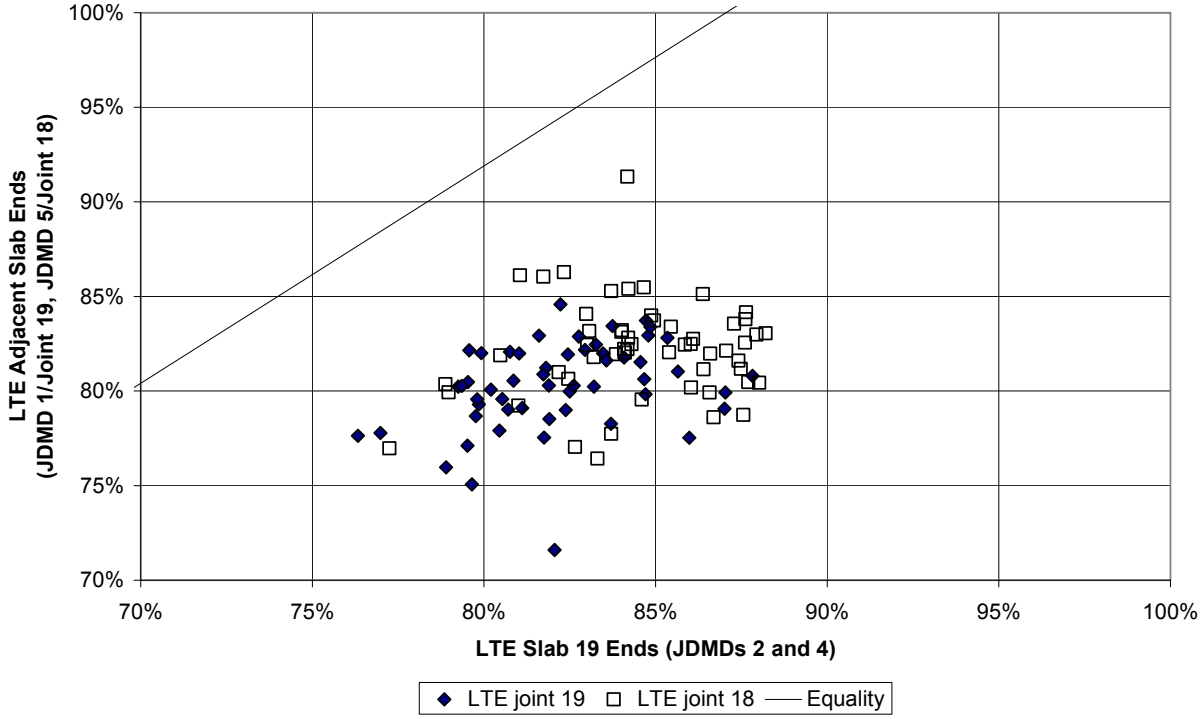

Figure 83. Comparison of LTE at each end of Slab 19 (Joints 18 and 19), Test 538FD.

4.8 Test 539FD

Test 539FD was performed on Slabs 10, 11, and 12 on the North Tangent. Slab 11 (total length of 3.85 m, total width 4.26 m) was fully tested together with some area on either side of Joints 10 and 11. The test was conducted under ambient temperature conditions (no temperature control chamber).

Test 539FD was the first of 3 tests on Section 11 on the North Tangent. Section 11 consisted of 200-mm FSHCC test pavement with dowels and an asphalt shoulder (no tie bars). The design lane width was increased 4.26 m (an increase from the typical 3.66-m regular lane width); the sections were designated “widened truck lane” sections.

The test was begun with a 40-kN (690-kPa) dual wheel load and was kept constant up to 13,342 repetitions, after which the dual wheel load was increased to 70 kN (690 kPa). This load

was applied for 500 repetitions until 13,842 repetitions. The load was then increased to a 90-kN (690-kPa) dual wheel load for 305,004 repetitions. The test was stopped after 318,846 repetitions. The whole test was performed in a nominally dry state with no water added to the pavement. Bi-directional trafficking was applied throughout the test.

One important difference between the trafficking of all tests done on Section 11 (in contrast to tests conducted on Sections 7 and 9) is that loading was not applied right on the edge of the slabs, as is illustrated in the placement of the HVS wheelpath in Figure 11. In places where widened truck lanes are used on in-service pavements, road striping keeps traffic following the alignment of a regular 3.6 m width slab so that the extended width serves as a concrete shoulder. Thus, to simulate real traffic patterns, the HVS load wheel was run next 0.6 m from the edge of the slab, where the striping would be on the widened truck lane slabs (where a normal 3.66-m lane width would have ended).

The philosophy behind the widened truck lane design is that because the traffic is directed 0.6 m away from the slab edge, the load is moved away from the critical location and edge stresses and strains will be less. This should lead to longer pavement life than traditional concrete slabs subjected to edge loading.

Standard 40-kN (690-kPa) dual wheel load pavement response measurements were not performed for the duration of the test. Therefore, all pavement response data are reported at the indicated trafficking load level. In the tables, data for the three different load levels are shown.

4.8.1 Visual Observations

The crack pattern that developed is shown schematically in Figure 84. Figure 85 presents a composite image of the test section at the completion of HVS trafficking. The orientation of the

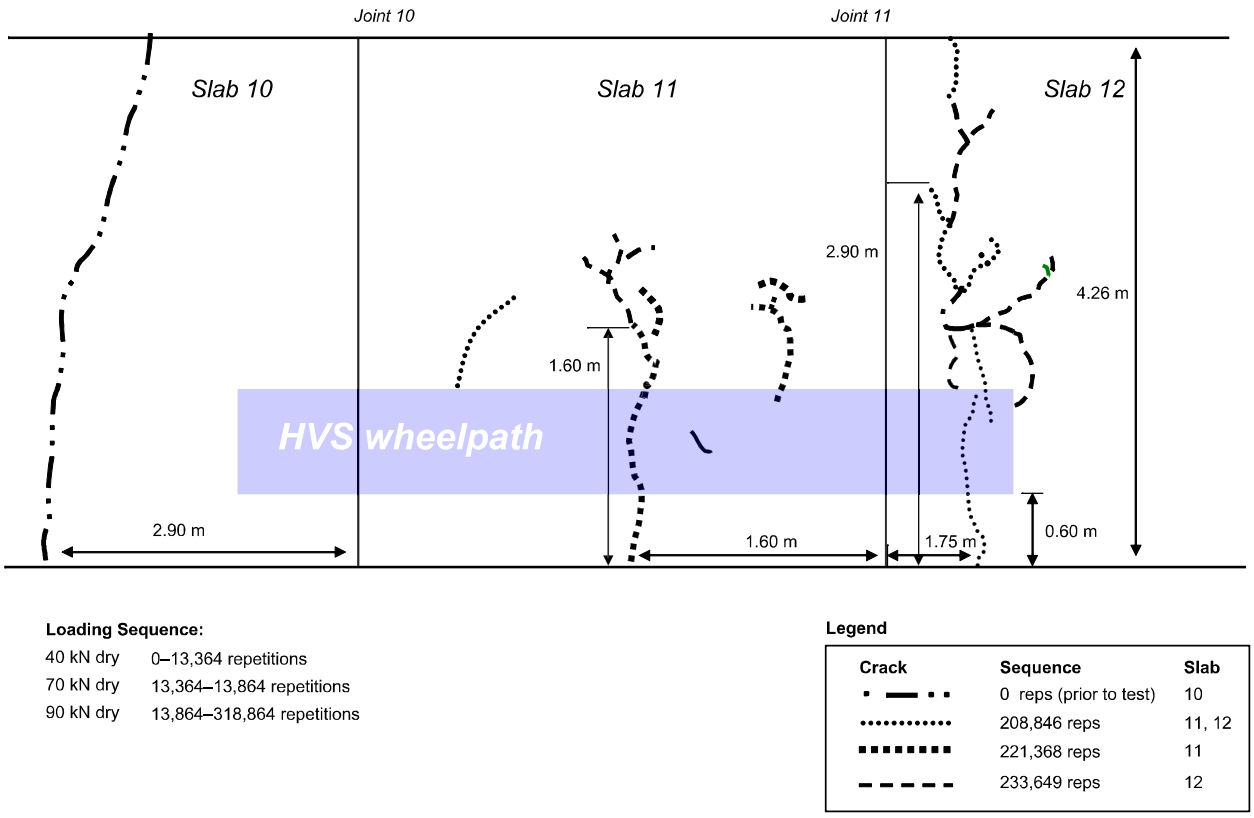

Figure 84. Schematic of crack pattern, Test 539FD.

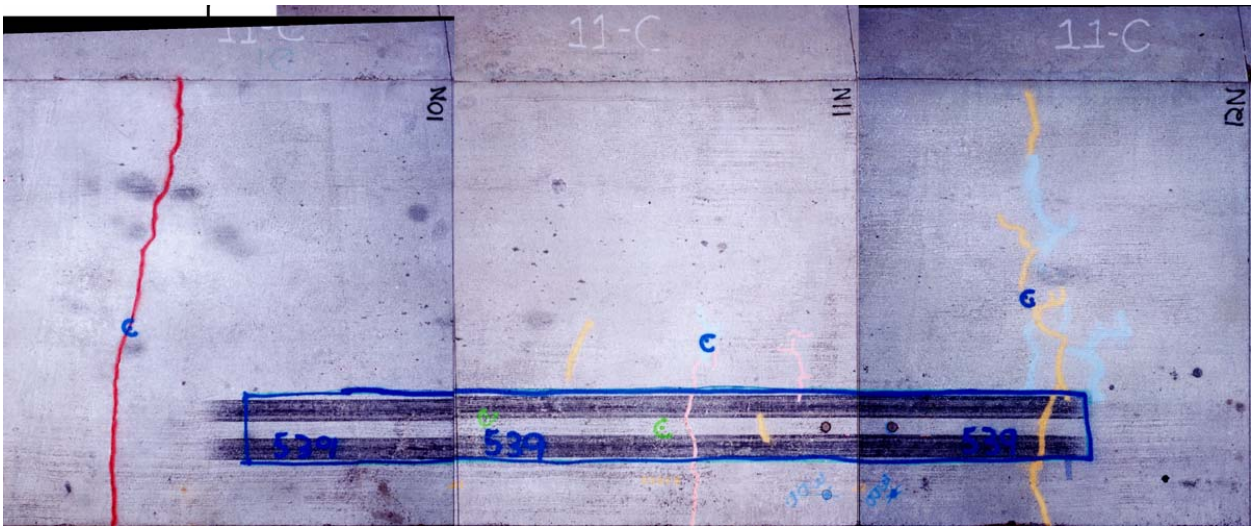

Figure 85. Composite image of Test 539FD showing cracks.

figure is such that the outer shoulder is at the bottom of the page (the trailer side) and the inner shoulder (the opposing traffic side) is at the top of the page. The first cracks developed after 208,846 repetitions in the center area of Slab 11 outside the testing area next to the test section and approximately 1,750 mm from Joint 11 on Slab 12. All were transverse cracks. This was followed by cracks developing after 221,368 repetitions at mid-span of Slab 11 across the test section, as well as a crack developing at quarter span of Slab 11 closer to Joint 11.

4.8.2 Joint Deflection Measuring Device (JDMD) Results

Four Joint Displacement Monitoring Devices (JDMD) were placed on either side of Joints 10 and 11 (transverse joints of Slab 11) and one at the mid-span edge of Slab 11. One JDMD was placed horizontally between the transverse joint of Slab 11 and Slab 12 (Joint 11). These instruments were used to record the elastic movement of the concrete slab under the influence of the HVS wheel load (see Figure 10). Table 20 summarizes maximum vertical deflections at the edge of the midpoint of Slab 11, corner edge deflections on either side of the two joints (Joints 10 and 11), maximum horizontal deflection at the center of Joint 11, and temperature data.

The data are also graphically displayed in Figure 86. These data should be analyzed together with the crack pattern as displayed in Figure 84 to enable clear interpretation.

It is first important to realize the effect of temperature on the measured deflection values. It appears as if an inverse relationship exists between the temperature and the vertical elastic deflections, which agrees with all previous tests.

A comparison of vertical deflections measured at the two corners indicates that vertical deflections of Slab 12 were slightly higher than those of Slab 11. Vertical deflections of Slab 11

Table 20 JDMD Deflections (Test loads 40 kN, 70 kN, 90 kN), Test 539FD

Repetitions	Test Load kN	Deflection (mm)						Temperature (ºC)	
		Corner, Joint 11		Mid-span, Slab 11	Corner, Joint 10		Horizontal Joint 11	Surface	Difference (top - bottom)
		Slab 12	Slab 11		Slab 11	Slab 10			
		JDMD 1	JDMD 2	JDMD 3	JDMD 4	JDMD 5	JDMD 6		
0	40	0.838	0.817	0.233	0.675	0.680	0.007	22.3	-1.0
13,342		0.885	0.859	0.249	0.729	0.727	0.008	20.5	-1.3
13,354	70	0.975	0.958	0.273	0.796	0.806	0.007	21.3	-1.1
13,844		0.984	0.957	0.276	0.819	0.826	0.008	20.5	-1.9
13,856	90	1.020	0.989	0.283	0.851	0.864	0.006	21.6	-1.3
53,847		1.157	1.124	0.321	0.985	1.000	0.008	21.8	-1.2
103,847		1.287	1.255	0.477	1.158	1.172	0.009	27.9	1.5
153,846		1.333	1.300	0.530	1.259	1.261	0.011	27.8	-0.7
203,846		1.234	1.211	0.578	1.181	1.161	0.014	28.2	-1.9
253,847		1.033	1.010	0.563	1.027	1.011	0.012	30.0	-1.4
308,846		1.482	1.435	0.672	1.388	1.382	0.013	18.9	-4.3
313,846		1.506	1.467	0.748	1.457	1.461	0.017	20.8	-4.3

were slightly higher than those of Slab 10. This may be related to slab length because Slab 12 was shorter than Slab 11, which was shorter than Slab 10.

A comparison of the vertical deflections measured at the corners of the two slabs and at mid-span of the slab indicates that the deflections at mid-span were only 25 to 50 percent of the magnitude of the elastic deflections at the corners of the two slabs. Similar fluctuations were observed for the data from the various instruments.

The horizontal movement measured at mid-span of Joint 11 was almost negligible when compared with the vertical elastic deflections, although they also increased with increased load levels and repetitions. Horizontal movements were on the order of 1 percent of the vertical movements (note scale on right side of Figure 86.).

In summary, it appears that the applied loads, slab lengths, and temperatures affected the vertical and horizontal elastic deflections. Comparing deflections observed during Test 539FD to deflection observed during tests on sections with the normal lane width (Tests 532FD–535FD), the following is noted:

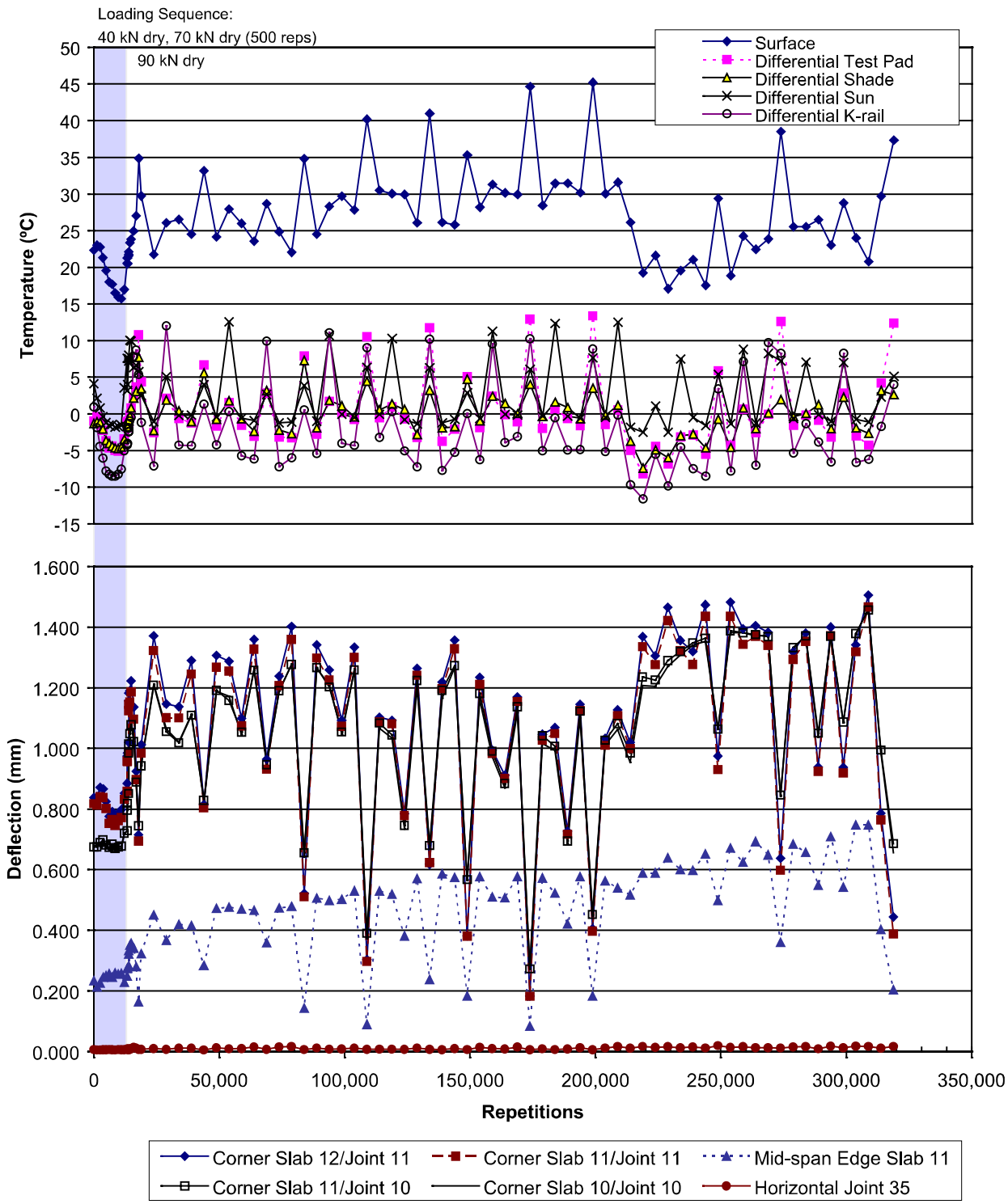

Figure 86. Plot of JDMD deflections and temperature versus load repetitions, Test 539FD.

- The corner deflections of the widened lanes (4.26 m) are significantly lower than those of standard width lanes (3.66 m): a nearly 50-percent reduction in deflections was observed.
- The mid-span edge deflections of the widened lanes were similar to those of the standard width lanes (around 0.7 mm).

Likely causes for these observations are that Tests 532FD–535FD had no load transfer devices, which produced high corner deflections. Dowels installed in Test 539FD resulted in lower corner deflections. Remember that during the tests conducted on Section 11 (widened truck lane sections) the trafficking load was not applied at the edge, but the deflection measurement devices were still placed along the edge of the concrete slabs.

It is also important to note that no significant reduction in mid-span edge deflections was observed. The additional slab width can be concluded to have had a limited influence in controlling the edge deflections at mid-span. One possible explanation for this behavior may be the upward curling effect caused by differential shrinkage and temperature differentials between the top and the bottom of the slab. Slab lift-off will cause significant edge deflections regardless of the additional width of the slabs.

4.8.3 Joint Load Transfer Efficiency (LTE)

The Load Transfer Efficiency (LTE) was calculated at Joints 10 and 11 adjacent to the center slab (Slab 11). LTE is defined as the ratio between the deflections on the unloaded slab with respect to the deflection on the loaded slab at the joint. LTE was calculated for the HVS wheel running in the cabin to tow end direction. The calculated LTEs are shown in Table 21 for the beginning and end of each of the three stages of the test (40 kN, 70 kN, and 90 kN). No clear

trend is seen with increased trafficking, formation of cracks, or pavement temperature. LTE values indicate that full load transfer took place for the duration of the test without any decrease.

Table 21 Load Transfer Efficiency, Test 539FD

Repetitions	Test Load, kN	Load Transfer Efficiency (%)				Temperature (ºC)	
		Corner, Joint 11		Corner, Joint 10			
		Slab 12	Slab 11	Slab 11	Slab 10		
		JDMD 1	JDMD 2	JDMD 4	JDMD 5	Surface	Difference (top – bottom)
0 –	40	99.8	99.6	99.0	98.2	22.3	-1.0
13,342		99.4	99.7	99.6	99.7	20.5	-1.3
13,354 –		99.5	98.8	99.7	99.4	21.3	-1.1
13,444 –	70	99.9	100.0	99.5	99.8	20.5	-1.9
13,844		99.7	99.6	99.9	99.6	21.6	-1.3
13,856–		99.6	99.8	99.6	99.2	21.8	-1.2
53,847–		99.5	99.1	99.5	98.6	27.9	1.5
103,847–		99.6	99.0	99.4	99.3	27.8	-0.7
153,846–	90	99.8	99.8	99.4	99.3	28.2	-1.9
203,846–		99.2	99.6	99.3	99.1	30.0	-1.4
253,847–		99.4	97.9	99.7	99.6	18.9	-4.3
313,846		99.3	99.3	99.6	99.6	29.7	4.2

4.8.4 Multi-Depth Deflectometer (MDD) Elastic Deflection Results

Two MDDs were installed on Test 539FD. They were positioned 300 mm from either side of Joint 11, one in Slab 11 (MDD 5) and one in Slab 12 (MDD 4) (see Figure 10). Both were installed between the wheel paths of the dual wheels about 900 mm from the edge of the slab. MDD modules were placed at the surface and at depths of 200, 425, and 650 mm. The peak MDD elastic deflections can be seen in Tables 22 (MDD 5) and 23 (MDD 4) and in Figures 87 (MDD 5) and 88 (MDD 4).

The vertical elastic deflections measured on the surface and at a depth of 200 mm were very affected by the temperatures on the concrete pavement (Figure 87). A clear trend could not be identified with increasing load repetitions. The vertical elastic deflections of the two lower

Table 22 MDD 5 Deflections (Test Loads 40 kN, 70 kN, 90 kN), Test 539FD

Repetitions	Test Load, kN	Deflection (mm) MDD 11, Slab 32				Temperature (°C)	
		0 mm	200 mm	425 mm	650 mm	Surface	Difference (top – bottom)
0–	40	327	270	30	14	22.3	-1.0
13,342		353	292	25	11	20.5	-1.3
13,354–	70	394	327	28	20	21.3	-1.1
13,444–		406	338	29	14	20.5	-1.9
13,844		460	384	39	16	21.6	-1.3
13,856–	90	485	417	30	20	21.8	-1.2
53,847–		481	428	30	19	27.9	1.5
103,847–		420	392	21	19	27.8	-0.7
153,846–		336	327	32	28	28.2	-1.9
203,846–		516	449	43	25	30.0	-1.4
253,847–		512	447	58	36	18.9	-4.3
313,846		320	277	95	60	29.7	4.2

Table 23 MDD 4 Deflections (Test loads 40 kN, 70 kN, 90 kN) Test 539FD

Repetitions	Test Load, kN	Deflection (mm) MDD 11, Slab 32				Temperature (°C)	
		0 mm	200 mm	425 mm	650 mm	Surface	Difference (top – bottom)
0–	40	510	429	41	16	22.3	-1.0
13,342		561	425	30	20	20.5	-1.3
13,354–	70	637	500	47	18	21.3	-1.1
13,444–		645	512	42	15	20.5	-1.9
13,844		726	606	66	15	21.6	-1.3
13,856–	90	795	630	90	29	21.8	-1.2
53,847–		838	620	74	28	27.9	1.5
103,847–		770	572	76	30	27.8	-0.7
153,846–		632	512	107	40	28.2	-1.9
203,846–		882	624	66	28	30.0	-1.4
253,847–		885	641	97	42	18.9	-4.3
313,846		543	489	155	73	29.7	4.2

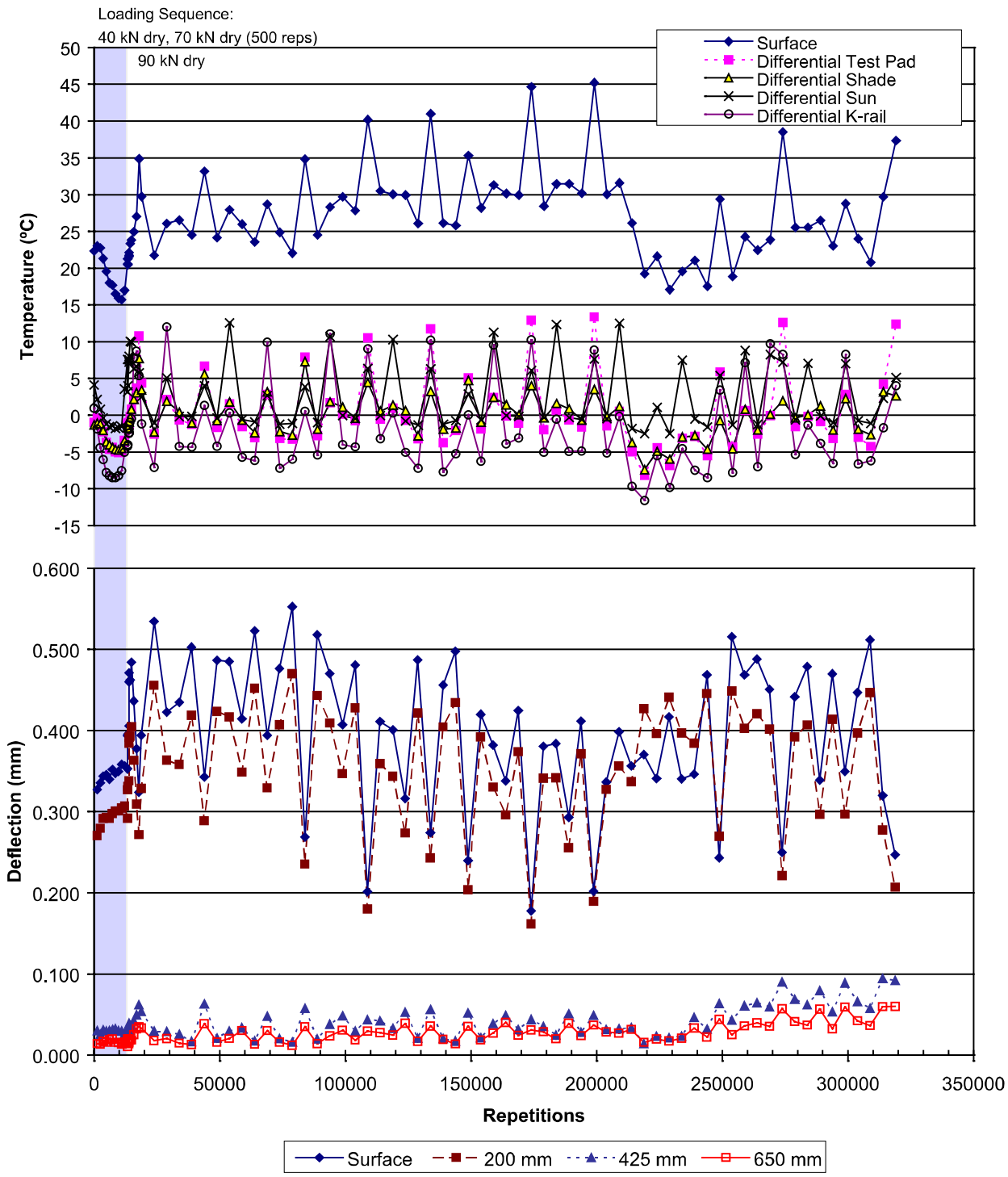

Figure 87. Plot of MDD 5 deflections and temperature versus load repetitions, Test 539FD.

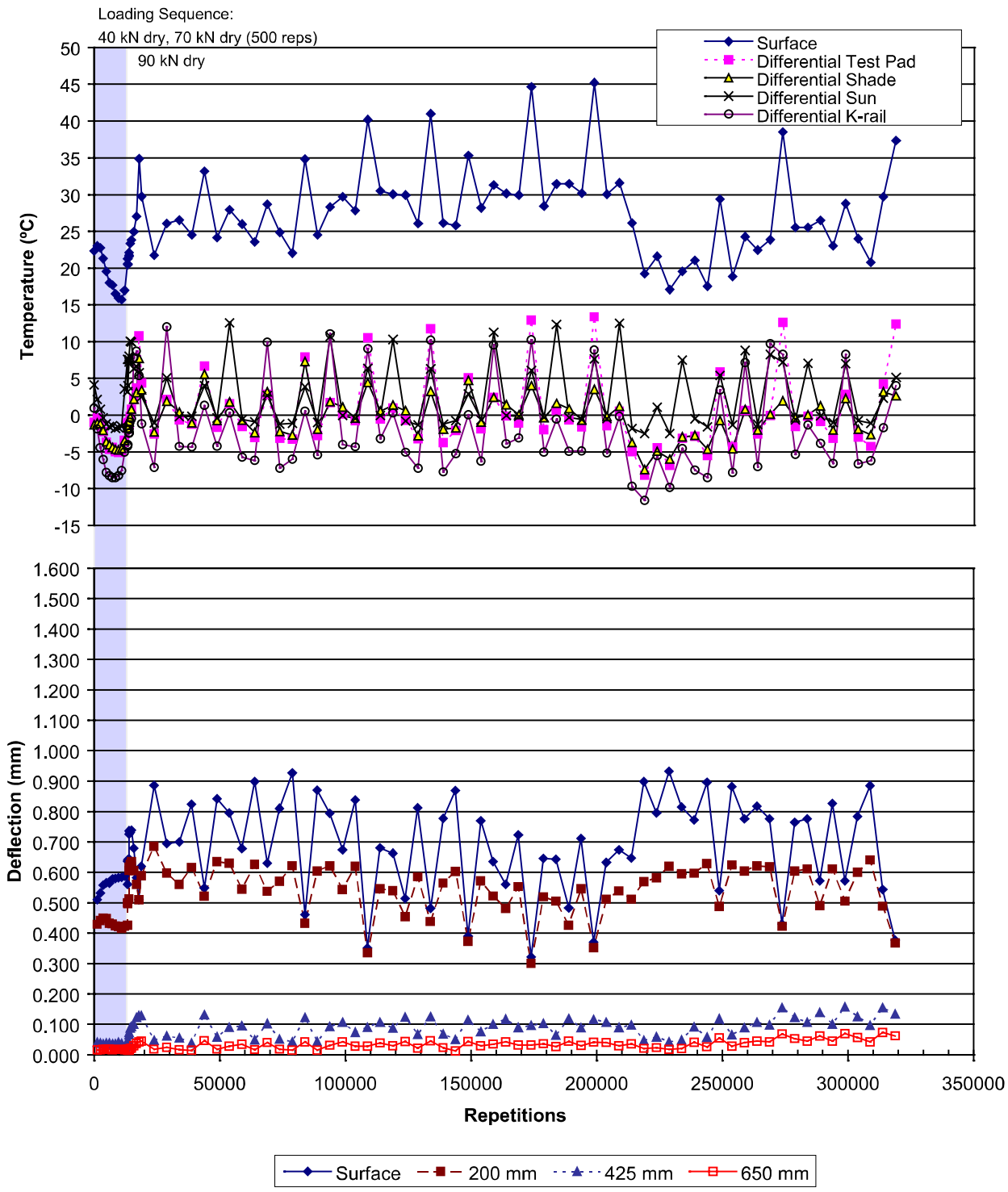

Figure 88. Plot of MDD 4 deflections and temperature versus load repetitions, Test 539FD.

MDD modules (425 mm and 650 mm) were substantially lower than those of the two upper modules, which indicates a high degree of stress dissipation with depth in the sub-structure.

The vertical elastic deflections measured on Slab 12 (MDD 4) were slightly higher than those measured on Slab 11 (MDD 5) for all the load levels and repetitions. This is in agreement with trends recorded by the JDMDs.

Comparing the MDD data from the widened truck lane test to those of the normal slab width tests (532FD–535FD) leads to the following conclusions:

- The MDD surface deflections are significantly lower in the widened truck lane test. Recorded surface deflections for the widened truck lane section were on the order of 0.85 mm (MDD 4) and 0.45 mm (MDD 5) for the 90-kN load whereas MDD surface deflections in excess of 2.2 mm were measured during Tests 532FD–535FD. This difference, representing a reduction in surface deflection of more than 60 percent using the same load (90 kN), highlights the beneficial effect of the widened lane. The lower deflections should lead to longer pavement life.
- The base course deflections (at 200 mm depth) were significantly higher in the widened truck lane test. Base course deflections on the order of 0.6 mm (MDD 4) and 0.4 mm (MDD 5) were recorded towards the end of the test (90-kN load) in comparison with values in the order of 0.2 mm for Tests 532FD–535FD.

One possible reason for these differences in deflection behavior is the position of the MDDs with respect to the longitudinal edge of the slabs. In Tests 532FD–535FD, the MDDs were placed about 300 mm from the edge (between the dual wheels). At this spot, differential shrinkage, slab warp, and curling effects produced slab lift-off resulting in high MDD surface deflections and low base course deflections. In Section 539FD (widened truck lane), the MDDs

were placed 600 mm farther away from the longitudinal edge of the slab. At this spot (900 mm from the edge), the slab was in contact with the base course and significantly higher base deflections were recorded. Furthermore, the wider slab had better support from the sub-structure which resulted in lower surface deflections.

4.8.5 Multi-Depth Deflectometer (MDD) Permanent Deformation Results

The permanent deformation of the upper part of the pavement was measured using the two MDDs. Permanent deformations were recorded at the surface and depths of 200, 425 and 650 mm. Results are summarized in Tables 24 (MDD 5) and 25 (MDD 4) and in Figures 89 (MDD 5) and 90 (MDD 4).

The data indicates a clear temperature-related trend with measured values increasing and decreasing with fluctuating daily temperatures. This gives rise to "negative" permanent deformation values at some load repetitions. However, it is connected to the behavior of the MDD as reported for the vertical elastic deflections.

The data further indicates a trend of higher deflections with increasing number of load repetitions. There is a significant drop followed by increasing permanent deformation values after approximately 220,000 repetitions (Figures 89 and 90). This change in behavior is possibly due to the transverse crack that appeared at mid-span after approximately 220,000 load repetitions (Figure 84). Another important observation is that the deformation in the base was very similar to what was recorded at the surface. This result further substantiates the conclusion that in the case of the widened lane, the concrete slabs were in full contact with the base at a distance of 900 mm from the longitudinal edge.

Table 24 MDD 5 Permanent Deformation, Test 539FD

Repetitions	Test Load, kN	Permanent Deformation (mm)			
		MDD 5, Slab 11			
		0 mm	200 mm	425 mm	650 mm
1,223	40	0.042	0.045	0.005	0.000
13,342		-0.054	-0.022	-0.001	-0.006
13,354	70	-0.114	-0.073	-0.013	-0.007
13,444		-0.108	-0.069	-0.015	-0.006
13,844		-0.068	-0.039	-0.015	-0.008
13,856	90	-0.061	-0.029	-0.015	-0.008
53,847		0.302	0.319	0.056	0.002
103,847		0.338	0.355	0.063	0.003
153,846		0.396	0.454	0.083	0.016
203,846		0.577	0.594	0.114	0.039
253,847		0.370	0.455	0.092	0.021
303,846		0.589	0.619	0.113	0.029
313,846		0.761	0.785	0.121	0.036

Table 25 MDD 4 Permanent Deformation, Test 539FD

Repetitions	Test Load, kN	Permanent Deformation (mm)			
		MDD 4, Slab 12			
		0 mm	200 mm	425 mm	650 mm
1,223–	40	0.068	0.061	0.005	-0.004
13,342		-0.099	-0.072	-0.006	-0.010
13,354–	70	-0.189	-0.157	-0.027	-0.005
13,444–		-0.179	-0.148	-0.026	-0.005
13,844		-0.118	-0.105	-0.026	-0.007
13,856–	90	-0.101	-0.084	-0.018	-0.002
53,847–		0.472	0.325	0.157	0.013
103,847–		0.501	0.351	0.200	0.025
153,846–		0.636	0.433	0.253	0.042
203,846–		0.909	0.598	0.321	0.072
253,847–		0.612	0.461	0.303	0.065
303,846–		0.928	0.670	0.365	0.078
313,846		1.267	0.855	0.392	0.093

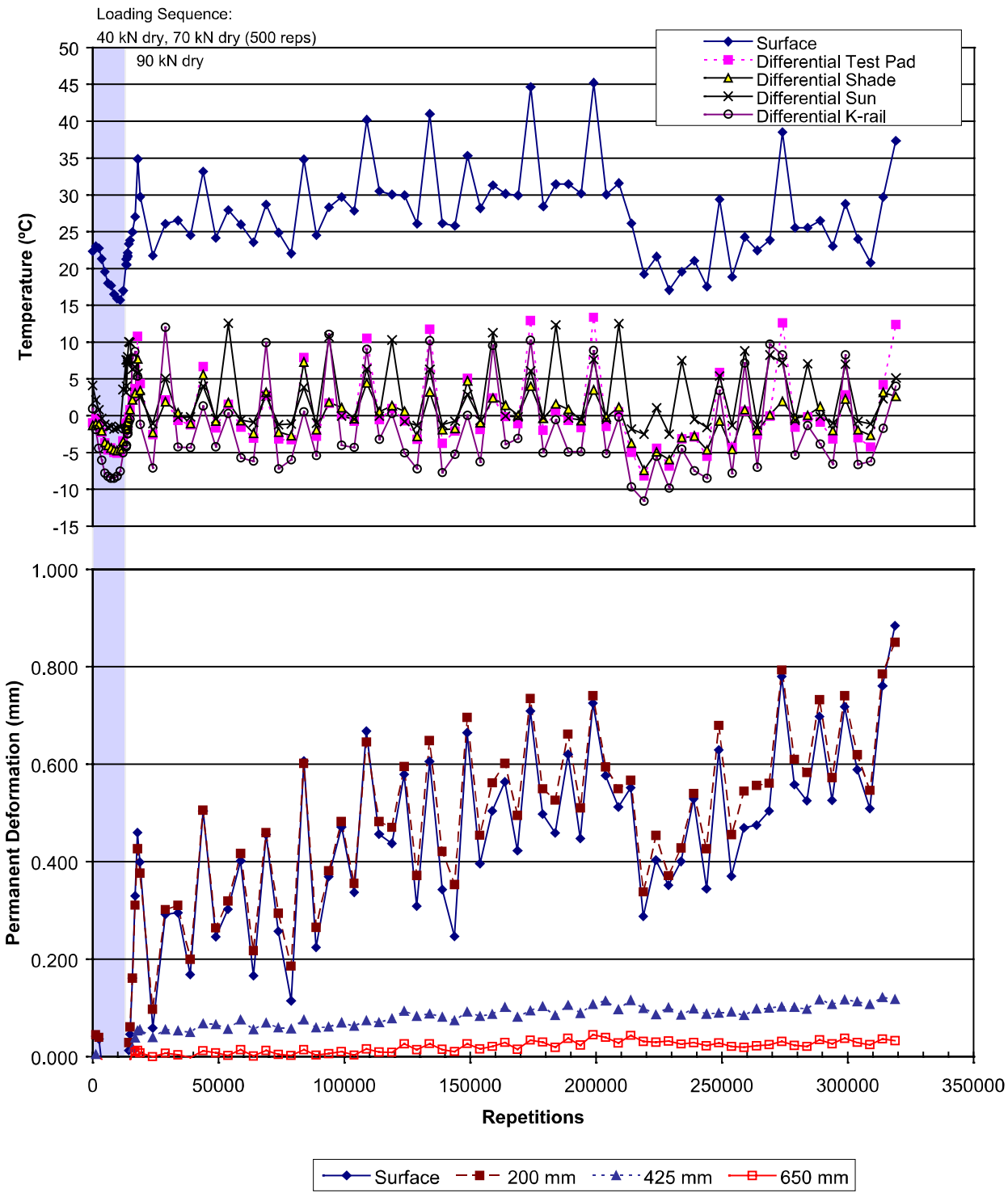

Figure 89. Plot of MDD 5 permanent deformation and temperature versus load repetitions, Test 539FD.

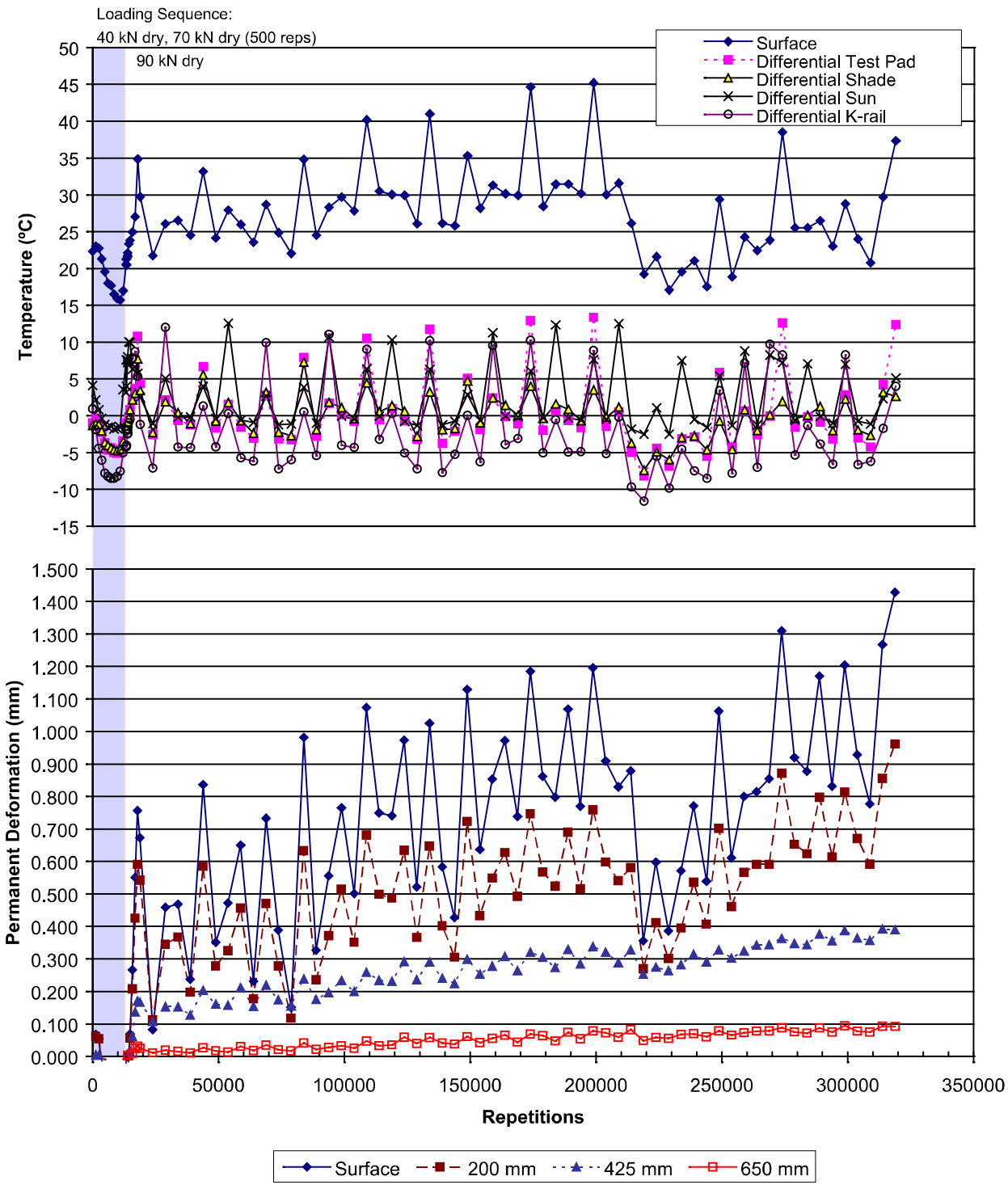

Figure 90. Plot of MDD 4 permanent deformation and temperature versus load repetitions, Test 539FD.

4.9 Test 540FD

Test 540FD was conducted on Slabs 6, 7, and 8 on the North Tangent. Slab 7 (total length 3.80 m, total width 4.26 m) was fully tested, together with some area on either side of Joints 6 and 7. The temperature control chamber was used during this test and the test was performed at a nominal temperature of 20ºC. This was the second of three tests on Section 11 on the North Tangent (200-mm FSHCC test pavement with dowels and asphalt shoulder, 4.26-m widened truck lanes).

The test was begun with a 40-kN (690-kPa) dual wheel load up to 13,003 repetitions after which the dual wheel load was increased to 70 kN (690 kPa). This load was applied for 392,062 repetitions until 405,065 total repetitions. At this point, the dual truck tires were replaced with a single aircraft tire and the load was increased from 70 kN to 150 kN (1100 kPa). This load was applied for an additional 142,398 repetitions until a total of 547,463 load repetitions was reached. The whole test was performed in the nominally dry state with no water added to the pavement. Bi-directional trafficking was utilized throughout the test.

Standard 40-kN (690-kPa) dual wheel load pavement response measurements were not performed during Test 540FD and so all pavement response data are reported at the indicated trafficking load level. Data for the three different load levels are boxed in the tables for easy differentiation.

4.9.1 Visual Observations

The crack pattern as it developed with time is shown in Figure 91. A composite image of the completed test section is shown in Figure 92. The orientation of the figure is such that the outer shoulder is at the bottom of the figure (the trailer side) and the inner shoulder (the opposing

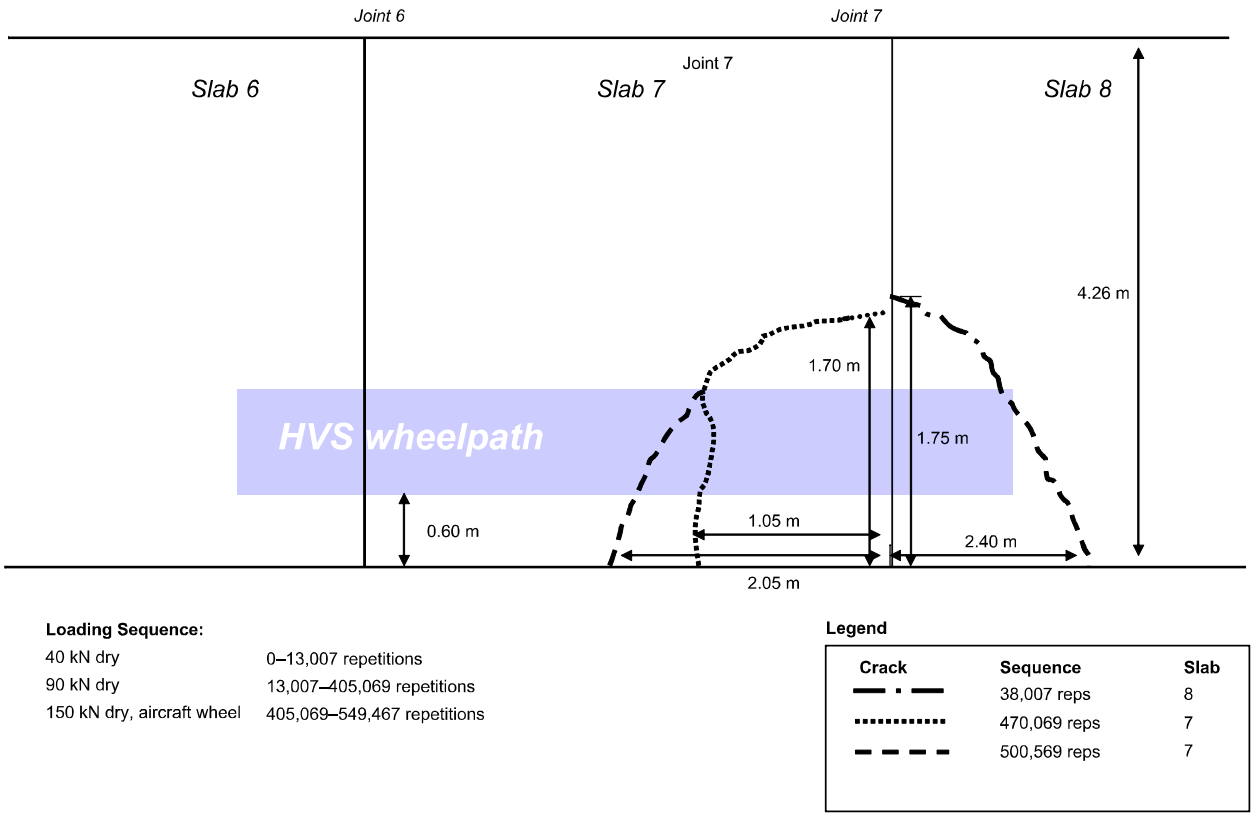

Figure 91. Schematic of crack pattern, Test 540FD.

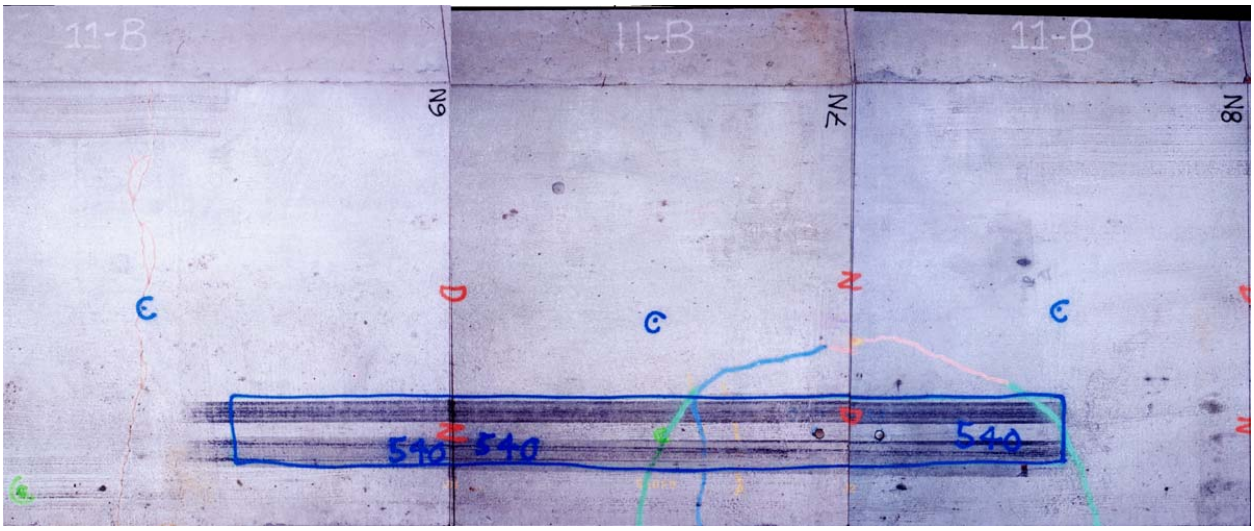

Figure 92. Composite image of Section 540FD showing crack pattern.

traffic side) is at the top of the figure. The first cracks developed after 38,007 repetitions on Slabs 7 and 8. The cracks were located about 1700 mm from the edge across Joint 7. The two cracks developed into two corner cracks on either side of Joint 7. After 500,569 repetitions, another transverse crack that connected with the previous corner crack appeared in the middle of Slab 7.

4.9.2 Joint Deflection Measuring Device (JDMD) Results

Four JDMDs were placed on either side of Joints 6 and 7 (the two sides of Slab 7) and one was placed on the edge of Slab 7 midway between the two joints. One JDMD was placed horizontally across the transverse joint of Slab 7 and Slab 8. These instruments were used to record the elastic movement of the slab under the influence of the HVS wheel loading (see Figure 11). Table 26 summarizes the results of the maximum vertical deflections at the edge of the midpoint of Slab 7 and the corner edge deflections on either side of the transverse joints (Joints 6 and 7), maximum horizontal deflection at the center of Joint 7, and temperature data.

JDMD data is graphically presented in Figure 93. These data should be analyzed together with the crack pattern shown in Figure 91 to enable clear interpretation.

It is important to acknowledge the effect of temperature on the measured deflection values. It appears as if an inverse relationship exists between the temperature and the vertical elastic deflections. As in the previous test (Test 539FD), this may have been caused by movement of the edges of the concrete slab, which was not linked structurally via dowels to the asphalt shoulder on the side where the measurements were taken.

A comparison of vertical deflections measured at the two corners indicates that vertical deflections of Slab 8 were mostly higher than those of Slab 7. Vertical deflections of Slab 7 were higher than the vertical deflections of Slab 6. This may be related to the direction of trafficking

Table 26 JDMD Deflections, (Test Load 40 kN, 90 kN, 150 kN) Test 540FD

		Deflection (mm)						Temperature (ºC)	
	Test	Corner, Joint 7		Mid-span,	Corner, Joint 6		Horizontal		Difference
	Load	Slab 8	Slab 7	Slab 7	Slab 7	Slab 6	Joint 7		(top -
Repetitions	kN	JDMD 1	JDMD 2	JDMD 3	JDMD 4	JDMD 5	JDMD 6	Surface	bottom)
0	40	0.779	0.765	0.244	0.499	0.493	0.008	20.6	-2.3
13,003		0.810	0.792	0.250	0.512	0.499	0.009	20.4	-2.6
13,016	90	1.335	1.317	0.462	1.030	1.015	0.014	19.2	-2.5
53,006		1.778	1.750	0.606	1.353	1.357	0.017	19.1	-1.3
103,005		1.752	1.707	0.613	1.365	1.376	0.021	20.0	-1.0
153,005		1.776	1.750	0.614	1.417	1.377	0.015	20.5	-1.0
203,005		1.780	1.758	0.619	1.442	1.401	0.018	19.7	-0.5
253,006		1.514	1.504	0.503	1.104	1.126	0.019	18.6	-0.9
298,006		1.316	1.315	0.403	0.895	0.963	0.014	22.2	0.2
348,005		1.452	1.443	0.500	1.130	1.211	0.014	19.0	-1.3
403,006		1.121	1.117	0.325	0.795	0.848	0.012	21.5	0.6
405,065		1.092	1.081	0.404	0.748	0.795	0.012	21.5	0.6
405,076	150	1.760	1.748	0.724	1.251	1.364	0.015	0.0	0.0
425,067		2.424	2.390	0.923	1.752	1.798	0.019	18.4	-0.6
450,068		2.074	1.998	0.737	1.566	1.555	0.018	21.9	0.9
475,067		1.801	1.727	0.517	1.507	1.474	0.018	25.1	1.9
500,067		1.159	1.100	0.835	1.986	1.965	0.044	20.0	-2.2
525,067		0.942	0.879	0.732	1.881	1.827	0.054	19.7	-0.4
547,463		0.878	0.799	0.698	1.936	1.916	0.057	20.8	0.2

when the measurements were performed and possibly to the fact that Slabs 7 and 8 were shorter than Slab 6. The surface temperature also appears to directly influence these differences. A decrease in deflections that may be directly related to the formation of a crack can be observed after approximately 500,000 load applications (see Figure 91).

A comparison of vertical deflections measured at the corners of the two slabs and at mid-span of the slab indicates that the deflections at mid-span were between 25–50 percent of the magnitude of the elastic deflections at the corners of the two slabs. Similar fluctuations were observed for the data from the various instruments.

Horizontal movement measured at mid-span of Joint 7 was almost negligible when compared with the vertical elastic deflections, although it also increased with increased load

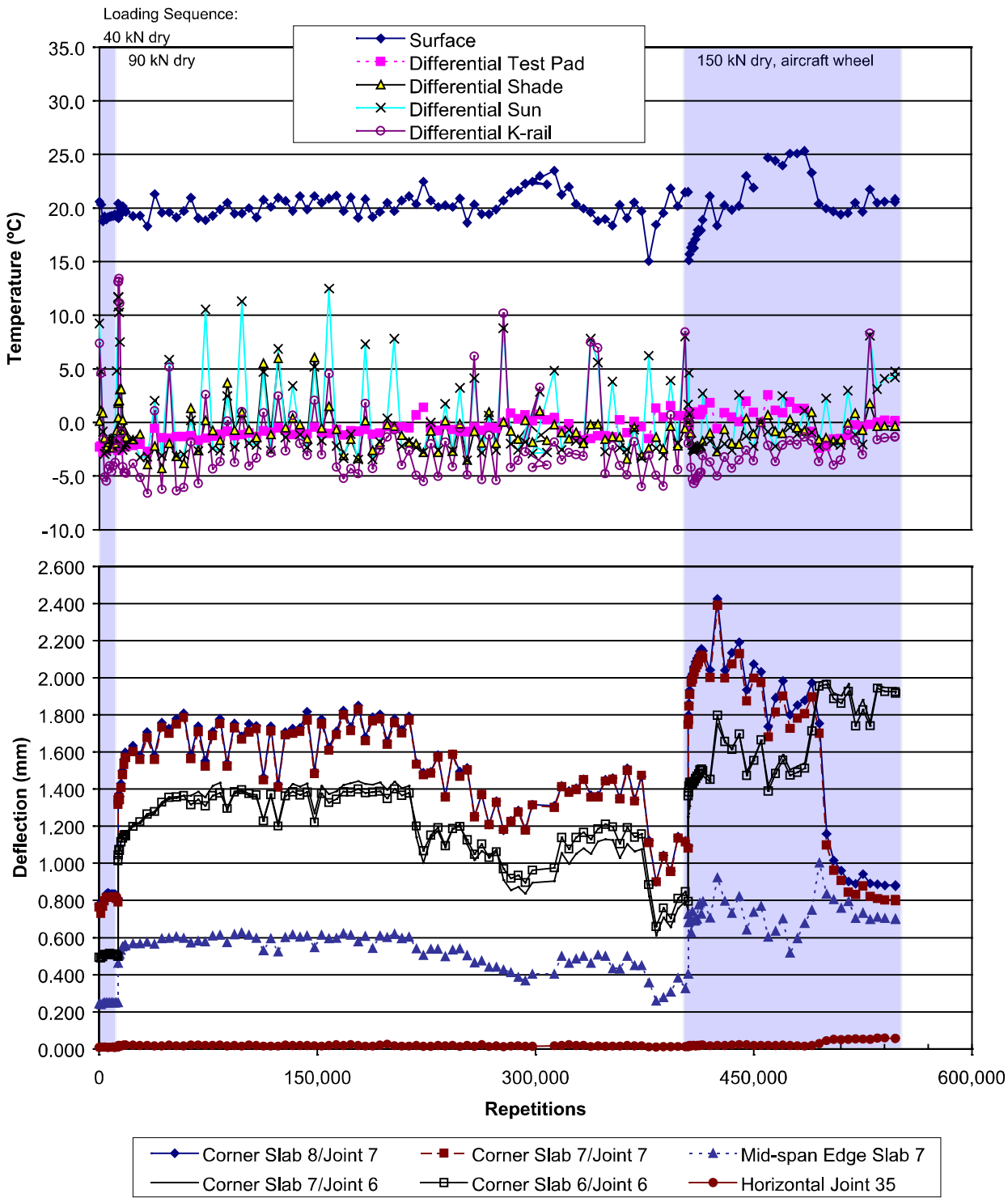

Figure 93. Plot of JDMD deflections and temperature versus load repetitions, Test 540FD.

levels and repetitions. Horizontal movement also appears to have increased after the formation of the crack at approximately 470,000 load repetitions.

In summary it appears that the applied loads, slab lengths, crack development, and temperatures affected the vertical and horizontal elastic deflections.

4.9.3 Joint Load Transfer Efficiency (LTE)

LTE was calculated at the two joints (Joints 6 and 7) adjacent to the center slab (Slab 7). LTE values were calculated for the HVS wheel running in the cabin to tow end direction. The calculated LTEs are shown in Table 27 for the beginning and end of each of the three stages of the test (40 kN, 90 kN and 150 kN).

Table 27 Load Transfer Efficiency, Test 540FD

		Load Transfer Efficiency (%)				**Temperature (ºC)**	
		Corner, Joint 7		**Corner, Joint 6**			
	Test	**Slab 8**	**Slab 7**	**Slab 7**	**Slab 6**		**Difference**
Repetitions	**Load, kN**	**JDMD 1**	**JDMD 2**	**JDMD 4**	**JDMD 5**	**Surface**	**(top – bottom)**
0	40	99.3	99.7	99.8	99.2	20.6	-2.3
13,003		99.2	99.6	98.9	99.3	20.4	-2.6
13,016	90	99.6	99.8	99.3	99.7	19.2	-2.5
405,065		98.8	99.2	99.2	99.1	21.5	0.6
405,076	150	98.4	97.8	98.5	98.7	0.0	0.0
547,463		97.5	98.2	98.6	98.1	20.8	0.2

No significant variation in LTE values could be detected and almost 100 percent load transfer was achieved throughout the whole test. With the use of the aircraft tire at 150 kN and a tire pressure of 1100 kPa, the LTE values drop somewhat, but it is clear that the dowels used in this test did extremely well in transferring the applied loads across the slabs. No significant deterioration in load transfer was detected.

4.9.4 Multi-Depth Deflectometer (MDD) Elastic Deflection Results

Two MDDs were installed on Test 540FD. They were positioned 300 mm from either side of Joint 7, one in Slab 7 (MDD 3) and one in Slab 8 (MDD 2) (see Figure 11). Both were installed between the wheel paths of the dual wheels about 900 mm from the edge of the slab. The MDDs included one module at the surface of the concrete slab (0 mm) and the other modules at depths of 200, 425, and 650 mm. A summary of the peak MDD elastic deflections is presented in Tables 28 (MDD 2) and 29 (MDD 3) and in Figures 94 (MDD 2) and 95 (MDD 3).

The first significant observation is that very little deflection originated in the sub-structure at MDD 2 (Slab 7) (Figure 94). Deflections on the order of 0.4 mm (at 200 mm depth) were recorded only after the corner crack developed (see Figure 91) and the load was increased to 150 kN. Surface deflections were above 1.0 mm. This result again suggests a significant amount of slab lift-off occurred under Slab 7 near Joint 7. This effect was not observed at MDD 3 (Slab 8) where significant deflections were recorded at 200 mm. One explanation for this behavior is that the module placed at 200 mm may have been in contact with the bottom of the slab instead of the base layer.

The second interesting observation is that prior to the appearance of the corner cracks (before 400,000 repetitions) the surface deflections for both MDDs dropped. It is likely that during the development of the corner cracks, the slab made better contact with the base layer. The additional support caused the observed reduction in surface deflection measurements.

Note that even with the application of a 150-kN wheel load, the surface deflections did not increase substantially from the deflections recorded during the application of the 90-kN load. This indicates that the pavement structure showed no fatigue damage even with the application of this very heavy 150-kN aircraft wheel load.

Table 28 MDD 2 Deflections (Test load 40 kN, 90 kN, 150 kN), Test 540FD

Repetitions	Test Load, kN	Deflection (mm) MDD 2, Slab 7			
		0 mm	200 mm	425 mm	650 mm
0	40	0.516	0.036	0.019	0.036
13,003		0.538	0.038	0.019	0.051
13,016	90	0.842	0.088	0.021	0.078
53,006		1.142	0.078	0.022	0.085
103,005		1.096	0.084	0.023	0.080
153,005		1.131	0.074	0.024	0.064
203,005		1.148	0.048	0.021	0.133
253,006		0.991	0.087	0.028	0.089
303,006		0.732	0.129	0.055	0.049
348,005		0.949	0.097	0.039	0.067
403,006		0.727	0.159	0.075	0.071
405,065		0.722	0.171	0.078	0.069
405,076	150	0.998	0.246	0.127	0.106
425,067		1.417	0.347	0.173	0.195
450,068		1.249	0.389	0.192	0.127
475,067		1.114	0.427	0.210	0.087
500,067		0.807	0.475	0.250	0.072
525,067		0.691	0.480	0.249	0.083
547,463		0.665	0.472	0.247	0.070

Table 29 MDD 3 Deflections (Test load 40 kN, 90 kN, 150 kN), Test 540FD

Repetitions	Test Load, kN	Deflection (mm) MDD 3, Slab 8			
		0 mm	200 mm	425 mm	650 mm
0	40	0.502	0.506	0.123	0.025
13,003		0.523	0.521	0.127	0.022
13,016	90	0.864	0.780	0.198	0.039
53,006		1.191	1.068	0.126	0.052
103,005		1.157	1.019	0.136	0.060
153,005		1.174	1.026	0.135	0.052
203,005		1.201	1.035	0.104	0.039
248,005		0.996	0.854	0.130	0.061
303,006		0.751	0.667	0.165	0.086
353,006		0.988	0.871	0.139	0.054
403,006		0.755	0.691	0.206	0.097
405,065	150	0.756	0.689	0.204	0.102
405,076		1.032	0.936	0.299	0.155
425,067		1.517	1.331	0.374	0.195
450,068		1.342	1.196	0.411	0.222
475,067		1.200	1.089	0.434	0.239
500,067		0.855	0.802	0.472	0.284
525,067		0.725	0.706	0.475	0.293
547,463		0.693	0.663	0.460	0.283

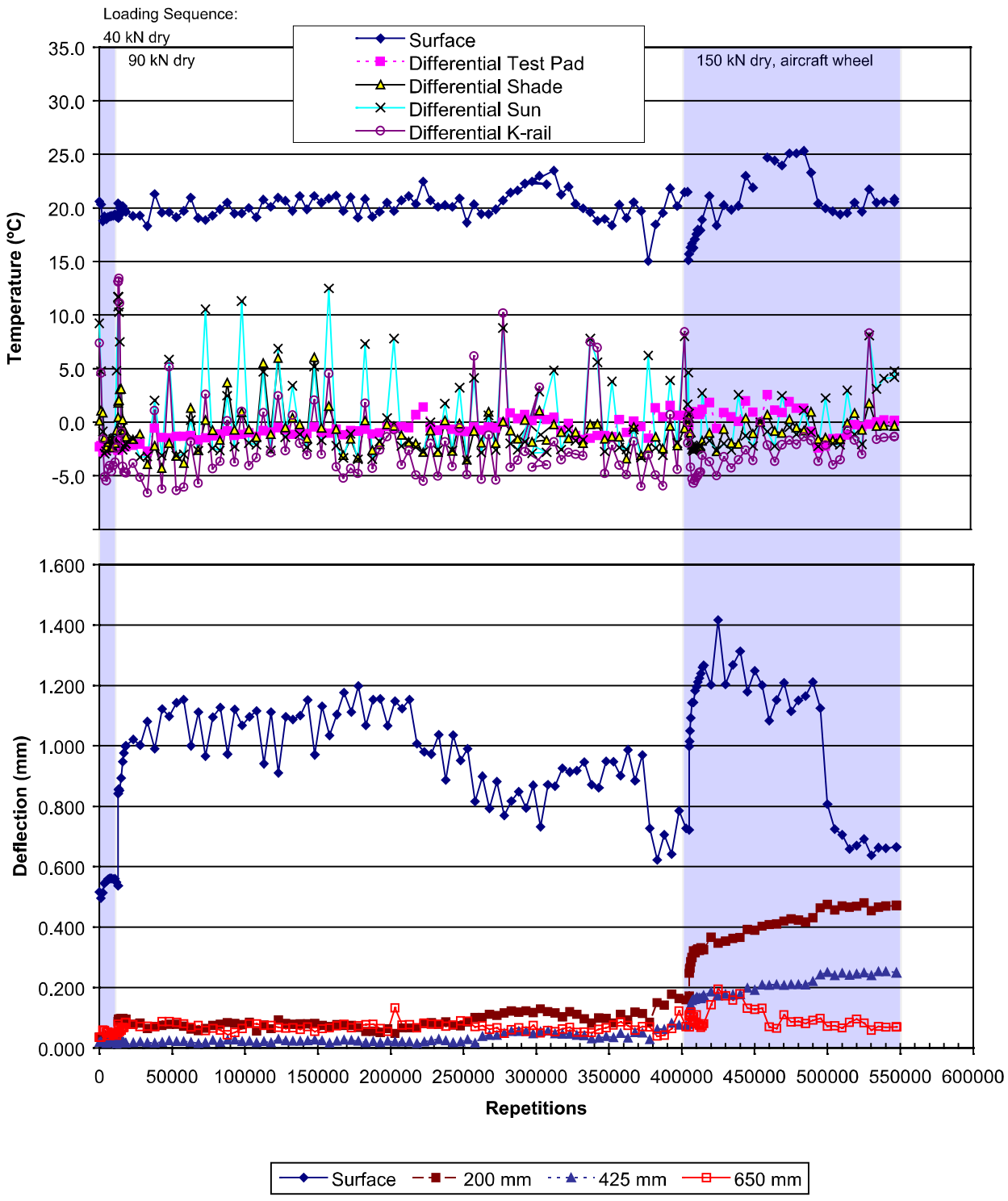

Figure 94. Plot of MDD 2 deflections and temperature versus load repetitions, Test 540FD.

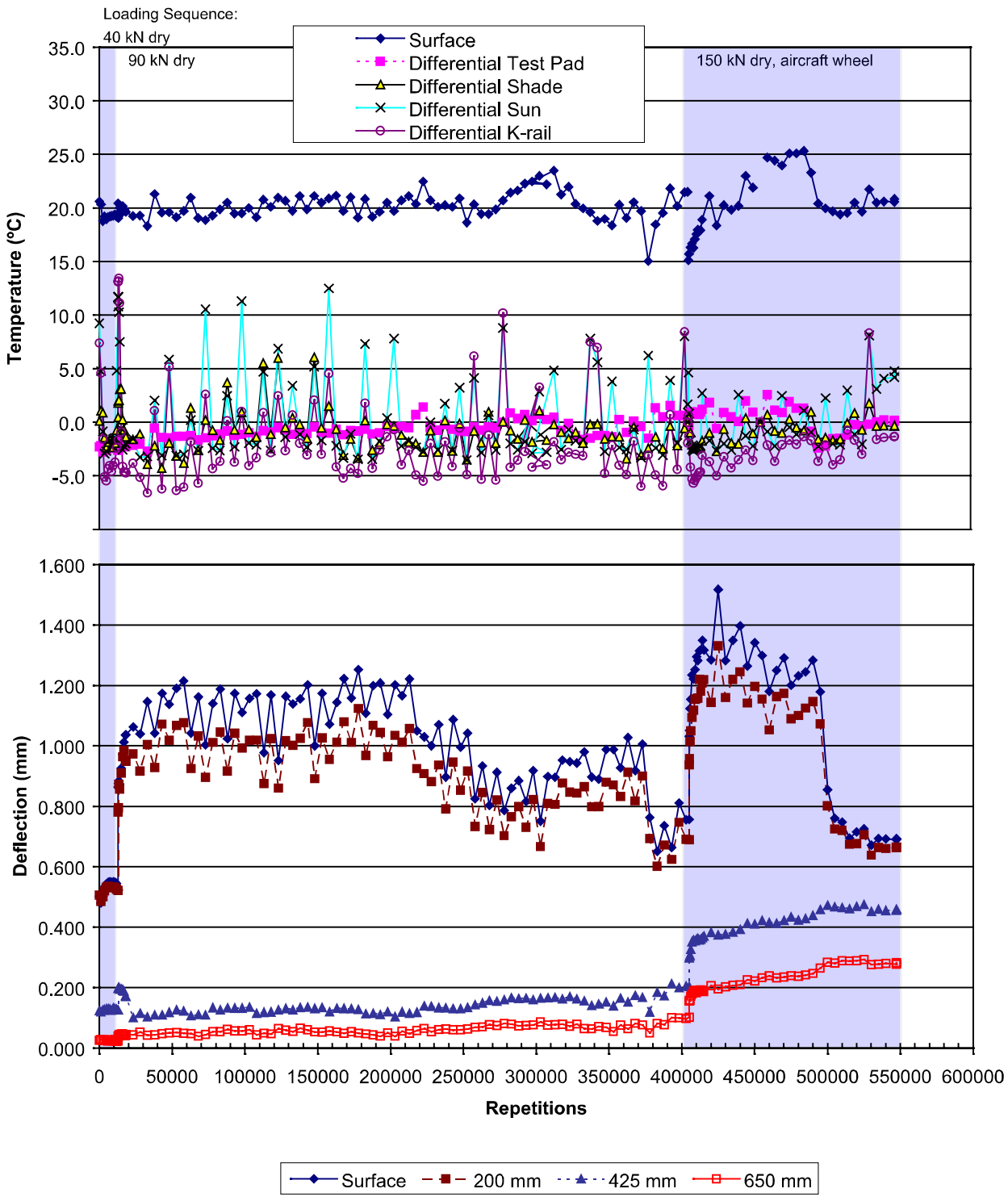

Figure 95. Plot of MDD3 deflections and temperature versus load repetitions, Test 540FD.

4.9.5 Multi-Depth Deflectometer (MDD) Permanent Deformation Data

The permanent deformation of the upper part of the pavement was measured using the two MDDs. Permanent deformation was recorded at the surface and depths of 200, 425, and 650 mm. The results are presented in Tables 30 (MDD 2) and 31 (MDD 3) and in Figures 96 (MDD 2) and 97 (MDD 3).

The data indicates a clear temperature-related trend with measured values increasing and decreasing with fluctuating temperatures. This gives rise to "negative" permanent deformation values at some load repetitions. This trend was also observed in the data sets of the elastic deflections.

The development of the corner crack on Slab 7 had a significant influence on the permanent deformation as recorded by MDD 2 (Figure 96). From the start of the test until about 200,000 repetitions very little permanent deformation could be detected and the deformation was in the order of 0.4 mm. Between 200,000 and 400,000 there is a marked increase in the surface deformation with values higher than 0.8 mm were recorded.

After the development of the cracks and the application of the 150-kN load, a steep increase in the permanent deformation is evident. At the end of the test, a total of over 2.7 mm of surface deformation was recorded.

Note that the two MDD surface modules placed on either side of Joint 7 recorded similar values and trends. It is clear that the dowels placed at Joint 7 were very effective in keeping the two slabs (Slabs 7 and 8) well intact. No joint faulting developed during this test.

Table 30 MDD 2 Permanent Deformation, Test 540FD

Repetitions	Test Load, kN	Deflection (mm) MDD 2, Slab 7			
		0 mm	200 mm	425 mm	650 mm
0	40	0.000	0.000	0.000	0.000
13,003		-0.021	-0.013	-0.045	-0.005
13,016	90	0.138	0.023	-0.028	0.007
53,006		0.266	0.129	-0.005	0.000
103,005		0.422	0.148	0.008	-0.002
153,005		0.412	0.152	0.028	-0.019
203,005		0.361	0.159	-0.042	-0.008
248,005		0.557	0.135	-0.008	-0.023
303,006		0.972	0.153	0.046	-0.058
353,006		0.715	0.146	0.030	-0.065
403,006		0.693	0.149	0.027	-0.065
405,065	150	1.088	0.142	0.043	-0.126
405,076		1.093	0.139	0.045	-0.128
425,067		0.902	0.164	0.023	-0.115
450,068		1.103	0.380	0.022	-0.084
475,067		1.506	0.475	0.075	-0.069
500,067		1.857	0.573	0.097	-0.049
525,067		2.410	0.696	0.135	-0.017
547,463		2.658	0.786	0.196	0.017

Table 31 MDD 3 Permanent Deformation, Test 540FD

Repetitions	Test Load, kN	Deflection (mm) MDD 3, Slab 8			
		0 mm	200 mm	425 mm	650 mm
0	40	0.000	0.000	0.000	0.000
13,003		-0.023	-0.009	0.000	-0.005
13,016	90	0.118	0.194	0.024	0.001
53,006		0.125	0.233	0.164	0.000
103,005		0.289	0.395	0.198	-0.006
153,005		0.287	0.413	0.200	-0.018
203,005		0.204	0.345	0.178	-0.028
248,005		0.431	0.536	0.156	-0.048
303,006		0.924	0.993	0.246	-0.036
353,006		0.659	0.735	0.242	-0.048
403,006		0.628	0.701	0.233	-0.048
405,065	150	1.026	1.051	0.209	-0.105
405,076		1.040	1.062	0.217	-0.106
425,067		0.848	0.918	0.219	-0.106
450,068		0.982	1.085	0.406	-0.099
475,067		1.424	1.480	0.516	-0.088
500,067		1.777	1.795	0.605	-0.071
525,067		2.367	2.320	0.708	-0.042
547,463		2.638	2.571	0.830	-0.009

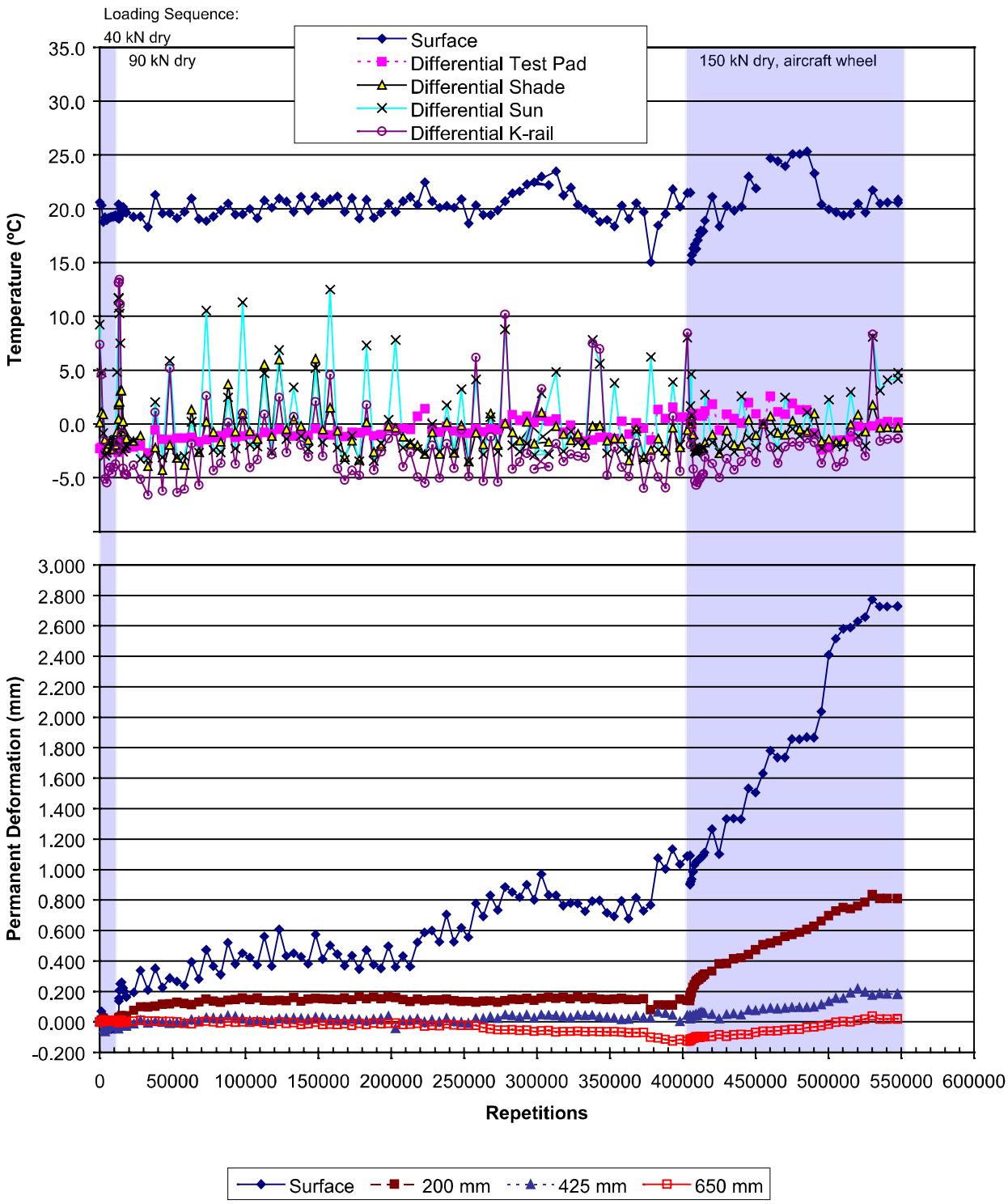

Figure 96. Plot of MDD 2 permanent deformation and temperature versus load repetitions, Test 540FD.

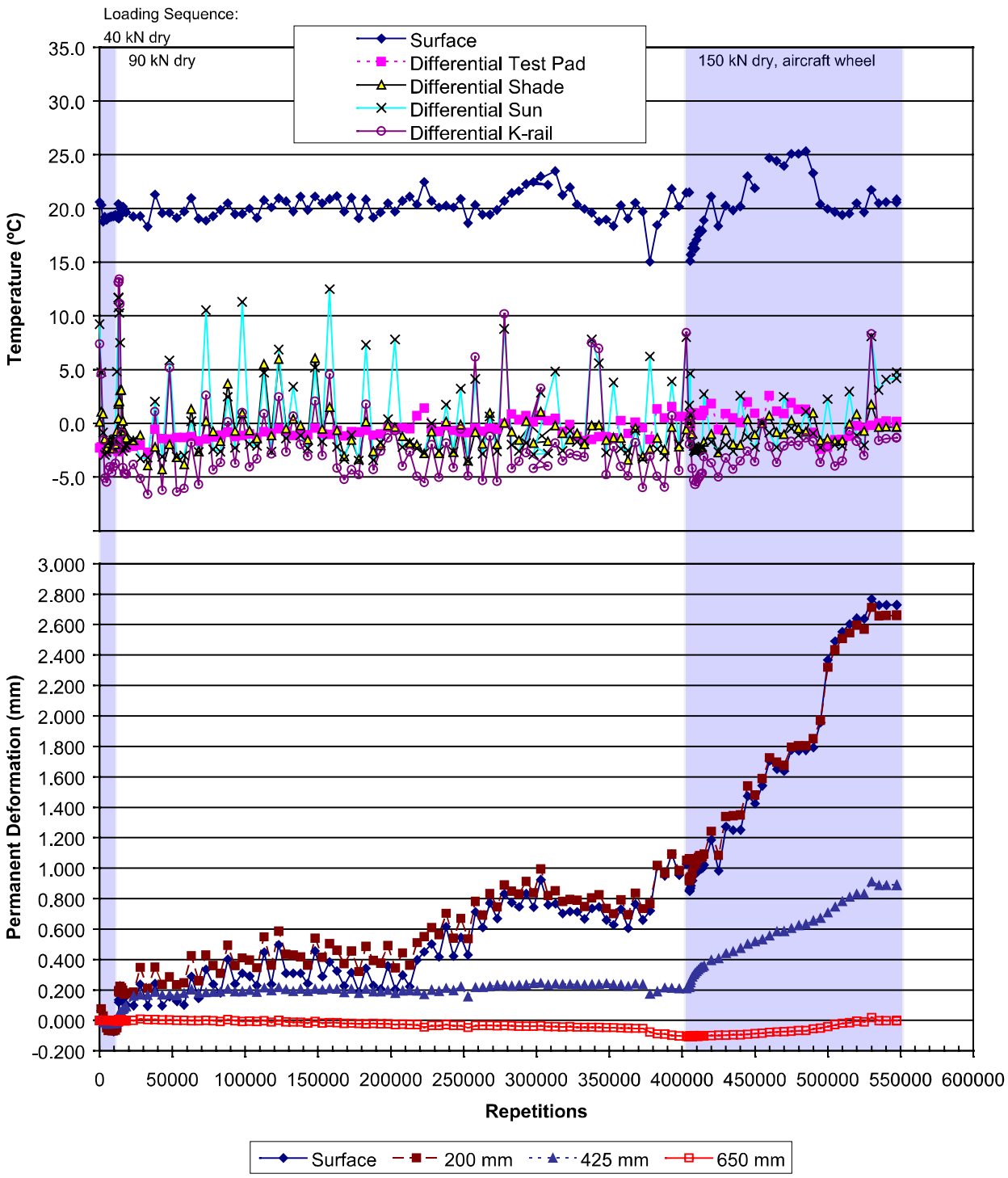

Figure 97. Plot of MDD 3 permanent deformation and temperature versus load repetitions, Test 540FD.

4.10 Test 541FD

Test 541FD was conducted on Slabs 2, 3, and 4 on the North Tangent. Slab 3 (total length of 3.80 m, total width 4.26 m) was fully tested together with some area on either side of Joints 2 and 3. The temperature control chamber was not used during this test so the test was performed at ambient temperature. MDDs were not installed for this test.

This test was the last of three tests on Section 11 on the North Tangent (200-mm FSHCC test pavement with dowels and asphalt shoulder, 4.26-m widened truck lanes). Test 541FD was also the last test conducted on the North Tangent on State route 14 near Palmdale.

The test started with a 70-kN (690-kPa) dual wheel load up to 500 repetitions after which the dual wheel load was increased to 90 kN (690 kPa). This load was applied for 167,777 repetitions until 168,277 total repetitions. At this point, the dual truck tires were replaced with a single aircraft tire and the loading was increased to 150 kN with a tire pressure of 1,100 kPa. This load was applied for 110,011 repetitions. The test was stopped after 278,288 total repetitions. The whole test was performed in the nominally dry state with no water added to the pavement. Bi-directional trafficking was applied throughout the test.

Standard 40-kN (690 kPa) dual wheel load pavement response measurements were not performed during the test and so all pavement response data are reported at the indicated trafficking load level.

4.10.1 Visual Observations

No visible cracks developed on the three slabs tested during Test 541FD. The test section was still in a visually good condition at the end of the test program. One transverse crack was

visible prior to the start of the test, as shown in Figure 98. This crack is situated at about the midspan of Slab 2 and was outside the HVS trafficked area.

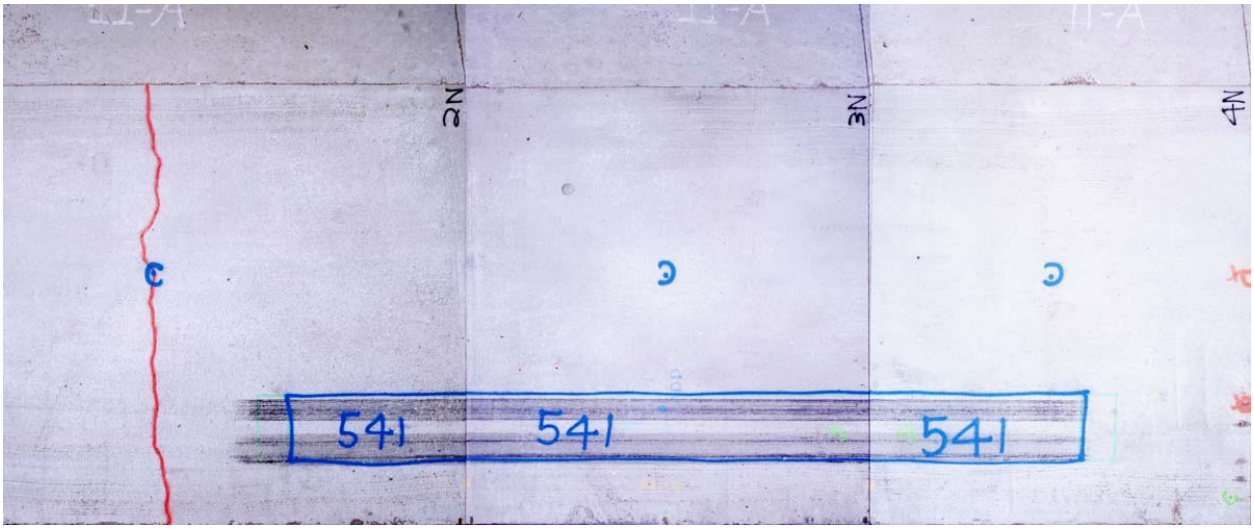

Figure 98. Composite image of Test Section 541FD.

4.10.2 Joint Deflection Measuring Device (JDMD) Results

Four JDMDs were placed on either side of Joints 2 and 3 (the two sides of Slab 3). One JDMD one was placed on the edge of Slab 3 midway between the two joints. One JDMD was placed horizontally across Joint 3 between Slabs 3 and 4.

Table 32 summarizes the results of the maximum vertical deflections at the edge of the midpoint of Slab 3 and the corner edge deflections on either side of the two joints (Joints 2 and 3), the maximum horizontal deflection at the center of Joint 3, and temperature data. Data are presented graphically in Figure 99.

Table 32 JDMD Deflections (Test Loads 70 kN, 90 kN, 150 kN) Test 541FD

Repetitions	Test Load kN	Deflection (mm)						Temperature (°C)	
		Corner, Joint 3		Mid-span, Slab 3	Corner, Joint 2		Horizontal Joint 3	Surface	Difference (top - bottom)
		Slab 4	Slab 3		Slab 3	Slab 2			
		JDMD 1	JDMD 2	JDMD 3	JDMD 4	JDMD 5	JDMD 6		
0	70	0.683	0.658	0.211	0.523	0.519	0.012	16.7	1.4
500		0.625	0.601	0.180	0.469	0.464	0.013	17.0	2.0
590	90	0.615	0.590	0.156	0.451	0.447	0.013	18.3	3.2
5,490		1.058	1.016	0.308	0.743	0.746	0.016	14.9	-0.7
25,491		1.269	1.218	0.410	0.947	0.958	0.018	13.5	-3.2
50,491		0.987	0.942	0.295	0.683	0.685	0.017	19.2	1.8
100,490		1.157	1.119	0.341	0.840	0.851	0.015	13.7	-2.4
150,491		1.372	1.309	0.389	1.058	1.086	0.021	9.8	-4.4
168,277		1.157	1.109	0.375	0.851	0.873	0.017	12.7	0.0
168,289	150	1.414	1.363	0.426	0.996	1.011	0.017	14.2	1.5
168,379		1.455	1.402	0.459	1.017	1.033	0.020	14.0	1.2
175,279		2.011	1.935	0.648	1.459	1.503	0.019	11.3	-2.6
203,278		2.372	2.253	0.770	1.738	1.798	0.024	12.2	-3.3
248,278		2.210	2.124	0.747	1.593	1.627	0.021	17.1	-1.4
278,278		2.551	2.380	0.906	1.956	2.006	0.024	13.0	-3.6

It is important to realize the effect of temperature on the measured deflection values. An inverse relationship appears to exist between the vertical elastic deflections and the temperatures as in the previous tests.

A comparison of vertical deflections measured at the two corners indicates that vertical deflections at Joint 3 were consistently higher than those at Joint 2. This may be related to the direction of trafficking when the measurements were taken and possibly to the fact that Slab 4 is shorter than Slab 3, which is shorter than Slab 2. The surface temperature also appears to directly influence these differences. The increase in deflections around 170,000 load repetitions is attributed to the increased load of 150 kN applied by the aircraft tire with a higher tire pressure.

A comparison of vertical deflections measured at the corners of the two slabs and at mid-span of the slab indicates that the deflections at mid-span were approximately 25 to 50 percent of the magnitude of the elastic deflections at the corners of the two slabs.

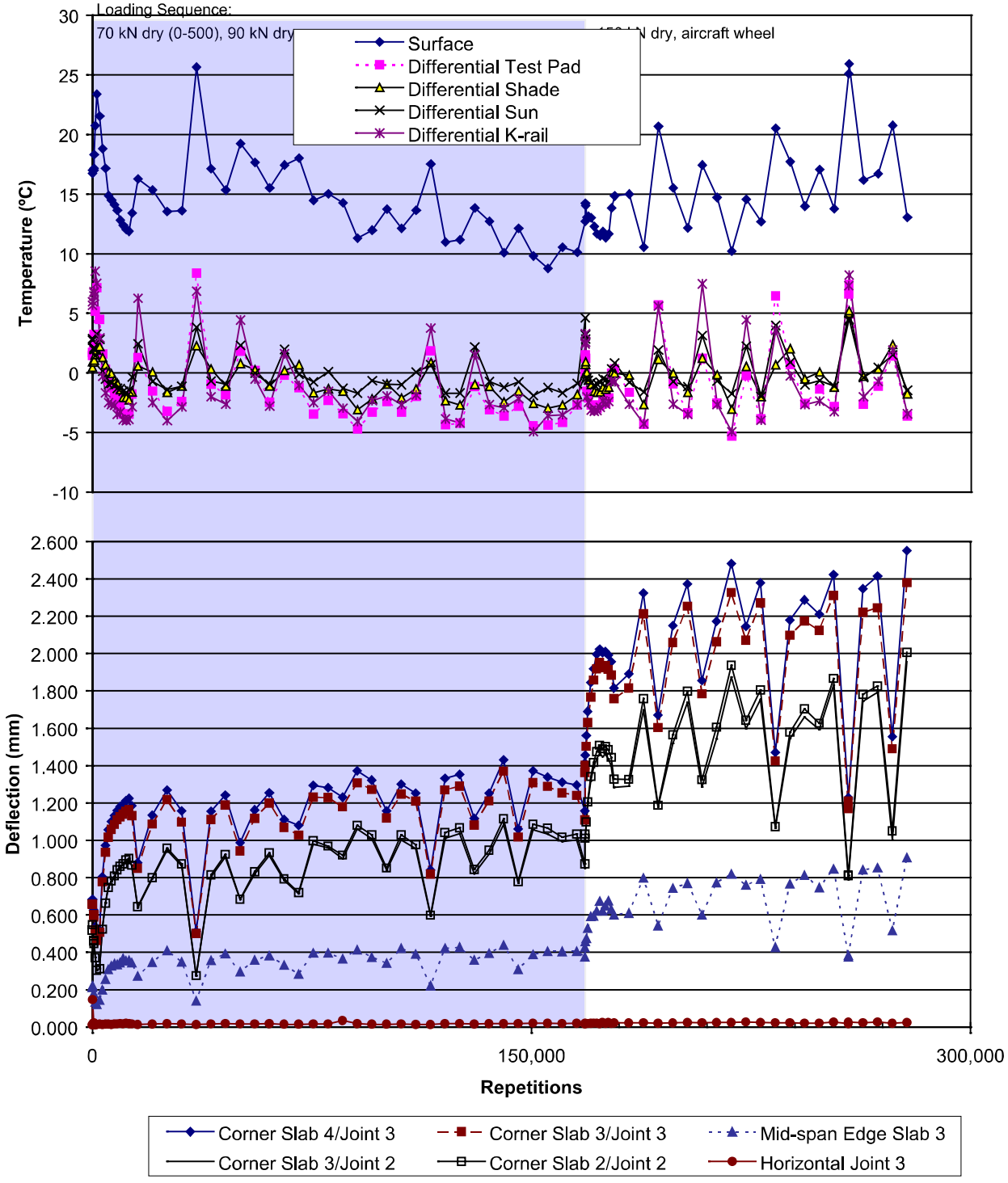

Figure 99. Plot of JDMD deflections and temperature versus load repetitions, Test 541FD.

The horizontal movement measured at the midpoint of Joint 3 was almost negligible (0.01 to 0.05 mm) when compared to the vertical elastic deflections. However, horizontal movement also increased with increased load levels and trafficking.

Differential movement between the slabs at the joints was also negligible (about 0.02 mm). This indicates that the dowels kept the slabs well intact without any loss in load transfer, even after application of the 150-kN aircraft wheel load.

4.10.3 Joint Load Transfer Efficiency (LTE)

The Load Transfer Efficiency (LTE) was calculated at the two joints (Joints 2 and 3) adjacent to the center slab (Slab 3). The LTE was calculated for the HVS wheel running in the cabin to tow end direction. In Table 33, the calculated LTE is shown at the beginning and end of each of the three stages of the test (70 kN, 90 kN and 150 kN). No clear trend with either increased trafficking or pavement temperature could be identified in the data. However, LTE values calculated at the corner of Joint 2 decreased slightly with increasing traffic. The 150-kN test load generally caused lower LTE values than the two lighter test loads. The influence of the aircraft tire's substantially higher inflation pressure is unclear.

Table 33 Load Transfer Efficiency, Test 541FD

		Load Transfer Efficiency (%)				**Temperature (ºC)**	
		Corner, Joint 7		**Corner, Joint 6**			
	Test	**Slab 8**	**Slab 7**	**Slab 7**	**Slab 6**		**Difference**
Repetitions	**Load, kN**	**JDMD 1**	**JDMD 2**	**JDMD 4**	**JDMD 5**	**Surface**	**(top – bottom)**
0	70	98.1	98.6	99.2	99.3	16.7	1.4
500		98.8	97.8	98.8	99.0	17.0	2.0
590	90	99.6	98.7	99.2	98.9	18.3	3.2
168,277		98.9	99.5	97.5	98.3	12.7	0.0
168,289	150	98.0	96.1	96.6	97.7	14.2	1.5
278,278		98.5	97.3	97.3	95.9	13.0	-3.6

As with the previous tests done on sections with dowel bars, the LTE values started very high and stayed constant for the duration of the entire test. Even with the application of the aircraft wheel, no significant drop in LTE values was observed. This is a clear indication of the positive effects of dowel bars and their ability to spread load across joints.

4.11 Test 541FD Phase II

After the completion of HVS Test 541FD on December 27, 2001, the HVS was moved to Ukiah, California to traffic a series of dowel bar retrofit (DBR) sections (*5*). Following completion of the Ukiah DBR tests, the HVS was transported back to Palmdale to continue testing Section 541FD. To avoid confusion, this series of tests is called 541FD Phase II. Testing was begun March 20, 2003 and completed June 14, 2003.

Test 541FD Phase II was conducted on the widened truck lane sections with dowels (Section 11A) and asphalt shoulder on Slabs 2, 3, and 4 on the North Tangent. Slab 3 (total length of 3.80 m, total width 4.26 m) was fully tested, together with some area on either side of Joints 2 and 3. The trafficked area is exactly the as Test 541FD (see Section 4.11). The test was performed at ambient temperature (no temperature control chamber was used).

The test was conducted using the aircraft wheel with a test load of 150 kN and a tire pressure of 1100 kPa. The test was stopped after 1,426,599 repetitions. In total, Section 541FD was subjected to 1,704,887 repetitions (278,288 repetitions from 541FD Phase I and 1,426,599 repetitions from Phase II testing). The entire test was performed in the nominally dry state with no water added to the pavement. Bi-directional trafficking was applied for the duration of the test.

Standard 40-kN (690-kPa) dual wheel load pavement response measurements were performed at intervals of approximately 100,000 repetitions as well as deflection measurements at test loads of 90 kN and 150 kN, although all trafficking was done with the 150-kN applied load.

4.11.1 Visual Observations

No visible cracks developed during the test. The test section was still in a visually good condition at the completion of loading. The final condition of the test section is shown in Figure 100.

One transverse crack was visible prior to the start of the test. This crack is situated at approximately midspan of Slab 2 (total length 5.91 m) and is, therefore, dividing the slab in approximately equal lengths of 2.92 m. This crack falls outside the HVS trafficked area.

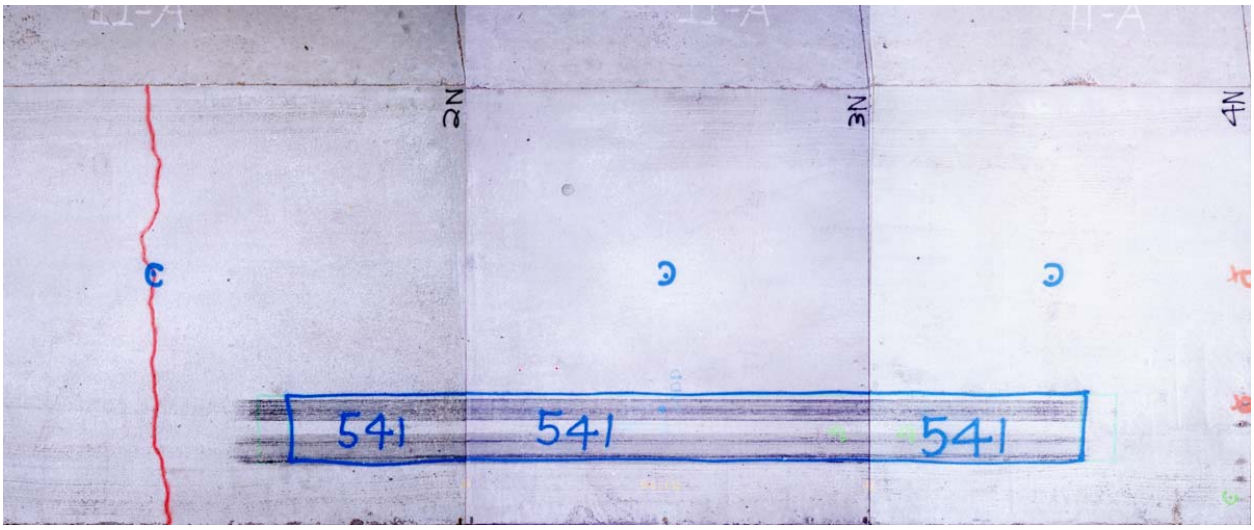

Figure 100. Composite image of Test 541FD phase II.

4.11.2 Joint Deflection Measuring Device (JDMD) Results

Four JDMDs were placed on either side of Joints 2 and 3 (the two sides of Slab 3) and one was placed on the edge of Slab 3 at midspan. One JDMD was placed horizontally across Joint 3 between Slabs 3 and 4. The instrumentation layout is similar to that of the previous 541FD test (see Figure 12).

Prior to the start of the loading cycle, deflection measurements were taken at three load levels: 40, 90, and 150 kN. The deflections measured with all the JDMDs under the influence of these loads are presented in Figure 101 and Table 34. Comparing the responses of the various JDMDs, it is noted that a linear relationship between applied load and measured deflection exists and that the mid-span edge area is the least load sensitive.

Table 34 Relationship between Test Loads and Measured Deflections, Test 541FD Phase II

Test Load kN	Deflection (mm)					
	Corner, Joint 3		Mid-span, Slab 3	Corner, Joint 2		Horizontal
	Slab 4	Slab 3		Slab 3	Slab 2	Joint 3
	JDMD 1	JDMD 2	JDMD 3	JDMD 4	JDMD 5	JDMD 6
40	0.471	0.347	.0120	0.331	0.331	0.007
90	0.633	0.485	0.163	0.429	0.436	0.009
150	0.832	0.651	0.231	0.585	0.588	0.012

Although the test was conducted at a wheel load of 150 kN, 40- and 90-kN deflections were recorded at approximately 100,000 repetition intervals. This was done to investigate the degree of damage over time with a standard 40-kN test load. The results are summarized in Tables 35 and 36 for the 40- and 90-kN test load cases, respectively. The data are also graphically shown in Figures 102, 103, and 104, for the 40-, 90-, and 150-kN test loads.

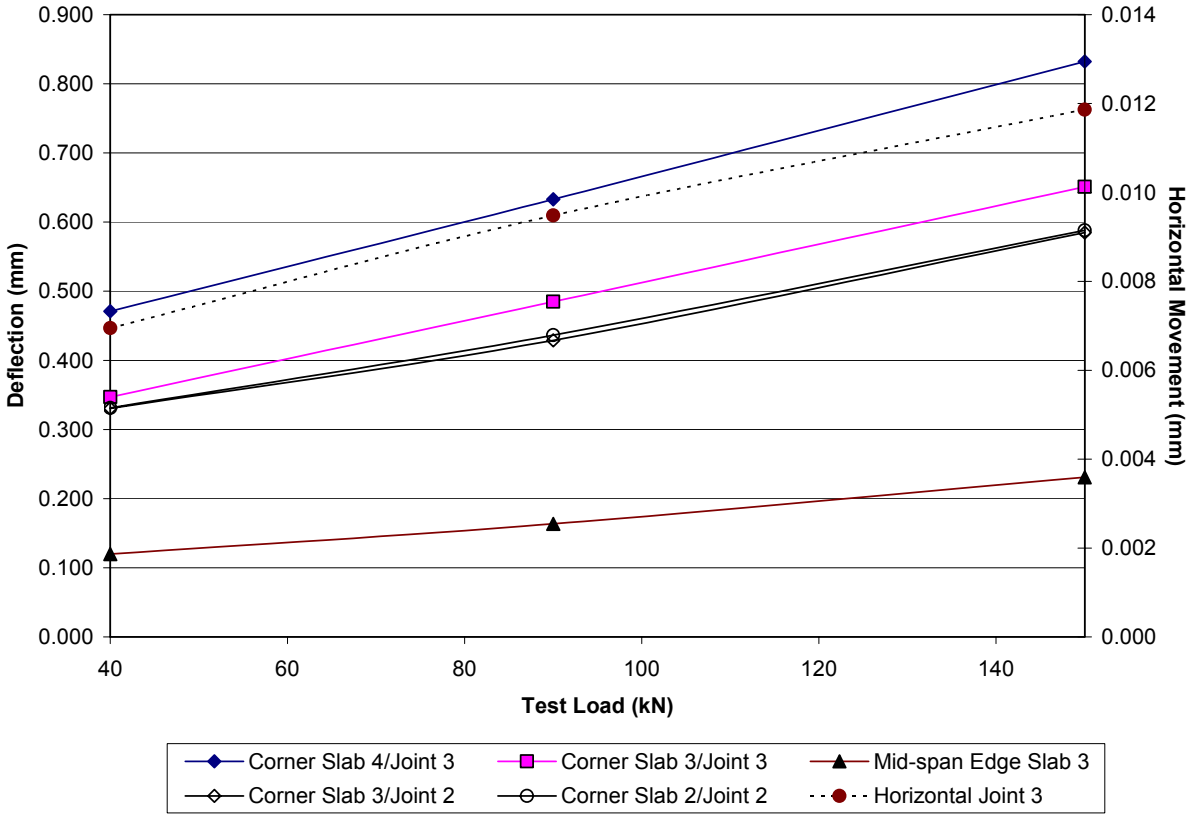

Figure 101. Plot of JDMD deflections versus test load at the start of Test 541FD Phase II.

Table 35 JDMD Deflections, Test Load 40 kN, Test 541FD Phase II

	Deflection (mm)						Temperature (ºC)	
	Corner, Joint 3		Mid-span,	Corner, Joint 2		Horizontal		
	Slab 4	Slab 3	Slab 3	Slab 3	Slab 2	Joint 3		Difference
Repetitions	JDMD 1	JDMD 2	JDMD 3	JDMD 4	JDMD 5	JDMD 6	Surface	(top -bottom)
0	0.471	0.347	0.120	0.331	0.331	0.007	13.7	0.5
91,433	1.143	1.720	0.260	0.759	0.770	0.010	20.4	4.3
200,012	1.073	1.614	0.280	0.777	0.788	0.009	18.5	0.5
320,406	1.102	1.908	0.333	0.992	1.003	0.011	15.0	-2.2
433,854	1.074	1.061	0.385	1.099	1.101	0.009	13.3	2.2
538,258	1.198	1.184	0.454	1.398	1.402	0.008	10.9	-1.8
661,874	1.165	1.351	0.538	1.319	1.244	0.009	16.9	4.1
774,212	1.171	1.545	0.626	1.108	1.093	0.011	16.5	1.5
885,286	1.325	1.841	0.660	1.047	1.052	0.010	16.3	-1.1
1,233,173	1.060	1.787	0.494	0.617	0.641	0.006	29.0	3.1

Table 36 JDMD Deflections, Test Load 90 kN, Test 541FD Phase II

	Deflection (mm)						Temperature (ºC)	
	Corner, Joint 3		Mid-span, Slab 3	Corner, Joint 2		Horizontal Joint 3		
	Slab 4	Slab 3		Slab 3	Slab 2			Difference
Repetitions	JDMD 1	JDMD 2	JDMD 3	JDMD 4	JDMD 5	JDMD 6	Surface	(top -bottom)
0	0.633	0.485	0.163	0.429	0.436	0.009	13.7	0.5
91,433	1.263	1.125	0.268	0.785	0.800	0.010	20.4	4.3
200,012	1.389	1.059	0.329	0.908	0.920	0.012	18.5	0.5
320,406	1.487	1.271	0.448	1.288	1.290	0.014	15.0	-2.2
433,854	1.388	1.363	0.453	1.326	1.333	0.010	13.3	2.2
538,258	1.646	1.621	0.616	1.787	1.790	0.009	10.9	-1.8
661,874	1.703	1.925	0.373	0.808	0.752	0.012	16.9	4.1
774,212	1.560	2.055	0.602	0.961	0.968	0.011	16.5	1.5
885,286	1.866	2.156	0.409	0.561	0.564	0.012	16.3	-1.1
1,426,471	1.630	2.140	0.515	0.874	0.880	0.013	20.8	-0.1

From the data, it is concluded that no significant amount of damage could be detected during this test. Even after the application of 1.4 million 150-kN load applications, neither cracking nor any significant increase in deflections was observed. The variation in deflections as presented in the tables is mainly due to temperature changes and no significant increase or trend regarding the amount of deflections with increased repetitions could be detected. The 40-kN and 90-kN deflections recorded at the start of the test (at zero repetitions) are significantly lower than all subsequent deflections. This may be due to settling and in-bedding, which is normally observed with all HVS testing.

The deflections recorded at Joint 3 were in general the highest of all recorded deflections. The average of all 40-kN deflections is shown in Table 37.

Because of the bi-directional trafficking and the use of the dowel bars, it was not expected that any particular corner would have higher deflections developing with time and the observation that Joint 3 (JDMDs 1 and 2) has significantly higher deflections is probably due to the variability in all the parameters that influence deflections (e.g., slab thickness, support

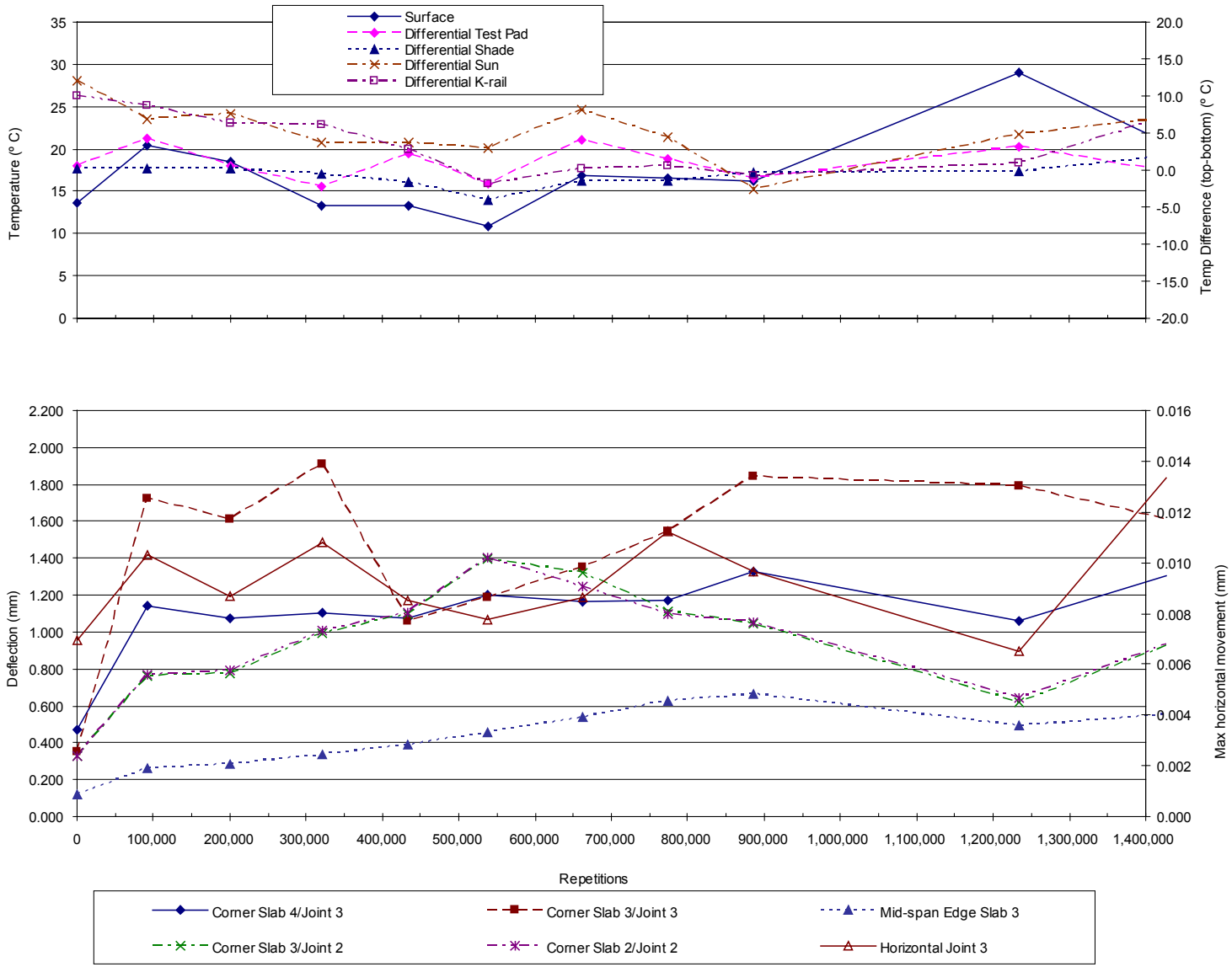

Figure 102. Plot of JDMD deflections and temperature versus load repetitions (40-kN test load), Test 541FD Phase II.

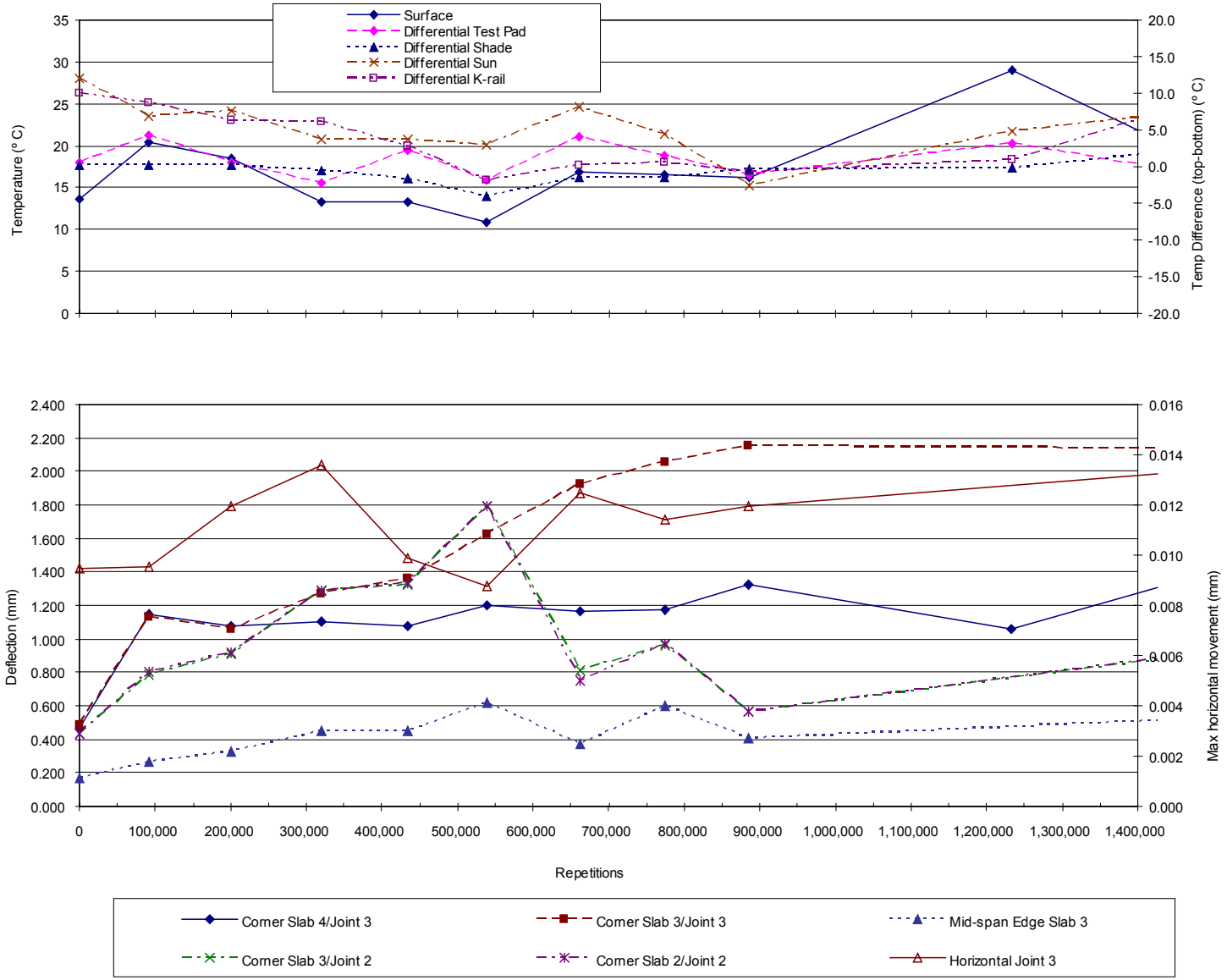

Figure 103. Plot of JDMD deflections and temperature versus load repetitions (90-kN test load), Test 541FD Phase II.

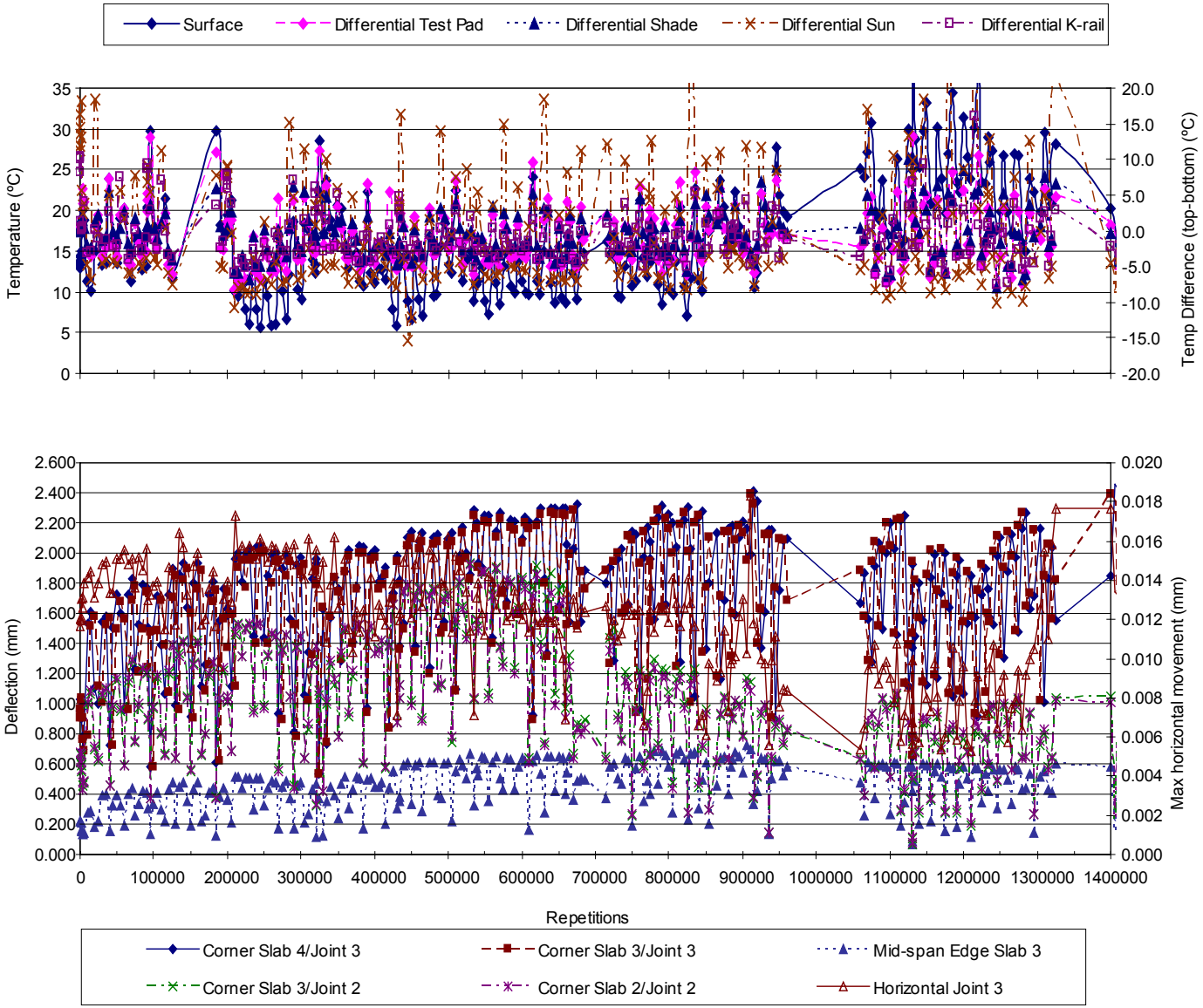

Figure 104. Plot of JDMD deflections and temperature versus load repetitions (150-kN test load), Test 541FD Phase II.

Table 37 Average of all 40-kN Deflection, Test 541FD

Instrument	Position	Average Deflection (mm)
JDMD 1	Slab 4, Joint 3	1.099
JDMD 2	Slab 3, Joint 3	1.452
JDMD 3	Slab 3, mid-span edge	0.427
JDMD 4	Slab 3, Joint 2	0.943
JDMD 5	Slab 2, Joint 2	0.941
JDMD 6	Horizontal, Joint 3	0.009

conditions, condition of the dowels, etc.). It may also be related to the differences in slab lengths. Slab 4 (3.67 m) and Slab 3 (3.89 m) are significantly shorter than Slab 2 (5.91 m) (see Table 2 in Chapter 3). Although a crack was formed in the middle of Slab 2, it is quite possible that aggregate interlock could have still play a major role in keeping the slab structurally intact during the testing period.

Similar to what was observed during Test 541FD, the mid-span edge deflections are approximately 30 to 40 percent of those recorded at the corners.

It is important to realize the effect of temperature on the measured deflection values. Although the use of dowels minimizes these effects, it is still evident from Figure 104 that significant variations in deflection data are due to daily temperature fluctuation.

The horizontal movement measured at the mid-span of Slab 3 was almost negligible when compared to the vertical elastic deflections. Movements between .009 and .014 mm were recorded. These values are significantly lower than those recorded during Test 535FD (Section 7, no dowels), for which the range of horizontal movements measured were ranged from approximately .060 to .080 mm, using a 90-kN test load (see Table 13). One possible explanation for this is that the dowels installed in 541FD may have somewhat restricted the ability of the slabs to move horizontally.

4.11.3 Joint Load Transfer Efficiency (LTE)

The Load Transfer Efficiency (LTE) was calculated at the two joints on either side of the center slab (Slab 3), Joint 2 (between Slabs 2 and 3) and Joint 3 (between Slabs 3 and 4). In Table 38, the calculated LTE is shown right at the beginning of the test at test load levels of (40, 90, and 150 kN).

Table 38 Load Transfer Efficiency at Various Loads, Test 541FD Phase II

	LTE (%)			
	Corner, Joint 3		**Corner, Joint 2**	
	Slab 4	**Slab 3**	**Slab 3**	**Slab 2**
Test Load, kN	**JDMD 1**	**JDMD 2**	**JDMD 4**	**JDMD 5**
40	98.6	99.0	98.2	98.8
90	98.9	99.6	99.3	98.3
150	99.1	99.5	99.6	98.9

No noticeable degree of deterioration in LTE was detected using the various test loads. LTE remained close to 100 percent. LTE was also calculated throughout the test and a summary of the 40-kN test load LTE is shown in Table 39.

Table 39 Load Transfer Efficiency, Test Load 40 kN, Test 541FD Phase II

	LTE (%)			
	Corner, Joint 3		**Corner, Joint 2**	
	Slab 4	**Slab 3**	**Slab 3**	**Slab 2**
Repetitions	**JDMD 1**	**JDMD 2**	**JDMD 4**	**JDMD 5**
0	98.6	99.0	98.2	98.8
91,433	97.4	96.7	99.1	98.1
200,012	98.7	99.0	99.7	99.6
320,406	97.7	97.5	99.1	98.6
433,854	98.9	98.0	98.1	98.5
538,258	97.7	96.9	97.5	97.4
661,874	96.7	97.7	99.3	99.6
774,212	98.9	98.4	98.0	99.4
885,286	98.6	98.4	97.6	99.3
1,233,173	99.5	99.8	99.4	99.8
1,426,471	99.6	99.9	99.4	99.2

No clear trend with increased trafficking, increased loading, or pavement temperature could be identified in the data. The load transfer across the joints via the dowels stayed close to 100 percent even after the application of over 1.4 million 150-kN load applications. It is clear that the use of dowels was very beneficial in controlling the differential movements between the two adjacent slabs. No degree of deterioration was visible even after the application of a total of 1,704,887 repetitions (278,288 repetitions from 541FD Phase I and 1,426,599 repetitions from Phase II testing) of which the bulk were applied with a 150-kN wheel load.

4.11.4 Permanent Deformation

The permanent deformation of the slab edge under the influence of the environment and loading was measured with the JDMDs. The slab edge movement during the first 125,000 repetitions is shown in Figure 105 while the complete data set (all 1.4 million repetitions) can bee seen in Figure 106. This is done to clearly identify the influence that daily temperature variations have on the movement of the edge of the slabs. The sign convention of the graphs is such that decreasing values of permanent movement represent downward movements along the edge of the slab and vice-versa.

As shown in Figure 105, the influence of daily temperature variation and temperature differentials (top–bottom) on the movement of the edge of the slab is significant. For instance, as shown in Figure 105, at 95,000 repetitions the corner of Slab 4 at Joint 3 experienced a total vertical movement of 2.2 mm under the influence of a total surface temperature change of 18ºC during the 24-hour cycle.

The total long term permanent displacement of the edge of the slab for the whole test can be seen in Figure 106. Apart from the daily cyclic variation, it is clear that the slab moved

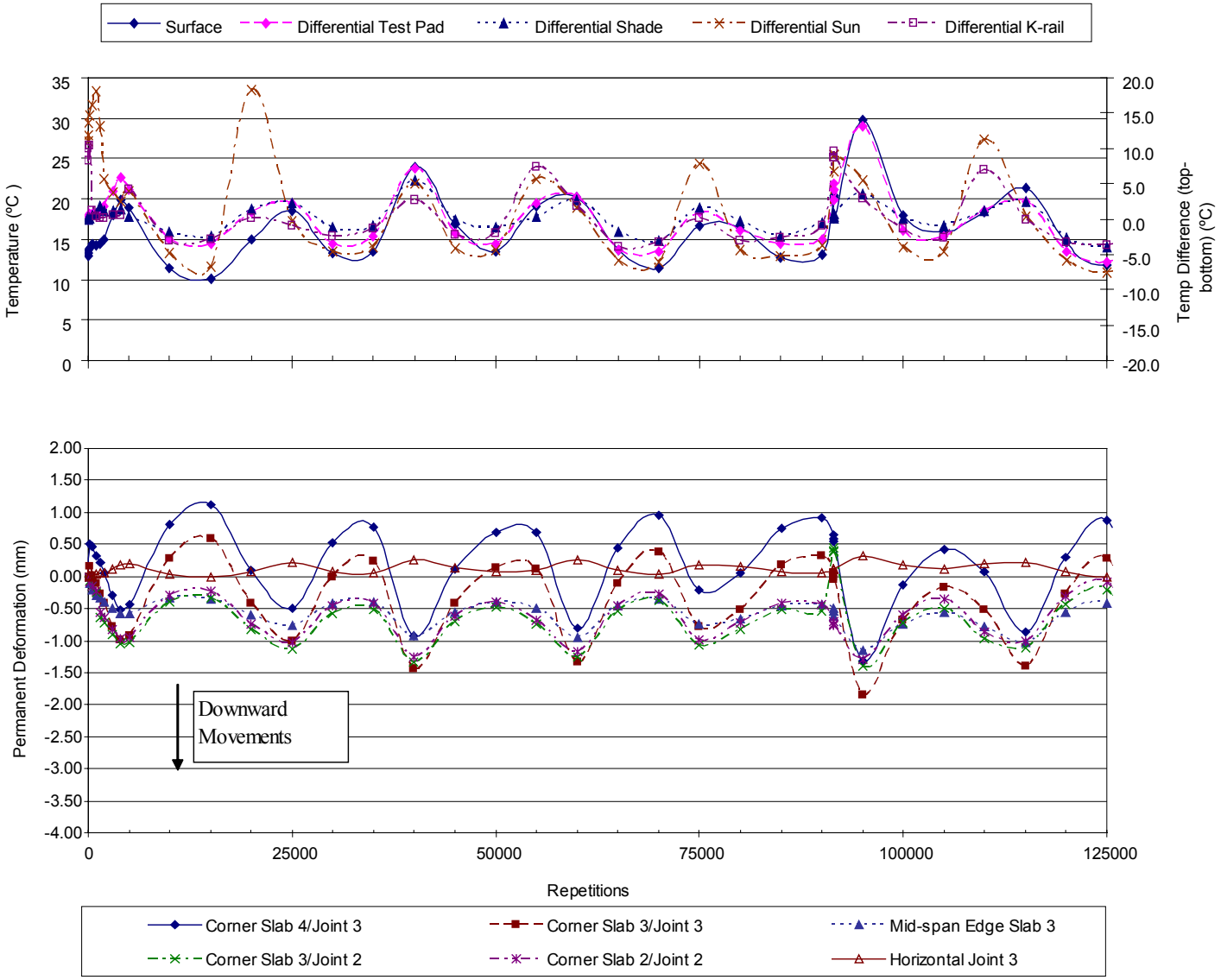

Figure 105. Plot of JDMD permanent deformation and temperature versus load repetitions (first 125,000 repetitions), Test 541FD Phase II.

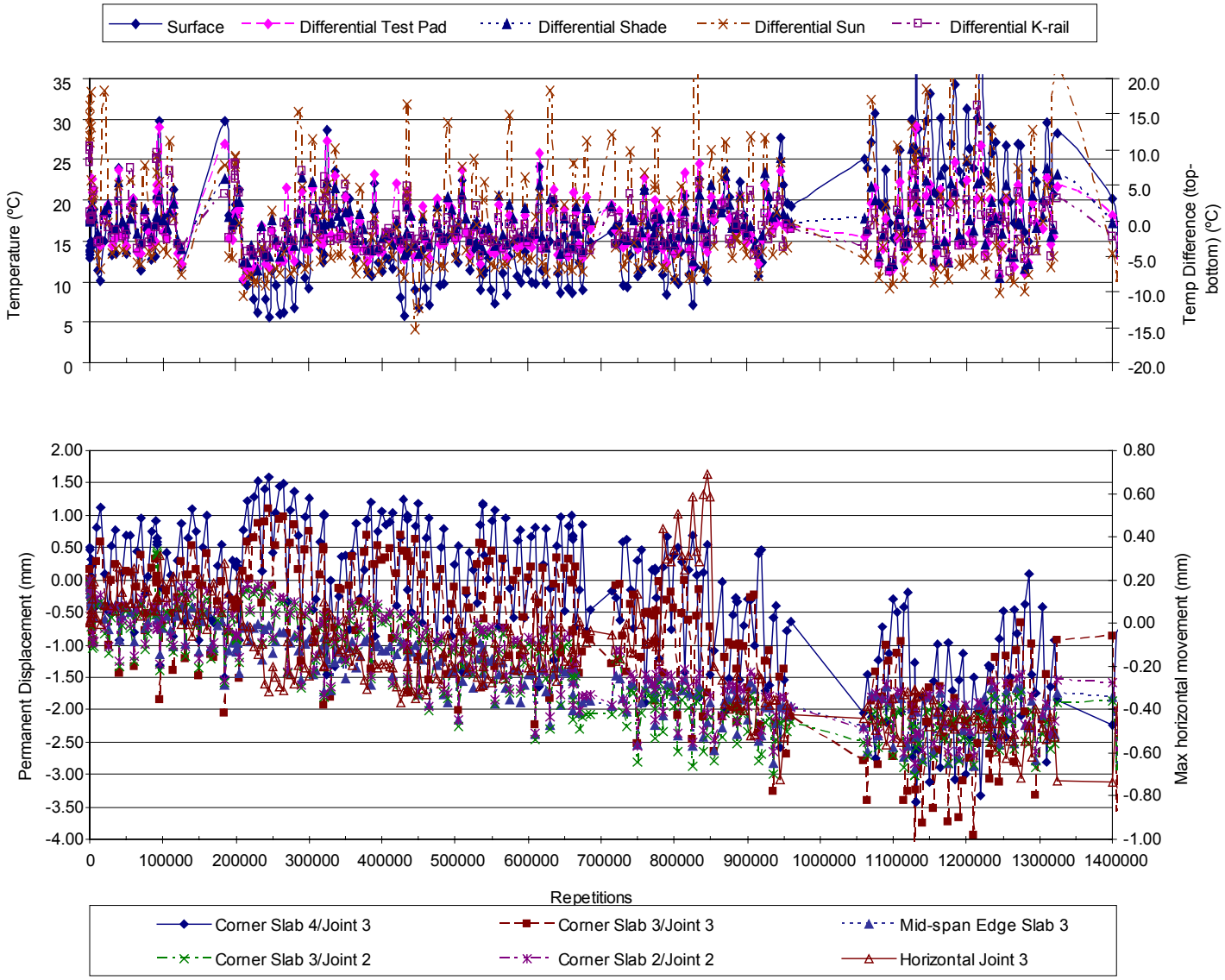

Figure 106. Plot of JDMD permanent displacement and temperature versus load repetitions, Test 541FD Phase II.

downwards with time. On average, Slabs 2, 3, and 4 moved approximately 2 to 2.5 mm downwards after the application of 1,426 million load repetitions. Due to the high loads applied to the test slabs, it is possible that the slabs got pushed into the base layer with time. This also explains why the slab could absorb such an aggressive loading history without showing signs of deterioration. Due to the settling and in-bedding of the PCC slab in the base, the support of the slab from the bottom increased with time. This additional uniform support obviously increased the ability of the slab to withstand the high loads imposed on them without any deterioration such as the formation of cracks.

5.0 FALLING WEIGHT DEFLECTOMETER (FWD) RESULTS

This chapter presents Falling Weight Deflectometer (FWD) data recorded before and after Heavy Vehicle Simulator (HVS) testing. FWD data was recorded at various stages after construction and also at different temperatures including day and night measurements within a 24-hour period. The FWD data thus provide an indication of the structural response of the slabs and joints over different seasons as well as before and after HVS trafficking. The analysis presented here focuses on two main aspects: (1) structural stiffness, characterized by center slab deflections and back-calculated concrete stiffness, and (2) Load Transfer Efficiency (LTE), measured at longitudinal and transverse joints.

Chapter 5.1 presents a summary of available data and of the approach to and assumptions made for the presentation and analysis of available information.

Chapter 5.2 presents maximum deflection variation for different test sections and loading conditions, with summary statistics and graphics for principal effects. Data used for this chapter excludes data recorded on slabs that were affected by HVS testing. Also, the deflections measured at slab centers (as opposed to joints) were isolated in order to focus on overall structural stiffness.

Chapter 5.3 presents the measurement of load transfer over joints, including a discussion of main parameters and a presentation of load transfer efficiency at different stations and loading conditions. In this chapter, deflections measured at joints and corners were isolated in order to focus on load transfer over joints.

Chapter 5.4 presents the effect of HVS loading on deflections measured at the slab center and over joints for those slabs affected by HVS testing, including deflections and load transfer efficiencies measured before and after HVS testing.

Chapter 5.5 includes back-calculated stiffnesses of pavement layers at several periods after construction and for several loading conditions, focusing on concrete stiffness back-calculated from center slab deflections.

Chapter 5.6 contains the summary and conclusions from FWD testing.

To maintain continuity, most of the data relating to principal effects are presented in graphical or tabular format in this chapter, together with discussions of key observations. Appendix A contains supporting stripmaps and data.

5.1 Available Data and Analysis Methodology

The relevant FWD raw data files recorded as part of the North Tangent tests are summarized in Table 40. Figure 107 shows the schedule relationship between the FWD measurements and the HVS test program.

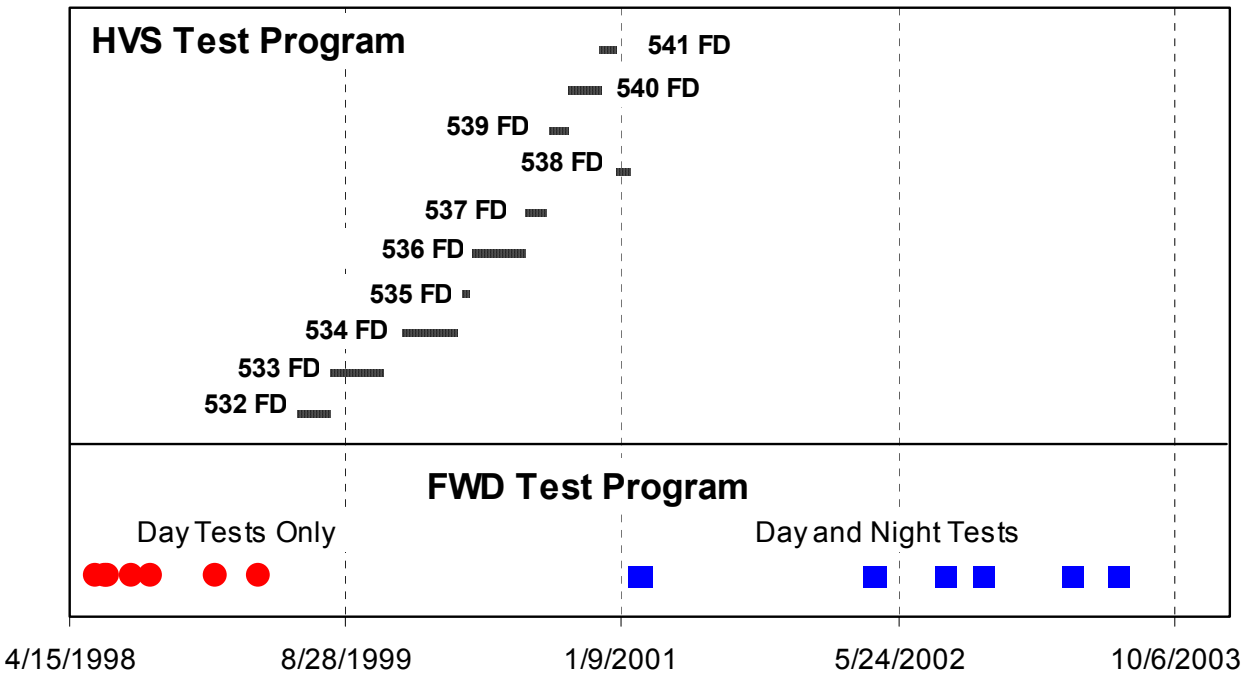

Figure 107. FWD measurement program relative to HVS program.

Table 40 Summary of Relevant FWD Tests Performed on North Tangent

	Filename	Record Date	Days Before (-) or After (+) Construction	Drop Locations			Time of Day	Approximate Pressure (kPa)		
				Center	Shoulder	K-rail		Drop 1	Drop 2	Drop 3
Before Concrete Construction	1nhvs2ex.fwd	1998/03/19	-90	Yes	No	No	Day	722	976	1554
	2nhvsrwa.fwd	1998/04/08	-70	Yes	No	No	Day	373	562	1075
	2nhvsrwb.fwd	1998/04/08	-70	Yes	No	No	Day	373	488	669
	3nhvsrwa.fwd	1998/06/02	-15	Yes	No	No	Day	562	867	1323
	3nhvsrwb.fwd	1998/06/02	-15	Yes	No	No	Day	548	849	1295
	4nc&e1d.fwd	1998/06/19	1	Yes	Yes	No	Day	831	1272	No Drop
Before HVS Testing	5nc&e7d.fwd	1998/06/23	7	Yes	Yes	No	Day	825	1267	No Drop
	6nc&e49d.fwd	1998/08/05	49	Yes	Yes	No	Day	818	1042	No Drop
	7nc&e90D.fwd	1998/09/10	90	Yes	Yes	No	Day	957	1238	No Drop
	8nc&e200.fwd	1999/01/06	200	Yes	Yes	No	Day	675	1203	No Drop
	9nc&e270.fwd	1999/03/23	270	Yes	Yes	No	Day	581	886	No Drop
After HVS Testing	11NC&Ed2.fwd	2001/02/07	966	Yes	No	Yes	Day	694	1119	No Drop
	11NCtrday.FWD	2001/02/07	966	Yes	No	No	Day	699	1182	No Drop
	11NCtrnit.FWD	2001/02/08	966	Yes	No	No	Night	659	963	No Drop
	11NEdgday.FWD	2001/02/07	966	No	No	Yes	Day	689	1055	No Drop
	11SCtrday.FWD	2001/02/07	966	Yes	No	No	Day	669	924	No Drop
	11SCtrnit.FWD	2001/02/07	966	Yes	No	No	Night	710	1041	No Drop
	11NC&En2.fwd	2001/02/08	967	Yes	No	Yes	Night	663	979	No Drop
	11NEdgnit.FWD	2001/02/08	967	No	No	Yes	Night	668	995	No Drop
	pmndc.fwd	2001/02/10	969	Yes	No	No	Day	618	914	1262
	pmnnc.fwd	2001/02/10	969	Yes	No	No	Night	625	923	1274
	pmnns.fwd	2001/02/10	969	No	Yes	No	Night	620	919	1280
	pmndk.fwd	2001/02/10	969	No	No	Yes	Day	629	935	1290
	pmnds.fwd	2001/02/11	970	No	Yes	No	Day	607	910	1267
	pmnnk.fwd	2001/02/11	970	No	No	Yes	Night	612	920	1285
	4NCTRDAY.FWD	2002/04/08	1391	Yes	No	No	Day	613	959	996
	4NEDGDAY.FWD	2002/04/08	1391	No	No	Yes	Day	617	957	No Drop
	4NCTRNIT.FWD	2002/04/10	1393	Yes	No	No	Night	603	931	No Drop
	4NEDGNIT.FWD	2002/04/10	1393	No	No	Yes	Night	583	901	No Drop
	5NCTRDAY.FWD	2002/08/14	1519	Yes	No	No	Day	554	831	No Drop
	5NEDGDAY.FWD	2002/08/14	1519	No	No	Yes	Day	535	792	No Drop
	5NCTRNIT.FWD	2002/08/15	1520	Yes	No	No	Night	544	806	No Drop
	5NEDGNIT.FWD	2002/08/15	1520	No	No	Yes	Night	511	744	No Drop

Table 40 continued

	Filename	Record Date	Days Before (-) or After (+) Construction	Drop Locations			Time of Day	Approximate Pressure (kPa)		
				Center	Shoulder	K-rail		Drop 1	Drop 2	Drop 3
After HVS Testing	12NCTRDY.FWD	2002/10/24	1590	Yes	No	No	Day	434	704	No Drop
	12NEDGDY.FWD	2002/10/24	1590	No	No	Yes	Day	407	653	No Drop
	12NCTRNT.FWD	2002/10/25	1591	Yes	No	No	Night	414	668	No Drop
	12NEDGNT.FWD	2002/10/25	1591	No	No	Yes	Day	389	623	No Drop
	13NCTRDY.FWD	2003/04/01	1749	Yes	No	No	Day	440	632	No Drop
	13NCTRNT.FWD	2003/04/02	1750	Yes	No	No	Night	424	600	No Drop
	13NEDGDY.FWD	2003/04/01	1750	No	No	Yes	Day	434	622	No Drop
	13NEDGNT.FWD	2003/04/02	1750	No	No	Yes	Night	417	590	No Drop
	14NCTRDY.FWD	2003/06/23	1832	Yes	No	No	Day	442	729	No Drop
	14NS11DY.FWD	2003/06/23	1832	No	Yes	No	Day	432	692	No Drop
	14NCTRNT.FWD	2003/06/24	1833	Yes	No	No	Night	428	687	No Drop
	14NED2NT.FWD	2003/06/24	1833	No	No	Yes	Night	405	648	No Drop
	14NED2DY.FWD	2003/06/25	1834	No	No	Yes	Day	439	714	No Drop
	14NEDRNT.FWD	2003/06/25	1834	No	Yes	No	Night	411	658	No Drop
	14NEDRDY.FWD	2003/06/25	1834	No	Yes	No	Day	434	713	No Drop
	14NS11NT.FWD	2003/06/25	1834	No	Yes	No	Night	391	621	No Drop

The set of measurements summarized in Table 40 represents a large data collection of more than 65,000 deflection bowls in which the following parameters are varied: (1) joint construction, (2) station position, (3) load level, (4) age after construction, (5) trafficking (HVS and other), and (6) temperature. All of these FWD files are now in the Pavement Research Center Database.

5.2 Test Configuration

FWD testing was performed on all North Tangent concrete slabs including those trafficked by the HVS. For most of the FWD tests, deflections were measured along the centerline of the slabs, and along the K-rail (trafficked edge) and shoulder of the slab, as shown in Figure 108. For deflections measured along the centerline of the slab, one deflection was measured at the center of the slab, and every other deflection was measured across the transverse joint. A similar protocol was followed along the K-rail edge of the slabs. However, for this line of measurement, the second and third sensors were arranged so that they measured joint transfer efficiency across the longitudinal joint. Figure 109 shows the typical measurement arrangement and sensor spacing for measurements taken across transverse and longitudinal joints.

5.2.1 Principal Effects

Analysis of the pavement surface temperature recorded during testing showed that, within a specific test run, there is generally less than 5ºC overall variation in surface temperature recorded at different stations during testing. Thus, within a specific test, temperature is not considered to be a principal effect. This can also be seen from the deflection and LTE versus

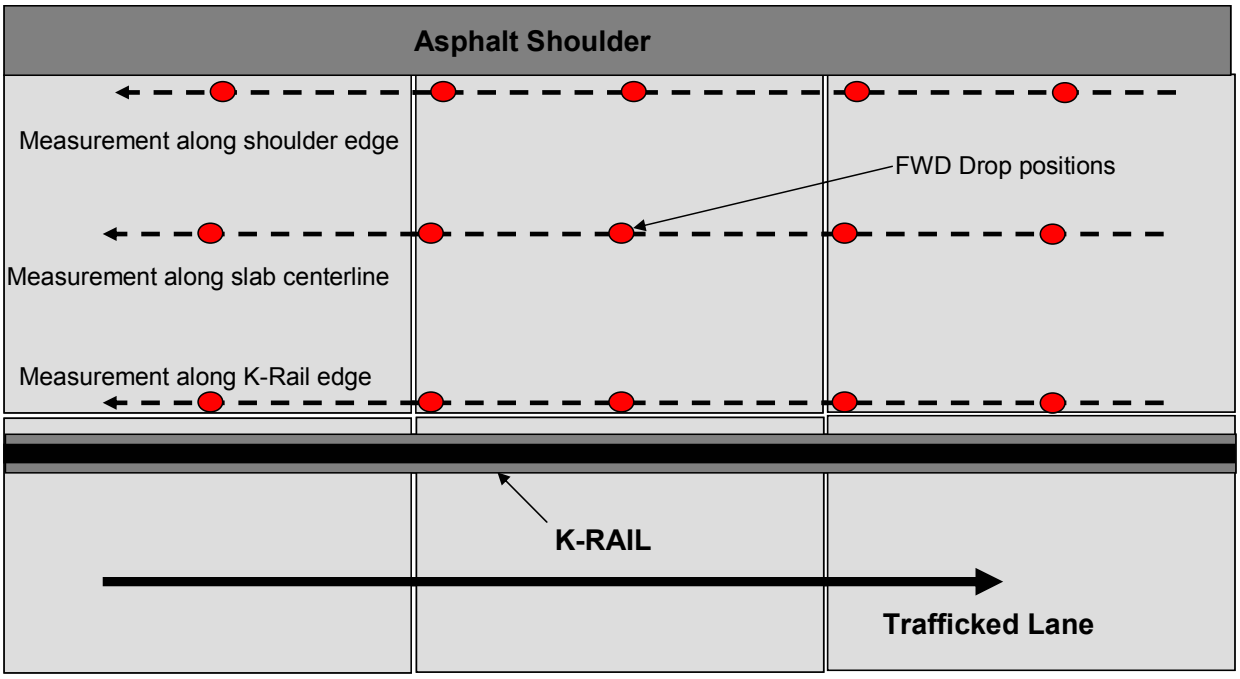

Figure 108. General setup for FWD measurement locations.

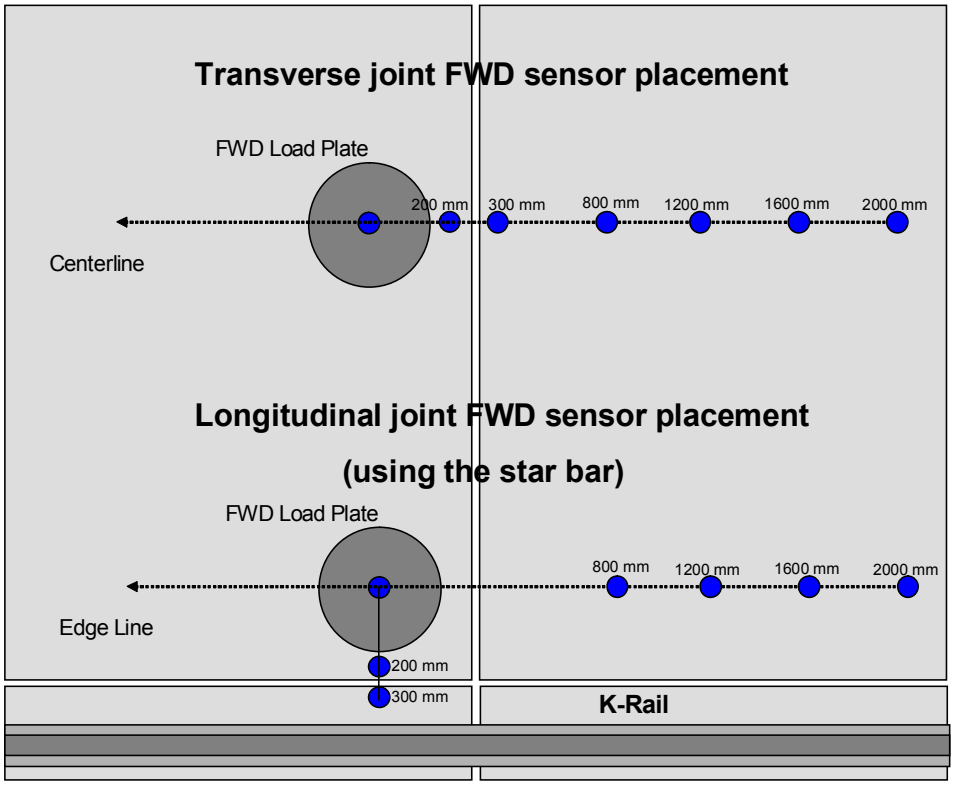

Figure 109. Sensor setup for measurements across transverse and longitudinal joints.

station graphs in Appendix A, which exhibit little or no correlation between surface temperature and test result.

The variation in the average surface temperature recorded for different tests does, however, vary significantly, and has a significant effect on measured results. This aspect will be discussed subsequently.

Another principal effect on FWD measurements is the applied pressure, or load level used during deflection testing. It will be noted from Table 40 that the deflections measured at various times after construction were recorded at widely differing loads. In order to compare the different load pressures at different times, a standard load level of 943 kPa, or 66.7 kN (15,000 lbs.) was used. Because of minor surface irregularities, the actual pressure applied by the FWD differs from station to station. To compensate for these variations, all deflections shown in this chapter were normalized to a common load level of 66.7 kN before plotting or calculation of statistics.

An important aspect noted during data analysis was the interaction between concrete age (quantified by the number of days after concrete construction) and the test temperature (quantified by the average surface temperature recorded during FWD testing).

For the tests performed before HVS testing (up to 270 days after construction, as shown in Table 40), the recorded surface temperature was always above 10ºC and mostly above 20ºC. In contrast, for the deflections recorded after HVS testing, the recorded surface temperature was often below 10ºC and sometimes below 0ºC. One reason for this is that FWD tests performed after HVS testing includes both daytime and nighttime measurements. These tests therefore were performed at a greater temperature range than those tests performed before HVS testing.

Because temperature has a significant effect on deflections, and on LTE in particular (as discussed in a later subchapter of this chapter), it is to be expected that the deflections measured after HVS testing will exhibit a greater variation compared to those measured before HVS testing. It should thus be kept in mind that the slab temperature always affects the apparent effects of concrete age on deflections. This aspect will be discussed in more detail in later subchapters.

5.3 Analysis of Maximum Deflections

5.3.1 Measurements Recorded Prior to Concrete Construction

Figures 110 and 111 show the maximum deflection measured approximately 16 days before construction of the concrete slabs. Data shown in these figures were measured at a load of approximately 60 kN and were normalized to 66.7 kN to facilitate comparisons. Both figures show that, apart from a single point situated at approximately 150 m, the support conditions are largely similar for the three joint construction types.

If both the centerline and K-rail side measurements are considered, then Section 11 (4.26-m widened lane, dowels at joints, asphalt shoulder without tie bars) seems to have slightly better support conditions and a lower variation in support condition than Sections 7 (no dowels or tie bars) and 9 (dowels and tie bars).

A comparison of Figures 110 and 111 also shows that measurements taken along the K-rail edge consistently show a larger variation in maximum deflection than the measurements taken along the centerline.

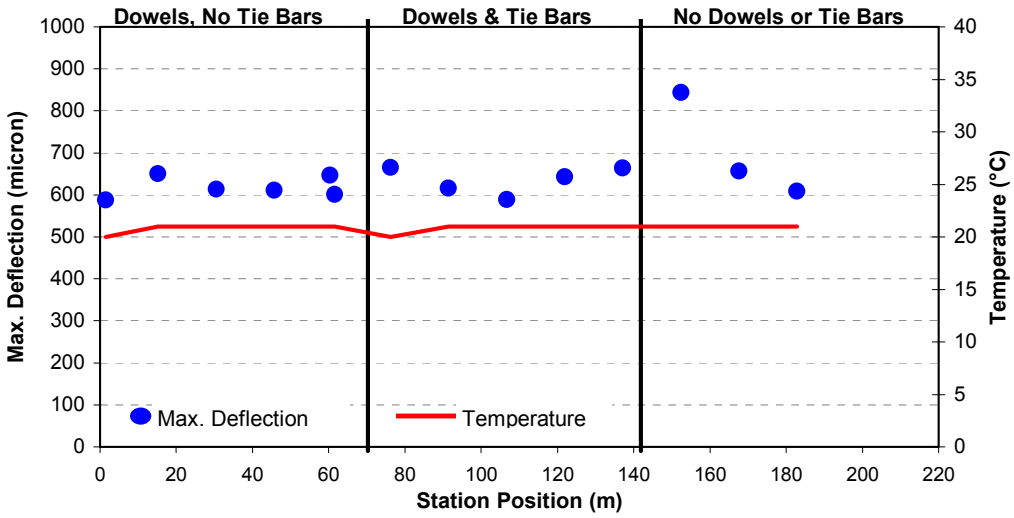

Dowels, No Tie Bars	
Parameter	Value
Mean	618
Std. Dev	24.9
85th %	647
15th %	598
COV (%)	4.0%

Dowels and Tie Bars	
Parameter	Value
Mean	635
Std. Dev	33.0
85th %	664
15th %	605
COV (%)	5.2%

No Dowels, No Tie Bars	
Parameter	Value
Mean	703
Std. Dev	124.3
85th %	788
15th %	623
COV (%)	17.7%

Figure 110. Maximum deflection measured along slab centerline prior to concrete construction.

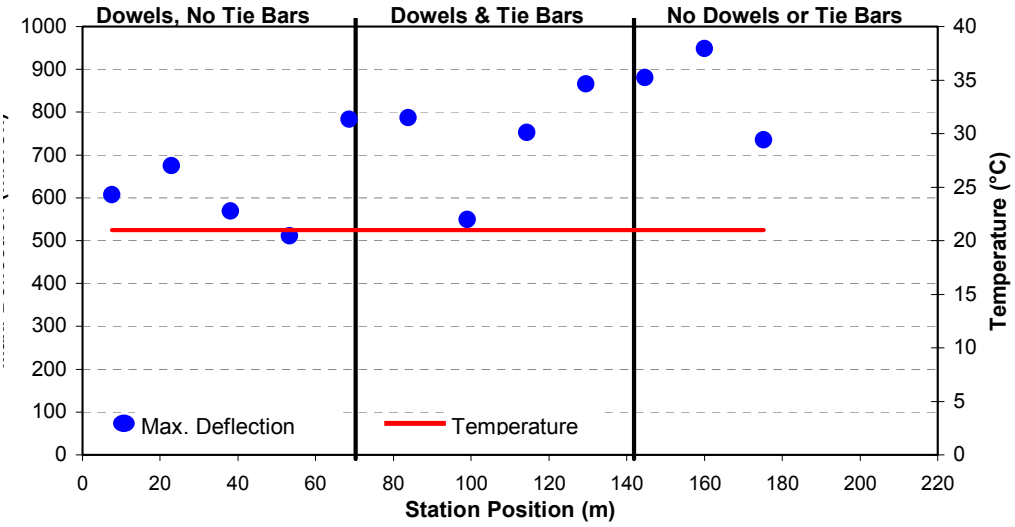

Dowels, No Tie Bars	
Parameter	Value
Mean	629
Std. Dev	104.9
85th %	718
15th %	546
COV (%)	16.7%

Dowels and Tie Bars	
Parameter	Value
Mean	738
Std. Dev	134.5
85th %	830
15th %	641
COV (%)	18.2%

No Dowels, No Tie Bars	
Parameter	Value
Mean	854
Std. Dev	108.8
85th %	928
15th %	779
COV (%)	12.7%

Figure 111. Maximum deflection measured along K-rail edge prior to concrete construction.

5.3.2 Measurements Taken After Concrete Construction

The central deflections (i.e., measured at the center of the FWD loading plate) measured at different times after construction are summarized in Tables 41 and42 for the centerline and K-rail edge measurements, respectively. The data shown in these tables are the average central deflection values for deflections measured over each test section at the construction age shown.

It should be noted that the data in these tables include only those measurements taken at the slab center (in longitudinal direction). Thus, measurements taken at transverse joints and corners are not considered in Tables 41 and 42. Furthermore, the data considered for this chapter excludes all deflections measured on slabs which were tested by the HVS. The reason for this is that the aim was to compare deflection measurements on slabs which were only exposed to environmental factors and not HVS loading.

The data shown in Tables 41 and 42 are represented graphically in Figures 112–123. In these figures, two legends are used to distinguish between deflections recorded during daytime and nighttime.

As expected, deflections measured at the longitudinal edge (K-rail side, Table 42) are consistently much higher than those measured at the center of the slab (Table 41). This effect can be partly attributed to the poorer support conditions along the K-rail edge, as noted in the previously.

The central deflections measured at the slab center (Table 41 and Figures 112–117), prompt the following observations:

- The central deflection data do not exhibit a clear pattern or relationship between either central deflection and concrete age, or central deflection and surface temperature.

- Considering the large variation in concrete age and temperature, as well as the combined influence of these two effects, Section 11 (dowels, no tie bars) shows a remarkably consistent average deflection that ranges roughly from .090 to .160 mm.
- Surprisingly, Section 9, which is equipped with both dowels and tie bars, shows a larger variation in average deflection than Section 7, with deflections that range from approximately .100 to .190 mm.
- The data for all test sections show only marginal differences between the deflections measured at day and those measured at night at the same time after concrete construction.

Table 41 Summary of Average Central Deflections Along Slab Centerline

Concrete Age (days)	Temperature, ºC	Average Central Deflection Normalized to 66.7 kN (mm)		
		Dowels, No Tie Bars	Dowels and Tie Bars	No Dowels or Tie Bars
-90 (on CTB)	16	0.145	0.156	0.155
2	28	0.087	0.108	0.107
6	24	0.090	0.099	0.090
49	39	0.106	0.142	0.110
85	22	0.111	0.157	0.110
203	13	0.120	0.193	0.128
279	13	0.125	0.169	0.122
966	6	0.121	0.171	0.135
967	-1	0.132	0.158	0.142
969	3	0.134	0.128	0.172
969	3	0.130	0.131	0.171
1391	21	0.133	0.122	0.122
1393	13	0.144	0.140	0.158
1519	35	0.132	0.129	0.124
1520	25	0.127	0.134	0.143
1590	17	0.127	0.178	0.143
1591	8	0.157	0.179	0.138
1749	19	0.149	0.146	0.152
1750	7	0.122	0.153	0.138
1832	21	0.138	0.130	0.132
1833	10	0.124	0.154	0.182

Note: Transverse joint deflections are excluded.

Table 42 Summary of Average Central Deflection Measured Along Slab Edge (K-rail Side)

Concrete Age (days)	Temperature, ºC	Average Central Deflection Normalized to 66.7 kN (mm)		
		Dowels, No Tie Bars	Dowels and Tie Bars	No Dowels or Tie Bars
966	4	0.432	0.485	0.361
967	-1	0.561	0.506	0.441
969	4	0.448	0.414	0.374
970	2	0.575	0.433	0.454
1391	69	0.154	0.309	0.218
1393	55	0.275	0.593	0.406
1519	33	0.233	0.330	0.236
1520	26	0.353	0.656	0.336
1590	14	0.477	0.788	0.379
1591	8	0.671	0.957	0.569
1749	17	0.166	0.242	0.205
1750	7	0.257	0.639	0.272

Note: Corner deflections are excluded.

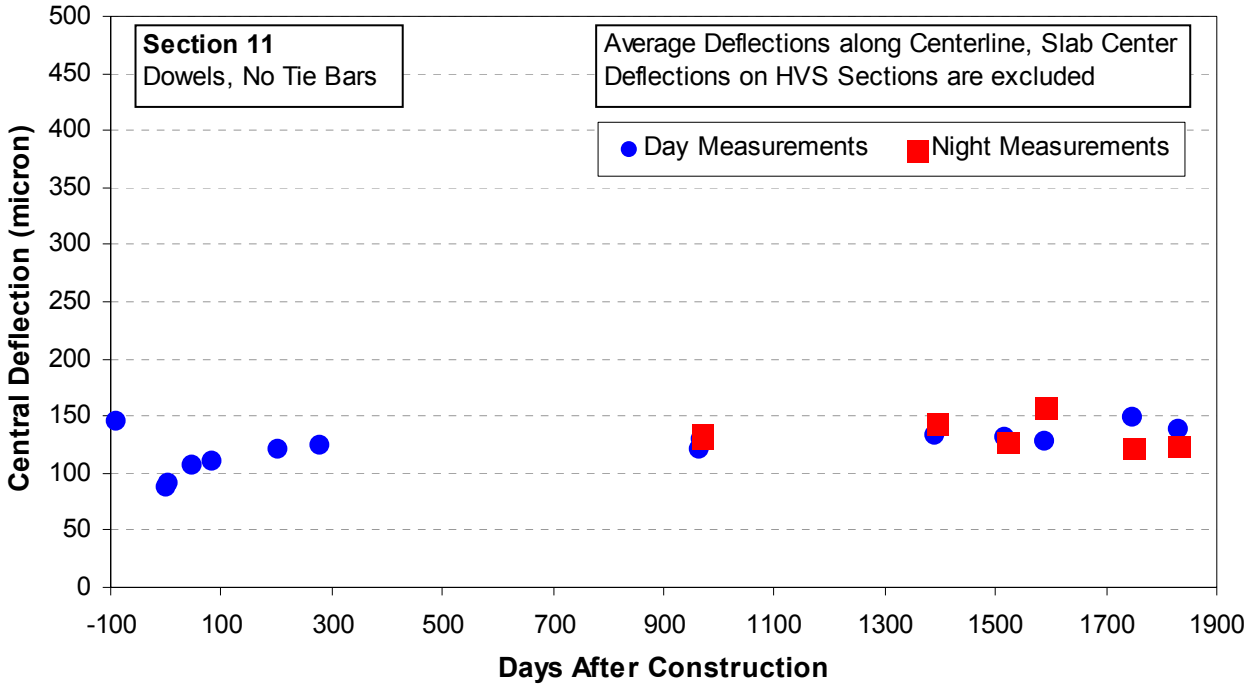

Figure 112. Central deflection along centerline at different concrete ages, Section 11 (doweled joints with asphalt concrete shoulder and widened truck lane).

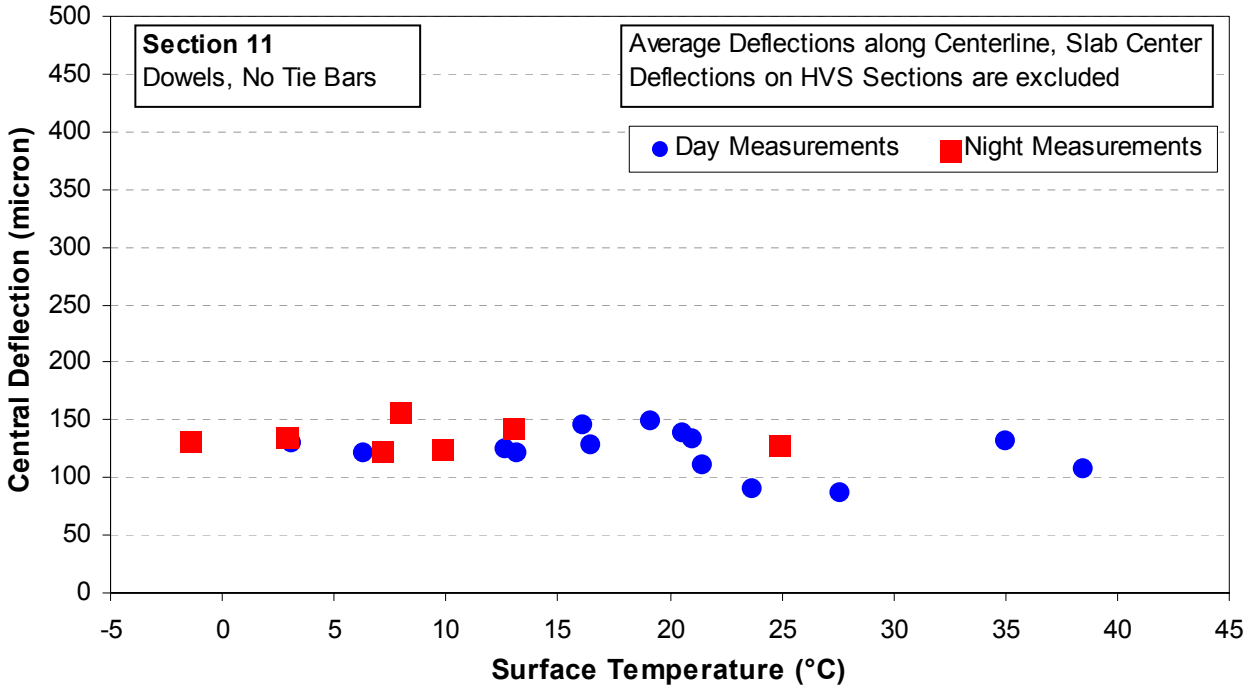

Figure 113. Central deflection along centerline at different surface temperatures, Section 11 (doweled joints with asphalt concrete shoulder and widened truck lane),

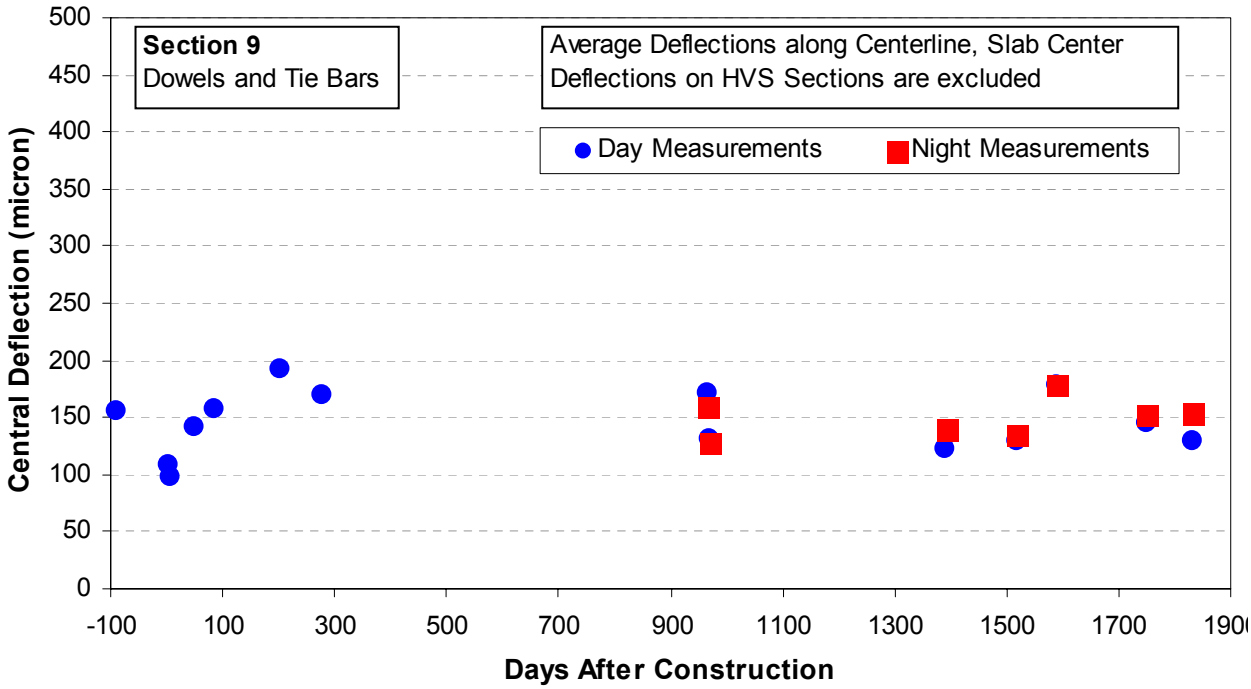

Figure 114. Central deflection along centerline at different concrete ages, Section 9 (doweled joints and tie bars at concrete shoulder).

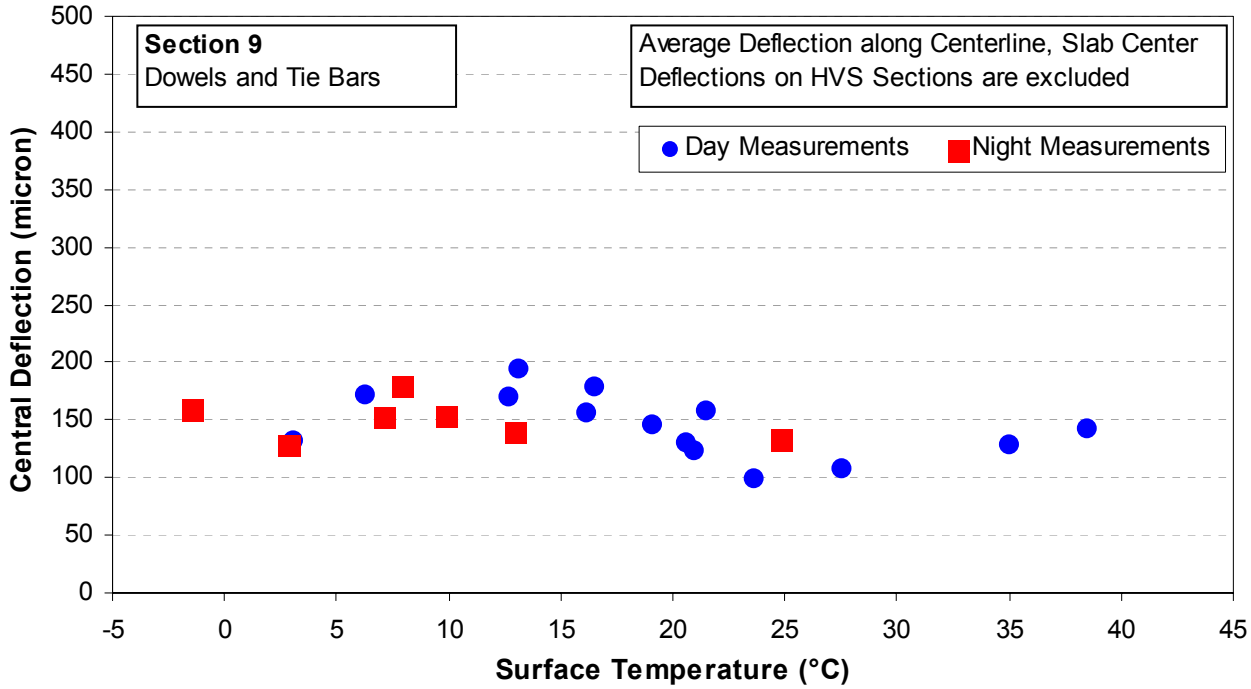

Figure 115. Central deflection along centerline at different temperatures, Section 9 (doweled joints and tie bars at concrete shoulder).

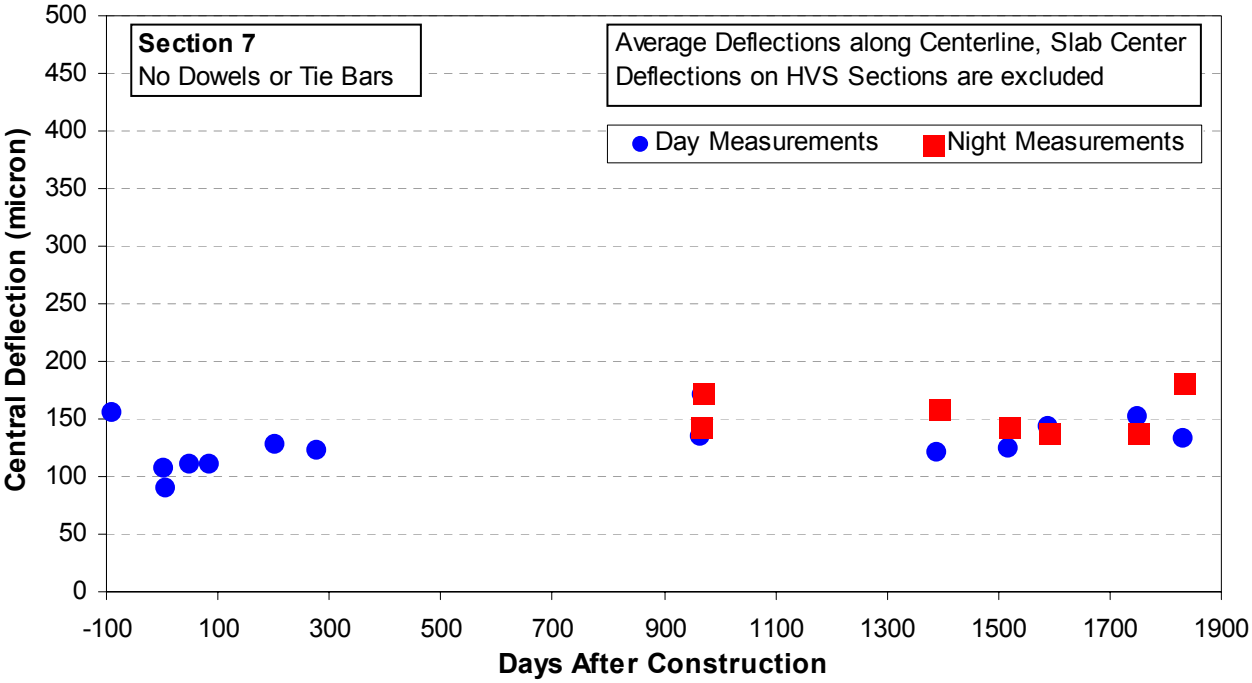

Figure 116. Central deflection along centerline at different concrete ages, Section 7 (no dowels or tie bars, asphalt concrete shoulder).

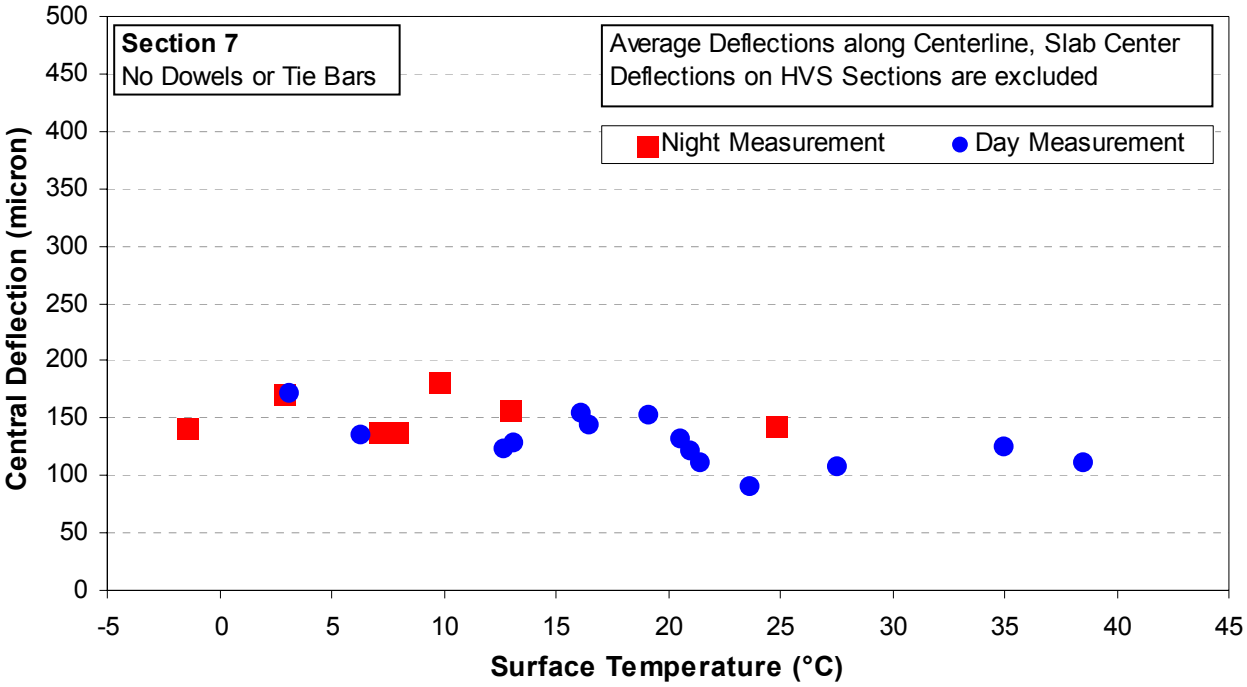

Figure 117. Central deflection along centerline at different temperatures, Section 7 (no dowels or tie bars, asphalt concrete shoulder).

The deflections measured along the longitudinal joint at the K-rail side (Table 42 and Figures 118–123) prompt the following observations:

- Compared to the deflections measured along the slab centerline (see Figures 112–117), the deflections measured along the K-rail edge exhibit a greater difference between daytime and nighttime measurements. All three test sections consistently show significant difference between the deflections recorded during the day and those recorded at night.
- For all construction types, the deflections recorded at night are significantly higher than those recorded during the day. Nighttime deflections are consistently higher than daytime deflections recorded at the same concrete age (see for example, Figures 118and 122).

- Because these measurements were recorded at a longitudinal joint, the higher deflections at night (i.e., at lower temperatures) are expected and are partly attributable to a reduced LTE at lower temperatures when joints are more open than at higher temperatures.
- A clear pattern between central deflection and concrete age is not noted for any of the sections. Similarly, there is no clear relationship between central deflection and surface temperature. The lack of relationship between surface temperature and central deflection suggests that the difference between day and night measurements is not caused only by temperature, but is influenced by other factors. Also, it is expected that the confounded effect of concrete age and slab temperature masks any clear relationship that may exist between central deflection and either concrete age or slab temperature.

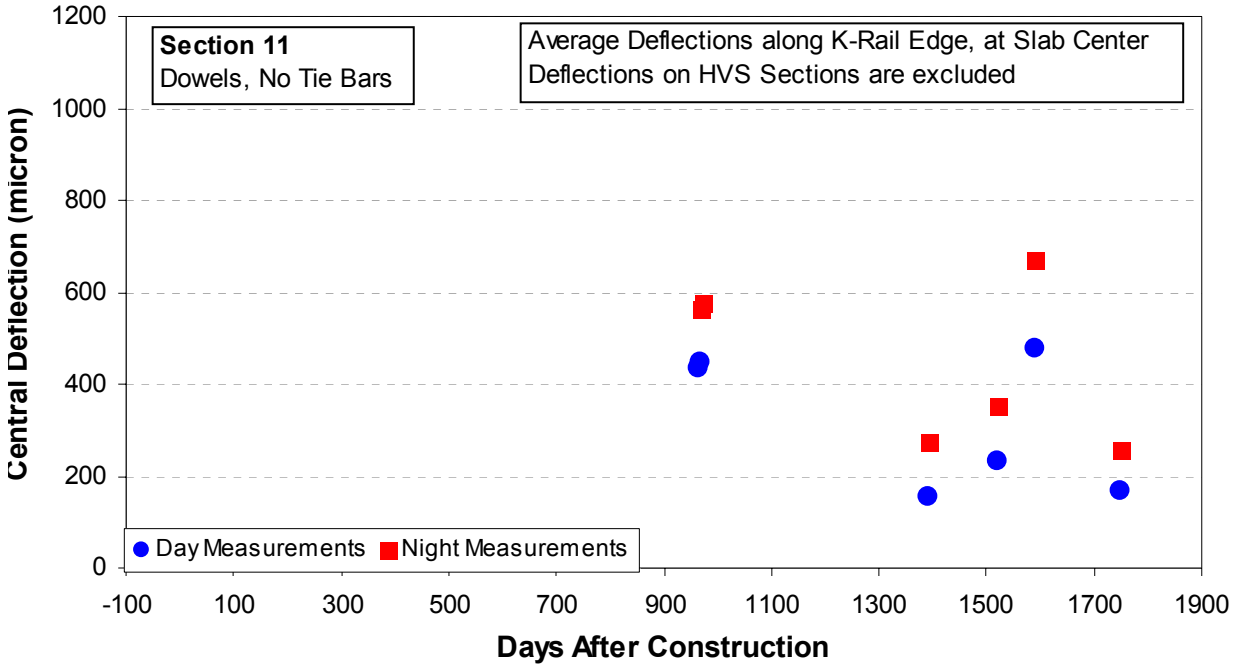

Figure 118. Central deflection along K-rail at different concrete ages, Section 11 (doweled joints with asphalt concrete shoulder and widened truck lane).

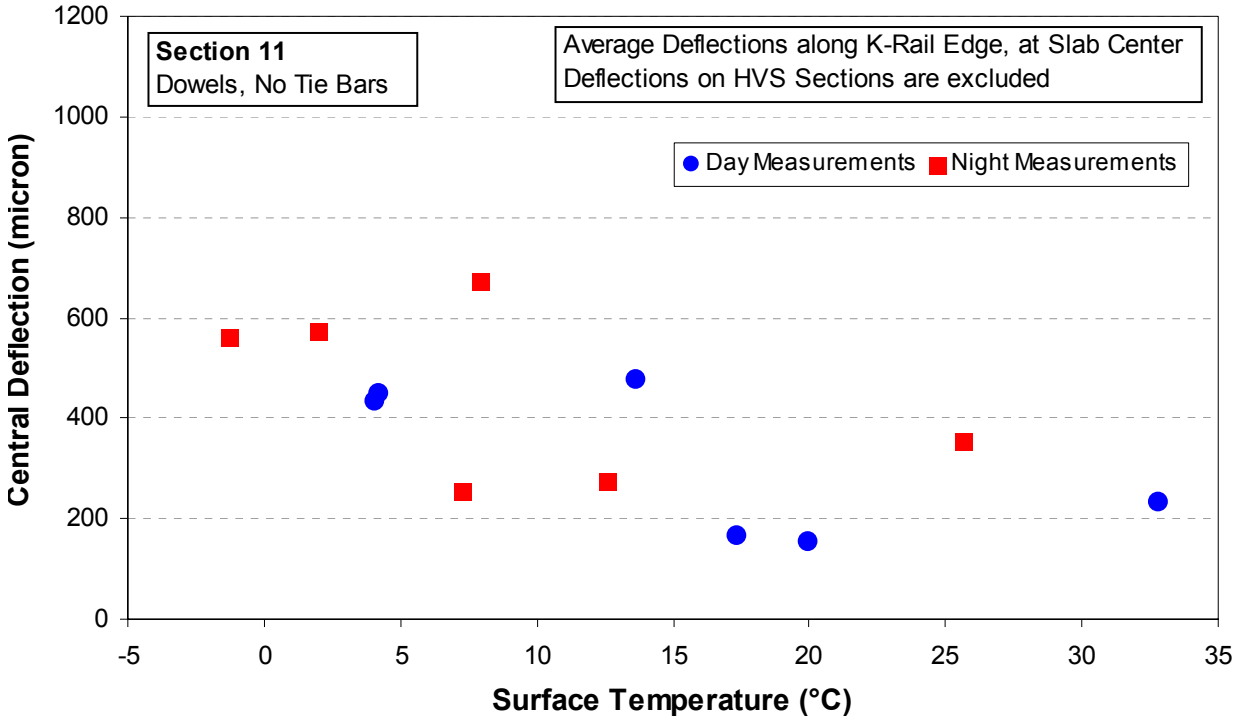

Figure 119. Central deflection along K-rail at different temperatures, Section 11 (doweled joints with asphalt concrete shoulder and widened truck lane).

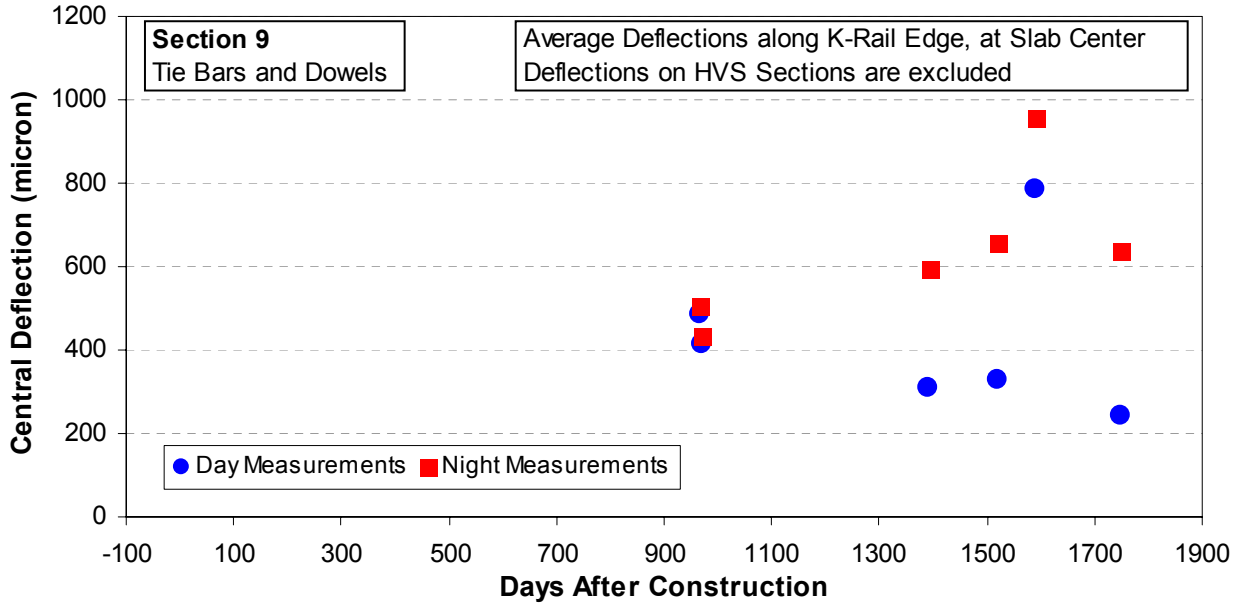

Figure 120. Central deflection along K-rail at different concrete ages, Section 9 (doweled joints and tie bars at concrete shoulder).

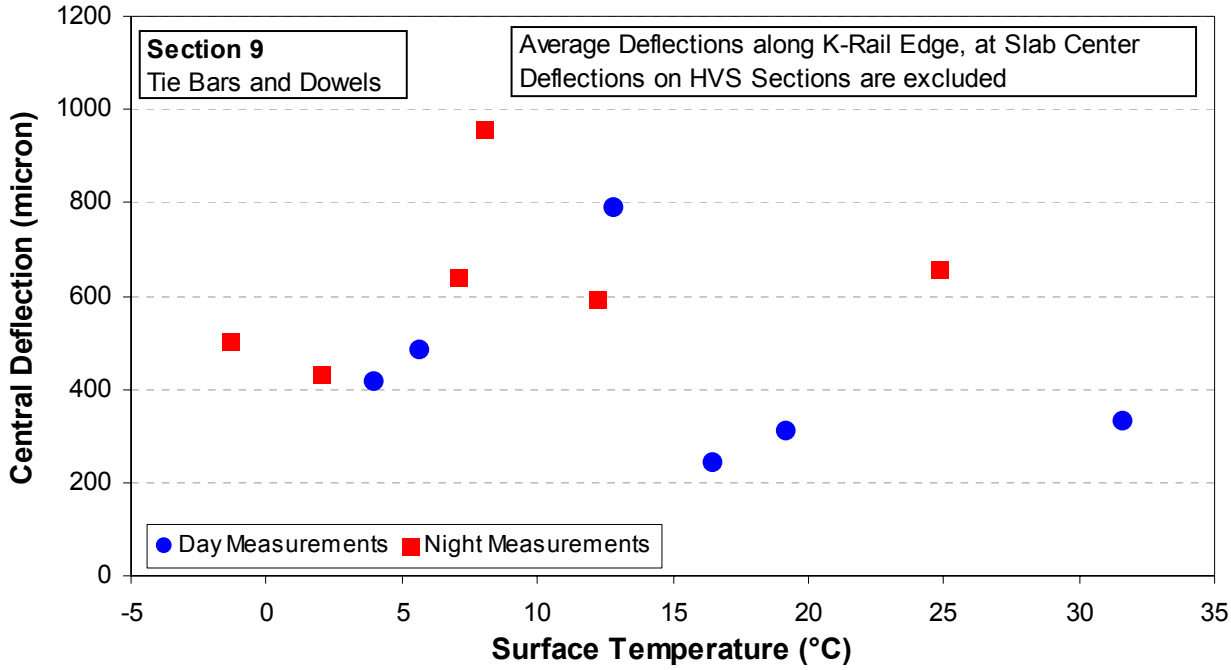

Figure 121. Central deflection along K-rail at different temperatures, Section 9 (doweled joints and tie bars at concrete shoulder).

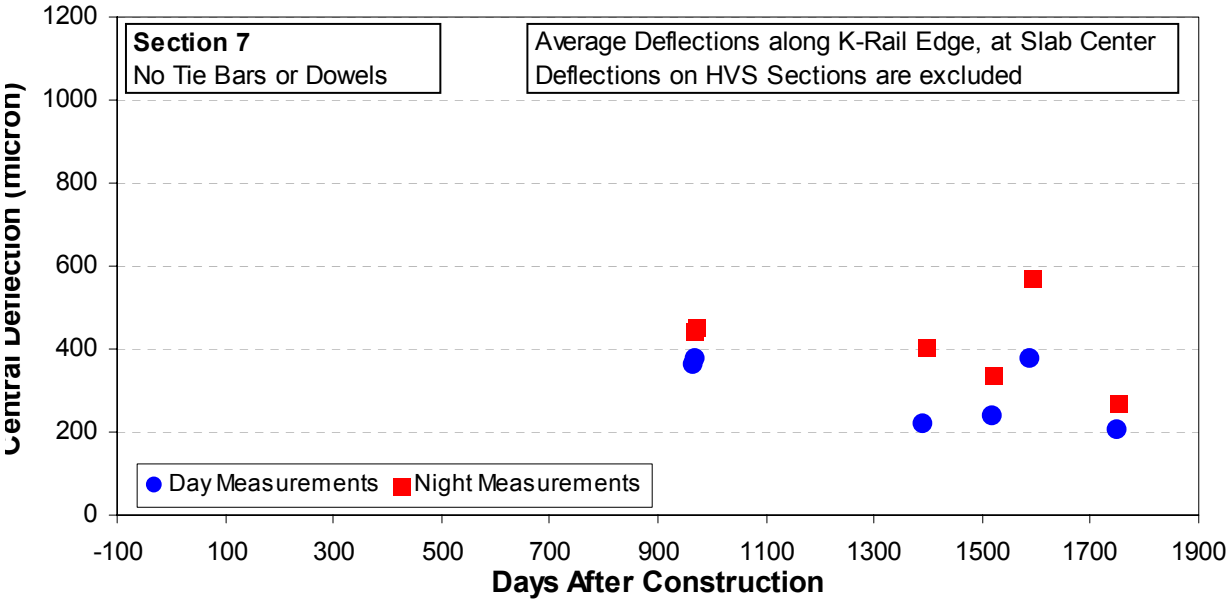

Figure 122. Central deflection along K-rail at different concrete ages, Section 7 (no dowels or tie bars, asphalt concrete shoulder).

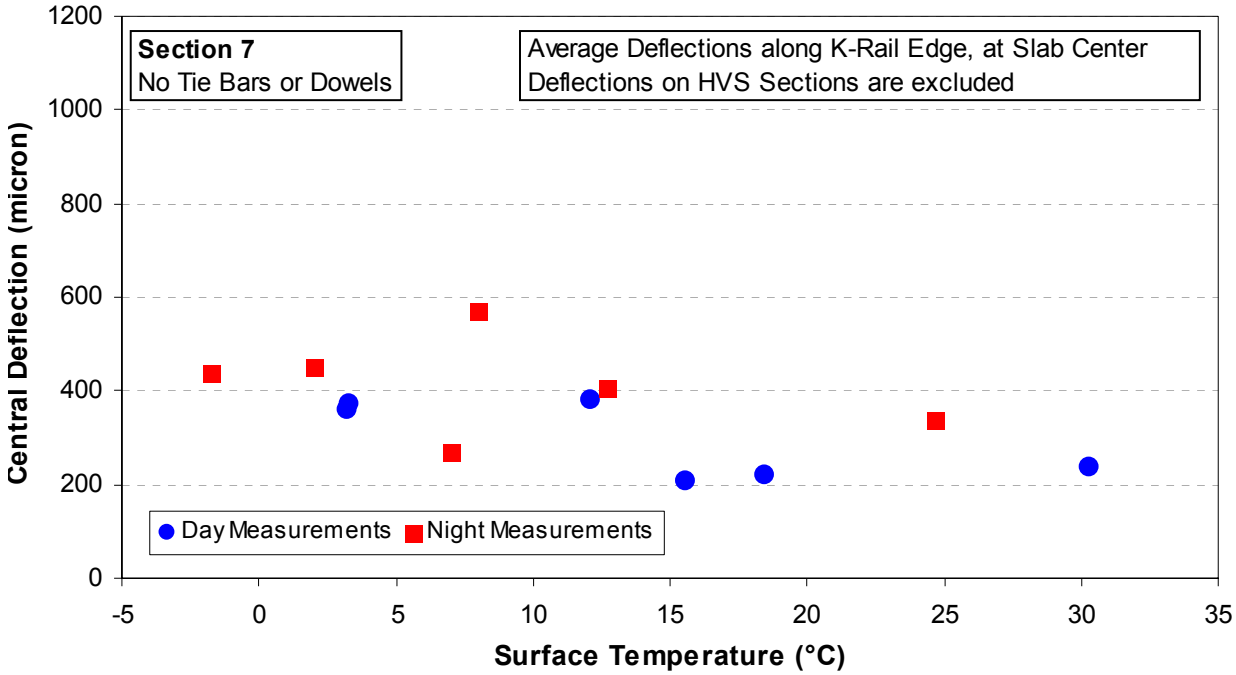

Figure 123. Central deflection along K-rail at different temperatures, Section 7 (no dowels or tie bars, asphalt concrete shoulder).

5.4 Load Transfer Efficiency Across Joints

For the analysis presented here, the load transfer efficiency (LTE) across joints is quantified by the deflection ratio over joints. This parameter is obtained by dividing the deflection measured closest to the joint on the unloaded side by the deflection measured closest to the joint on the loaded side of the joint. (The setup for FWD measurement of deflections across joints is discussed in Chapter 5.2.2, and is summarized in Figure 109).

An example of this calculation is shown in Figure 124, which shows a typical deflection profile measured across a transverse joint for measurements taken along the slab centerline. Figure 125 shows a typical deflection profile measured across a longitudinal joint (along slab edge, K-rail side) at the same date and at roughly the same location.

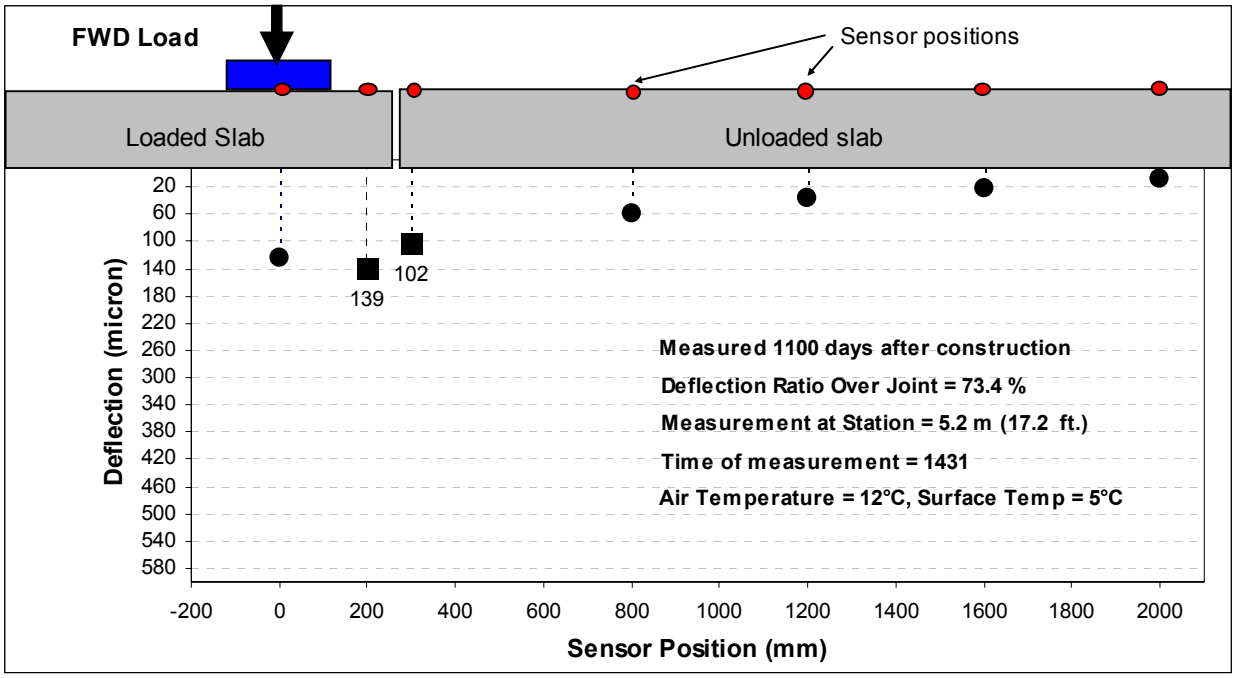

Figure 124. Typical deflection profile measured across a transverse joint along slab centerline.

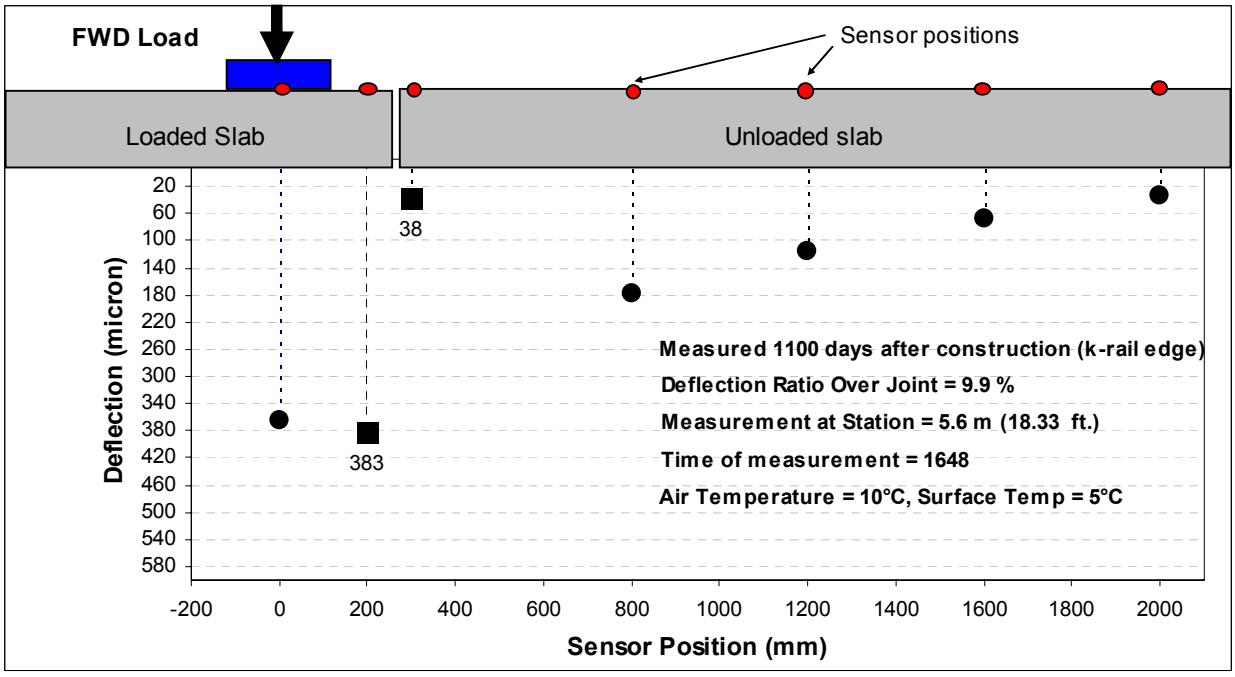

Figure 125. Typical deflection profile measured across a transverse joint along slab edge (K-rail side).

It is clear from Figures 124 and 125 that the load transfer efficiency can be significantly different at transverse and longitudinal joints. The data presented in the rest of this chapter is aimed at summarizing the main effects noted for transverse and longitudinal joint load transfer efficiency for the three joint construction types used on the North Tangent.

Tables 43–45 summarize the LTE quantified by the deflection ratio for the different joint construction types at different times of construction. Data shown in Table 43 represent LTE measured over transverse joints along the slab centerline, while the data shown in Table 44 and 5.6 represent the LTE measured across the longitudinal joint along the slab edge at the K-rail side, and at the slab center and corner positions, respectively. Deflections falling within HVS test sections are excluded from the data shown in Tables 43–45.

Table 43 Summary of LTE Across Transverse Joints Along Slab Centerline

Concrete Age (days)	Temperature, ºC	Average LTE (%) at 66.7 kN along Slab Centerline		
		Dowels, No Tie Bars	Dowels and Tie Bars	No Dowels or Tie Bars
2	28	78	83	84
6	24	80	80	60
49	39	86	86	62
85	21	84	86	58
203	13	82	87	37
279	13	81	84	32
966	6	82	85	33
967	-1	81	85	20
969	3	59	59	38
969	3	62	62	40
1391	21	93	92	94
1393	13	88	90	73
1519	35	94	94	94
1520	25	92	92	93
1590	17	84	89	72
1591	8	86	91	62
1749	19	94	94	94
1750	7	88	87	68
1832	20	92	92	93
1833	10	88	94	77

Table 44 Summary of LTE Across Longitudinal Joints Along K-Rail Edge, Slab Center

Concrete Age (days)	Temperature, ºC	Average LTE (in %) at 66.7 kN along K-Rail Edge, Slab Center		
		Dowels, No Tie Bars	Dowels and Tie Bars	No Dowels or Tie Bars
966	6	10	15	24
967	-1	5	13	11
969	4	8	12	24
970	2	4	10	11
1391	19	73	19	71
1393	12	59	3	59
1519	32	92	55	87
1520	25	79	20	70
1590	13	32	2	47
1591	8	28	1	17
1749	17	83	56	73
1750	7	72	3	63

Table 45 Summary of LTE Across Longitudinal Joints Along K-Rail Edge, At Slab Corner

Concrete Age (days)	Temperature, ºC	Average LTE (in %) at 66.7 kN along K-Rail Edge, Slab Corner		
		Dowels, No Tie Bars	Dowels and Tie Bars	No Dowels or Tie Bars
966	6	7	13	12
967	-1	3	10	8
969	4	6	10	9
970	2	3	8	6
1391	19	59	18	39
1393	13	26	4	25
1519	32	89	56	75
1520	25	60	16	63
1590	13	45	3	32
1591	8	14	2	12
1749	16	78	54	60
1750	7	37	5	32
1833	10	90	95	82
1834	29	93	94	93

The data shown in Tables 43 to 45 are summarized graphically in Figures 126–145. Specifically, Figures 126–133 summarize the LTE effects over transverse joints at the slab center, while Figures 134–145 summarizes the LTE effects noted over longitudinal joints.

Tables 43–45 show that the LTE measured across transverse joints is consistently higher (i.e., better load transfer) than that measured across the longitudinal joint. As expected, the LTE measured across the transverse joints show a dependency on the joint construction type, whereas the LTE measured along the longitudinal joint shows little or no systematic variation. This is discussed in more detail subsequently.

The data measured along the slab centerline across transverse joints (Table 44), prompt the following observations:

- The transverse joint LTEs of Sections 9 and 11 (both fitted with dowels) show no significant dependency on age or temperature. These two sections exhibit very similar LTEs, which range from 80 to 100 percent in almost all cases, regardless of concrete age or temperature (see Figure 128–131).
- In contrast to Sections 9 and 11, which are both fitted with dowels, the LTE measured on Section 7 (no dowels) shows a definite dependency on concrete temperature (see Figure 133).
- At concrete ages of roughly less than 300 days, the LTE of Section 7 is significantly lower than that of Sections 9 and 11, regardless of the measurement temperature (see Figure 126).
- At concrete ages of roughly 950 days and longer, the LTEs of Section 7 differ from those of Sections 9 and 11 only when the slab temperature is roughly below 15ºC. This effect is highlighted in Figure 127.

- Section 7 (no dowels or tie bars) shows a consistent difference between LTE measured during the day and that measured at night (see Figure 133). In contrast, there is very little difference between daytime LTEs and nighttime LTEs for Sections 9 and 11 (both fitted with dowels).
- Section 7 (no dowels or tie bars) shows a clear correlation between concrete temperature and LTE. The correlation is especially clear for the nighttime measurements (see Figure 133). It is believed that the relationship is less clear in the case of the daytime measurements because these measurements include concrete aging effects, which are quite pronounced for concrete ages of less than 300 days (see Figure 132).

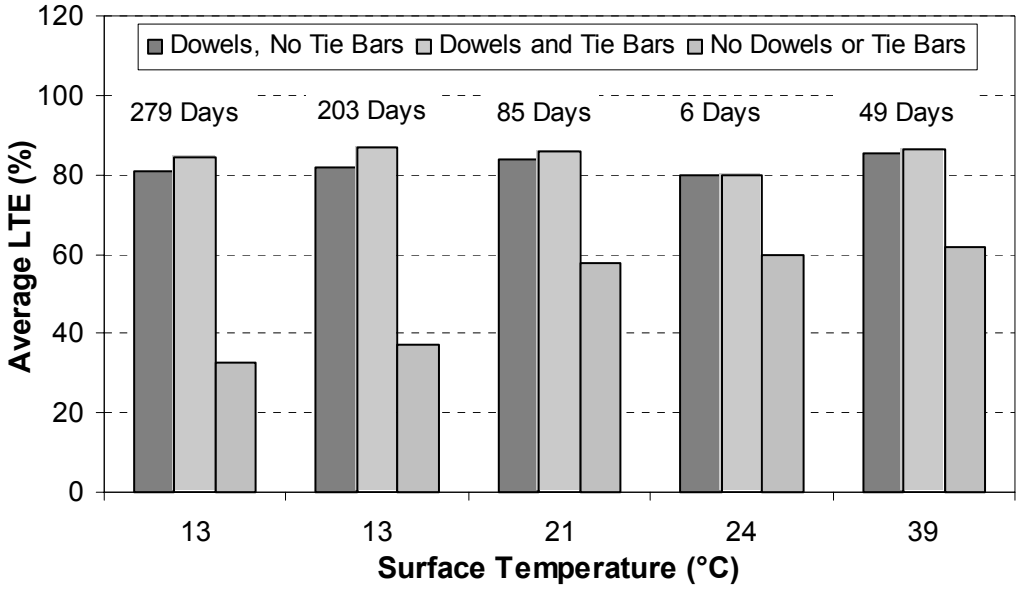

Figure 126. LTE across transverse joints at concrete ages of less than 300 days.

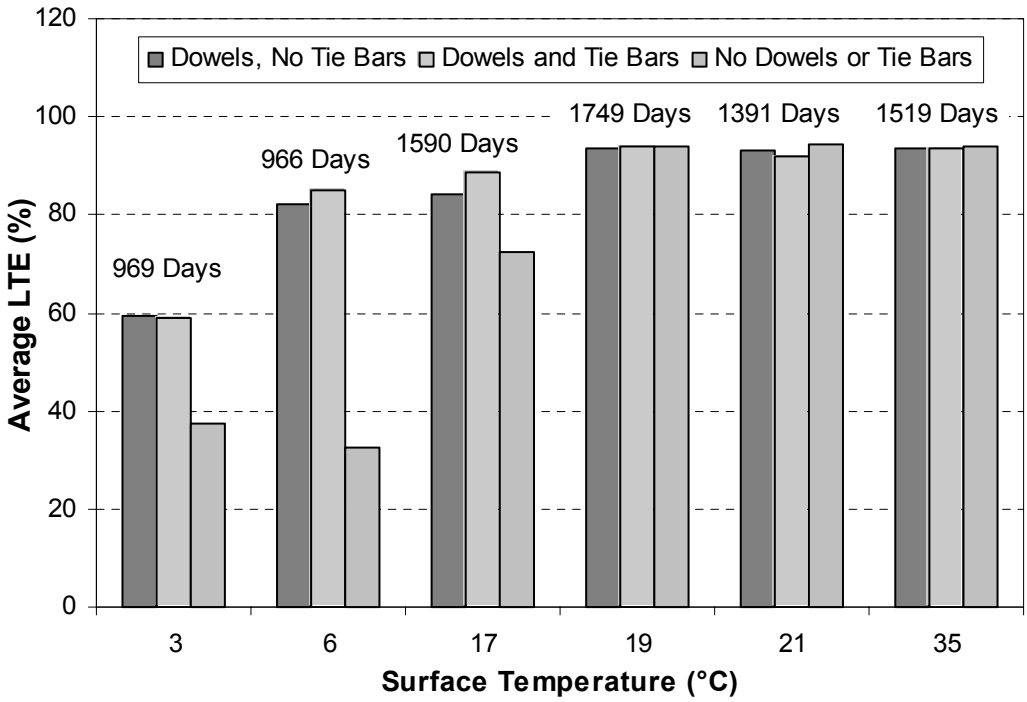

Figure 127. LTE across transverse joints at concrete ages of more than 900 days (only day measurements are shown).

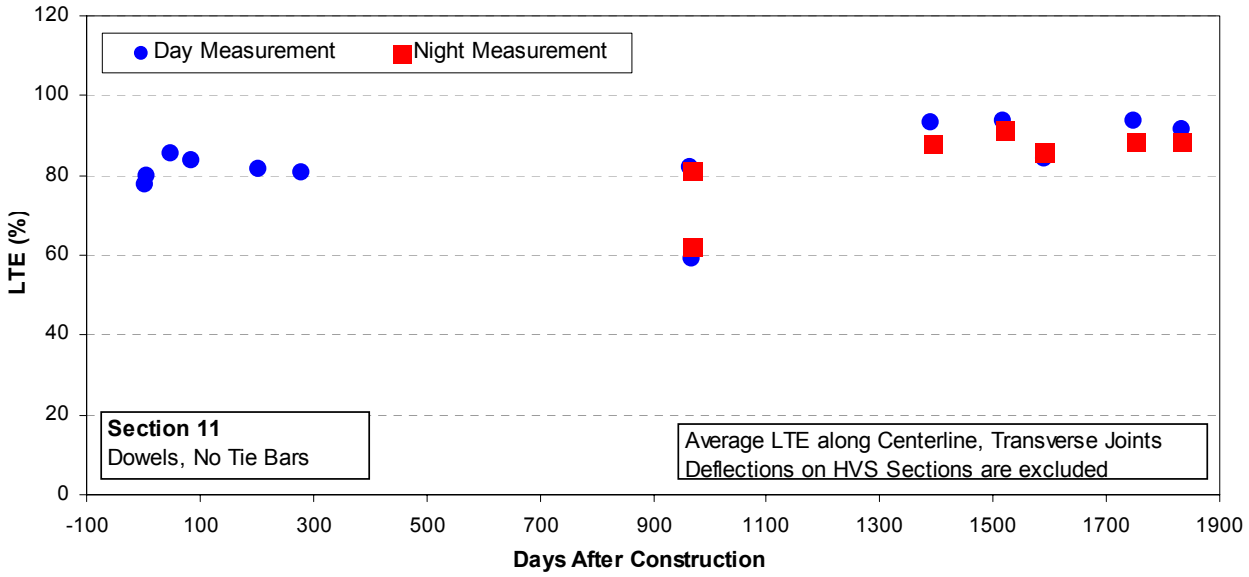

Figure 128. Transverse joint LTE versus concrete age, Section 11 (doweled joints with asphalt concrete shoulder and widened truck lane).

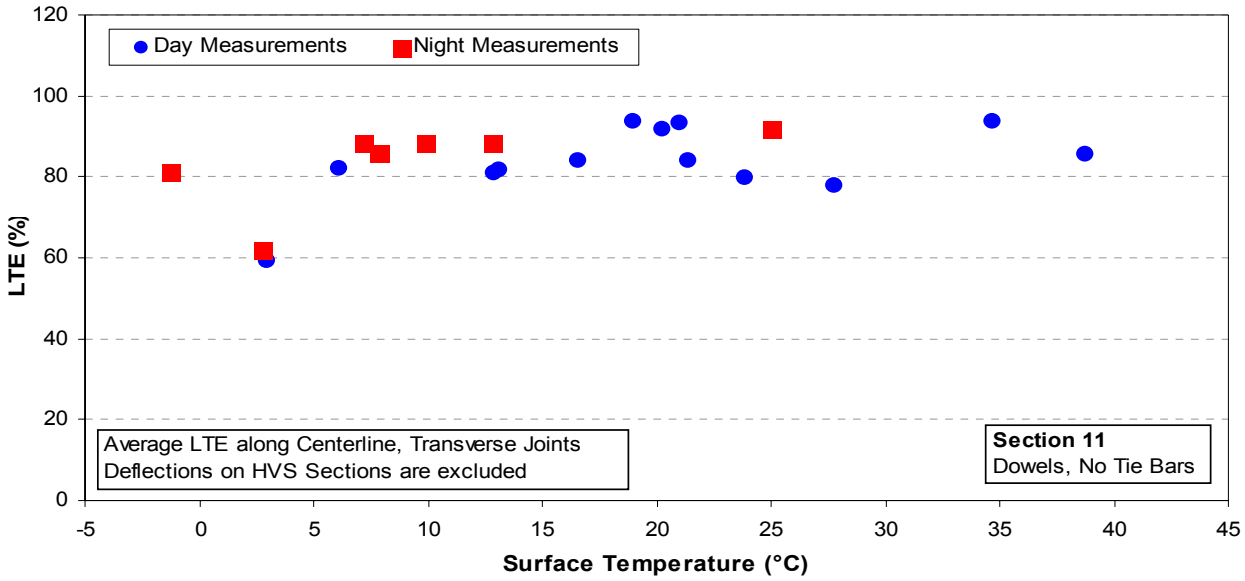

Figure 129. Transverse joint LTE versus surface temperature, Section 11 (doweled joints with asphalt concrete shoulder and widened truck lane).

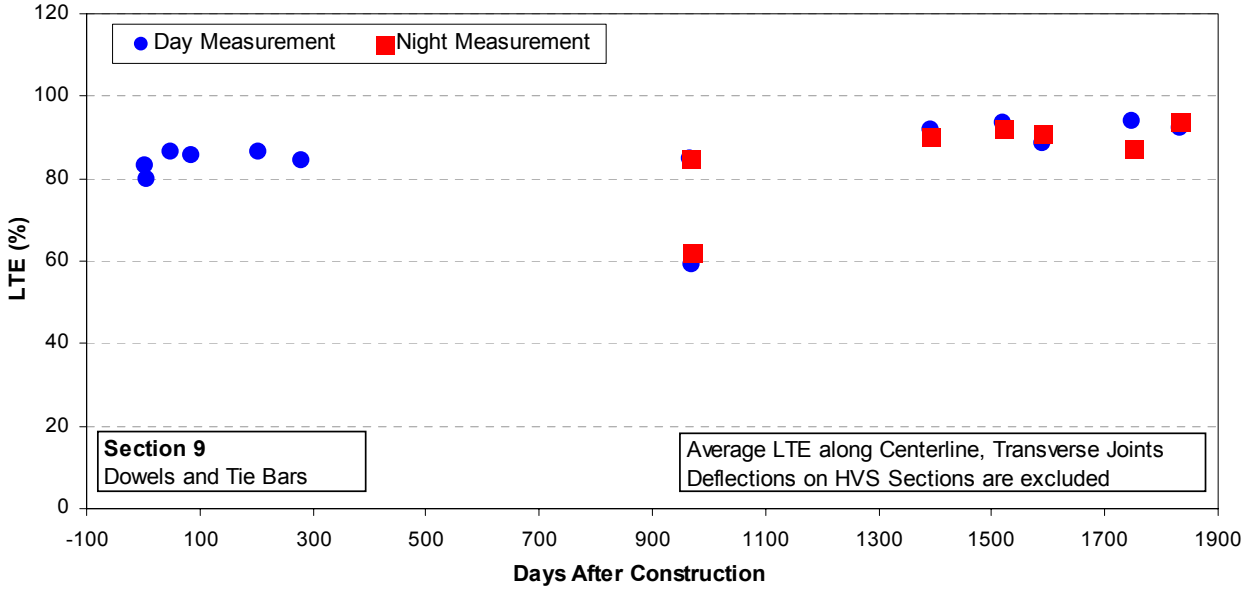

Figure 130. Transverse joint LTE versus concrete age, Section 9 (doweled joints and tie bars at concrete shoulder).

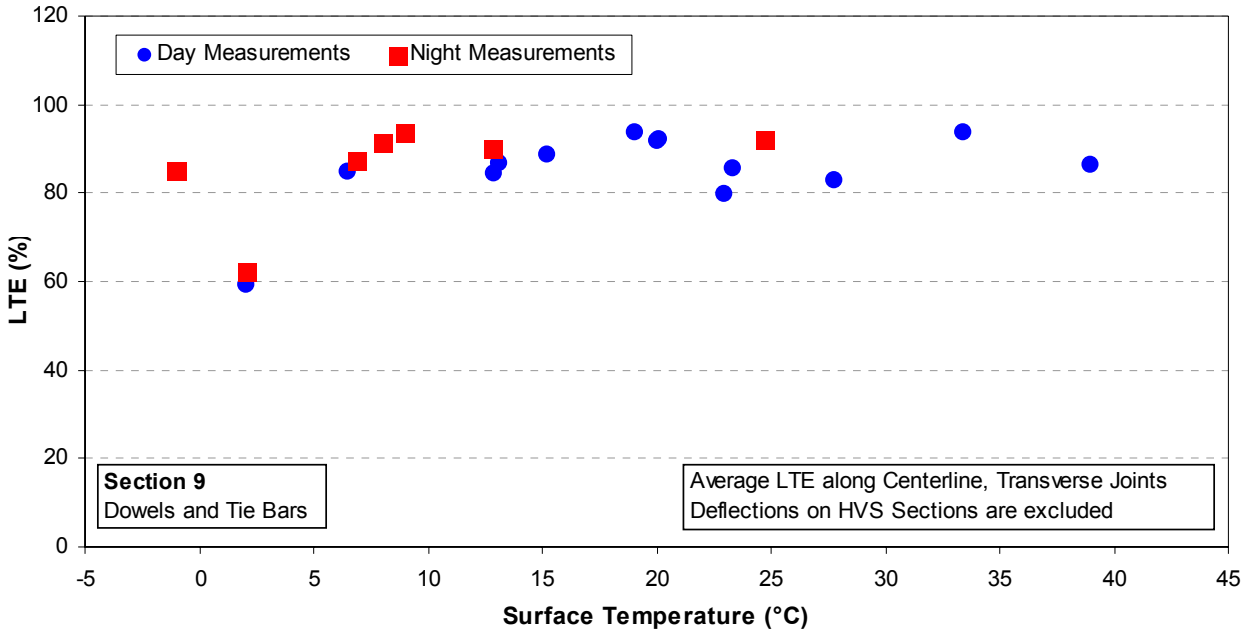

Figure 131. Transverse joint LTE versus surface temperature, Section 9 (doweled joints and tie bars at concrete shoulder).

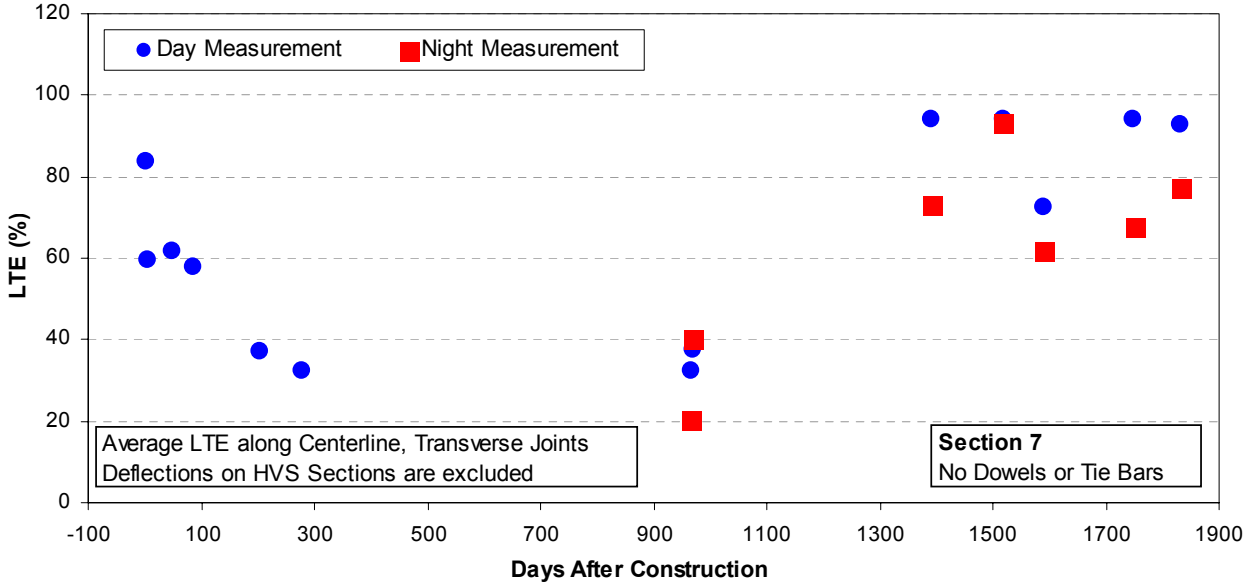

Figure 132. Transverse joint LTE versus concrete age, Section 7 (no dowels or tie bars, asphalt concrete shoulder).

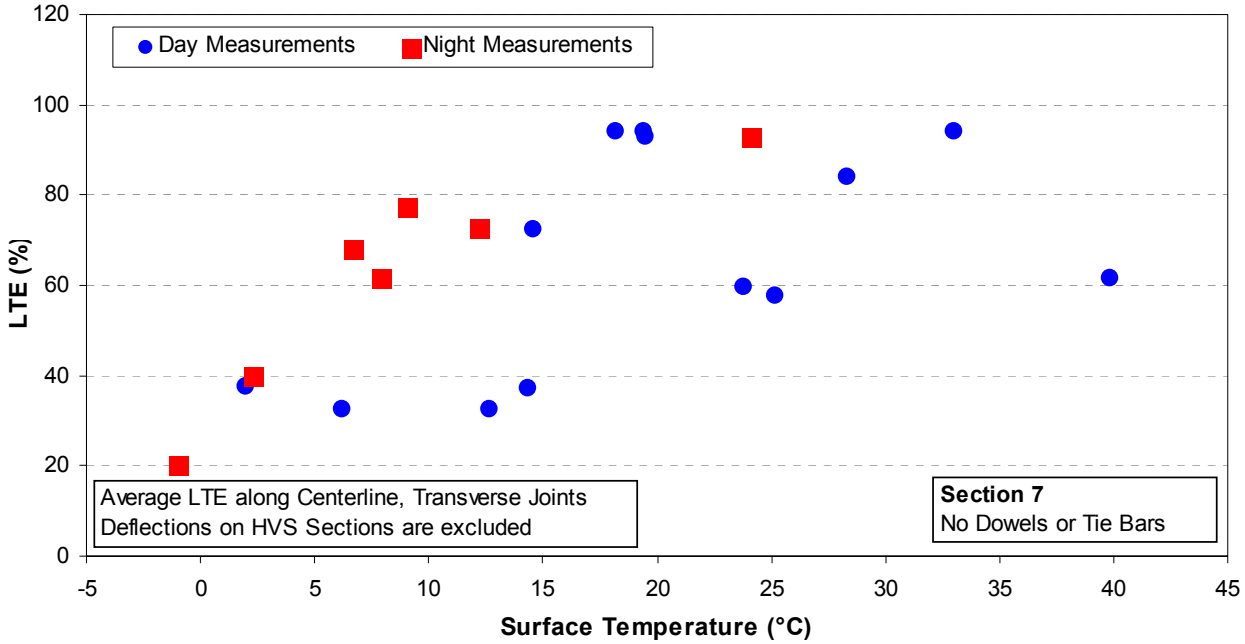

Figure 133. Transverse joint LTE versus surface temperature, Section 7 (no dowels or tie bars, asphalt concrete shoulder).

The data measured across the longitudinal joint at the K-rail side at the slab center (Table 44 and Figures 134–139) prompt the following observations:

- The longitudinal joint LTE for all sections show a clear dependency on slab temperature.
- The relationship between LTE and temperature is clearest in the case of Section 7 (no dowels or tie bars—see Figure 139), and the least clear in the case of Section 9 (dowels and tie bars—see Figure 137).
- Section 9 (dowels and tie bars) show the greatest variation in longitudinal joint LTE and (surprisingly) also has the lowest overall LTE over longitudinal joints (see Table 44).

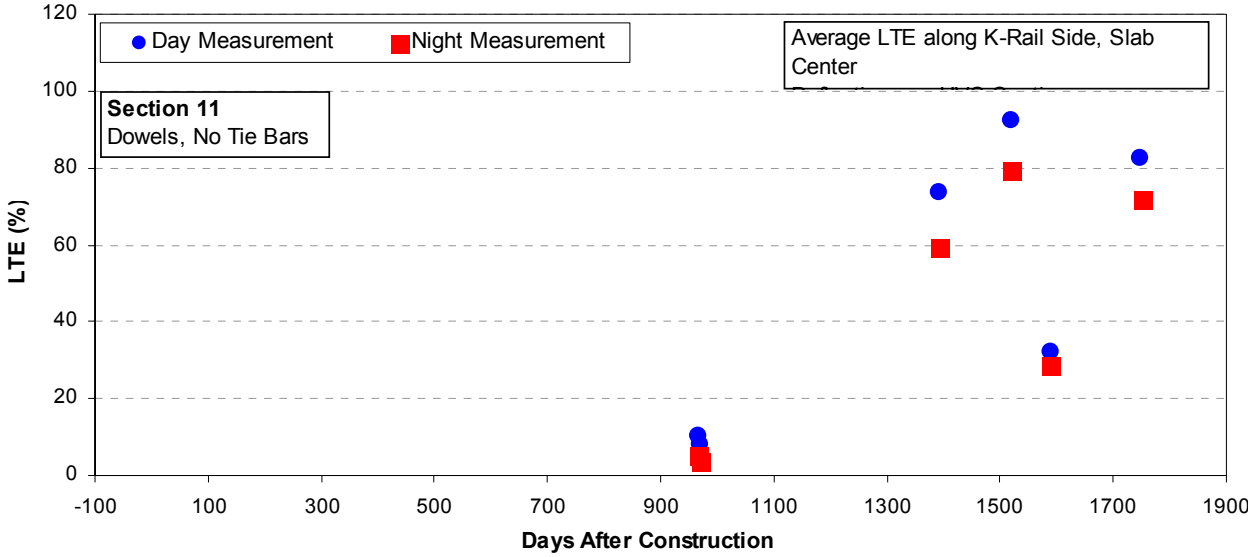

Figure 134. Longitudinal joint LTE versus concrete age at slab center along K-rail edge, Section 11 (doweled joints with asphalt concrete shoulder and widened truck lane).

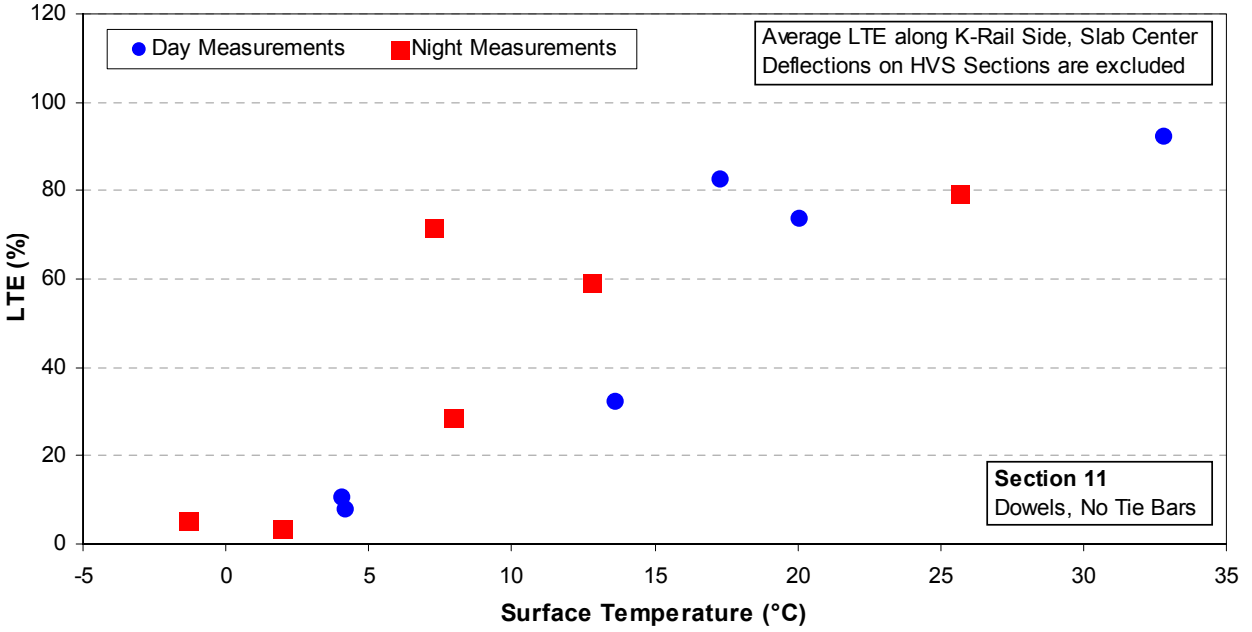

Figure 135. Longitudinal joint LTE versus surface temperature at slab center along K-rail edge, Section 11 (doweled joints with asphalt concrete shoulder and widened truck lane).

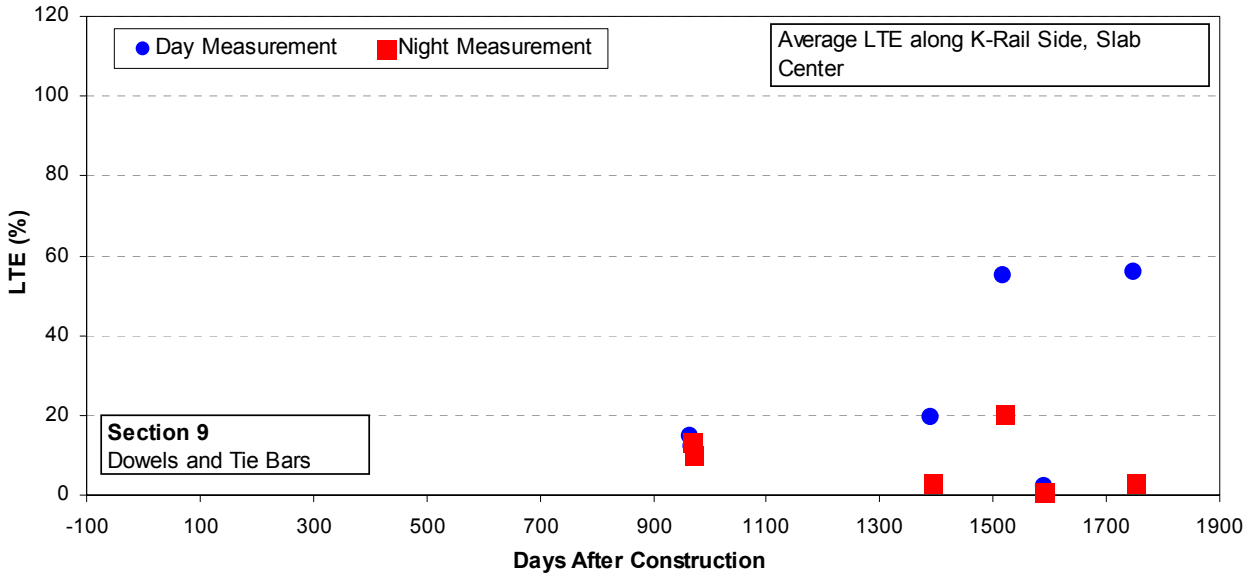

Figure 136. Longitudinal joint LTE versus concrete age at slab center along K-rail edge, Section 9 (doweled joints and tie bars at concrete shoulder).

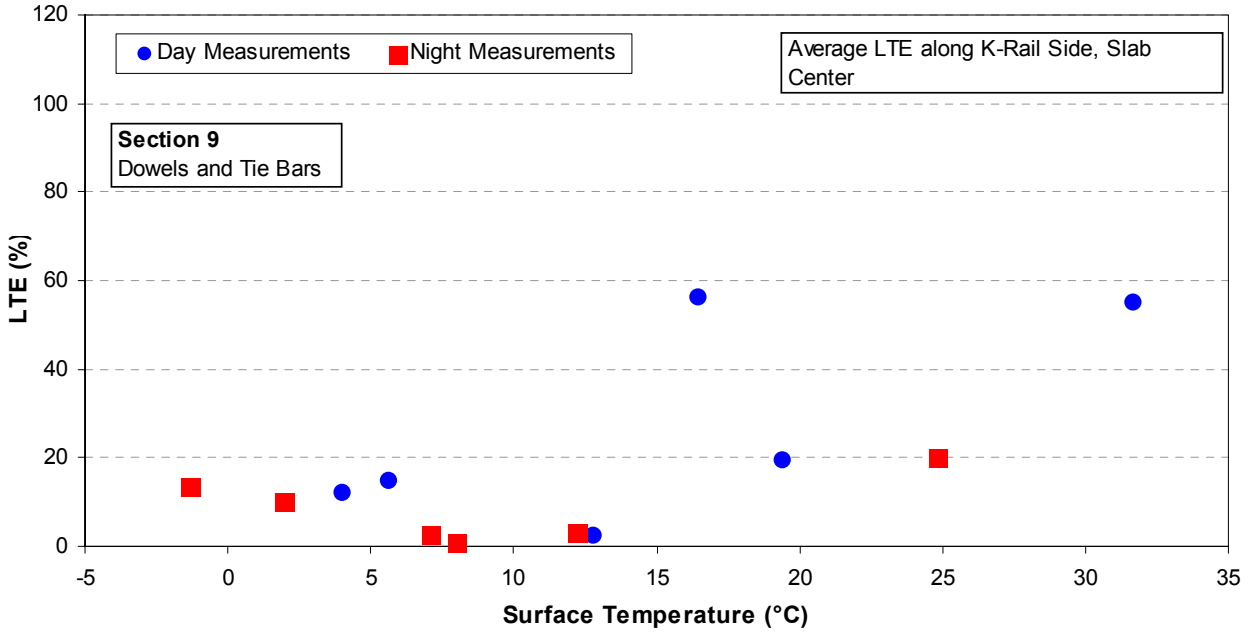

Figure 137. Longitudinal joint LTE versus surface temperature at slab center along K-rail edge, Section 9 (doweled joints and tie bars at concrete shoulder).

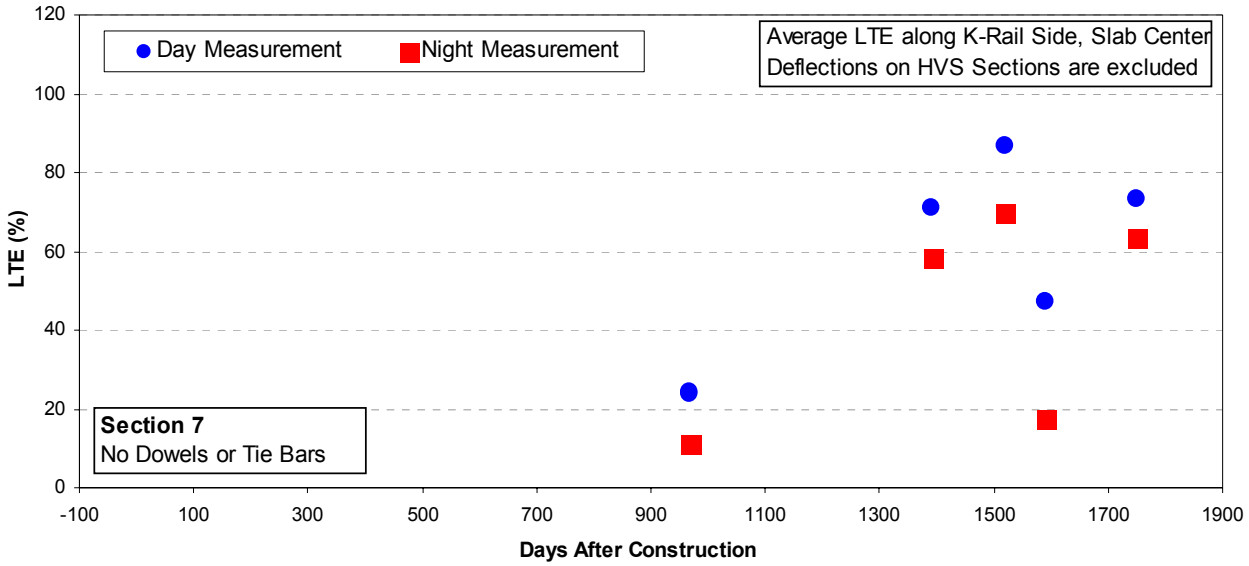

Figure 138. Longitudinal joint LTE versus concrete age at slab center along K-rail edge, Section 7 (no dowels or tie bars, asphalt concrete shoulder).

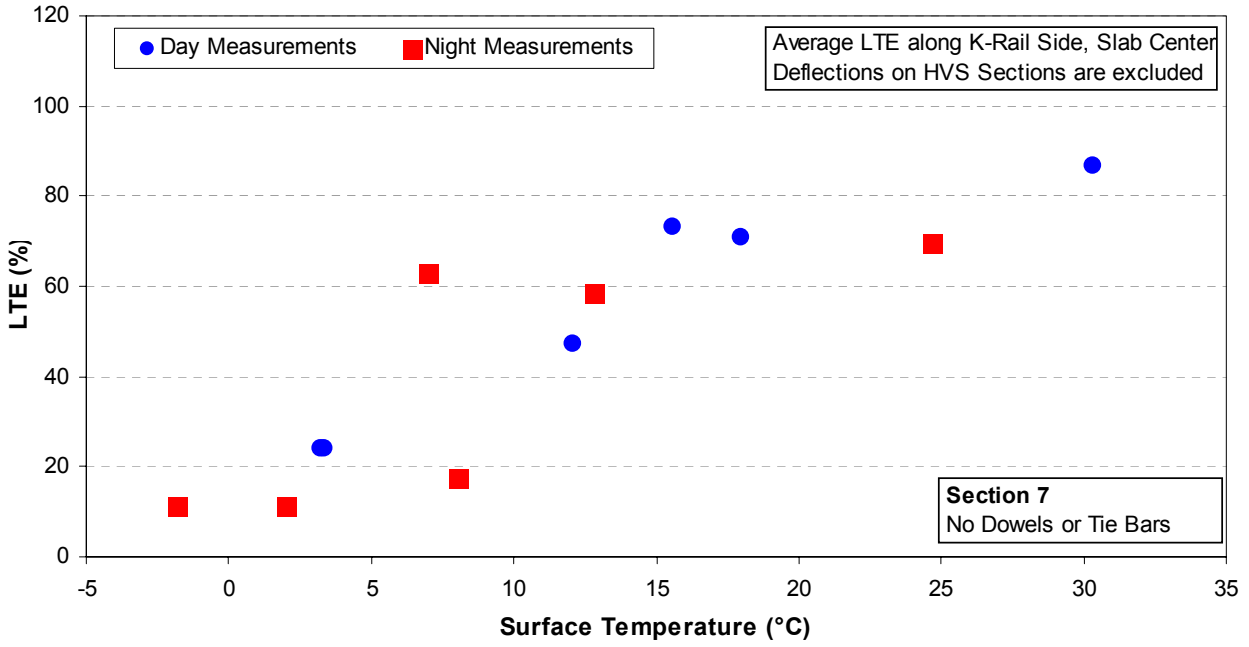

Figure 139. Longitudinal joint LTE versus surface temperature at slab center along K-rail edge, Section 7 (no dowels or tie bars, asphalt concrete shoulder).

The data measured over the longitudinal joint at the K-rail side at the slab corner (Table 45 and Figures 140–145) prompt the following observations:

- The longitudinal joint LTEs for all sections show a clear dependency on slab temperature.
- As with LTE measured at the slab center, the relationship between LTE and temperature is clearest in the case of Section 7 (no dowels or tie bars—see Figure 145), and the least clear in the case of Section 9 (dowels and tie bars—see Figure 143).

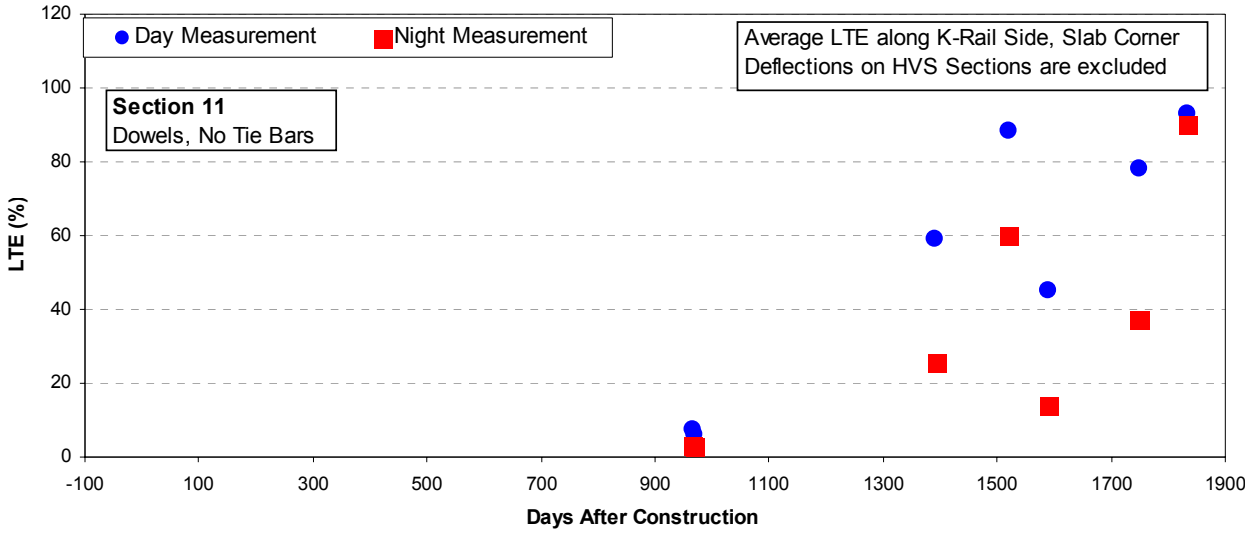

Figure 140. Longitudinal joint LTE versus concrete age at slab corner along K-rail edge, Section 11 (doweled joints with asphalt concrete shoulder and widened truck lane).

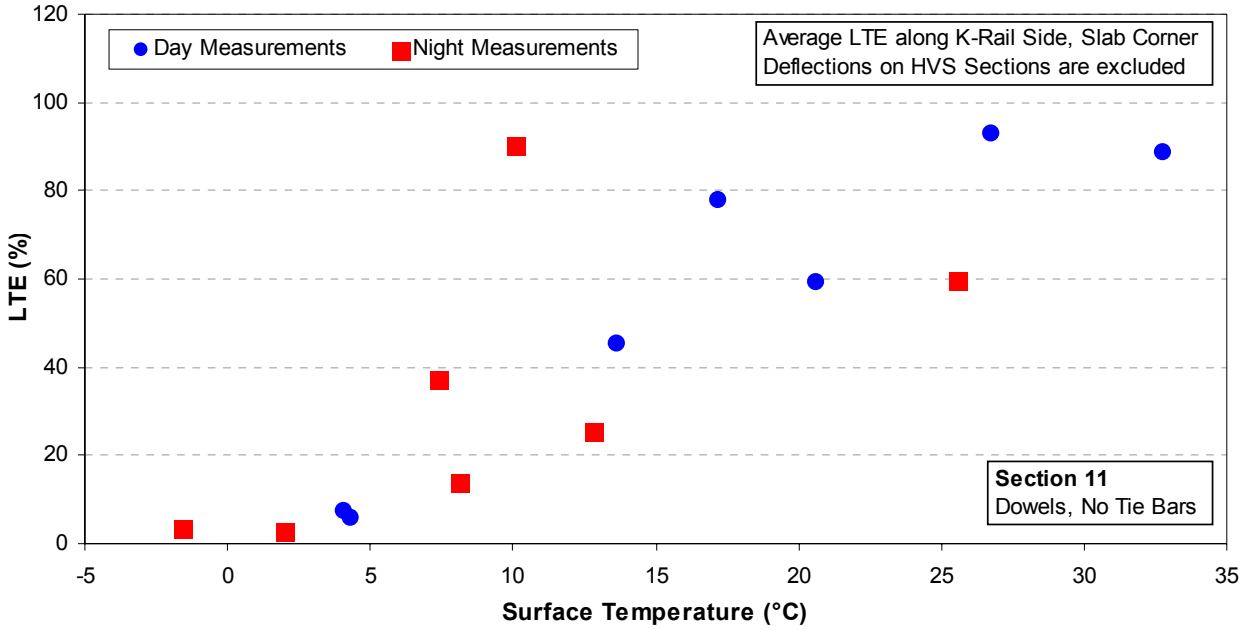

Figure 141. Longitudinal joint LTE versus surface temperature at slab corner along K-rail edge, Section 11 (doweled joints with asphalt concrete shoulder and widened truck lane).

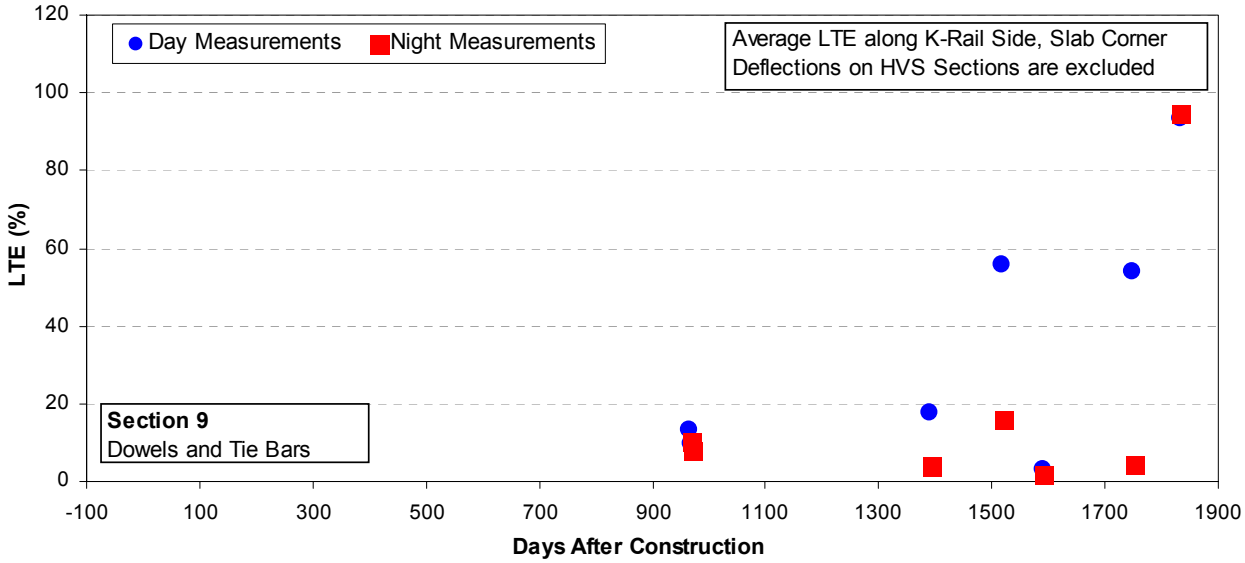

Figure 142. Longitudinal joint LTE versus concrete age at slab corner along K-rail edge, Section 9 (doweled joints and tie bars at concrete shoulder).

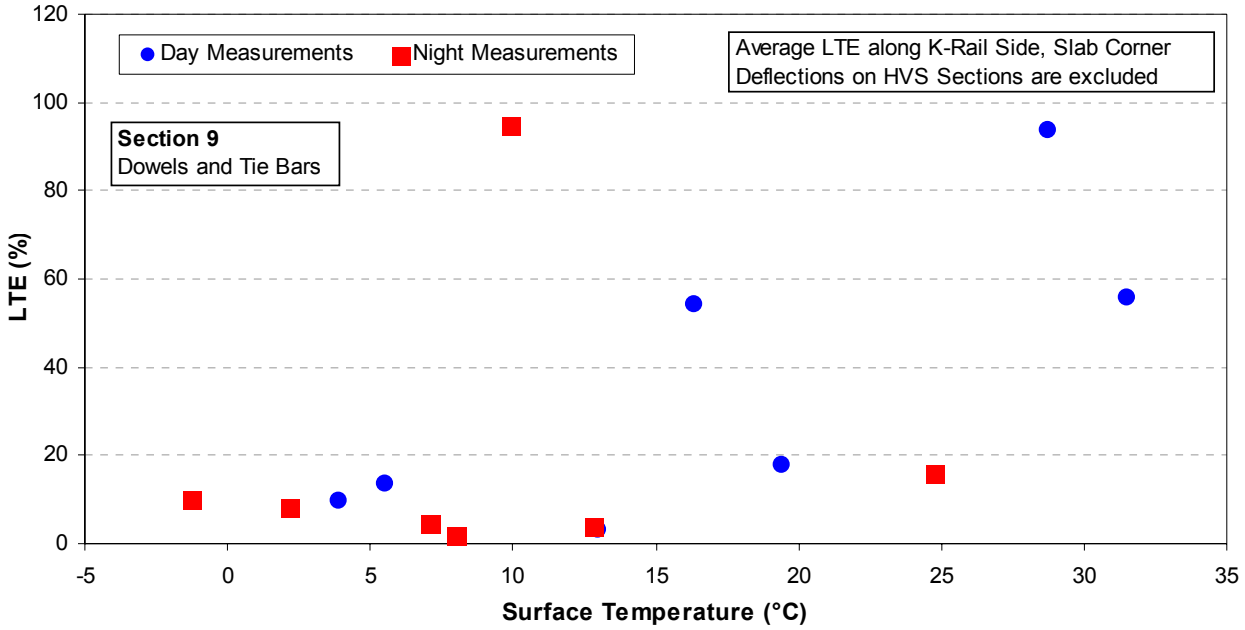

Figure 143. Longitudinal joint LTE versus surface temperature at slab corner along K-rail edge, Section 9 (doweled joints and tie bars at concrete shoulder).

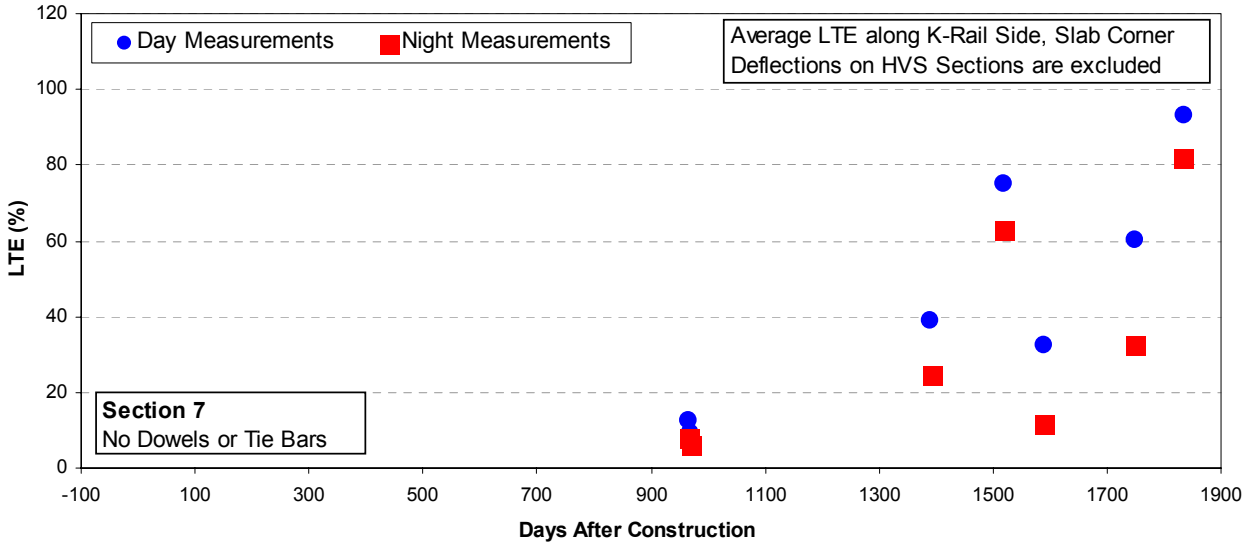

Figure 144. Longitudinal joint LTE versus concrete age at slab corner along K-rail edge, Section 7 (no dowels or tie bars, asphalt concrete shoulder).

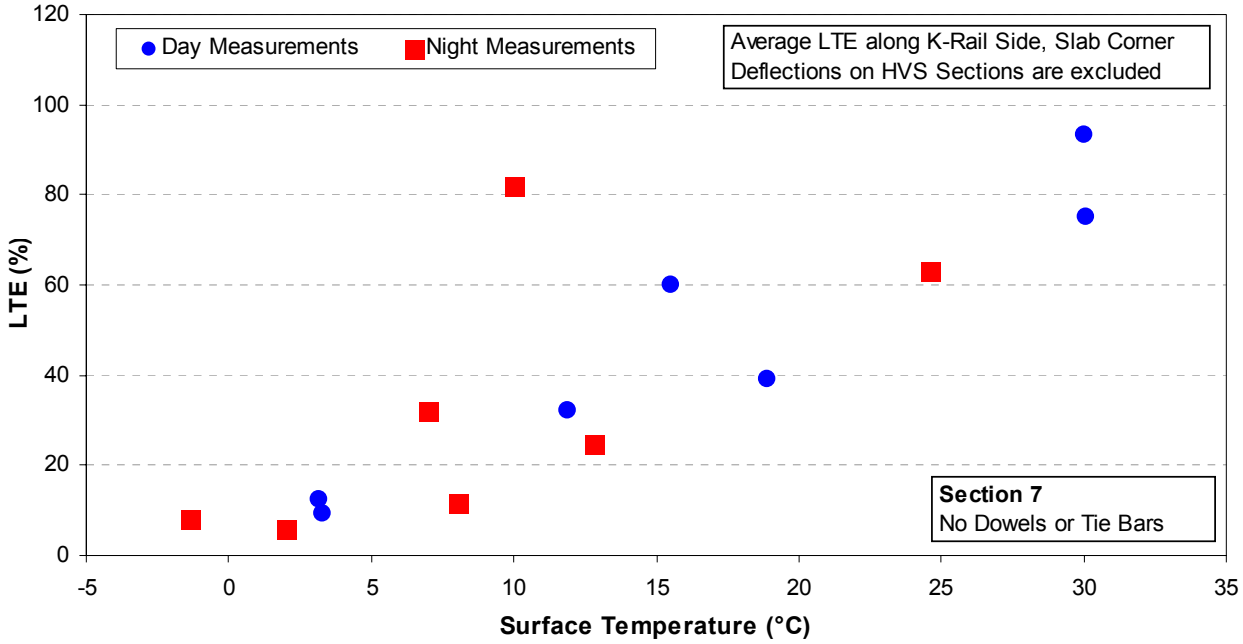

Figure 145. Longitudinal joint LTE versus surface temperature at slab corner along K-rail edge, Section 7 (no dowels or tie bars, asphalt concrete shoulder).

5.5 Deflections Before and After HVS Testing

In this chapter, FWD data recorded before and after HVS testing is shown for each of the HVS test sections. Data shown in Figures 146–165 include only the deflection bowls recorded on slabs that were tested by the HVS. The primary objective is to investigate the impact, if any, that HVS testing had on the general deflection behavior of slabs.

HVS tests were always performed either along the shoulder or the K-rail side. However, FWD data was only consistently recorded along the slab centerline (see Table 40), and therefore the only complete record of deflections before and after HVS testing involves deflections recorded along the centerline of the slab. It should thus be noted that, because the data shown in this chapter include only deflections recorded along the slab centerline, any conclusions drawn are related to the overall change (if any) in slab behavior due to HVS testing and not to localized effects at the specific location on the slab where the HVS test was performed.

5.5.1 Test 532FD (Section 7: No Dowels or Tie Bars)

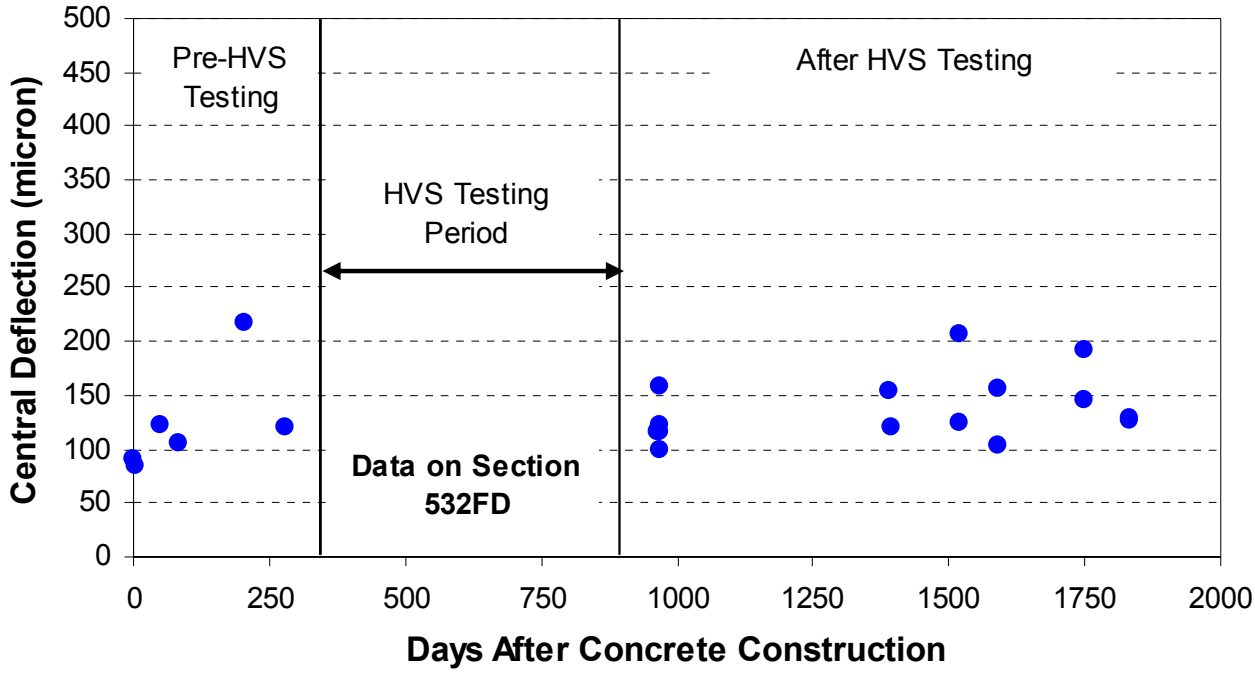

Figure 146. Impact of HVS testing on central deflection measured at slab center (Test 532FD).

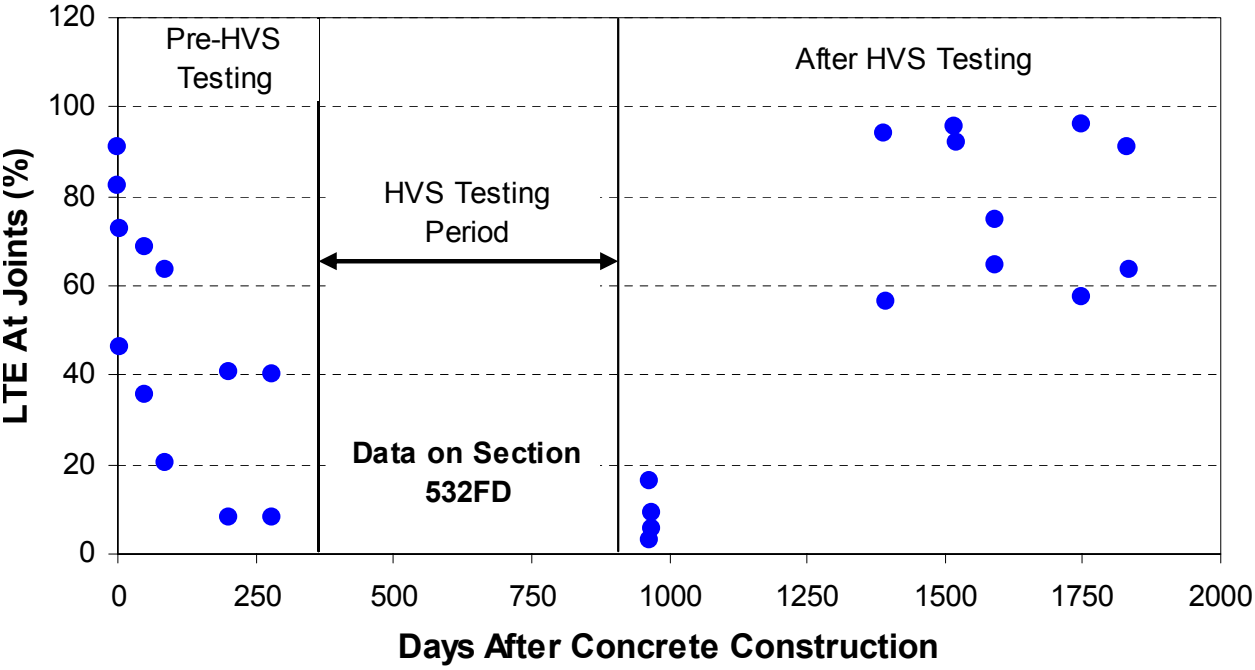

Figure 147. Impact of HVS testing on LTE at transverse joints measured along slab centerline (Test 532FD).

5.5.2 Test 533FD (Section 7: No Dowels or Tie Bars)

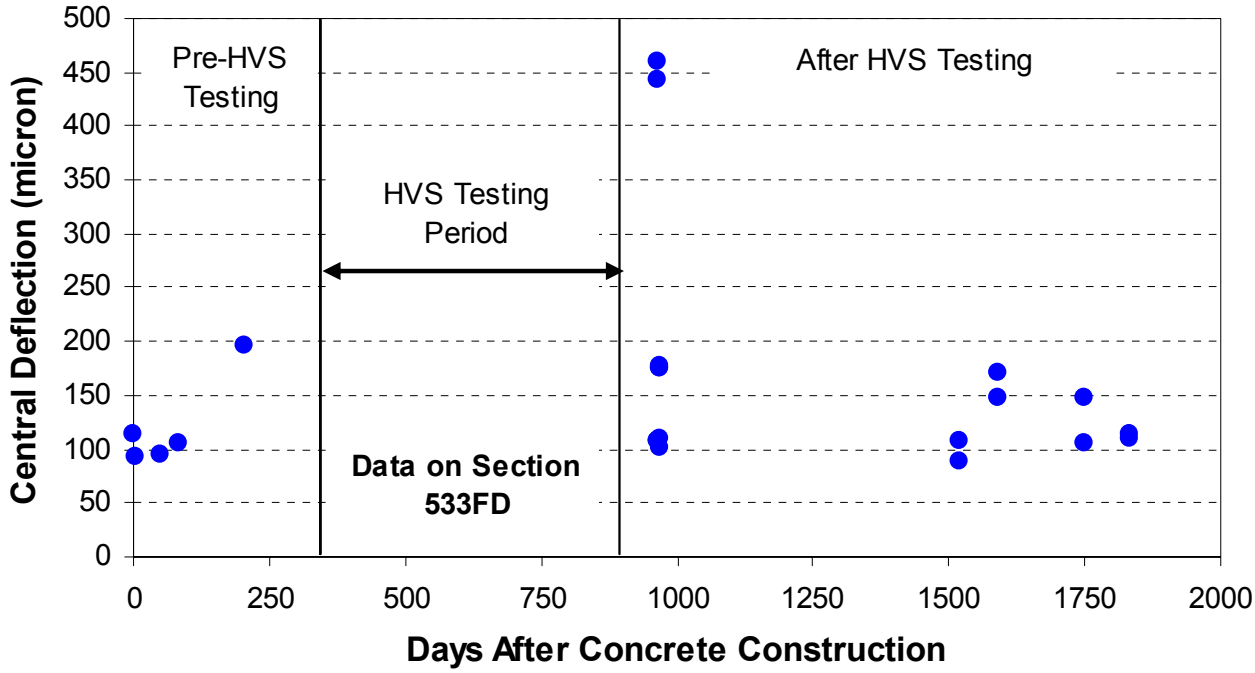

Figure 148. Impact of HVS testing on central deflection measured at slab center (Test 533FD).

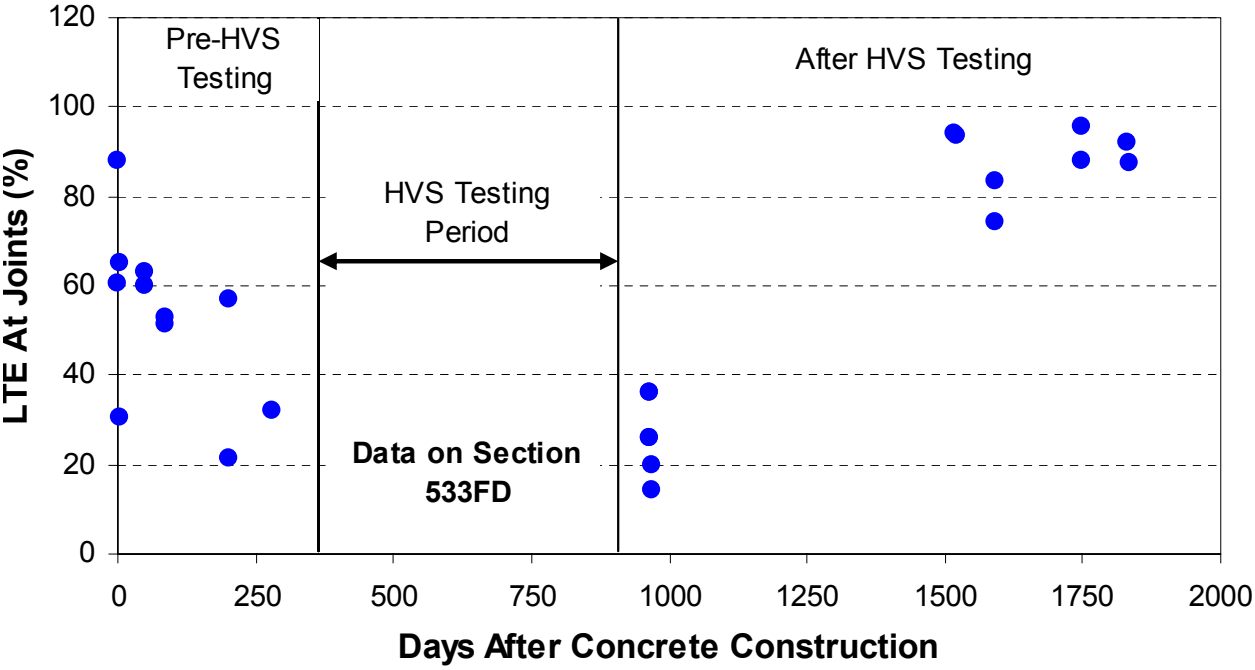

Figure 149. Impact of HVS testing on LTE measured at transverse joints along slab centerline (Test 533FD).

5.5.3 Test 534FD (Section 7: No Dowels or Tie Bars)

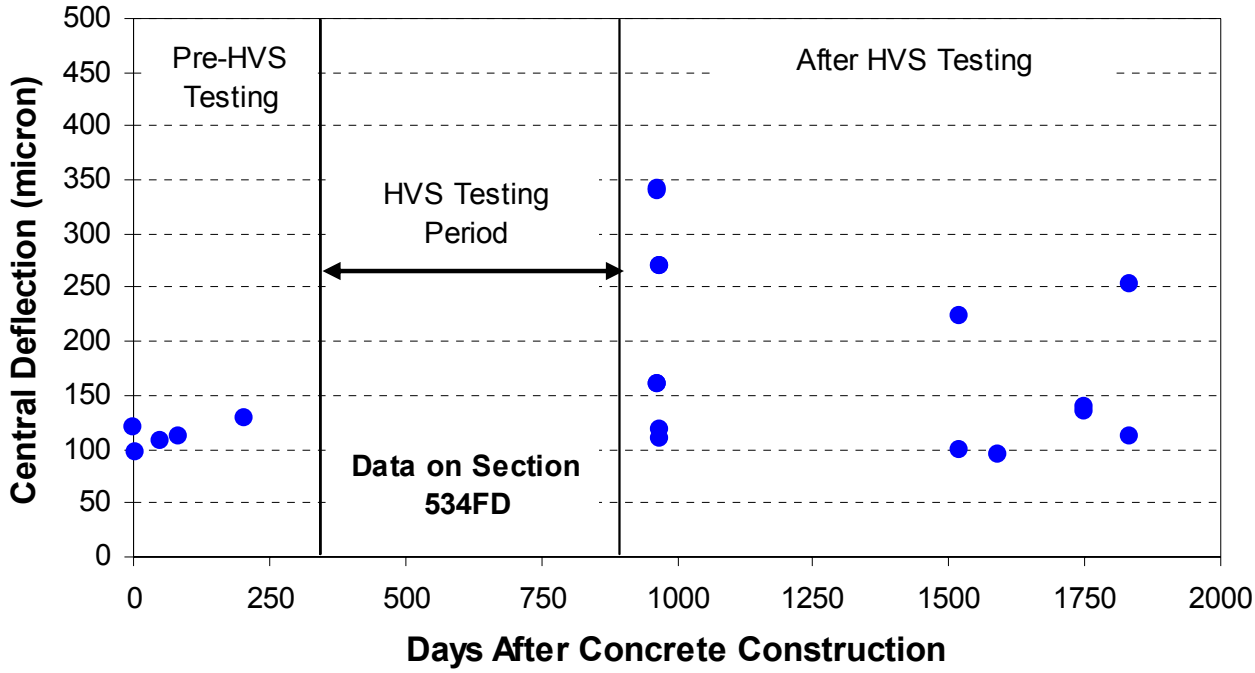

Figure 150. Impact of HVS testing on central deflection measured at slab center (Test 534FD).

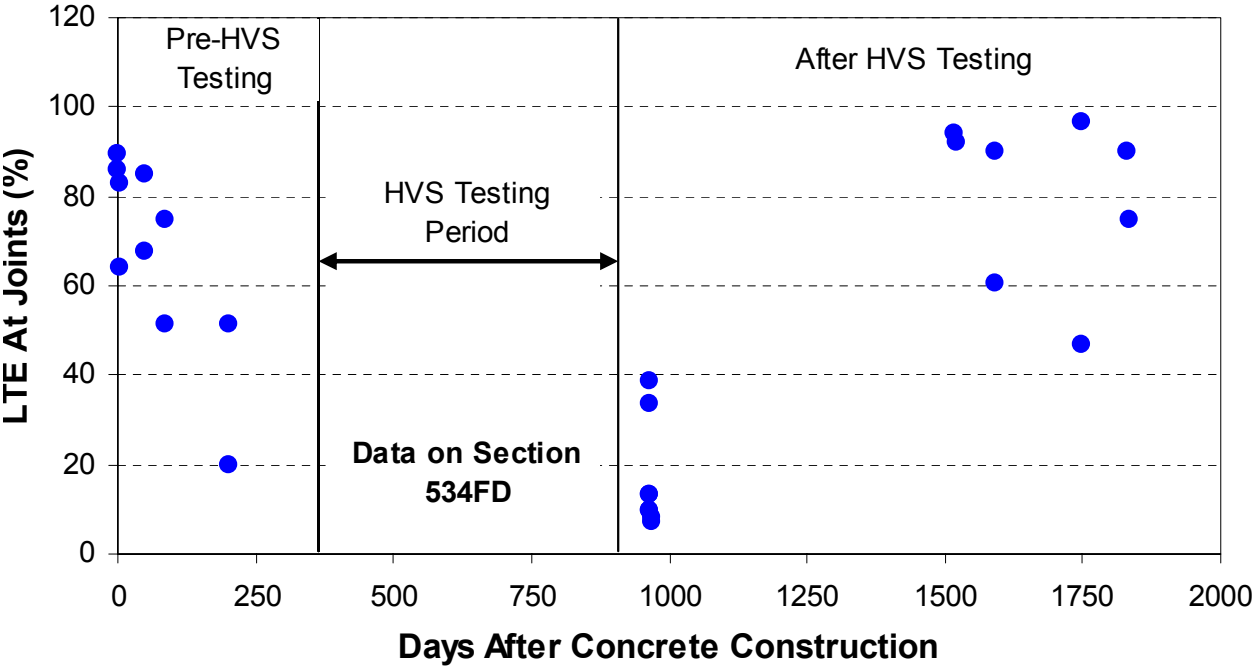

Figure 151. Impact of HVS testing on LTE measured at transverse joints along slab centerline (Test 534FD).

5.5.4 Test 535FD (Section 7: No Dowels or Tie Bars)

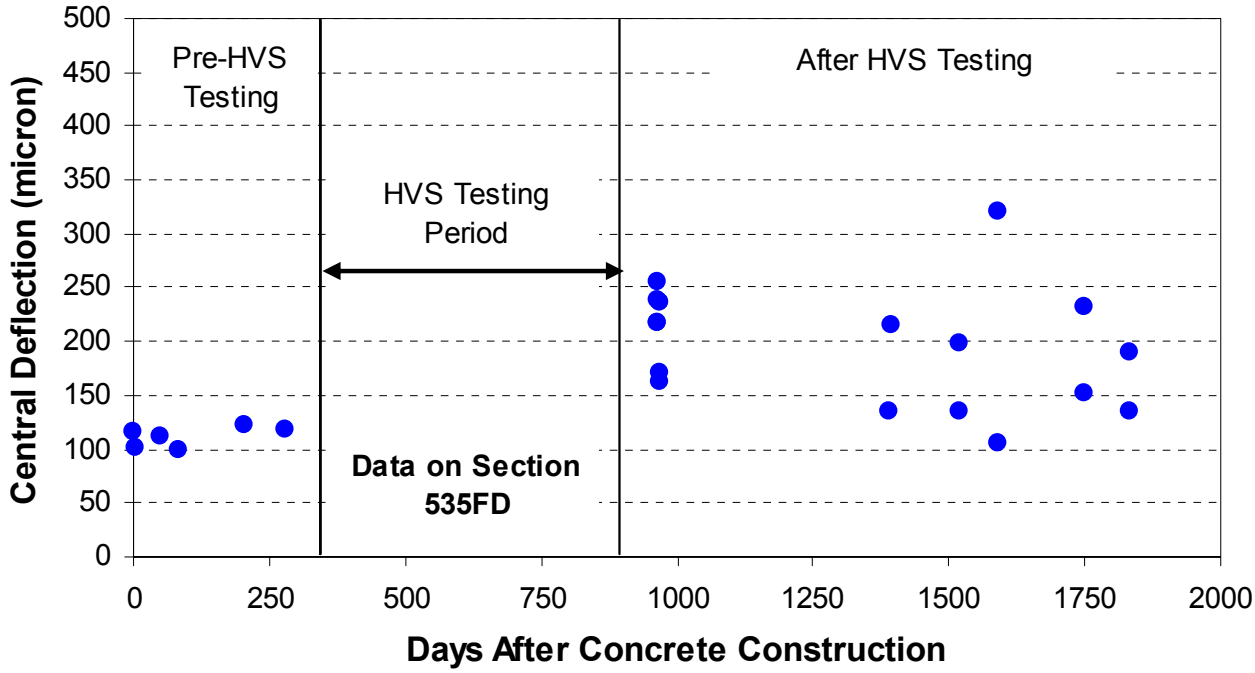

Figure 152. Impact of HVS testing on central deflection measured at slab center (Test 535FD).

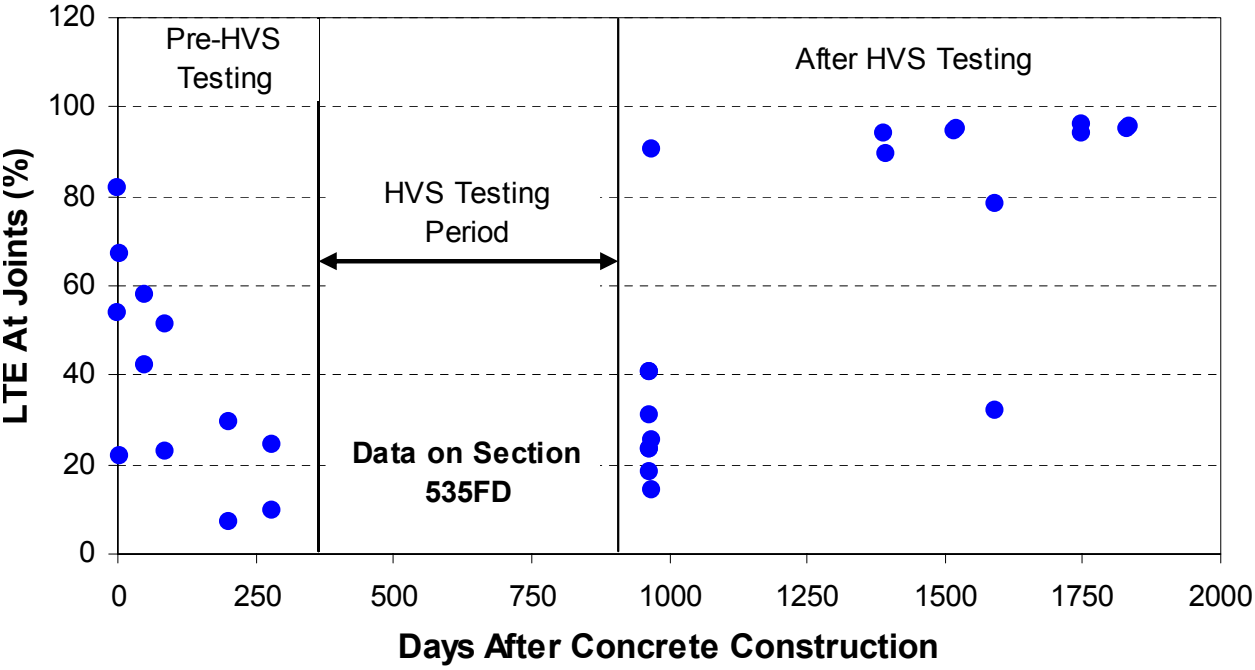

Figure 153. Impact of HVS testing on LTE measured at transverse joints along slab centerline (Test 535FD).

5.5.5 Test 536FD (Section 9: Dowels and Tie Bars)

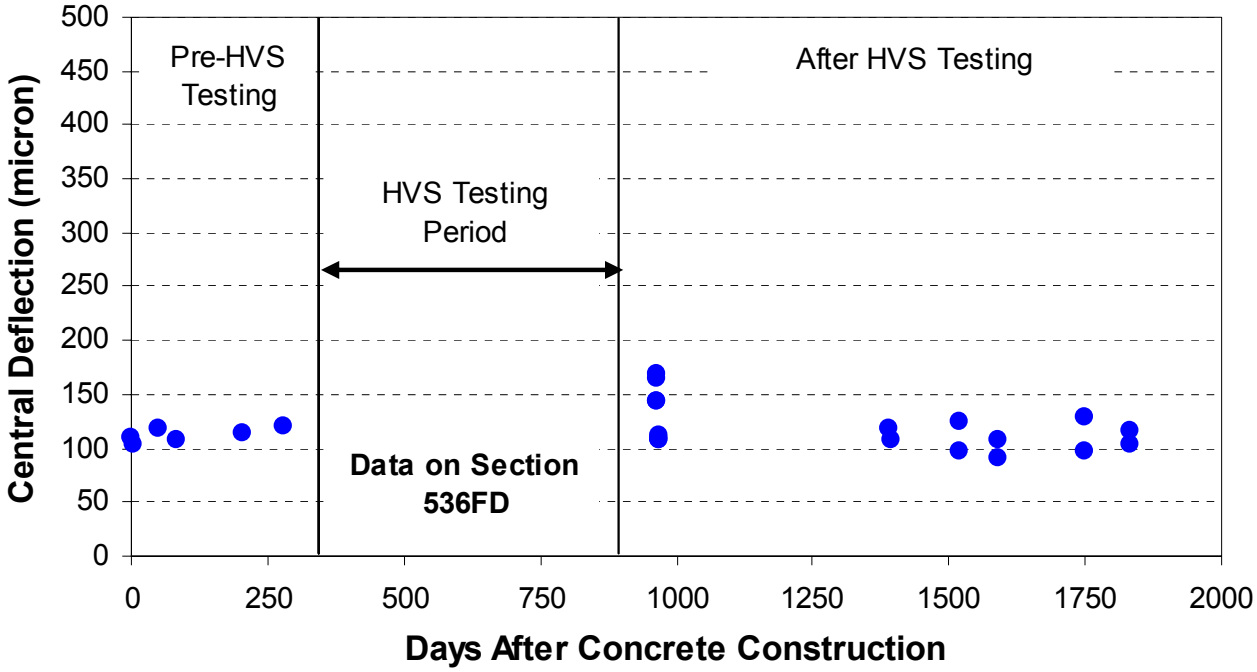

Figure 154. Impact of HVS testing on central deflection measured at slab center (Test 536FD).

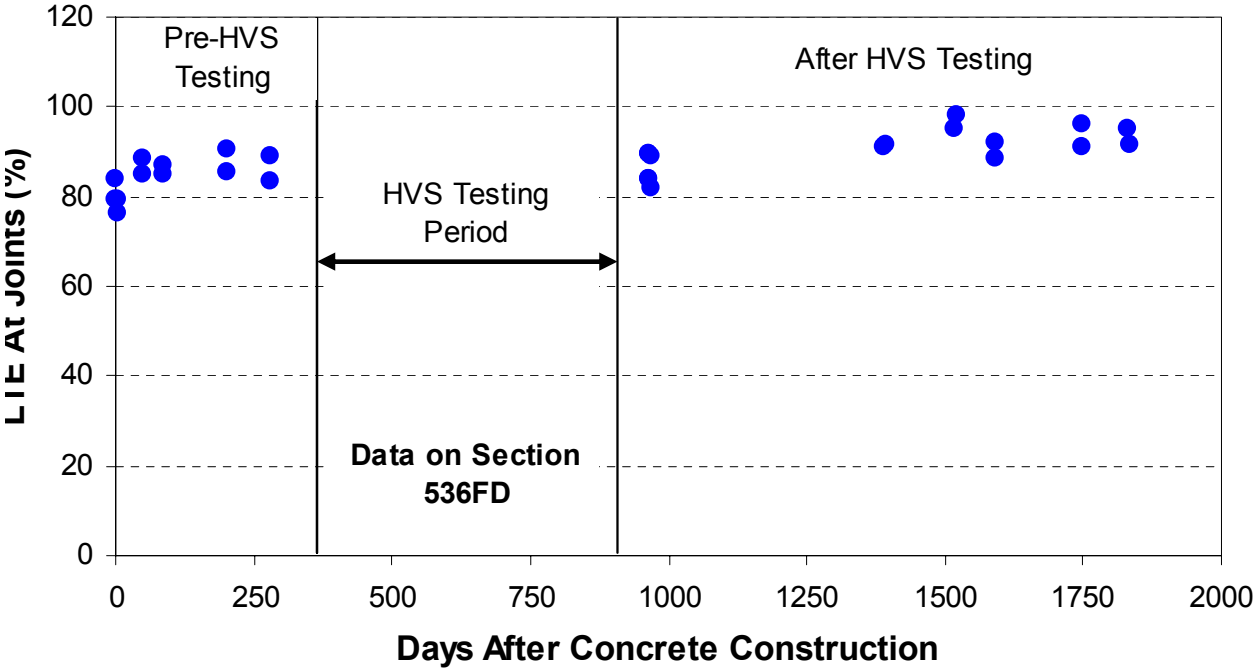

Figure 155. Impact of HVS testing on central LTE measured at transverse joints along slab centerline (Test 536FD).

5.5.6 Test 537FD (Section 9: Dowels and Tie Bars)

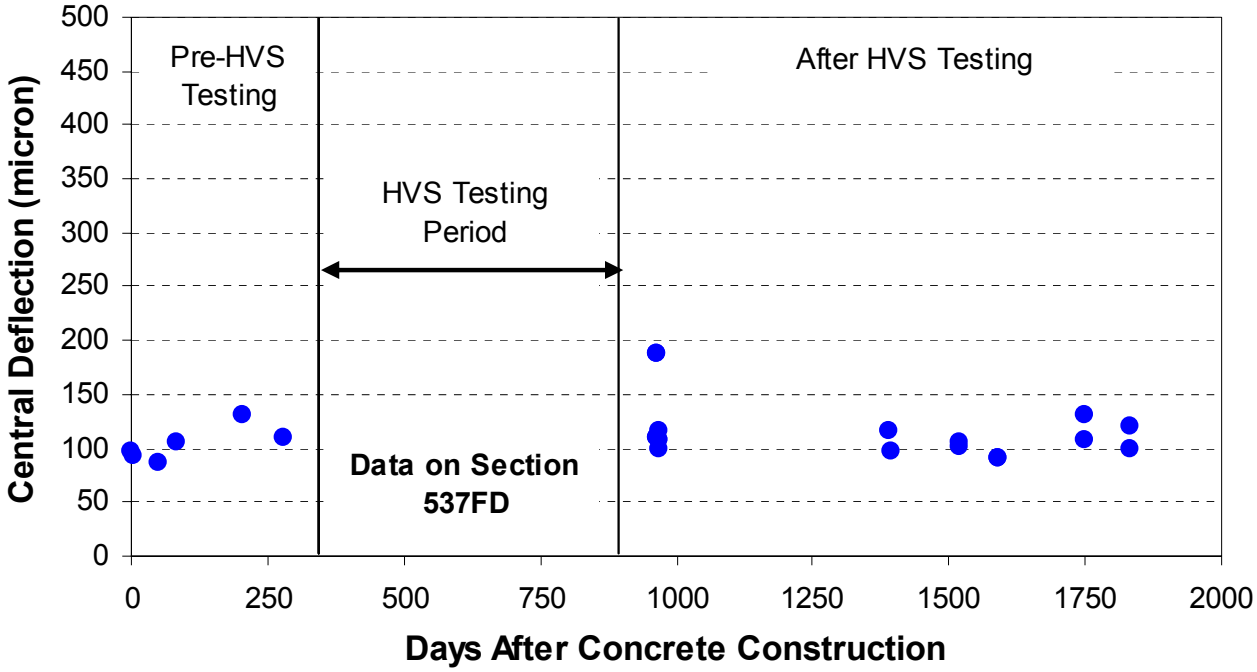

Figure 156. Impact of HVS testing on central deflection measured at slab center (Test 537FD).

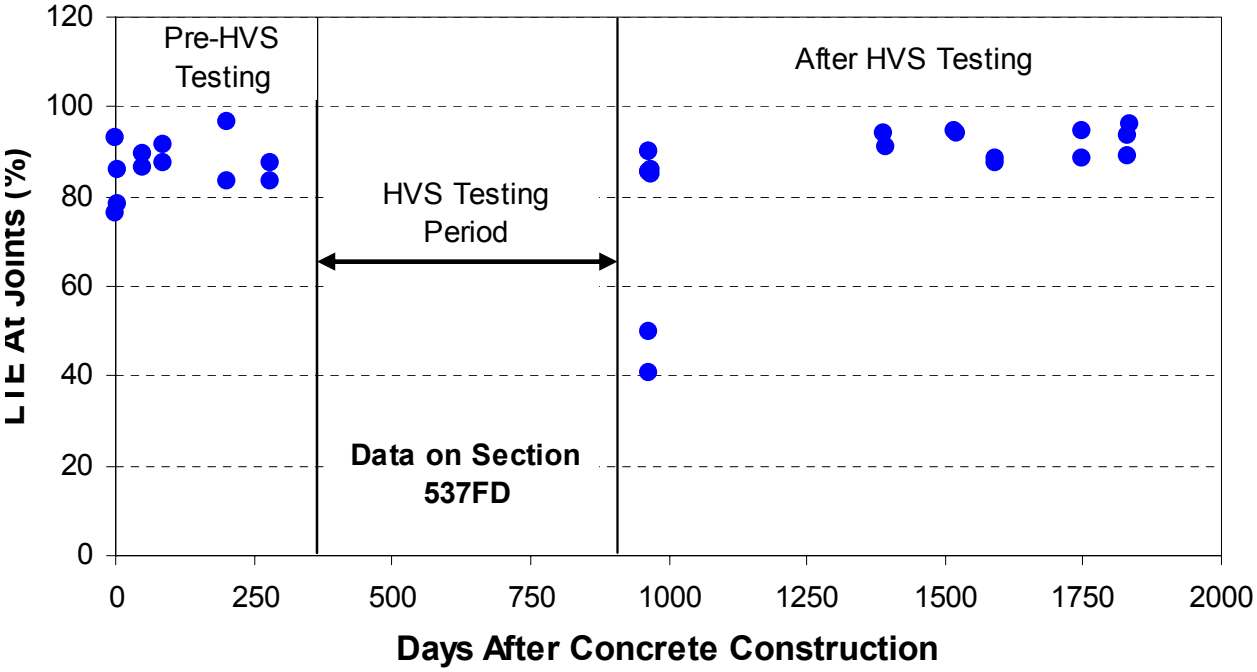

Figure 157. Impact of HVS testing on LTE measured at transverse joints along slab centerline (Test 537FD).

5.5.7 Test 538FD (Section 9: Dowels and Tie Bars)

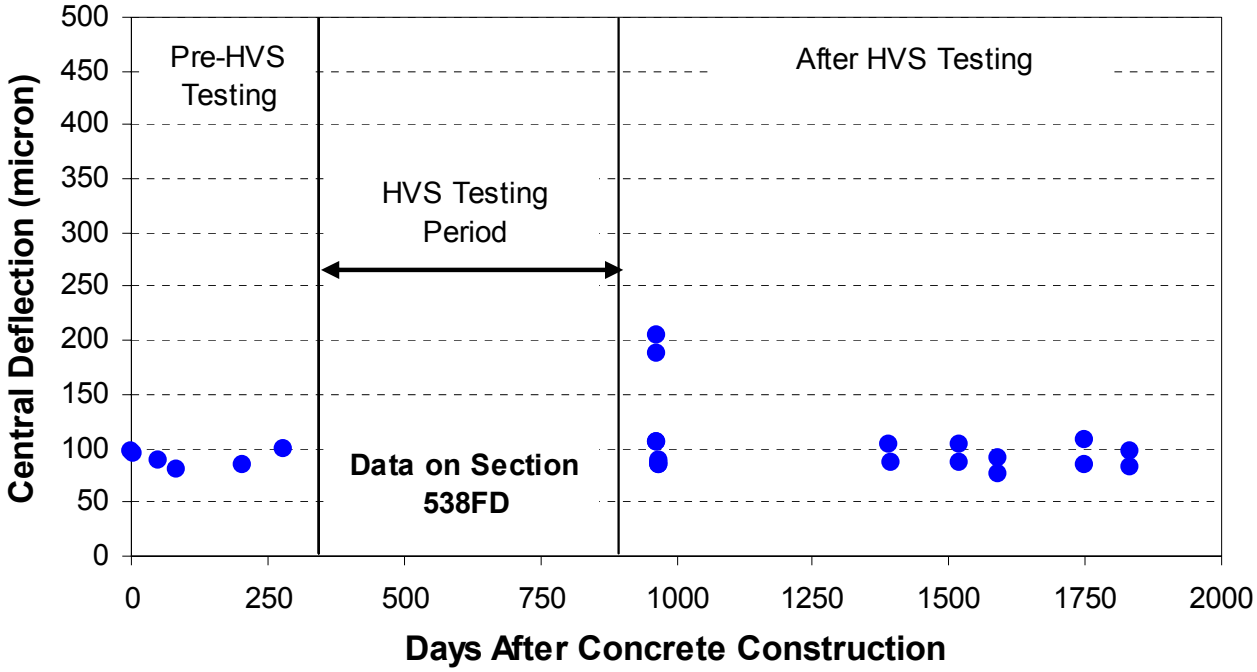

Figure 158. Impact of HVS testing on central deflection measured at slab center (Test 538FD).

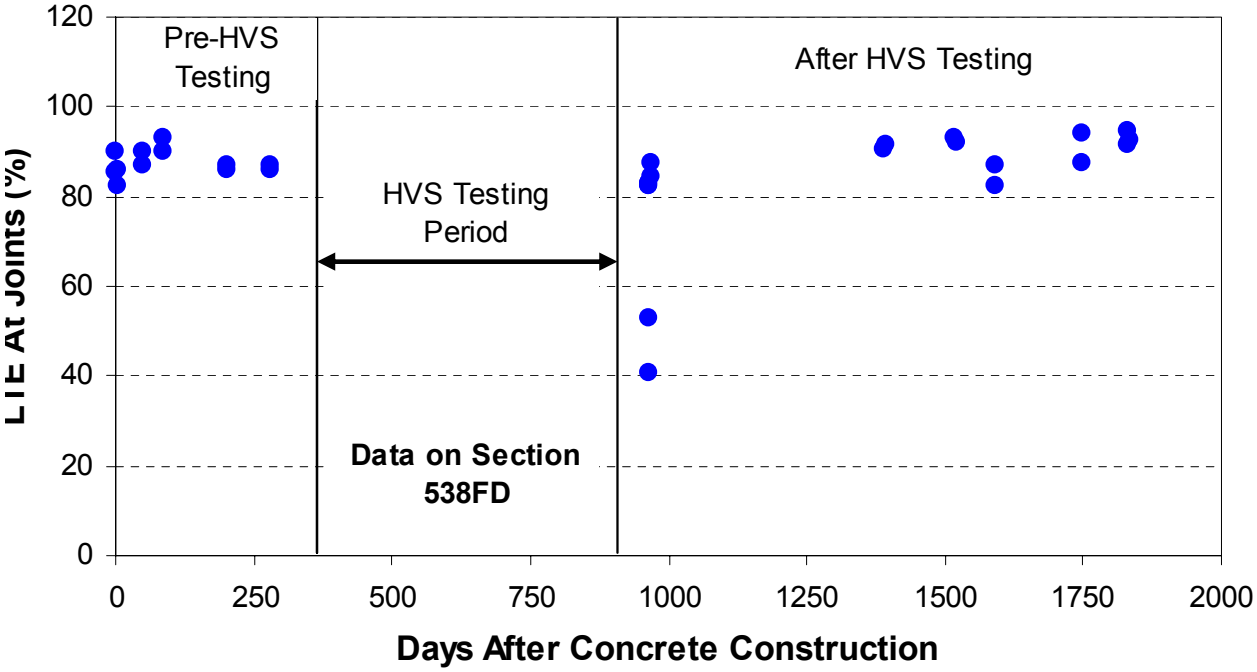

Figure 159. Impact of HVS testing on LTE measured at transverse joint along slab centerline (Test 538FD).

5.5.8 Test 539FD (Section 11: Dowels, No Tie Bars, Widened Truck Lane)

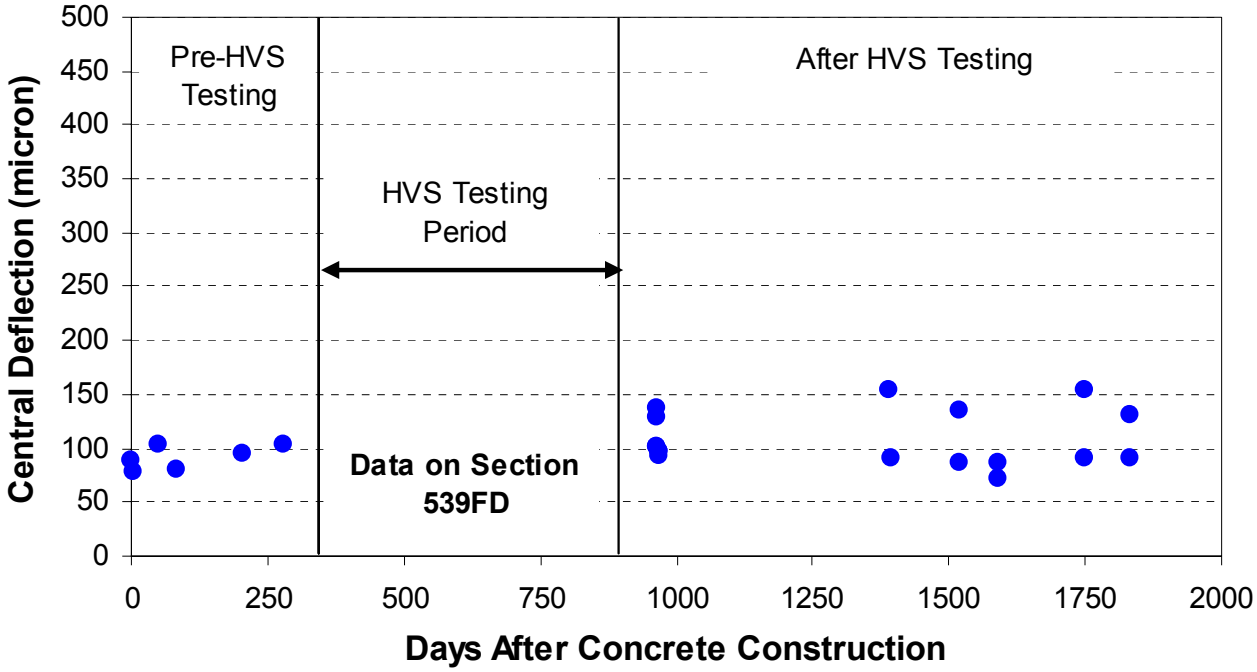

Figure 160. Impact of HVS testing on central deflection measured at slab center (Test 539FD).

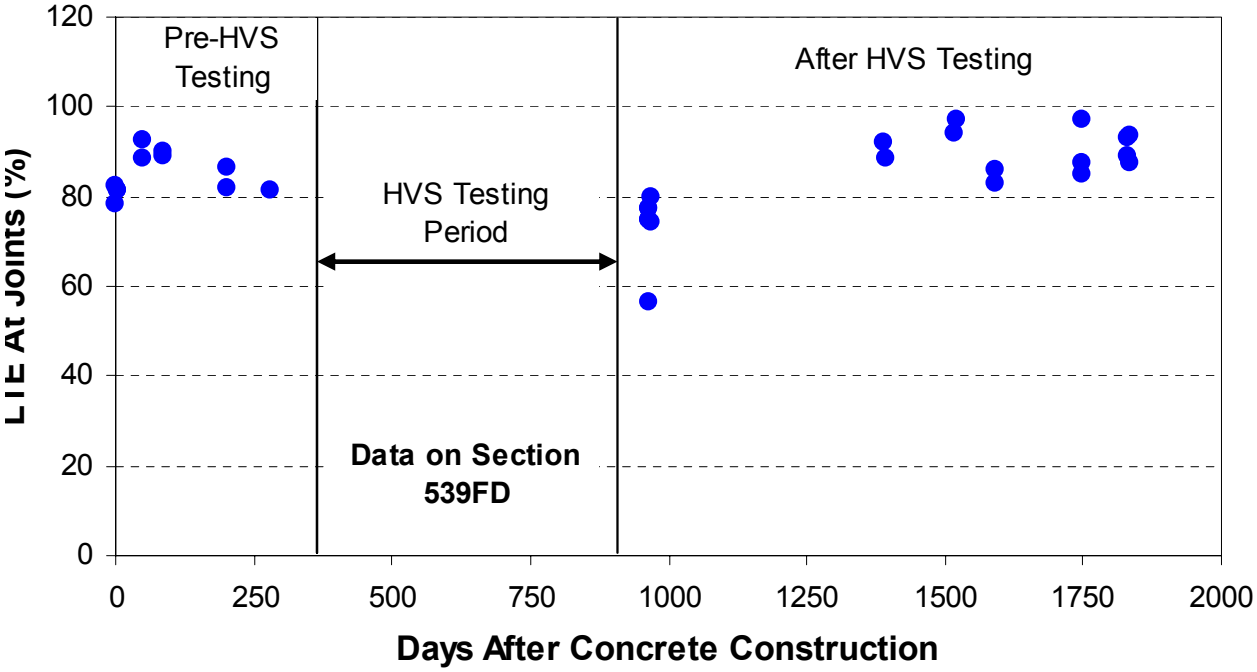

Figure 161. Impact of HVS testing on LTE measured at transverse joints along slab centerline (Test 539FD).

5.5.9 Test 540FD (Section 11: Dowels, No Tie Bars, Widened Truck Lane)

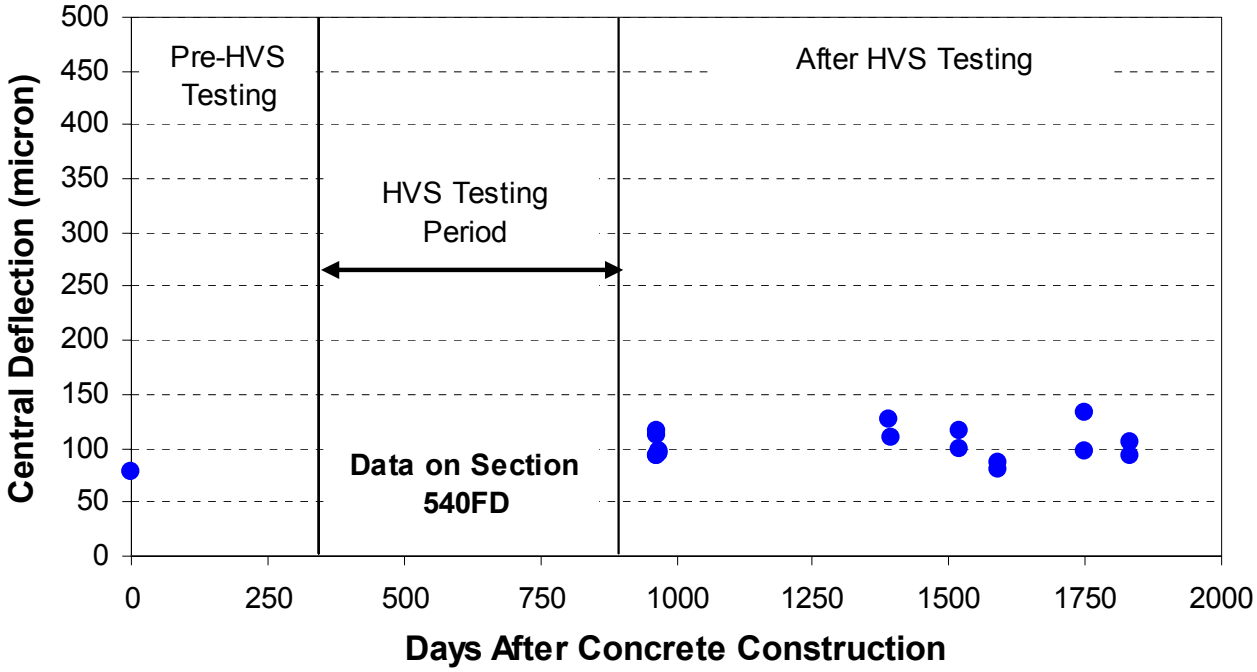

Figure 162. Impact of HVS testing on central deflection measured at slab center (Test 540FD).

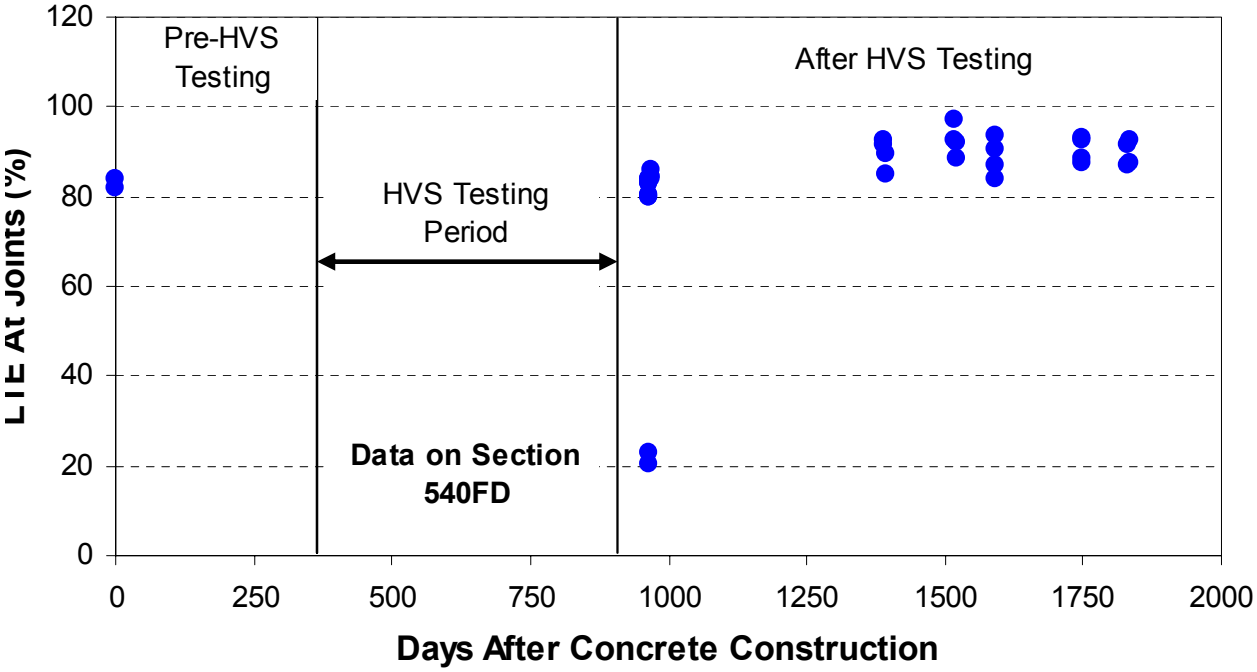

Figure 163. Impact of HVS testing on LTE measured at transverse joints along slab centerline (Test 540FD).

5.5.10 Test 541FD (Section 11: Dowels, No Tie Bars, Widened Truck Lane)

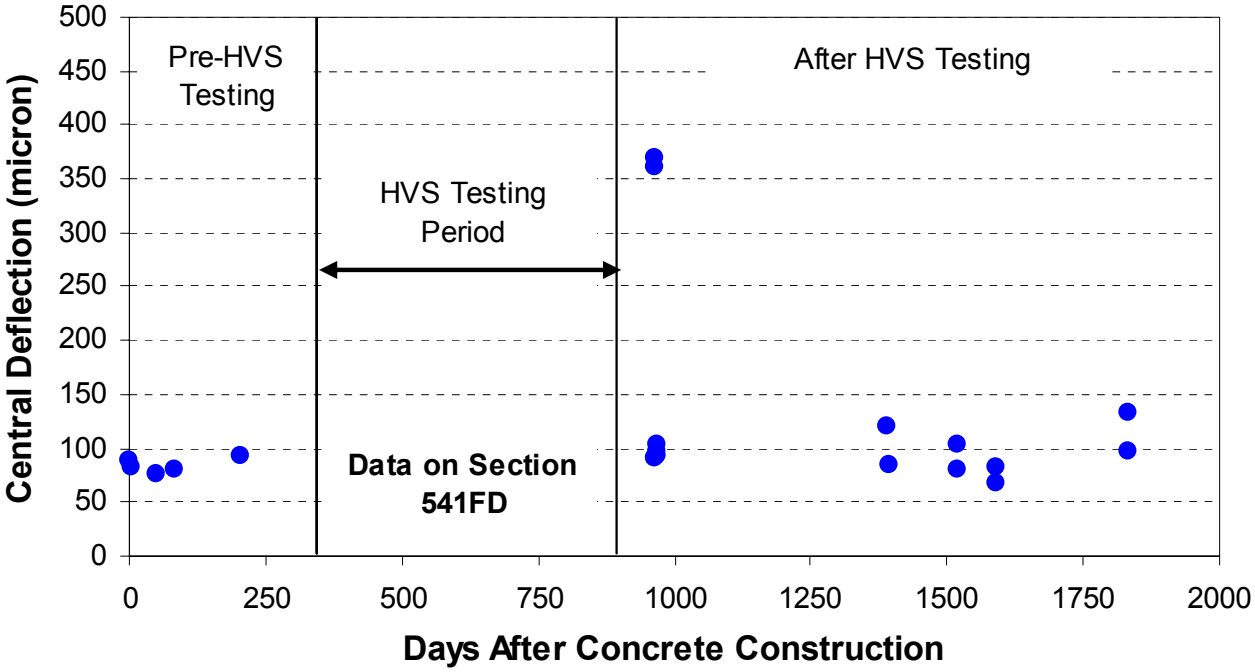

Figure 164. Impact of HVS testing on central deflection measured at slab center (Test 541FD).

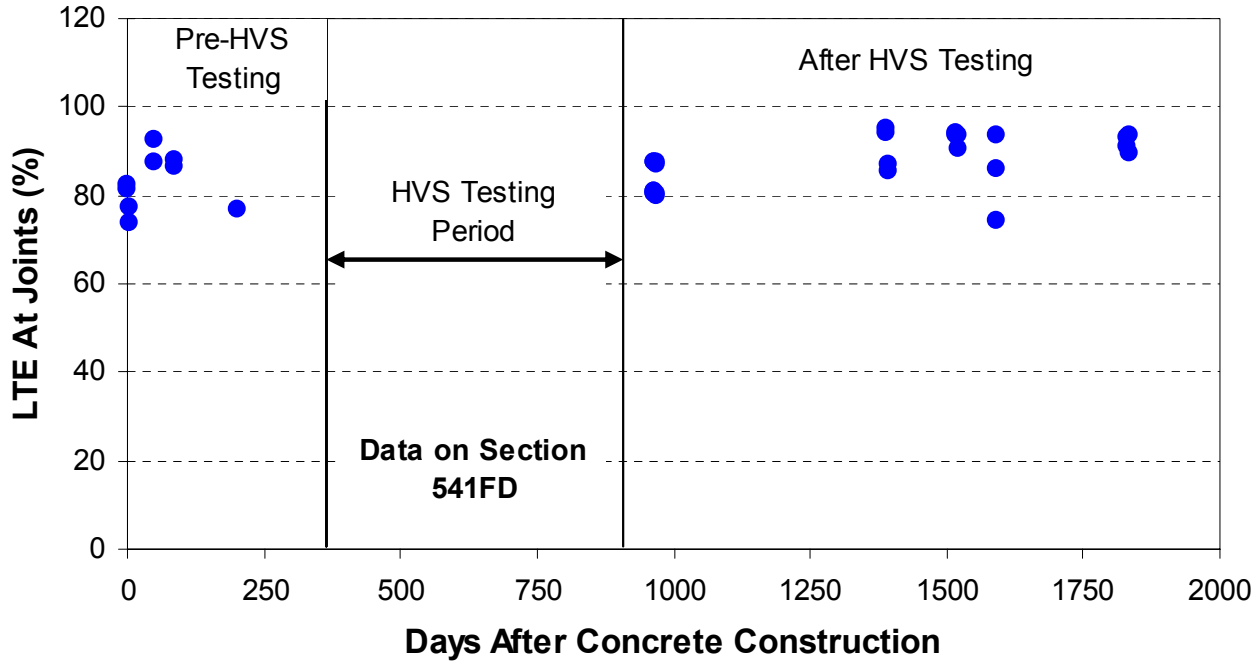

Figure 165. Impact of HVS testing on LTE measured at transverse joints along slab centerline (Test 541FD).

5.5.11 Observations and Conclusions

The deflections and load transfer efficiencies measured before and after HVS testing generally suggest that the HVS tests did not significantly affect the manner in which a tested slab as a whole reacts to FWD loading. The central deflection at the slab center as well as the LTE at the transverse joints generally exhibit a pattern that is consistent before and after HVS testing. However, as noted in Chapter 5.5.1, this observation is based on deflections taken at the slab center, which is not where HVS testing was conducted.

A possible exception to the above observation is Test 535FD, conducted on Slab 39 which is located in Section 7 (no dowels or tie bars). This section shows a slight increase in deflections after HVS testing, as well as a clear increase in variability of deflections after HVS testing. However, it should be noted that the deflections recorded before HVS testing was conducted were all recorded during the day. The tests conducted after HVS testing, on the other hand, were conducted both during the day and night. Because of this, it is expected that the data recorded after HVS testing will exhibit increased variance owing to the larger temperature range during FWD testing.

As expected, the HVS test sections located in Sections 9 and 11 (both fitted with dowels), exhibit a consistently higher LTE both before and after HVS testing when compared to the HVS sections located on Section 7 (no dowels).

5.6 Back-calculated Stiffnesses

Back-calculation of concrete stiffness was performed for most of the FWD measurements recorded before HVS testing. Back-calculation results reported in this chapter were obtained using the ELMOD program (Version 3) (*6*) which uses the Odemark-Bousinesq theory to back-

calculate pavement layer stiffnesses. Back-calculation results reported in this chapter are based only on those deflections measured at the center of the concrete slabs.

For this analysis, the pavement was modeled as a three-layer system with a constant subbase stiffness of approximately 1400 MPa (200 ksi) for the cement treated subbase. Thus the only variables determined by the back-calculation were the concrete stiffness and the subgrade stiffness.

Figures 166–176 show the back-calculated stiffness of the concrete and subgrade at different times after concrete construction. The main trends in back-calculated stiffness over time are summarized in Figures 174–179. These figures prompt the following observations:

- In general, the back-calculated stiffness for the concrete slabs and the subgrade show little or no clear trends for different ages and temperatures. The exception is that the concrete shows a slight increase in stiffness variation for all joint construction types with increasing age (see Figures 174–176). This trend is most apparent in the case of Section 9 (dowels and tie bars, Figure 175). As noted previously, it is likely that this trend is caused by reduced temperature during testing rather than by concrete effects.
- Decreased subgrade stiffness and decreased variation in subgrade stiffness seems more evident in Figure 177 (dowels, no tie bars) and Figure 178 (no dowels, no tie bars), than in Figure 179 (dowels and tie bars).

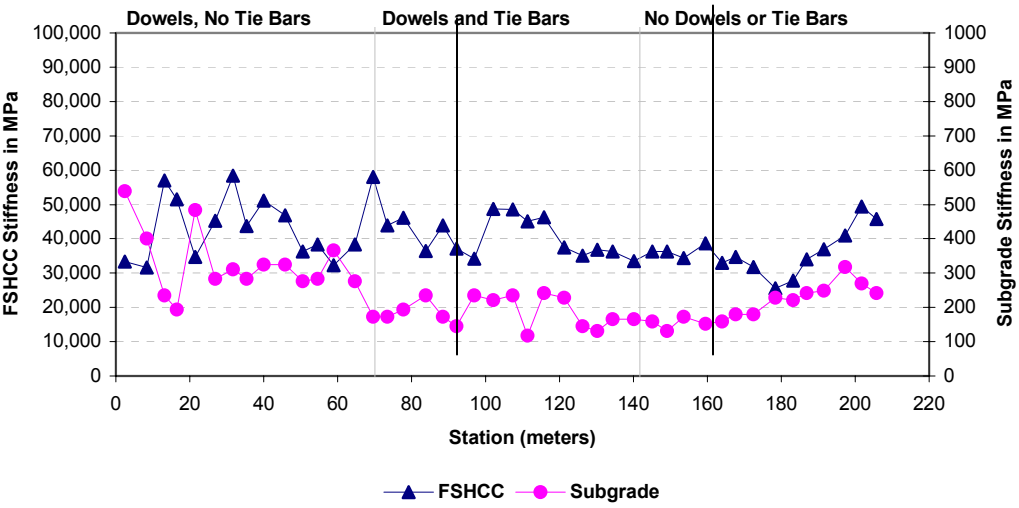

Parameter	Dowels, No Tie Bars		Dowels and Tie Bars		No Dowels or Tie Bars	
	FSHCC	Subgrade	FSHCC	Subgrade	FSHCC	Subgrade
Mean	43775	316	40614	187	36100	207
Stdev	9644	98	5511	43	6316	53
15th %	33440	239	35182	145	31539	158
85th %	56362	397	46238	235	41223	249
COV (%)	22	31	14	23	17	26

Figure 166. Back-calculated stiffness 1 day after concrete construction.

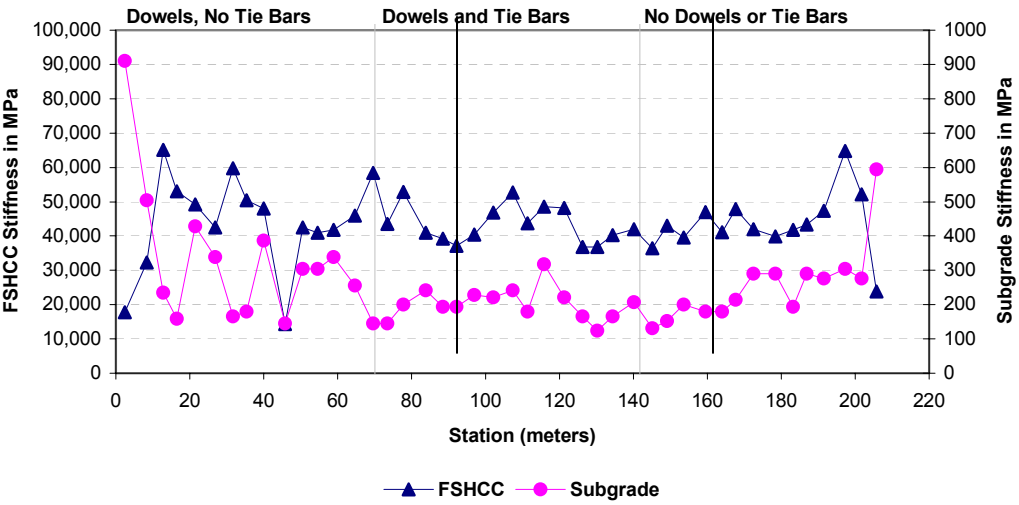

Parameter	Dowels, No Tie Bars		Dowels and Tie Bars		No Dowels or Tie Bars	
	FSHCC	Subgrade	FSHCC	Subgrade	FSHCC	Subgrade
Mean	44150	320	43301	203	43590	255
Stdev	14119	197	5419	47	8959	113
15th %	33239	159	37348	166	39352	178
85th %	57818	424	48465	240	48115	290
COV (%)	32	62	13	23	21	45

Figure 167. Back-calculated stiffness 7 days after concrete construction.

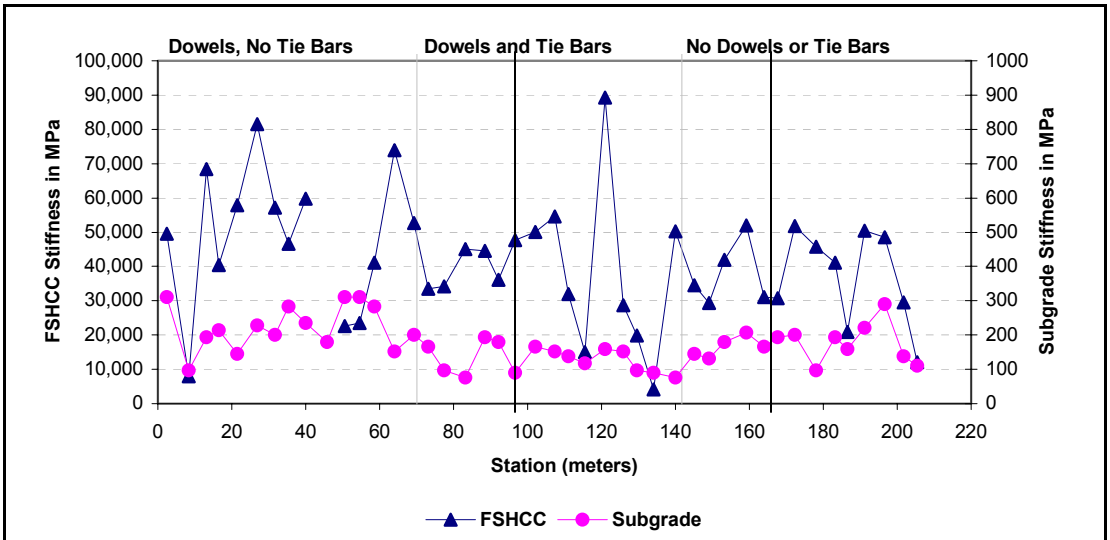

Parameter	Dowels, No Tie Bars		Dowels and Tie Bars		No Dowels or Tie Bars	
	FSHCC	Subgrade	FSHCC	Subgrade	FSHCC	Subgrade
Mean	45534	223	38997	130	37122	173
Stdev	23502	66	19904	40	12246	50
15th %	22760	155	20755	90	28998	130
85th %	67519	308	50302	166	50555	208
COV (%)	52	30	51	31	33	29

Figure 168. Back-calculated stiffness 49 days after concrete construction.

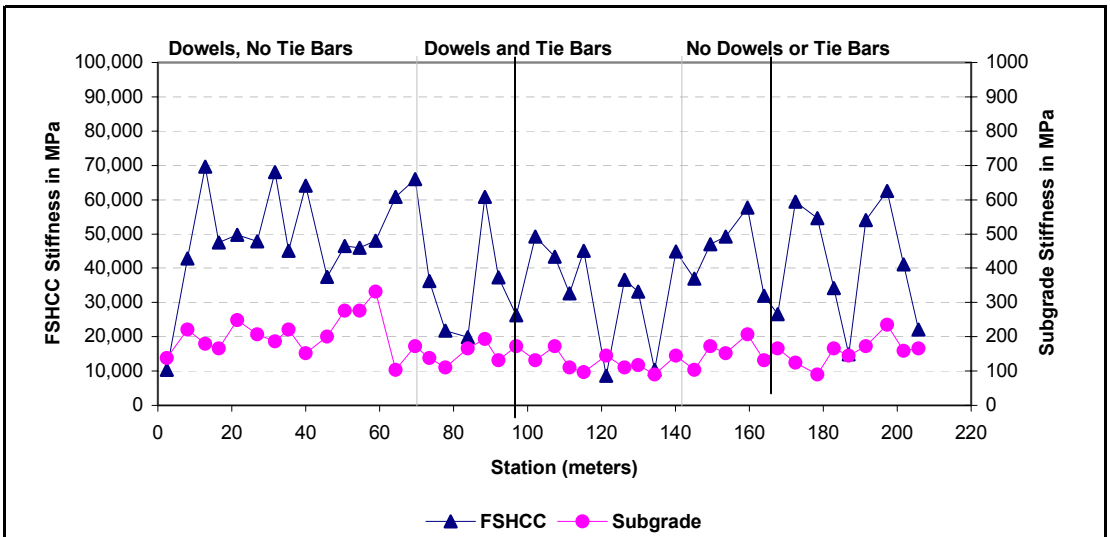

Parameter	Dowels, No Tie Bars		Dowels and Tie Bars		No Dowels or Tie Bars	
	FSHCC	Subgrade	FSHCC	Subgrade	FSHCC	Subgrade
Mean	49978	205	33731	135	42285	156
Stdev	14925	60	14416	31	14960	38
15th %	43021	153	20061	110	26354	123
85th %	65761	273	44990	172	57806	174
COV (%)	30	29	43	23	35	24

Figure 169. Back-calculated stiffness 90 days after concrete construction.

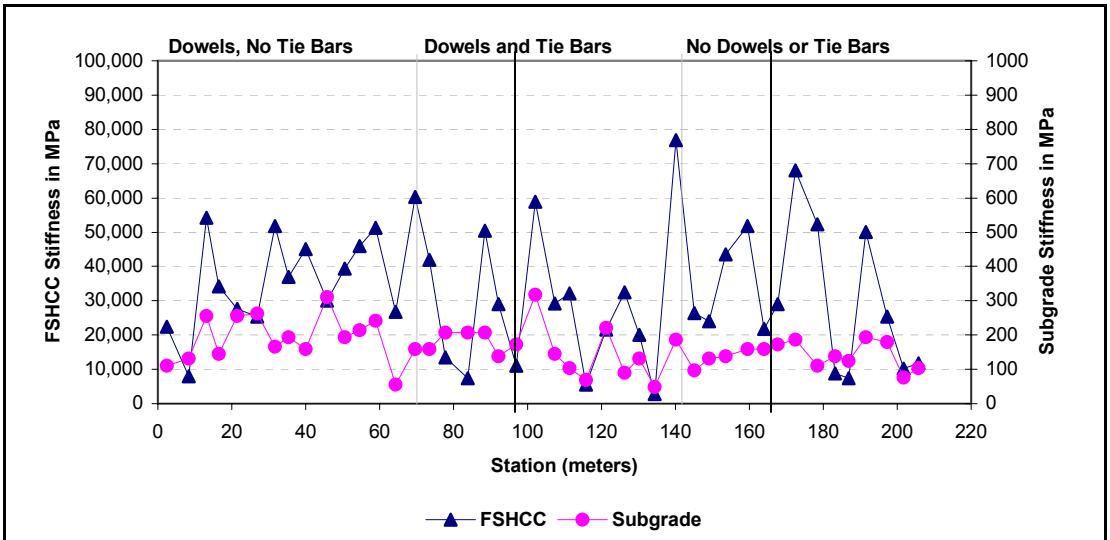

Parameter	Dowels, No Tie Bars		Dowels and Tie Bars		No Dowels or Tie Bars	
	FSHCC	Subgrade	FSHCC	Subgrade	FSHCC	Subgrade
Mean	37289	190	28869	160	30771	140
Stdev	14293	68	21091	69	19251	36
15th %	25460	132	7858	91	10144	103
85th %	51758	255	49580	207	51852	180
COV (%)	38	36	73	43	63	26

Figure 170. Back-calculated stiffness 200 days after concrete construction.

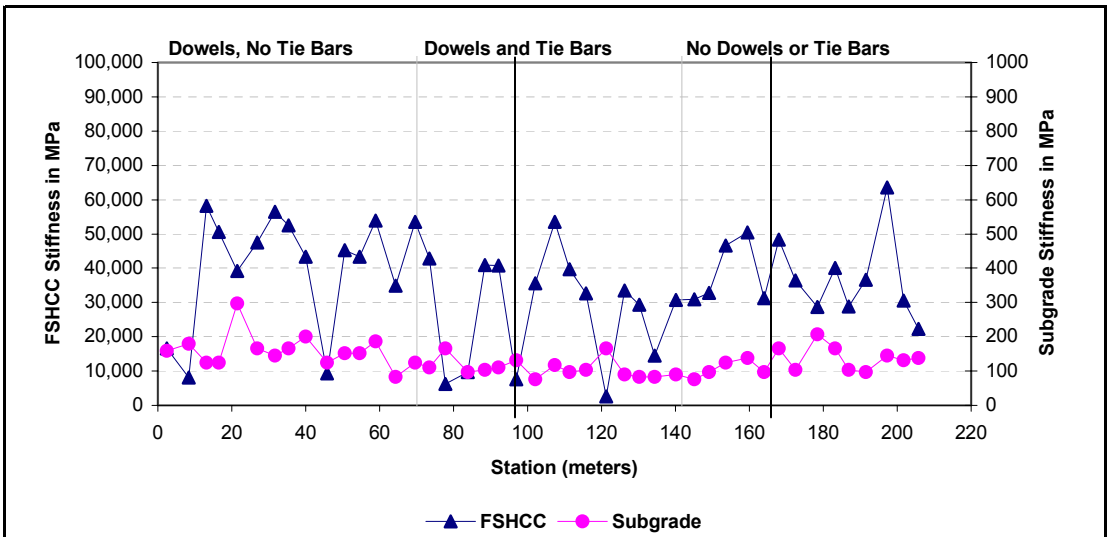

Parameter	Dowels, No Tie Bars		Dowels and Tie Bars		No Dowels or Tie Bars	
	FSHCC	Subgrade	FSHCC	Subgrade	FSHCC	Subgrade
Mean	40858	159	28024	108	37676	128
Stdev	16622	48	15842	27	11062	36
15th %	18379	124	7830	83	28810	97
85th %	53899	186	40906	130	48523	166
COV (%)	41	31	57	25	29	28

Figure 171. Back-calculated stiffness 270 days after concrete construction.

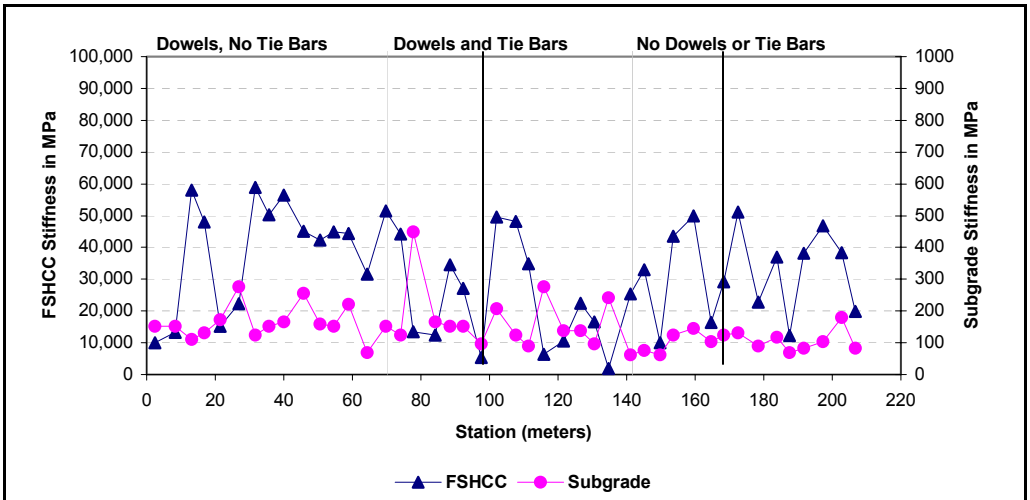

Parameter	Dowels, No Tie Bars		Dowels and Tie Bars		No Dowels or Tie Bars	
	FSHCC	Subgrade	FSHCC	Subgrade	FSHCC	Subgrade
Mean	39472	163	23545	167	30866	104
Stdev	16767	53	15858	97	14079	33
15th %	15842	125	6773	97	14812	70
85th %	55982	216	43321	238	46463	130
COV (%)	42	33	67	58	46	32

Figure 172. Back-calculated stiffness 966 days after concrete construction (daytime measurement).

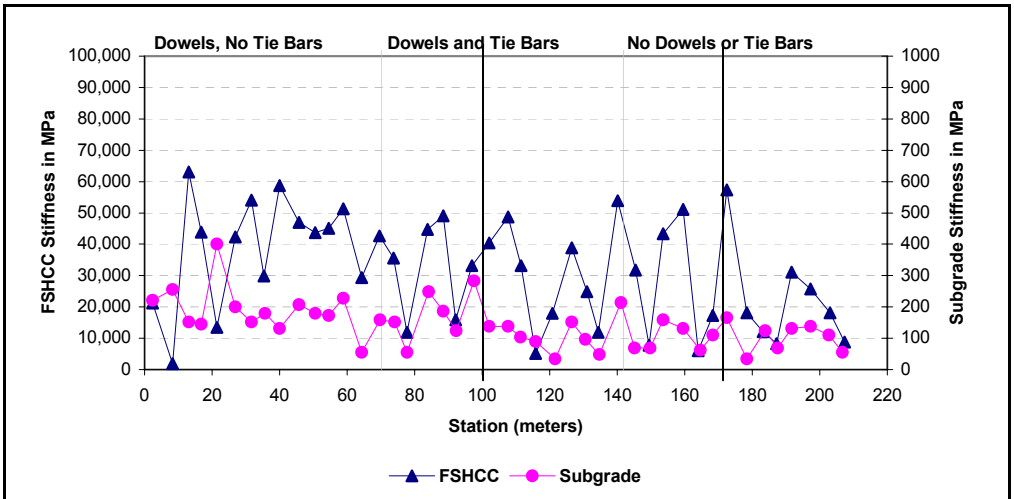

Parameter	Dowels, No Tie Bars		Dowels and Tie Bars		No Dowels or Tie Bars	
	FSHCC	Subgrade	FSHCC	Subgrade	FSHCC	Subgrade
Mean	39176	189	31014	138	23488	100
Stdev	16968	75	15509	72	16319	41
15th %	22019	146	12315	59	8278	63
85th %	53832	227	48271	211	42225	137
COV (%)	43	40	50	52	69	41

Figure 173. Back-calculated stiffness 966 says after concrete construction (daytime measurement).

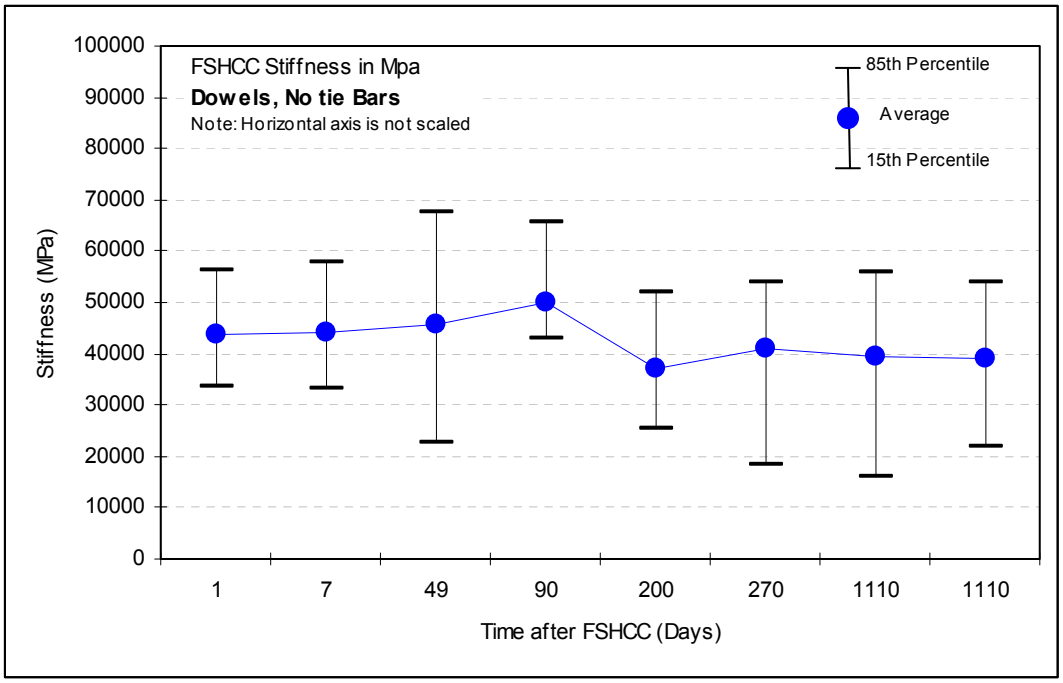

Figure 174. Concrete stiffness at different ages, Section 11 (doweled joints with asphalt concrete shoulder and widened truck lane).

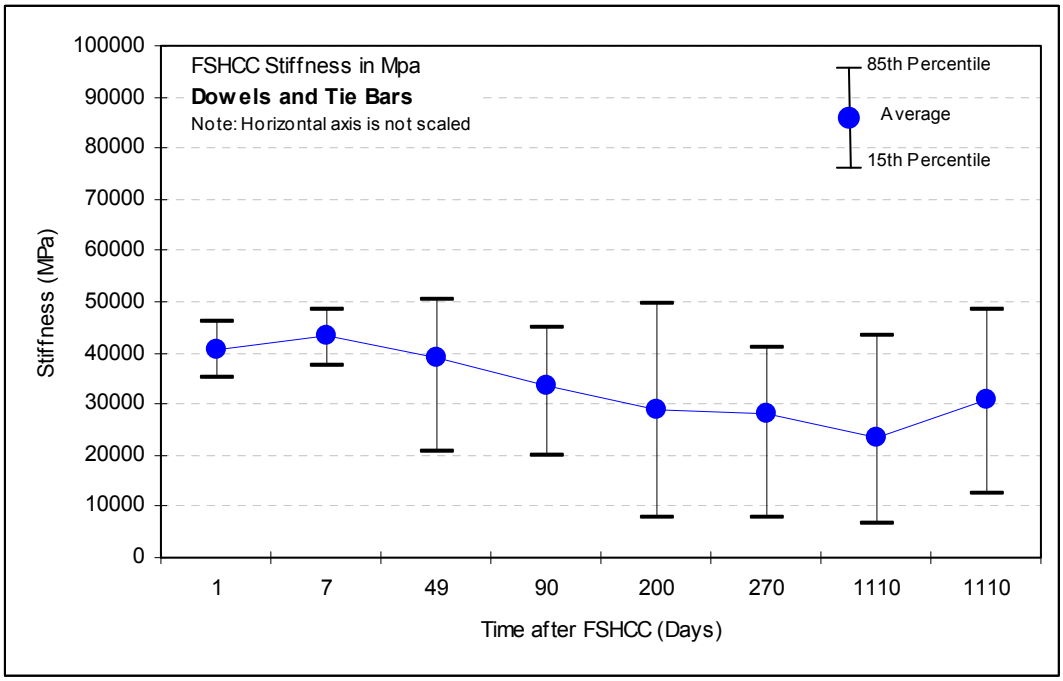

Figure 175. Concrete stiffness at different ages, Section 9 (doweled joints and tie bars at concrete shoulder).

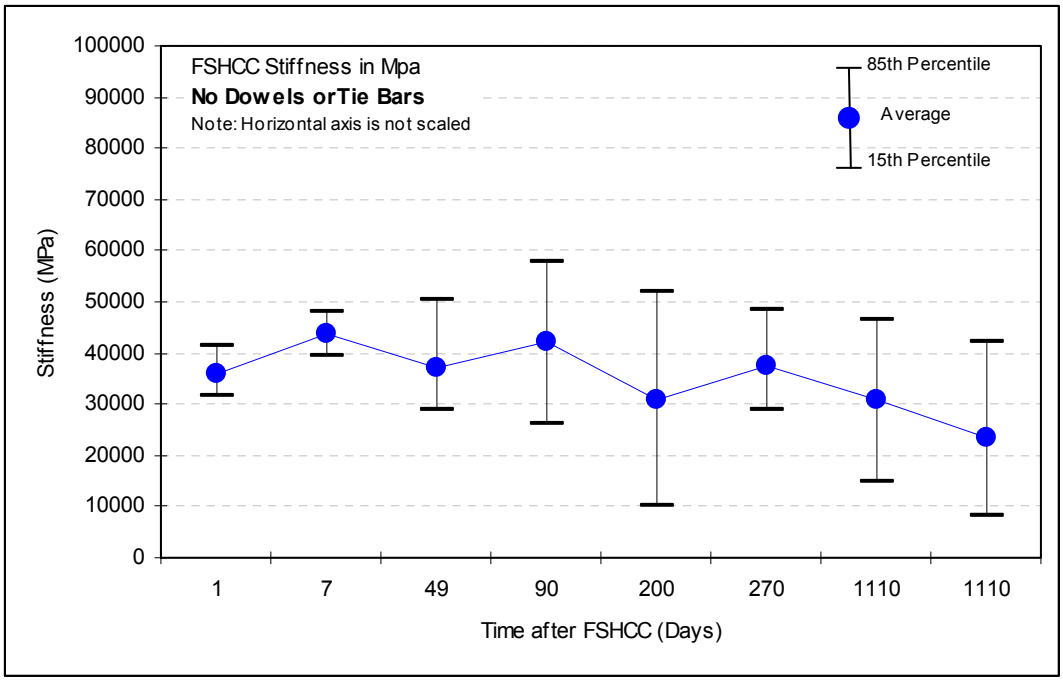

Figure 176. Concrete stiffness at different ages, Section 7 (no dowels or tie bars, asphalt concrete shoulder).

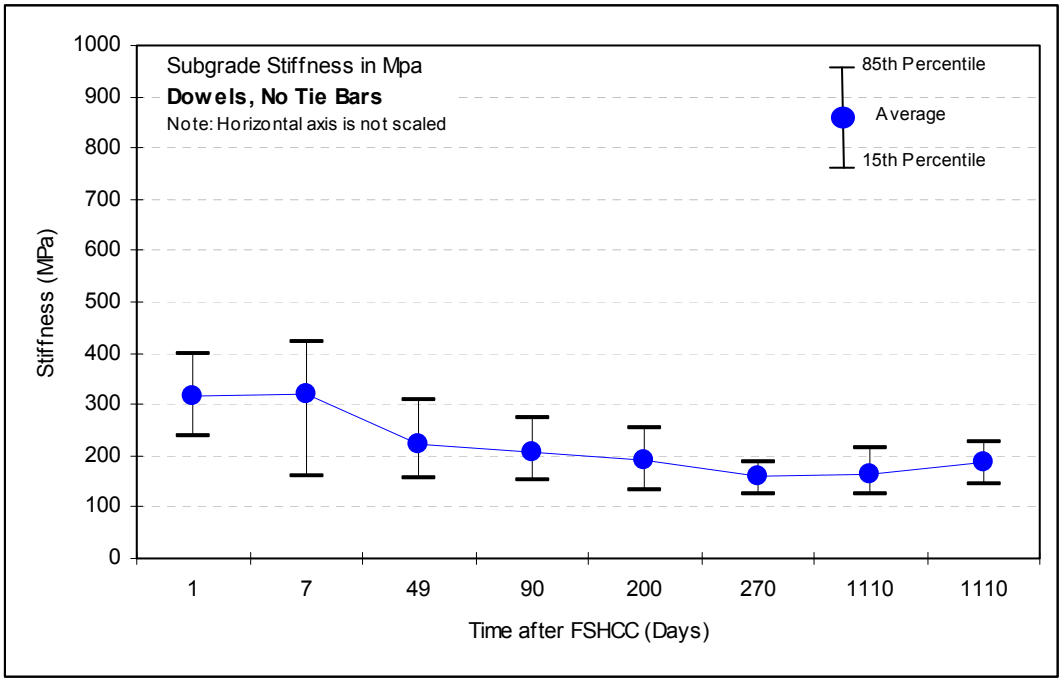

Figure 177. Subgrade stiffness at different ages, Section 11 (doweled joints with asphalt concrete shoulder and widened truck lane).

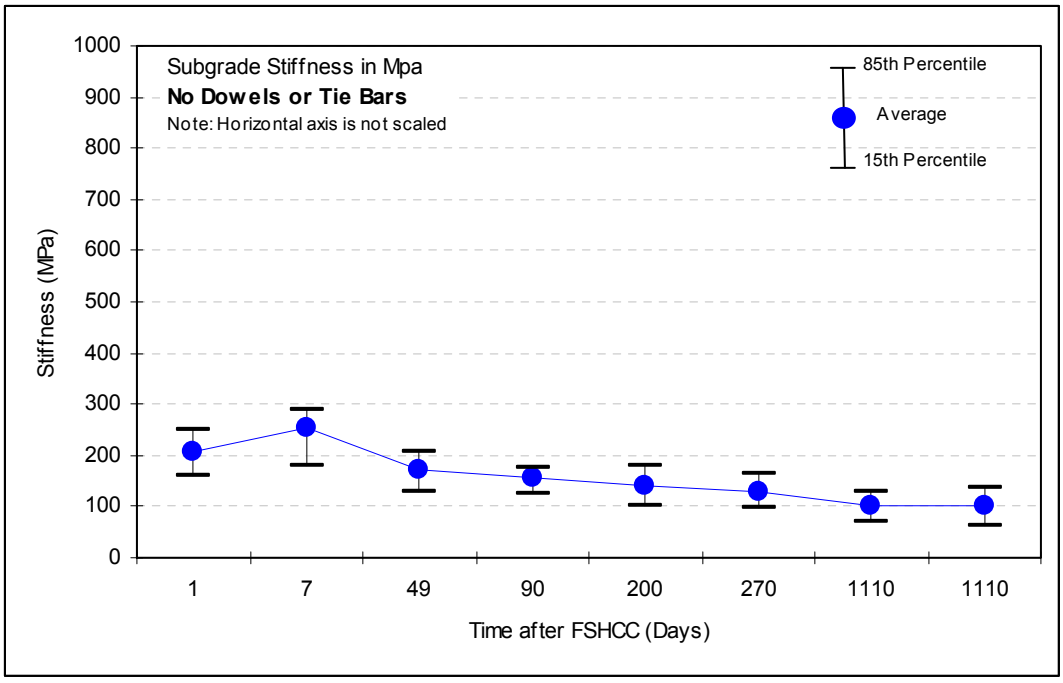

Figure 178. Subgrade stiffness at different ages, Section 7 (no dowels or tie bars, asphalt concrete shoulder).

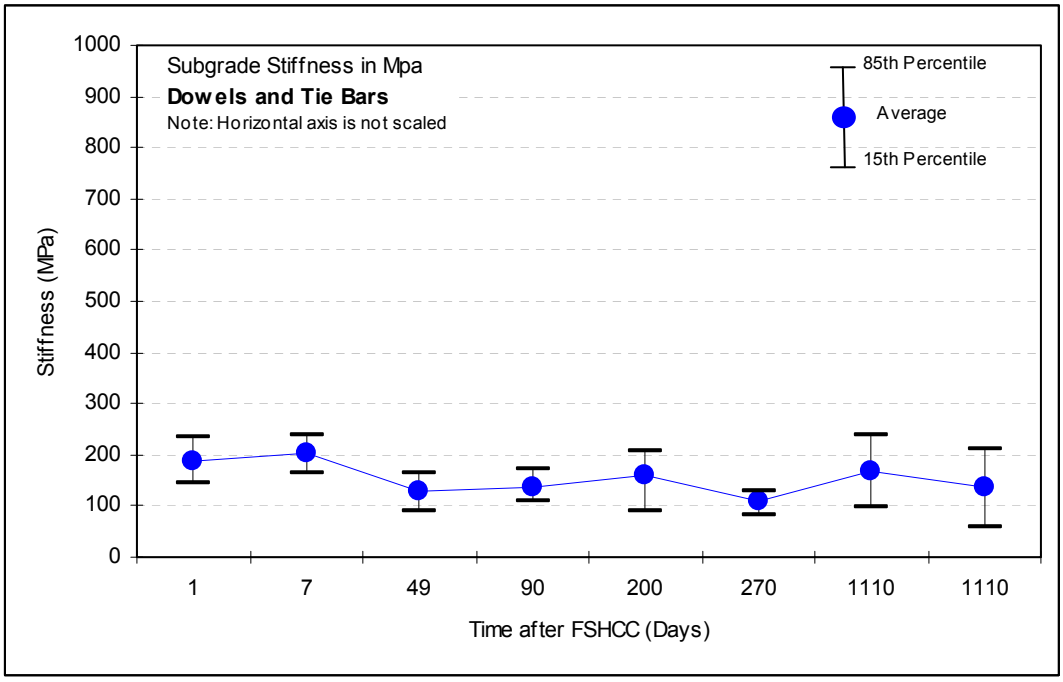

Figure 179. Subgrade stiffness at different ages, Section 9 (doweled joints and tie bars at concrete shoulder).

5.7 Summary and Conclusions

Observations related to maximum deflections, LTE and back-calculated stiffness are noted in the relevant chapters. Some of the more significant observations include:

- The support conditions, as tested prior to concrete construction, are largely similar for the three joint construction types. Section 11 (dowels, no tie bars), appears to have a slightly more uniform and better support than the other two sections (Figure 166).
- The maximum deflection and back-calculated stiffnesses at the slab center show little systematic variation for sections with different joint construction types.
- The central deflection recorded along the slab centerline and K-rail edge show little or no correlation with concrete age or slab temperature at the time of testing.
- As expected, the central deflection is always higher at the longitudinal edge (K-rail side) of the pavement when compared to the centerline. Similarly, LTE is lower along the edge (i.e., at corners) in contrast to the centerline (i.e., at transverse joints).
- At transverse joints, the LTE shows a clear dependency on joint construction type. At temperatures below roughly 15ºC, Section 7 (no dowels) shows a significantly lower LTE than Sections 9 and 11 (both constructed with dowels). However, this dependency decreases significantly at higher temperatures, and also somewhat as concrete age increases. At temperatures of roughly greater than 20ºC and at concrete ages greater than 300 days, there is little difference between the LTE recorded on the doweled and undoweled sections.
- There is no appreciable difference in the transverse joint LTE for Sections 9 (with dowels and tie bars) and 11 (with dowels, no tie bars).

- Sections 9 and 11 show little change in transverse joint LTE with changing age and temperature. In contrast, Section 7 (no dowels or tie bars) shows a significant dependency on age and temperature.
- At longitudinal joints (measured along the K-rail side), there is little or no systematic variation in LTE for different transverse joint construction types.
- FWD data recorded before and after HVS testing suggest that the HVS test did not significantly affect slab behavior as characterized by center slab deflection and transverse joint LTE (recorded at the slab centerline).

Perhaps the clearest and most significant observation that follows from the FWD test program is the improved transverse joint LTE for Sections 9 (dowels and tie bars) and 11 (dowels, no tie bars) when compared to that of Section 7 (no dowels or tie bars), at temperatures below 15ºC.

It should be noted, however, that the main effects were not evaluated statistically during the first level analysis presented here. It is therefore recommended that further analysis include statistical evaluation of the main effects at an appropriate significance level to ensure that apparent trends are indeed statistically significant.

6.0 PCC CORE MEASUREMENTS (NORTH TANGENT)

This chapter briefly outlines the most significant results from a post mortem coring investigation, which was conducted on the concrete sections on the north tangent. Coring was conducted at three stages during HVS testing:

3. Approximately 40 days after construction (early August 1998),
4. during February 2001 after all HVS testing on the North Tangent was completed, and
5. in October 2001 on specific joints and cracks.

The main objectives of the coring investigation were to verify the following concrete slab characteristics:

- As-built slab thicknesses in comparison with the design thickness;
- Density and strength measurements of the in-place concrete;
- As-built placement of strain gauges;
- Characterization of cracks;
- Saw-cut joint widths;
- Influence of slab expansion and contraction on joint and crack widths; and
- As-built placement and orientation of dowel bars.

6.1 Cores taken 40 days after construction

All the measured core properties with some useful statistics are shown in Table 46.

Table 46 Properties and Statistics of Cores Taken Approximately 40 Days After Construction

Section	Core ID	Location	Measured Properties		
			Thickness (mm)	Density Parafilm (kg/m^3)	Compressive Strength (MPa)
7	7A-32	North 7-A	220	2461.02	32.41
	7B-35	North 7-B	228	2311.37	41.26
	7C-39	North 7-C	220	2240.74	17.47
	7D-43	North 7-D	237	2361.91	33.14

	Statistics		
	Thickness (mm)	Density Parafilm (kg/m^3)	Compressive Strength (MPa)
Average	226	2343.76	31.07
Low	220	2240.74	17.47
High	237	2461.02	41.26
Std. Dev.	8	92.63	9.91
50^{th} percentile	224	2336.64	32.78
90^{th} percentile	234	2431.29	38.82
10^{th} percentile	220	2261.93	21.95

Section	Core ID	Location	Measured Properties		
			Thickness (mm)	Density Parafilm (kg/m^3)	Compressive Strength (MPa)
9	9A-27	North 9-A	220	2357.78	33.43
	9B-20	North 9-B	221	2384.33	38.7
	9C-23	North 9-C	213	2294.95	41.13
	9D-17	North 9-D	230	2428.51	40.61

	Statistics		
	Thickness (mm)	Density Parafilm (kg/m^3)	Compressive Strength (MPa)
Average	221	2366.39	38.47
Low	213	2294.95	33.43
High	230	2428.51	41.13
Std. Dev.	7	55.85	3.52
50^{th} percentile	220	2371.06	39.66
90^{th} percentile	227	2415.26	40.97
10^{th} percentile	215	2313.80	35.01

Table 46 continued

Section	Core ID	Location	Measured Properties		
			Thickness (mm)	Density Parafilm (kg/m^3)	Compressive Strength (MPa)
11	11A-3	North 11-A	244	2390.31	32.87
	11B-7	North 11-B	223	2418.33	43.31
	11C-11	North 11-C	203	2416.18	35.78
	11D-14	North 11-D	220	2381.71	43.15

	Statistics		
	Thickness (mm)	Density Parafilm (kg/m^3)	Compressive Strength (MPa)
Average	222	2401.63	38.78
Low	203	2381.71	32.87
High	244	2418.33	43.31
Std. Dev.	17	18.40	5.28
50^{th} percentile	222	2403.25	39.47
90^{th} percentile	237	2417.69	43.26
10^{th} percentile	208	2384.29	33.74

	Statistics of All Sections Together		
	Thickness (mm)	Density Parafilm (kg/m^3)	Compressive Strength (MPa)
Average	223	2370.6	36.11
Low	203	2240.74	17.47
High	244	2461.02	43.31
Std. Dev.	11	62.46	7.18
50^{th} percentile	221	2383.02	37.24
90^{th} percentile	236	2427.5	42.96
10^{th} percentile	213	2296.6	32.46

6.1.1 Slab Thickness

The true heights of the cores were measured to determine the as-built slab thicknesses. The design slab thickness on all sections on the North Tangent is 200 mm. A total of 12 cores were investigated. All the measured properties are summarized in Table 46.

In the case of Section 7, the average core thickness was 226.0 mm with a maximum of 237.0 mm and a minimum of 219.5 mm. These values are approximately 13 percent higher than the design thickness of 200 mm. In the case of Section 9, the average thickness value is 220.8 mm with a maximum value of 230.0 mm and a minimum of 212.8 mm. This represents a 10 percent increase from the original design thickness. For Section 11, the average thickness is 222.4 mm with a maximum of 243.5 mm and a minimum of 220.0 mm (11 percent increase from the design thickness).

In general, it can be said that the slab thicknesses measured from the cores drilled from each section are on average about 20 mm thicker than the design of 200 mm. Taking into consideration that only a limited number of samples were taken, the distribution of the slab thickness seems to be skewed to the high side. The variability in core thickness is however significantly less than observed in cores extracted from the South Tangent (*3*).

6.1.2 Core Densities

Some useful statistics of the core densities taken from Sections 7, 9, and 11 are also shown in Table 46. Core densities calculated using the Parafilm procedure is shown in the table. The corresponding volumetric densities as calculated from measured sample dimensions and weights are (as can be expected) somewhat higher than the Parafilm densities with an average conversion factor of 0.9768. This conversion factor is very consistent and applies to both the

North Tangent and South Tangent data set. The average Parafilm densities of all the samples taken on the north tangent is 2,370.60 kg/m^3, with a maximum value of 2,461.02 kg/m^3 and a minimum value of 2,240.74 kg/m^3.

6.1.3 Compressive Strength

The average compressive strength of all the samples taken from Sections 7, 9, and 11 is 36.11 MPa with a high of 43.31 MPa (corresponding to the third highest core density value of 2,418.33 kg/m^3). The lowest strength recorded is 17.47 MPa, which corresponds to the lowest Parafilm density measured of 2,240.74 kg/m^3. The results indicate that compressive strength is very sensitive to concrete density. A 7.3 percent drop in density (from 2,418.33 to 2,240.74 kg/m^3) caused a 59.7 percent drop in the compressive strength (43.31 MPa to 17.47 MPa) as indicated in Figure 180.

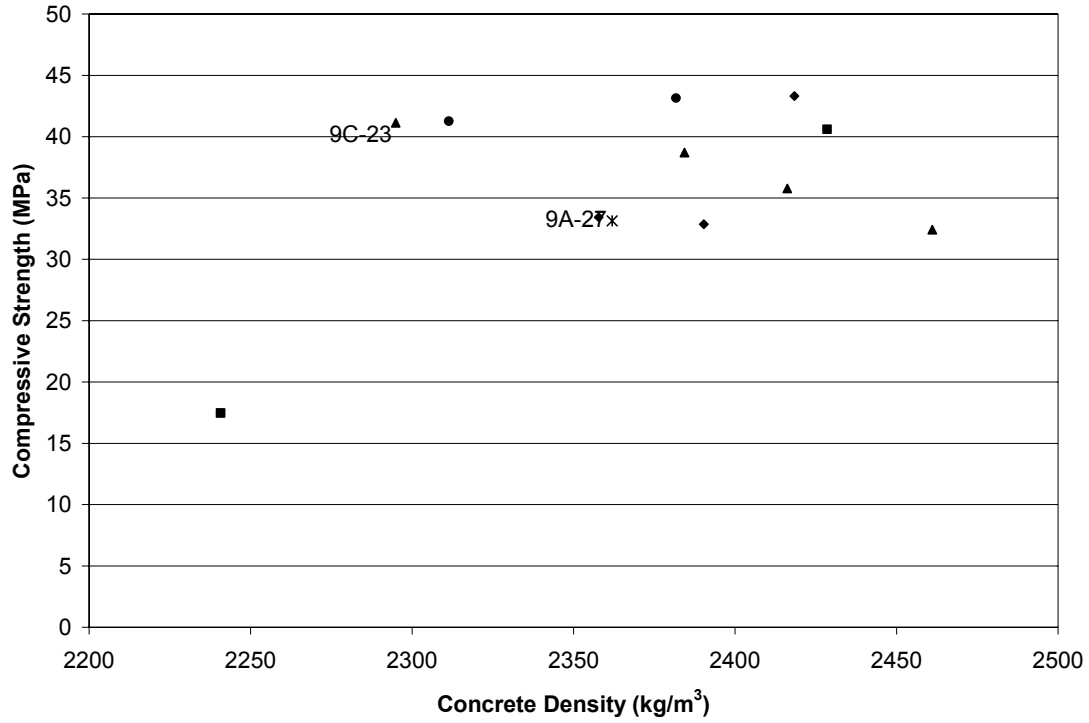

Figure 180. Relationship between compressive strength and concrete density.

It appears that a density of 2,300 kg/m^3 is a threshold in terms of compressive strength. As indicated in Figure 180, there is no clear trend between density and compressive strength with samples with densities above 2,300 kg/m^3. Through investigation of both the South Tangent and North Tangent core data sets, a significant drop in compressive strength was observed on samples with densities less than 2,300 kg/m^3.

6.2 Observations from Cores Taken After HVS Testing

A number of 100-mm diameter cores were drilled from the concrete slabs on the North Tangent after all HVS testing was completed (February 2001). The objectives of coring were to investigate the characteristics of the cracks, which formed on the various concrete slabs to determine slab thickness under HVS tested slabs, and to verify the position and orientation of some of the strain sensors.

A total of 46 samples were cored: 15 cores from Section 7, 15 cores from Section 9, and 16 cores from Section 11.

6.2.1 Slab Thickness

The thickness of each core was measured to verify the constructed slab thickness. Table 47 presents the core height statistics from the four HVS tests on Section 7 (532FD–535FD), Table 48 presents the core data from Section 9 (Tests 536 FD–538 FD), and Table 49 presents the core data from Section 11 (539 FD–541 FD). Table 50 summarizes all the data collected from all tests.

Table 47 Core Height Statistics of Cores Taken after HVS Testing on Section 7

HVS Test	Core Number	True Height (mm)	Statistics of Core Height (mm)	
532FD	42N	240	**Average**	222
	43N	217	**Low**	208
	44N	208	**High**	240
			Std. Dev.	17
			50th percentile	217
			90th percentile	235
			10th percentile	210
533FD	38N-Center	219	**Average**	222
	38N-SE	235	**Low**	215
	39N-Center	221	**High**	235
	40N-Center	215	**Std. Dev.**	8
	40N-WP	222	**50th percentile**	221
			90th percentile	230
			10th percentile	217
534FD	34N-C	223	**Average**	232
	35N-C	230	**Low**	223
	35N-E	240	**High**	240
	36N-Center	233	**Std. Dev.**	7
			50th percentile	232
			90th percentile	238
			10th percentile	225
535FD	31N-C	223	**Average**	224
	32N C-E	225	**Low**	223
	33N-C	224	**High**	225
			Std. Dev.	1
			50th percentile	224
			90th percentile	225
			10th percentile	223

Table 48. Core Height Statistics of Cores Taken After HVS Testing on Section 9

HVS Test	Core Number	True Height (mm)	Statistics of Core Height (mm)	
536FD	26N-N	220	**Average**	219
	26N-W	204	**Low**	204
	26N-C	220	**High**	225
	27N-C	223		8
	27N-NW	220	**50th percentile**	220
	28N-C	225	**90th percentile**	224
			10th percentile	212
537FD	22N-C	215	**Average**	209
	23N-W	205	**Low**	203
	23N-C	211	**High**	215
	24N-C	203	**Std. Dev.**	6
			50th percentile	208
			90th percentile	214
			10th percentile	204
538FD	18N-C	210	**Average**	218
	19N-C	226	**Low**	210
	20N-C	212	**High**	226
	20N-W	223	**Std. Dev.**	8
			50th percentile	218
			90th percentile	225
			10th percentile	211

Table 49 Core Height Statistics of Cores Taken After HVS Testing on Section 11

HVS Test	Core Number	True Height (mm)	Statistics of Core Height (mm)	
539FD	10N	219	**Average**	213
	11N-SE	218	**Low**	205
	11N-CE	212	**High**	219
	11N-C	210	**Std. Dev.**	6
	12N-C	205	**50th percentile**	212
			90th percentile	219
			10th percentile	207
540FD	6N	226	**Average**	220
	6N-SE	216	**Low**	216
	7N	220	**High**	226
	7N-Center	222	**Std. Dev.**	4
	8N-Center	218	**50th percentile**	220
			90th percentile	224
			10th percentile	217
541FD	2N	228	**Average**	227
	3N Center	241	**Low**	221
	3N-NE	221	**High**	241
	4N-Center	224	**Std. Dev.**	7
	4N-North East	224	**50th percentile**	225
	4N-SE	226	**90th percentile**	235
			10th percentile	223

Table 50 Summary of Core Height Statistics

	Core Height		
	Section 7 (mm)	**Section 9 (mm)**	**Section 11 (mm)**
Average	227	216	221
Low	221	203	205
High	241	226	241
Std. Dev.	7	8	8
50th percentile	225	220	221
90th percentile	235	225	227
10th percentile	223	204	211

The slab thickness on Section 9 is the lowest with an average of 216 mm, a low of 203 mm (Slab 24, Test 537 FD), and a high of 226 mm (Slab 19, Test 538FD). Section 7 has the highest slab thickness with an average thickness of 225 mm and a high of 240 mm.

The average slab thickness on HVS test sections were:

- Section 7: 225 mm,
- Section 9: 216 mm; and
- Section 11: 220 mm.

In conclusion it is noted that on average the slab thickness on the North Tangent HVS sections are approximately 10 percent higher than the design thickness of 200 mm.

6.2.2 Instrument Positioning

The main aim of this coring investigation was to verify correct vertical and horizontal location and orientation of various types of strain gauges placed inside the concrete slab on the North Tangent during construction. Three types of strain gauges of different configurations were placed inside the concrete from manufacturers Dynatest, Tokyo Sokki, and Carlson, as discussed in Reference (*1*). The specified vertical positions of these instruments inside the 200-mm thick concrete were 40 mm from top of the slab, in the case of the top strain gauges and 40 mm from the bottom of the slab in the case of the gauges placed at the bottom of the slab. The vertical instrument positions were measurable on 10 of the 46 cores.

The vertical positions of the Dynatest strain gauges (design depth 40 mm from the top) were obtained from 7 of the 10 cores. Eight cores revealed the true position of the PMR strain gauges and one core was used to check the position of a Carlson strain gauge (also supposed to be 40 mm from the top of the slab). The findings are summarized in Table 51.

Table 51 Strain Gauge Positioning as Measured from Cores after HVS Testing

Core Number	Location (Section Number)	Core Height (mm)	Instrument Type				
			Dynatest		Tokyo Sokki		Carlson
			Distance from		Distance from		Distance from
			Top (mm)	Bottom (mm)	Top (mm)	Bottom (mm)	Top (mm
3N-NE	11	221	180	41	61.5	159.5	N/A
4N-SE	11	226	N/A	N/A	67.5	158.5	N/A
6N-SE	11	216	N/A	N/A	N/A	N/A	60
7N	11	220	185	35	N/A	N/A	N/A
11N-CE	11	212	176	36	56	156	N/A
20N-W	9	223	185	38	60	163	N/A
23N-W	9	205	166	39	37	168	N/A
27N-NW	9	220	177	43	45	175	N/A
35N-E	7	240	208	32	80	160	N/A
40N-WP	7	222	182	40	72	150	N/A

6.2.2.1 Dynatest Strain Gauges (Specified Distance from the Top of the Slab = 40 mm)

Analysis of the data indicates that the vertical positioning achieved during the installation of the Dynatest strain gauges was accurate. Although the distances taken from the bottom of the drilled cores vary from 32 mm to 43 mm (refer to Table 51), the average distance from the bottom of the slab for all the Dynatest gauges was 38 mm, which is very close to the target of 40 mm.

6.2.2.2 Tokyo Sokki Strain Gauges (Specified Position = 40 mm from the Top of the Slab)

The vertical distances measured from the top of the slabs of the PMR gauges varies from 37 mm (on Section 9, Test 537 FD, where the slab thickness is 205 mm), to 80 mm (on Section 7, Test 534 FD, where the slab thickness is 240 mm). This variation is clearly a function of the slab thickness at the specific point where coring took place. It is clear that the positioning of the gauges was controlled from the bottom of the slab (i.e., the top of the subbase) during

construction. If the specified slab thickness of 200 mm was achieved during construction, the positioning would have been very accurate. The average distance from the bottom of the slab of all the gauges is 161 mm, which is equal to the design target of 160 mm (200 mm – 40 mm).

6.2.2.3 Carlson Strain Gauges (Specified Position = 40 mm from the Top of the Slab)

Only one Carlson gauge was found through the coring process. The slab thickness at that point is 216 mm (see Core 6N-SE in Table 51) and the strain gauge was found 60 mm from the top of the slab. This means that the gauge was placed 156 mm from the bottom of the slab, which is acceptable in comparison with the design placement depth of 160 mm. The limited information indicates that the positioning of the Carlson gauges follows the same trend as the Tokyo Sokki gauges (i.e., their position relative to the top of the slab is a function of the concrete slab thickness at the point).

6.2.3 Crack Mechanisms

Twenty cores were drilled through cracks to study crack origin (top-down versus bottom-up), crack openings, and probable cause of the cracks. Twelve cores were drilled from HVS test slabs on Section 7, and five cores each on Sections 9 and 11. Observations from these cores are summarized in Tables 52, 53, and 54.

Cracks that developed only during HVS testing were attributed to fatigue while other cracks (mostly mid-slab transverse cracking) were attributed to concrete shrinkage. Shrinkage cracks are generally full-depth cracks with similar dimensions at the top and bottom of the slab with crack openings of 1 to 2 mm. Fatigue crack depths and openings vary in dimensions and

Table 52 Observations from Cores Taken Through Cracks on Section 7

HVS Test	Core Number	Slab Length (m)	Crack Origin for Full Depth Cracks	Crack Origin for Other Cracks	Crack Opening (mm)				Comments	Probable Cause
					Top 1	Top 2	Bottom 1	Bottom 2		
532FD	42N	5.82	Top	-	0.7	0.55	N/A	N/A	Crack developed prior to HVS testing. Completely cracked. Crack is skewed (ends on lateral side of core).	Shrinkage
	44N	3.64	Top	-	0.55	0.55	< 0.4	< 0.4	Crack developed during HVS testing	Fatigue
533FD	38N-Center	5.79	Not sure	Not sure	N/A	N/A	N/A	N/A	Crack all the way through and split the core in 2;couldn't measure crack widths.	Shrinkage
	39	4.03	No crack	No crack	-	-	-	-	Core intact, no cracks	-
	40N-Center	3.65	-	Top	< 0.4	< 0.4	-	-	Fine crack top down. Not completely cracked to bottom	Fatigue
534FD	34N-C	5.91	-	Top	0.55	0.47	N/A	N/A	Crack developed prior to HVS testing, not through to bottom	Shrinkage
	35N-C	3.86	-	Top	0.47	0.47	N/A	N/A	Fine crack top down. Not completely cracked to bottom	Fatigue
	36	3.9	No crack	No crack	-	-	-	-	Core intact, no cracks	-
535FD	31N-C	4.11	-	Top	0.55	0.55	N/A	N/A	Small crack on surface only	Fatigue
	32N C-E	3.71	Bottom	-	0.55	0.4	2.24	2.24	Core separated in two parts longitudinally.	Fatigue
	33N-C	5.35	-	Top	< 0.4	< 0.4	N/A	N/A	Very small crack on surface only	Fatigue

Table 53 Observations from Cores Taken Through Cracks on Section 9

HVS Test	Core Number	Slab Length (m)	Crack Origin for Full Depth Cracks	Crack Origin for Other Cracks	Crack Opening (mm)				Comments	Probable Cause
					Top 1	Top 2	Bottom 1	Bottom 2		
536FD	26N-C	5.81	Top	_	3.15	3.15	0.82	0.82	Core separated in two parts longitudinally.	Shrinkage
537FD	22N-C	5.78	Not sure	Not sure	0.61	0.61	Couldn't be measured		Crack developed prior to HVS testing.	Shrinkage
	23N-W	3.94	_	Top	< 0.4	< 0.4	No	No	Hairline crack on surface	Fatigue
	23N-C	3.94	_	Top	< 0.4	< 0.4	No	No	Hairline crack on surface	Fatigue
538FD	18N-C	5.86	Not sure	Not sure	1.9	1.9	1.1	1.1	Crack developed prior to HVS testing. Core separated in two parts longitudinally.	Shrinkage
	20N-C	3.75	Top		< 0.4	< 0.4	No	No	Hairline crack on surface	Fatigue

Table 54 Observations from Cores Taken Through Cracks on Section 11

HVS Test	Core Number	Slab Length (m)	Crack Origin for Full Depth Cracks	Crack Origin for Other Cracks	Crack Opening (mm)				Comments	Probable Cause
					Top 1	Top 2	Bottom 1	Bottom 2		
539FD	10N	5.86	?	?	1.9	1.9	1.9	1.9	Crack developed prior to HVS testing. Could not detect origin of crack	Shrinkage
	11N-C	3.85	_	Top	< 0.4	< 0.4	No	No	Hairline crack on surface only	Fatigue
	12N-C	3.71	_	Top	< 0.4	< 0.4	No	No	Hairline crack on surface only	Fatigue
540FD	6N	5.86	Top		N/A	N/A	N/A	N/A	Crack developed prior to HVS seting. Core split in 2 parts.	Shrinkage
	7N	3.8	_	Top	0.7	0	No	No	Crack only detected on one face on the upper part of the core. Crack did not propagate to the bottom.	Fatigue
541FD	2N	5.91	Top		1.1	1.1	1.1	1.1	Crack developed prior to HVS testing.	Shrinkage

depending on the position of the load it can originate from either the top or the bottom of the slab.

The following information was recorded through physical investigations of each core as reported in Tables 52–54:

- Core positions in terms of HVS test numbers and slab lengths.
- Crack widths, where available, were measured on both edges of the top (referred to as top 1 and top 2), and the bottom (referred to as bottom 1 and bottom 2) of each core. In the tables, any crack smaller than 0.4 is indicated as < 0.4 due to the limitation of the smallest feeler gauge used in this investigation.
- Attempts were also made to characterize the crack origin (i.e. top-down or bottom-up), and the crack depth (i.e. completely cracked through the 200-mm slab or partially cracked).
- Comments on the appearance and probable cause of each crack.

Through the comparison of Tables 52–54, it is evident that the bigger measurable cracks originated through shrinkage. The cracks with the greatest widths were all outside the influence of HVS testing and appeared prior to any HVS testing. The fatigue cracks due to HVS loading were small in width and in almost all the cases, originated at the surface, and did not propagate through the depth of the 200-mm thick slabs. The fatigue cracks of Section 7 (no dowels and an asphalt shoulder) were bigger than those of Sections 9 and 11 where dowels and tie bars were used.

From the data, it can be concluded that the use of dowels restricted the amount and severity of fatigue cracks in comparison to the HVS sections without dowels.

6.3 Observations and Comments on Day/Night Cores Taken in February 2001

Twelve pairs of cores were extracted from sections on the North Tangent to investigate day/night differences in crack and joint widths. Ten pairs of cores were taken on joints, one of each pair during daytime and one during nighttime on the same joint. The other two pairs were taken on two different cracks, again one during daytime and one during nighttime on the same crack. The following data were collected from these cores:

- Core height (slab thickness);
- Saw-cut depth;
- Saw-cut width, both at the top and bottom of the cut on both sides of the core;
- Crack widths at the bottom of the cores. All cores had cracks between the bottom of the core and the bottom of the saw-cut joints; and
- Where possible, the position of dowel bar.

The data are summarized in Tables 55 and 56. Table 55 contains data collected on the widths of the joints and Table 56 presents the data on the cracks, which connected the bottom of the saw-cut to the bottom of the slab.

In order to do a more meaningful analysis of the differences between the values measured during the day versus those measured at night, it is important to record the surface and in-depth temperature at time of data collection. Unfortunately this was not possible. Nighttime coring was performed between 03:00 and 07:00 hours and daytime coring between 13:00 and 17:00 hours. Coring was conducted during the first week in October 2001. Surface temperatures were however recorded together with FWD testing, which was conducted during that same week.

The surface temperature recorded during the daytime with the FWD was around 5ºC and –2ºC during the night. The total surface temperature change was therefore 7 degrees.

Table 55 Saw-cut and Core Height Statistics, Day/Night Cores

Daytime Data Collection							
	Core Height (mm)	**Saw-cut depth (mm)**	**Saw-cut width (mm)**				
			Top		**Bottom**		
			Side 1	**Side 2**	**Side 1**	**Side 2**	**Average**
Average	221.3	68.6	4.9	4.9	4.5	4.4	4.7
Low	212.0	67.0	4.4	4.4	4.1	4.0	
High	256.0	69.0	5.6	5.8	5.3	4.9	
Std. Dev.	12.1	0.8	0.4	0.4	0.4	0.3	
50th percentile	216.5	69.0	4.9	4.8	4.5	4.3	
90th percentile	229.5	69.0	5.2	5.3	4.8	4.8	
10th percentile	213.2	67.0	4.5	4.5	4.2	4.1	
Nighttime Data Collection							
	Core Height (mm)	**Saw-cut depth (mm)**	**Saw-cut width (mm)**				
			Top		**Bottom**		
			Side 1	**Side 2**	**Side 1**	**Side 2**	**Average**
Average	219.6	68.8	5.5	5.5	4.8	4.8	5.1
Low	203.0	66.0	4.8	4.5	4.3	4.3	
High	235.0	70.0	6.5	6.5	5.4	5.4	
Std. Dev.	9.3	1.1	0.4	0.6	0.3	0.4	
50th percentile	218.0	69.0	5.5	5.6	4.7	4.8	
90th percentile	232.0	69.2	5.8	6.2	5.1	5.2	
10th percentile	210.0	68.4	5.1	5.0	4.4	4.4	

6.3.1 Day/Night Measurements of Cores at Joints

The saw-cut depths from all the cores were very consistent with an average depth of around 69 mm, which relates to a percentage depth of about 31 per cent. The data is summarized in Table 55.

No significant differences between widths of the top and the bottom of the saw-cut joints were detected.

From the statistics for ten pairs of cores shown in Table 55, there seems to be a slight increase in the saw cut openings (< 0.5 mm) during the night. This applies to measurements both

Table 56 Day/Night Crack Widths at Bottom of Cores Drilled through Joints on the North Tangent

Section	Core Number	Crack Width (at Bottom of Core) (mm)			
		Daytime Cores		Nighttime Cores	
		Bottom 1	Bottom 2	Bottom 1	Bottom 2
Section 11: Dowels, Asphalt Shoulder, Widened (4.26-m) Truck Lane	3N/4N DAY	0.61	0.61		
	4N/5N NIGHT			<0.4	<0.4
	5N/6N DAY	0.90	0.90		
	5N/6N NIGHT			<0.4	<0.4
	6N/7N DAY	0.47	0.47		
	6N/7N NIGHT			<0.4	<0.4
	7N/8N DAY	0.61	0.61		
	7N/8N NIGHT			0.40	0.40
	8N/9N DAY	<0.4	<0.4		
	8N/9N NIGHT			<0.4	<0.4
Section 9: Dowels and Tied Concrete Shoulder	17N/18N DAY	<0.4	<0.4		
	17N/18N NIGHT			<0.4	<0.4
	18N/19N DAY	0.47	0.47		
	18N/19N NIGHT			<0.4	<0.4
	19N/20N DAY	0.61	0.61		
	19N/20N NIGHT			<0.4	<0.4
	20N/21N DAY	<0.4	<0.4		
	20N/21N NIGHT			<0.4	<0.4
	21N/22N DAY	<0.4	<0.4		
	21N/22N NIGHT			<0.4	<0.4

at the top and bottom of the saw-cut and is probably due to the concrete expansion and contraction under the influence of the 7ºC surface temperature change.

6.3.2 Day/Night Measurements of Cracks through Joints

Ten pairs of day/night measurements of crack widths are shown in Table 56.

There seems to be a small decrease in the crack widths at nighttime compared to the crack widths measured during the day. Unfortunately, 0.4 mm was the smallest feeler gauge size and all cracks smaller than 0.4 mm was recorded as < 0.4 mm.

Daytime measurements varies from < 0.4 mm to 0.90 mm while nighttime crack widths were all < 0.5 mm. These differences are small and given the variation in the results of the manual measuring method it is concluded that no significant differences between the crack widths could be detected. What is more important is the comparison of the joint crack widths of the North Tangent with those of the South Tangent. Table 57 presents the data from cores taken from the South Tangent.

Table 57 Day/Night Crack Widths at Bottom of Cores Drilled through Joints on the South Tangent

	Crack Width (at Bottom of Core) (mm)			
	Daytime Cores		**Nighttime Cores**	
Core Number	**Bottom 1**	**Bottom 2**	**Bottom 1**	**Bottom 2**
32S/33S DAY	1.10	1.10		
32S/33S NIGHT			0.55	0.55
33S/34S DAY	0.94	0.94		
33S/34S NIGHT			1.10	0.94
34S/35S DAY	1.40	1.40		
34S/35S NIGHT			0.70	0.70
35S/36S DAY	0.70	0.70		
35S/36S NIGHT			0.70	0.70
36S/37S DAY	1.60	1.60		
36S/37S NIGHT			0.82	0.82
37S/38S DAY	0.90	0.90		
37S/38S NIGHT			0.70	0.70
Average	*1.11*		*0.75*	

The total average of the crack widths from all the daytime and nighttime cores is 0.9 mm. This is higher than those recorded on the north tangent where almost all the crack widths are less than 0.4 mm. This is probably due to the use of the dowel bars, which restricted the degree of horizontal slab separation. On the South Tangent, no dowel bars were installed, which caused the cracks at each joint to be more open. Sections 9 and 11 on the north tangent were constructed with dowel bars. The negative influences of bigger crack widths are twofold:

- The saw-cut joints act as collection channels for water and once the cracks below the saw-cut joints are big enough, water will penetrate into the subbase. Due to the dynamic influences of traffic, this will cause pumping that will erode the subbase and voids will form all along the edge under the slab at the joints. This loss of support from the subbase finally leads to joint faulting.
- Aggregate interlock provides a vital function in transferring loads from one slab to another. Smaller crack widths under saw-cut joints lead to a higher degree of aggregate interlock and, therefore, a higher degree of load transfer.

6.3.3 Day/Night Measurements of Normal Surface Cracks

Two pairs of cores were taken on cracks not related to HVS testing. The data is summarized in Table 58.

Table 58 Day/Night Crack Widths from Cores Drilled on Cracks on the South Tangent

	Crack Width (at Bottom of Core) (mm)			
	Daytime Cores		Nighttime Cores	
Core Number	Bottom 1	Bottom 2	Bottom 1	Bottom 2
5N CRACK DAY	1.40	0.70		
5N CRACK NIGHT			1.90	1.10
21N CRACK DAY	2.22	1.10		
21N CRACK NIGHT			2.65	N/A

The first core taken on a crack had a daytime crack width of 1.4 mm at the surface of the slab and 0.7 mm at the bottom, which increased to 1.9 mm and 1.1 mm respectively at night. The second core had a crack width on the surface of 2.2 mm (daytime) and 2.6 mm (nighttime).

This data set is too small to draw any broad conclusions but it is obvious that the crack widths are significantly larger than the bottom (cracked portion) of the saw-cut joints. The differences in the various measurements probably are from slab expansion and contraction under the influences of day/night temperature variations.

A second observation is that the crack widths at the surface appear to be bigger than those found at the bottom of the slab. This suggests a top-down mode of crack growth and is probably the result of temperature fluctuations and concrete shrinkage.

6.3.4 Dowel Bar Placement Measurements

Only 5 of the cores drilled through joints had dowel bars in them. Although this sample set is too small for general conclusions, the results were documented to verify:

- whether the dowels were placed perfectly horizontally, and
- the placement depth of the dowels.

The data is summarized in Table 59.

Table 59 Dowel Bar Placement Statistics

Core Number	Dowel Bar Depths (mm)		True Measured Slab Thickness (mm)	Percent Deviation from Ideal Mid-depth Placement
	Side 1	Side 2		
7N/8N DAY	102	103	215	4.2
17N/18N DAY	116	116	222	-4.5
18N/19N NIGHT	111	113	215	-5.1
20N/21N NIGHT	107	107	216	0.9
21N/22N DAY	117	118	220	-7.3

The dowels visible in the cores were measured at both faces of the cores and distances were recorded from the bottom of the core to the center point of the dowel. All dowels placed on the North Tangent were 38 mm in diameter.

From Table 59 it is clear that all dowels found inside the cores were all placed very close to perfectly horizontal (compare the results from columns 2 and 3 in Table 59). Only one core, 18N/29N, had a change in measurement of 2 mm, which is not substantial given that the steel bar diameter is 38 mm.

The second important observation is that of the in-depth placement. The design of the dowel bars required that they should be placed at mid-depth, on the neutral axis of the concrete slabs. The design thickness of the slabs on the North Tangent was 200 mm, which means that the dowels should have been placed 100 mm from the bottom. The true slab thicknesses did, however, deviate from the design thickness and the as built data is displayed in Table 59. It is clear that the objective of placing the dowels at mid-depth was successfully met. In most cases the deviation from the target was less than 5 percent.

It must be noted that given that more than 300 dowels were placed on the North Tangent, a sample size of 5 is not sufficient to make general conclusions. The results from this study, nevertheless, suggest that the design requirements were successfully met in terms of dowel orientation and placement inside the concrete slabs.

7.0 DISCUSSION OF HVS TEST RESULTS AND CONCLUSIONS

The principal indicator of the slab behavior under HVS trafficking has been monitoring of slab elastic and plastic movements with JDMDs situated on either side of slab joints and at slab midspan edges. The term "deflection" has been used consistently throughout for these measurements, which is an accurate and readily understood description. However, it is important to clarify that these deflections should not be confused with pavement deflections as commonly used in structural evaluations derived usually from a deflection beam (Benkelman beam type equipment) or a Falling Weight Deflectometer (FWD). The deflections obtained from these devices are based on change in radius of curvature for a particular section between the unloaded to loaded case during the test, which is primarily governed by the stiffness (modulus value) of the uppermost layers.

PCC pavement slabs have by far the highest stiffness of any paving material and would therefore normally have the lowest deflections. Values of 0.1 mm or less (under standard test loadings) would be expected, even with development of microcracking (provided no major discontinuity such as significant cracking, or presence of a joint, makes the reading unrepresentative).

The deflection measurements made during HVS testing of the concrete slabs at the Palmdale HVS test site can be regarded as absolute indications of movement of the particular test point from its datum level. As evident from the preceding discussion of the various tests, the deflection changes recorded by the JDMDs were usually far greater than 0.1 mm.

The movement variations measured during these tests were influenced by the continuous shape-changes of the slabs due to temperature and moisture differentials (upward and downward curling), differential shrinkage, and the condition of the slab (cracked or intact, dowels or plain

jointed). These movements are most amplified at the corners and near the slab edges and will therefore contribute to various degrees to the movement under load.

Interpretation of the results is, therefore, complicated on two counts. First, without any trafficking and no test load, the measuring instruments would measure movement variation due to environmental influences. Although steps were taken to minimize the effects of temperature with the use of a temperature controlled chamber during some tests, the data suggests that a high degree of correlation existed between temperature variations outside the temperature box and the responses measured inside the box. Second, in order to isolate the effects of loading on various pavement structures (like plain jointed or doweled concrete sections) the loading regime should ideally be kept the same in all cases (Sections 7, 9, and 11). Unfortunately, because of the differences in the various test plans it is not possible to directly compare behavior of the various structures.

In this chapter, brief summaries and concluding remarks are given and it should be seen in the light of the above-mentioned limitations.

7.1 Deflection Profiles

Figures 181 to 183 give the JDMD deflection results for Sections 7, 9, and 11, respectively. The results for each test on a particular section are all plotted to the same vertical and horizontal scales for ease of comparison. In order to evaluate the additional damage caused by the loading, all JDMD readings displayed in the graphs are relative to the initial reading, taken just prior to HVS trafficking (called the N10 reading), and shown on a vertical scale of +/– 2 mm. The horizontal scale represents 500,000 HVS wheel-load repetitions in each case. Tests

534FD (Section 7), 536FD (Section 9) and 540FD (Section 11) each have greater trafficking history but this scale allows realistic comparison.

The sign convention used in all figures is that movement in the positive (upward) direction represents increasing deflections (or downward movement of the concrete surface) relative to what was measured at the start of the test (N10).

From studying the raw data presented in Chapter 4, it is clear that deflection variations caused by daily and seasonal temperature changes in almost all the cases masked the deflections caused by repetitive loading. The data indicate that lower surface temperatures (and negative temperature differentials) are associated with high deflection measurements and visa versa. An inversely proportional relationship could be found between surface temperature, the temperature difference between the top and the bottom of the PCC layer, and the deflections measured.

This behavior is in agreement with what is expected to happen: during the night (low surface temperatures), the slabs were warmer at the bottom than the top, causing the slabs to curl upwards and slab lift-off from the base layers occurred. Deflection measurements taken during these times were high due to the loss in support from the substructure. During the day, the slabs were warmer at the top than the bottom, resulting in downward curling of the slabs and low deflections. For cases in which the temperature control box was used, it is clear that heat and cold migration from the exposed areas affected the behavior inside the box where deflection measurements were recorded (*7*). From these observations it is clear that the temperature control box was not sufficiently large enough to isolate the effects caused by temperature variations. It seems as if a box at least the size of 3 slabs would be required to achieve this goal.

The following three subchapters summarizes main conclusions drawn from Figures 181 to 183 where the incremental changes with respect to the first (N10) readings are compared

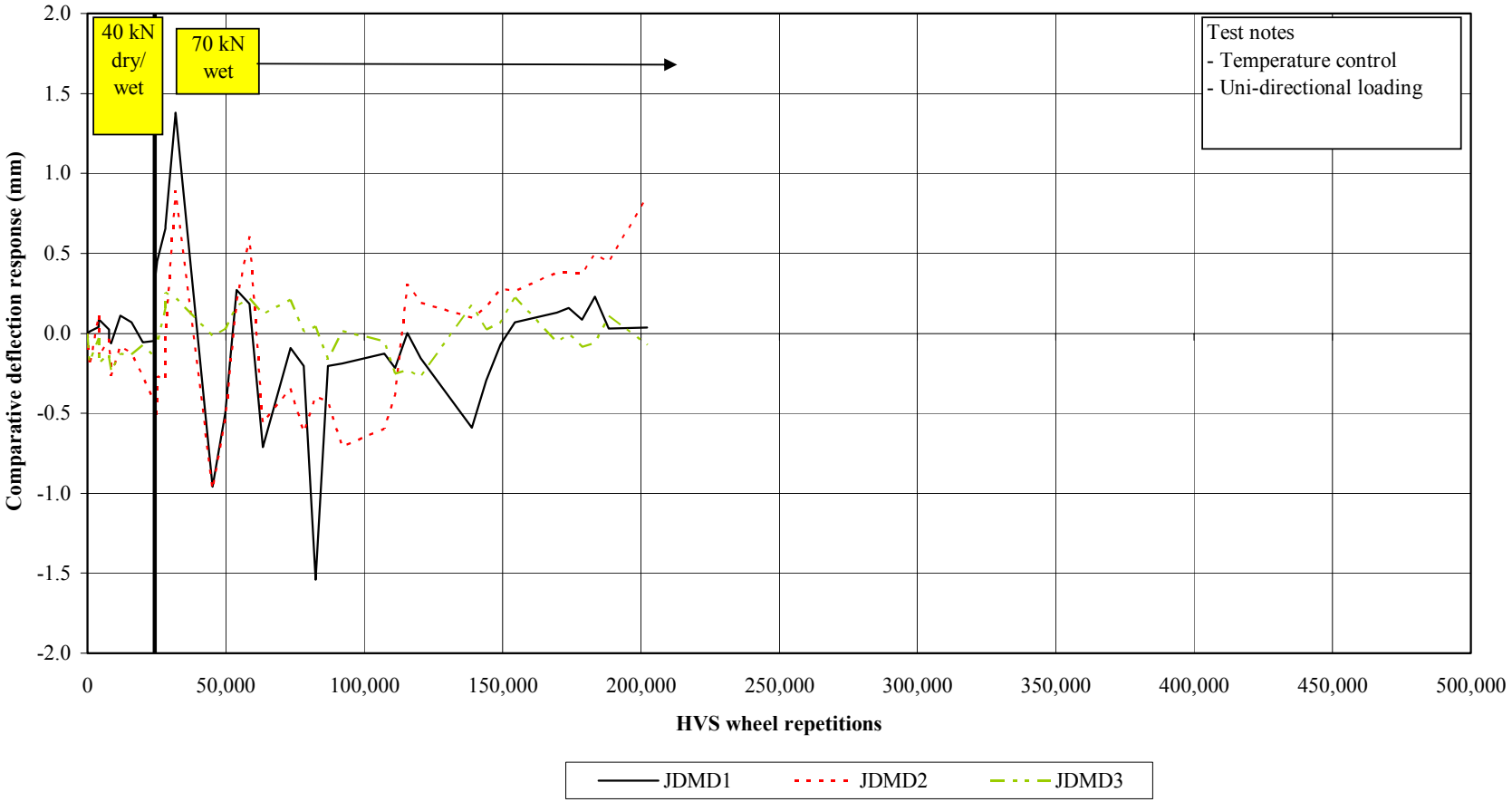

Figure 181a. Variation in deflection with respect to N10, Section 7 (no dowels or tie bars, asphalt concrete shoulder), Test 532FD.

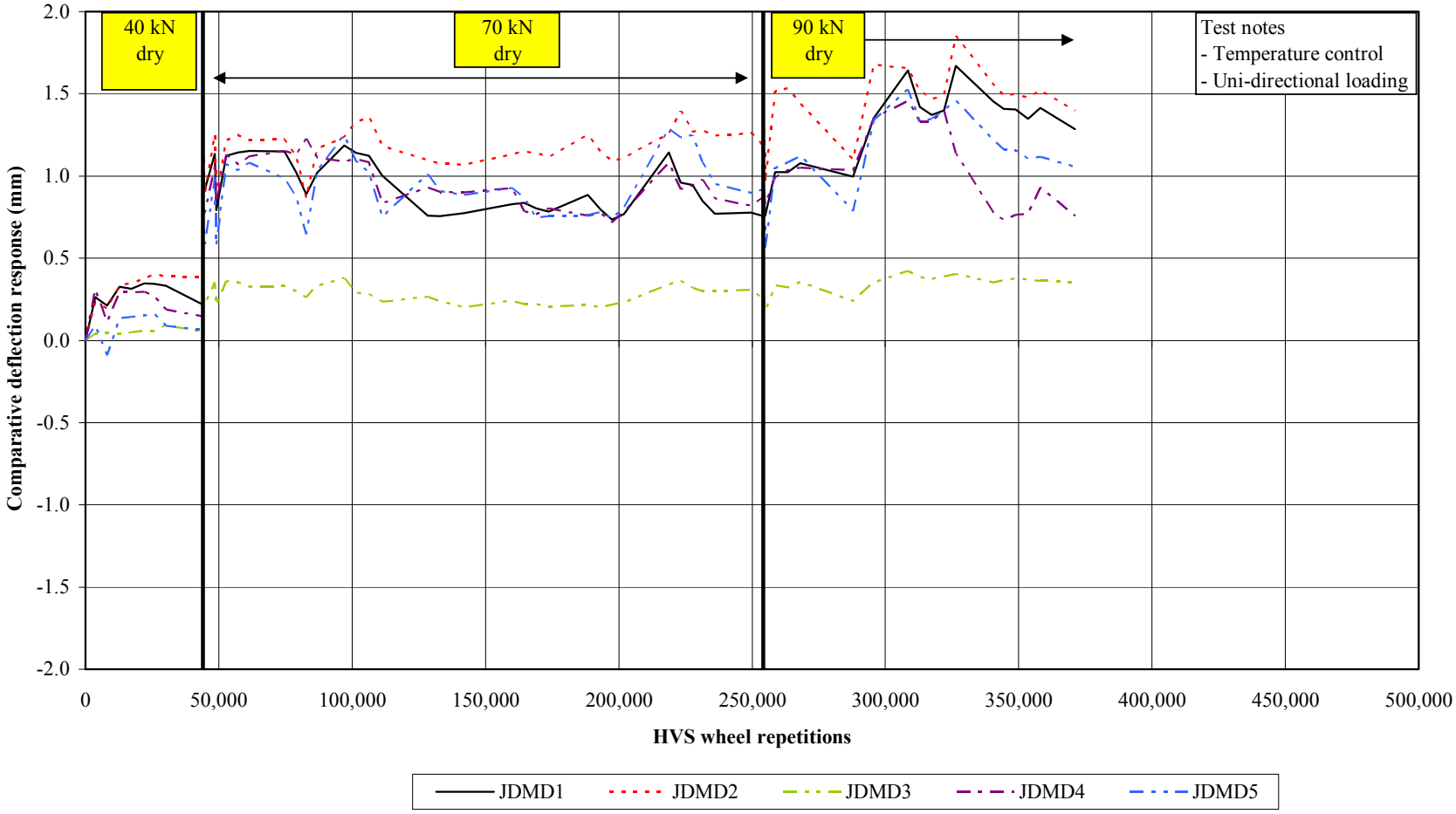

Figure 181b. Variation in deflection with respect to N10, Section 7 (no dowels or tie bars, asphalt concrete shoulder), Test 534FD.

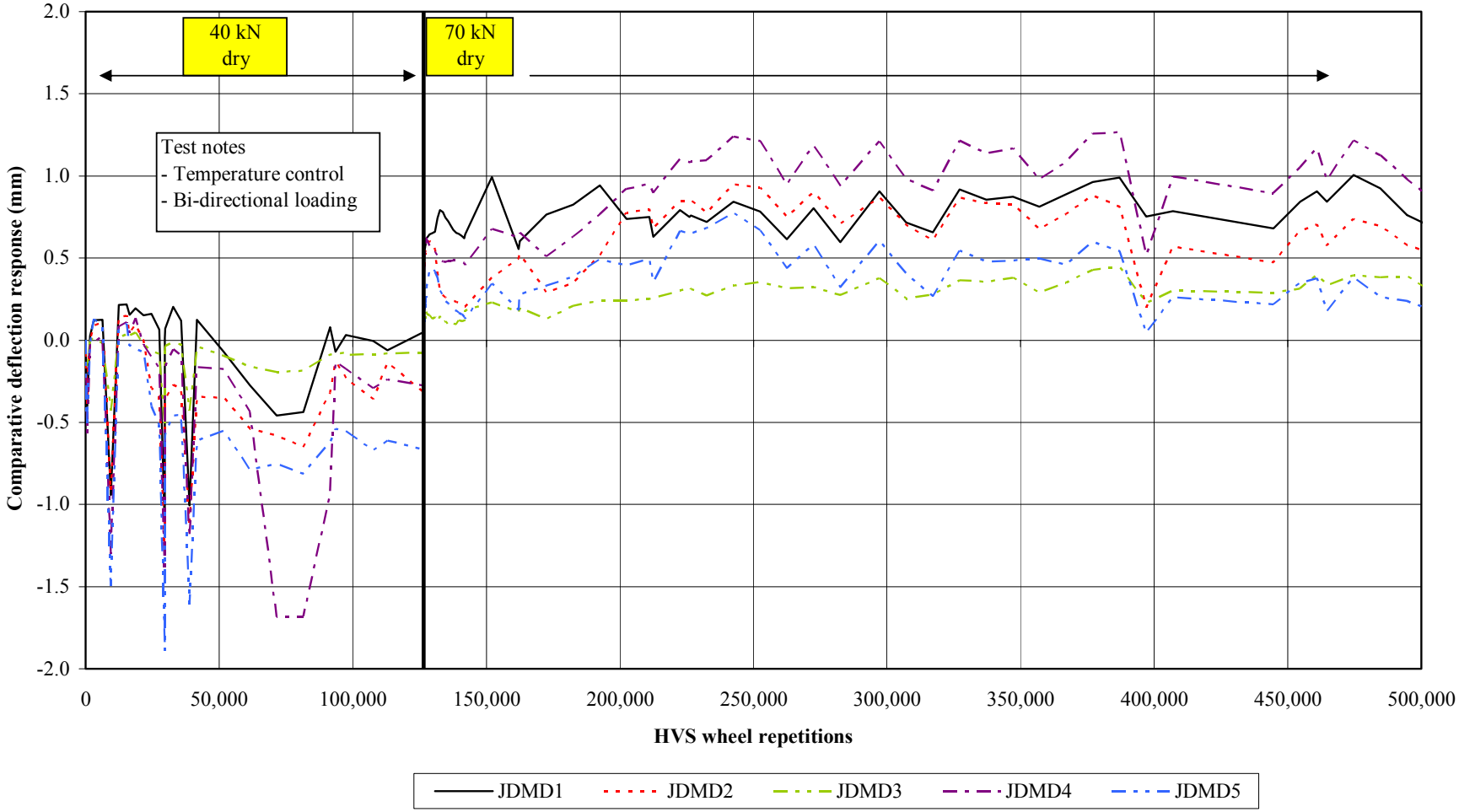

Figure 181c. Variation in deflection with respect to N10, Section 7 (no dowels or tie bars, asphalt concrete shoulder), Test 533FD.

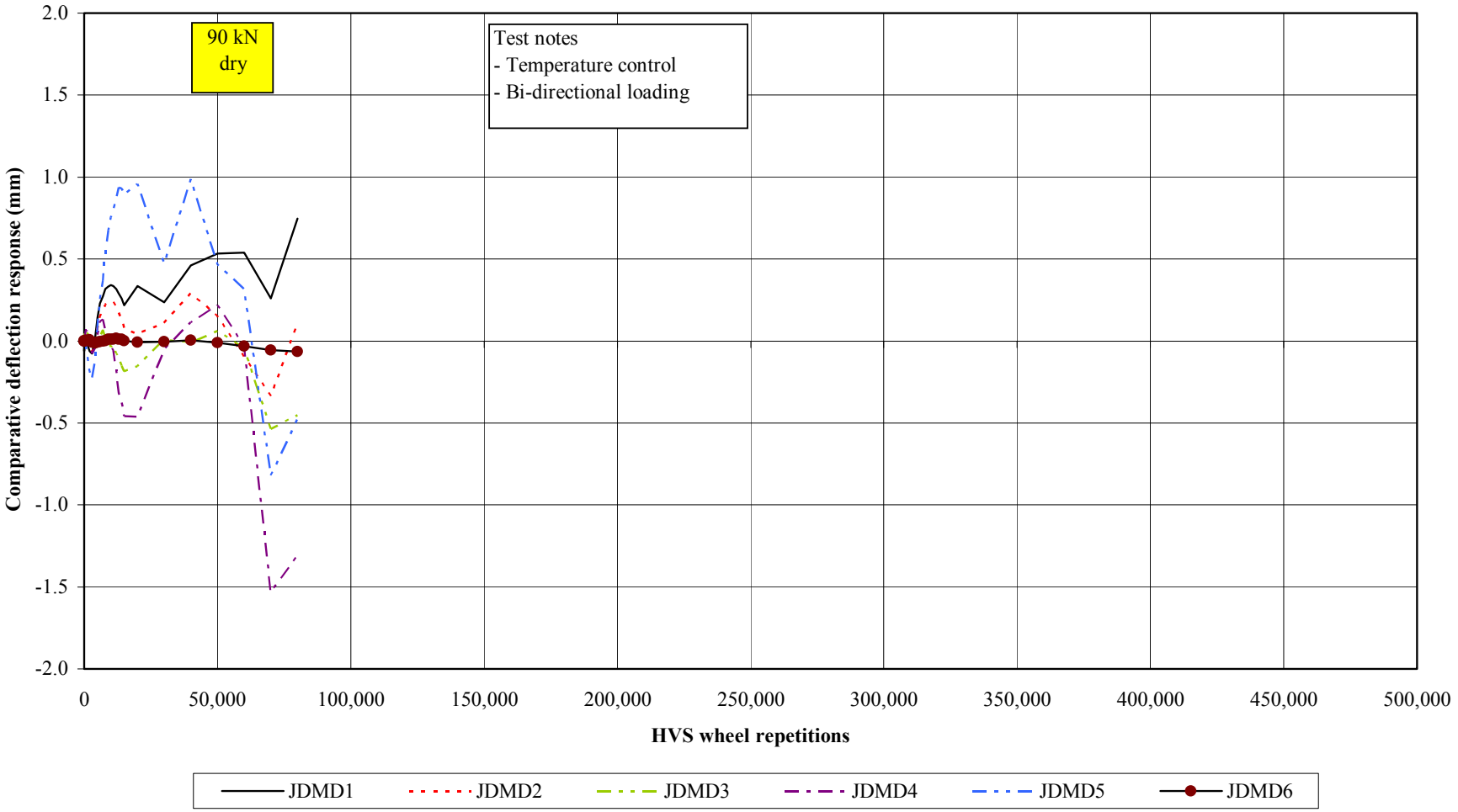

Figure 181d. Variation in deflection with respect to N10, Section 7 (no dowels or tie bars, asphalt concrete shoulder), Test 535FD.

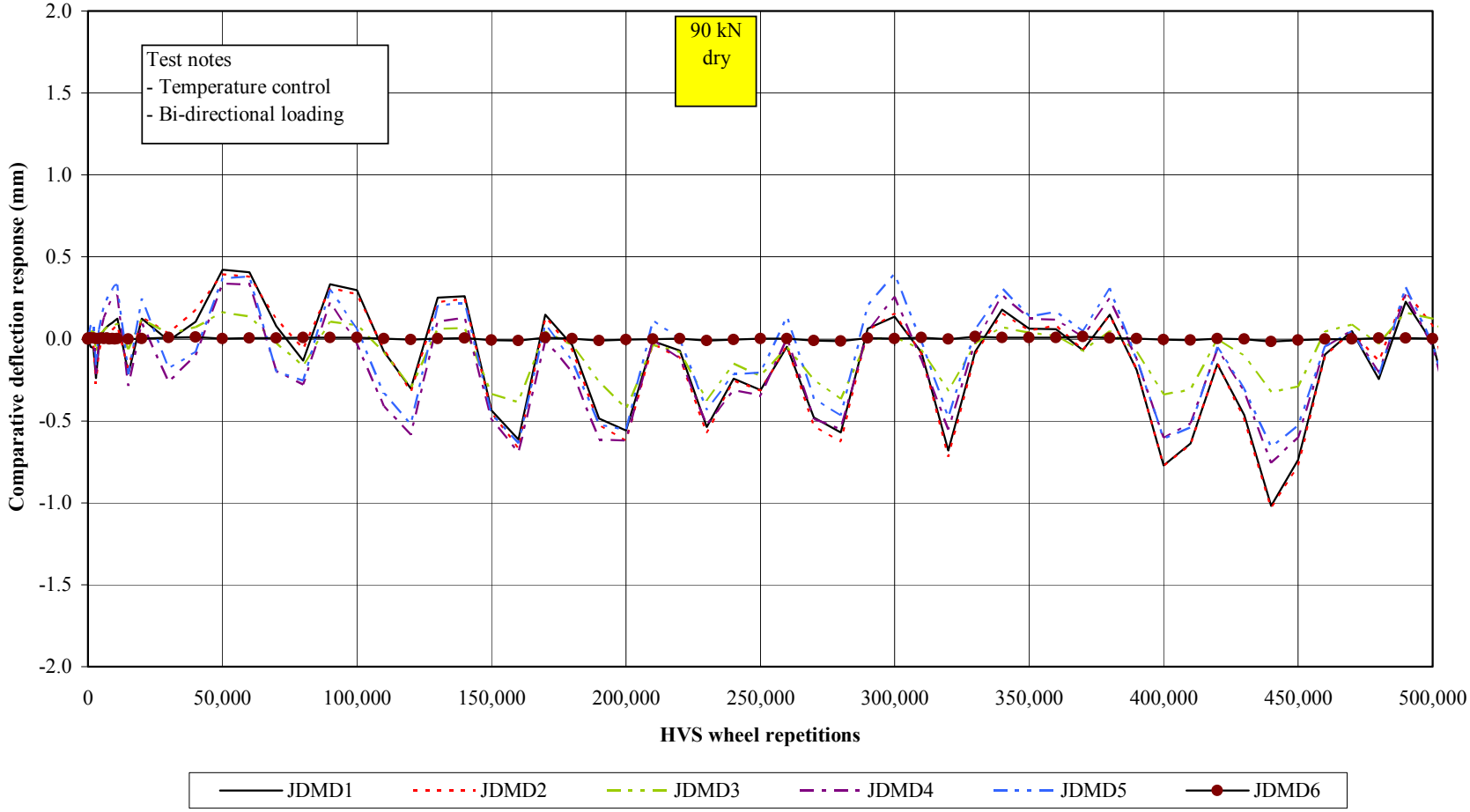

Figure 182a. Variation in deflection with respect to N10, Section 9 (doweled joints and tie bars at concrete shoulder), Test 536FD.

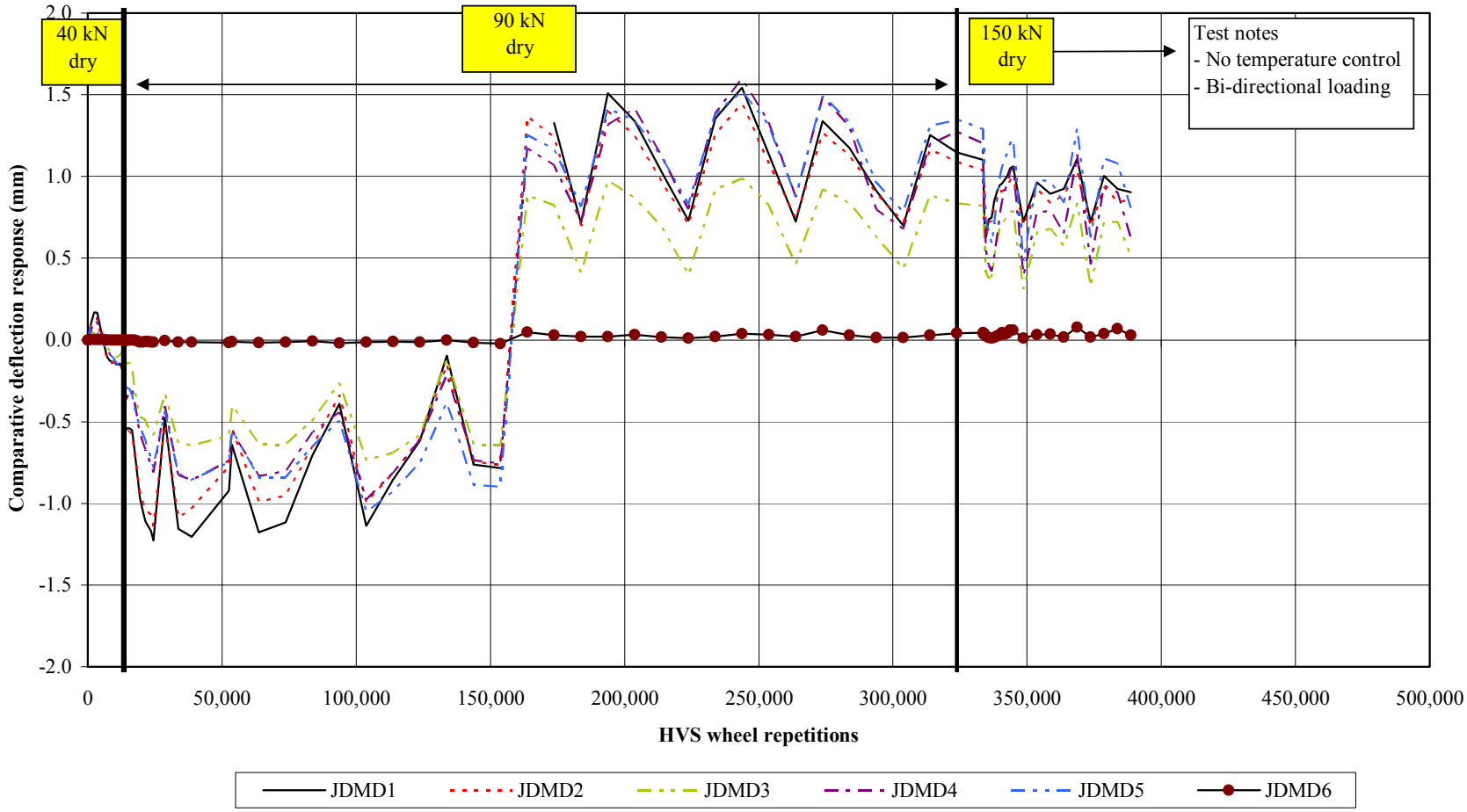

Figure 182b. Variation in deflection with respect to N10, Section 9 (doweled joints and tie bars at concrete shoulder), Test 537FD.

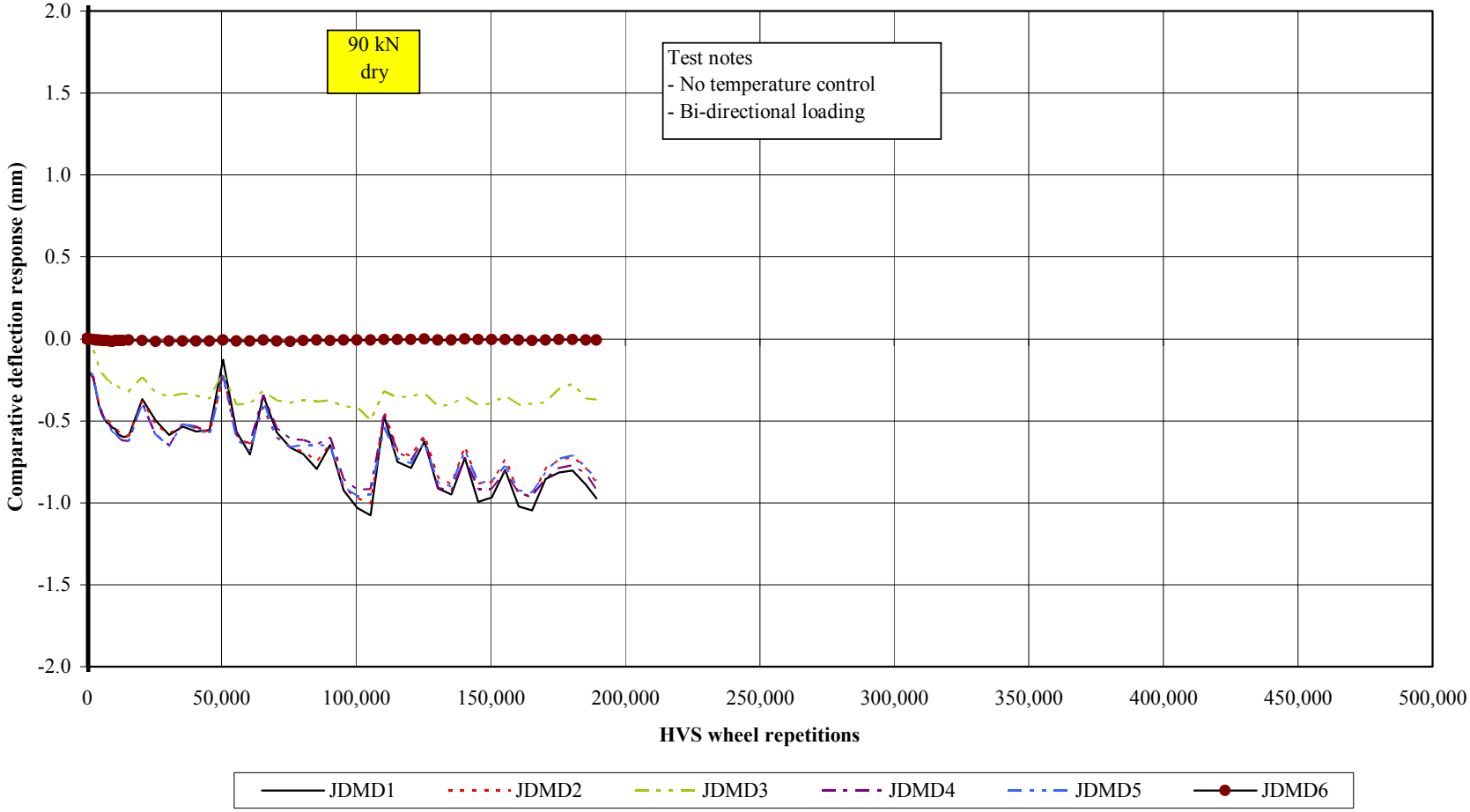

Figure 182c. Variation in deflection with respect to N10, Section 9 (doweled joints and tie bars at concrete shoulder), Test 538FD.

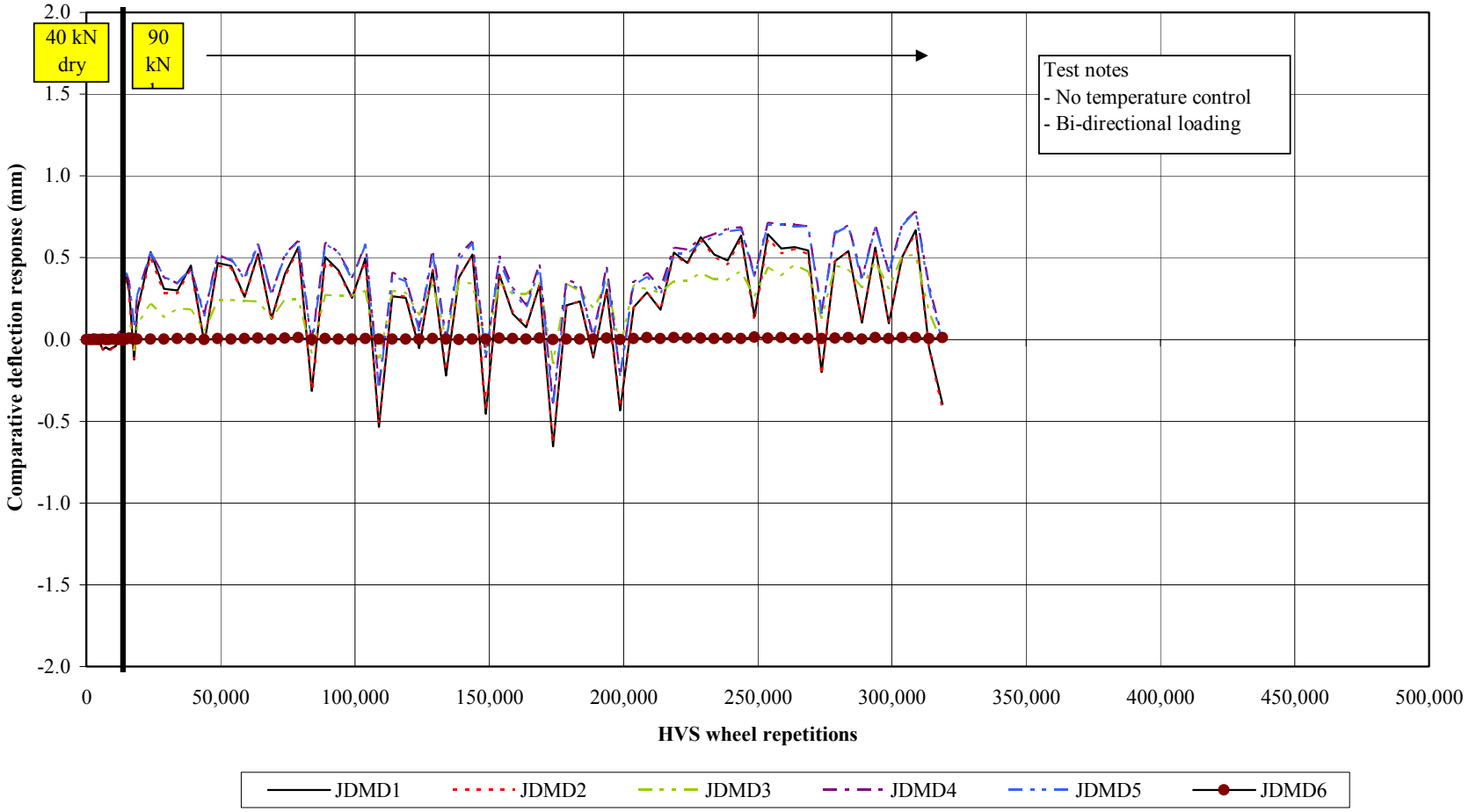

Figure 183a. Variation in deflection with respect to N10, Section 11 (doweled joints with asphalt concrete shoulder and widened truck lane). Test 539FD.

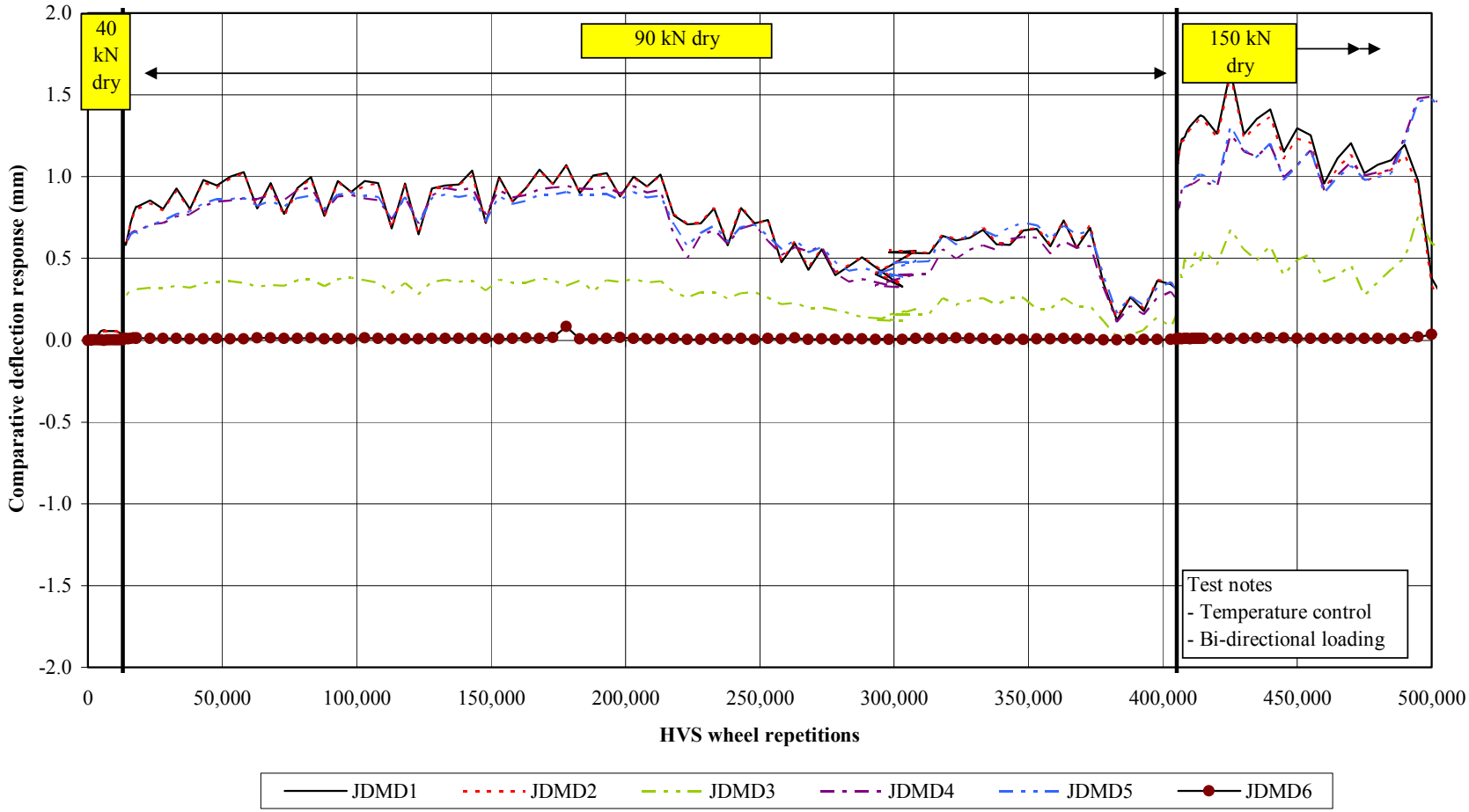

Figure 183b. Variation in deflection with respect to N10, Section 7 (no dowels or tie bars, asphalt concrete shoulder), Test 540FD.

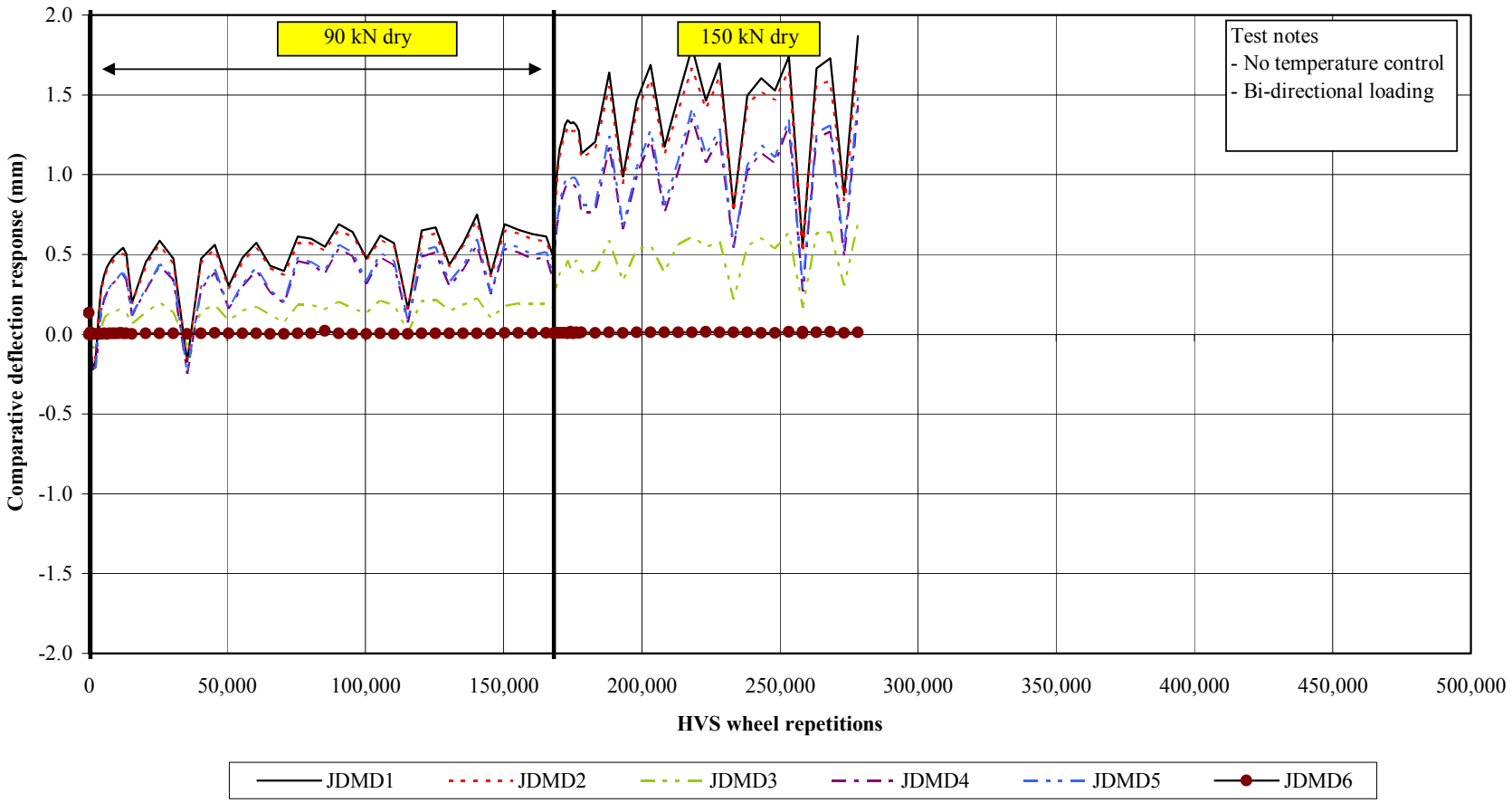

Figure 183c. Variation in deflection with respect to N10, Section 7 (no dowels or tie bars, asphalt concrete shoulder), Test 541FD.

7.1.1 Section 7: No Dowels, No Tie Bars, Asphalt Shoulder (Tests 532–535FD)

Each of the tests was conducted with temperature control so the variations from thermal effects should be minimized. The results, nevertheless, show movements with major variations of up to 2 mm observed over short trafficking periods (Tests 532FD and 534FD in particular, as shown in Figure 181).

It is also evident that the increase in load from 40 to 70 kN (Tests 532FD, 533FD, and 534FD), occurring at the end of the first and start of the second trafficking phase, seemed to give increased movements near the joint of 0.5 mm or more.

In line with this observation, it is assumed that this indicates that the slab sections in each case were neither significantly cracked nor in contact with the support layer at the measurement locations after the first phase of 40-kN loading. The deflection change is therefore considered to be an increased movement caused by the higher 70-kN load, where little or no support is contributed from the underlying layer and substantial movement is attributable to slab curl.

Subsequent deflections during the 70-kN load phase show variations (to varying degrees, with Test 532FD giving most marked variations, and Tests 533FD and 534FD broadly similar) that would be inconsistent with marked cracking and structural deterioration. The variations are attributed to changes in slab curl (and effective support around the measurement position) even within the temperature controlled test regime, for which top surface temperature variation was minimal within the temperature control box.

As mentioned previously, the instrumentation layout representations for these tests (Figures 4–7) shows that the temperature control box did not cover the whole of the three directly affected slabs during each test, and it can only be surmised that the deflection variations

observed will be influenced by the overall temperature regime of the trafficked slabs and possibly even their neighboring slabs.

Even considering only the three directly affected slabs during each test would suggest an extremely complex temperature regime for their top surfaces, and presumably this would indicate a complex and varying temperature gradient within the slabs. In consequence, direct comparisons of deflections for the same test load after different stages of trafficking are difficult because it is highly unlikely that the same slab temperature conditions exist at any stage. The level of variation in measurement values, even for these temperature chamber controlled tests, tends to mask any underlying trends that would be associated with slab deterioration.

The hypothesis of the slab not being in full contact with the base layer has been substantiated by the responses of the MDD measurements. As illustrated by Figures 30 and 36, the MDD module (situated 200 mm deep in the base layer) only recorded significant movement after the formation of a crack in the same slab.

7.1.2 Section 9: Dowels, Tied Concrete Shoulder (Tests 536FD–538FD)

The first of these tests was conducted with temperature control and the other two without. Each was trafficked entirely or predominantly with a 90-kN wheel load using bi-directional trafficking.

From Figure 182, it can be seen that the general level of response variation for all the tests in the 90-kN trafficking phase is broadly similar and in fact slightly lower on the non-temperature controlled Test 536FD. This variation is also distinctly lower than that observed on all the Section 7 temperature controlled tests discussed in Chapter 5.2.2, especially in the case of

Test 536FD. Apart from the obvious effect of increasing loading, the variation from the N10 reading suggests that the dowels had a significant influence in controlling the edge movements.

Table 60 summarizes the deflections recorded at the end of the 90-kN load phase for the various tests. Note that variations in temperature, crack patterns, and loading history make the direct comparison as displayed in Table 60 difficult but, in general, it is obvious that Section 9 (with dowels) was more successful in controlling corner edge deflections than the plain jointed sections without tie bars and dowels.

Table 60 Deflection Comparison: Plain Jointed versus Doweled Sections

Section	Test	Repetitions	90 kN Deflections (mm)			
			JDMD 1	JDMD 2	JDMD 4	JDMD 5
7 (No Dowels)	532FD	202,302	1.76	2.46	N/A	N/A
	533FD	371,149	2.57	2.49	2.40	1.98
	534FD	1,284,360	3.42	2.86	1.97	3.73
	535FD	80,000	2.68	2.20	1.62	2.31
9 (Dowels)	536FD	750,518	0.79	0.71	0.46	0.59
	537FD	323,734	1.15	1.09	1.27	1.35
	538FD	189,382	1.84	1.65	1.54	1.49

As indicated previously, the lack of a common loading history compounds the difficulty of more meaningful comparisons.

In the case of Test 537FD (Figure 182), the displacement in the positive direction represents an increase in deflection at the measurement points (and detected by all gauges) that could be concomitant with distinct crack formation. However, as discussed in Chapter 4.6, this does not correspond with the observed crack formation on the section as detailed in Figure 53. This result is somewhat surprising in the light of the two well-established corner cracks around Joint 23.

The downward trend (decreasing deflection) in Test 538FD can be attributed to some slab deterioration and increased contact with the supporting layer with trafficking. The smaller variation in measurements (compared with the other two tests on Section 9) was also attributed to greater initial support contact (detailed discussion, Chapter 4.7).

7.1.3 Section 11: Dowels, Asphalt Shoulder, Widened (4.26-m) Truck Lane (Tests 539FD–541FD)

These tests were conducted without temperature control and each was trafficked predominantly with a 90-kN wheel load using bi-directional trafficking. In this respect, the tests more closely align with those on Section 9 (Chapter 7.2.3 above).

Many of the observations from the previous test series apply including distinct deflection increases with change in test wheel load, the thermal-influenced measurement patterns, and difference in responses of one test section versus another.

Direct comparison with the behavior of Section 9 (Figure 182 compared with Figure 183) suggests that the peak/trough variations were somewhat less on Section 11, but in terms of the wheel load repetitions they occurred more frequently. This is because of the recording schedule differences between the tests. During Section 11 testing, a higher frequency of data recording was conducted than the frequency of Section 9, which translates to improved characterization of the daily peak/trough variations.

Of the three tests on Section 11, Test 540FD gave smaller variations in deflections and also showed a downward trend (decreasing deflections) from about 200,000 repetitions, compared with the other two tests. As noted for Test 536FD (Section 9), which also exhibited this type of response when compared with the other tests, it suggests that the particular slab(s)

were already in better contact with the support layers (limiting downward deflections) and that deterioration occurred under trafficking to seat the slabs at the measurement points.

7.2 Influence of Main Test Variables

The primary objective of this series of HVS testing was to evaluate the performance of full-scale pavements with the following design features:

- plain aggregate interlock joints (no dowels)
- dowels and tied slabs, and
- widened (4.26-m) truck lanes

under traffic loading with respect to fatigue cracking, corner cracking and joint distress to determine whether they will provide adequate performance.

While much of the preceding discussion has dealt with the difficulties of drawing any fundamental conclusions due to the influence of other essentially unquantified parameters, the following provides some insight into the effect of the abovementioned experimental variables as indicated within these test series. These observations are based only on mainly the monitored deflection responses, since it is considered that these will be the most reliable of any monitoring methods.

7.2.1 Dowels

Section 7 had no dowels, while Sections 9 and 11 included dowels, the latter also having an asphalt shoulder as Section 7 although with a widened (4.26-m) slab. In terms of general responses, slabs with dowels showed what would be expected from greater continuity between

slabs: more uniform (less variable) responses (see Figures 181 and 183 from Sections 7 and 11), and more obvious correlation of cracking across joints.

Dowels also provide greater load transfer efficiency (LTE), as broadly indicated during these tests, although comments on the validity of the evaluation method adopted (particularly regarding the apparent increase in LTE as slabs deteriorate) should be borne in mind.

A clear deterioration of LTE values was observed during the testing of the plain jointed concrete sections (Section 7), especially after the formation of cracks (Figures 16 and 20). Values on the order of 20 to 25 percent were recorded during the post-cracked phase towards the end of the test.

The following brief conclusions are drawn regarding Load Transfer Efficiency of the doweled sections:

- Even after the application of 150-kN loading, no obvious LTE deterioration could be detected (Figures 51, 69 and 82). Values above of well above 80 percent and even above 90 percent were commonly recorded after extensive HVS testing.
- During Tests 537FD, 539FD, and 540FD, significant cracks developed during the testing period (Figures 53, 84, and 91), but no significant drop in LTE values could be detected after the formation of the cracks, which is an indication of the effectiveness of the dowels to transfer load across joints.

7.2.2 Widened (4.26-m) Truck Lane Slabs

As can be inferred from the preceding discussion, the influence of the greater slab width for Section 11 is regarded as likely to be secondary to the influence of either dowels or tied concrete shoulders on pavement performance.

Table 61, an expansion of Table 60, shows the various corner and edge deflections for all tests for the end of the 90-kN test phase.

Table 61 Summary of JDMD Deflections for All Sections, 90-kN Test Load

Section	Test	Repetitions	90 kN Deflections (mm)				
			JDMD 1	JDMD 2	JDMD 3	JDMD 4	JDMD 5
7	532FD	202,302	1.76	2.46	0.59	N/A	N/A
	533FD	371,149	2.57	2.49	0.81	2.40	1.98
	534FD	1,284,360	3.42	2.86	1.39	1.97	3.73
	535FD	80,000	2.68	2.20	0.60	1.62	2.31
9	536FD	750,518	0.79	0.71	0.39	0.46	0.59
	537FD	323,734	1.15	1.09	0.84	1.27	1.35
	538FD	189,382	1.84	1.65	0.61	1.54	1.49
11	539FD	313,846	0.79*	0.76*	0.40*	1.00*	0.99*
	540FD	405,065	1.09	1.08	0.40	0.75	0.80
	541FD	168,277	1.16	1.11	0.38	0.85	0.87

*data highly variable (see Figure 86)

Note that the same limitations apply to the analysis of Table 61 as those mentioned for Table 60.

Within the test matrix represented by Sections 7, 9 and 11 and with the monitoring regime used, it is difficult to quantify the influence of widened slabs. It is obvious that a significant reduction in corner deflections could be detected comparing Section 11 with 7, and to a lesser extend comparing Section 9 with 11.

The mid-span edge deflection (JDMD 3) reveals that no real difference could be detected for all three sections.

A comparison of the crack patterns reveals the following conclusion: although a direct comparison is difficult due to the different loading regimes per test, it seems as if the formation of corner cracks on the widened lane section took longer time to develop (compare Figure 53 to

Figure 91) than the doweled section, and both Sections 9 and 11 (doweled, and doweled and widened lane) outperform Section 7, the un-doweled section.

7.3 General Conclusions

A number of shortcomings in the program applied during this series of tests have been identified that impact the ability to make direct comparisons between the responses of the various slab structures on the North Tangent.

The definition and calculation of LTE should be reviewed. It seems that the present definition and calculation will return values of 100 percent if uniform deterioration takes place on each side of a given joint, implying similar changes in deflection responses, but not necessarily identifying joint deterioration per se.

The influence of temperature variations on the elastic response of concrete pavements is clearly highlighted in this series of tests. Results show that deflection variations caused by daily temperature fluctuations are as extensive as the damaging effect of repetitive loading.

In any further field work on concrete pavements in which the significant influence of thermal effects is seen throughout the tests, it must be recognized that use of the HVS temperature box is probably not merited. Changing the surface temperature of a relatively small area within the total area of influence complicates the thermal regime. This is distinctly different from the case of field testing of asphalt pavement structures, where the area of influence of temperature is much more localized and can be controlled with the temperature chamber.

The field study, nevertheless, illustrates the advantages of dowels and tie bars in restricting relative movement between joints, preventing joint faulting and ultimately prolonging pavement life.

8.0 REFERENCES

1. University of California Berkeley, Dynatest Consulting Inc., and CSIR, Division of Roads and Transport Technology. *Test Plan for CAL/APT Goal LLPRS-Rigid Phase III*. Test Plan prepared for California Department of Transportation. April 1998. Palmdale Construction Report

2. du Plessis, L., D. Bush, F. Jooste, D. Hung, C. Scheffy, J. Roesler, L Popescu, J. T. Harvey. *HVS Test Results on Fast-Setting Hydraulic Cement Concrete, Palmdale, California Test Sections, South Tangent.* Draft report prepared for the California Department of Transportation. Pavement Research Center, Institute of Transportation Studies, University of California, Berkeley. July 2002.

3. Lea, J. and L. Popescu. *The Design and Implementation of the Pavement Research Center Heavy Vehicle Simulator Database.* Draft report prepared for the California Department of Transportation. Pavement Research Center, Institute of Transportation Studies, University of California. February 2003.

4. Harvey, J. T., A. Ali, D. Hung, J. Uhlmeyer, L Popescu, D. Bush, K Grote, J. Lea, C. Scheffy. *Construction and Test Results from Dowel Bar Retrofit HVS Test Sections 553FD, 554FD and 555FD: US 101, Ukiah, Mendocino County*. Draft report prepared for the California Department of Transportation. Pavement Research Center, Institute of Transportation Studies, University of California. February 2003.

5. Dynatest Consulting, Inc. ELMOD Version 3.0 1988, Version 4.0 1999, Ojai, California.

6. du Plessis, L. and J. T. Harvey. *Environmental Influences on the Curling of Concrete Slabs at the Palmdale HVS Test Site.* Draft report prepared for the California Department of Transportation. Pavement Research Center, Institute of Transportation Studies, University of California. June 2003.

9.0 APPENDIX A: STRIPMAPS SHOWING FWD DEFLECTIONS

The graphics in this appendix show the FWD deflections measured at several times after construction, and at different offset positions from the slab centreline. Each graphic, or "stripmap," shows the section layout (i.e., construction type), slab layout, and HVS test sections, in conjunction with the main FWD parameters and surface temperature at the time of recording.

Some data strips show summary statistics for the FWD parameters for each construction type. These strips have titles ending with "Statistics" or "Stats." The statistics shown in these data strips contain the 15^{th} percentile value, the mean, and the 85^{th} percentile value for the construction section, in the following format:

15^{th} percentile – (Mean) – 85^{th} percentile

Thus a value of 78-(80)-84 indicates that for the section under consideration, the 15^{th} percentile value was 78, the mean was 80, and the 85^{th} percentile was 84. The units for these numbers are the same was that of the stripmap immediately above the statistics data strip.

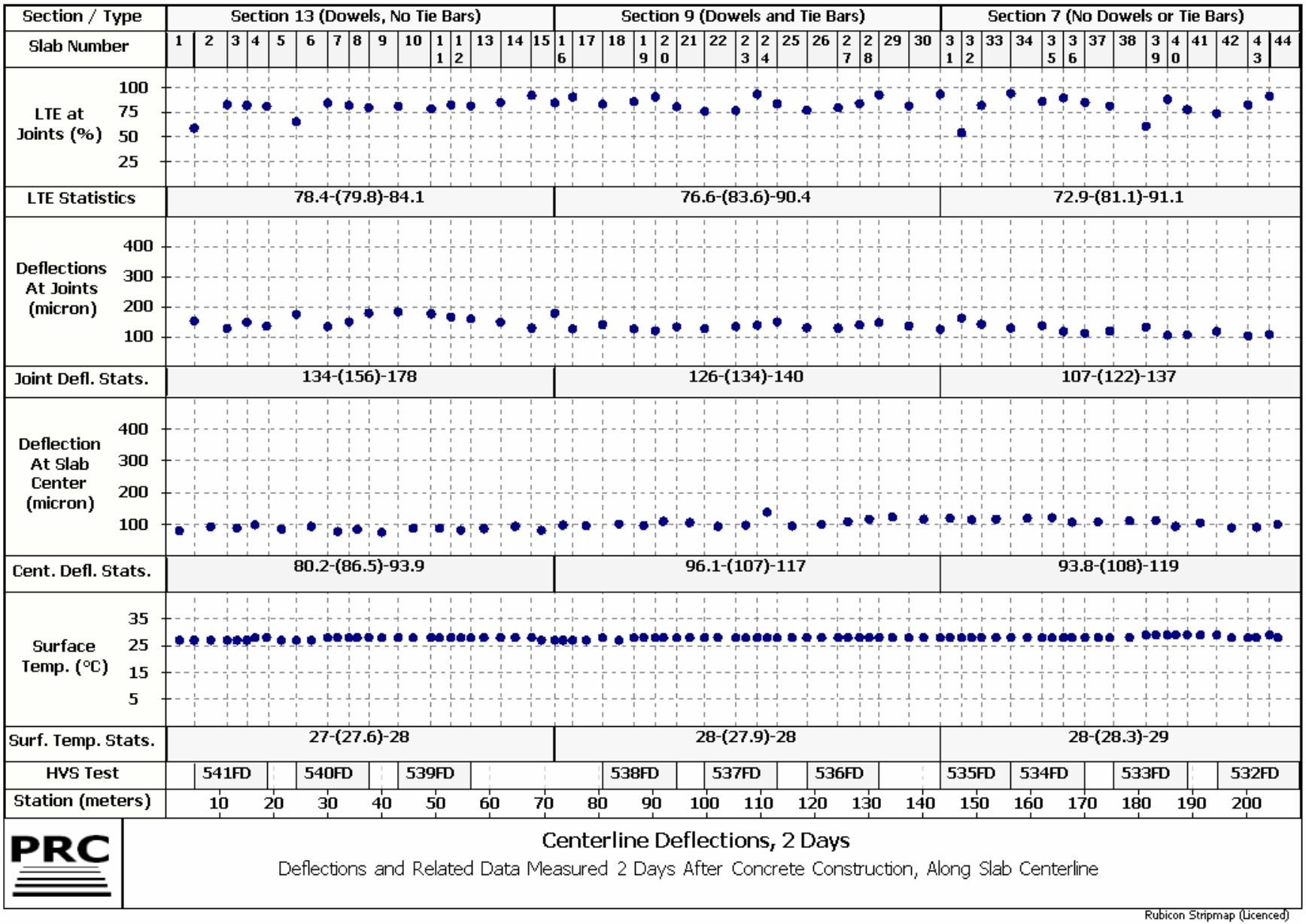
Section / Type
Section 13 (Dowels, No Tie Bars)
Section 9 (Dowels and Tie Bars)
Section 7 (No Dowels or Tie Bars)
Slab Number
1 2 3 4 5 6 7 8 9 10 11 12 13 14 15 16 17 18 19 20 21 22 23 24 25 26 27 28 29 30 31 32 33 34 35 36 37 38 39 40 41 42 43 44
LTE at Joints (%)
100
75
50
25
LTE Statistics
78.4-(79.8)-84.1
76.6-(83.6)-90.4
72.9-(81.1)-91.1
Deflections At Joints (micron)
400
300
200
100
Joint Defl. Stats.
134-(156)-178
126-(134)-140
107-(122)-137
Deflection At Slab Center (micron)
400
300
200
100
Cent. Defl. Stats.
80.2-(86.5)-93.9
96.1-(107)-117
93.8-(108)-119
Surface Temp. (°C)
35
25
15
5
Surf. Temp. Stats.
27-(27.6)-28
28-(27.9)-28
28-(28.3)-29
HVS Test
541FD
540FD
539FD
538FD
537FD
536FD
535FD
534FD
533FD
532FD
Station (meters)
10 20 30 40 50 60 70 80 90 100 110 120 130 140 150 160 170 180 190 200
PRC
Centerline Deflections, 2 Days
Deflections and Related Data Measured 2 Days After Concrete Construction, Along Slab Centerline
Rubicon Stripmap (Licenced)

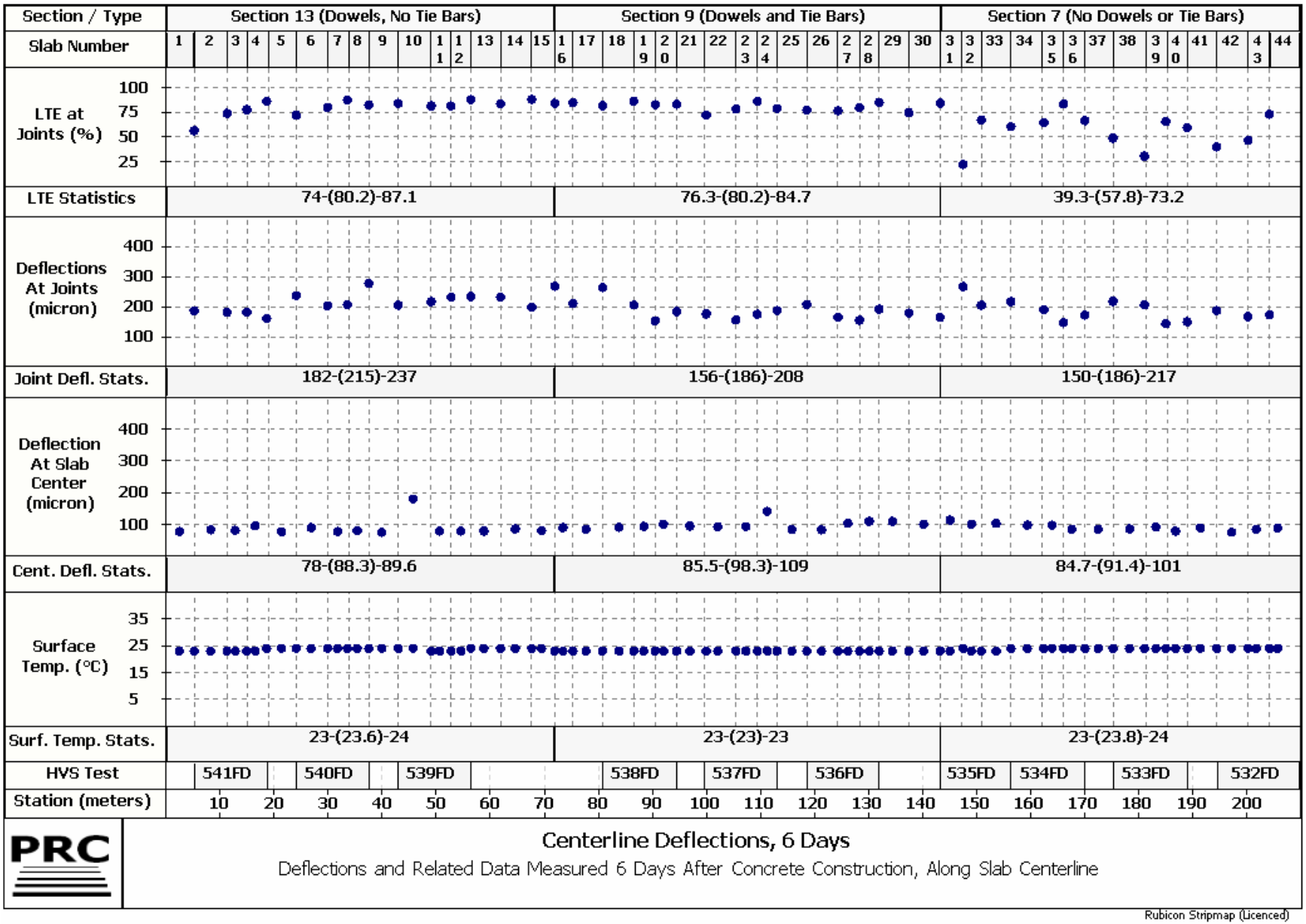
Section / Type
Section 13 (Dowels, No Tie Bars)
Section 9 (Dowels and Tie Bars)
Section 7 (No Dowels or Tie Bars)
Slab Number
1 2 3 4 5 6 7 8 9 10 11 12 13 14 15 16 17 18 19 20 21 22 23 24 25 26 27 28 29 30 31 32 33 34 35 36 37 38 39 40 41 42 43 44
LTE at Joints (%)
100
75
50
25
LTE Statistics
74-(80.2)-87.1
76.3-(80.2)-84.7
39.3-(57.8)-73.2
Deflections At Joints (micron)
400
300
200
100
Joint Defl. Stats.
182-(215)-237
156-(186)-208
150-(186)-217
Deflection At Slab Center (micron)
400
300
200
100
Cent. Defl. Stats.
78-(88.3)-89.6
85.5-(98.3)-109
84.7-(91.4)-101
Surface Temp. (°C)
35
25
15
5
Surf. Temp. Stats.
23-(23.6)-24
23-(23)-23
23-(23.8)-24
HVS Test
541FD
540FD
539FD
538FD
537FD
536FD
535FD
534FD
533FD
532FD
Station (meters)
10 20 30 40 50 60 70 80 90 100 110 120 130 140 150 160 170 180 190 200
PRC
Centerline Deflections, 6 Days
Deflections and Related Data Measured 6 Days After Concrete Construction, Along Slab Centerline
Rubicon Stripmap (Licenced)

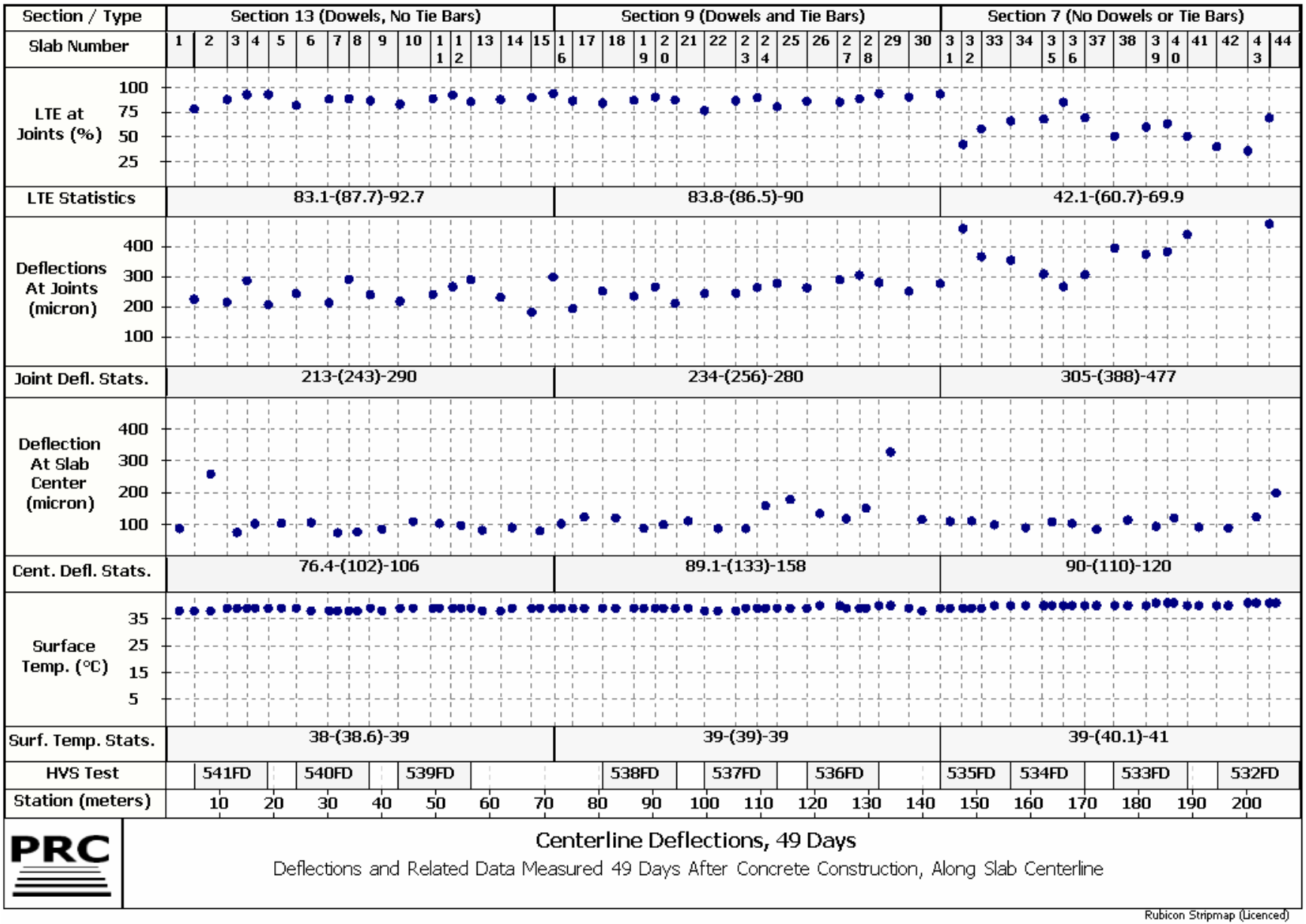
Section / Type
Section 13 (Dowels, No Tie Bars)
Section 9 (Dowels and Tie Bars)
Section 7 (No Dowels or Tie Bars)
Slab Number
1 2 3 4 5 6 7 8 9 10 11 12 13 14 15 16 17 18 19 20 21 22 23 24 25 26 27 28 29 30 31 32 33 34 35 36 37 38 39 40 41 42 43 44
LTE at Joints (%)
100
75
50
25
LTE Statistics
83.1-(87.7)-92.7
83.8-(86.5)-90
42.1-(60.7)-69.9
Deflections At Joints (micron)
400
300
200
100
Joint Defl. Stats.
213-(243)-290
234-(256)-280
305-(388)-477
Deflection At Slab Center (micron)
400
300
200
100
Cent. Defl. Stats.
76.4-(102)-106
89.1-(133)-158
90-(110)-120
Surface Temp. (°C)
35
25
15
5
Surf. Temp. Stats.
38-(38.6)-39
39-(39)-39
39-(40.1)-41
HVS Test
541FD
540FD
539FD
538FD
537FD
536FD
535FD
534FD
533FD
532FD
Station (meters)
10 20 30 40 50 60 70 80 90 100 110 120 130 140 150 160 170 180 190 200
PRC
Centerline Deflections, 49 Days
Deflections and Related Data Measured 49 Days After Concrete Construction, Along Slab Centerline
Rubicon Stripmap (Licenced)

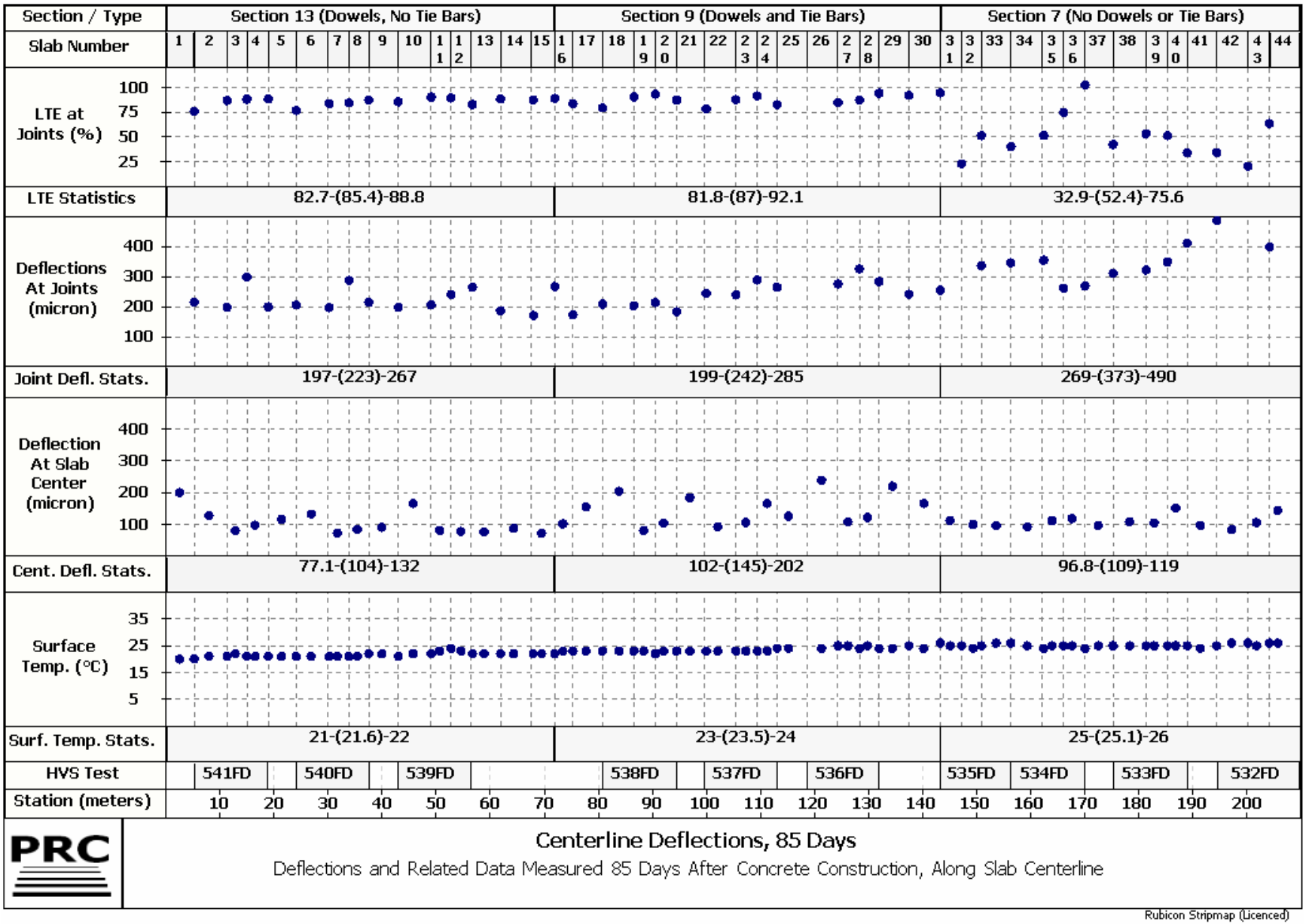

PRC

Centerline Deflections, 85 Days

Deflections and Related Data Measured 85 Days After Concrete Construction, Along Slab Centerline

Rubicon Stripmap (Licenced)

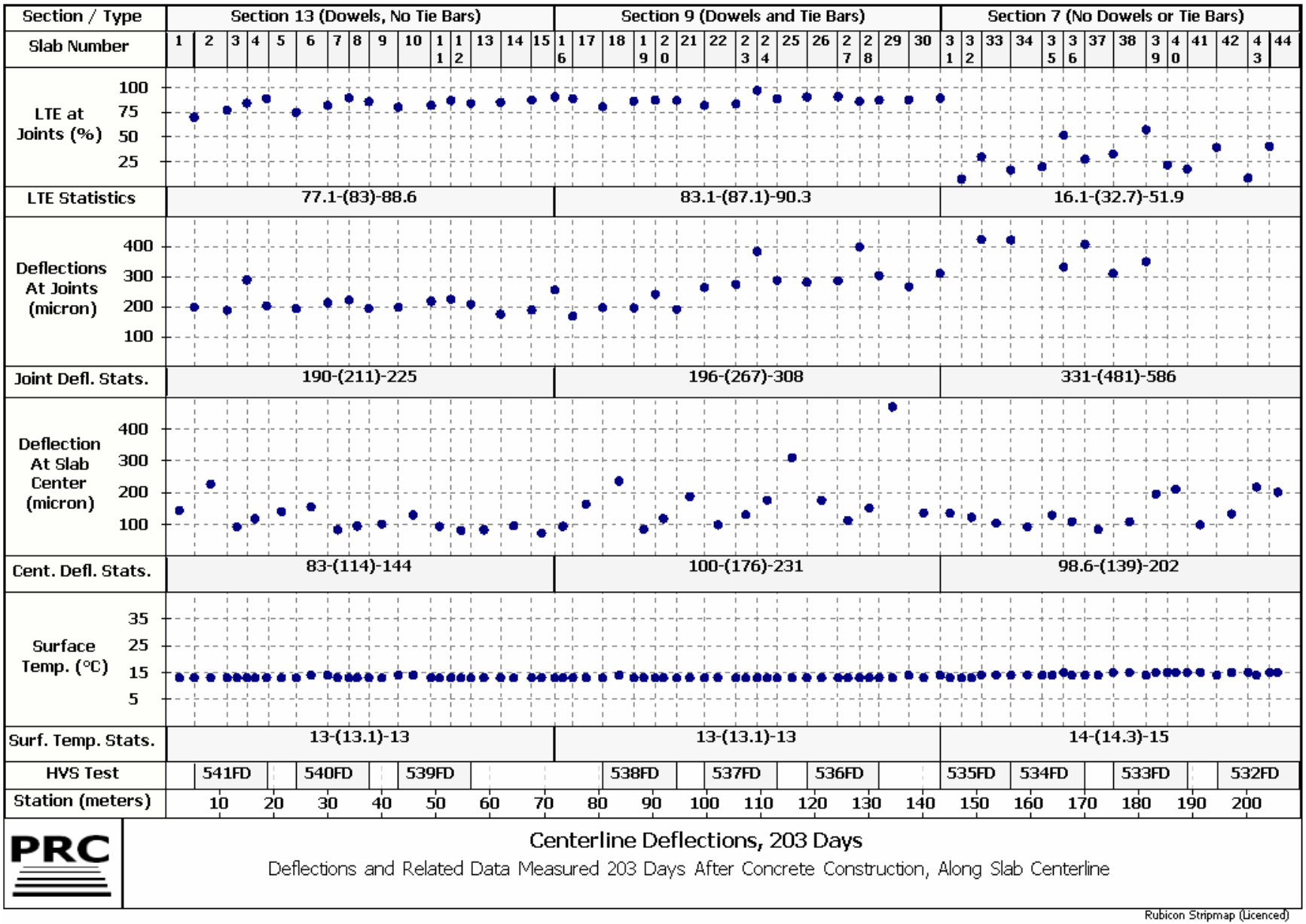
Section / Type
Section 13 (Dowels, No Tie Bars)
Section 9 (Dowels and Tie Bars)
Section 7 (No Dowels or Tie Bars)
Slab Number
1 2 3 4 5 6 7 8 9 10 11 12 13 14 15 16 17 18 19 20 21 22 23 24 25 26 27 28 29 30 31 32 33 34 35 36 37 38 39 40 41 42 43 44
LTE at Joints (%)
100
75
50
25
LTE Statistics
77.1-(83)-88.6
83.1-(87.1)-90.3
16.1-(32.7)-51.9
Deflections At Joints (micron)
400
300
200
100
Joint Defl. Stats.
190-(211)-225
196-(267)-308
331-(481)-586
Deflection At Slab Center (micron)
400
300
200
100
Cent. Defl. Stats.
83-(114)-144
100-(176)-231
98.6-(139)-202
Surface Temp. (°C)
35
25
15
5
Surf. Temp. Stats.
13-(13.1)-13
13-(13.1)-13
14-(14.3)-15
HVS Test
541FD
540FD
539FD
538FD
537FD
536FD
535FD
534FD
533FD
532FD
Station (meters)
10 20 30 40 50 60 70 80 90 100 110 120 130 140 150 160 170 180 190 200
PRC
Centerline Deflections, 203 Days
Deflections and Related Data Measured 203 Days After Concrete Construction, Along Slab Centerline
Rubicon Stripmap (Licenced)

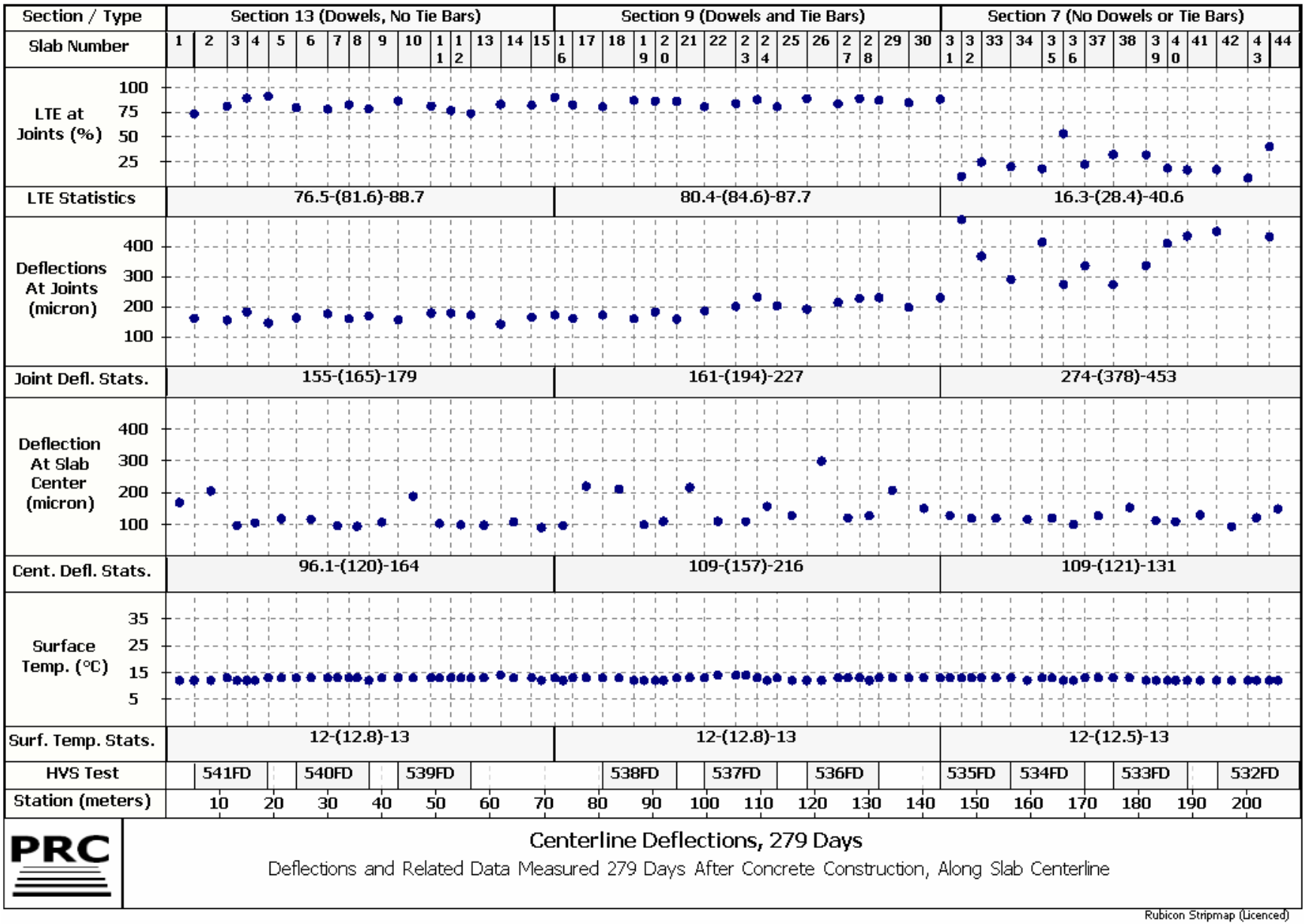
Section / Type
Section 13 (Dowels, No Tie Bars)
Section 9 (Dowels and Tie Bars)
Section 7 (No Dowels or Tie Bars)
Slab Number
1 2 3 4 5 6 7 8 9 10 11 12 13 14 15 16 17 18 19 20 21 22 23 24 25 26 27 28 29 30 31 32 33 34 35 36 37 38 39 40 41 42 43 44
LTE at Joints (%)
100
75
50
25
LTE Statistics
76.5-(81.6)-88.7
80.4-(84.6)-87.7
16.3-(28.4)-40.6
Deflections At Joints (micron)
400
300
200
100
Joint Defl. Stats.
155-(165)-179
161-(194)-227
274-(378)-453
Deflection At Slab Center (micron)
400
300
200
100
Cent. Defl. Stats.
96.1-(120)-164
109-(157)-216
109-(121)-131
Surface Temp. (°C)
35
25
15
5
Surf. Temp. Stats.
12-(12.8)-13
12-(12.8)-13
12-(12.5)-13
HVS Test
541FD
540FD
539FD
538FD
537FD
536FD
535FD
534FD
533FD
532FD
Station (meters)
10 20 30 40 50 60 70 80 90 100 110 120 130 140 150 160 170 180 190 200
PRC
Centerline Deflections, 279 Days
Deflections and Related Data Measured 279 Days After Concrete Construction, Along Slab Centerline
Rubicon Stripmap (Licenced)

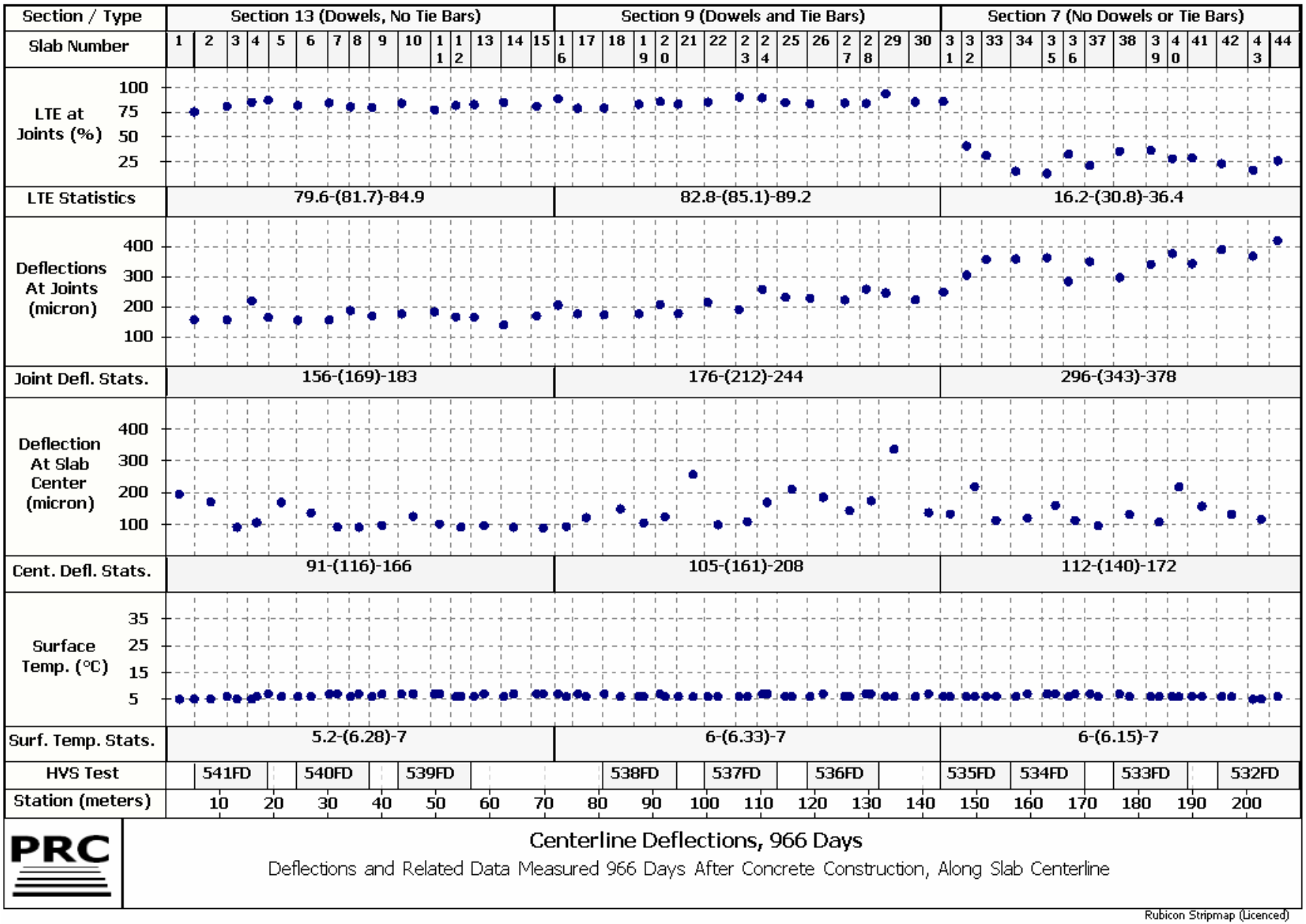
Section / Type
Section 13 (Dowels, No Tie Bars)
Section 9 (Dowels and Tie Bars)
Section 7 (No Dowels or Tie Bars)
Slab Number
1 2 3 4 5 6 7 8 9 10 11 12 13 14 15 16 17 18 19 20 21 22 23 24 25 26 27 28 29 30 31 32 33 34 35 36 37 38 39 40 41 42 43 44
LTE at Joints (%)
100
75
50
25
LTE Statistics
79.6-(81.7)-84.9
82.8-(85.1)-89.2
16.2-(30.8)-36.4
Deflections At Joints (micron)
400
300
200
100
Joint Defl. Stats.
156-(169)-183
176-(212)-244
296-(343)-378
Deflection At Slab Center (micron)
400
300
200
100
Cent. Defl. Stats.
91-(116)-166
105-(161)-208
112-(140)-172
Surface Temp. (°C)
35
25
15
5
Surf. Temp. Stats.
5.2-(6.28)-7
6-(6.33)-7
6-(6.15)-7
HVS Test
541FD
540FD
539FD
538FD
537FD
536FD
535FD
534FD
533FD
532FD
Station (meters)
10 20 30 40 50 60 70 80 90 100 110 120 130 140 150 160 170 180 190 200
PRC
Centerline Deflections, 966 Days
Deflections and Related Data Measured 966 Days After Concrete Construction, Along Slab Centerline
Rubicon Stripmap (Licenced)

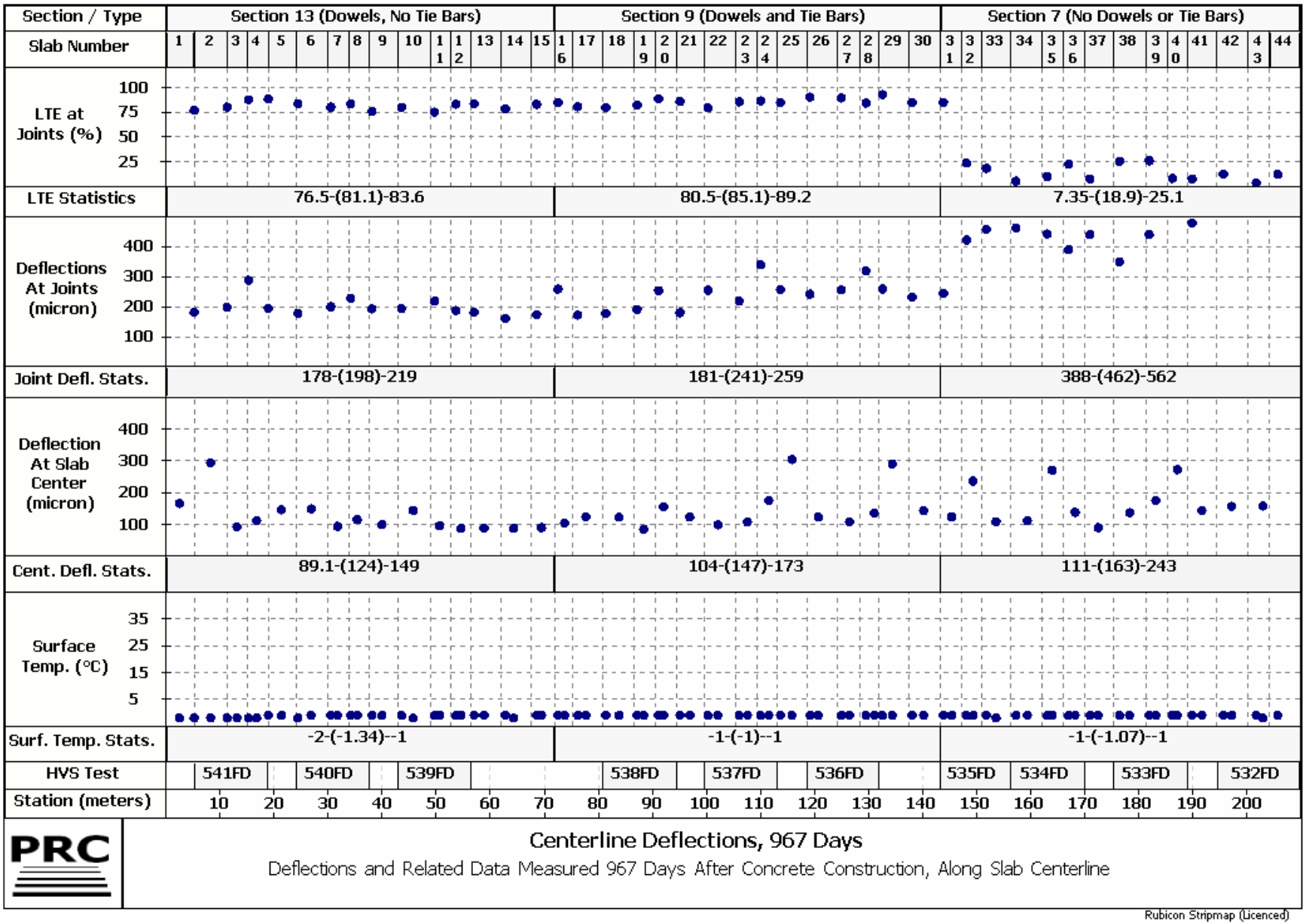
Section / Type
Section 13 (Dowels, No Tie Bars)
Section 9 (Dowels and Tie Bars)
Section 7 (No Dowels or Tie Bars)
Slab Number
1 2 3 4 5 6 7 8 9 10 11 12 13 14 15 16 17 18 19 20 21 22 23 24 25 26 27 28 29 30 31 32 33 34 35 36 37 38 39 40 41 42 43 44
LTE at Joints (%)
100
75
50
25
LTE Statistics
76.5-(81.1)-83.6
80.5-(85.1)-89.2
7.35-(18.9)-25.1
Deflections At Joints (micron)
400
300
200
100
Joint Defl. Stats.
178-(198)-219
181-(241)-259
388-(462)-562
Deflection At Slab Center (micron)
400
300
200
100
Cent. Defl. Stats.
89.1-(124)-149
104-(147)-173
111-(163)-243
Surface Temp. (°C)
35
25
15
5
Surf. Temp. Stats.
-2-(-1.34)--1
-1-(-1)--1
-1-(-1.07)--1
HVS Test
541FD
540FD
539FD
538FD
537FD
536FD
535FD
534FD
533FD
532FD
Station (meters)
10 20 30 40 50 60 70 80 90 100 110 120 130 140 150 160 170 180 190 200
PRC
Centerline Deflections, 967 Days
Deflections and Related Data Measured 967 Days After Concrete Construction, Along Slab Centerline
Rubicon Stripmap (Licenced)

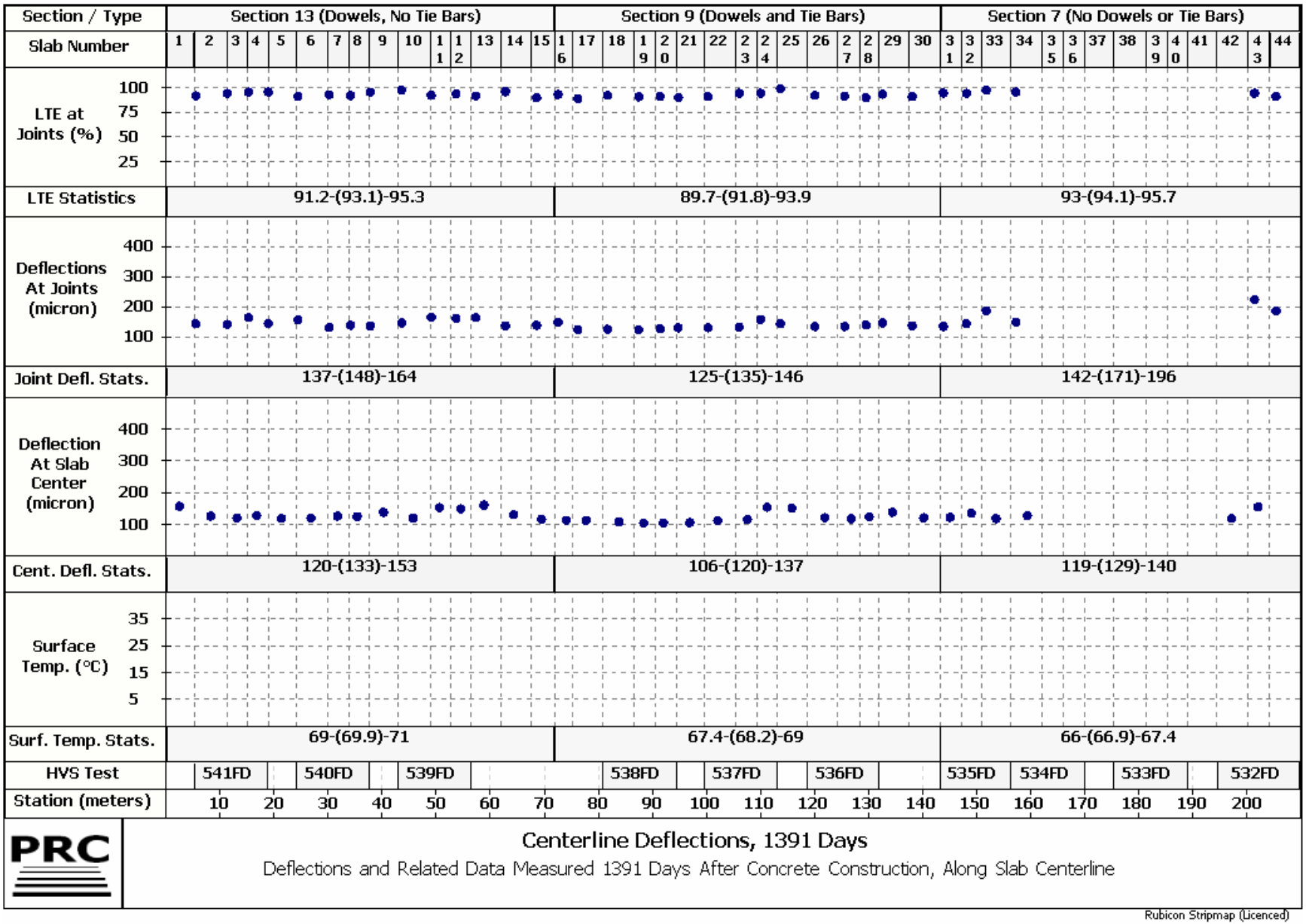
Section / Type
Section 13 (Dowels, No Tie Bars)
Section 9 (Dowels and Tie Bars)
Section 7 (No Dowels or Tie Bars)
Slab Number
1 2 3 4 5 6 7 8 9 10 11 12 13 14 15 16 17 18 19 20 21 22 23 24 25 26 27 28 29 30 31 32 33 34 35 36 37 38 39 40 41 42 43 44
LTE at Joints (%)
100
75
50
25
LTE Statistics
91.2-(93.1)-95.3
89.7-(91.8)-93.9
93-(94.1)-95.7
Deflections At Joints (micron)
400
300
200
100
Joint Defl. Stats.
137-(148)-164
125-(135)-146
142-(171)-196
Deflection At Slab Center (micron)
400
300
200
100
Cent. Defl. Stats.
120-(133)-153
106-(120)-137
119-(129)-140
Surface Temp. (°C)
35
25
15
5
Surf. Temp. Stats.
69-(69.9)-71
67.4-(68.2)-69
66-(66.9)-67.4
HVS Test
541FD
540FD
539FD
538FD
537FD
536FD
535FD
534FD
533FD
532FD
Station (meters)
10 20 30 40 50 60 70 80 90 100 110 120 130 140 150 160 170 180 190 200
PRC
Centerline Deflections, 1391 Days
Deflections and Related Data Measured 1391 Days After Concrete Construction, Along Slab Centerline
Rubicon Stripmap (Licenced)

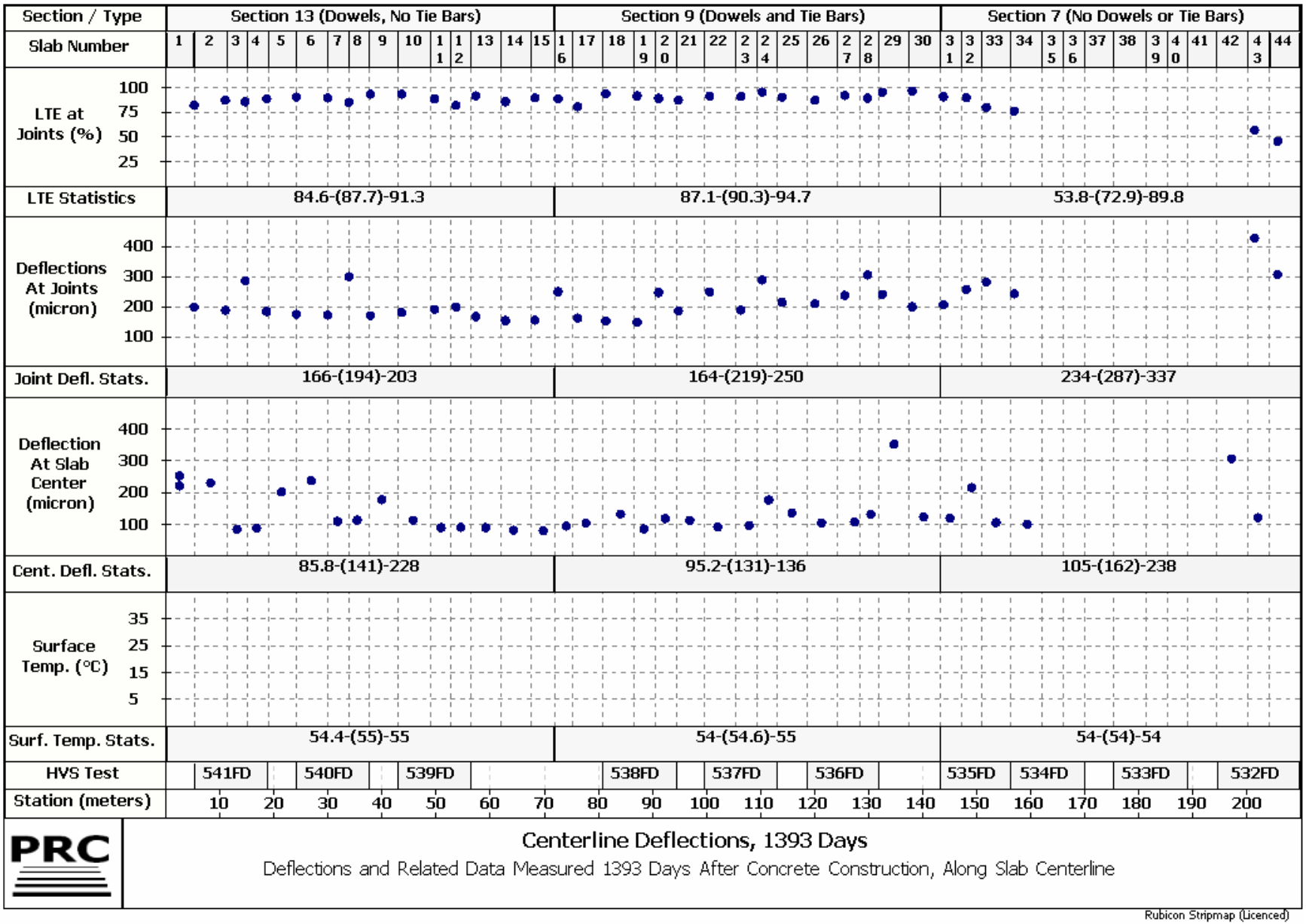
Section / Type
Section 13 (Dowels, No Tie Bars)
Section 9 (Dowels and Tie Bars)
Section 7 (No Dowels or Tie Bars)
Slab Number
1 2 3 4 5 6 7 8 9 10 11 12 13 14 15 16 17 18 19 20 21 22 23 24 25 26 27 28 29 30 31 32 33 34 35 36 37 38 39 40 41 42 43 44
LTE at Joints (%)
100
75
50
25
LTE Statistics
84.6-(87.7)-91.3
87.1-(90.3)-94.7
53.8-(72.9)-89.8
Deflections At Joints (micron)
400
300
200
100
Joint Defl. Stats.
166-(194)-203
164-(219)-250
234-(287)-337
Deflection At Slab Center (micron)
400
300
200
100
Cent. Defl. Stats.
85.8-(141)-228
95.2-(131)-136
105-(162)-238
Surface Temp. (°C)
35
25
15
5
Surf. Temp. Stats.
54.4-(55)-55
54-(54.6)-55
54-(54)-54
HVS Test
541FD
540FD
539FD
538FD
537FD
536FD
535FD
534FD
533FD
532FD
Station (meters)
10 20 30 40 50 60 70 80 90 100 110 120 130 140 150 160 170 180 190 200
PRC
Centerline Deflections, 1393 Days
Deflections and Related Data Measured 1393 Days After Concrete Construction, Along Slab Centerline
Rubicon Stripmap (Licenced)

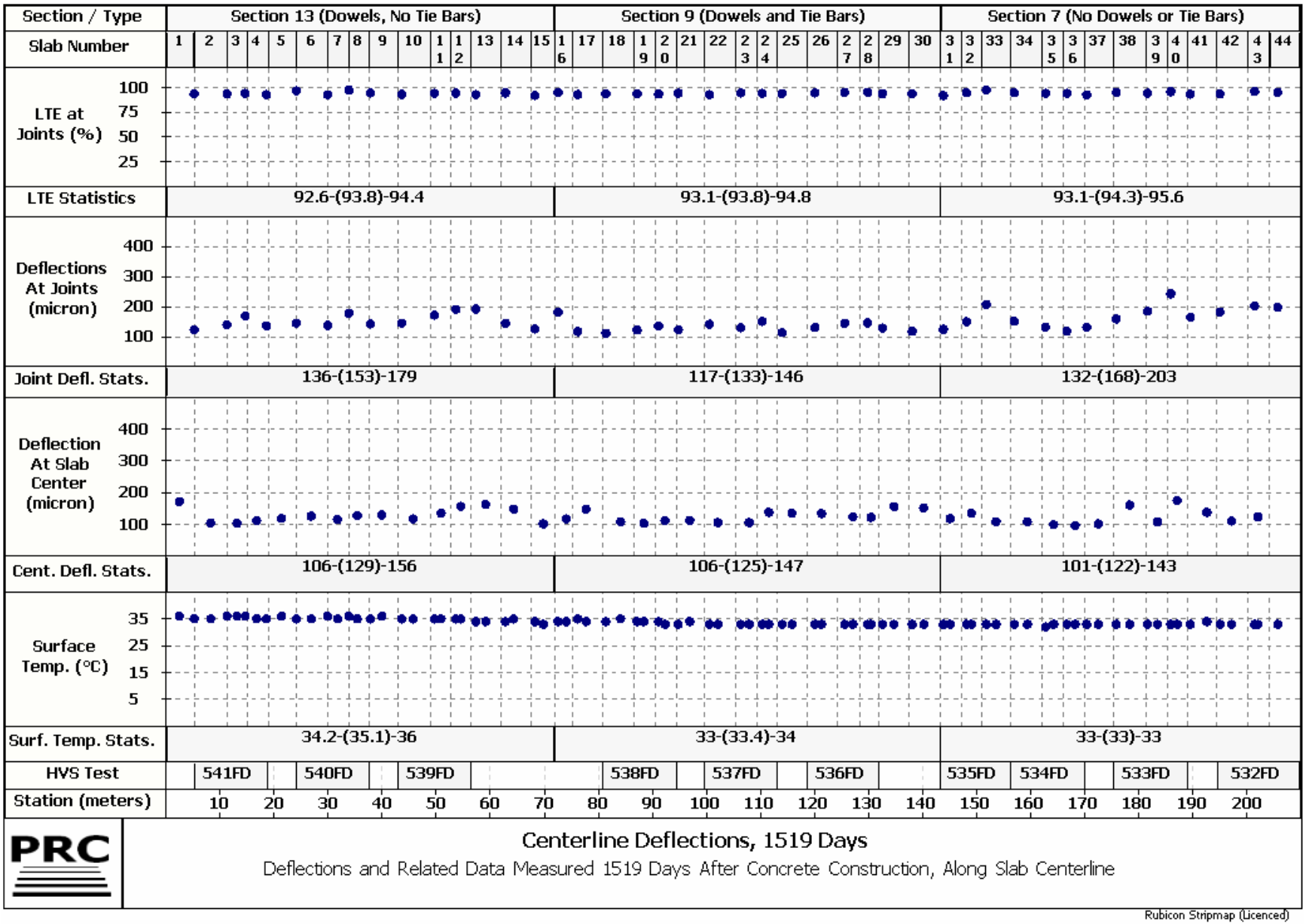
Section / Type
Section 13 (Dowels, No Tie Bars)
Section 9 (Dowels and Tie Bars)
Section 7 (No Dowels or Tie Bars)
Slab Number
1 2 3 4 5 6 7 8 9 10 11 12 13 14 15 16 17 18 19 20 21 22 23 24 25 26 27 28 29 30 31 32 33 34 35 36 37 38 39 40 41 42 43 44
LTE at Joints (%)
100
75
50
25
LTE Statistics
92.6-(93.8)-94.4
93.1-(93.8)-94.8
93.1-(94.3)-95.6
Deflections At Joints (micron)
400
300
200
100
Joint Defl. Stats.
136-(153)-179
117-(133)-146
132-(168)-203
Deflection At Slab Center (micron)
400
300
200
100
Cent. Defl. Stats.
106-(129)-156
106-(125)-147
101-(122)-143
Surface Temp. (°C)
35
25
15
5
Surf. Temp. Stats.
34.2-(35.1)-36
33-(33.4)-34
33-(33)-33
HVS Test
541FD
540FD
539FD
538FD
537FD
536FD
535FD
534FD
533FD
532FD
Station (meters)
10 20 30 40 50 60 70 80 90 100 110 120 130 140 150 160 170 180 190 200
PRC
Centerline Deflections, 1519 Days
Deflections and Related Data Measured 1519 Days After Concrete Construction, Along Slab Centerline
Rubicon Stripmap (Licenced)

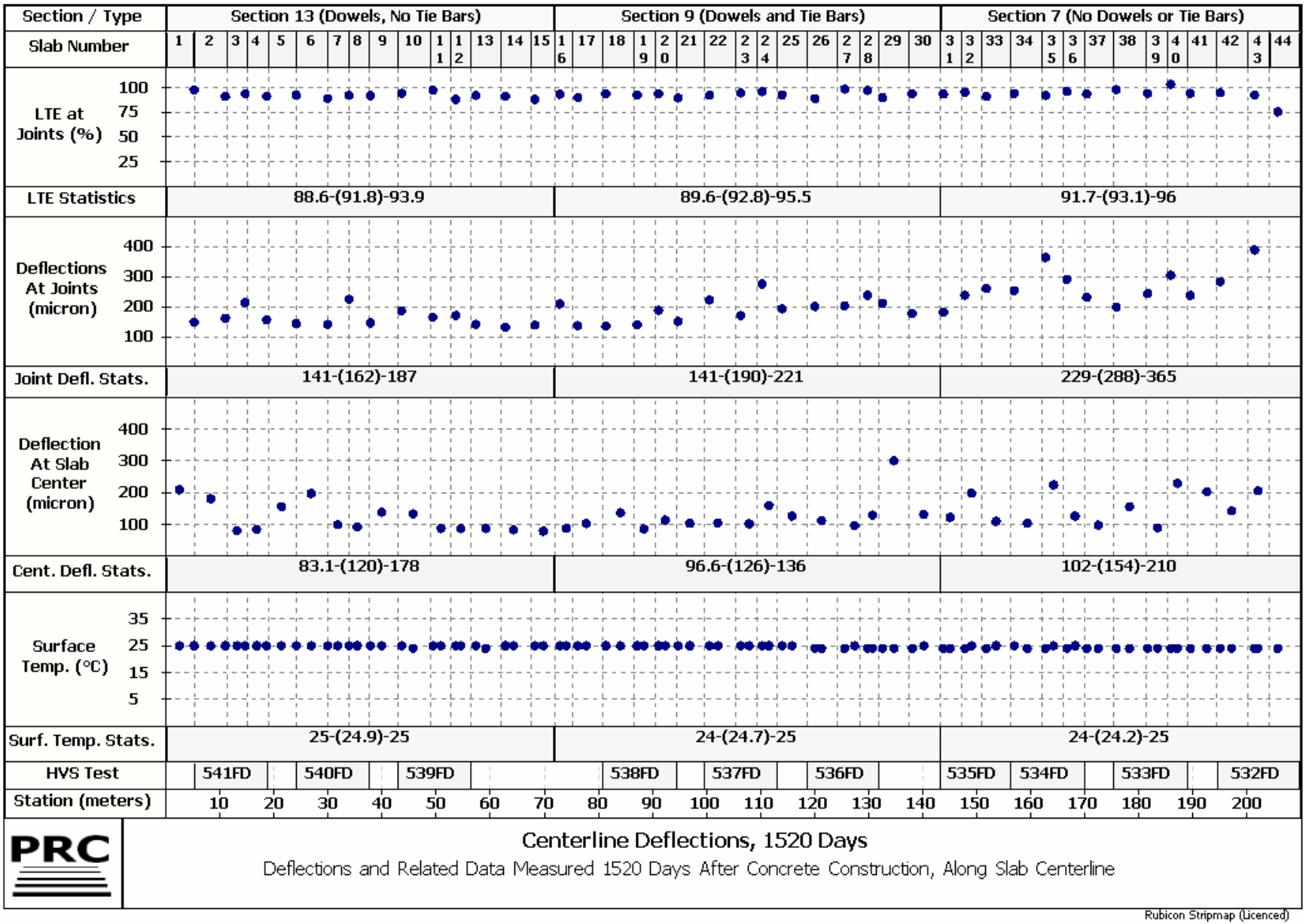
Section / Type
Section 13 (Dowels, No Tie Bars)
Section 9 (Dowels and Tie Bars)
Section 7 (No Dowels or Tie Bars)
Slab Number
1 2 3 4 5 6 7 8 9 10 11 12 13 14 15 16 17 18 19 20 21 22 23 24 25 26 27 28 29 30 31 32 33 34 35 36 37 38 39 40 41 42 43 44
LTE at Joints (%)
100
75
50
25
LTE Statistics
88.6-(91.8)-93.9
89.6-(92.8)-95.5
91.7-(93.1)-96
Deflections At Joints (micron)
400
300
200
100
Joint Defl. Stats.
141-(162)-187
141-(190)-221
229-(288)-365
Deflection At Slab Center (micron)
400
300
200
100
Cent. Defl. Stats.
83.1-(120)-178
96.6-(126)-136
102-(154)-210
Surface Temp. (°C)
35
25
15
5
Surf. Temp. Stats.
25-(24.9)-25
24-(24.7)-25
24-(24.2)-25
HVS Test
541FD
540FD
539FD
538FD
537FD
536FD
535FD
534FD
533FD
532FD
Station (meters)
10 20 30 40 50 60 70 80 90 100 110 120 130 140 150 160 170 180 190 200
PRC
Centerline Deflections, 1520 Days
Deflections and Related Data Measured 1520 Days After Concrete Construction, Along Slab Centerline
Rubicon Stripmap (Licenced)

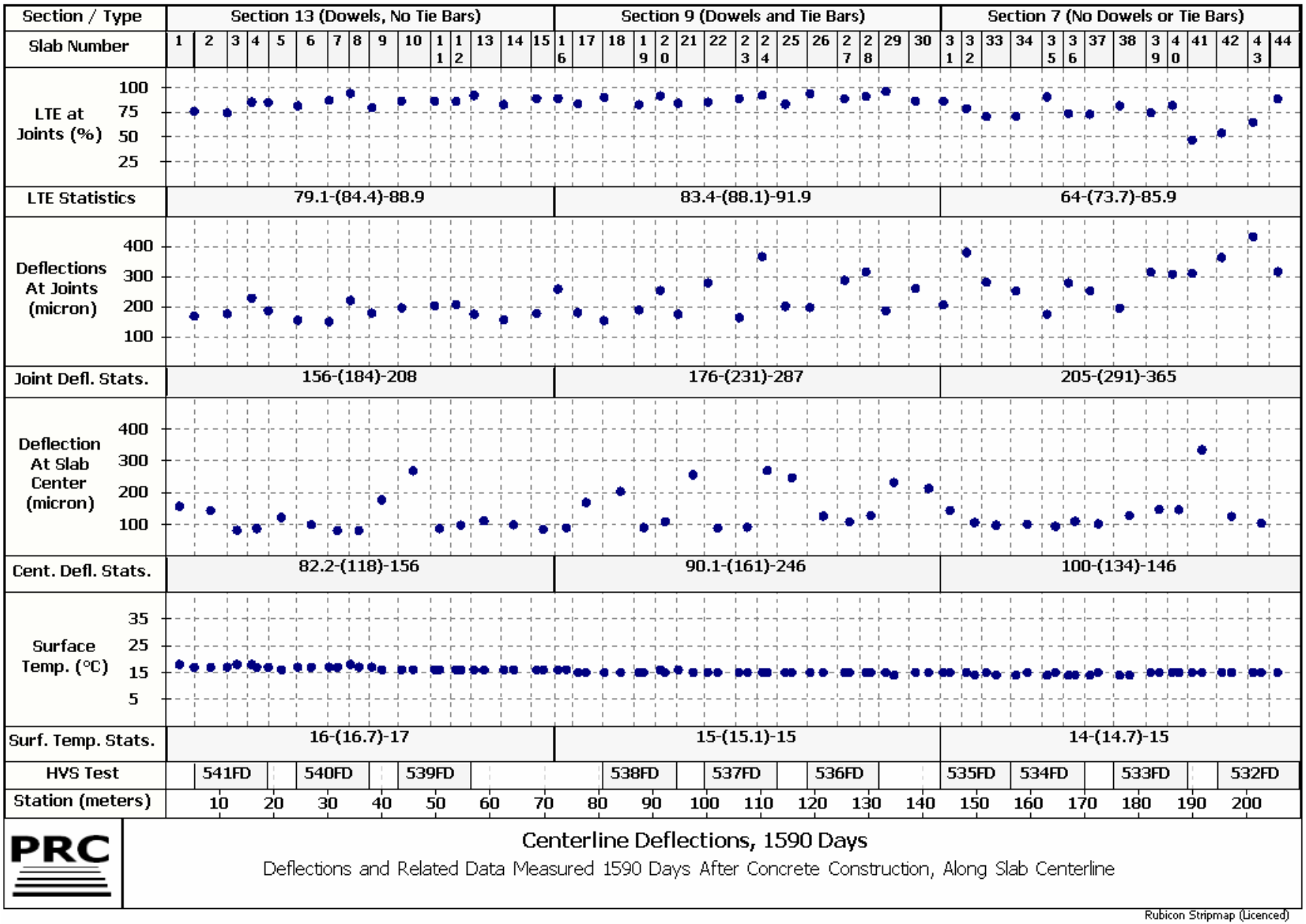
Section / Type
Section 13 (Dowels, No Tie Bars)
Section 9 (Dowels and Tie Bars)
Section 7 (No Dowels or Tie Bars)
Slab Number
1 2 3 4 5 6 7 8 9 10 11 12 13 14 15 16 17 18 19 20 21 22 23 24 25 26 27 28 29 30 31 32 33 34 35 36 37 38 39 40 41 42 43 44
LTE at Joints (%)
100
75
50
25
LTE Statistics
79.1-(84.4)-88.9
83.4-(88.1)-91.9
64-(73.7)-85.9
Deflections At Joints (micron)
400
300
200
100
Joint Defl. Stats.
156-(184)-208
176-(231)-287
205-(291)-365
Deflection At Slab Center (micron)
400
300
200
100
Cent. Defl. Stats.
82.2-(118)-156
90.1-(161)-246
100-(134)-146
Surface Temp. (°C)
35
25
15
5
Surf. Temp. Stats.
16-(16.7)-17
15-(15.1)-15
14-(14.7)-15
HVS Test
541FD
540FD
539FD
538FD
537FD
536FD
535FD
534FD
533FD
532FD
Station (meters)
10 20 30 40 50 60 70 80 90 100 110 120 130 140 150 160 170 180 190 200
PRC
Centerline Deflections, 1590 Days
Deflections and Related Data Measured 1590 Days After Concrete Construction, Along Slab Centerline
Rubicon Stripmap (Licenced)

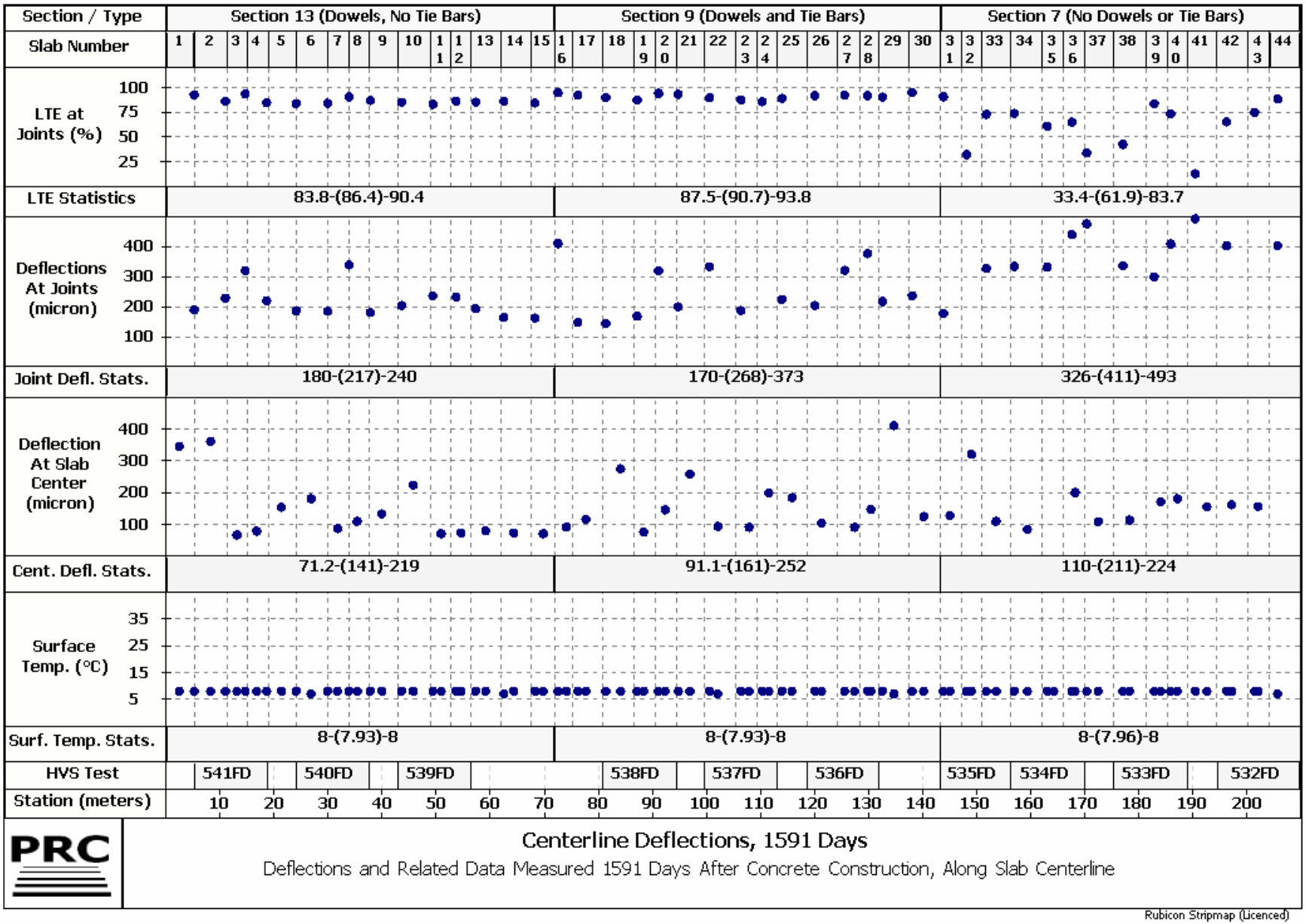
Section / Type
Section 13 (Dowels, No Tie Bars)
Section 9 (Dowels and Tie Bars)
Section 7 (No Dowels or Tie Bars)
Slab Number
1 2 3 4 5 6 7 8 9 10 11 12 13 14 15 16 17 18 19 20 21 22 23 24 25 26 27 28 29 30 31 32 33 34 35 36 37 38 39 40 41 42 43 44
LTE at Joints (%)
100
75
50
25
LTE Statistics
83.8-(86.4)-90.4
87.5-(90.7)-93.8
33.4-(61.9)-83.7
Deflections At Joints (micron)
400
300
200
100
Joint Defl. Stats.
180-(217)-240
170-(268)-373
326-(411)-493
Deflection At Slab Center (micron)
400
300
200
100
Cent. Defl. Stats.
71.2-(141)-219
91.1-(161)-252
110-(211)-224
Surface Temp. (°C)
35
25
15
5
Surf. Temp. Stats.
8-(7.93)-8
8-(7.93)-8
8-(7.96)-8
HVS Test
541FD
540FD
539FD
538FD
537FD
536FD
535FD
534FD
533FD
532FD
Station (meters)
10 20 30 40 50 60 70 80 90 100 110 120 130 140 150 160 170 180 190 200
PRC
Centerline Deflections, 1591 Days
Deflections and Related Data Measured 1591 Days After Concrete Construction, Along Slab Centerline
Rubicon Stripmap (Licenced)

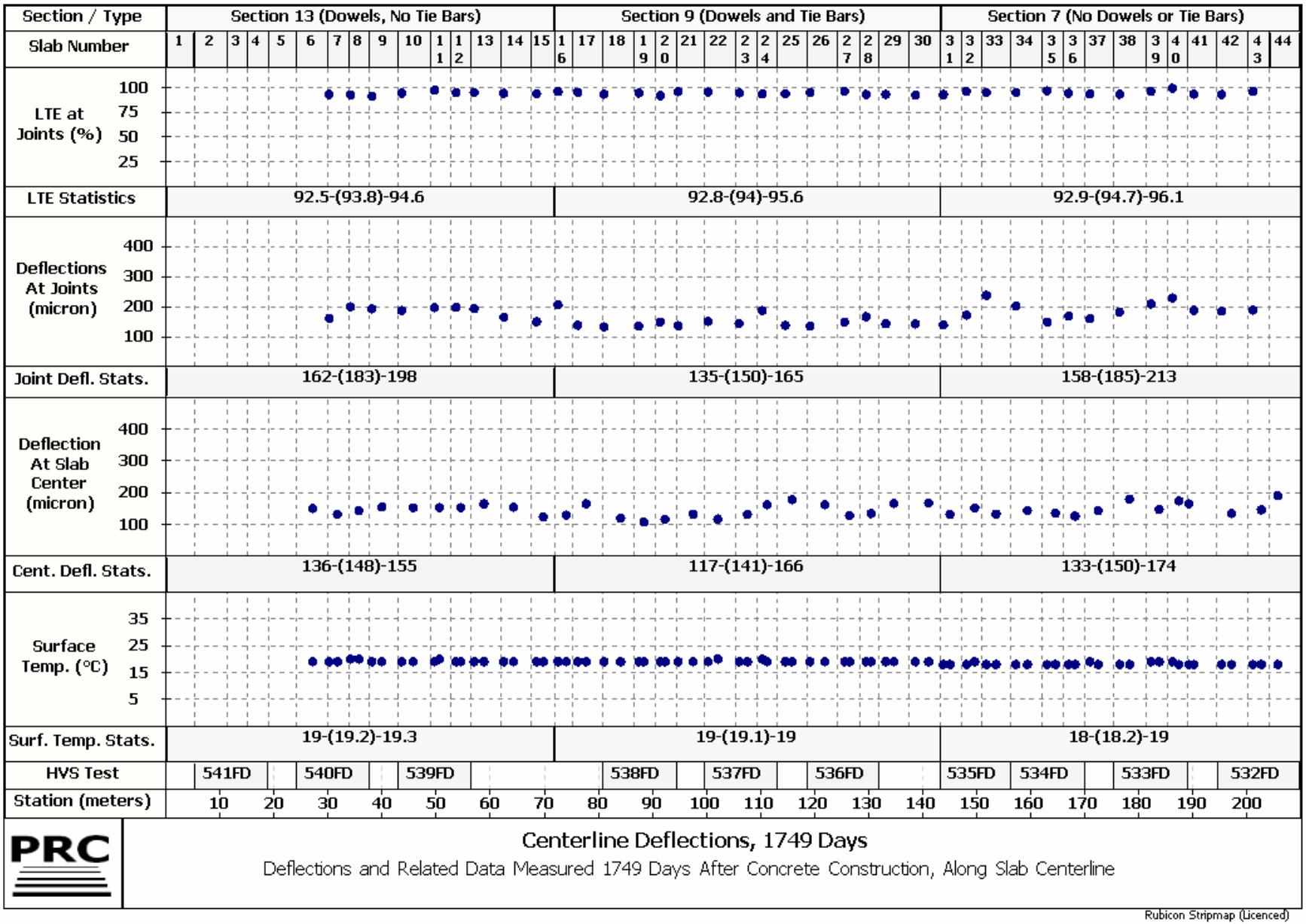
Section / Type
Section 13 (Dowels, No Tie Bars)
Section 9 (Dowels and Tie Bars)
Section 7 (No Dowels or Tie Bars)
Slab Number
1 2 3 4 5 6 7 8 9 10 11 12 13 14 15 16 17 18 19 20 21 22 23 24 25 26 27 28 29 30 31 32 33 34 35 36 37 38 39 40 41 42 43 44
LTE at Joints (%)
100
75
50
25
LTE Statistics
92.5-(93.8)-94.6
92.8-(94)-95.6
92.9-(94.7)-96.1
Deflections At Joints (micron)
400
300
200
100
Joint Defl. Stats.
162-(183)-198
135-(150)-165
158-(185)-213
Deflection At Slab Center (micron)
400
300
200
100
Cent. Defl. Stats.
136-(148)-155
117-(141)-166
133-(150)-174
Surface Temp. (°C)
35
25
15
5
Surf. Temp. Stats.
19-(19.2)-19.3
19-(19.1)-19
18-(18.2)-19
HVS Test
541FD
540FD
539FD
538FD
537FD
536FD
535FD
534FD
533FD
532FD
Station (meters)
10 20 30 40 50 60 70 80 90 100 110 120 130 140 150 160 170 180 190 200
PRC
Centerline Deflections, 1749 Days
Deflections and Related Data Measured 1749 Days After Concrete Construction, Along Slab Centerline
Rubicon Stripmap (Licenced)

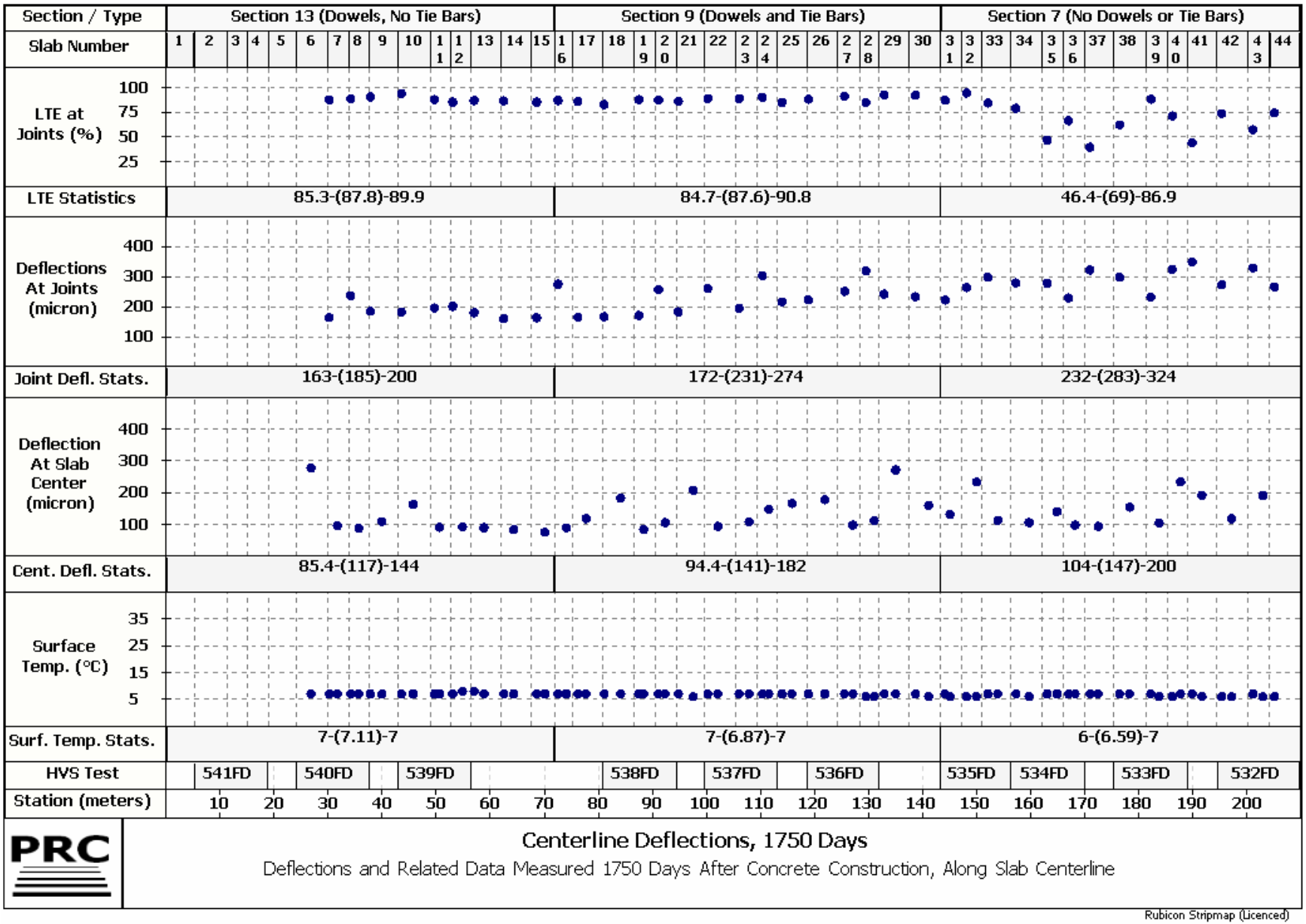
Section / Type
Section 13 (Dowels, No Tie Bars)
Section 9 (Dowels and Tie Bars)
Section 7 (No Dowels or Tie Bars)
Slab Number
1 2 3 4 5 6 7 8 9 10 11 12 13 14 15 16 17 18 19 20 21 22 23 24 25 26 27 28 29 30 31 32 33 34 35 36 37 38 39 40 41 42 43 44
LTE at Joints (%)
100
75
50
25
LTE Statistics
85.3-(87.8)-89.9
84.7-(87.6)-90.8
46.4-(69)-86.9
Deflections At Joints (micron)
400
300
200
100
Joint Defl. Stats.
163-(185)-200
172-(231)-274
232-(283)-324
Deflection At Slab Center (micron)
400
300
200
100
Cent. Defl. Stats.
85.4-(117)-144
94.4-(141)-182
104-(147)-200
Surface Temp. (°C)
35
25
15
5
Surf. Temp. Stats.
7-(7.11)-7
7-(6.87)-7
6-(6.59)-7
HVS Test
541FD
540FD
539FD
538FD
537FD
536FD
535FD
534FD
533FD
532FD
Station (meters)
10 20 30 40 50 60 70 80 90 100 110 120 130 140 150 160 170 180 190 200
PRC
Centerline Deflections, 1750 Days
Deflections and Related Data Measured 1750 Days After Concrete Construction, Along Slab Centerline
Rubicon Stripmap (Licenced)

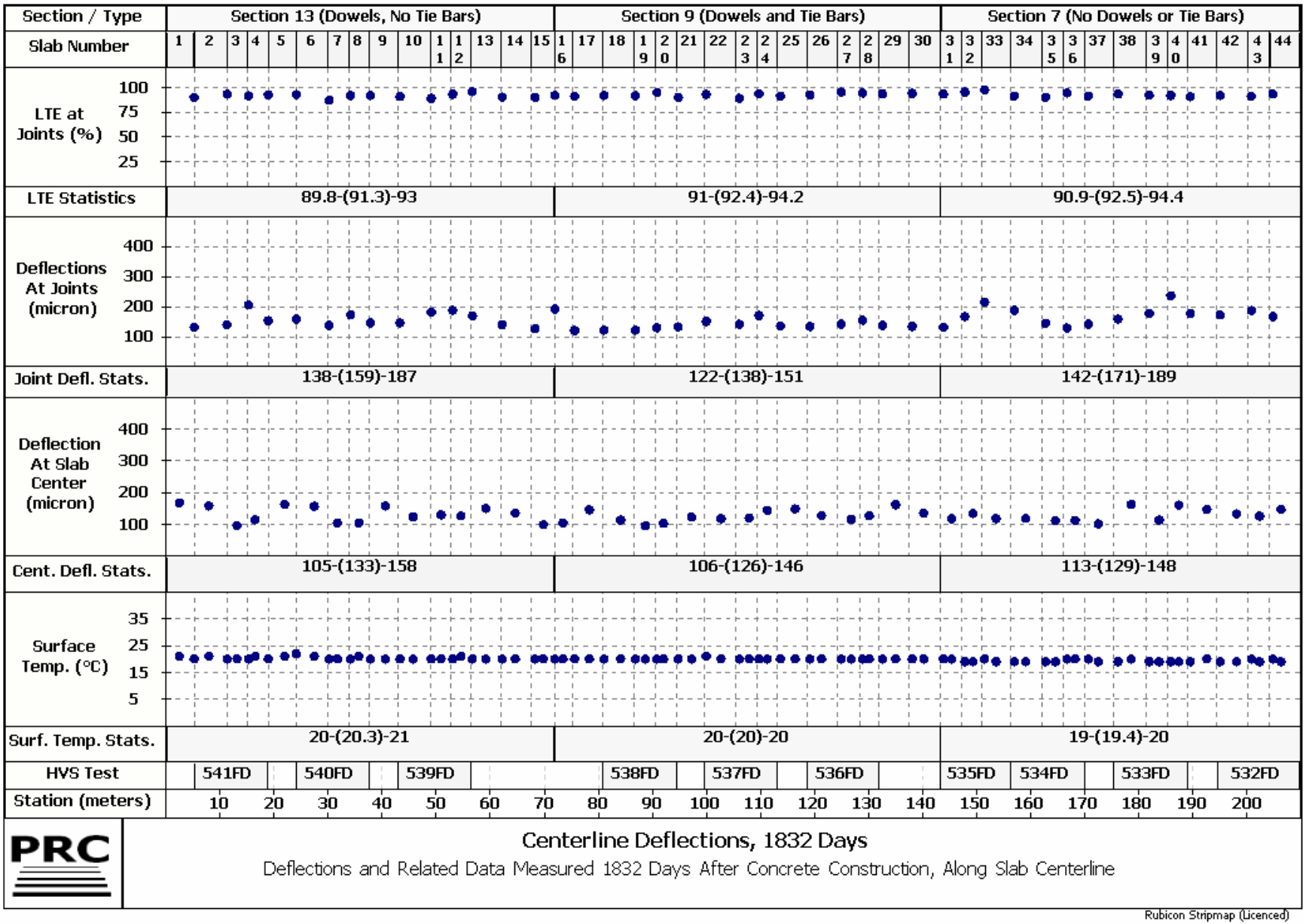
Section / Type
Section 13 (Dowels, No Tie Bars)
Section 9 (Dowels and Tie Bars)
Section 7 (No Dowels or Tie Bars)
Slab Number
1 2 3 4 5 6 7 8 9 10 11 12 13 14 15 16 17 18 19 20 21 22 23 24 25 26 27 28 29 30 31 32 33 34 35 36 37 38 39 40 41 42 43 44
LTE at Joints (%)
100
75
50
25
LTE Statistics
89.8-(91.3)-93
91-(92.4)-94.2
90.9-(92.5)-94.4
Deflections At Joints (micron)
400
300
200
100
Joint Defl. Stats.
138-(159)-187
122-(138)-151
142-(171)-189
Deflection At Slab Center (micron)
400
300
200
100
Cent. Defl. Stats.
105-(133)-158
106-(126)-146
113-(129)-148
Surface Temp. (°C)
35
25
15
5
Surf. Temp. Stats.
20-(20.3)-21
20-(20)-20
19-(19.4)-20
HVS Test
541FD
540FD
539FD
538FD
537FD
536FD
535FD
534FD
533FD
532FD
Station (meters)
10 20 30 40 50 60 70 80 90 100 110 120 130 140 150 160 170 180 190 200
PRC
Centerline Deflections, 1832 Days
Deflections and Related Data Measured 1832 Days After Concrete Construction, Along Slab Centerline
Rubicon Stripmap (Licenced)

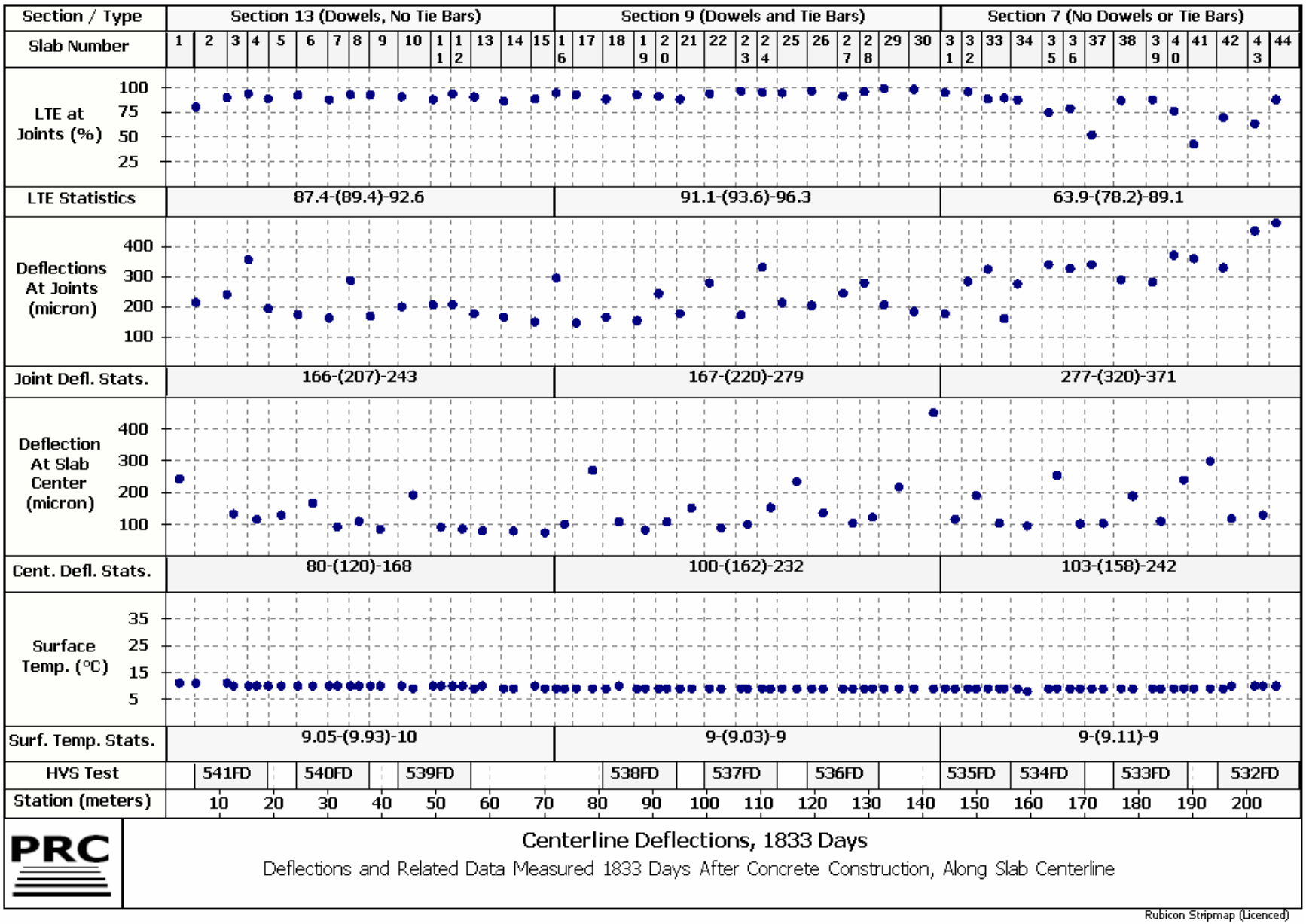
Section / Type
Section 13 (Dowels, No Tie Bars)
Section 9 (Dowels and Tie Bars)
Section 7 (No Dowels or Tie Bars)
Slab Number
1 2 3 4 5 6 7 8 9 10 11 12 13 14 15 16 17 18 19 20 21 22 23 24 25 26 27 28 29 30 31 32 33 34 35 36 37 38 39 40 41 42 43 44
LTE at Joints (%)
100
75
50
25
LTE Statistics
87.4-(89.4)-92.6
91.1-(93.6)-96.3
63.9-(78.2)-89.1
Deflections At Joints (micron)
400
300
200
100
Joint Defl. Stats.
166-(207)-243
167-(220)-279
277-(320)-371
Deflection At Slab Center (micron)
400
300
200
100
Cent. Defl. Stats.
80-(120)-168
100-(162)-232
103-(158)-242
Surface Temp. (°C)
35
25
15
5
Surf. Temp. Stats.
9.05-(9.93)-10
9-(9.03)-9
9-(9.11)-9
HVS Test
541FD
540FD
539FD
538FD
537FD
536FD
535FD
534FD
533FD
532FD
Station (meters)
10 20 30 40 50 60 70 80 90 100 110 120 130 140 150 160 170 180 190 200
PRC
Centerline Deflections, 1833 Days
Deflections and Related Data Measured 1833 Days After Concrete Construction, Along Slab Centerline
Rubicon Stripmap (Licenced)

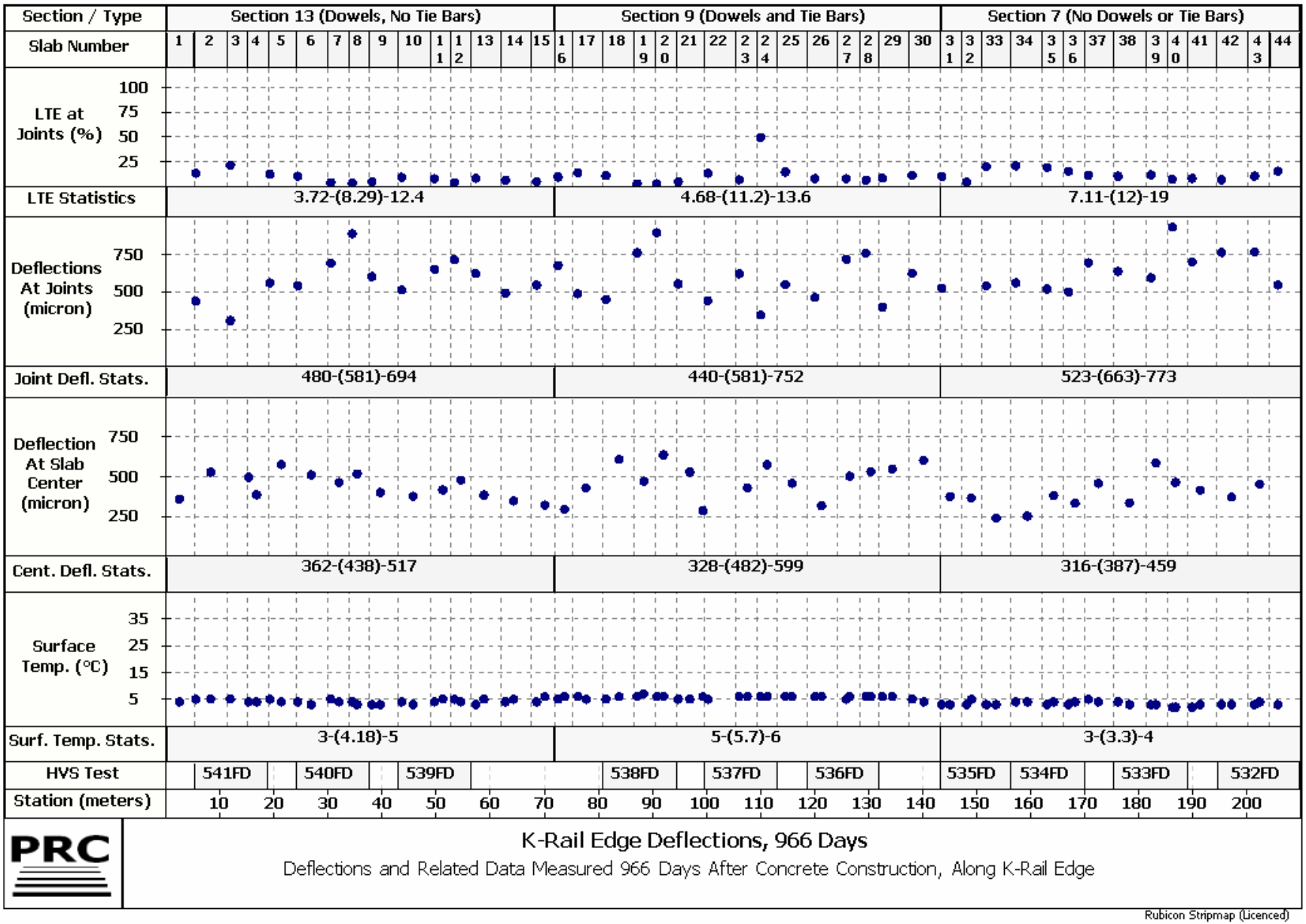
Section / Type
Section 13 (Dowels, No Tie Bars)
Section 9 (Dowels and Tie Bars)
Section 7 (No Dowels or Tie Bars)
Slab Number
1 2 3 4 5 6 7 8 9 10 11 12 13 14 15 16 17 18 19 20 21 22 23 24 25 26 27 28 29 30 31 32 33 34 35 36 37 38 39 40 41 42 43 44
LTE at Joints (%)
100
75
50
25
LTE Statistics
3.72-(8.29)-12.4
4.68-(11.2)-13.6
7.11-(12)-19
Deflections At Joints (micron)
750
500
250
Joint Defl. Stats.
480-(581)-694
440-(581)-752
523-(663)-773
Deflection At Slab Center (micron)
750
500
250
Cent. Defl. Stats.
362-(438)-517
328-(482)-599
316-(387)-459
Surface Temp. (°C)
35
25
15
5
Surf. Temp. Stats.
3-(4.18)-5
5-(5.7)-6
3-(3.3)-4
HVS Test
541FD
540FD
539FD
538FD
537FD
536FD
535FD
534FD
533FD
532FD
Station (meters)
10 20 30 40 50 60 70 80 90 100 110 120 130 140 150 160 170 180 190 200
PRC
K-Rail Edge Deflections, 966 Days
Deflections and Related Data Measured 966 Days After Concrete Construction, Along K-Rail Edge
Rubicon Stripmap (Licenced)

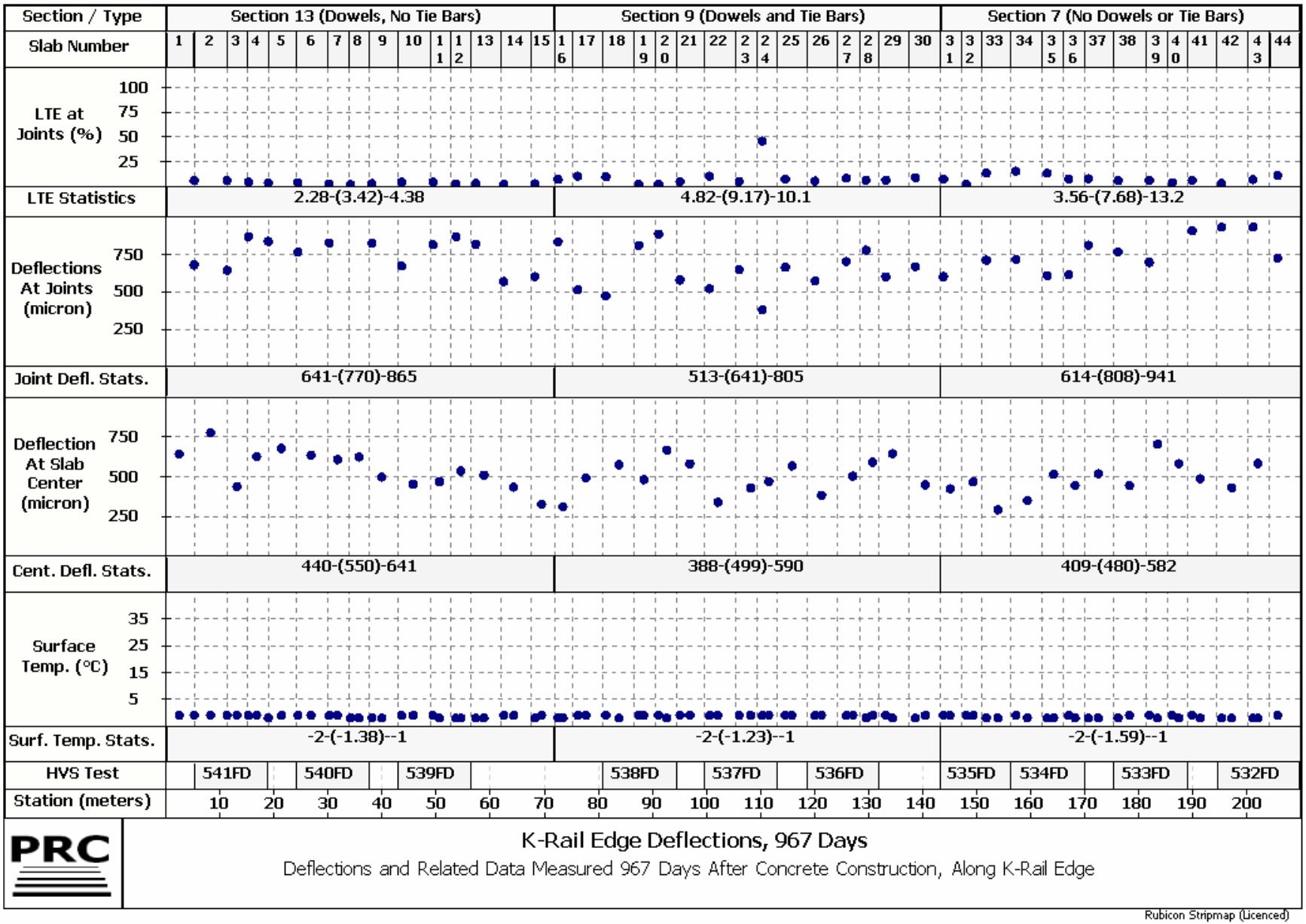
Section / Type
Section 13 (Dowels, No Tie Bars)
Section 9 (Dowels and Tie Bars)
Section 7 (No Dowels or Tie Bars)
Slab Number
1 2 3 4 5 6 7 8 9 10 11 12 13 14 15 16 17 18 19 20 21 22 23 24 25 26 27 28 29 30 31 32 33 34 35 36 37 38 39 40 41 42 43 44
LTE at Joints (%)
100
75
50
25
LTE Statistics
2.28-(3.42)-4.38
4.82-(9.17)-10.1
3.56-(7.68)-13.2
Deflections At Joints (micron)
750
500
250
Joint Defl. Stats.
641-(770)-865
513-(641)-805
614-(808)-941
Deflection At Slab Center (micron)
750
500
250
Cent. Defl. Stats.
440-(550)-641
388-(499)-590
409-(480)-582
Surface Temp. (°C)
35
25
15
5
Surf. Temp. Stats.
-2-(-1.38)--1
-2-(-1.23)--1
-2-(-1.59)--1
HVS Test
541FD
540FD
539FD
538FD
537FD
536FD
535FD
534FD
533FD
532FD
Station (meters)
10 20 30 40 50 60 70 80 90 100 110 120 130 140 150 160 170 180 190 200
PRC
K-Rail Edge Deflections, 967 Days
Deflections and Related Data Measured 967 Days After Concrete Construction, Along K-Rail Edge
Rubicon Stripmap (Licenced)

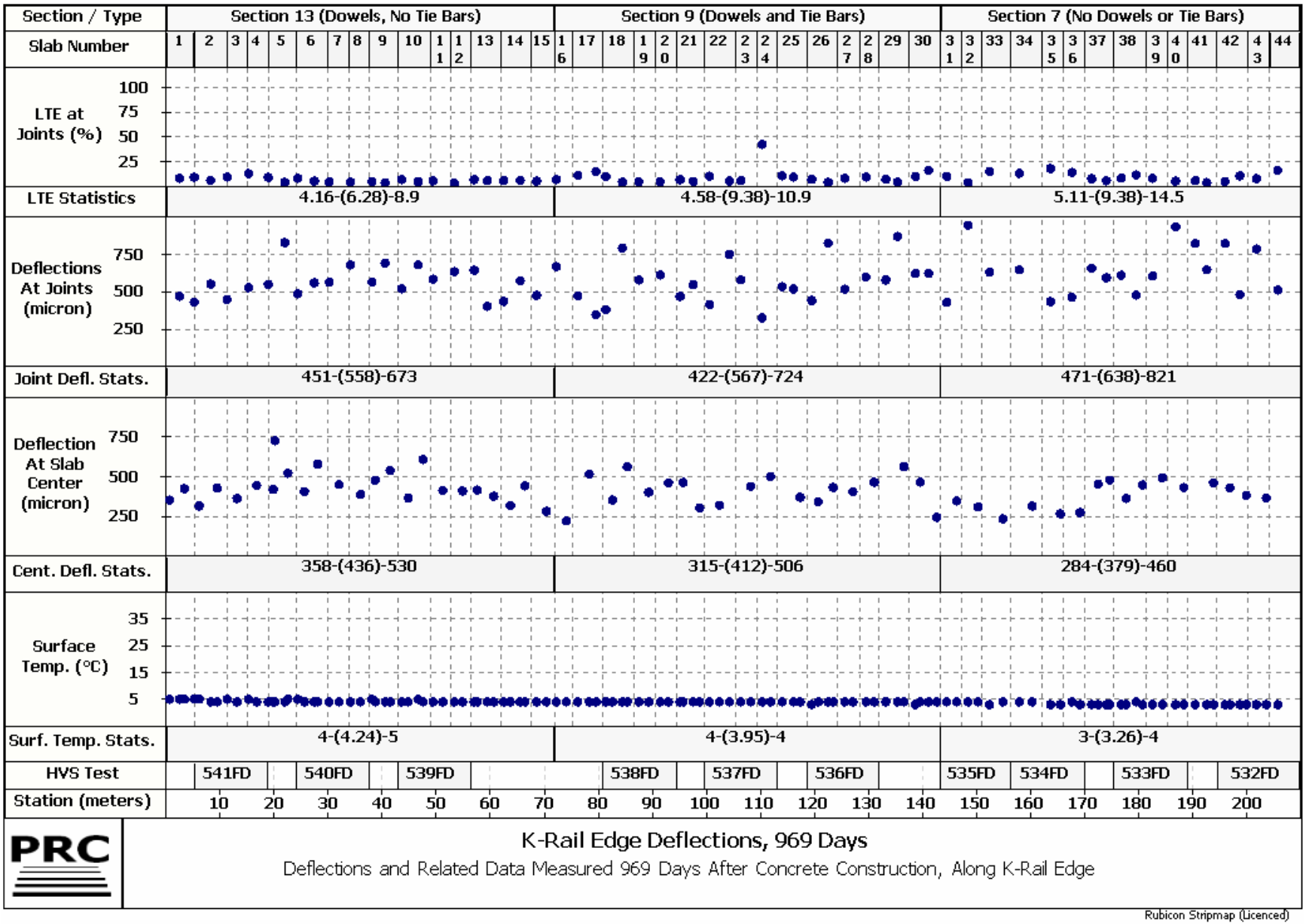
Section / Type
Section 13 (Dowels, No Tie Bars)
Section 9 (Dowels and Tie Bars)
Section 7 (No Dowels or Tie Bars)
Slab Number
1 2 3 4 5 6 7 8 9 10 11 12 13 14 15 16 17 18 19 20 21 22 23 24 25 26 27 28 29 30 31 32 33 34 35 36 37 38 39 40 41 42 43 44
LTE at Joints (%)
100
75
50
25
LTE Statistics
4.16-(6.28)-8.9
4.58-(9.38)-10.9
5.11-(9.38)-14.5
Deflections At Joints (micron)
750
500
250
Joint Defl. Stats.
451-(558)-673
422-(567)-724
471-(638)-821
Deflection At Slab Center (micron)
750
500
250
Cent. Defl. Stats.
358-(436)-530
315-(412)-506
284-(379)-460
Surface Temp. (°C)
35
25
15
5
Surf. Temp. Stats.
4-(4.24)-5
4-(3.95)-4
3-(3.26)-4
HVS Test
541FD
540FD
539FD
538FD
537FD
536FD
535FD
534FD
533FD
532FD
Station (meters)
10 20 30 40 50 60 70 80 90 100 110 120 130 140 150 160 170 180 190 200
PRC
K-Rail Edge Deflections, 969 Days
Deflections and Related Data Measured 969 Days After Concrete Construction, Along K-Rail Edge
Rubicon Stripmap (Licenced)

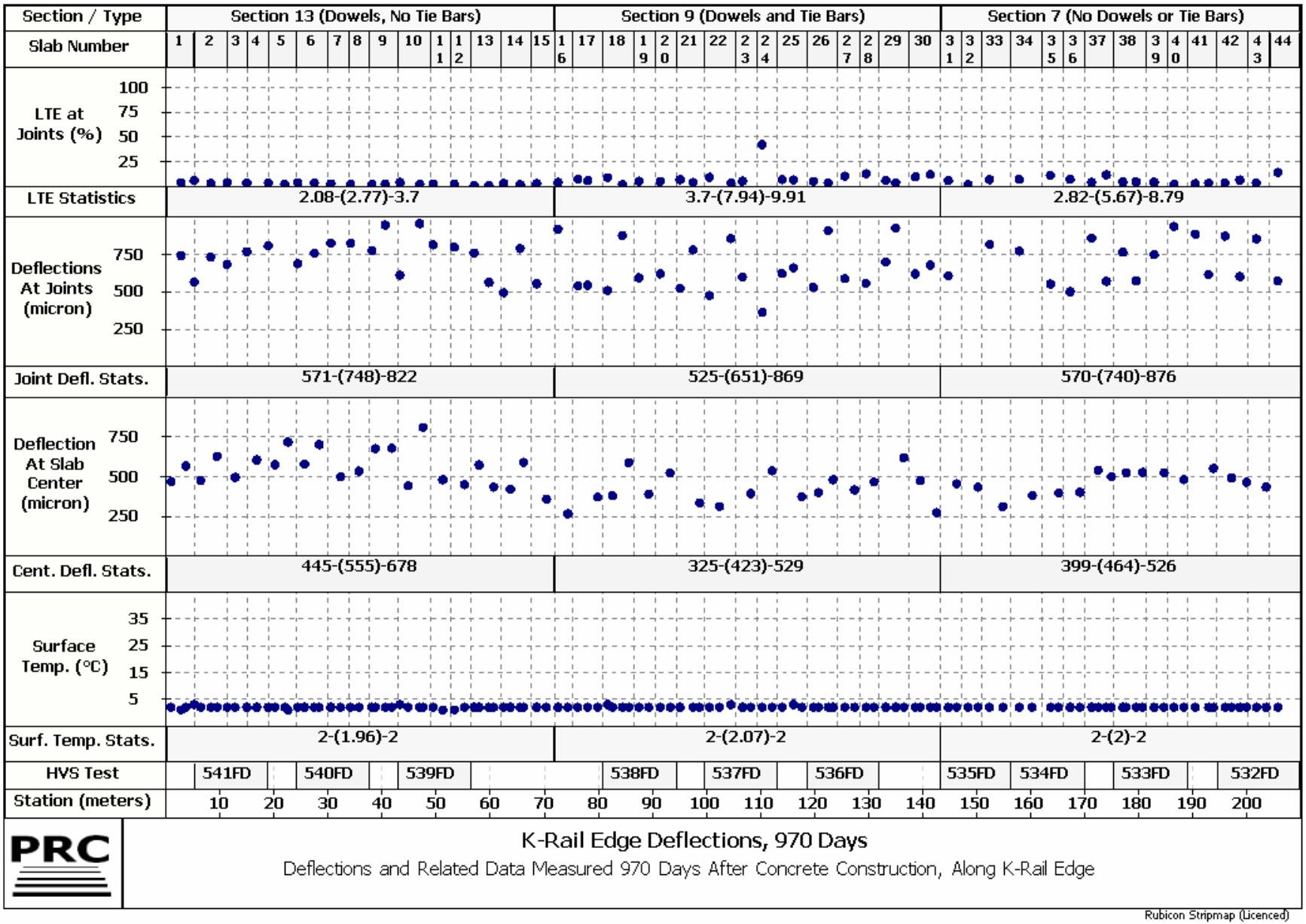

PRC

K-Rail Edge Deflections, 970 Days

Deflections and Related Data Measured 970 Days After Concrete Construction, Along K-Rail Edge

Rubicon Stripmap (Licenced)

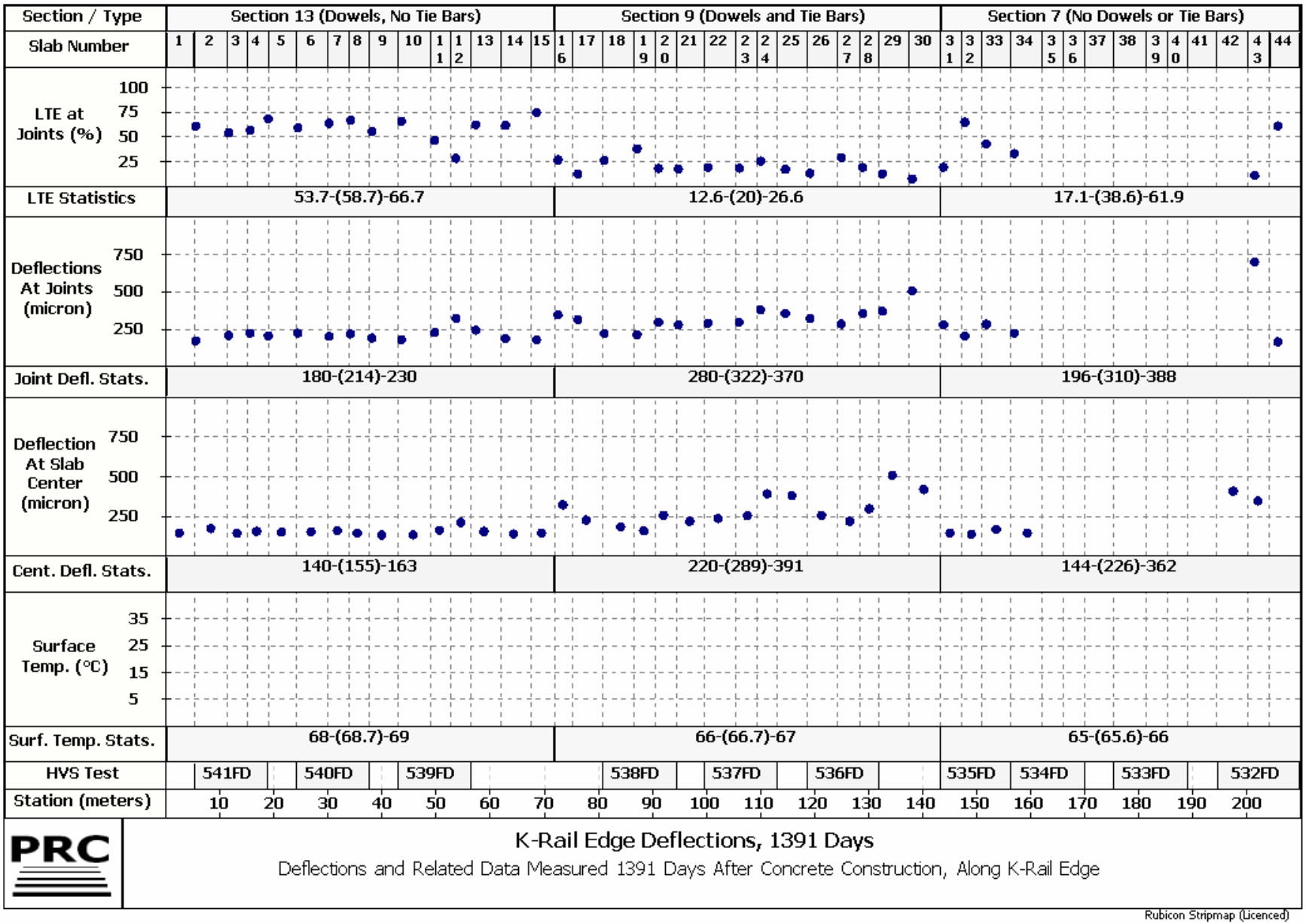

PRC

K-Rail Edge Deflections, 1391 Days

Deflections and Related Data Measured 1391 Days After Concrete Construction, Along K-Rail Edge

Rubicon Stripmap (Licenced)

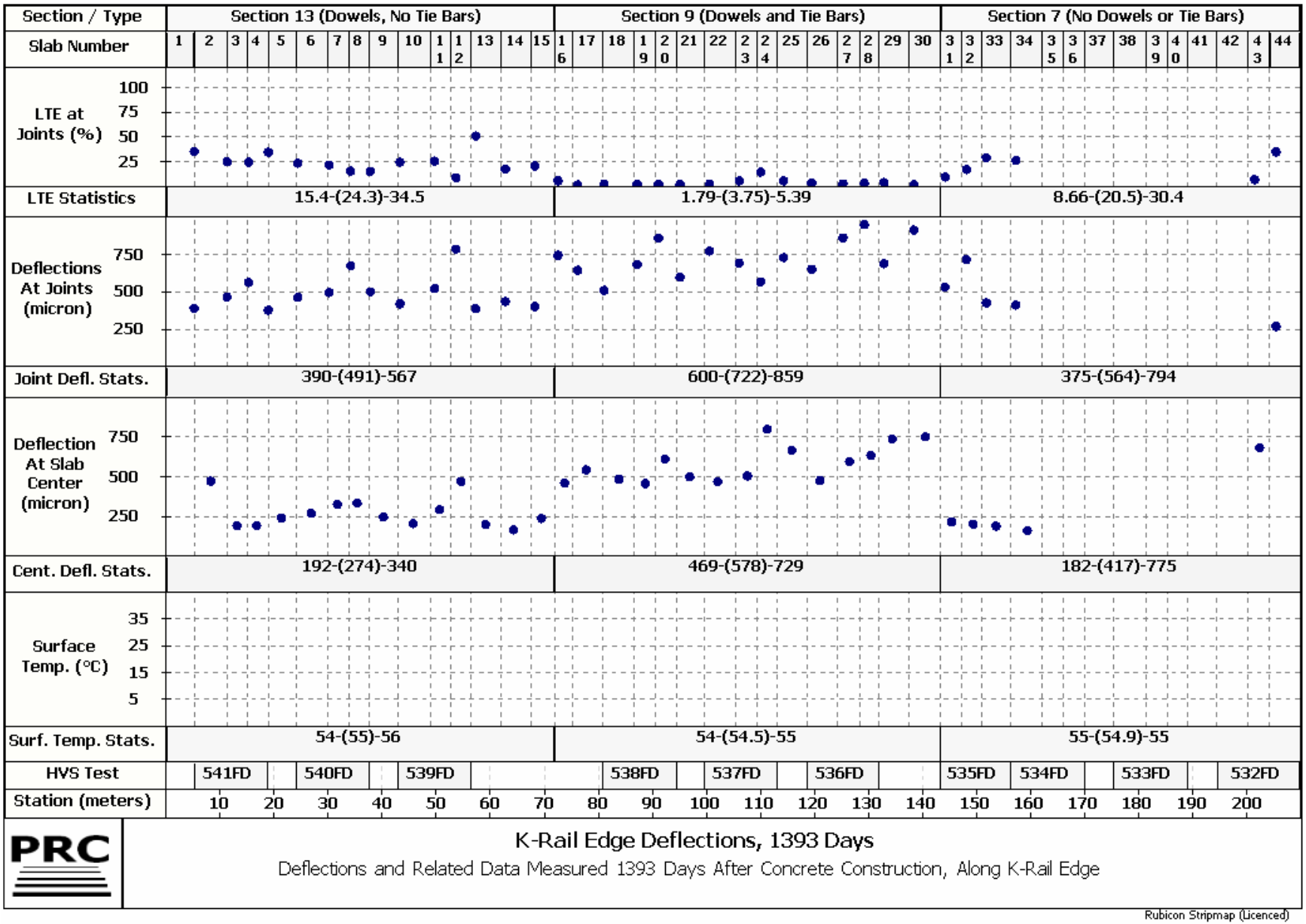
Section / Type
Section 13 (Dowels, No Tie Bars)
Section 9 (Dowels and Tie Bars)
Section 7 (No Dowels or Tie Bars)
Slab Number
1 2 3 4 5 6 7 8 9 10 11 12 13 14 15 16 17 18 19 20 21 22 23 24 25 26 27 28 29 30 31 32 33 34 35 36 37 38 39 40 41 42 43 44
LTE at Joints (%)
100
75
50
25
LTE Statistics
15.4-(24.3)-34.5
1.79-(3.75)-5.39
8.66-(20.5)-30.4
Deflections At Joints (micron)
750
500
250
Joint Defl. Stats.
390-(491)-567
600-(722)-859
375-(564)-794
Deflection At Slab Center (micron)
750
500
250
Cent. Defl. Stats.
192-(274)-340
469-(578)-729
182-(417)-775
Surface Temp. (°C)
35
25
15
5
Surf. Temp. Stats.
54-(55)-56
54-(54.5)-55
55-(54.9)-55
HVS Test
541FD
540FD
539FD
538FD
537FD
536FD
535FD
534FD
533FD
532FD
Station (meters)
10 20 30 40 50 60 70 80 90 100 110 120 130 140 150 160 170 180 190 200
PRC
K-Rail Edge Deflections, 1393 Days
Deflections and Related Data Measured 1393 Days After Concrete Construction, Along K-Rail Edge
Rubicon Stripmap (Licenced)

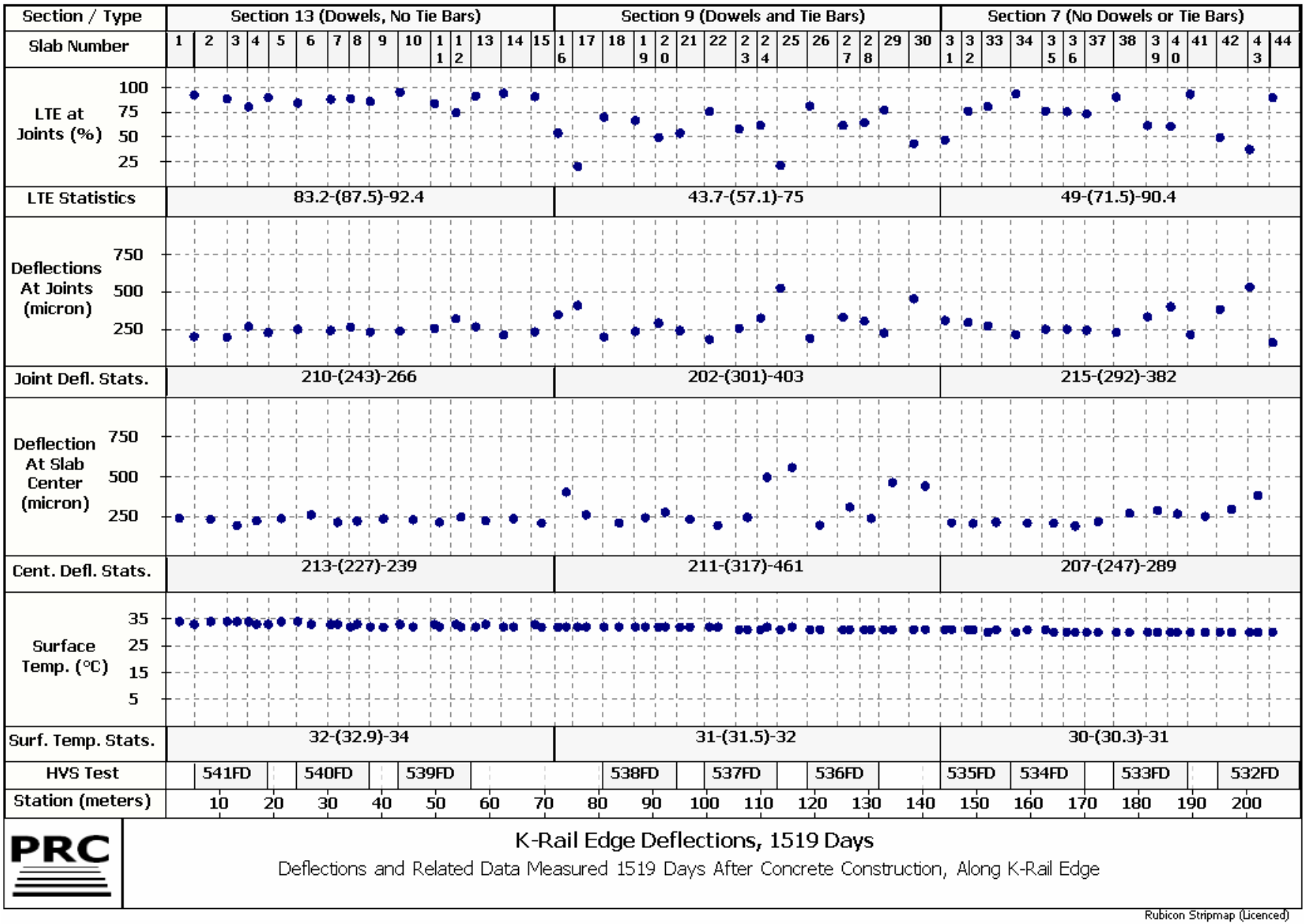
Section / Type
Section 13 (Dowels, No Tie Bars)
Section 9 (Dowels and Tie Bars)
Section 7 (No Dowels or Tie Bars)
Slab Number
1 2 3 4 5 6 7 8 9 10 11 12 13 14 15 16 17 18 19 20 21 22 23 24 25 26 27 28 29 30 31 32 33 34 35 36 37 38 39 40 41 42 43 44
LTE at Joints (%)
100
75
50
25
LTE Statistics
83.2-(87.5)-92.4
43.7-(57.1)-75
49-(71.5)-90.4
Deflections At Joints (micron)
750
500
250
Joint Defl. Stats.
210-(243)-266
202-(301)-403
215-(292)-382
Deflection At Slab Center (micron)
750
500
250
Cent. Defl. Stats.
213-(227)-239
211-(317)-461
207-(247)-289
Surface Temp. (°C)
35
25
15
5
Surf. Temp. Stats.
32-(32.9)-34
31-(31.5)-32
30-(30.3)-31
HVS Test
541FD
540FD
539FD
538FD
537FD
536FD
535FD
534FD
533FD
532FD
Station (meters)
10 20 30 40 50 60 70 80 90 100 110 120 130 140 150 160 170 180 190 200
PRC
K-Rail Edge Deflections, 1519 Days
Deflections and Related Data Measured 1519 Days After Concrete Construction, Along K-Rail Edge
Rubicon Stripmap (Licenced)

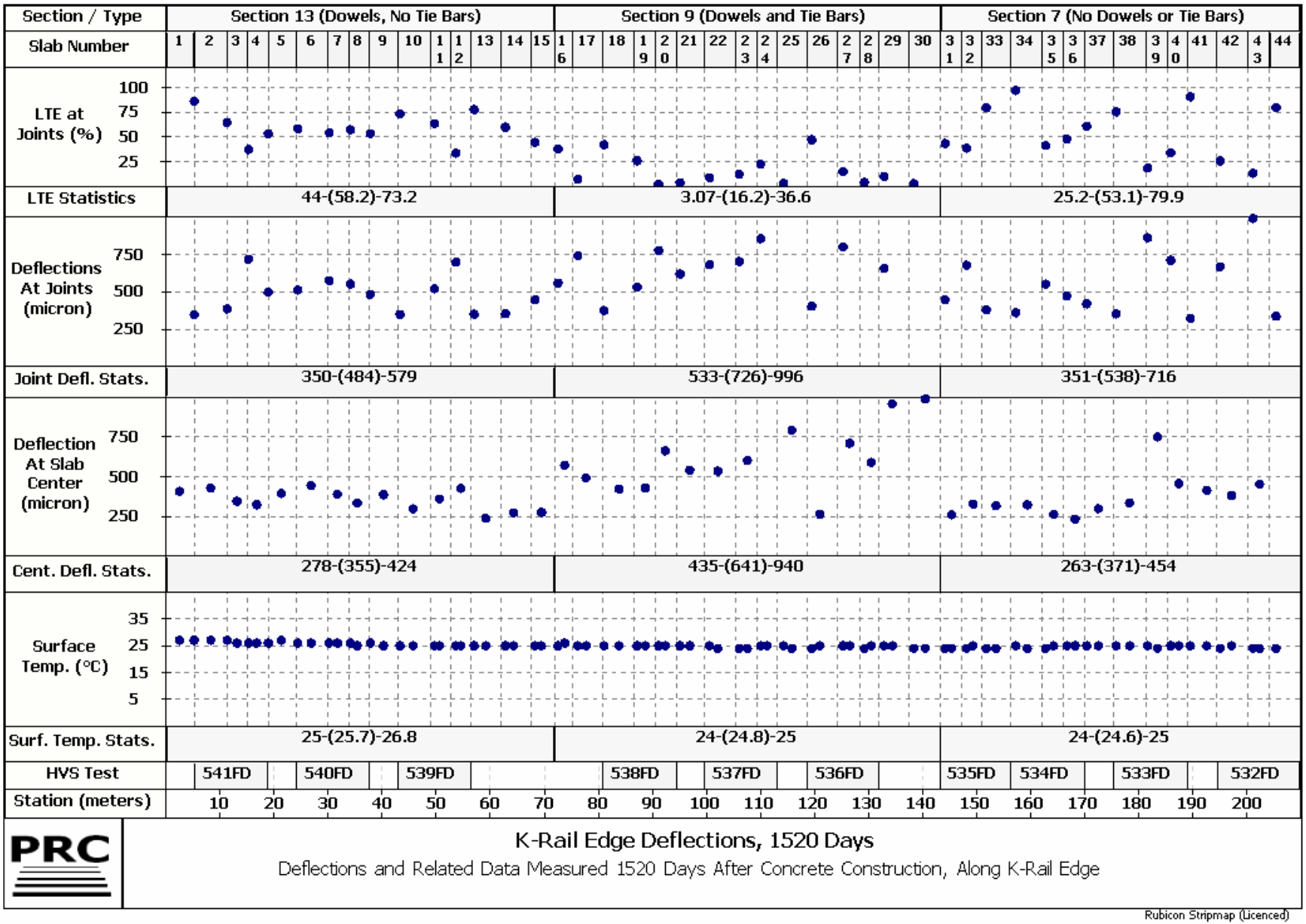
Section / Type
Section 13 (Dowels, No Tie Bars)
Section 9 (Dowels and Tie Bars)
Section 7 (No Dowels or Tie Bars)
Slab Number
1 2 3 4 5 6 7 8 9 10 11 12 13 14 15 16 17 18 19 20 21 22 23 24 25 26 27 28 29 30 31 32 33 34 35 36 37 38 39 40 41 42 43 44
LTE at Joints (%)
100
75
50
25
LTE Statistics
44-(58.2)-73.2
3.07-(16.2)-36.6
25.2-(53.1)-79.9
Deflections At Joints (micron)
750
500
250
Joint Defl. Stats.
350-(484)-579
533-(726)-996
351-(538)-716
Deflection At Slab Center (micron)
750
500
250
Cent. Defl. Stats.
278-(355)-424
435-(641)-940
263-(371)-454
Surface Temp. (°C)
35
25
15
5
Surf. Temp. Stats.
25-(25.7)-26.8
24-(24.8)-25
24-(24.6)-25
HVS Test
541FD
540FD
539FD
538FD
537FD
536FD
535FD
534FD
533FD
532FD
Station (meters)
10 20 30 40 50 60 70 80 90 100 110 120 130 140 150 160 170 180 190 200
PRC
K-Rail Edge Deflections, 1520 Days
Deflections and Related Data Measured 1520 Days After Concrete Construction, Along K-Rail Edge
Rubicon Stripmap (Licenced)

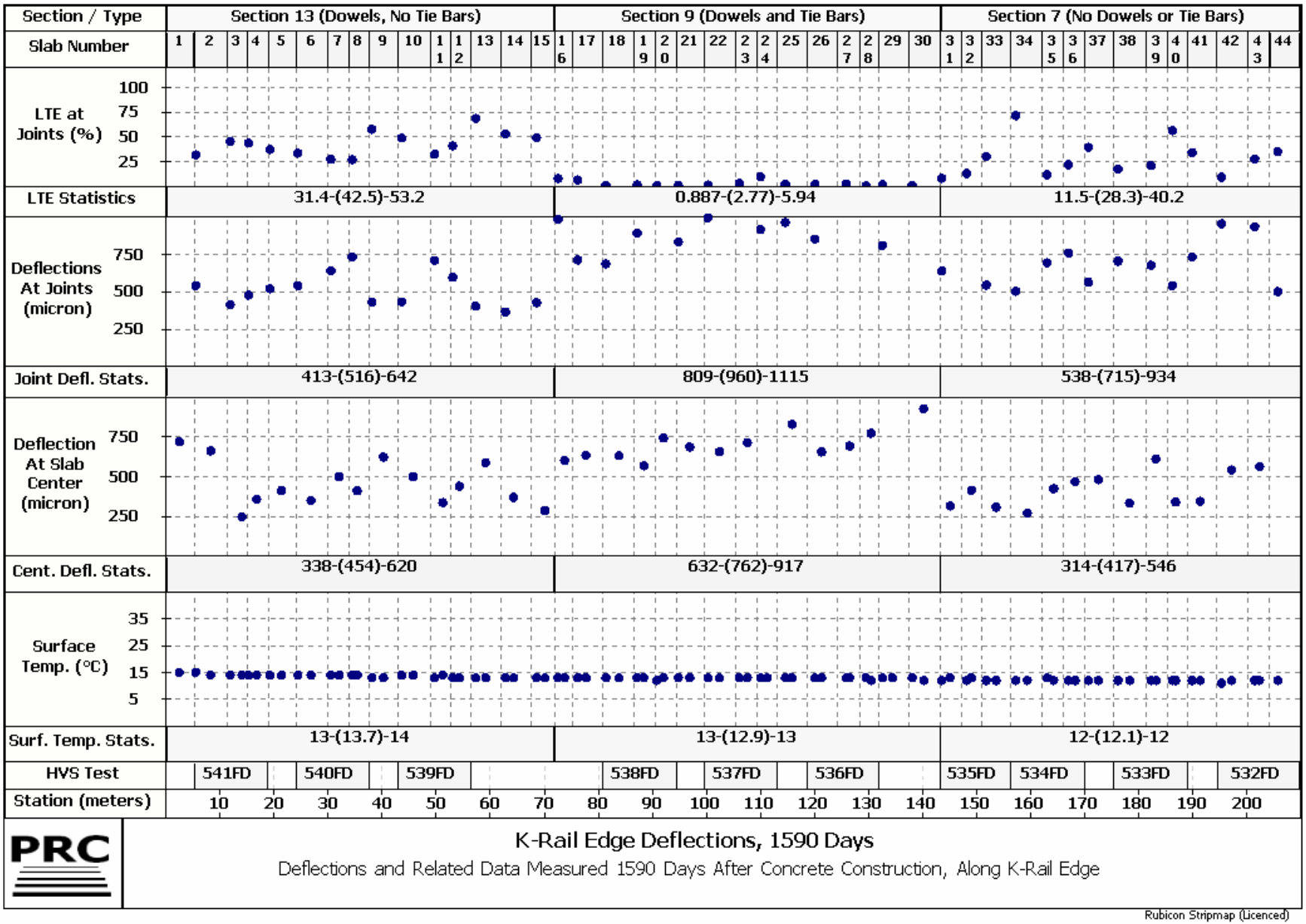
Section / Type
Section 13 (Dowels, No Tie Bars)
Section 9 (Dowels and Tie Bars)
Section 7 (No Dowels or Tie Bars)
Slab Number
1 2 3 4 5 6 7 8 9 10 11 12 13 14 15 16 17 18 19 20 21 22 23 24 25 26 27 28 29 30 31 32 33 34 35 36 37 38 39 40 41 42 43 44
LTE at Joints (%)
100
75
50
25
LTE Statistics
31.4-(42.5)-53.2
0.887-(2.77)-5.94
11.5-(28.3)-40.2
Deflections At Joints (micron)
750
500
250
Joint Defl. Stats.
413-(516)-642
809-(960)-1115
538-(715)-934
Deflection At Slab Center (micron)
750
500
250
Cent. Defl. Stats.
338-(454)-620
632-(762)-917
314-(417)-546
Surface Temp. (°C)
35
25
15
5
Surf. Temp. Stats.
13-(13.7)-14
13-(12.9)-13
12-(12.1)-12
HVS Test
541FD
540FD
539FD
538FD
537FD
536FD
535FD
534FD
533FD
532FD
Station (meters)
10 20 30 40 50 60 70 80 90 100 110 120 130 140 150 160 170 180 190 200
PRC
K-Rail Edge Deflections, 1590 Days
Deflections and Related Data Measured 1590 Days After Concrete Construction, Along K-Rail Edge
Rubicon Stripmap (Licenced)

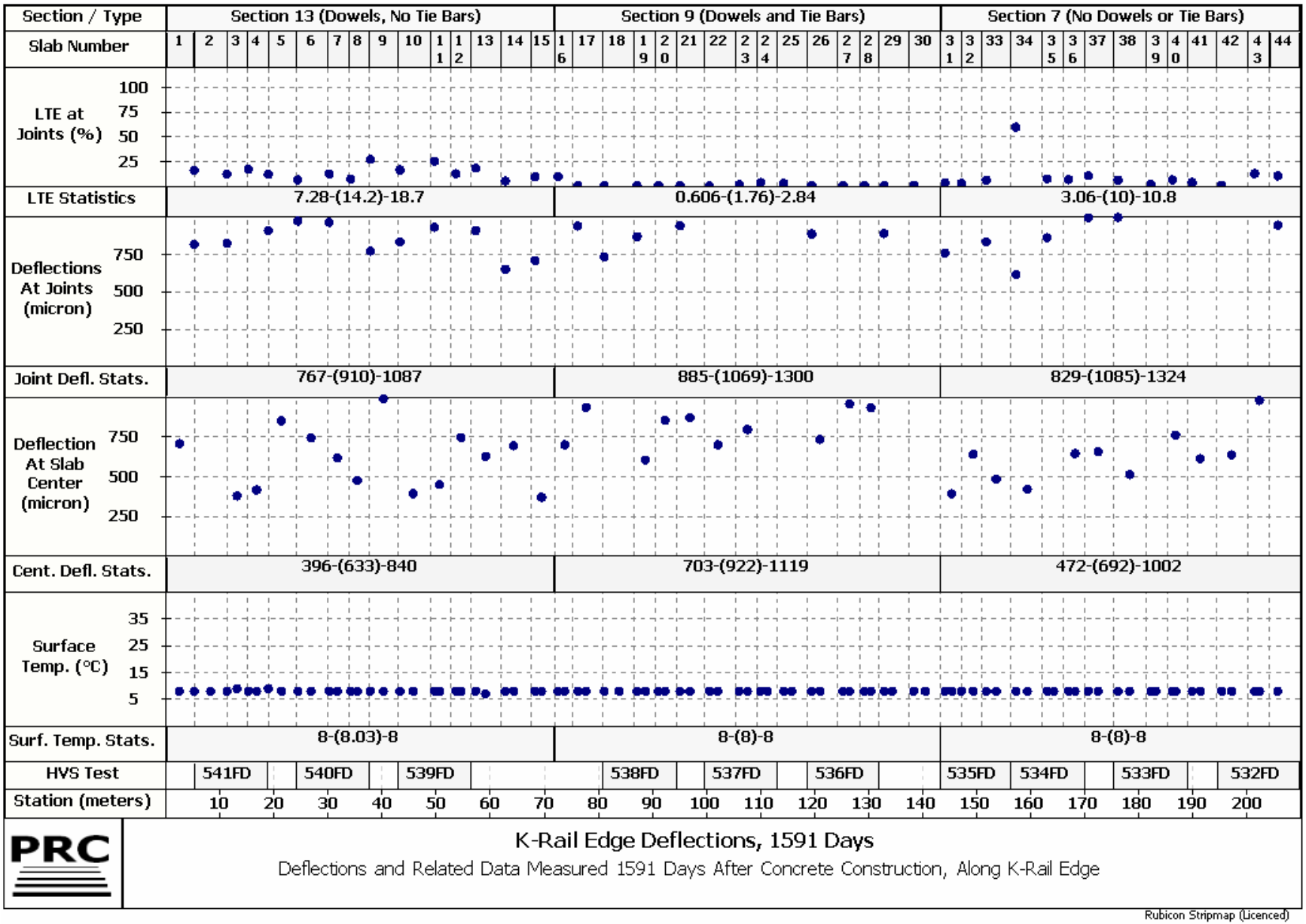

PRC

K-Rail Edge Deflections, 1591 Days

Deflections and Related Data Measured 1591 Days After Concrete Construction, Along K-Rail Edge

Rubicon Stripmap (Licenced)

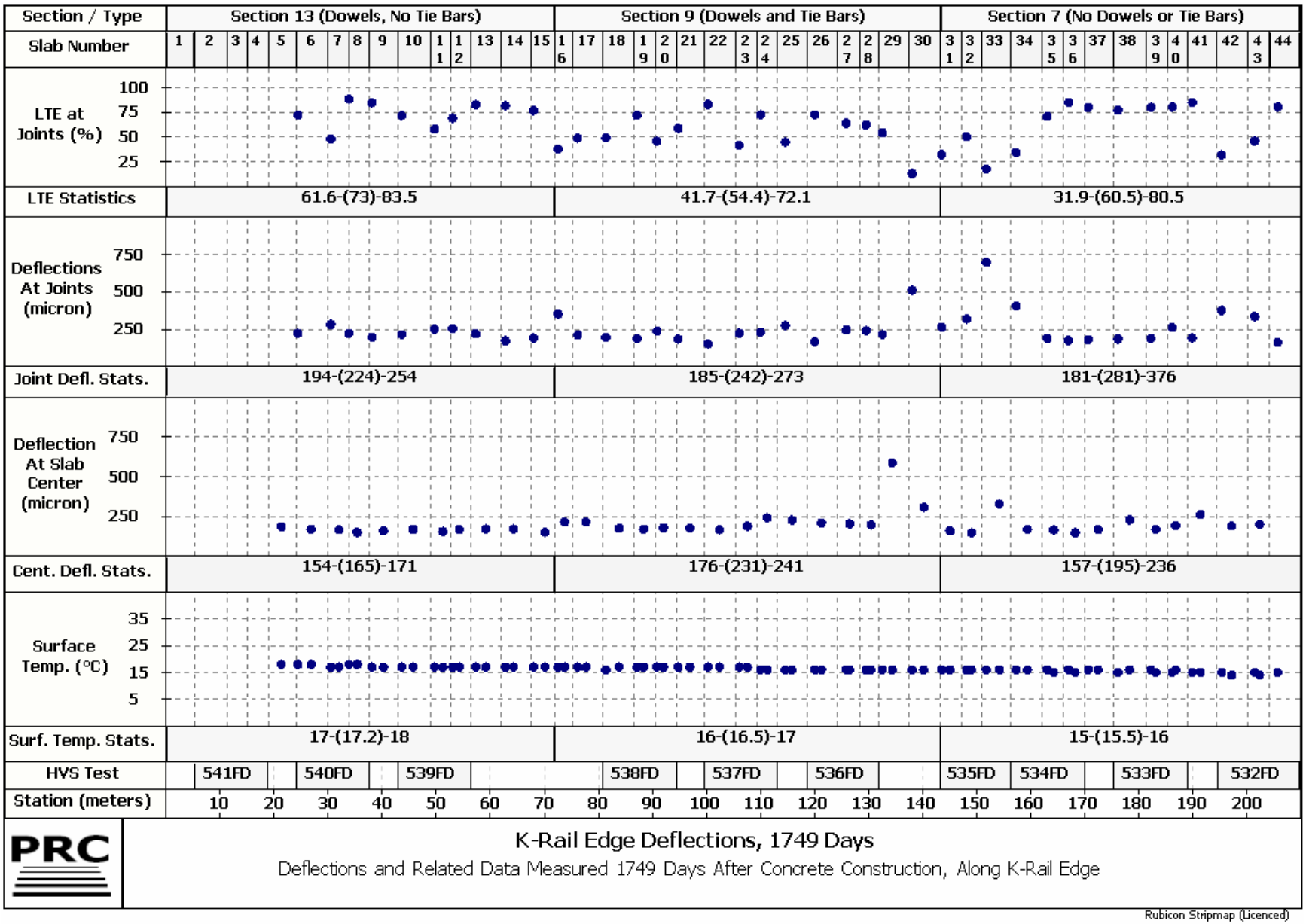
Section / Type
Section 13 (Dowels, No Tie Bars)
Section 9 (Dowels and Tie Bars)
Section 7 (No Dowels or Tie Bars)
Slab Number
1 2 3 4 5 6 7 8 9 10 11 12 13 14 15 16 17 18 19 20 21 22 23 24 25 26 27 28 29 30 31 32 33 34 35 36 37 38 39 40 41 42 43 44
LTE at Joints (%)
100
75
50
25
LTE Statistics
61.6-(73)-83.5
41.7-(54.4)-72.1
31.9-(60.5)-80.5
Deflections At Joints (micron)
750
500
250
Joint Defl. Stats.
194-(224)-254
185-(242)-273
181-(281)-376
Deflection At Slab Center (micron)
750
500
250
Cent. Defl. Stats.
154-(165)-171
176-(231)-241
157-(195)-236
Surface Temp. (°C)
35
25
15
5
Surf. Temp. Stats.
17-(17.2)-18
16-(16.5)-17
15-(15.5)-16
HVS Test
541FD
540FD
539FD
538FD
537FD
536FD
535FD
534FD
533FD
532FD
Station (meters)
10 20 30 40 50 60 70 80 90 100 110 120 130 140 150 160 170 180 190 200
PRC
K-Rail Edge Deflections, 1749 Days
Deflections and Related Data Measured 1749 Days After Concrete Construction, Along K-Rail Edge
Rubicon Stripmap (Licenced)

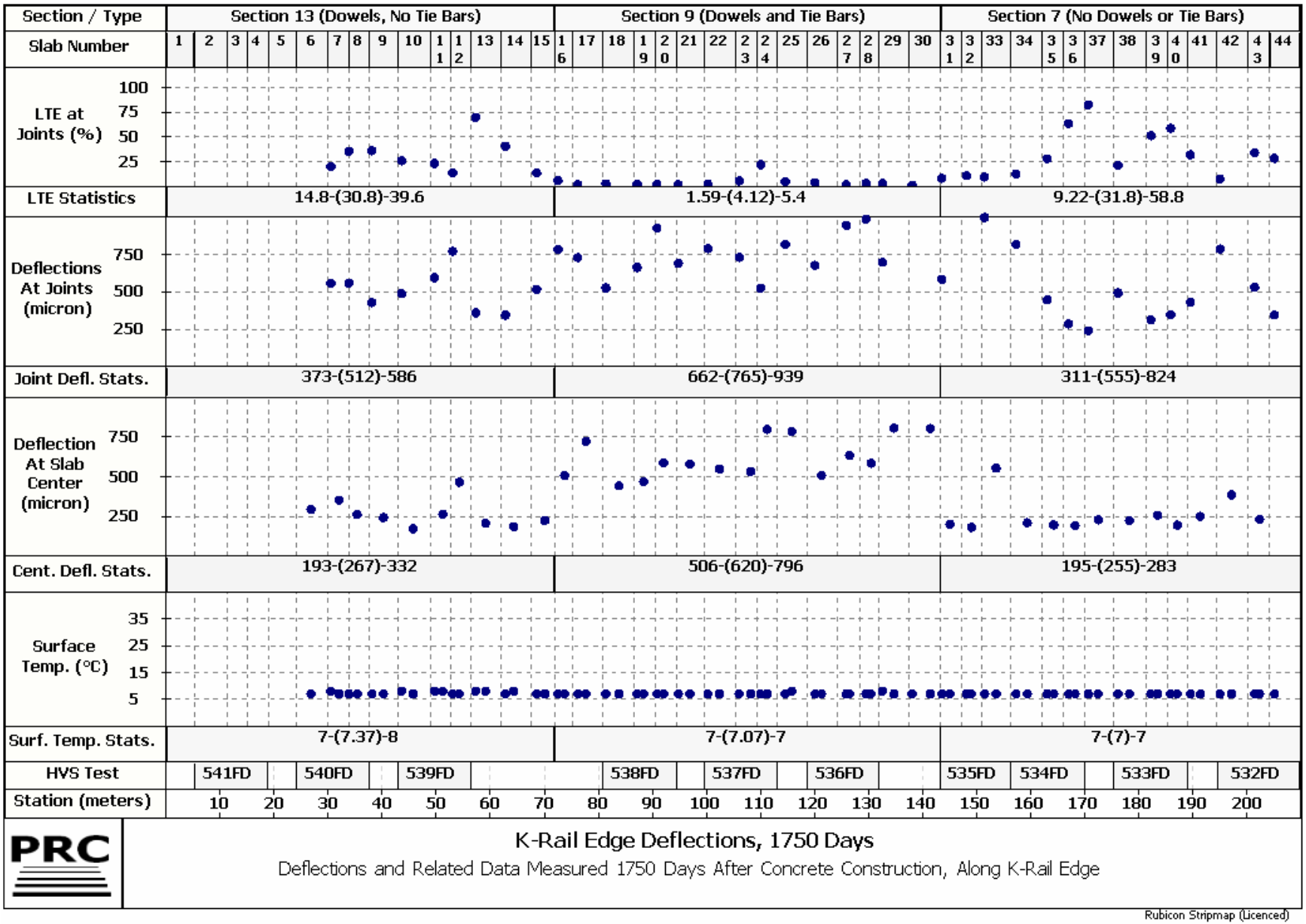
Section / Type
Section 13 (Dowels, No Tie Bars)
Section 9 (Dowels and Tie Bars)
Section 7 (No Dowels or Tie Bars)
Slab Number
1 2 3 4 5 6 7 8 9 10 11 12 13 14 15 16 17 18 19 20 21 22 23 24 25 26 27 28 29 30 31 32 33 34 35 36 37 38 39 40 41 42 43 44
LTE at Joints (%)
100
75
50
25
LTE Statistics
14.8-(30.8)-39.6
1.59-(4.12)-5.4
9.22-(31.8)-58.8
Deflections At Joints (micron)
750
500
250
Joint Defl. Stats.
373-(512)-586
662-(765)-939
311-(555)-824
Deflection At Slab Center (micron)
750
500
250
Cent. Defl. Stats.
193-(267)-332
506-(620)-796
195-(255)-283
Surface Temp. (°C)
35
25
15
5
Surf. Temp. Stats.
7-(7.37)-8
7-(7.07)-7
7-(7)-7
HVS Test
541FD
540FD
539FD
538FD
537FD
536FD
535FD
534FD
533FD
532FD
Station (meters)
10 20 30 40 50 60 70 80 90 100 110 120 130 140 150 160 170 180 190 200
PRC
K-Rail Edge Deflections, 1750 Days
Deflections and Related Data Measured 1750 Days After Concrete Construction, Along K-Rail Edge
Rubicon Stripmap (Licenced)

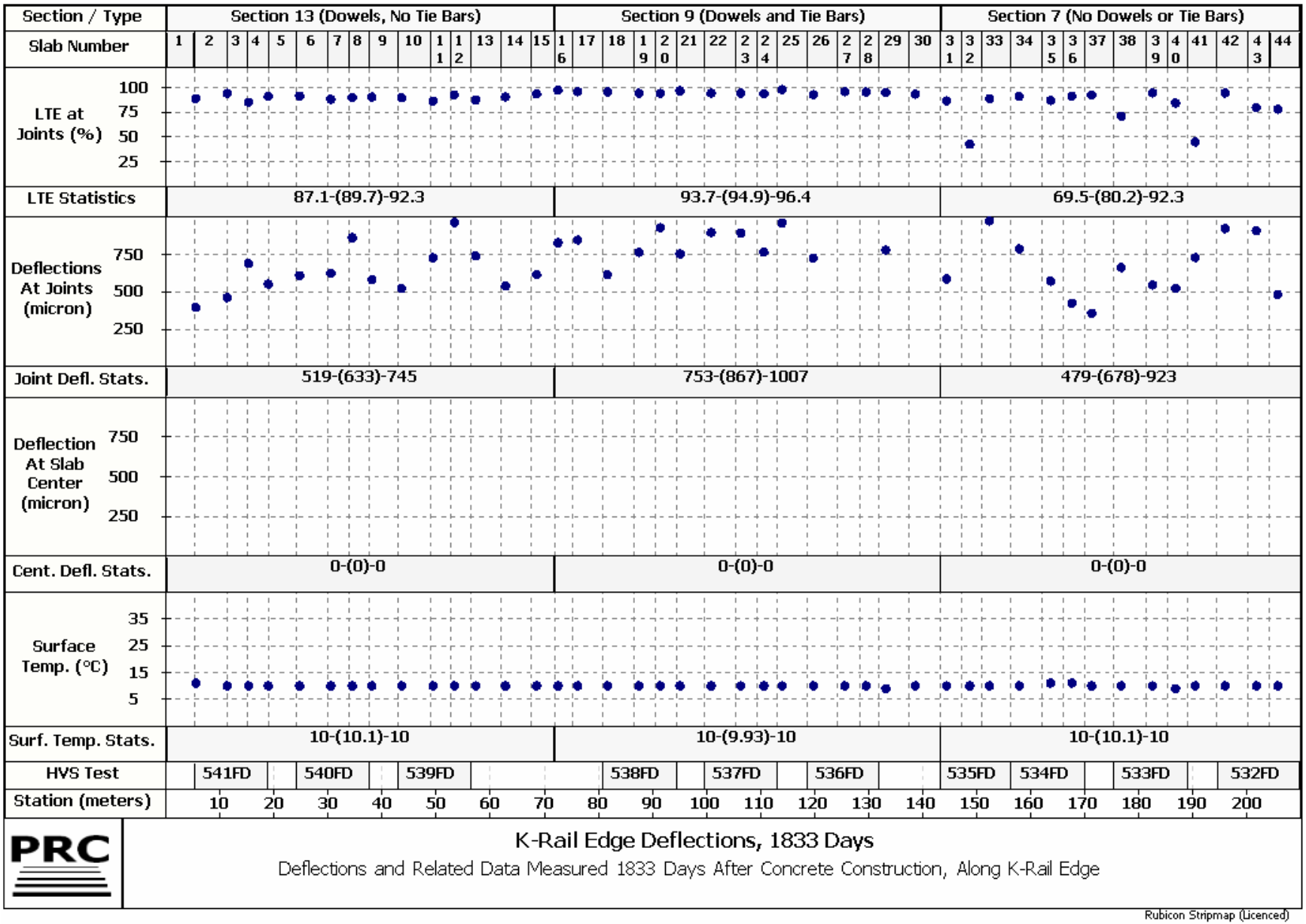
Section / Type
Section 13 (Dowels, No Tie Bars)
Section 9 (Dowels and Tie Bars)
Section 7 (No Dowels or Tie Bars)
Slab Number
1 2 3 4 5 6 7 8 9 10 11 12 13 14 15 16 17 18 19 20 21 22 23 24 25 26 27 28 29 30 31 32 33 34 35 36 37 38 39 40 41 42 43 44
LTE at Joints (%)
100
75
50
25
LTE Statistics
87.1-(89.7)-92.3
93.7-(94.9)-96.4
69.5-(80.2)-92.3
Deflections At Joints (micron)
750
500
250
Joint Defl. Stats.
519-(633)-745
753-(867)-1007
479-(678)-923
Deflection At Slab Center (micron)
750
500
250
Cent. Defl. Stats.
0-(0)-0
0-(0)-0
0-(0)-0
Surface Temp. (°C)
35
25
15
5
Surf. Temp. Stats.
10-(10.1)-10
10-(9.93)-10
10-(10.1)-10
HVS Test
541FD
540FD
539FD
538FD
537FD
536FD
535FD
534FD
533FD
532FD
Station (meters)
10 20 30 40 50 60 70 80 90 100 110 120 130 140 150 160 170 180 190 200
PRC
K-Rail Edge Deflections, 1833 Days
Deflections and Related Data Measured 1833 Days After Concrete Construction, Along K-Rail Edge
Rubicon Stripmap (Licenced)

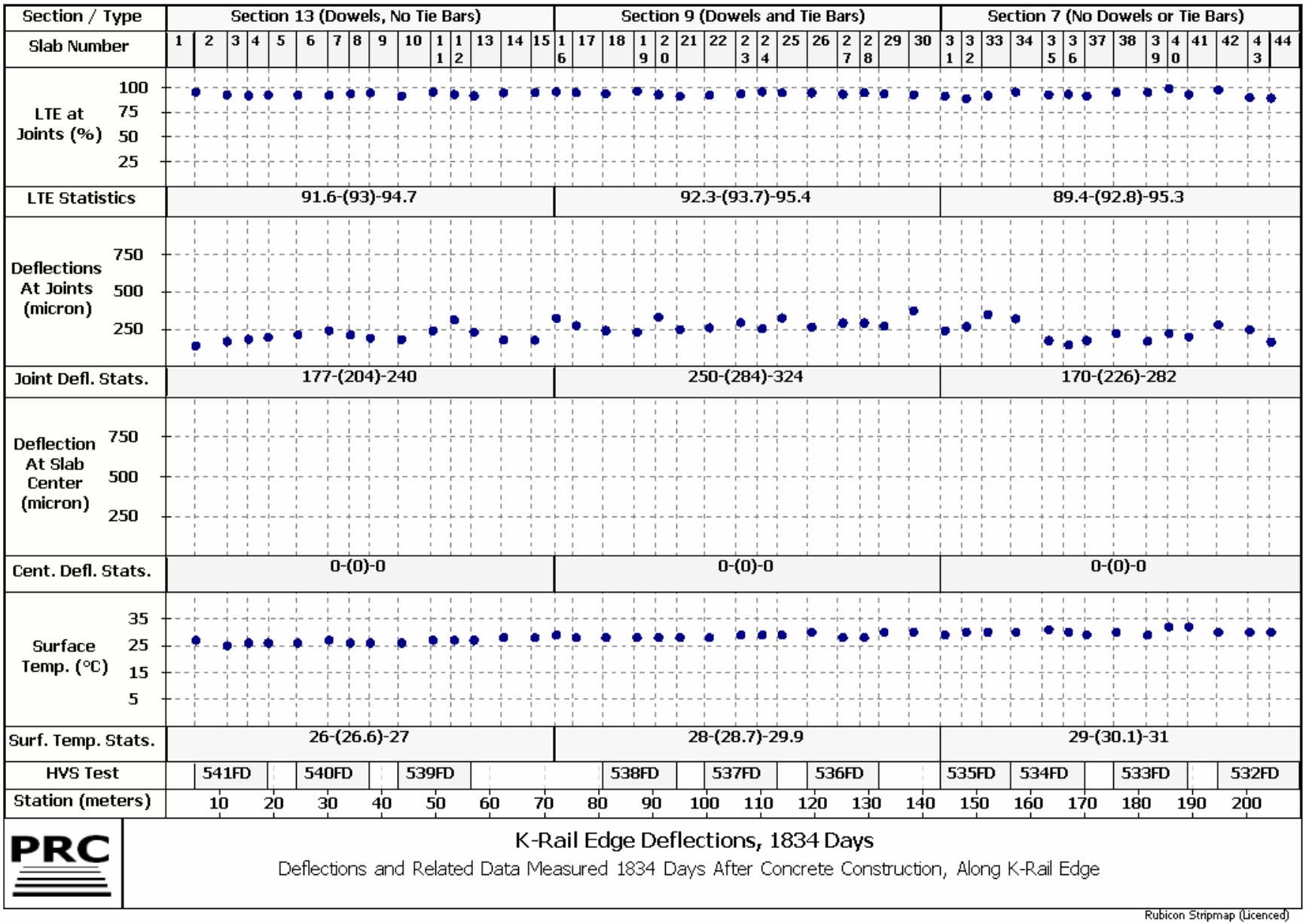
Section / Type
Section 13 (Dowels, No Tie Bars)
Section 9 (Dowels and Tie Bars)
Section 7 (No Dowels or Tie Bars)
Slab Number
1 2 3 4 5 6 7 8 9 10 11 12 13 14 15 16 17 18 19 20 21 22 23 24 25 26 27 28 29 30 31 32 33 34 35 36 37 38 39 40 41 42 43 44
LTE at Joints (%)
100
75
50
25
LTE Statistics
91.6-(93)-94.7
92.3-(93.7)-95.4
89.4-(92.8)-95.3
Deflections At Joints (micron)
750
500
250
Joint Defl. Stats.
177-(204)-240
250-(284)-324
170-(226)-282
Deflection At Slab Center (micron)
750
500
250
Cent. Defl. Stats.
0-(0)-0
0-(0)-0
0-(0)-0
Surface Temp. (°C)
35
25
15
5
Surf. Temp. Stats.
26-(26.6)-27
28-(28.7)-29.9
29-(30.1)-31
HVS Test
541FD
540FD
539FD
538FD
537FD
536FD
535FD
534FD
533FD
532FD
Station (meters)
10 20 30 40 50 60 70 80 90 100 110 120 130 140 150 160 170 180 190 200
PRC
K-Rail Edge Deflections, 1834 Days
Deflections and Related Data Measured 1834 Days After Concrete Construction, Along K-Rail Edge
Rubicon Stripmap (Licenced)

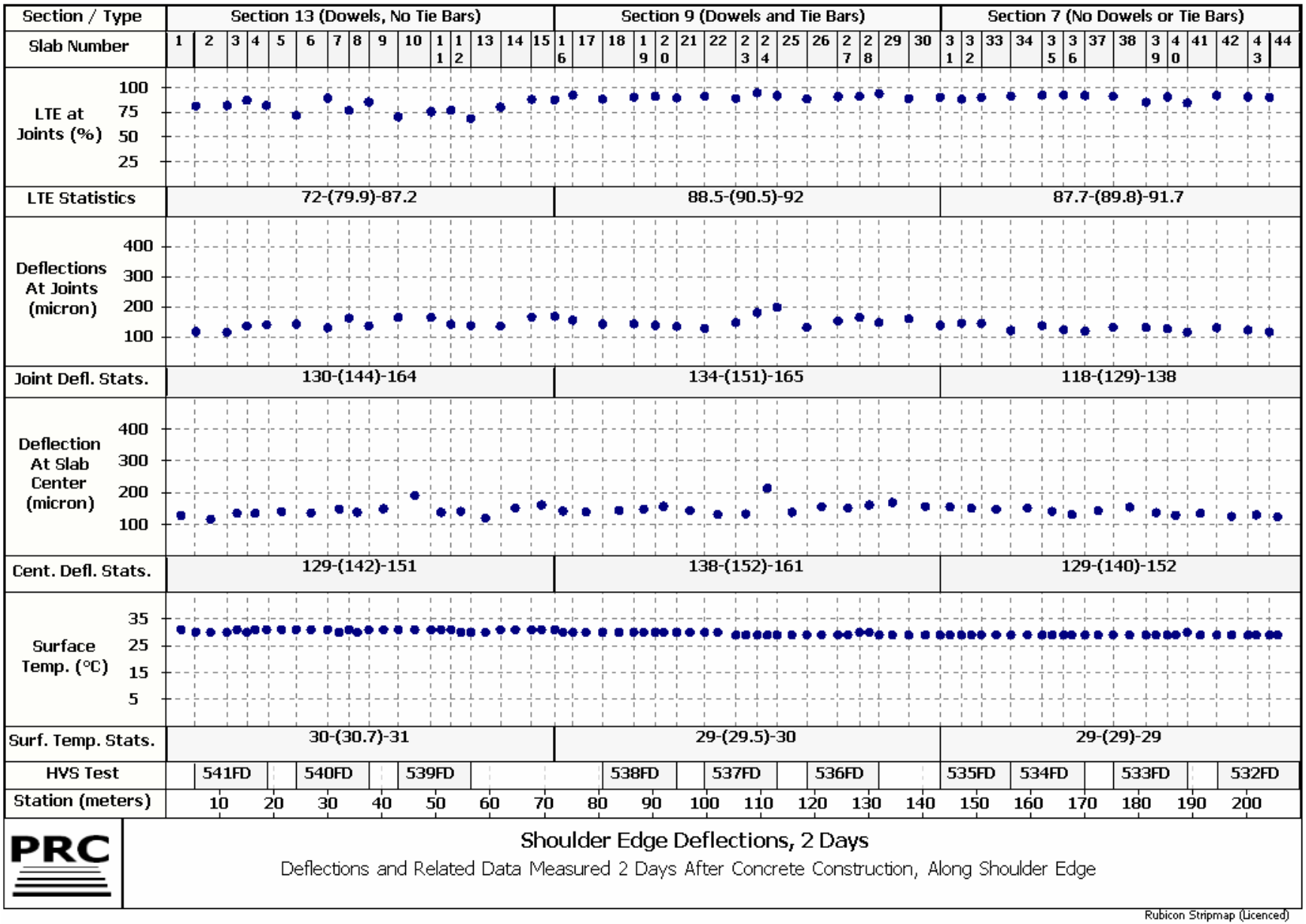
Section / Type
Section 13 (Dowels, No Tie Bars)
Section 9 (Dowels and Tie Bars)
Section 7 (No Dowels or Tie Bars)
Slab Number
1 2 3 4 5 6 7 8 9 10 11 12 13 14 15 16 17 18 19 20 21 22 23 24 25 26 27 28 29 30 31 32 33 34 35 36 37 38 39 40 41 42 43 44
LTE at Joints (%)
100
75
50
25
LTE Statistics
72-(79.9)-87.2
88.5-(90.5)-92
87.7-(89.8)-91.7
Deflections At Joints (micron)
400
300
200
100
Joint Defl. Stats.
130-(144)-164
134-(151)-165
118-(129)-138
Deflection At Slab Center (micron)
400
300
200
100
Cent. Defl. Stats.
129-(142)-151
138-(152)-161
129-(140)-152
Surface Temp. (°C)
35
25
15
5
Surf. Temp. Stats.
30-(30.7)-31
29-(29.5)-30
29-(29)-29
HVS Test
541FD
540FD
539FD
538FD
537FD
536FD
535FD
534FD
533FD
532FD
Station (meters)
10 20 30 40 50 60 70 80 90 100 110 120 130 140 150 160 170 180 190 200
PRC
Shoulder Edge Deflections, 2 Days
Deflections and Related Data Measured 2 Days After Concrete Construction, Along Shoulder Edge
Rubicon Stripmap (Licenced)

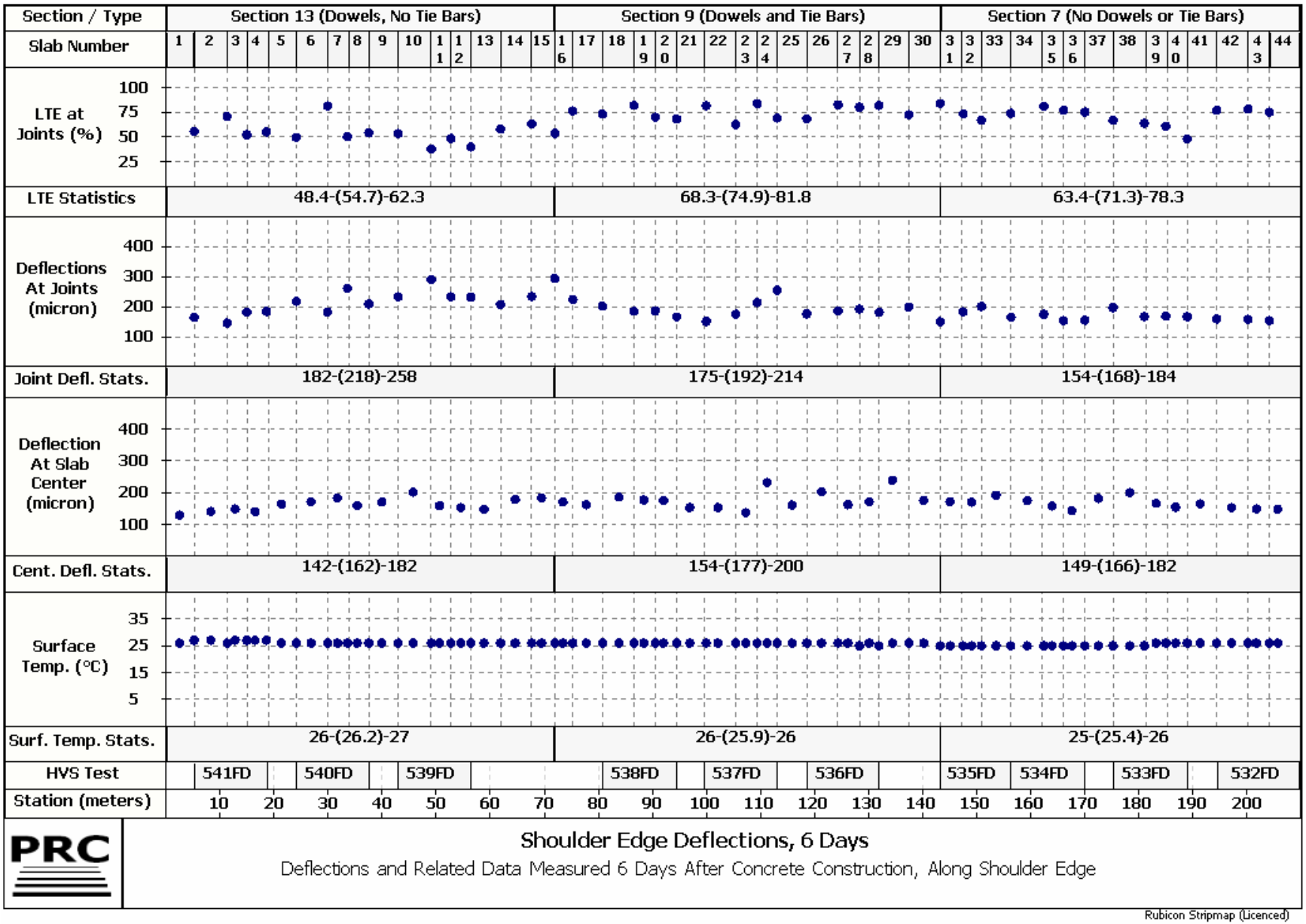
Section / Type
Section 13 (Dowels, No Tie Bars)
Section 9 (Dowels and Tie Bars)
Section 7 (No Dowels or Tie Bars)
Slab Number
1 2 3 4 5 6 7 8 9 10 11 12 13 14 15 16 17 18 19 20 21 22 23 24 25 26 27 28 29 30 31 32 33 34 35 36 37 38 39 40 41 42 43 44
LTE at Joints (%)
100
75
50
25
LTE Statistics
48.4-(54.7)-62.3
68.3-(74.9)-81.8
63.4-(71.3)-78.3
Deflections At Joints (micron)
400
300
200
100
Joint Defl. Stats.
182-(218)-258
175-(192)-214
154-(168)-184
Deflection At Slab Center (micron)
400
300
200
100
Cent. Defl. Stats.
142-(162)-182
154-(177)-200
149-(166)-182
Surface Temp. (°C)
35
25
15
5
Surf. Temp. Stats.
26-(26.2)-27
26-(25.9)-26
25-(25.4)-26
HVS Test
541FD
540FD
539FD
538FD
537FD
536FD
535FD
534FD
533FD
532FD
Station (meters)
10 20 30 40 50 60 70 80 90 100 110 120 130 140 150 160 170 180 190 200
PRC
Shoulder Edge Deflections, 6 Days
Deflections and Related Data Measured 6 Days After Concrete Construction, Along Shoulder Edge
Rubicon Stripmap (Licenced)

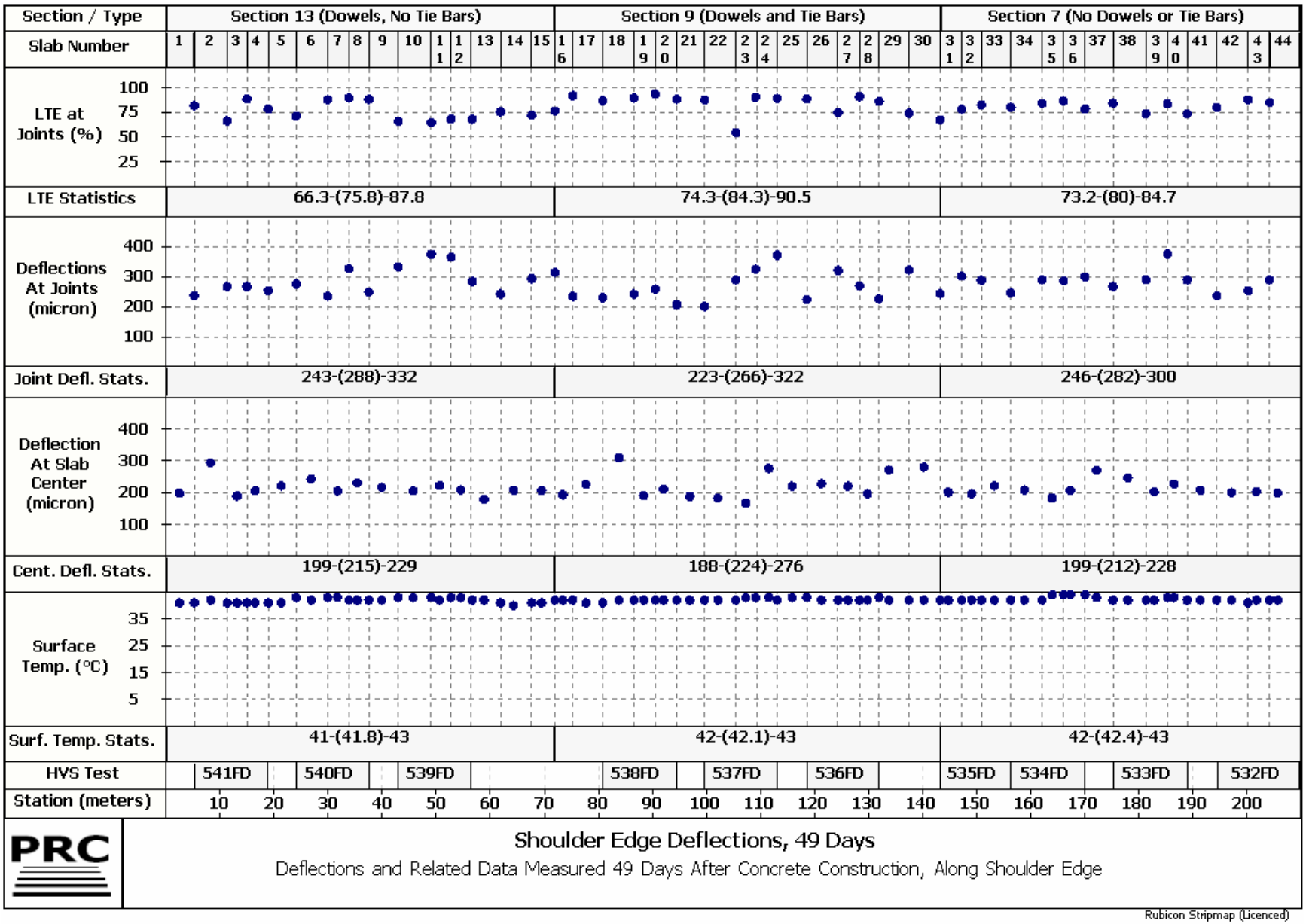
Section / Type
Section 13 (Dowels, No Tie Bars)
Section 9 (Dowels and Tie Bars)
Section 7 (No Dowels or Tie Bars)
Slab Number
1 2 3 4 5 6 7 8 9 10 11 12 13 14 15 16 17 18 19 20 21 22 23 24 25 26 27 28 29 30 31 32 33 34 35 36 37 38 39 40 41 42 43 44
LTE at Joints (%)
100
75
50
25
LTE Statistics
66.3-(75.8)-87.8
74.3-(84.3)-90.5
73.2-(80)-84.7
Deflections At Joints (micron)
400
300
200
100
Joint Defl. Stats.
243-(288)-332
223-(266)-322
246-(282)-300
Deflection At Slab Center (micron)
400
300
200
100
Cent. Defl. Stats.
199-(215)-229
188-(224)-276
199-(212)-228
Surface Temp. (°C)
35
25
15
5
Surf. Temp. Stats.
41-(41.8)-43
42-(42.1)-43
42-(42.4)-43
HVS Test
541FD
540FD
539FD
538FD
537FD
536FD
535FD
534FD
533FD
532FD
Station (meters)
10 20 30 40 50 60 70 80 90 100 110 120 130 140 150 160 170 180 190 200
PRC
Shoulder Edge Deflections, 49 Days
Deflections and Related Data Measured 49 Days After Concrete Construction, Along Shoulder Edge
Rubicon Stripmap (Licenced)

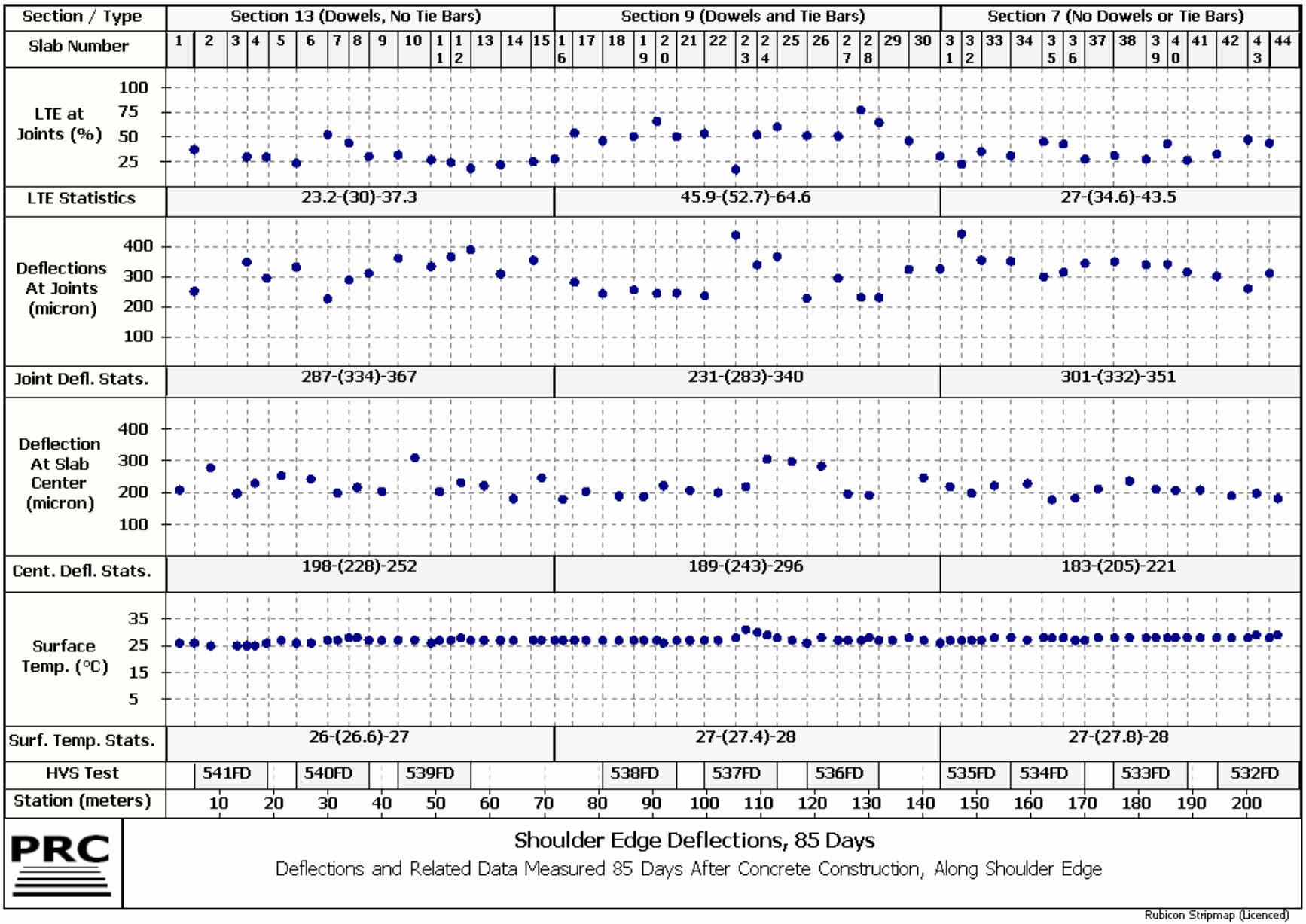
Section / Type
Section 13 (Dowels, No Tie Bars)
Section 9 (Dowels and Tie Bars)
Section 7 (No Dowels or Tie Bars)
Slab Number
1 2 3 4 5 6 7 8 9 10 11 12 13 14 15 16 17 18 19 20 21 22 23 24 25 26 27 28 29 30 31 32 33 34 35 36 37 38 39 40 41 42 43 44
LTE at Joints (%)
100
75
50
25
LTE Statistics
23.2-(30)-37.3
45.9-(52.7)-64.6
27-(34.6)-43.5
Deflections At Joints (micron)
400
300
200
100
Joint Defl. Stats.
287-(334)-367
231-(283)-340
301-(332)-351
Deflection At Slab Center (micron)
400
300
200
100
Cent. Defl. Stats.
198-(228)-252
189-(243)-296
183-(205)-221
Surface Temp. (°C)
35
25
15
5
Surf. Temp. Stats.
26-(26.6)-27
27-(27.4)-28
27-(27.8)-28
HVS Test
541FD
540FD
539FD
538FD
537FD
536FD
535FD
534FD
533FD
532FD
Station (meters)
10 20 30 40 50 60 70 80 90 100 110 120 130 140 150 160 170 180 190 200
PRC
Shoulder Edge Deflections, 85 Days
Deflections and Related Data Measured 85 Days After Concrete Construction, Along Shoulder Edge
Rubicon Stripmap (Licenced)

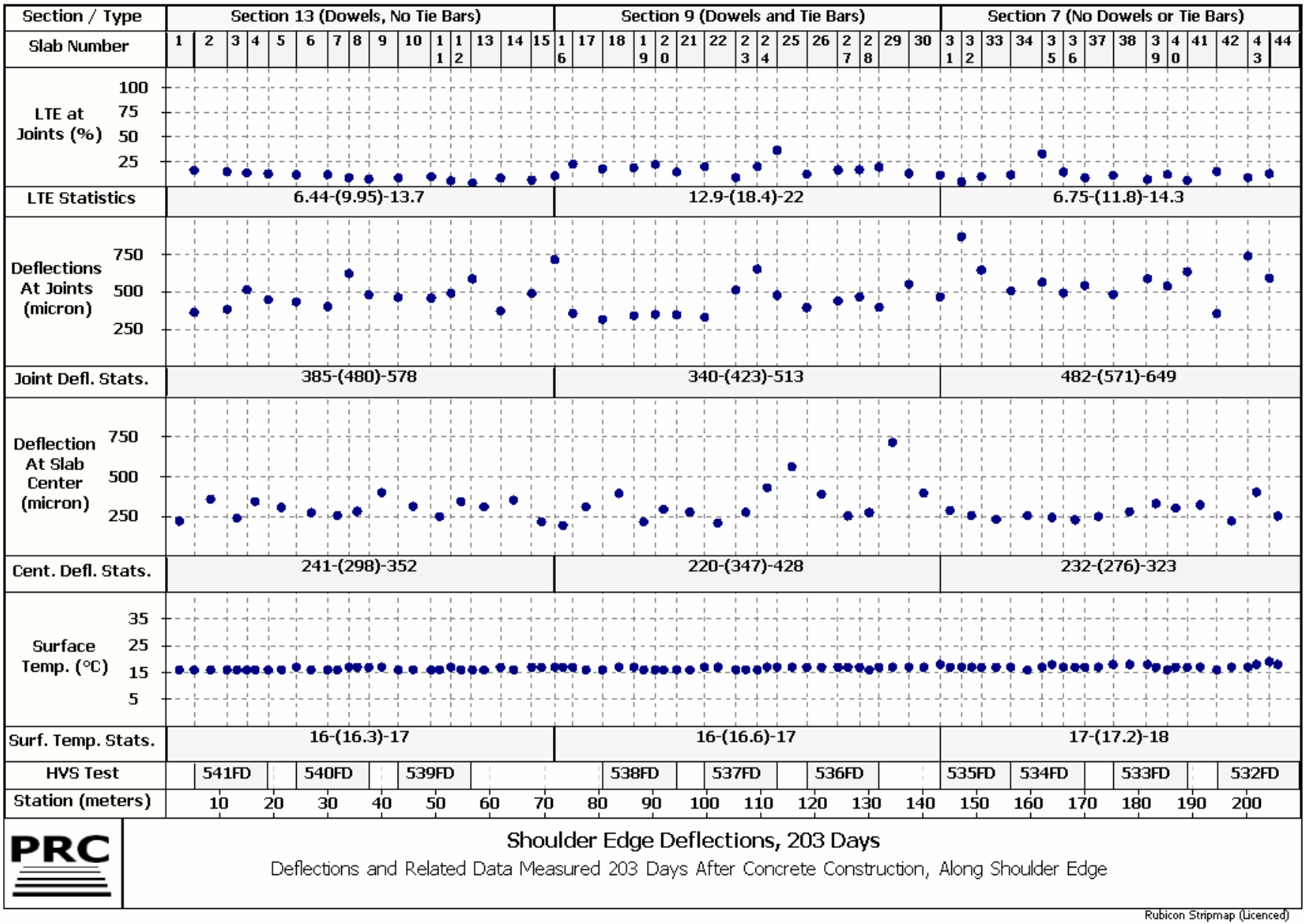
Section / Type
Section 13 (Dowels, No Tie Bars)
Section 9 (Dowels and Tie Bars)
Section 7 (No Dowels or Tie Bars)
Slab Number
1 2 3 4 5 6 7 8 9 10 11 12 13 14 15 16 17 18 19 20 21 22 23 24 25 26 27 28 29 30 31 32 33 34 35 36 37 38 39 40 41 42 43 44
LTE at Joints (%)
100
75
50
25
LTE Statistics
6.44-(9.95)-13.7
12.9-(18.4)-22
6.75-(11.8)-14.3
Deflections At Joints (micron)
750
500
250
Joint Defl. Stats.
385-(480)-578
340-(423)-513
482-(571)-649
Deflection At Slab Center (micron)
750
500
250
Cent. Defl. Stats.
241-(298)-352
220-(347)-428
232-(276)-323
Surface Temp. (°C)
35
25
15
5
Surf. Temp. Stats.
16-(16.3)-17
16-(16.6)-17
17-(17.2)-18
HVS Test
541FD
540FD
539FD
538FD
537FD
536FD
535FD
534FD
533FD
532FD
Station (meters)
10 20 30 40 50 60 70 80 90 100 110 120 130 140 150 160 170 180 190 200
PRC
Shoulder Edge Deflections, 203 Days
Deflections and Related Data Measured 203 Days After Concrete Construction, Along Shoulder Edge
Rubicon Stripmap (Licenced)

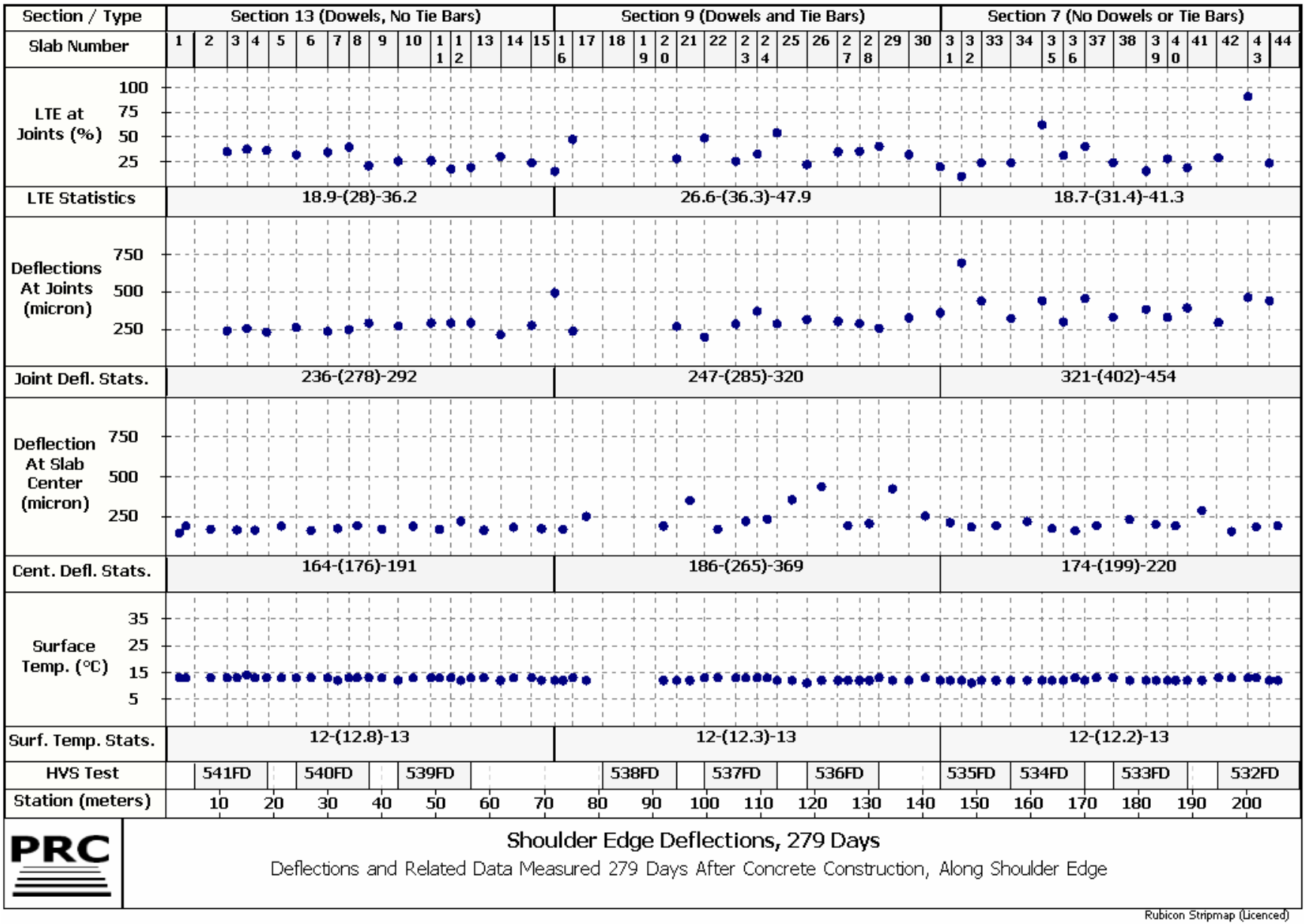
Section / Type
Section 13 (Dowels, No Tie Bars)
Section 9 (Dowels and Tie Bars)
Section 7 (No Dowels or Tie Bars)
Slab Number
1 2 3 4 5 6 7 8 9 10 11 12 13 14 15 16 17 18 19 20 21 22 23 24 25 26 27 28 29 30 31 32 33 34 35 36 37 38 39 40 41 42 43 44
LTE at Joints (%)
100
75
50
25
LTE Statistics
18.9-(28)-36.2
26.6-(36.3)-47.9
18.7-(31.4)-41.3
Deflections At Joints (micron)
750
500
250
Joint Defl. Stats.
236-(278)-292
247-(285)-320
321-(402)-454
Deflection At Slab Center (micron)
750
500
250
Cent. Defl. Stats.
164-(176)-191
186-(265)-369
174-(199)-220
Surface Temp. (°C)
35
25
15
5
Surf. Temp. Stats.
12-(12.8)-13
12-(12.3)-13
12-(12.2)-13
HVS Test
541FD
540FD
539FD
538FD
537FD
536FD
535FD
534FD
533FD
532FD
Station (meters)
10 20 30 40 50 60 70 80 90 100 110 120 130 140 150 160 170 180 190 200
PRC
Shoulder Edge Deflections, 279 Days
Deflections and Related Data Measured 279 Days After Concrete Construction, Along Shoulder Edge
Rubicon Stripmap (Licenced)

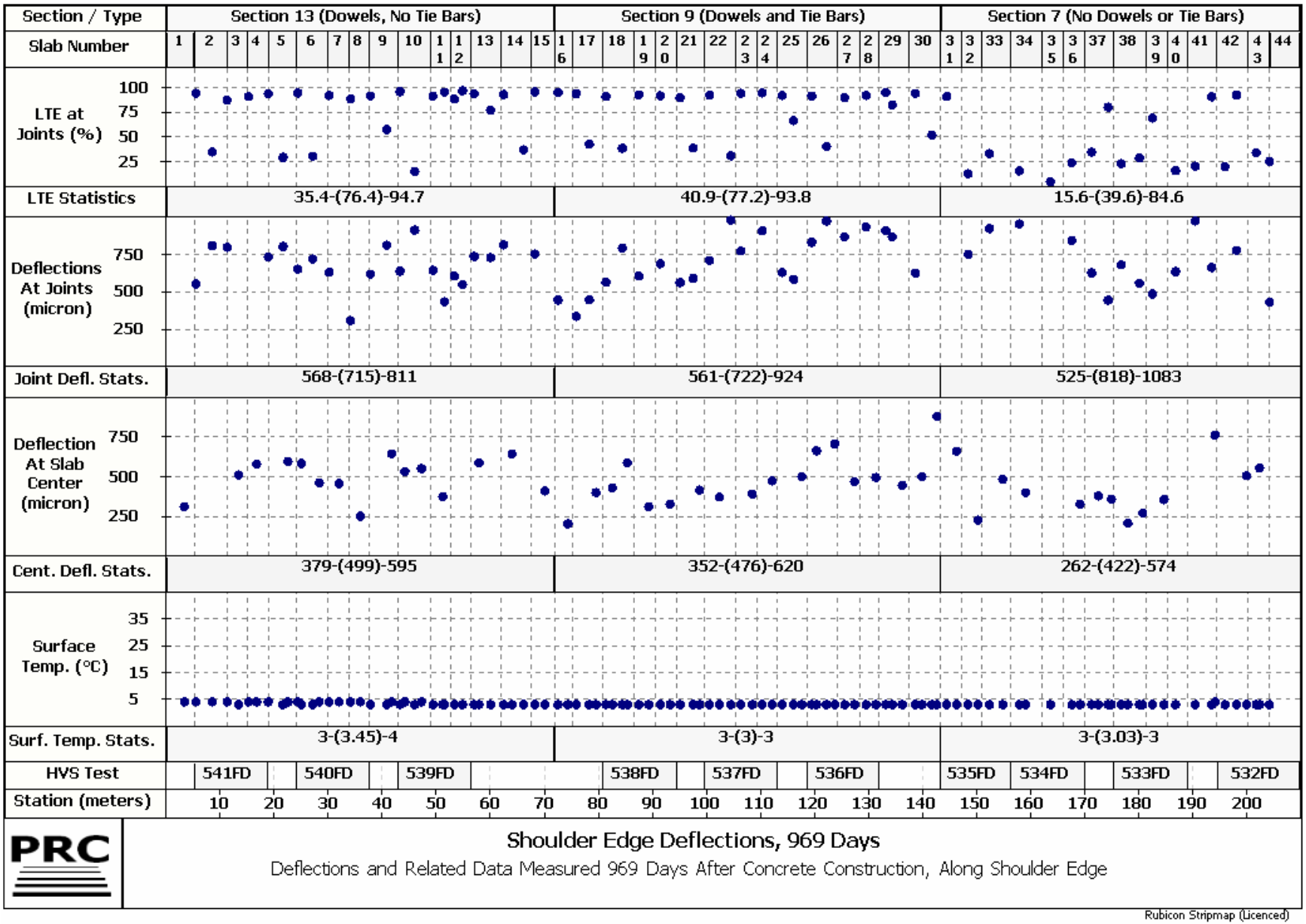
Section / Type
Section 13 (Dowels, No Tie Bars)
Section 9 (Dowels and Tie Bars)
Section 7 (No Dowels or Tie Bars)
Slab Number
1 2 3 4 5 6 7 8 9 10 11 12 13 14 15 16 17 18 19 20 21 22 23 24 25 26 27 28 29 30 31 32 33 34 35 36 37 38 39 40 41 42 43 44
LTE at Joints (%)
100
75
50
25
LTE Statistics
35.4-(76.4)-94.7
40.9-(77.2)-93.8
15.6-(39.6)-84.6
Deflections At Joints (micron)
750
500
250
Joint Defl. Stats.
568-(715)-811
561-(722)-924
525-(818)-1083
Deflection At Slab Center (micron)
750
500
250
Cent. Defl. Stats.
379-(499)-595
352-(476)-620
262-(422)-574
Surface Temp. (°C)
35
25
15
5
Surf. Temp. Stats.
3-(3.45)-4
3-(3)-3
3-(3.03)-3
HVS Test
541FD
540FD
539FD
538FD
537FD
536FD
535FD
534FD
533FD
532FD
Station (meters)
10 20 30 40 50 60 70 80 90 100 110 120 130 140 150 160 170 180 190 200
PRC
Shoulder Edge Deflections, 969 Days
Deflections and Related Data Measured 969 Days After Concrete Construction, Along Shoulder Edge
Rubicon Stripmap (Licenced)

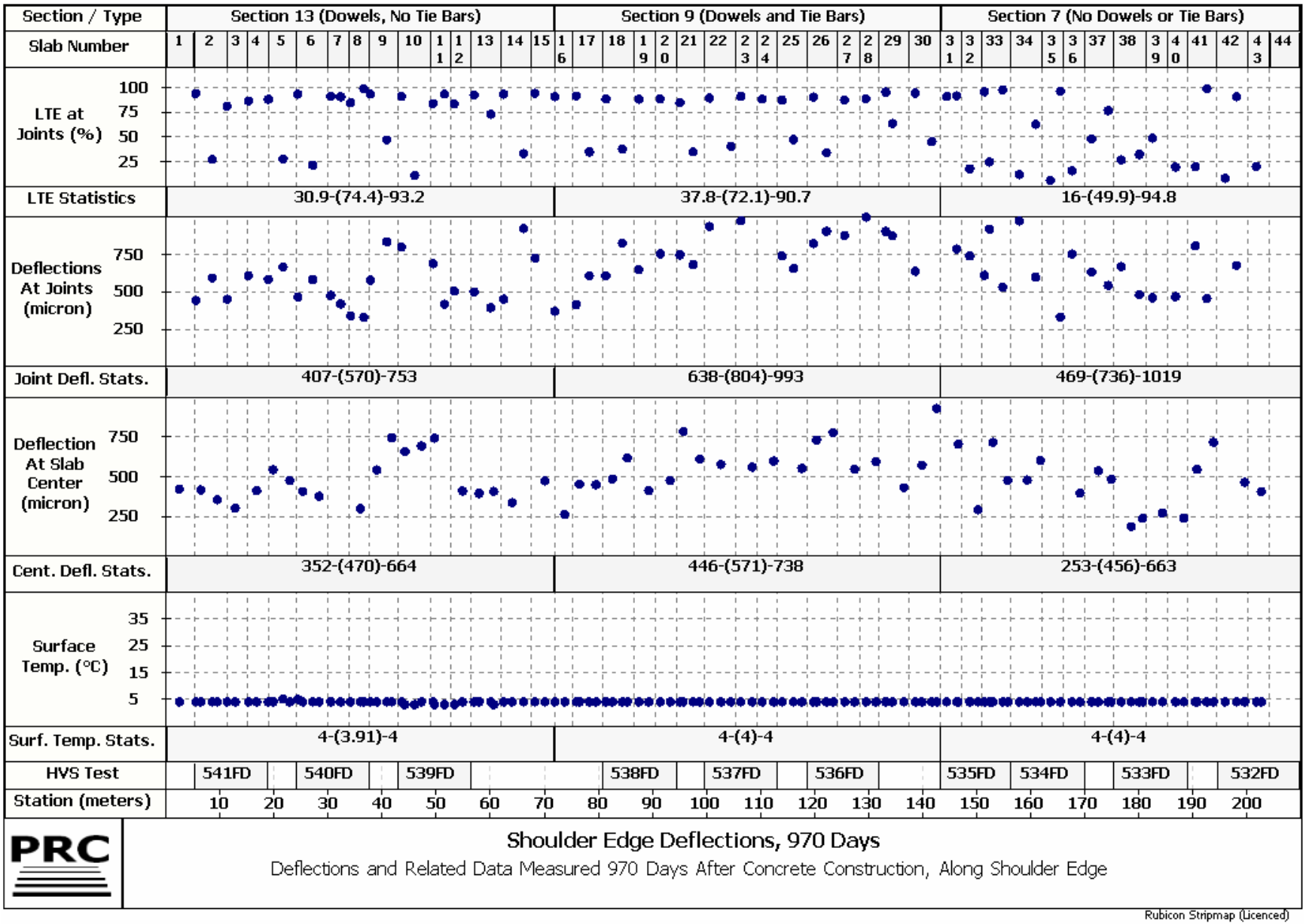
Section / Type
Section 13 (Dowels, No Tie Bars)
Section 9 (Dowels and Tie Bars)
Section 7 (No Dowels or Tie Bars)
Slab Number
LTE at Joints (%)
LTE Statistics
30.9-(74.4)-93.2
37.8-(72.1)-90.7
16-(49.9)-94.8
Deflections At Joints (micron)
Joint Defl. Stats.
407-(570)-753
638-(804)-993
469-(736)-1019
Deflection At Slab Center (micron)
Cent. Defl. Stats.
352-(470)-664
446-(571)-738
253-(456)-663
Surface Temp. (°C)
Surf. Temp. Stats.
4-(3.91)-4
4-(4)-4
4-(4)-4
HVS Test
541FD
540FD
539FD
538FD
537FD
536FD
535FD
534FD
533FD
532FD
Station (meters)
Shoulder Edge Deflections, 970 Days
Deflections and Related Data Measured 970 Days After Concrete Construction, Along Shoulder Edge
Rubicon Stripmap (Licenced)